july 1960

the institute of radio engineers

Proceedings of the IRE

in this issue

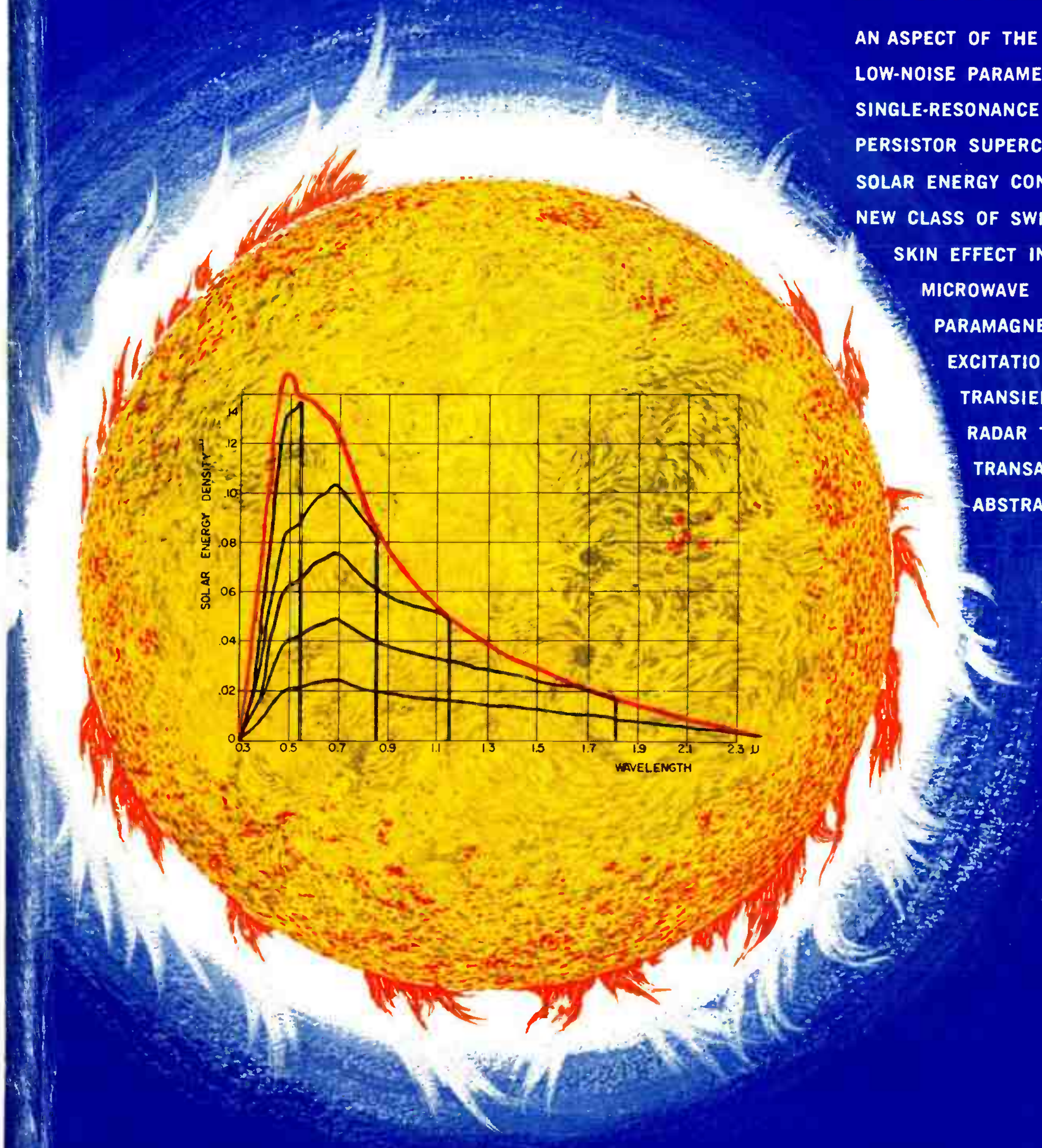

Solar Energy Conversion: Page 1246

FOR YOUR
SPECIAL APPLICATIONS
The bulk of UTC production is on special units designed to specific customers' needs. Illustrated below are some typical units and some unusual units as manufactured for special applications. We would be pleased to advise and quote to your special requirements.
FILTERS
All types for frequencies from .1 cycle to 400 MC.
400 ~ telemetering, 3 db at ± 7.5%, 40 db at 230 and 700 ~, 5/8 x 1¼ x 2"
15 ~ BP filter, 20 db at 30 ~, 45 db at 100 ~, phase angle at CF less than 3° from —40 to +100°C.
LP filter within 1 db to 49 KC, stable to .1 db from 0 to 85°C., 45 db at 55 KC.
LP filter less than .1 db 0 to 2.5 KC, 50 db beyond 3 KC.
PULSE TRANSFORMERS
From miniature blocking oscillator to 10 megawatt.
Wound core unit .01 micro-second rise time.
Pulse current transformer 100 Amp.
Pulse output to magnatron, bifilar filament.
Precise wave shape pulse output, 2500 V. 3 Amps.
HIGH Q COILS
Toroid, laminated, and cup structures from .1 cycle to 400 MC.
Tuned DO-T servo amplifier transformer, 400 ~ .5% distortion.
Toroid for printed circuit, Q of 90 at 15 KC.
Dual toroid, Q of 75 at 10 KC, and Q of 120 at 5 KC.
HVC tapped variable inductor for 3 KC oscillator.
SPECIALTIES
Saturable reactors, reference transformers, magnetic amplifiers, combined unit.
RF saturable inductor for sweep from 17 MC to 21 MC.
Voltage reference transformer .05% accuracy.
Multi-control magnetic amplifier for airborne servo.
Input, output, two tuned interstages, peaking network, and BP filter, all in one case.
POWER COMPONENTS
Standard and high temperature . . . hermetic, molded, and encapsulated.
Multi-winding 140 VA, 6 KC power transformer 1¼ x 1¼ x 1"
200° C. power transformer, 400 ~, 150 VA.
400 ~ scope transformer, 20 KV output.
60 ~ current limiting filament transformer, Sec. 25 Mmfd., 30 KV hipot.
plus OVER 1,000 STOCK ITEMS with UTC High Reliability
write for catalog
UNITED TRANSFORMER CORP.
150 VARICK STREET, NEW YORK 13, N. Y.
PACIFIC MFG. DIVISION: 4008 W. JEFFERSON BLVD., LOS ANGELES 16, CALIF.
EXPORT DIVISION: 13 EAST 40th STREET, NEW YORK 16, N. Y. CABLES: "ARLAB"

VOLUME 48, NUMBER 7

July, 1960

published monthly by The Institute of Radio Engineers, Inc.

Proceedings of the IRE®

contents

COVER

The efficiency of solar energy converters is limited by the energy gap of the semiconductor materials used. This is demonstrated by the diagram of the energy spectrum of the sun, which shows the amount of the spectrum utilized by materials with different energy-gap levels. This is one of several factors which affect the performance of solar cells, as discussed on page 1246.

JULY

published monthly by The Institute of Radio Engineers, Inc.

Proceedings of the IRE®

continued

PROCEEDINGS OF THE IRE, published monthly by The Institute of Radio Engineers, Inc. at 1 East 79 Street, New York 21, N. Y. Manuscripts should be submitted in triplicate to the Editorial Department. Responsibility for contents of papers published rests upon the authors, and not the IRE or its members. All republication rights, including translations, are reserved by the IRE and granted only on request. Abstracting is permitted with mention of source.

Thirty days advance notice is required for change of address. Price per copy: members of the Institute of Radio Engineers, one additional copy $1.25; non-members $2.25. Yearly subscription price: to members $9.00, one additional subscription $13.50; to non-members in United States, Canada, and U. S. Possessions $18.00; to non-members in foreign countries $19.00. Second-class postage paid at Menasha, Wisconsin under the act of March 3, 1879. Acceptance for mailing at a special rate of postage is provided for in the act of February 28, 1925, embodied in Paragraph 4, Section 412, P. L. and R., authorized October 26, 1927. Printed in U.S.A.

DIFILM® DUAL DIELECTRIC

gives new BLACK BEAUTY® series of small, low-cost capacitors outstanding performance characteristics

- withstand 105C operation with no voltage derating
- moderate capacitance change with temperature
- excellent retrace under temperature cycling
- superior long-term capacitance stability
- very high insulation resistance

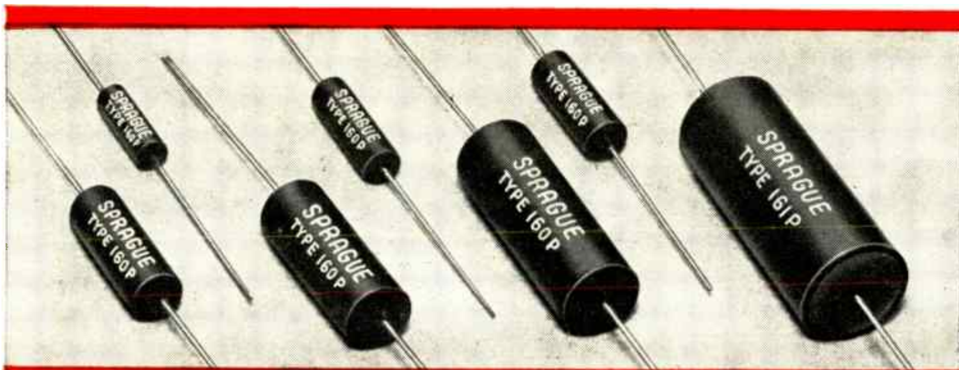

NEW!... DIFILM Type 160P fully-molded case and Type 161P pre-molded case capacitors in 5/16" to 1" diameters for general commercial and entertainment electronics.

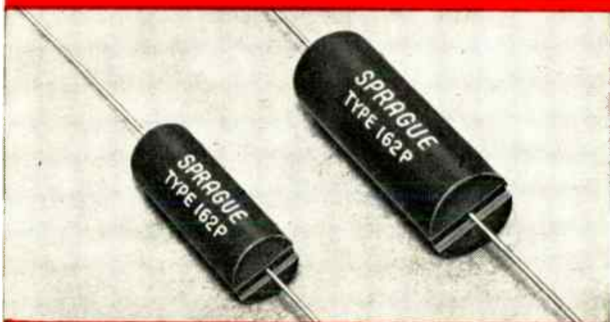

NEW!... DIFILM Type 162P slotted-base multi-purpose molded case capacitors for auto radios and other severe vibration applications. Slot prevents collection of moisture around leads when capacitor is end-mounted against chassis.

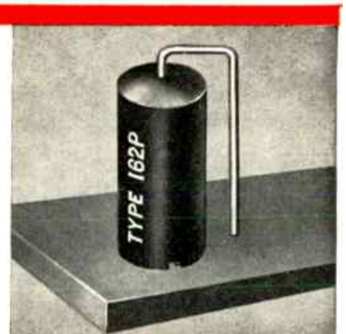

● New DIFILM Black Beauty Capacitors represent a basic advance in paper tubular capacitor design. DIFILM Capacitors combine the proven long life of paper capacitors with the effective moisture protection of plastic capacitors . . . by using a *dual dielectric of both cellulose and polyester film that's superior to all others for small, yet low cost, capacitors.*

● Just check the characteristics listed above. This overall performance is fully protected by HCX®, an exclusive Sprague hydrocarbon material which impregnates the windings, filling all voids and pinholes before it polymerizes. The result is a solid rock-hard capacitor section, further protected by an outer molding of humidity-resistant phenolic. *These capacitors are designed for operating temperatures ranging up to 105°C (221°F) . . . at high humidity levels . . . without voltage derating!*

For complete specifications on DIFILM Black Beauty Capacitors, write for Bulletin 2025 to Technical Literature Section, Sprague Electric Company, 235 Marshall Street, North Adams, Massachusetts.

SPRAGUE®
THE MARK OF RELIABILITY

SPRAGUE COMPONENTS:

CAPACITORS • RESISTORS • MAGNETIC COMPONENTS • TRANSISTORS • INTERFERENCE FILTERS • PULSE NETWORKS • HIGH TEMPERATURE MAGNET WIRE • CERAMIC-BASE PRINTED NETWORKS • PACKAGED COMPONENT ASSEMBLIES

This month's "advertisement" was prepared by Dr. C. J. Hubbard, of our Research Group. "Rex" Hubbard's main preoccupation for some time has been the subject of thermoelectricity. In this writeup he tells about an interesting and possibly useful laboratory by-product of our research program.

THERMOELECTRICITY AND ESAKI DIODES

Some of us at AIL have recently been intrigued by the difficulty of obtaining a simple and efficient d.c. power supply for equipment utilizing considerable numbers of Esaki diodes and operating from the a.c. power mains. The difficulty is that this diode requires a bias of approximately one hundred millivolts, which must be extremely ripple free. Since conventional rectifiers do not operate with any degree of efficiency in this low voltage region, one is forced to find an alternative.

Possibly a nonlinear device can be found that will rectify efficiently at the hundred millivolt level; one is nonetheless faced with a vary nasty filtering problem due to the low impedance level involved. To obtain stability, Esaki diodes must be biased from an impedance substantially lower than the negative resistance at the diode operating point. Presently available diodes display negative resistances between ten and one hundred ohms, and if a substantial number are to be powered simultaneously, the supply impedance must be a small fraction of this, necessitating inconveniently large filter condensers.

An intriguing alternate solution to this problem occurred to us in the course of a program of research on various aspects of thermoelectricity. We noted that a single-stage semiconductor thermocouple, heated by a resistance heater, would be uniquely suited for use as just such a power supply. In the first place, the output voltage would be of the right magnitude with a quite moderate hot junction temperature. Secondly, the output impedance would be extremely low. In fact, it is rather difficult to build such a thermocouple with an impedance higher than a few tens of milliohms. Furthermore, due to the thermal time constants of the materials involved, the output should be virtually ripple free.

Nor is the thermoelectric converter at a disadvantage in the matter of efficiency. The efficiency of a conventional rectifier power supply, together with the voltage divider necessary to obtain a very low voltage, turns out to be of the order of a percent or two. On the other hand, a thermoelectric generator can easily be made to deliver up to five or more percent, depending on the degree of impedance match permitted by conditions of load regulation and diode stability.

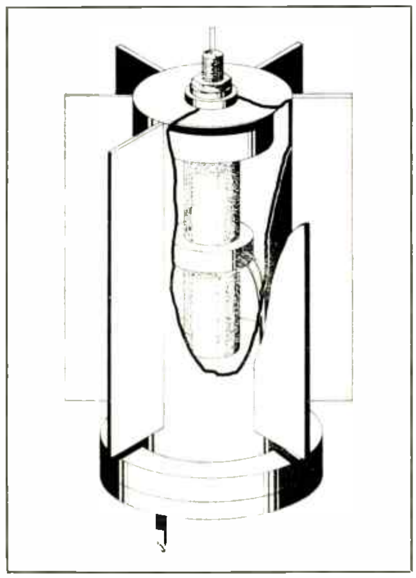

As an interesting (and possibly useful) by-product of our research, we decided to build such a thermoelectric power supply. The result is shown in the accompanying illustration, approximately three quarters life size, from which the simplicity of construction is apparent. For a heater we used a conventional 6.3 volt vacuum tube heater, embedded in an iron capsule which furnished the hot junction. The thermoelements are lead telluride, doped respectively p and n type, and are used to support the heater assembly in a sandwich arrangement held together by spring pressure. One cold junction is electrically, but not thermally, insulated from the can, and is brought out to a stud at the top for one output terminal. The other junction is the can itself. The entire unit is hermetically sealed to prevent oxidation of the thermoelements, and cooling fins were provided as a precaution.

When completed, the generator fulfilled our fondest expectations. Outputs of up to 240 millivolts were obtained (depending on the heater voltage applied), and the output impedance was approximately 20 milliohms at all outputs. The output ripple was less than 10 microvolts. The efficiency, when operating into a matched load, proved to be approximately 5%.

The can temperature, when operated at 100 millivolts output, measured 35°C (95°F), and rose to only 45°C at full output, showing that perhaps we were overcautious in appending fins. Incidentally, this unit has been running continuously for the last two months and shows no sign of deterioration.

Another possible use for this power supply, that has subsequently occurred to us, is in conjunction with the single-stage thermoelectric spot coolers that have recently been introduced for use with critical electronic components. These tiny refrigerators present load impedances of a few milliohms, and require about one hundred millivolts of direct current. The mismatch between one of these and a conventional power supply seems to be the greatest drawback to their usefulness in small numbers. Admittedly, the overall coefficient of performance of a system consisting of a thermoelectric cooler powered by a thermoelectric generator is rather low. Nevertheless, the natural impedance match between the two devices may render this the most efficient method of powering these coolers available at the present time.

Perhaps some of our readers will think of other uses for this interesting new power supply. If so, we would certainly appreciate hearing about them.

A complete bound set of our fourth series of articles is available on request. Write to Harold Hechtman at AIL for your set.

Airborne Instruments Laboratory
A DIVISION OF CUTLER-HAMMER, INC.
DEER PARK, LONG ISLAND, N. Y.
Phone MYrtle 2-6100

ALL UNITS ACTUAL SIZE

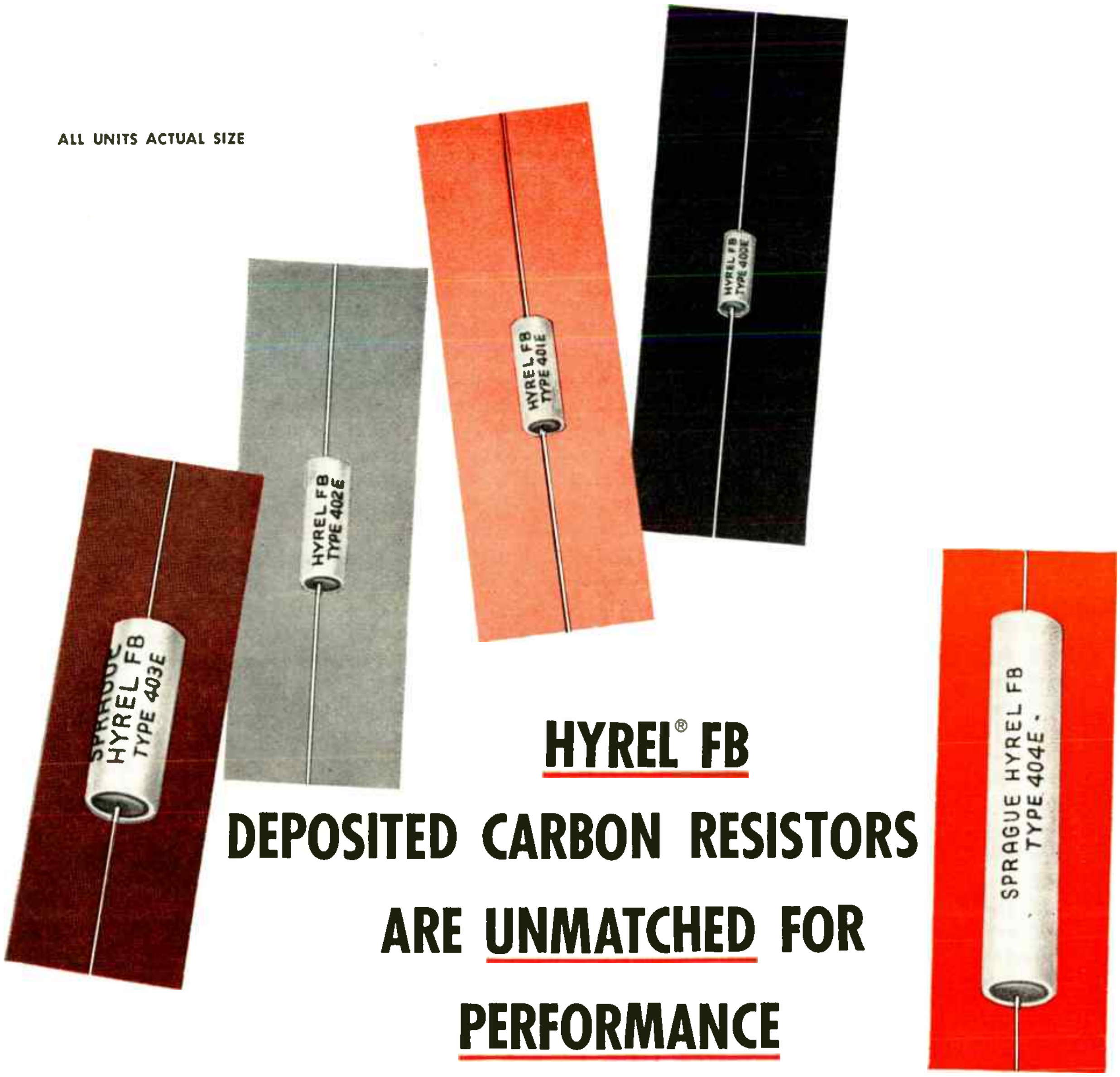

HYREL® FB DEPOSITED CARBON RESISTORS ARE UNMATCHED FOR PERFORMANCE

★ ★ ★ ★ ★ ★ ★ ★ ★ ★ ★ ★ ★ ★ ★ ★ ★ ★ ★ ★

HYREL® FB DEPOSITED CARBON RESISTORS
are hermetically sealed in ceramic jackets against moisture and vapor . . . safely protected against mechanical abuse. The Hyrel FB series is intended for applications in military, commercial and telephone equipment where long life under high humidity, small size, and stability of electrical characteristics are important.

WRITE FOR ENGINEERING BULLETIN 7010B
SPRAGUE ELECTRIC COMPANY
235 MARSHALL STREET • NORTH ADAMS, MASS.

SPRAGUE®
THE MARK OF RELIABILITY

Made to far exceed MIL-R-10509C Specifications

SPRAGUE COMPONENTS:
CAPACITORS • RESISTORS • MAGNETIC COMPONENTS • TRANSISTORS • INTERFERENCE FILTERS • PULSE NETWORKS
HIGH TEMPERATURE MAGNET WIRE • CERAMIC-BASE PRINTED NETWORKS • PACKAGED COMPONENT ASSEMBLIES

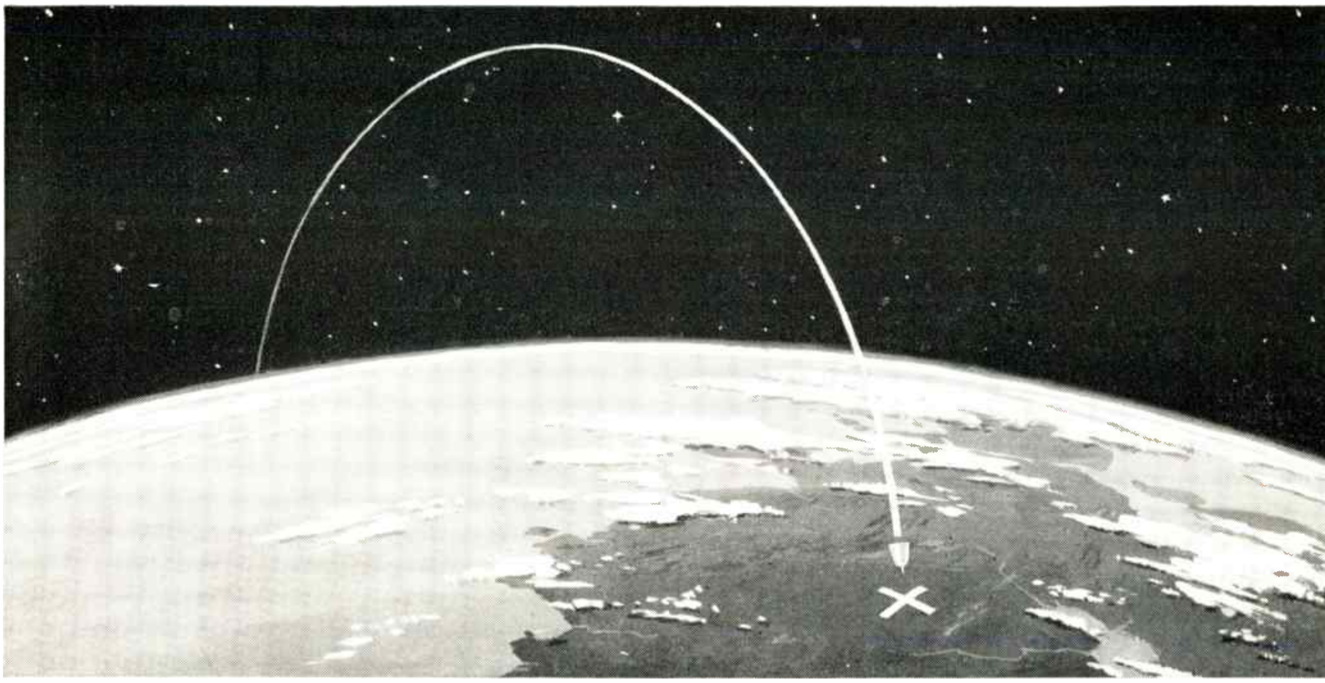

ASSIGNMENT: HIT A TARGET 6000 MILES AWAY

Can you guide a 110-ton Air Force Titan missile far up into the sky, to bring its nuclear warhead down with pinpoint accuracy on a target one-fourth the way around the globe—a target you not only can't see but which continually moves with the spinning earth?

This was the problem in missile guidance the Air Force presented to Bell Telephone Laboratories and its manufacturing partner, Western Electric. The answer was the development of a command guidance system which steers the Titan with high accuracy.

Unlike self-contained systems which demand complex guidance equipment in the missile itself, Bell Laboratories Command Guidance System keeps its master control equipment on the ground where it can be used over and over again. Thus a minimum of equipment is carried in the missile, and the ground station has full control of the missile during its guided flight. Techniques drawn from the communications art render the system immune to radio jamming.

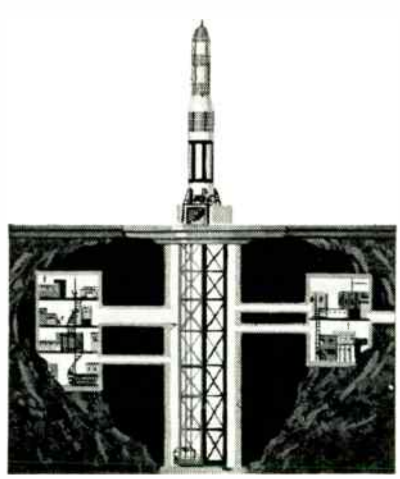

Bell Laboratories scientists and engineers designed the transmission and switching systems for the world's most versatile telephone network, developed much of our nation's radar, and pioneered in missile systems. From their vast storehouse of knowledge and experience comes the guidance system for the Titan.

BELL TELEPHONE LABORATORIES

WORLD CENTER OF COMMUNICATIONS RESEARCH AND DEVELOPMENT

HIGH SPEED SILICON COMPUTER DIODES with uniformly typical recovery time of 2 millimicroseconds were first made available in commercial quantities one year ago by Microwave Associates.

Today, Microwave Associates silicon mesa switching diodes are setting the computer industry standard. Extremely low reverse leakage (even at elevated temperatures), excellent forward characteristics, and superb reliability under severe mechanical and environmental conditions make these diodes suitable for a very wide range of applications. Major users have called these diodes excellent "universal switching diodes."

Production quantities are now replacing germanium and silicon computer diodes of both standard and newer types. They are priced competitively for large volume orders and delivery is off-the-shelf.

Faster, more sophisticated diodes for tomorrow's computers are on the way from Microwave Associates. Our leadership in this field is the result of years of experience with silicon semiconductor devices which operate at tomorrow's speeds. This experience, added to your own, will accelerate your computer progress.

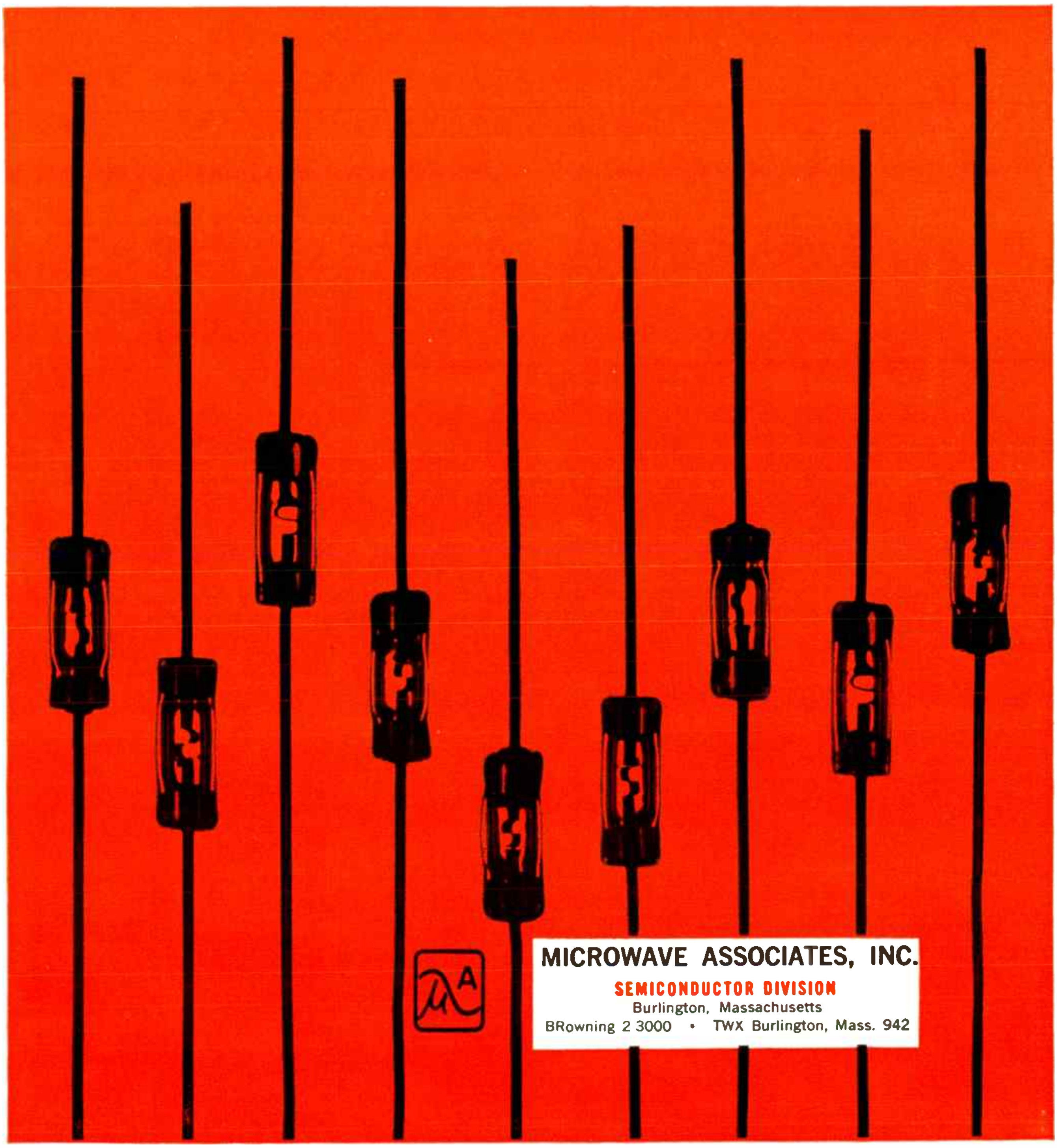

Meetings with Exhibits

● As a service both to Members and the industry, we will endeavor to record in this column each month those meetings of IRE, its sections and professional groups which include exhibits.

August 1-3, 1960
Fourth Global Communications Symposium, Hotel Statler, Washington, D.C.
Exhibits: Mr. Robert F. Brady, Office of the Chief Signal Officer, U. S. Army Signal Corps, Pentagon, Washington, D.C.

August 23-26, 1960
WESCON, Western Electronic Show and Convention, Memorial Sports Arena, Los Angeles, Calif.
Exhibits: Mr. Don Larson, WESCON, 1435 LaCienega Blvd., Los Angeles, Calif.

September 9-10, 1960
Conference on Communications, Tomorrow's Techniques—A Survey. Roosevelt Hotel, Cedar Rapids, Iowa.
Exhibits: Mr. D. O. McCoy, 2315 Blake Blvd., Cedar Rapids, Iowa.

September 19-22, 1960
National Symposium on Space Electronics & Telemetry, Shoreham Hotel, Washington, D.C.
Exhibits: Mr. Leon King, Jansky and Bailey, Inc., 1339 Wisconsin Ave., N.W., Washington, D.C.

October 3-5 1960
Sixth National Communications Symposium, Hotel Utica & Utica Municipal Auditorium, Utica, N.Y.
Exhibits: Mr. R. E. Bischoff, 19 Westminster Road, Utica, N.Y.

October 10-12, 1960
National Electronics Conference, Hotel Sherman, Chicago, Ill.
Exhibits: National Electronics Conference, Inc., 228 North La Salle St., Chicago 1, Ill.

October 19-21, 1960
Symposium on Space Navigation, Deshler-Hilton Hotel & Civic Center, Columbus, Ohio
Exhibits: Mr. William P. McNally, 35 Laurel St., Floral Park, L.I., N.Y.

October 24-26, 1960
East Coast Aeronautical & Navigational Electronics Conference, Lord Baltimore Hotel, Baltimore, Md.
Exhibits: Dr. Harold Schutz, Westinghouse Electric Corp., Air Arm Div., P.O. Box 746, Baltimore, Md.

October 26-28, 1960
Fifth Annual Conference on Non-Linear Magnetics and Magnetic Amplifiers, Bellevue-Stratford Hotel, Philadelphia, Pa.
Exhibits: J. L. Whitlock Associates, 6044 Ninth St., North, Arlington 5, Va.

(Continued on page 10A)

KAY KAY KAY

KAY *Ligna-Sweep*® SKV

SWEEPING OSCILLATOR

Cat. No. 935-A

AUDIO—VIDEO—VHF . . . IN ONE INSTRUMENT!

- FREQUENCY RANGE—200 CPS TO 220 MC.
- SWEEP REPETITION RATES FROM 0.2 TO 60 CPS.
- LINEAR AND LOGARITHMIC SWEEPS.
- AUDIO SWEEP—200 CPS TO 20,000 CPS.

- 3 Highly Stable Video Bands—1 kc to 12 mc., Variable or in Single Sweep.
- RF Output of 1 Volt rms into 70 Ohms ±.5 db Over Widest Sweep Width.
- 8 Narrow Customer Selected Fixed Frequency Bands—20 kc to 12 mc.
- 9 Fundamental Frequency, Wide VHF Bands—10 mc to 220 mc.

SPECIFICATIONS

VARIABLE FREQUENCY RANGES: .5-12 mc, .1-12 mc, 10 kc-12 mc, 10-220 mc (9 bands)

FIXED FREQUENCIES: Up to max. of 8 center frequencies (20 kc to 12 mc—Customer selected)

AUDIO RANGE: 200 cps to 20 kc.

SWEEP WIDTHS: Selected for maximum stability 1-10 mc on .5-12 mc band; .2-2 mc on .1-12 mc band; 20-200 kc on 10 kc-12 mc band; 6% to 60% of center freq. to 50 mc and 3 mc to 30 mc above 50 mc on 10-220 mc bands. 2-20 kc on fixed frequencies and audio range.

OUTPUT LEVEL: Continuously variable from 1 volt rms down to 65 db below 1 volt, ±5% over widest sweep. AGC. Audio range: variable .5-1 volt rms.

IMPEDANCE: 70 ohms nominal (50 ohms on request). Audio range: 600 ohms.

SWEEP OUTPUT and REPETITION RATES: Sawtooth for horizontal deflection of oscilloscope. Approx. 7 volts peak to peak—Output Impedance 1000 ohms nom.; fixed 60 cps, line locked; fixed 30 cps, logarithmic (for audio and video application) 3 cont. var. ranges—.2-1 cps, 1-5 cps, 5-30 cps.

MARKERS: Swept signal available for operation of *Vari-Marker SKV* Generator.

Optional Internal Markers. Limited number of sharp, crystal-controlled pulse-type markers at customer specified frequencies can be provided. Please inquire before ordering.

POWER SUPPLY: Input approx. 220 Watts, 117v (±10%), 50-60 cps. B+ electronic regulation.

PRICE: $995.00 f.o.b. factory. Fixed freq bands add $17.00 per band.

The wide range of frequency and repetition rate in the *Ligna-Sweep Model SKV* make it ideally suited for alignment and testing of a wide variety of electronic instruments—audio amplifiers, filters, communication receivers, radar IF channels, TV receivers and transmitters.

The unit is stable and carefully shielded and filtered to prevent spurious signals on beat frequency video bands. A wide range of sweep repetition rates makes viewing easy on conventional oscilloscopes. Low repetition rates used with long persistence screens permit study of high Q circuitry, LF limits of band circuits and observation of the "ring" characteristics of tuned circuits.

Ligna-Sweep® MODEL CP

SWEEPING OSCILLATORS

Cat. No. 932-A: Variable bands between 100 kc and 215 mc. Price: $750.00 f.o.b. factory. 18 pulse-type markers avail. at customer specified freq., $17.00 each.

Cat. No. 932-B: Continuous coverage from 100 kc—150 mc. Price: $750.00 f.o.b. factory. 18 pulse-type markers avail. at customer specified freq., $17.00 each.

WRITE FOR NEW KAY CATALOG

SEE US AT THE WESCON SHOW
BOOTHS #2062, #2063

KAY ELECTRIC COMPANY

DEPT. 1-7, MAPLE AVENUE, PINE BROOK, N. J. CApitol 6-4000

KAY KAY KAY

Meetings with Exhibits

(*Continued from page 8A*)

Oct. 31-Nov. 2, 1960

13th Annual Conference on Electrical Techniques in Medicine & Biology, Sheraton-Park Hotel, Washington, D.C.

Exhibits: Mr. Lewis Winner, 152 West 42nd St., New York 36, N.Y.

November 14-16, 1960

Mid-American Electronics Convention (MAECON), Hotel Muehlebach, Kansas City, Mo.

Exhibits: Dr. L. R. Crissman, Trans World Airlines, Kansas City, Mo.

November 15-17, 1960

Northeast Electronics Research & Engineering Meeting (NEREM), Boston Commonwealth Armory, Boston, Mass.

Exhibits: Miss Shirley Whitcher, IRE Boston Office, 73 Tremont St., Boston, Mass.

December 1-2, 1960

PGVC Annual Meeting, Sheraton Hotel, Philadelphia, Pa.

Exhibits: Mr. E. B. Dunn, Atlantic Refining Co., 260 S. Broad St., Philadelphia 1, Pa.

December 11-14, 1960

Eastern Joint Computer Conference, Hotel New Yorker, New York, N.Y.

Exhibits: Mr. Alan D. Meacham, 120 E. 41st St., New York 17, N.Y.

January 9-11, 1961

Seventh National Symposium on Reliability and Quality Control in Electronics, Bellevue-Stratford Hotel, Philadelphia, Pa.

Exhibits: Mr. James H. Goodman, Burroughs Research Center, Building #3, Room 3307, Paoli, Pa.

March 20-23, 1961

International Radio and Electronics Show, Waldorf-Astoria Hotel and New York Coliseum, New York, N.Y.

Exhibits: Mr. William C. Copp, Institute of Radio Engineers, 72 West 45th Street, New York 36, N.Y.

April 26-28 1961

Seventh Region Technical Conference and Trade Show, Westward Ho Hotel, Phoenix, Ariz.

Exhibits: Dr. Frank Holman, Boeing Airplane Co., 10708 39th Ave., S.W., Seattle 66, Wash.

Note on Professional Group Meetings: Some of the Professional Groups conduct meetings at which there are exhibits. Working committeemen on these groups are asked to send advance data to this column for publicity information. You may address these notices to the Advertising Department and of course listings are free to IRE Professional Groups.

At The Ramo-Wooldridge Laboratories... integrated programs of research & development of electronic systems and components.

The new Ramo-Wooldridge Laboratories in Canoga Park provide an environment for creative work in an academic setting. Here, scientists and engineers seek solutions to the technological problems of today. The Ramo-Wooldridge research and development philosophy places major emphasis on the imaginative contributions of the members of the technical staff. ■ There are outstanding opportunities for scientists and engineers. *Write* Dr. Richard C. Potter, Head, Technical Staff Development, Department 31-G.

THE RAMO-WOOLDRIDGE LABORATORIES
8433 FALLBROOK AVENUE, CANOGA PARK, CALIFORNIA

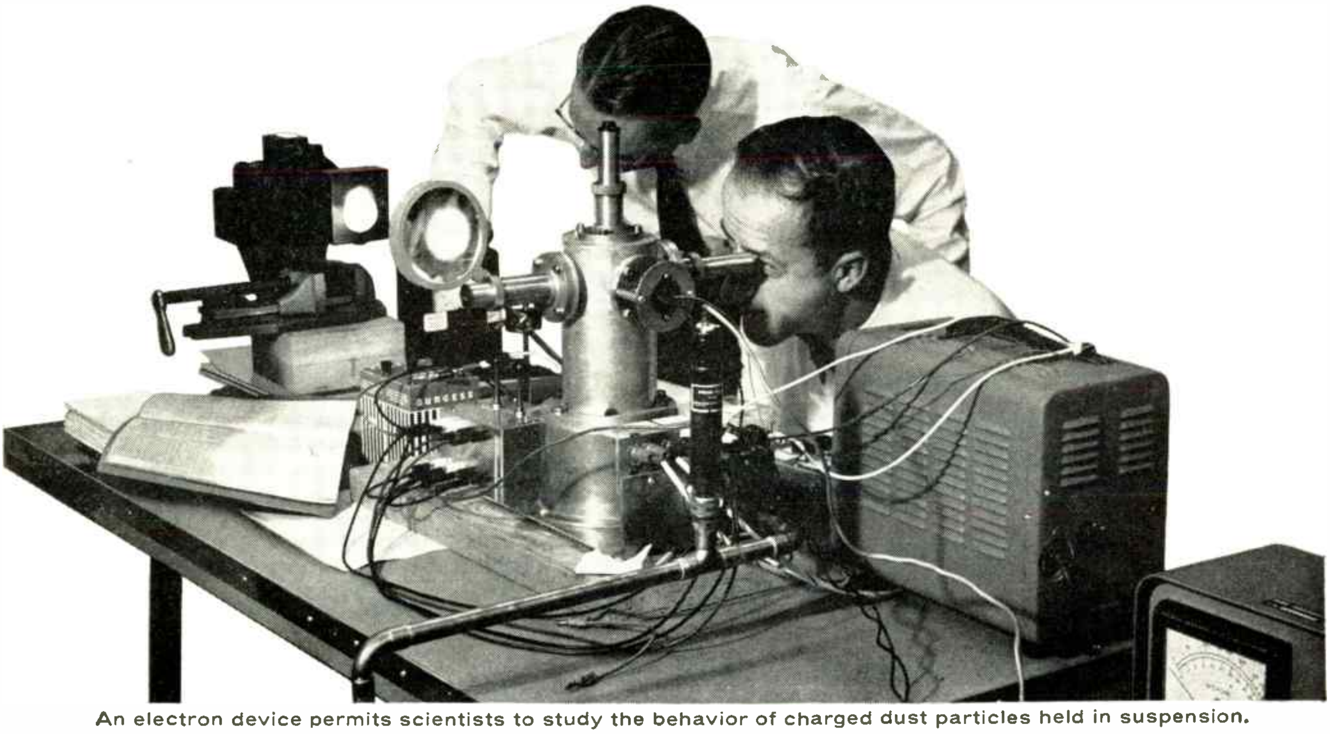

An electron device permits scientists to study the behavior of charged dust particles held in suspension.

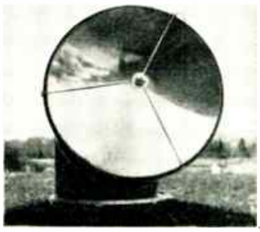

KENNEDY **CYCLOCONIC MOUNTING**

an advanced concept in antenna mounting

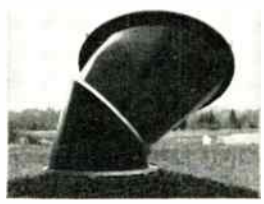

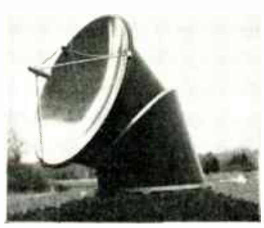

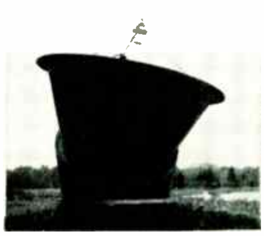

KENNEDY *Cycloconic* mounting has several significant advantages over conventional two-axis arrangements. With the *Cycloconic* method of mounting reflectors, two axes are provided, one vertical (azimuth) and one non-orthogonal (inclined) to the vertical. The reflector axis is at an angle to the inclined axis. By combination of rotations any direction of pointing may be achieved.

Cycloconic mounting eliminates the need for mechanical stops or limit switches. The large working diameters on *both* axes insure high angular accuracy. Continuous unidirectional motion about the azimuth and inclined axes provides meridian scanning with simple harmonic motion of the antenna beam.

The inclined axis of the *Cycloconic* mount provides a convenient "Vernier" for measurement of true elevation angle. For example, in satellite tracking low angle passes of short duration can yield quite precise elevation data.

The inherent stability and absence of mechanical limits of the *Cycloconic* mount result in a high survival capability under extreme environmental conditions. This extra ruggedness and rigidity make it ideal for mounting large antennas for radio telescopes. Dishes from 300 feet in diameter up may be *Cycloconic* mounted with total dependability. Loads on the antenna from dead weight, inertia and wind are handled with positive reliability.

KENNEDY *Cycloconic* mounts may be custom made to meet your specific requirements. They are the products of D. S. KENNEDY & CO., designers and builders of more tracking antennas, tropo-scatter systems and radio telescopes than anyone else in the field. The backlog of structural design and antenna technology gained through more than 15 years of activity in antenna installations has been applied to the design of this advanced mounting technique. You can consider *Cycloconic* mounting for your application with complete confidence. It will meet your highest performance standards.

Kennedy gives you experience you can't buy elsewhere.

D. S. KENNEDY & CO.

Antenna Division, Cohasset, Mass.
EVergreen 3-1200 Twx COH 311

Anchor Metals Division, Hurst, Texas
(Fort Worth) ATlas 4-2583

TRACKING ANTENNAS • RADIO TELESCOPES • RADAR ANTENNAS • SCATTER COMMUNICATIONS ANTENNAS • MICROWAVE RESEARCH AND DEVELOPMENT • TRANSMISSION TOWERS • SWITCHYARD STRUCTURES

TI low cost germanium general purpose transistors give you 250 mw dissipation

...with beta spreads as low as 2:1

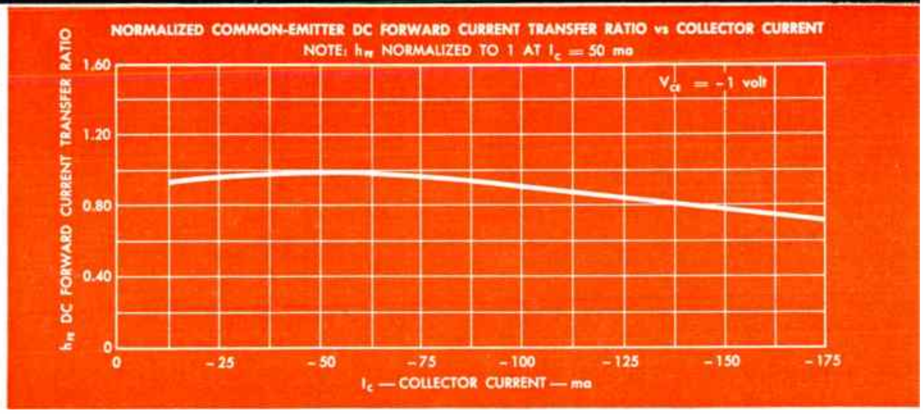

Available in commercial production quantities, TI 2N1372 series germanium P-N-P alloy transistors make possible low-cost applications that provide linear beta, high power gain and low distortion characteristics. These general purpose economy transistors are especially suited for your medium frequency switching circuits, audio amplifiers and motor control applications.

Fully automatic testing and classification by CAT (Centralized Automatic Testing) completely eliminates human error and assures uniformity and reliability . . . ideal for your production assembly and testing requirements.

Evaluate the specifications below and contact your nearby TI distributor or TI sales office for the devices most suited to your particular requirements.

maximum ratings at 25° C ambient		2N1372	2N1373	2N1374	2N1375	2N1376	2N1377	2N1378	2N1379	2N1380	2N1381	Unit
Collector—Base Voltage		−25	−45	−25	−45	−25	−45	−12	−25	−12	−25	v
Collector Current		−200	−200	−200	−200	−200	−200	−200	−200	−200	−200	ma
Total Device Dissipation		250	250	250	250	250	250	250	250	250	250	mw
Storage Temperature Range						−55 to +100						°C
electrical characteristics at 25° C ambient												
I_{CBO} Collector Reverse Current												
(V_{CB} = −12v I_E = 0)	(max)							−7		−14		μa
(V_{CB} = −20v I_E = 0)	(max)	−7	−7	−7	−7	−7	−7		−7		−14	μa
(V_{CB} = −1.5v I_E = 0)	(typ)	−3	−3	−3	−3	−3	−3	−3	−3	−3	−3	μa
h_{FE} dc Forward Current Transfer Ratio*	(min)	30	30	50	50	75	75	95	95	30	30	
(V_{CE} = −1v I_C = −50 ma)	(typ)	45	45	80	80	95	95	200	200	100	100	
	(max)	95	95	150	150	150	150	300	300	300	300	
$f_{\alpha b}$ Common-Base Alpha-Cutoff Frequency (V_{CB} = −5v I_C = −1 ma)	(typ)	1.5	1.5	2	2	2	2	3	3	2	2	mc
Noise Figure 1000 cps†	(typ)	7.0	7.0	6.5	6.5	5.5	5.5	4	4	5.5	5.5	db

*Tolerance on all values ±10% for test set correlation. †Conventional noise compared to 1000 cps and 1 cycle bandwidth.

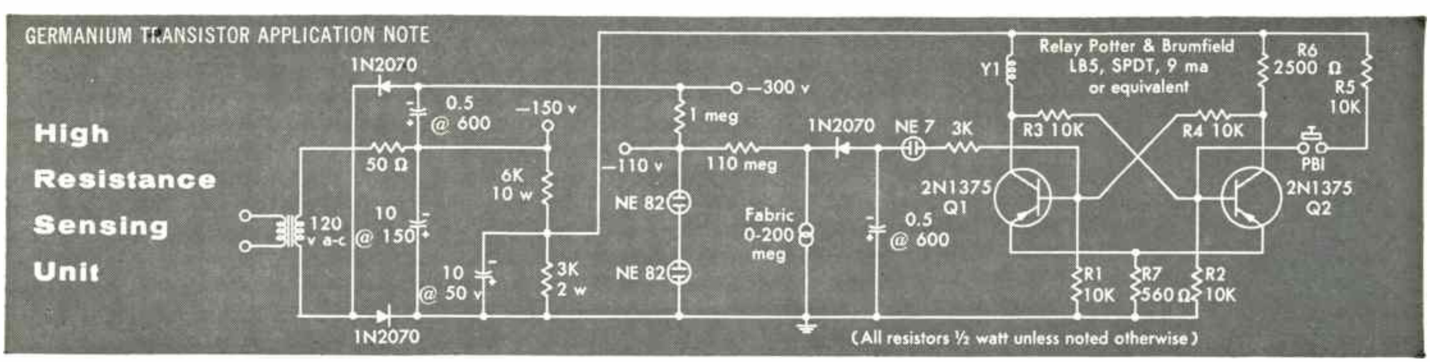

Write on your company letterhead for complete high resistance sensing circuit application report.

DESIGN LEADERSHIP IN QUALITY GERMANIUM TRANSISTORS

TEXAS INSTRUMENTS INCORPORATED
SEMICONDUCTOR-COMPONENTS DIVISION
13500 N. CENTRAL EXPRESSWAY
POST OFFICE BOX 312 · DALLAS, TEXAS

IRE News and Radio Notes

Current IRE Statistics

(As of May 31, 1960)

Membership—81,833
Sections*—107
Subsections*—26
Professional Groups*—28
Professional Group Chapters—269
Student Branches†—191

* See May, 1960, issue for a list.
† See this issue for a list.

Calendar of Coming Events and Authors' Deadlines*

1960

7th Ann. Symp. on Computers and Data Processing, Stanley Hotel, Estes Park, Colo., July 28–29.

5th Global Communications Symp., Hotel Statler, Washington, D. C., Aug. 1–3.

AIEE Pacific Gen. Mtg., El Cortez Hotel, San Diego, Calif., Aug. 9–12.

WESCON, Los Angeles Mem. Sports Arena, Los Angeles, Calif., Aug. 23–26.

Int'l. Information Theory Mtg., London, Eng., Aug. 29–Sept. 2.

Int'l Conf. on Electrical Engrg. Education, Sagamore Conf. Center, Syracuse Univ., Syracuse, N. Y., Sept.

EIA Conf. on Value Engrg., Disneyland Hotel, Anaheim, Calif., Sept. 7–8.

URSI 13th Gen. Assembly, Univ. of London, London, Eng., Sept. 5–15.

Joint Automatic Control Conf., M.I.T., Cambridge, Mass., Sept. 7–9.

Conf. on Communications, Roosevelt Hotel, Cedar Rapids, Iowa, Sept. 9–10.

4th Ann. Joint Mil. Ind. Electronic Test Equip. Symp., Chicago, Ill., Sept. 14–15.

8th Ann. Engrg. Management Conf., Morrison Hotel, Chicago, Ill., Sept. 15–16.

Benelux Section–PGCS Int'l Symp. on Data Transmission, Delft, Netherlands, Sept. 19–20,

Space Electronics and Telemetry Conv. and Symp., Shoreham Hotel, Washington, D. C., Sept. 19–22.

Industrial Elec. Symp., Manger Hotel, Cleveland, Ohio, Sept. 21–22,

10th Ann. Broadcast Symp., Willard Hotel, Washington, D. C., Sept. 23–24.

Sixth Natl. Communications Symp., Hotel Utica and Utica Municipal Aud., Utica, N. Y., Oct. 3–5. (DL*: June 1, B. H. Baldridge, 25 Bolton Rd., New Hartford, N. Y.)

PGNF 7th Ann. Mtg, Gatlinburg, Tenn., Oct. 3–5.

6th Conf. on Radio Interference Reduction, Chicago, Ill., Oct. 4–6.

Natl. Elec. Conf., Hotel Sherman, Chicago, Ill., Oct. 10–12. (DL*: May 1960 Prof. T. F. Jones, Jr., School of E.E., Purdue Univ., Lafayette, Ind.)

* DL = Deadline for submitting abstracts.

(Continued on page 15A)

Electron Devices Meeting Issues Call for Papers

The annual technical meeting of the Professional Group on Electron Devices will be held on October 27 and 28, 1960 at the Shoreham Hotel in Washington, D. C.

An informative abstract of approximately 200 words will be required for each paper to be considered for presentation at the meeting. Final deadline for acceptance of abstracts is August 1, 1960, but earlier submission is requested, if possible. Abstracts, including an original and four copies, should be sent to the technical program chairman, H. W. Welch, Jr., Motorola, Inc., 8201 E. McDowell Rd., Scottsdale, Ariz.

Papers to be presented at this meeting should deal with material of an applied or development nature in the broad field of electron devices. This includes electron tubes, semiconductor devices, masers, tunnel diodes, parametric amplifiers and other solid state device configurations. This meeting is intended not to overlap with the Research Conferences, which comprise papers dealing with new ideas and concepts. Papers for this meeting should be concerned primarily with the device itself, or important new device technology, rather than with its application or circuitry, except insofar as circuitry is built into the device itself. Papers related to microelectronics will be welcome if they are specific in nature and deal with the active device.

The Chairman of the General Committee is Dr. J. A. Hornbeck, Bell Telephone Labs., Murray Hill, N. J. Other members of the General Committee are Dr. C. P. Marsden, Jr., National Bureau of Standards, Local Arrangements; Dr. E. L. Steele, National Bureau of Standards, Local Arrangements; Dr. E. L. Steele, National Bureau of Standards, Publications; and H. S. Renne, Bell Telephone Labs., Publicity.

PGNS Holds Seventh Annual Meeting

The Seventh Annual Meeting of the Professional Group on Nuclear Science of the Institute of Radio Engineers is to be held in Gatlinburg, Tenn. on October 3–5, 1960. The meeting, jointly sponsored by PGNS and Oak Ridge National Laboratory, will feature papers on Solid State Radiation Detectors and low noise amplifiers, and their applications to nuclear science. Exhibits, appropriate to the meeting theme, will be on display and a tour of the ORNL "Project Sherwood" Thermonuclear Facilities will be available to those interested.

The title and an approximately fifty-word description of papers appropriate to the above theme must be submitted by August 1, 1960 to: H. E. Banta, Oak Ridge National Laboratory, P. O. Box "X," Oak Ridge, Tenn.

Call for Papers

1961 IRE International Convention

March 20–23, 1961

Waldorf-Astoria Hotel and New York Coliseum, New York, N. Y.

Prospective authors are requested to submit all of the following information by:

October 21, 1960

1. 100-word abstract *in triplicate*, title of paper, name and address
2. 500-word summary *in triplicate*, title of paper, name and address
3. Indicate the technical field in which your paper falls:

Aeronautical & Navigational Electronics
Antennas & Propagation
Audio
Automatic Control
Bio-Medical Electronics
Broadcast & Television Receivers
Broadcasting
Circuit Theory
Communications Systems
Component Parts
Education
Electron Devices
Electronic Computers
Engineering Management
Engineering Writing & Speech
Human Factors in Electronics
Industrial Electronics
Information Theory
Instrumentation
Microwave Theory & Techniques
Military Electronics
Nuclear Science
Production Techniques
Radio Frequency Interference
Reliability & Quality Control
Space Electronics & Telemetry
Ultrasonics Engineering
Vehicular Communications

Note: Only original papers which have not been published or presented prior to the 1961 IRE International Convention will be considered; any necessary military or company clearance of paper is to be granted prior to submittal.

Address all material to: Dr. Gordon K. Teal, Chairman
1961 Technical Program Committee
The Institute of Radio Engineers, Inc.
1 East 79 Street, New York 21, N. Y.

National Science Academy Elects 4 IRE Members; Names Berkner Treasurer

The National Academy of Sciences elected 35 members, among them 4 IRE members, in April. At the same time, Lloyd V. Berkner (A'26–M'34–SM'43–F'47) was named treasurer of the Academy.

IRE members chosen as members of the Academy are Allen V. Astin (SM'50–F'54), Director of the National Bureau of Standards, Washington, D. C.; Nicolaas Bloembergen (SM'58), Professor of Applied Physics, Harvard University, Cambridge, Mass.; Henry G. Booker (SM'45–F'53), Professor of Electrical Engineering, Cornell University, Ithaca, N. Y.; and Jerome B. Wiesner (S'36–A'40–SM'48–F'52), Director of the research laboratory for electronics, Massachusetts Institute of Technology, Cambridge, Mass.

Call for Papers, 6th Annual Magnetism and Magnetic Materials Conference

The Sixth Annual Conference on Magnetism and Magnetic Materials will be held in New York City, November 14–17, 1950, at the New Yorker Hotel. This conference is sponsored jointly by the AIEE and the American Institute of Physics, in cooperation with the Office of Naval Research, the IRE, and the Metallurgical Society of the AIME.

Authors should submit titles and abstracts of proposed papers by August 26 to A. M. Colgston or R. C. Fletcher, Program Chairmen, Bell Telephone Laboratories, Murray Hill, N. J. Further conference details can be obtained from the Local Chairman, L. R. Bickford, Jr., I.B.M. Research Center, Yorktown Heights, N. Y.

Purdue To Sponsor Fall Symposium

A two-day Symposium on Engineering Applications of Probability and Random Function Theory sponsored by Purdue University will be held November 15–16, 1960, at Lafayette, Ind. The symposium will stress applications of probability and random function theory to problems associated with factors of safety in structures, reliability of structures and systems, optimization of systems of all types which are subject to random disturbances, jet and rocket engine noise fields and traffic control. Professors M. Kac of Cornell, A. J. F. Siegert of Northwestern, and E. W. Montroll of the University of Maryland have already agreed to participate. A detailed program will be released shortly.

Requests for further information should be addressed to either J. L. Bogdanoff or F. Kozin, co-chairmen of the Symposium, Division of Engineering Science, Purdue University, Lafayette, Ind.

Las Vegas Section Established by IRE

On April 21, 1960, the IRE Executive Committee approved the establishment of a new IRE Section, to be known as the Las Vegas Section, to encompass Clark and Nye counties in the State of Nevada.

Dr. Marvin Chodorow (*left*), Director of Microwave Laboratory, Stanford University, is shown presenting one of the early klystrons developed by the Varian Brothers to Dr. Donald A. Shelley (*right*), Director of the Edison Institute. The presentation was made in the presence of Dr. L. J. Giacoletto (*center*), Manager of the Electronics Department, Ford Motor Co. Scientific Laboratory, who is Chairman of the Detroit Section, during a special meeting of the Section held in cooperation with the Henry Ford Museum and the Greenfield Village of Dearborn, Mich. The klystron will be part of a special exhibit of velocity modulation devices which will be on display at the Henry Ford Museum during the summer months. (Photo courtesy of the Henry Ford Museum, Dearborn, Mich.)

Calendar of Coming Events and Authors' Deadlines*

Continued from page 14A)

2nd Natl. Ultrasonics Symp., Boston, Mass., Oct.

Engrg. Writing and Speech Symp., Bismark Hotel, Chicago, Ill., Oct. 13–14.

Symp. on Space Navigation, Deshler-Hilton Hotel, Columbus, Ohio, Oct. 19–21, (DL*: July 15, J. D. Kraus, Ohio State Univ. Radio Observatory, Columbus.)

East Coast Conf. on ANE, Lord Baltimore Hotel, Baltimore, Md., Oct. 24–26. (DL*: June 6, S. Hershfield, The Martin Co., Baltimore, Md.)

5th Ann. Conf. on Nonlinear Magnetics and Magnetic Amplifiers, Bellevue-Stratford Hotel, Philadelphia, Pa., Oct. 26–28.

Electron Devices Mtg., Hotel Shoreham, Washington, D. C., Oct. 27–29.

13th Ann. Conf. on Elec. Tech. in Med. and Bio., Sheraton Park Hotel, Washington, D. C., Oct. 31, Nov. 1–2.

Radio Fall Mtg., Hotel Syracuse, Syracuse, N. Y., Oct. 31, Nov. 1–2.

Symp. on Communications, Queen Elizabeth Hotel, Montreal, Quebec, Canada, Nov. 4–5.

Symp. on Space Instrumentation, Washington, D. C., Nov. 8–9.

6th Ann. Conf. on Magnetism and Magnetic Materials, New Yorker Hotel, N. Y., N. Y., Nov. 14–17. (DL*: Aug. 26, A. M. Clogston, R. C. Fletcher, Bell Tel. Labs., Murray Hill, N. J.)

Mid-Amer. Elec. Conv., Hotel Muehlebach, Kansas City, Mo., Nov. 15–16. (DL*: June 15, J. Austin, Bendix Aviation Corp., 95 and Troost, Kansas City, Mo.)

PGPT Ann. Conf., Boston, Mass., Nov. 15–16. (DL*: June 1, C. W. Watt, Raytheon Co., Waltham, Mass.)

Symp. on Engineering Applications of Probability and Random Function Theory, Purdue University, Lafayette, Ind., Nov. 15–16.

1960 NEREM (Northeast Electronics Res. & Engrg. Mtg.), Boston, Mass., Nov. 15–17.

PGVC Ann. Mtg., Sheraton Hotel, Philadelphia, Pa., Dec. 1–2, (DL*: July 15, W. G. Chaney, American Telephone and Telegraph Co., 195 Broadway, N. Y. 7, N. Y.)

3rd EIA Conf. on Maintainability of Electronic Equipment, Hilton Hotel, San Antonio, Tex., Dec. 5–7.

Eastern Joint Computer Conf., New Yorker Hotel, New York, N. Y., Dec. 13–15. (DL, papers: Aug. 13, E. Kubie, Computer Usage Co., 18 E. 41 St., N. Y. 17, N. Y.)

1961

7th Natl. Symp. on Reliability and Quality Control, Bellevue-Strafford Hotel, Philadelphia, Pa., Jan. 9–11 (DL*: May 9, 1960, R. E. Kuehn, IBM Corp., Owego, N. Y.) 1961.

Solid State Circuits Conference, University of Pennsylvania and Sheraton Hotel, Philadelphia, Pa., February 15–17 (DL*: Oct. 14, 1960, J. J. Suran, Bldg. 3, Rm. 115 GE Co., Electronics Park, Syracuse, N. Y.)

* DL = Deadline for submitting abstracts.

Dr. Yasujiro Niwa (A'53–F'54), President of Tokyo Electrical Engineering College and former Vice President of the IRE, was presented the Order of Culture by the Emperor of Japan on November 3, 1959. The Order of Culture is Japan's highest honor in science and art. Only 107 persons have received the Order during its history, of which number 50 are still living. Dr. Niwa is one of 25 persons from the field of science who hold the honor today.

Yasujiro Niwa

Dr. Niwa was instrumental in forming the Tokyo Section of the IRE, serving as its Vice Chairman in 1955–1956, and Chairman in 1957–1959. He served as Vice President and Director of the IRE in 1957.

In addition to receiving many honors during his career, Dr. Niwa has served as President of the following societies: Institute of Communication Engineers of Japan, Japan Radio Society, Institute of Electrical Engineers of Japan, Television Society of Japan, and Acoustical Society of Japan.

At a recent meeting of the 1960 NEREM committee in Newton, Mass., plans for the November 15–17 meeting were formalized. (Seated, *left to right*): G. Cooper, publicity; R. Wall, secretary; A. Winston, conference chairman; and R. Purinton, Jr., treasurer. (Standing, *left to right*): L. Winner, public relations coordinator; G. Rudenberg, IRE Boston Section; H. Alberts, special arrangements; S. Gibson, exhibits; and J. Cattanach, arrangements. The committee also includes J. Meagher, registration, and J. H. Mulligan, Jr., program chairman.

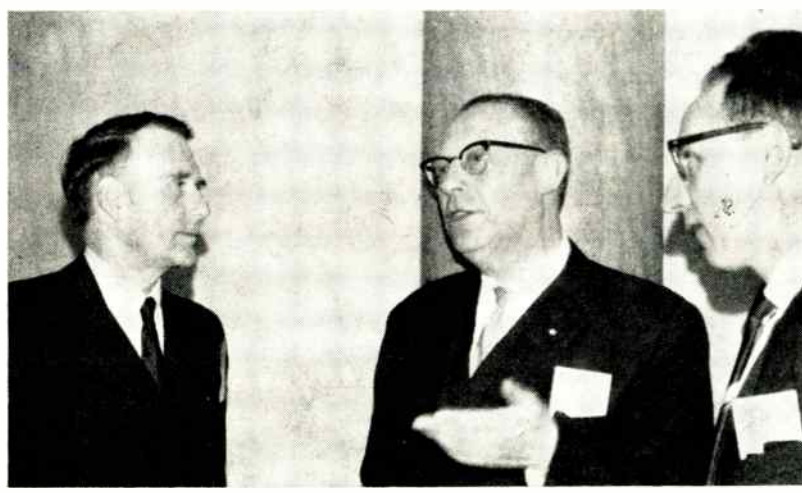

This photograph was taken during intermission at the Benelux Section meeting of April 25, 1960, at which J. A. Ratcliffe, Vice President of the IRE, was a guest speaker. From *left to right*, Mr. Ratcliffe, H. Rinia, Chairman of the Benelux Section, and J. M. L. Janssen, Chairman of the Meetings and Papers Committee.

Papers Now Available from 1960 Nuclear Congress

Copies of the papers produced for presentation during the 1960 Nuclear Congress are available from: 1960 Nuclear Congress, 29 West 39th St., New York 18, N. Y.

For those who found it impossible to attend the 1960 Nuclear Congress, and to obtain printed copies of papers at the Congress, provision has been made for mail order distribution. This facility has been provided as a part of the first objective of the Congress, "to provide free exchange of knowledge in the subject area between engineers and scientists and the industry which is dependent upon such information."

The Nuclear Congress, held in New York City's Coliseum, April 4–7, produced new information in a variety of subject areas related to the application of nuclear energy for mankind's benefit. A total of 62 papers were presented as part of the "streamlined" technical program. These papers were selected and invited so as not to duplicate any presented during other atomic conferences, and to fill gaps in information currently available.

Papers may be ordered individually or the complete set may be obtained. The price is 50¢ per paper, or $20 for the set.

International Solid-State Circuits Conference Call for Papers

The 1961 International Solid-State Circuits Conference, the 8th annual meeting, will be held on February 15–17, 1961, on the campus of the University of Pennsylvania and the Sheraton Hotel, Philadelphia, Pa.

The conference, sponsored jointly by the Institute of Radio Engineers, American Institute of Electrical Engineers and the University of Pennsylvania, will feature papers dealing with circuit properties, circuit philosophy and design techniques related to solid-state devices in the following general areas:

1) Solid-state memory, storage and logic elements, such as twistors, thin-film memories and associated circuits, photoelectronic circuitry, etc.
2) Solid-state microwave amplifying mechanisms, such as parametric amplifiers and masers.
3) Solid-state devices performing an integrated circuit function.
4) Cryogenic digital and linear applications.
5) Novel types of solid-state devices—in unique modes of operation—such as those utilizing the Hall effect, high-temperature circuit elements and solid-state filters and delay lines.
6) Advanced circuitry—with emphasis on significant developments in the art—to the exclusion of data on equipment design.

Papers representing original contributions in these and related fields are invited.

Abstracts—highlighting the nature of the contribution, its significance in the art and theoretical and experimental results—300 to 500 words in length, which can be accompanied by key illustrations, plus 50-word summaries for advance program mailings, should be submitted in double-spaced typewritten form (and in triplicate) on or before September 20, 1960, to J. J. Suran, Program Chairman, Building 3, Rm. 115, General Electric Company, Syracuse, N. Y.

Abstracts and summaries should be accompanied by author's name, company affiliation and position title, business and home address, telephone contact and brief biographical sketch.

Members of the 1961 conference committee include: Chairman, T. R. Finch, and Secretary, F. H. Blecher, Bell Telephone Laboratories, Murray Hill, N. J.; and Public Relations, L. Winner, 152 W. 42nd St., N. Y. 36, N. Y.

Get the complete story on microwave tubes and components in these two new booklets from BOMAC

What's new in microwave? You'll find full information in these 2 new Bomac booklets. One is a complete product catalog in a new, more convenient format (tubes are listed first by band, then by type) to make it easier and quicker for you to find the tube you want. The second booklet gives you facts and figures on any of Bomac's new components and test equipment. Put together, they give you a complete, concise picture of what's new in microwave for 1960.
Be sure to send for your copies today.

BOMAC laboratories, inc.
SALEM ROAD · BEVERLY, MASSACHUSETTS
Offices in major cities — A subsidiary of Varian Associates.

Leaders in the design, development and manufacture of TR, ATR, Pre-TR tubes; shutters; reference cavities; crystal protectors; silicon diodes; magnetrons; klystrons; duplexers; pressurizing windows; noise source tubes; high frequency triode oscillators; surge protectors.

Nominations for 1961 IRE Officers and Directors

At its April 22, 1960 meeting, the IRE Board of Directors voted to place the following nominees for officers and delegates-directors on the ballot, to be submitted to voting members by September 1, 1960. They are as follows:

President, 1961—Lloyd V. Berkner

Vice President, 1961 (residing in North America)—John F. Byrne

Vice President, 1961 (residing elsewhere than in North America)—Franz Ollendorff

Delegates-at-large-Directors-at-large, 1961–1963 (two to be elected)—E. Finley Carter, Charles Kimball, Emanuel R. Piore, and Lester C. Van Atta

Regional Delegates-Regional Directors, 1961–1962 (one to be elected in each Region):

Region 2—A. B. Giordano and A. C. Beck

Region 4—J. W. Coltman, M. Ferrence, Jr., R. W. Ittelson, and A. B. Bereskin

Region 6—D. Silverman, M. W. Bullock, J. W. Herbstreit, and G. E. Sheppard

Region 8—B. R. Tupper

According to Article VIII, Section 2 of the IRE Constitution, nominations by petition for any of the above offices may be made by letter to the Board of Directors setting forth the name of the proposed candidate and the office for which the candidate is desired to be nominated, provided such letter is received at the general offices of the IRE before noon on the Friday prior to August 15, 1960. Such a petition shall be signed by at least one per cent of the total number of voting members as listed in the official membership records of the IRE at the end of the previous year, but in no case shall the number be less than one hundred.

Biomedical Electronic Program Scope Expanded

The 13th Annual Conference on Electrical Techniques in Medicine and Biology, scheduled for the Sheraton-Park Hotel, Washington, D. C., October 31, November 1–2, 1960, will feature a diversified program on biomedical electronics, with emphasis on analytical techniques.

Among the subjects to be covered are:

1) General: Flowmetering, Ultrasonic Mapping, Densitometry, Electrophoresis, Mass Spectroscopy, Microwave Spectroscopy, etc.
2) Electroanalytical Techniques: Polarography, Specific Electrodes, Coulometry, Titrant Generators, etc.
3) Waveform Interpretation: Heart Sounds, Nerve and Muscle Potentials, Cardiovascular Pressure, etc.
4) Cell and Particle Counting and Sorting.
5) Analogs.
6) Automated Analytical Methods.
7) Physiological Monitoring: Patients, Astronauts, etc.

As in the past, this meeting will be sponsored by the Joint Executive Committee in Medicine and Biology representing the Institute of Radio Engineers, American Institute of Electrical Engineers and the Instrument Society of America.

The conference will publish—immediately prior to the meeting—a 100-page printed report with 600–1000 word digests for every paper, and supporting drawings and photographs, for distribution to all registrants. The book will also include illustrated profiles of every speaker. Post-conference cost of this record will be $5.00.

Another highlight of this meeting will be an exhibit of commercial, institutional and scientific developments in the biomedical-electronic field.

R. L. Bowman, National Institutes of Health, Bethesda, Maryland, has been named chairman of this year's conference. Others on the committee include: A. L. Henley, National Instrument Laboratories, secretary; A. Shapero, Litton Industries, treasurer; G. N. Webb, Johns Hopkins Hospital, technical program and W. A. Wildhack, National Bureau of Standards, local arrangements. Five have been named to a special editorial committee: L. E. Flory, RCA Labs.; A. L. Henley, National Instrument Labs.; G. C. Riggle, National Institutes of Health; J. C. Jacobs, General Electric Research Lab. and P. Frommer, National Institutes of Health. L. Winner, technical relations consultant, will handle public relations and exhibits.

Fourth Annual Symposium on Electronic Test Equipment To Be Held in Chicago

The Fourth Annual Joint Military-Industrial Electronic Test Equipment Symposium will be held in Chicago on September 14 and 15. This year, the symposium will be under joint sponsorship of the Office of the Director of Defense Research and Engineering and the Department of the Army Signal Corps, with the Armour Research Foundation of Illinois Institute of Technology serving as the host.

The theme of this year's conference deals with advanced instrumentation techniques. Technical sessions are now being planned to cover areas of new concepts in measurement, latest instrumentation design techniques, advanced data processing methods, etc. The program will be sufficiently diversified to attract industrial and government representatives, both at the practical and more technical levels.

If you have been involved in research, design or development of instrumentation devices or systems, or the application of instruments to new or unusual measurement problems, and if you feel these experiences would be of interest to others in this field, papers covering this work will be considered for presentation at the conference.

Special guests at the Welcoming Luncheon of the 12th Annual SWIRECO, held in Houston, Tex., on April 20, 1960 included (*left to right*); W. J. Greer, Houston, Tex.; G. W. Bailey, New York, N. Y.; Haraden Pratt, Pompano Beach, Fla.; C. W. Carnahan, Palo Alto, Calif.; R. J. Loofbourrow, Houston, Tex.; R. L. McFarlan, Chestnut Hill, Mass.; C. E. Harp, Norman, Okla.; B. M. Oliver, Palo Alto, Calif.; George Sinclair, Toronto, Ont., Canada; and K. O. Heintz, Houston, Tex.

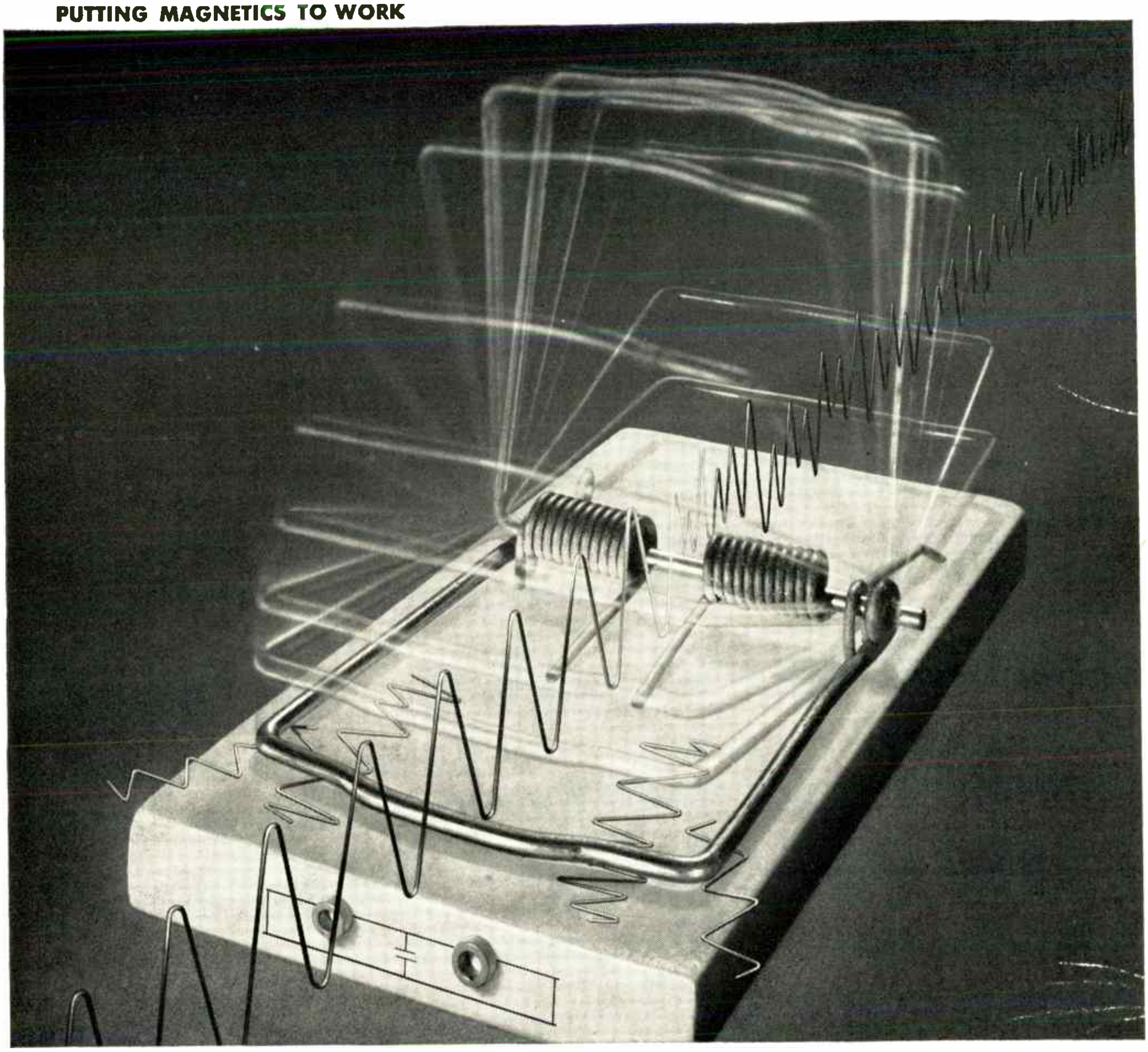

How to build a better (audio signal) trap!

Magnetics Inc. permalloy powder cores give filter designers new attenuation and stability standards—and miniaturization to boot!

The art of trapping unwanted frequencies has been advanced during the past year with a succession of improvements in molybdenum permalloy powder cores by Magnetics Inc. Most audio filter designers now work with smaller cores, more stable cores and cores whose attenuation characteristics are ultra-sharp. Do you?

Do you, for example, specify our 160-mu cores when space is a problem? With this higher inductance, you need at least 10 percent fewer turns for a given inductance than with the 125-mu core. What's more, you can use heavier wire, and thus cut down d-c resistance.

What about temperature stability? Our linear cores are used with polystyrene capacitors, cutting costs in half compared to temperature stabilized moly-permalloy cores with silvered mica capacitors. Yet frequency stability over a wide swing in ambient temperatures is increased!

And what do you specify when you must rigidly define channel cut-offs, with sharp, permanent attenuation at channel crossovers? Our moly-permalloy cores have virtually no resistive component, so there is almost no core loss. The resultant high Q means sharp attenuation of blocked frequencies in high and low band pass ranges.

Why not write for complete information? Like all of our components, molybdenum permalloy powder cores are *performance-guaranteed* to standards unsurpassed in the industry. *Magnetics Inc., Dept. P-82, Butler, Pa.*

MAGNETICS inc. ®

VISIT OUR BOOTH 521-522 AT THE WESCON SHOW

Professional Groups*

Aeronautical & Navigational Electronics (G-11)—L. M. Sherer, RTCA, Bldg. T-5, 16 and Constitution Ave., N.W., Washington 25, D. C.; H. R. Mimno, Harvard Univ., Cambridge, Mass.

Antennas & Propagation (G-3)—E. C. Jordan, Elec. Engrg. Dept., Univ. of Illinois, Urbana, Ill.; S. A. Bowhill, Pennsylvania State Univ., University Park, Pa.

Audio (G-1)—H. S. Knowles, Knowles Electronics, 9400 Belmont Ave., Franklin Park, Ill.; Prof. A. B. Bereskin, E.E. Dept., Univ. of Cincinnati, Cincinnati 21, Ohio; M. Camras, Armour Res. Found. Tech. Ctr., Chicago 16, Ill.

Automatic Control (G-23)—J. M. Salzer, 909 Berkeley St., Santa Monica, Calif.; G. S. Axelby, Westinghouse Air Arm Div., Friendship Airport, Baltimore 3, Md.

Broadcast & Television Receivers (G-8)—R. R. Thalner, Sylvania Home Electronics, 700 Ellicott St., Batavia, N. Y.; C. W. Sall, RCA, Bldg. 13-4, Camden, N. J.

Broadcasting (G-2)—G. E. Hagerty, Westinghouse Elec. Corp., 122 E. 42 St., Suite 2100, N. Y. 17, N. Y.; W. L. Hughes, E.E. Dept., Iowa State College, Ames, Iowa.

Circuit Theory (G-4)—S. Darlington, Bell Telephone Labs., Murray Hill, N. J.; W. Bennett, Bell Telephone Labs., Murray Hill, N. J.

Communications Systems (G-19)—C. L. Engleman, Engleman & Co., Inc., 2480 16th St., N.W., Washington 9, D. C.; M. R. Donaldson, Electronic Comm. Inc., St. Petersburg, Fla.

Component Parts (G-21)—F. E. Wenger, Headquarters ARDC, Andrews AFB, Washington 25, D. C.; G. Shapiro, Engineering Electronics Sec., Div. 1.6, NBS, Connecticut Ave. and Van Ness St., Washington, D. C.

* Names listed are Group Chairmen and TRANSACTIONS Editors.

Education (G-25)—J. G. Truxal, Head, Dept. of E.E., Polytechnic Inst. of Brooklyn, Brooklyn, N. Y.; W. R. LePage, Dept. of E.E., Syracuse Univ., Syracuse, N. Y.

Electron Devices (G-15)—W. M. Webster, Semi-Conductor Div., RCA, Somerville, N. J.; E. L. Steele, Hughes Prods., Inc., International Airport Station, Los Angeles 45, Calif.

Electronic Computers (G-16)—A. A. Cohen, Remington Rand Univac, St. Paul 16, Minn.; R. O. Endres, Rese Engrg. Co., Philadelphia, Pa.; H. E. Tompkins, Moore School of E.E., Univ. of Pennsylvania, Philadelphia.

Engineering Management (G-14)—H. M. O'Bryan, General Telephone & Electronics Lab., 730 3rd Ave., N. Y. 17, N. Y.; A. H. Rubenstein, Northwestern Univ., Evanston, Ill.

Engineering Writing and Speech (G-16)—T. T. Patterson, Jr., RCA, Bldg. 13-2, Camden, N. J.; H. B. Michaelson, IBM Res. Center, Box 218, Yorktown Heights, N. Y.

Human Factors in Electronics (G-28)—C. M. Jansky, Royal McBee Corp., Portchester, N. Y.; J. I. Elkind, Bolt, Beranek and Newman, Cambridge, Mass.

Industrial Electronics (G-13)—J. E. Eiselein, RCA Victor Div., Camden, N. J.; R. W. Bull, Armour Res. Found., Chicago, Ill.

Information Theory (G-12)—P. Elias, M.I.T., Rm. 26-347, Cambridge 39, Mass.; A. Kohlenberg, Melpar Inc., 43 Leon St., Boston 15, Mass.

Instrumentation (G-9)—C. W. Little, C-Stellerator Assoc., Box 451, Princeton, N. J.; G. B. Hoadley, Dept. of E.E., North Carolina State College, Raleigh, N. C.

Medical Electronics (G-18)—H. P. Schwan, Univ. of Pennsylvania, School of Elec. Engrg., Philadelphia 4, Pa.; L. B. Lusted, Univ. of Rochester Medical School, Strong Memorial Hosp., Rochester 20, N. Y.

Microwave Theory and Techniques (G-17)—A. A. Oliner, Microwave Res. Inst., 55 Johnson St., Brooklyn 1, N. Y.; D. D. King, Electronic Comm., Inc., 1830 York Rd., Timonium, Md.

Military Electronics (G-24)—H. Randall, 1208 Seaton Lane, Falls Church, Va.; D. R. Rhodes, Radiation Lab., Instrument Div., Orlando, Fla.

Nuclear Science (G-5)—A. B. Van Rennes, United Res. Inc., Tech. Div., 128 Alewife Brook Pkwy., Cambridge, Mass.; R. F. Shea, Dig Power Plant Engrg., Knolls Atomic Power Lab., General Electric Co., Schenectady, N. Y.

Production Techniques (G-22)—L. M. Ewing, General Electric Co., HMEED CSP-3, Syracuse 1, N. Y.; A. R. Gray, Rte. #1, Box 940, Orlando Vineland Rd., Wintergarden, Fla.

Radio Frequency Interference (G-27)—R. M. Showers, Moore School of Elec. Engrg., 200 S. 33 St., Philadelphia 4, Pa.; P. O. Schreiber, Technical Wire Prods., Springfield, N. J.

Reliability and Quality Control (G-7)—P. K. McElroy, General Radio Co., 22 Baker Ave., West Concord, Mass.; E. J. Breiding, IBM Corp., Kingston, N. Y.

Space Electronics and Telemetry (G-10)—C. H. Hoeppner, Radiation, Inc., Melbourne, Fla.

Ultrasonics Engineering (G-20)—W. Roth, Roth Lab., 1240 Main St., Hartford 3, Conn.; O. Mattiat, Aerophysics Dev. Corp., P.O. Box 689, Santa Barbara, Calif.

Vehicular Communications (G-6)—A. A. MacDonald, Motorola, Inc., 4545 Augusta Blvd., Chicago 51, Ill.; R. P. Gifford, General Electric Co., Syracuse, N. Y.

Sections*

Akron (4)—C. D. Morrill, 2248 16th St., Cuyahoga Falls, Ohio; C. M. Kelly, 2915 Silver Lake Circle, Cuyahoga Falls, Ohio.

Alamogordo-Holloman (7)—U. C. Nolte, 2810 Quay, Holloman AFB, N. M.; W. F. Stotts, 1507 Michigan Ave., Alamogordo, N. M.

Albuquerque-Los Alamos (7)—R. C. Spence, 3020 W. Sandia Dr., Sandia Base, Albuquerque, N. Mex.; E. C. Davis, Neely Enterprises, Box 8366, Station "C," Albuquerque, N. M.

Anchorage (7)—R. O. Voight, HQ Alaskan Command, APO 942, Seattle, Wash.; J. T. Little, Star Route B, Box 3453, Spenard, Alaska.

* Numerals in parentheses following sections designate region number. First name designates Chairman, second name Secretary.

Atlanta (3)—W. L. Fattig, 1643 N. Gatewood Rd., Atlanta 6, Ga.; R. L. Ellis, Jr., 77 Karland Dr., N.W., Atlanta, Ga.

Baltimore (3)—B. Wolfe, 6112 Talles Rd., Baltimore 7, Md.; J. T. Wilner, 2610 No. Charles St., Sta. WBAL, Baltimore 18, Md.

Bay of Quinte (8)—H. L. Blacker, Northern Electric Co., Ltd., 250 Sidney St., Belleville, Ont., Canada; G. M. Turney, R.R.2, Carrying Place, Ont., Canada.

Beaumont-Port Arthur (6)—L. O. Senneville, 2519 Poe St., Lake Charles, La.; C. A. O'Shaugnessy, 19 East End Blvd., Maplewood, La.

Benelux—Herre Rinia, Parklaan 24, Eindhoven, Netherlands; B. B. Barrow, S.A.D.T.C., Box 174, The Hague, Netherlands.

Binghamton (1)—B. H. Rudwick, 622 Lacey Dr., Johnson City, N. Y.; F. W. Schaaf, R.D. 1, Apalachin, N. Y.

Boston (1)—H. G. Rudenberg, 3 Lanthorn Lane, Beverly, Mass.; G. P. McCouch, Alcott Rd., Concord, Mass.

Buenos Aires—O. C. Fernandez, Transradio Internacional, 379 San Martin, Buenos Aires, Argentina; J. I. Steiner, 1345 20 H. Uriarte, 2do P. D. to H., Buenos Aires, Argentina.

Buffalo-Niagara (1)—J. P. Welsh, 544 Lisbon Ave., Buffalo 15, N. Y.; D. P. Sante, 30 Greenbriar Rd., Williamsville 21, N. Y.

Cedar Rapids (5)—D. M. Hodgin, Jr., 3206 Vine Ave., S.E. Cedar Rapids, Iowa; G. R. Marner, R. 3, Marion, Iowa.

Central Florida (3)—W. S. Hines, 1320 In-

dian River Dr., Eau Gallie, Fla.; M. Gould, 19 Azalea Dr., Cocoa Beach, Fla.

Central Pennsylvania (4)—C. R. Ammerman, 125 Grandview Rd., State College, Pa.; W. J. Ross, 105 Elec. Engrg. Dept., University Park, Pa.

Chicago (5)—K. E. H. Backman, 615 Winston Dr., Melrose Park, Ill.; B. G. Griffith, 2379 Oak Tree Lane, Park Ridge, Ill.

China Lake (7)—R. T. Merriam, 1501-B Smith Rd., China Lake, Calif.; L. D. Bryant, Box 333, Naval Ord. Test Sta., China Lake, Calif.

Cincinnati (4)—H. E. Hancock, Box 52, R.R.4, Branch Hill, Loveland, Ohio; J. P. Meehan, American Tel. & Tel. Co., 138 E. Court St., Cincinnati 2, Ohio.

Cleveland (4)—J. R. Hooper, Jr., 1606 Compton Rd., Cleveland Heights 18, Ohio; R. Kazarian, 2031 Lakeview Ave., Rocky River, Cleveland 16, Ohio.

Colombia—T. J. Meek, Apartado Aereo 78-15, Bogota, Colombia; F. S. Garbrecht, Apartado Nal. 2773, Bogota, Colombia.

Columbus (4)—D. F. Yaw, 2356 Farleigh Rd., Columbus 21, Ohio; F. A. Wolf, 354 Chatham Rd., Columbus 14, Ohio.

Connecticut (1)—A. R. Perrins, 951 Sperry Rd., Cheshire, Conn.; I. Flores, S. Huckleberry Dr., Norwalk, Conn.

Dallas (6)—H. J. Wisseman, 810 Knott Pl., Dallas 8, Texas; A. R. Teasdale, Jr., 6529 Lafayette Way, Dallas 30, Texas.

Dayton (4)—D. G. Clute, 4424 Appleton Pl., Kettering 40, Ohio; R. J. Framme, 316 Claranna, Dayton 9, Ohio.

Denver (6)—W. D. George, Natl. Bur. of Standards, Boulder, Colo.; F. P. Venditti, 2607 South Adams, Denver 10, Colo.

Detroit (4)—L. J. Giacoletto, Ford Motor Co., Scientific Lab., Box 2053, Dearborn, Mich.; H. W. Hale, Dept. of Elec. Engrg., Wayne State University, Detroit 2, Mich.

Egypt—H. M. Mahmoud, Faculty of Engrg., Fouad I University, Giza, Cairo, Egypt; El Garhi I. El Kashlan, Egyptian Broadcasting, 4, Shari Sherifein, Cairo, Egypt.

Elmira-Corning (1)—D. F. Aldrich, 1030 Hoffman St., Elmira, N. Y.; T. G. Keeton, 611 McDowell Pl., Elmira, N. Y.

El Paso (6)—W. H. DeBusk, 3017 Daisy, El Paso, Tex.; E. R. Flottman, 3236 Frankfort, El Paso, Texas.

Emporium (4)—H. V. Kalmer, Jr., 150 Elmwood Court, Emporium, Pa.; H. W. Herbert, Sylvania Elec. Prods., Inc., Emporium, Pa.

Erie (1)—P. E. Sterner, 322 Forest Dr., Erie, Pa.; B. Presutti, 1546 West 43 St., Erie, Pa.

Evansville-Owensboro (5)—R. M. Hughes, 1332 W. 15th St., Owensboro, Ky.; M. W. Russell, 1207 Farrier Place, Owensboro, Ky.

Florida West Coast (3)—R. Murphy, 12112 N. Edison Ave., Tampa 4, Fla.; R. E. Henning, Sperry Microwave Electronics Co., Box 1828, Clearwater, Fla.

Fort Huachuca (7)—J. C. Domingue, 62506 Barnes St., Fort Huachuca, Ariz.; A. S. Montasser, 368 Wolfe St., Sierra Vista, Ariz.

Fort Wayne (5)—T. Major, 5355 Meadowbrook Dr., Fort Wayne, Ind.; C. F. Mason, 1519½ Crescent Ave., Fort Wayne, Ind.

Fort Worth (6)—D. G. Harman, 5623 Volder Drive, Fort Worth 14, Texas; D. R. Robertson, 8279 Carrick St., Fort Worth 16, Tex.

Gainesville (3)—C. M. Veronda, 2232 N.W. 8th Ave., Gainesville, Fla.; M. E. Forsman, College of Engrg., Univ. of Florida, Gainesville, Fla.

Hamilton (8)—W. E. Jeynes, 67 Miller Dr., S. S. 2, Ancaster, Ont., Canada; W. A. Cheek, 102 Paradise Road, N., Hamilton, Ont., Can.

Hawaii (7)—M. S. Vittum, 218 Kuuhoa Pl., Kailua, Hawaii; G. Piety, 2030 Home Rule St., Honolulu 17, Hawaii.

Houston (6)—R. J. Loofbourrow, The Texas Co., Box 425, Bellaire 101, Tex.; W. P. Schneider, 8417 Bluegate, Houston, Tex.

Huntsville (3)—H. H. Hosenthien, 515 Madison St., Huntsville, Ala.; W. H. Cook, Jr., 2702 Evergreen St., S.E., Huntsville, Ala.

India—Officers to be elected.

Indianapolis (5)—G. R. Fraser, U. S. Naval Avionics Facility, 21 St. & Arlington Ave., Indianapolis 18, Ind.; C. E. David, 6110 E. 21 St., Indianapolis 18, Ind.

Israel—J. Shekel, Box 1, Kiryat, Mozkin, Israel; Secretary to be advised.

Italy—Algeri Marino, Via Guido d'Arezzo 14, Rome, Italy; Giuseppe P. Tarchini, Laboratorio Richerche Elettr., Via Del Parlamento N. 33, Borgolombardo, Milan, Italy.

Ithaca (1)—N. H. Bryant, School of Elec. Engrg., Cornell University, Ithaca, N. Y.; to be advised.

Kansas City (6)—H. L. Stout, 425 Volker Blvd., Kansas City 10, Mo.; E. A. McCall, 10004 East 34th St., Independence, Mo.

Kitchener-Waterloo (8)—T. W. R. East, Raytheon Canada Ltd., 61 Laurel St. E., Waterloo, Ont., Can.; W. J. Grey, 68 Plymouth Rd., Kitchener, Ont., Can.

Las Vegas (7)—R. B. Patton, 2204 Kirkland Ave., Las Vegas, Nev.; G. R. Luetkehans, 4901 Cannon Blvd., Las Vegas, Nev.

Little Rock (6)—V. L. Dillaplain, 203 S. Pine St., Little Rock Ark.; R. V. Anders, 5801 Windamere Dr., Little Rock, Ark.

London (8)—G. R. Hosker, Bach-Simpson Ltd., 1255 Brydges St., London, Ont., Can.; G. W. Parsons, 390 Princess Ave., Apt. 307, London, Ont., Can.

Long Island (2)—H. Jasik, 67-20A 193 Lane, Flushing 65, N. Y.; H. W. Redlien, Jr., Wheeler Labs., 122 Cutter Mill Road, Great Neck, N. Y.

Los Angeles (7)—B. Dempster, Electronic Engrg. Co. of California, 1601 E. Chestnut Ave., Santa Ana, Calif.; J. Lewi, Packard-Bell, 12333 W. Olympic, Los Angeles 64, Calif.

Louisville (5)—W. J. Ryan, 4216 Northwestern Pkwy., Louisville 12, Ky.; H. T. Smith, 2511 Saratoga Dr., Louisville, Ky.

Lubbock (6)—J. J. Criswell, 511 50 St., Lubbock, Tex.; J. P. Craig, Route 7, Lubbock, Tex.

Miami (3)—J. W. Keller, Jr., Miami Shipbuilding Corp., 615 S.W. Second Ave., Miami 36, Fla.; F. R. Macklin, 325 Malaga Ave., Coral Gables, Fla.

Milwaukee (5)—F. J. Lofy, 2258 S. 56 St., West Allis 19, Wis.; J. D. Horgan, 1530 N. Longwood Ave., Elm Grove, Wis.

Montreal (8)—R. B. Lumsden, 1680 Lepine St., St. Laurent 9, P.Q., Canada; H. H. Schwartz, 5212 King Edward Ave., Montreal 29, P.Q., Canada.

Newfoundland (8)—M. D. MacGray, Canadian Marconi Co., 3 Prescott St., St. John's, Newf., Canada; F. A. Mulloy, 55 Calver Ave., St. John's, Newf., Canada.

New Orleans (6)—J. C. Spencer, 1524 Shirley Dr., New Orleans 14, La. (Chairman and Acting Secretary).

New York (2)—Jerome Fox, Microwave Research Inst., Poly. Inst. of Bklyn., 55 Johnson St., Bklyn. 1, N. Y.; J. M. Kinn, 545 Madison Ave., N. Y., N. Y.

North Carolina (3)—W. G. McAvoy, 500 Magnolia St., Winston-Salem, N. C.; W. E. Lanford, 3260 Nottingham Rd., Winston-Salem, N. C.

Northern Alberta (8)—R. Usher, St. Albert, Alta., Canada; W. L. Storms, 12907 134 Ave., Edmonton, Alta., Canada.

Northern New Jersey (2)—G. M. Anderson, 9 Jeffrie Trail, Whippany, N. J.; J. R. Flegal, Bell Telephone Labs., Murray Hill, N. J.

Northwest Florida (3)—W. F. Kirlin, 312 May Circle, Bens Lake Area, Eglin AFB, Fla.; H. H. Hufnagle, 1 Katherine Ave., Fort Walton Beach, Fla.

Oklahoma City (6)—H. E. Phillips, 524 N.W. 19 St., Oklahoma City 3, Okla.; K. W. Kruger, 2328 N.W. 43 St., Oklahoma City, Okla.

Omaha-Lincoln (5)—B. L. Dunbar, 2921 S. 104 St., Omaha, Neb.; R. A. Stratbucker, University of Nebraska, College of Medicine, 42 & Dewey Ave., Omaha, Neb.

Orlando (3)—A. R. Gray, 6415 Vineland Rd., Orlando, Fla.; W. L. Eddy, 1711 Antilles Pl., Orlando, Fla.

Ottawa (8)—F. V. Cairns, Radio Div., National Res. Council, Ottawa, Ont., Canada; M. Yurko, 1295 Wesmar Drive, Ottawa, Ont., Canada.

Philadelphia (3)—W. T. Sumerlin, Box 215, Radnor, Pa.; R. G. Adamson, 524 South Bowman Ave., Merion, Pa.

Phoenix (7)—E. S. Shepard, Sr., 5716 N. 19th St., Phoenix, Ariz.; H. R. Hyder, III, 2523 N. 57th St., Phoenix, Ariz.

Pittsburgh (4)—A. E. Anderson, Westinghouse Res. Labs., Physics Proj. Labs., Beulah Rd., Churchill Borough, Pittsburgh 35, Pa.; W. P. Caywood, Jr., Box 179, RD 2, Murrysville, Pa.

Portland (7)—L. C. Hedrick, 35 S.W. 88 Ave., Portland 25, Ore.; M. L. Morgan, 12907 S.W. 62 St., Portland 19, Ore.

Princeton (2)—Sylvan Fich, College of Engineering, Rutgers Univ., New Brunswick, N. J.; R. D. Lohman, RCA, Somerville, N. J.

Quebec (8)—Paul Du Berger, 1267 Villars Ave., Sillery, P.Q., Canada; Theodore Wildi, 1365 De Longueiul, Quebec City, P.Q., Canada.

Regina (8)—L. E. McBride, 3211 Regina Ave., Regina, Sask., Canada; J. M. McNeil, 3147 Retallack St., Regina, Sask., Canada.

Rio de Janeiro—Joao A. Wiltgen, Caixa Postal 450, Rio de Janeiro, D. F., Brazil; L. C. Bahiana, Rua Bogari 70, Apt. 102, Lagoa, Rio de Janeiro, Brazil.

Rochester (1)—F. A. Mitchell, Stromberg-Carlson Co., 1400 N. Goodman St., Rochester 9, N. Y.; J. L. Wheeler, 535 Rondo Lane, Webster, N. Y.

Rome-Utica (1)—W. J. Kuehl, 5 Hoffman Road, New Hartford, N. Y.; R. A. Zachary, Jr., 11 Arbor Drive, New Hartford, N. Y.

Sacramento (7)—Nelis W. Godfrey, 3220 Fulton Ave., Sacramento 21, Calif.; A. O.

SAVE SPACE, WEIGHT AND MAINTENANCE with Versatile Compact MIL Spec Modules

For your electronic/electromechanical packaging problems, consult Oster specialists. Compact, transistorized, MIL spec, hermetically sealed, plug-in modules are available for numerous applications.

Typical building block basic units are illustrated. Temperature range is —55°C to +105°C. Basic units can be modified easily or completely redesigned to your specific requirement.

Oster engineers are specialists in creating densely packaged black boxes. These boxes can help you design more compactness and less weight into your systems. Phone or write your nearest John Oster office today.

GENERAL ENVIRONMENTAL CONDITIONS

A. Temperature—	—55°C to +75°C
B. Altitude—	—1000 Feet to +80,000 feet
C. Humidity—	Section 4.4.3 of MIL-E-5272
D. Vibration—	0.30 inch double excursion from 3 to 18 cycles per second and ± 2 g. acceleration from 18 to 500 cycles. (Without vibration isolators)
E. Crash Safety—	Repeated shocks of 30 g. with durations of 11 milliseconds
F. Salt Atmosphere—	Section 4.6.1 of MIL-E-5272
G. Fungus Growth—	Section 4.8.1 of MIL-E-5272
H. Sand and Dust—	Section 4.11.1 of MIL-E-5272

GENERAL PERFORMANCE SPECIFICATIONS

A. Gain Variation—	Less than 10% due to any given parameter extreme variation.
B. Linearity—	Better than 10% through the range of 3% to 80% of full output.
C. Noise—	Less than 5% of maximum output.
D. Phase Shift—	Less than 8 degrees.

Oster®

TYPE 9805-20—SYNCHRONIZER

Same as 9805-19 except Control Transformer Speed is 10 degrees/second—Min.

TYPE 9805-19—SYNCHRONIZER


Synchronizer

Motor Control Phase—
40/20 volts, 1.7 watts, 400 cycles
Motor Reference Phase—
57.5 volts, 2.2 watts, 400 cycles
Generator Excitation—
57.5 volts, 3.0 watts, 400 cycles
Generator Output—
0.3 volts/1000 R.N.M. Min.
Control Transformer Speed—
100 degrees/second-Min.
Control Transformer—
John Oster Mfg. Co. 4053-19
Motor Generator—
John Oster Mfg. Co. 6232-17

TYPE 9616-08—DEMODULATOR AMPLIFIER


Demodulator Amplifier

Input Impedance—
Greater than 25,000 ohms
Output Impedance—
2830 chms (Dual)
Voltage Gain—
Greater than 115
Supply Voltage—
28.0 D.C.

TYPE 9616-07—SYNCHRONIZER AMPLIFIER


Synchronizer Amplifier

Input Impedance—
Greater than 50,000 ohms
Voltage Gain—
Greater than 250
Load—
Control Phase of Motor Generator of 9805-19 or 9805-20

TYPE 9616-16—4-CHANNEL ISOLATION AMPLIFIER

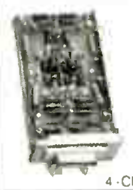
4-Channel Isolation Amplifier

Input Impedance—
1200 ohms per channel
Voltage Gain—
.98 ± .01 per channel
Load Impedance—
1200 ohms per channel
Supply Voltage—
48VDC

TYPE 9616-09—SERVO ACTUATOR AMPLIFIER


Servo Actuator Amplifier

Input Impedance—
Greater than 50,000 ohms
Output Impedance—
400 ohms
Voltage Gain—
Greater than 900
Supply Voltages—
100.0 volts D.C.
28.0 volts D.C.

TYPE 9616-15—RELAY AMPLIFIER


Relay Amplifier

Input Impedance—
Greater than 15,000 ohms
Relay Closing Voltage—
150-175 Millivolts, 400 cycles
Relay Opening Voltage—
125-150 Millivolts, 400 cycles
Relay Contacts—
4 Pole, Double Throw—Dry Circuit
Supply Voltage—
28.0 V. D.C.

TYPE 9616-06—SUMMING AMPLIFIER (DUAL)


Summing Amplifier

Summing Inputs—
10 (per channel)
Gain—
Nominal 1.0; variable from 0.1 to 10.0
Input Impedance—
Dependent on Summing Channel. (50,000 ohms—500,000 ohms)
Load Impedance—
Greater than 10,000 ohms
Supply Voltage—
28 V. D.C.

John Oster **MANUFACTURING CO.**
Specialists in Instrumentation and Display
Avionic Division
Racine, Wisconsin

OTHER PRODUCTS INCLUDE:
Servos, Synchros, Resolvers, Motor Tachs, DC Motors, Computers, Indicators, Servo Mechanisms, Servo Torque Units

EASTERN OFFICE
310 Northern Blvd.
Great Neck, Long Island, New York
Phone: HUnter 7-9030
TWX Great Neck N.Y. 2980

WESTERN OFFICE
5333 South Sepulveda Blvd.
Culver City, California
Phone: EXmont 1-5742 • UPton 0-1194
TWX S. Mon. 7671

Engineers For Advanced Projects Interesting varied work on designing transistor circuits and servo mechanisms.
Contact Mr. Dallas Nielsen, Personnel Manager, in confidence.

Rohde, 3160 Adams Road, Sacramento 25, Calif.

St. Louis (6)—R. L. Frazier, 9707 Willow Creek Lane, Rock Hill 19, Mo.; R. D. Hill, Jr., 363 Gray Ave., Webster Groves 19, Mo.

Salt Lake City (7)—C. L. Alley, Elec. Engrg. Dept., Univ. of Utah, Salt Lake City, Utah; J. E. Dalley, 3920 S. 1380 E., Salt Lake City 17, Utah.

San Antonio-Austin (6)—G. E. White, Box 9006, Allandale Station, Austin 17, Tex.; F. X. Bostick, Jr., 5002 Beverly Hills Dr., Austin 3, Tex.

San Diego (7)—R. E. Honer, 5462 Mary Lane Dr., San Diego 15, Calif.; E. W. Carlson, 2260 Clove St., San Diego 6, Calif.

San Francisco (7)—V. B. Corey, 385 Gravatt Dr., Berkeley 5, Calif.; S. F. Kaisel, Microwave Electronics Corp., 4061 Transport St., Palo Alto, Calif.

Schenectady (1)—T. R. Hoffman, 1471 Regent St., Schenectady 9, N. Y.; P. N. Hess, 1561 Clifton Park Rd., Schenectady 9, N. Y.

Seattle (7)—L. C. Perkins, Box 307, Des Moines, Wash.; H. H. Judson, Jr., 2006 14 Ave., N., Seattle 2, Wash.

Shreveport (6)—L. Hurley, 2736 Rosemont, Shreveport, La.; E. J. Culling, 3252 Sarah St., Bossier City, La.

South Bend-Mishawaka (5)—P. G. Cox, R.R. 2, 10251 Harrison Rd., Osceola, Ind.; E. L. Crosby, Jr., 400 S. Beiger St., Mishawaka, Ind.

South Carolina (3)—W. R. Boehm, Charleston Naval Shipyard, U. S. Naval Base, Code 210, Charleston, S. C.; H. L. Hunter, 49 Fort Dr., Rte. 6, N. Charleston, S. C.

Southern Alberta (8)—R. W. H. Lamb, Radio Sta. CFCN, 12th Ave. & 6th St. E., Calgary, Alta., Canada; J. D. Moore, Dept. of Transport, 404 Public Bldg., Calgary, Alta., Canada.

Syracuse (1)—R. N. Lothes, G. E. Co., DeWitt Engrg. Office, 3711 Erie Blvd., E., DeWitt, N. Y.; R. E. Gildersleeve, 110 S. Burdick St., Fayetteville, N. Y.

Tokyo—I. Koga, 254 8-Chome, Kami-Meguro, Tokyo, Japan; F. Minozuma, 16 Ohara-Machi, Meguro-Ku, Tokyo, Japan.

Toledo (4)—K. P. Herrick, 2516 Fulton St., Toledo 10, Ohio; R. B. Williams, Jr., 5945 Summit St., Sylvania, Ohio.

Toronto (8)—K. MacKenzie, McCurdy Radio Ind., Ltd., 22 Front St., W., Toronto 1, Ont., Canada; W. H. Anderson, 321 Sherbourne St., Apt. 110, Toronto 2, Ont., Canada.

Tucson (7)—Ernest L. Morrison, Jr., 4549 E. Eastland St., Tucson, Ariz.; Witsdoe Bastian, 7132 E. 31 St., Tuscon, Ariz.

Tulsa (6)—Robert Broding, 2820 E. 39th, Tulsa, Okla.; P. M. Ferguson, 1133 N. Lewis, Tulsa 10, Okla.

Twin Cities (5)—S. W. Schulz, 3132 Fourth St., S.E., Minneapolis 14, Minn.; H. D. Shekels, 1942 Beechwood, St. Paul 16, Minn.

Vancouver (8)—W. H. Thompson, 2958 West 28 Ave., Vancouver 8, B. C., Can.; P. A. Niblock, 745 Sylvan Ave., North Vancouver, B. C., Can.

Virginia (3)—R. W. Morton, Box 96, Denbigh, Va.; J. B. Spratley, Ellerson, Va.

Washington (3)—J. E. Durkovic, 10316 Colesville Rd., Silver Spring, Md.; Ben S. Melton, 3921 Mayfair Lane, Alexandria, Va.

Western Massachusetts (1)—J. J. Allen, 29 Sunnyside Dr., Dalton, Mass.; J. E. Mulford, Sprague Elec. Co., Marshall St., North Adams, Mass.

Western Michigan (4)—F. E. Castenholz, Police Headquarters, Jefferson & Walton Sta., Muskegon, Mich.; J. F. Giardina, 1528 Ball, N.E., R. 4, Grand Rapids 5, Mich.

Wichita (6)—J. W. D. Brown, 808 Governeour Road, Wichita, Kans.; R. F. Knowlton, 1200 North Derby, Derby, Kans.

Williamsport (4)—D. M. Jewart, 1400 Faxon Pkwy., Williamsport, Pa.; G. W. Deming, 1891 East 3rd., Williamsport, Pa.

Winnipeg (8)—P. F. Windrick, 669 Oxford St., Winnipeg 9, Man., Canada; R. I. Punshon, Canadian Broadcasting Corp., 540 Portage Ave., Winnipeg, Man., Canada.

Subsections

Buenaventura (7)—J. E. Bossoletti, 2004 South "K" St., Oxnard, Calif.; R. L. O'Bryan, 757 Devonshire Dr., Oxnard, Calif.

Burlington (5)—P. D. Keser, Box 123, Burlington, Iowa; Cleo D. Cherryholmes, 2072 Highland, Burlington, Iowa.

East Bay (7)—D. O. Pederson, Elec. Engrg. Dept., University of Calif., Berkeley 4, Calif.; Eugene A. Aas, 2684 Kennedy St., Livermore, Calif.

Eastern North Carolina (3)—W. J. Barclay, Dept. of Elec. Engrg., North Carolina State College, Raleigh, N. C.; W. J. Speed, 2718 E. Rothgeb Dr., Raleigh, N. C.

Fairfield County (1)—J. M. Hollywood, Fairfield House, 50 Lafayette Pl., Greenwich, Conn.; R. Townsend, 60 Du Bois St., Darien, Conn.

Lancaster (3)—F. S. Veith, 366 Arbor Rd., Lancaster, Pa.; J. Evans, 2109 Lyndell Dr., Lancaster, Pa.

Las Cruces-White Sands Proving Ground (6)—H. Coleman, Box 1238, Las Cruces, N. Mex.; Secretary to be advised.

Lehigh Valley (3)—H. A. Tooker, 2524 Fairview St., Allentown Pa.; M. C. Waltz, Bell Telephone Labs., 555 Union Blvd., Allentown, Pa.

Memphis (3)—Joseph J. Freymuth, 3205 Guernsey Ave., Memphis 12, Tenn.; Brother I. John Haas, Christian Brothers College, Memphis 4, Tenn.

Merrimac Valley (1)—Charles E. White, 16 Dale St., West Peabody, Mass.; Donald Christiansen, 12 Hay St., Newbury, Mass.

Mid-Hudson (2)—W. D. Reiner, 276 Manchester Rd., Poughkeepsie, N. Y.; Benjamin Agusta, 53 Colburn Drive, Poughkeepsie, N. Y.

Monmouth (2)—J. A. Young, Jr., 34 Kemp Ave., Fairhaven, N. J.; O. E. DeLange, Bell Telephone Labs., Holmdel, N. J.

Nashville (3)—Paul E. Dicker, 4208 Walker Lane, Nashville 12, Tenn.; R. L. Hucaby, 945 Caldwell Lane, Nashville 4, Tenn.

New Hampshire (1)—Ralph Baer, 134 Mayflower Dr., Manchester, N. H.; F. J. Safford, 71 Concord St., Nashua, N. H.

Northern Vermont (1)—F. Sichel, 35 Henderson Terrace, Burlington, Vt.; W. C. Chase, WDEV, 9 Stowe St., Waterbury, Vt.

Orange Belt (7)—G. D. Morehouse, 3703 San Simeon Way, Riverside, Calif.; W. G. Collins, 958 Dudley, Pomona, Calif.

Panama City (3)—S. B. Marley, 1912 Calhoun Ave., Panama City, Fla.; Robert C. Lowrey, 2342 Pretty Bayou Dr., Panama City, Fla.

Pasadena (7)—H. L. Richter, Jr., 4800 Oak Grove Dr., Pasadena, Calif.; Bertin N. Posthill, 56 Suffolk Ave., Sierra Madre, Calif.

Reading (3)—F. L. Rose, 42 Arlington St., Reading, Pa.; Harold S. Hauck, 216 Jameson Pl., Reading, Pa.

Richland (7)—P. Richard Kelly, 220 Delafield, Richland, Wash.; G. L. Erickson, 213 Armistead, Richland, Wash.

San Fernando (7)—R. A. Lamm, 15573 Briarwood Dr., Sherman Oaks, Calif.; Jack D. Wills, Systems Labs., Elec. Spec. Co., 5121 San Fernando Rd., Los Angeles 39, Calif.

Santa Ana (7)—T. W. Jarmie, 12345 Cinnabar Rd., Santa Ana, Calif.; R. F. Geiger, Aeronutronic, a Div. of Ford Motor Co., Ford Rd., Newport Beach, Calif.

Santa Barbara (7)—C. P. Hedges, 316 Coleman Ave., Santa Barbara, Calif.; J. A. Moseley, 4532 Via Huerto, Santa Barbara, Calif.

South Western Ontario (8)—W. A. Ruse, Bell Telephone Co., 1149 Goyeau St., Windsor, Ont., Canada; G. L. Virtue, 619 Lounsborough Rd., Sandwich-South, Windsor, Ont., Can.

Westchester County (2)—M. J. Lichtenstein, 52 Sprain Valley Rd., Scarsdale, N. Y.; Martin Ziserman, 121 Westmoreland Ave., White Plains, N. Y.

Western North Carolina (3)—L. L. Caudle, Jr., Box 2536, 1901–1925 N. Tryon St., Charlotte, N. C.; John I. Barron, Southern Bell T. & T. Co., Box 240, Charlotte, N. C.

This precision DC VTVM is also
a wide range, precision ohmmeter and ammeter!

1% accuracy 100 µv to 1,000 volts!

Also 2% accuracy, 1 µa to 1 amp full scale.

Measures 0.02 ohms to 5,000 megohms.

No zero adjustment. 1 minute warm-up.

Floating chassis. $1,000 worth of convenience for $350!

Haven't you wished for one compact, simple instrument that would make *precision* dc voltage, dc current and resistance measurements over a wide range?

The new ⓗⓟ 412A is it! In its VTVM circuit, the 412A uses an exclusive ⓗⓟ photo-chopper instead of old-style mechanical vibrators—no drift, no 60 cps pickup. Input is floating, with resistance increasing from 10 megohms on the 1 mv range to 200 megohms on ranges above 100 mv. Current and voltage ranges have a 10 db sequence for maximum readability and overlap. The ohmmeter is a modified Kelvin bridge eliminating lead resistance error; you measure resistance accurately on hook-up wire sections as short as 6″.

Model 412A also includes a 1 v or 1 ma recorder output, and 3 separate probes. Call your ⓗⓟ rep today for a demonstration on your bench. Price, $350.

HEWLETT-PACKARD COMPANY
1001D PAGE MILL ROAD • PALO ALTO, CALIFORNIA, U.S.A.
CABLE "HEWPACK" • DAVENPORT 6-7000
FIELD REPRESENTATIVES IN ALL PRINCIPAL AREAS

ⓗⓟ 400L LOGARITHMIC VOLTMETER—$325
New ⓗⓟ voltmeter covers 10 cps to 4 MC; accuracy high as ±2% of reading or 1% of full scale. Voltage range 0.3 mv to 300 v, 12 ranges, 1-3-10 sequence. Max. full scale sensitivity 1 mv. Large 5″ true log voltage scale, linear 12 db scale, generous overlap. High stability, high input impedance. Also useful as amplifier for small signals, or to monitor waveforms.

ⓗⓟ 400H PRECISION VOLTMETER—$325
Extreme accuracy as high as ±1% to 500 KC, ±2% to 1 MC, ±5% full range. Frequency coverage 10 cps to 4 MC. Large 5″ meter with precision mirror scale. Voltage range 0.1 mv to 300 v; max. full scale sensitivity 1 mv. High 10 megohm input impedance minimizes circuit disturbances. Amplifier with 56 db feedback insures lasting stability. Reads direct in db or volts.

ⓗⓟ 400D WIDE RANGE VOLTMETER—$225
Highest quality, extremely versatile. Covers 10 cps to 4 MC. Highly sensitive, accurate to within ±2% to 1 MC. Measures 0.1 mv to 300 v; max. full scale sensitivity 1 mv. Reads direct in dbm. High 10 megohm input impedance virtually eliminates circuit loading. 56 db amplifier feedback insures high stability and freedom from change due to external conditions.

Data subject to change without notice. Prices f.o.b. factory

5028

complete precision voltage measuring equipment

at Melpar...

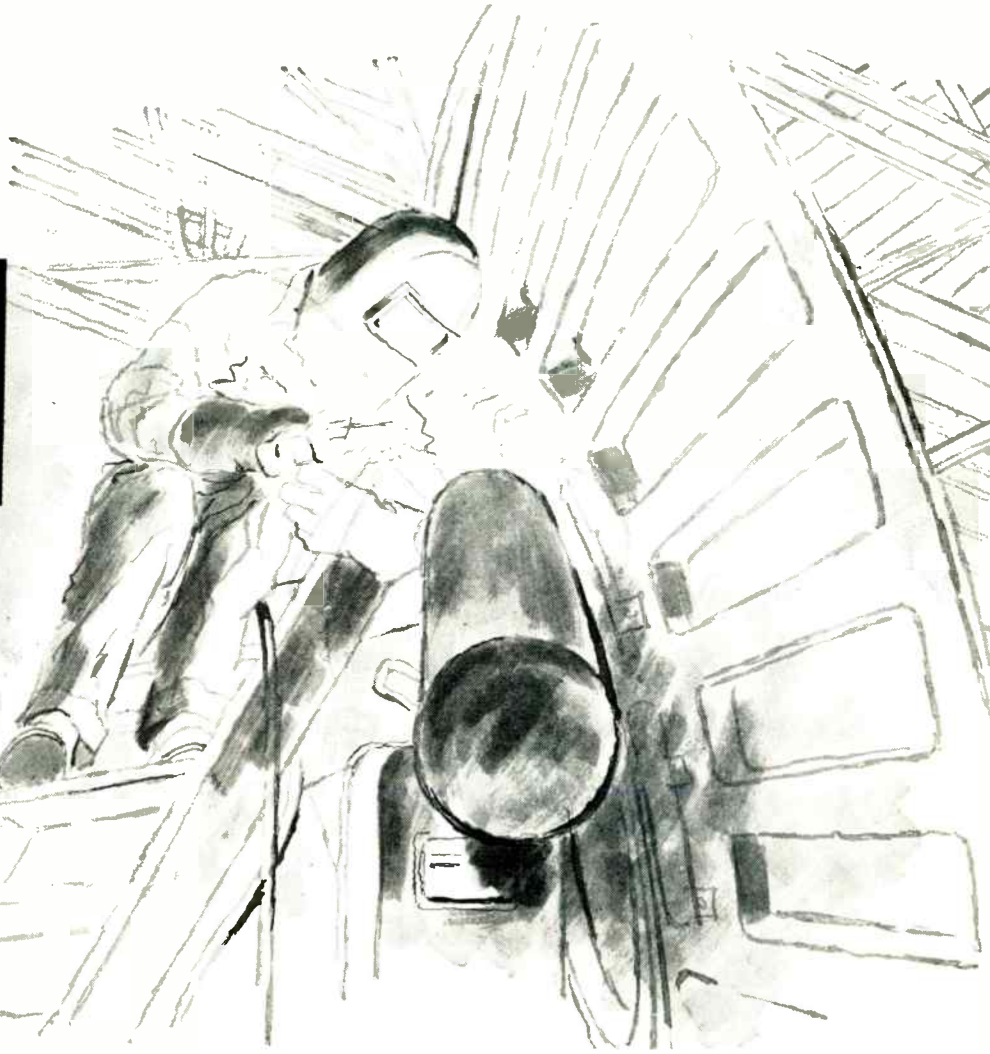

...parallel production, development

expedited production has been applied successfully in these major areas at Melpar

- Printed circuitry and materials
- Acoustic, audio and ultrasonic systems
- Electronic training devices
- Countermeasures systems
- Ordnance electronics
- Aids to navigation
- Flight simulators
- Radar systems
- Telemetry systems
- Antennas

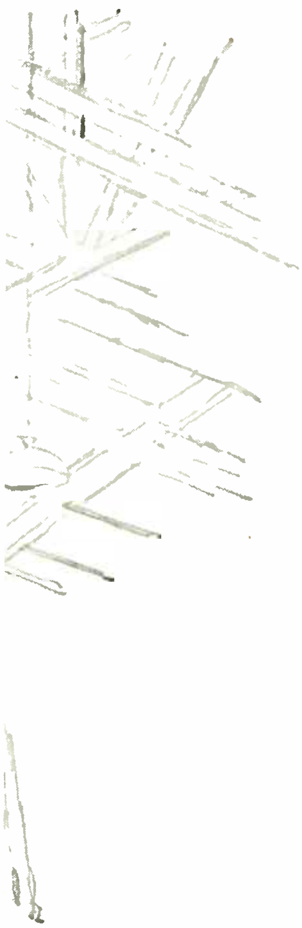

NEWS New Products

Hunter Named By CBS Electronics

Donald Hunter has been appointed semiconductor production superintendent for the **CBS Electronics Div., Columbia Broadcasting System, Inc.,** 900 Chelmsford St., Lowell, Mass., in an announcement by E. J. Quirk, semiconductor plant manager. Hunter was previously manager of production control.

He joined CBS Electronics in 1952 as a production supervisor. He also served as a general foreman with Transitron Electronic Corporation and as production manager for Clevite Transistor Products.

Hunter is a graduate of Northeastern University with a degree in industrial management. More recently he was graduaged from CBS Electronics' work factor and supervisory training programs.

Dole R. & D. Director of Ace Electronics

Ace Electronics Associates, Inc., Somerville, Mass., manufacturers of precision potentiometers, announces the appointment of Fred E. Dole as Director of Research & Development of Ace Electronics Associates, Inc. and its affiliates. His responsibilities include supervision of all matters of design, prototyping and production.

Dole has been a consultant to the electronic industry in the fields of precious metals, contacts, switches and other electromechanical component areas. For the past twelve years he has acted as Director of the Industrial Division of the J. M. Ney Company, Hartford, Conn. He served also as consultant for customer engineering for the Ney firm on a national basis, prior to establishing his own consulting firm.

Dole's wide experience in the precision potentiometer industry extends over twenty years, and his many major contributions to the state of the art have resulted in large degree in making the miniaturization of potentiometers possible. Dole began his career in this field in the potentiometer section of the Radiation Laboratory' M.I.T., where his responsibilities included all phases of potentiometer design and manufacturing, as well as liaison with all potentiometer manufacturers.

These manufacturers have invited PROCEEDINGS readers to write for literature and further technical information. Please mention your IRE affiliation.

Vibration Transmissibility Recorder

A new instrument which makes possible significant advances in recording vibration transmissibilities or other two-signal ratios, known as the Continuous Transmissibility Recorder, is being marketed by **Lord Manufacturing Co.,** Erie, Pa.

The Transmissibility Recorder permits continuous, direct recording of vibration transmissibilities with greater speed and accuracy than previous point-by-point manual methods. It records transmissibility directly as a function of frequency, giving a ready-to-use curve.

In addition to vibration testing, its versatility permits use with signal voltages representing any two phenomena of interest.

The recorder simultaneously accepts two synchronous signals in the frequency range of 10 to 5000 cps, measures their frequency, computes the average amplitude values and plots the ratio as a function of frequency. Data is recorded by ink writing in permanent, easy-to-read chart form. Special chart papers are available from the instrument manufacturer.

Results are acceptable to the ASESA in qualification testing to MIL specs.

The instrument can be used to determine these ratios: (1) input voltage vs frequency, (2) time-integral of input voltages vs frequency, (3) time-derivative of input voltages vs frequency. It features four operating scale ranges, high resolution capabilities, a built-in operating check and continuously adjustable sensitivity.

Range Time Decoder

Astrometrics, Inc., a division of **Arnoux Corp.,** 11924 W. Washington Blvd., Los Angeles 66, Calif., announced this week the development and manufacture of their new Range Time Decoder, the RTD 1501, a search and control device for automatic utilization of range time signals. Simple and extremely dependable, the RTD is economical and is smaller than existing equipment now available.

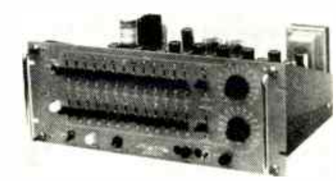

When a range time pulse is received, the sequential counter generates an output pulse summed with binary "one" detectors. Provision is made for storing coincidence. Sequential counter and memory circuits are reset during frame identification. When preselected pulses are present, a signal is generated during frame identification and applied to a second memory circuit. Reset is accomplished when the preselected pulse is generated. This pulse is used to start recorders, or as any start signal. A second set of switches permits a "stop" signal to be generated at any desired time. Further information may be obtained by writing Les Cole at the firm.

WWV Receiver

A new, transistorized WWV receiver, Model WVTR is announced by **Specific Products,** 21051 Costanso St., Woodland Hills, Calif. It is battery operated and requires 3½" rack space.

Instantaneous carrier frequency selectivity of 2.5, 5, 10, 15, 20 and 25 mc is crystal controlled. Double conversion, 1990 kc first IF crystal converter to 90 kc second IF. Sensitivity is 2 microvolts, selectivity is 10 kc at 20 db down, hi-lo impedance antenna inputs, "s" meter, and phone jack and speaker are provided. Battery or ac power pack available. Literature available on request. Price is $725.00.

(Continued on page 112A)

Creative Microwave Technology

Published by MICROWAVE AND POWER TUBE DIVISION, RAYTHEON COMPANY, WALTHAM 54, MASS., Vol. 1, No. 9

NEW RAYTHEON MAGNETRONS FOR A WIDE RANGE OF APPLICATIONS

Designed for C-band systems requiring tunability, the RK-7156 magnetron has a minimum peak power output rating of 250 kilowatts over a frequency range of 5,450 to 5,825 megacycles. Applications include a flight-tested, revolutionary airborne weather radar system. The RK-7156 is in quantity production.

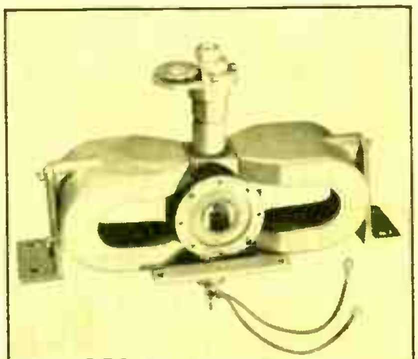

RK-7156

* * *

X-band magnetron for airborne search radar provides one megawatt minimum peak power and 875 watts average

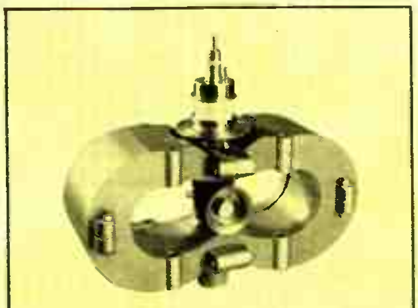

QK-624

power within a frequency range of 9,340 to 9,440 Mc. Designated QK-624, this pulsed-type tube is liquid cooled and should give at least 1,000 hours of reliable service.

* * *

For ground-based and airborne radar systems, the RK-7529 magnetron provides a 2.0 microsecond pulse of 3.5 megawatts minimum peak power over 2,700 to 2,850 Mc. This liquid-cooled tube is interchangeable with other fixed-frequency S-band tubes operating at similar power levels.

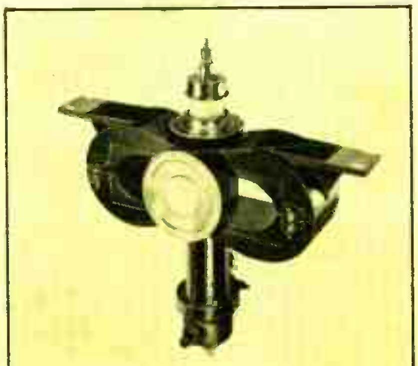

RK-7529

* * *

A one kilowatt beacon magnetron, the RK-7578 weighs only 14 ozs., yet will withstand vibrations of 15 G's at 20 to 2,000 cycles and shock up to 100 G's. It is

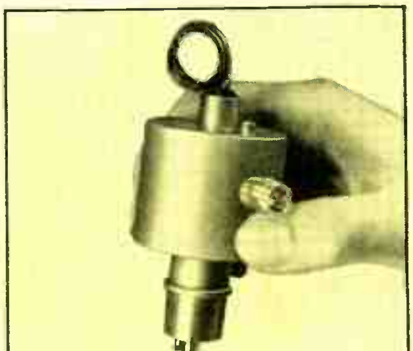

RK-7578

mechanically tunable and covers the 5,400 to 5,900 Mc range.

* * *

Developed to withstand extreme environmental conditions, the RK-7449 magnetron is a lightweight, compact tube with a minimum peak power output of 45 kilowatts at the operating frequency of 24 kmc. The RK-7449 is required to withstand re-

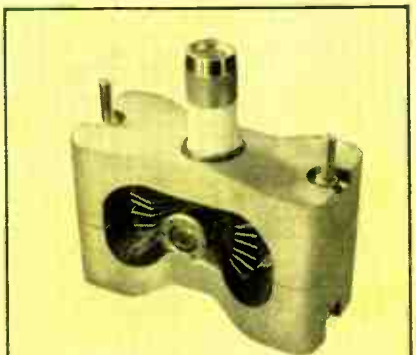

RK-7449

peated shocks of 50G. Stable operation is guaranteed at vibration frequencies up to 2,000 c.p.s. with 30G applied.

A Leader in Creative Microwave Technology RAYTHEON

IRE People

The appointment of **Frederick J. Anderson** (S'47–A'49–SM'55) as director of engineering for the Data Systems Operations of Sylvania Electronic Systems, a division of Sylvania Electric Products Inc., has been announced by Eugene J. Vigneron, General Manager of the Data Systems Operations. Sylvania is a subsidiary of General Telephone & Electronics Corp.

F. J. Anderson

He previously served as manager of the Data Processing Laboratory at the Data Systems Operations. The Needham facility is engaged in research, development and production activities in data processing, special and general-purpose computer systems, data transmission and allied fields.

An electronics officer in the U. S. Navy during World War II, he joined Sylvania in 1947 as an engineer working on design and construction of computing equipment. He was named manager of the computer department in 1954.

Mr. Anderson served successively as manager of the projects department, and assistant manager of the Avionics Laboratory in the division's Waltham Laboratories prior to assuming management of the Data Processing Laboratory in 1958.

A graduate of Stanford University with the B.S. degree in electrical engineering, he also studied at Nebraska Wesleyan University, and Northeastern University.

❖

The Board of Directors of the Wurlitzer Company has elected **A. Donald Arsem** (SM'52) a Vice President of the Company. He joined Wurlitzer March 17, 1958 as Manager, Engineering and Research of the North Tonawanda Division, and will continue in that capacity.

A. D. Arsem

He received the B.S. degree in electrical engineering from Massachusetts Institute of Technology, and did graduate work at Syracuse University. He is a member of the Scientific Research Society of America and the American Rocket Society. In 1943 and 1944 he served as Development Engineer at the U. S. Bureau of Standards on Proximity Fuzes. In 1945 he joined RCA Victor Division, Ground and Marine Radar Section, as Development Engineer. In 1949 he became associated with the General Electric Company Electronics Laboratory in Syracuse. He was responsible for development and system evaluation of the Hermes missile guidance systems as Assistant Head of the Missile Guidance Section of General Electric.

From 1951 to 1953 he headed the Magnetic Materials Application Section at General Electric. From 1953 to 1955 he was Manager of Advanced Product Development of General Electric's Electronics Laboratory, responsible for both commercial and military development programs.

In 1955 he became Manager of Engineering for Stewart-Warner Electronics in Chicago, with responsibility for such primary product fields as military communications, IFF equipment, automatic direction finders, micro-wave beacons, radar altimeters, and data processing systems.

❖

Dr. Chao C. Wang (A'43–SM'49–F'57), Electrical Engineering Department Head for Microwave Tube Research at Sperry Gyroscope Company, Great Neck, Long Island, has been awarded the VICTOR EMANUEL DISTINGUISHED PROFESSORSHIP at Cornell University's College of Engineering, for the Spring, 1960 term.

C. C. Wang

Professor Wang was selected in keeping with the original intent of conferring the honor on distinguished men who would be "brought to the campus chiefly for their ability to stimulate (Cornell) staff both academically and professionally." As the recipient of this award, Professor Wang is not required to hold formal classes at the University, but he is conducting seminars for graduate students and faculty members and is regularly conferring with men engaging in research in his field of interest.

A Sperry Gyroscope research scientist since 1946, he is known widely for his leadership in microwave science and especially for his many basic contributions in the electron physics and microwave tube fields. His defining works in the microwave fields of gridless klystron cavities, magnetic and space charge focusing systems for electron beams, theory of small and large signal interaction of microwave structures with electron beams, and especially in the use of computers in the research and develop-

(Continued on page 32A)

5/8 actual size

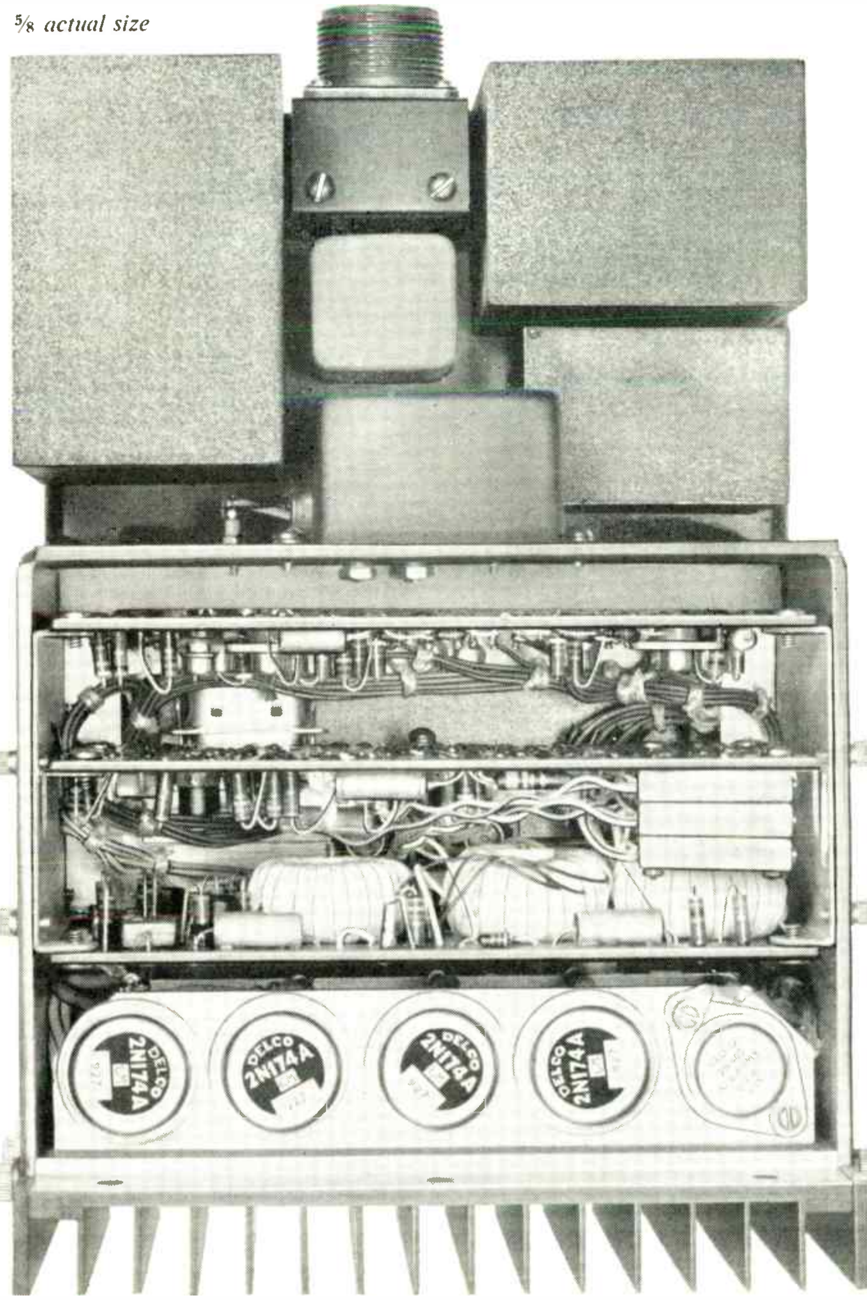

FROM DELCO RADIO NEW IDEAS FOR DEFENSE

HIGH CAPACITY STATIC INVERTERS WITH NO MOVING PARTS

Delco Radio's high capacity Static Inverters and Converters fill a critical need in missile guidance and control—offering extremely reliable, very highly regulated power of precise frequency. The Static Inverters use direct crystal-frequency control and digital logic circuits to produce accurate, single or polyphase power output. They have no moving parts. There is nothing that can get out of adjustment. Electrical characteristics are: High Capacity—150 to 4,000 volt-amperes. High Efficiency—65 to 90% depending on power and control (precision and regulation) required. Accurate Phase Angle Control—to 0.5 degree. Precise Frequency Control—up to 6 parts per million maximum variation under all load and environmental conditions. Voltage Amplitude Control—to ±1% no load to full load. Low Distortion—typically 2% total harmonic distortion. Delco Radio has developed and produced power supplies for missiles such as the Air Force's Ballistic Intermediate Range Thor, Intercontinental Titan, and the pilotless aircraft Mace. For further information on military electronics, write to our Sales Department. *Physicists and electronics engineers: Join Delco Radio's search for new and better products through Solid State Physics.*

PIONEERING PRECISION PRODUCTS THROUGH SOLID STATE PHYSICS

DELCO RADIO

Division of General Motors • Kokomo, Indiana

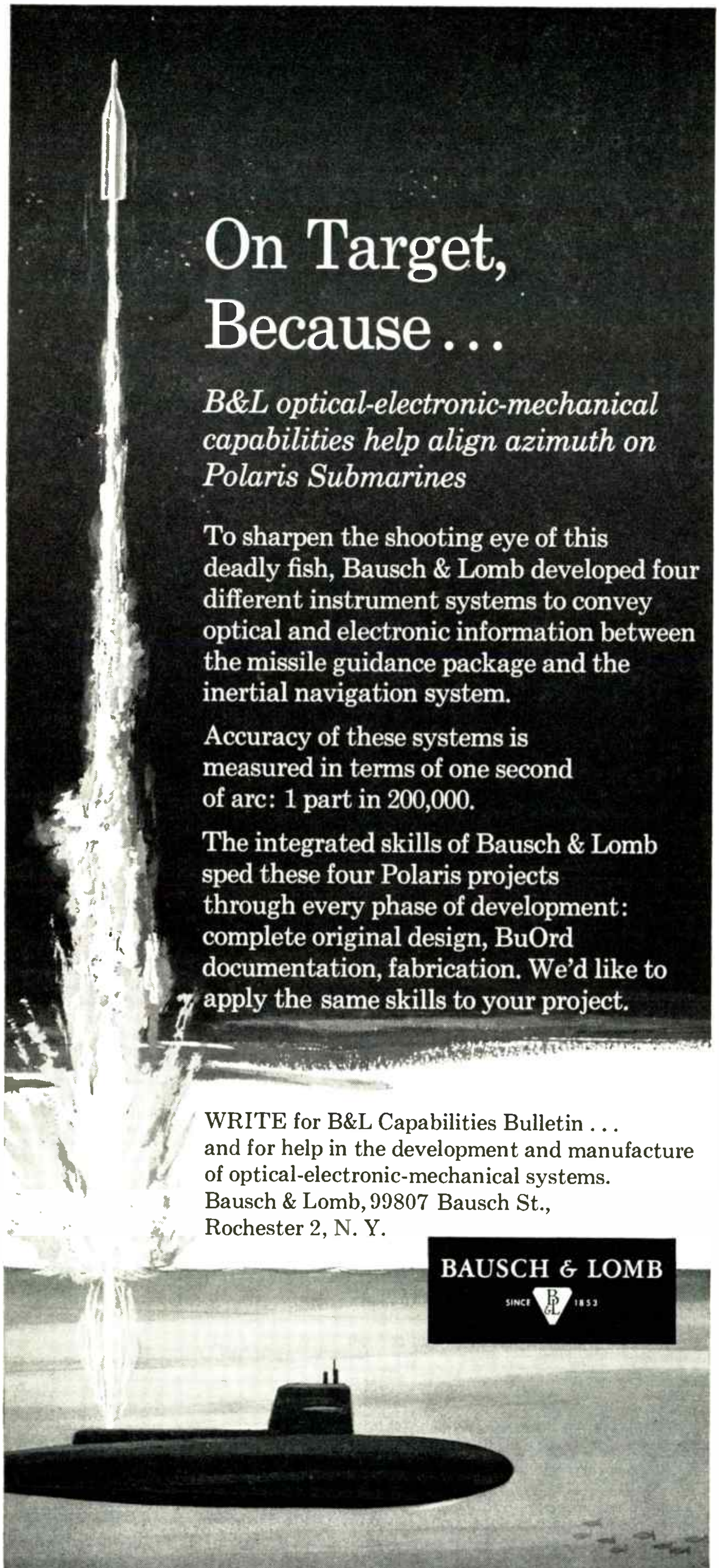

IRE People

(Continued from page 30A)

ment of microwave tubes have been an inspiration to his co-workers both at Sperry and elsewhere.

He was graduated from Hiao-Tung University in Shanghai with the B.S. Degree in 1936. He received the M.S. and Ph.D. Degrees in radio communications from Harvard University in 1938 and 1940.

Professor Wang is a member of the American Physical Society and the American Association for the Advancement of Science. He has published a number of papers on microwave tube theory and holds several patents.

❖

Appointment of **Richard H. Baker** (A'54–SM'56) as Manager of the Ballistic Missile Early Warning System (BMEWS) in the United Kingdom has been announced by D. Brainerd Holmes, Manager of BMEWS, Moorestown Missile and Surface Radar Division, Radio Corporation of America.

R. H. Baker

The announcement follows RCA's receipt of a letter contract, announced today by the U. S. Air Force, authorizing the implementation of the third BMEWS site at Fylingdales Moor in Yorkshire, England. This contract supplements RCA's prime contract for the BMEWS project.

Mr. Baker will have over-all responsibility for the management of the BMEWS program in the United Kingdom, working with RCA Great Britain Limited, of London, which has functional and administrative responsibilities. He will supervise the initial phases of planning, construction and implementation of equipment at the third BMEWS site, as well as maintaining liaison with RCA's major subcontractors at that location.

Plans to construct a BMEWS installation in England were announced jointly by the United States and British governments in February. BMEWS sites are already under construction in Thule, Greenland, and Clear, Alaska. Upon construction of the third site, the system will provide complete radar detection coverage of the U. S., Great Britain and Southern Canada against enemy ICBM attacks from beyond the Northern Polar regions and the Eurasian land mass.

Mr. Baker has been associated with the BMEWS program in various administrative capacities since it was started early in 1958. Before his recent appointment he was Manager, BMEWS Quality, Reliability and Subcontracted Projects. He joined RCA in 1954 as Manager of Standards En-

(Continued on page 35A)


Reliability in volume...
CLEVITE
TRANSISTOR
WALTHAM, MASSACHUSETTS

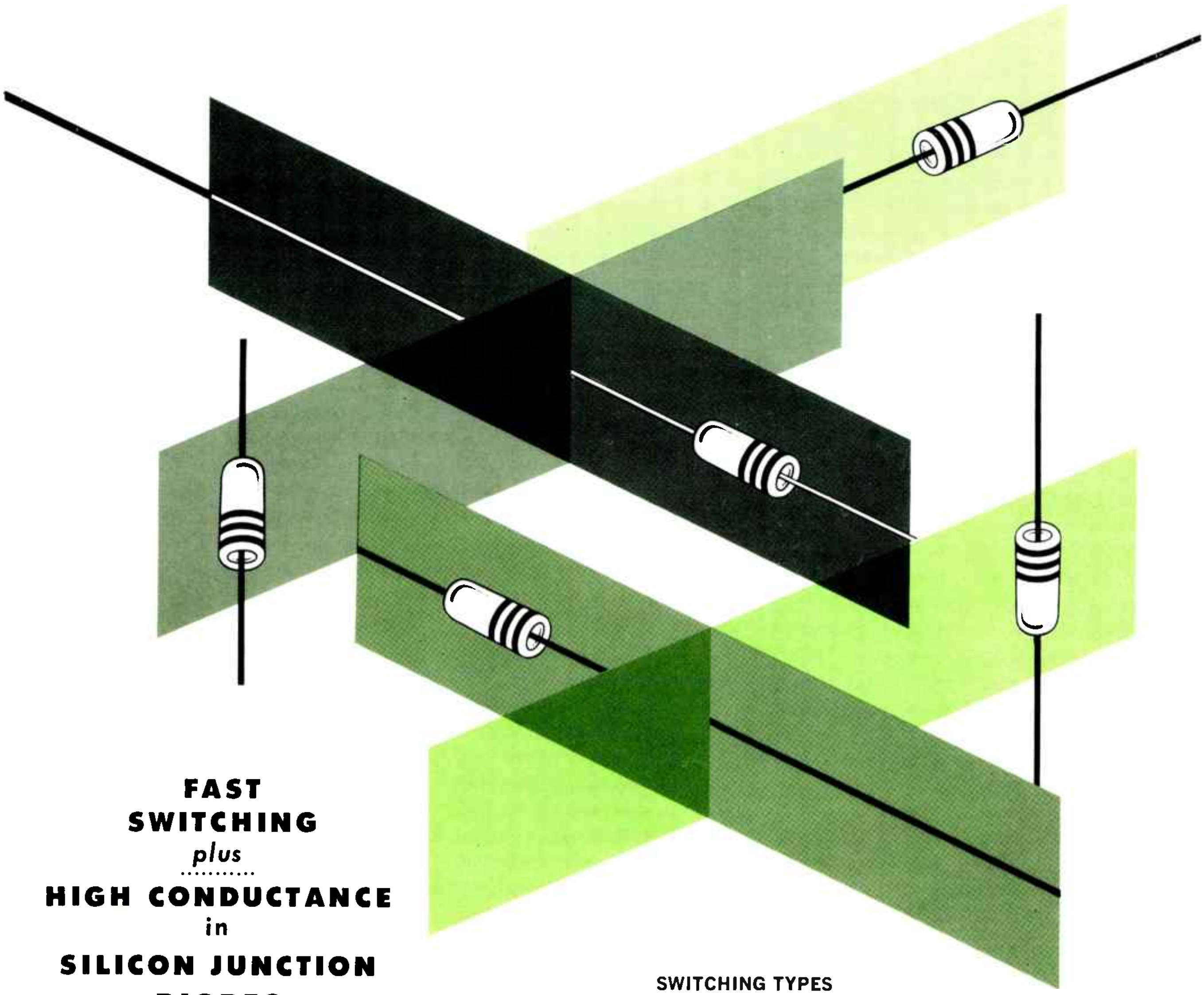

FAST SWITCHING
plus
HIGH CONDUCTANCE
in
SILICON JUNCTION DIODES

SWITCHING TYPES

New circuit possibilities for low impedance, high current applications are opened up by Clevite's switching diodes. Type CSD-2542, for example, switches from 30 ma to -35v. in 0.5 microseconds in a modified IBM Y circuit and has a forward conductance of 100 ma min@1 volt.

Combining high reverse voltage, high forward conductance, fast switching and high temperature operation, these diodes approach the ideal multi-purpose device sought by designers.

GENERAL PURPOSE TYPES

Optimum rectification efficiency rather than rate of switching has been built into these silicon diodes. They feature very high forward conductance and low reverse current. These diodes find their principal use in various instrumentation applications where the accuracy or reproduceability of performance of the circuit requires a diode of negligible reverse current. In this line of general purpose types Clevite has available, in addition to the JAN types listed below, commercial diodes of the 1N482 series.

MILITARY TYPES

JAN		SIGNAL CORPS	
1N457 –	MIL-E-1/1026	1N662 –	MIL-E-1/1139
1N458 –	MIL-E-1/1027	1N663 –	MIL-E-1/1140
1N459 –	MIL-E-1/1028	1N658 –	MIL-E-1/1160
		1N643 –	MIL-E-1/1171

All these diodes are available for immediate delivery. Write now for Bulletins B217A-1, B217A-2 and B217-4.

Reliability In Volume . . .

A DIVISION OF CLEVITE CORPORATION

CLEVITE TRANSISTOR

254 Crescent Street Waltham 54, Mass. Tel: TWinbrook 4-9330

IRE People

(Continued from page 32A)

gineering for Defense Electronic Products in Camden, New Jersey, and was later promoted to Manager, Central Services and Engineering.

A graduate of Case Institute of Technology in 1936, Mr. Baker has been employed in military defense industries for many years. He is a member of Tau Beta Pi and the American Ordnance Association. He is also a registered engineer in the States of California and New Jersey.

❖

George M. W. Badger (S'50–A'52–M'56) has been appointed to the newly-created position of Product Manager, Power Klystrons with Eitel-McCullough, Inc., San Carlos, Calif., manufacturer of Eimac electron-power tubes.

G. M. W. Badger

He joined Eimac in 1953 as research engineer. He was project engineer on early development of the company's power klystrons, and later was in charge of Eimac's color television laboratory.

Prior to joining Eimac, he helped pioneer development of the Lawrence color television picture tubes. He left the position of Eimac's Manager, Research and Development, to assume his present post.

Badger received the B.S. degree in electrical engineering from the University of California in Berkeley. He holds amateur radio license W6RXW.

❖

The creation of a new position of vice president, Electronics Systems and Equipment Operation, has been announced by the Crosley Division, Avco Corporation.

F. C. Reith, president of the Crosley Division and Avco vice president, said that **Jack L. Bowers** (A'44–SM'55) has been named to the new post.

As vice president of the Electronics Systems and Equipment Operation, he will be responsible for the Crosley Division's engineering, marketing, production and administration for radar, ground communications equipment and electronic systems.

Among the several products included in the Electronics Systems and Equipment Operation are the giant FPS-26 height finder radar designed and produced by Crosley for the U. S. Air Force. Electronic systems, including the ASG-15 fire control system used in the B-52, and the VRC-12 ground communications unit for the U. S. Army, are other products that will be handled by the operation headed by Mr. Bowers.

For the last four years as assistant chief

(Continued on page 36A)

IRE People

(Continued from page 35A)

engineer, design, he has been in charge of design of the Atlas intercontinental ballistic missile for Convair Astronautics, a division of General Dynamics Corporation. From 1946 to 1956 he held other positions in Convair related to missile and electronics development.

During World War II, he served three years with the U. S. Air Force and won the Legion of Merit for his work in electronic countermeasures and guidance at the Special Projects Laboratory at Wright-Patterson Air Force Base. At the end of World War II, he left the service with the rank of Captain.

Mr. Bowers is a native of Colorado Springs, Colorado, and Aberdeen, Washington. He holds the Bachelor of Science Degree in Electrical Engineering from the Carnegie Institute of Technology in Pittsburgh and has taken further graduate work at New York University and the University of California at Los Angeles. He has served as chairman of the Electronic Equipment Technical Committee of the Aerospace Industries Association.

❖

Dr. Charles R. Burrows (A'24–M'38–SM'43–F'43), internationally prominent scientist, has joined Page Communications Engineers, Inc. as Vice President and Director of Research and Development, Esterly C. Page, President, announced.

C. R. Burrows

Prior to joining Page, a Northrop subsidiary, Dr. Burrows was Vice President—Engineering for Radiation, Inc., Melbourne, Fla., where he established their advanced development division. At Page, he will be responsible for the technical administration of the firm's space and satellite communications projects, and continuing research in the fields of radio relay systems, navigational techniques and wave propagation.

Earlier, Dr. Burrows was Vice President for Engineering at the Ford Instrument Company Division of the Sperry Rand Corporation. From 1945 until 1956, Dr. Burrows was Professor of Electrical Engineering and Director of the School of Electrical Engineering at Cornell University.

During his 11 years at Cornell, Dr. Burrows organized a research program on radio astronomy, the first to be established in any American university. He was also a consultant to the University of Texas, Syracuse University, Bendix Aviation Company, the General Electric Company and the U. S. Navy Electronics Laboratory.

Dr. Burrows has had extensive experience in both radio and electrical engineering and contributed to the design of transmitters used for long-range telephone across the Atlantic.

Internationally known as an expert on electromagnetic wave propagation, Dr. Burrows was an Associate Chief Scientist of the General Electric Company's Advanced Electronics Center.

Just prior to World War II, Dr. Burrows worked on the development of the proximity fuse and later on electromagnetic counter measures and the development of high power radio equipment.

During the war, he was chairman of the Wave Propagation Committee of the National Defense Research Committee, coordinating all research work in this field affecting the war effort.

For 21 years, Dr. Burrows was a member of the technical staff of the Bell Telephone Laboratories, where he specialized in advanced electronics research.

He served as Vice President of the International Scientific Radio Union and is a Fellow and past director of the Institute of Radio Engineers. From 1946 to 1954 he was president of the Joint Commission on Radio Meteorology of the International Council of Scientific Unions.

Dr. Burrows received the A.M. and Ph.D. degrees in physics from Columbia University. He graduated from the University of Michigan in 1924 with the B.S.E. and later received the E.E. degree there.

He is a Fellow of the American Physical Society and is a member of the American

(Continued on page 38A)

New LAMBDA
Regulated Power Supplies
5 and 10 AMP 0-34 VDC

CONVECTION COOLED

3½″ ON 5 AMP MODELS

7″ ON 10 AMP MODELS

3½″ PANEL HEIGHT ON 5 AMP MODELS

- **Convection cooled—no internal blowers to wear out**
- **Guaranteed for a full 5 years**
- **Ambient temperature 50°C**
- **Excess ambient thermal protection**
- **Special, high purity foil, hermetically sealed long-life electrolytic capacitors**
- **Hermetically sealed transformer designed to MIL-T-27A**
- **Remote sensing and DC vernier**

New LAMBDA LA Series Condensed Data

DC OUTPUT:

(Regulated for line and load)

MODEL	VOLTAGE RANGE[1]	CURRENT RANGE[2]	PRICE
LA50-03A	0-34 VDC	0- 5A	$395
LA50-03AM	0-34 VDC	0- 5A	$425
LA100-03A	0-34 VDC	0-10A	$510
LA100-03AM	0-34 VDC	0-10A	$540

[1] The output voltage for each model is completely covered in four steps by selector switches plus vernier control and is obtained by summation of voltage steps and continuously variable DC vernier as follows:

MODEL	VOLTAGE STEPS
LA 50-03A, LA 50-03AM	2, 4, 8, 16 and 0-4 volt vernier
LA100-03A, LA100-03AM	2, 4, 8, 16 and 0-4 volt vernier

[2] Current rating applies over entire output voltage range

Regulation: Line: Better than 0.15 per cent or 20 millivolts (whichever is greater).
Load: Better than 0.15 per cent or 20 millivolts (whichever is greater).

Transient Response: Line or Load: Output voltage is constant within regulation specifications for step function line voltage change from 100-130 VAC or 130-100 VAC or for step-function load change from 0 to full load or full load to 0 within 50 microseconds after application.

Ripple and Noise: Less than 1 millivolt rms with either terminal grounded.

AC INPUT:
100-130 VAC, 60 ± 0.3 cycle. This frequency band amply covers standard commercial power lines in the United States and Canada.

OVERLOAD PROTECTION:

Electrical: Magnetic circuit breaker front panel mounted. Special transistor circuitry provides independent protection against transistor complement overload. Fuses provide internal failure protection. Unit cannot be injured by short circuit or overload.

REMOTE SENSING:
Provision is made for remote sensing to minimize effect of power output leads on DC regulation, output impedance and transient response.

PHYSICAL DATA:

Size: LA 50-03A. . .3½″ H x 19″ W x 14⅜″ D
LA100-03A. . .7″ H x 19″ W x 14⅜″ D

Panel Finish: Black ripple enamel (standard). Special finishes available to customers specifications at moderate surcharge. Quotation upon request.

Send today for complete data

λ LAMBDA ELECTRONICS CORP.
11-11 131 STREET • DEPT. 3 • COLLEGE POINT 56, N. Y. • INDEPENDENCE 1-8500

IRE People

(Continued from page 36A)

Rocket Society and the American Ordnance Association.

❖

Earl Chiswell (A'53–M'56) has been promoted to Central Regional Sales Manager and **J. Gordon Schontzler** (S'51–A'53–M'58) to Eastern Regional Sales Manager, it has been announced by Dr. E. M. Baldwin, Vice President and General Manager of the Rheem Semiconductor Corporation. This corporation, located in Mountain View, Calif., manufactures silicon diodes, transistors, and special assemblies.

Prior to joining Rheem, Mr. Chiswell was Director of Sales for General Electronic Controls, Inc.; Research Scientist in instrumentation laboratory for the University of Minnesota; Staff Consultant and Design Specialist at the University of Minnesota, and Head of Test Instrumentation for Propulsion Wind Tunnel, AEDC.

In his new position, he will have jurisdiction over the central United States region.

He graduated from the University of Toronto with a M.S. degree in electrical engineering. He is a member of the Institute of Aeronautical Sciences, the Instrument Society of America, and the Rocket Society of America.

Mr. Schontzler was formerly District Sales Manager in the Northeast District for Raytheon Company. For a period of three years he was employed as a member of the Technical Staff in the design of transistorized carrier equipment for Bell Telephone Laboratories.

In his new capacity, he will head the entire Eastern Region for Rheem Semiconductor Corporation. He is a graduate of Brown University and holds the B.S.E.E. degree from that school.

Before their promotions, Mr. Chiswell and Mr. Schontzler were employed as Sales Engineers for Rheem. Both men will report to Rudolph Maravich, Manager of Field Sales.

❖

H. S. Christensen (M'46) has joined the product management staff of the Avionics Group at Bendix Radio Division in Baltimore, according to an announcement by C. I. Rice, Manager of Avionic Products.

H. S. Christensen

Rice said that Christensen will be responsible for coordination and planning of the company's business aircraft product line. He further stated that this appointment was consistent with the Division's long range plans for expansion of the Avion-

(Continued on page 40A)

MEASUREMENT & COMMUNICATION

R&S NEWS

Another Example of ROHDE & SCHWARZ Contribution to Precise Measurement.

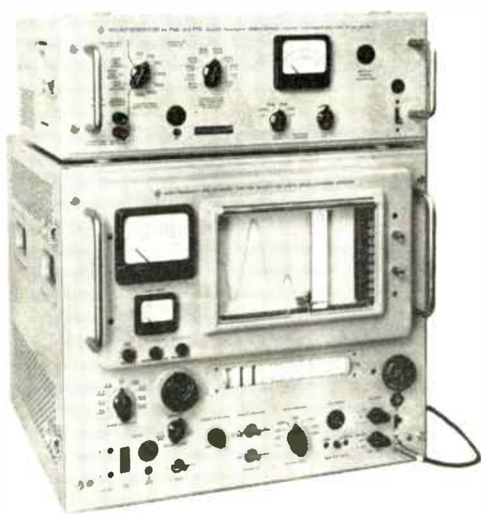

AUTOMATIC RECORDING AUDIO-FREQUENCY SPECTROGRAPH ANALYZER AND RESPONSE PLOTTER (TYPE FNA)

FEATURES

Automatic Spectrum Analyzer

- Built-in recorder with full 80 db coverage on one measurement range
- Narrow and wide band operation
- Slow and fast motor drive
- Any 4 kc within the range can be spread out over the entire range

With Synchronous Oscillator

- Synchronization of oscillator and analyzer-recorder by electronic means
- Single dial control for combined oscillator and analyzer
- Ideal for selective frequency-response measurements
  a) When wide attenuation range is required
  b) When hum and noise make wideband measurement impossible
- Permits plotting of loudspeaker characteristics in the presence of ambient noise
- Output voltage variable from microvolts to 100 volts

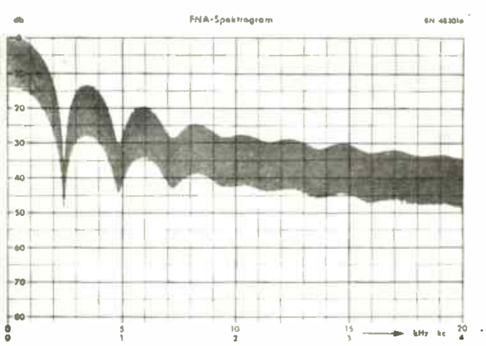

APPLICATIONS

- Fourier analysis of complex wave forms and pulse voltages
- Noise analysis
- Measurement of signal to noise ratio, of spurious frequencies and hum
- Measurement of harmonic distortion, intermodulation distortion and modulation products
- Analyses of sounds and complicated movements in conjunction with a suitable microphone or vibration pickup
- Complete frequency test assembly for amplifiers, filters, microphones, loudspeakers, etc., in conjunction with the synchronous oscillator

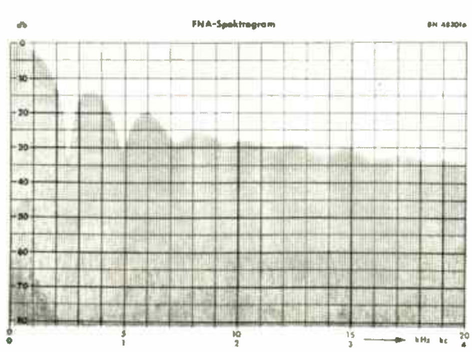

WRITE FOR DETAILED 6 PAGE DATA BULLETIN FNA

IN USE... AROUND THE WORLD

ROHDE & SCHWARZ

111 Lexington Ave., Passaic, New Jersey
Telephone: PRescott 3-8010
Cable Address: ROHDESCHWARZUSA

SEE ROHDE & SCHWARZ EQUIPMENT AT THE WESCON SHOW

IRE People

(Continued from page 38A)

ics product line to include equipment specifically designed for intermediate twin-engine aircraft.

Christensen comes to Bendix from the Aircraft Radio Corporation, where he was Commercial Sales Manager. Earlier activities at ARC, dating back to 1945, included operation of the Company's flight department, service as chief pilot, engineering liaison with government agencies, and the establishment of the commercial products sales division.

He has a long background in aviation and electronics. After a formal electrical engineering education at the University of Nebraska and the University of the Philippines, he spent several years in the broadcast industry. He holds a commercial pilot's instrument rating and has over 10,000 hours flight time, part of which dates back to the mid-1920s when he was first commissioned as a flying officer in the U. S. Army Air Corps. He qualified as a Naval Aviator in 1943.

He was officer-in-charge of Project CAST during World War II, the experimental flight test unit which evaluated many of the new electronic developments of the MIT Radiation Laboratory and Harvard's Radio Research Laboratory. He received the Legion of Merit for that assignment and is a retired Captain in the U. S. Naval Reserve.

He has served with various committees of The Radio Technical Commission on Aeronautics and as technical consultant to the Aircraft Industries Association.

❖

Formation of a new components division by Hughes Aircraft Company to develop and market commercial microwave components has been announced by Iden F. Richardson, vice president.

C. W. CURTIS

Charles W. Curtis (S'49–A'50–M'55) has been appointed manager of the new division; he has been acting manager of the company's microwave laboratory, which now becomes the nucleus for the new division. The components division will market a line of products including microwave components, antennas and advanced structures, with other new products to be developed.

Mr. Curtis, manager of the new division, has been at Hughes since 1949, when he joined the technical staff of its airborne systems group. He has served as head of various company microwave sections and departments, and in 1958 became head of the microwave engineering department of the microwave laboratory. In January of this year he was appointed acting manager of the microwave laboratory. He graduated from the University of California in 1947,

(Continued on page 42A)

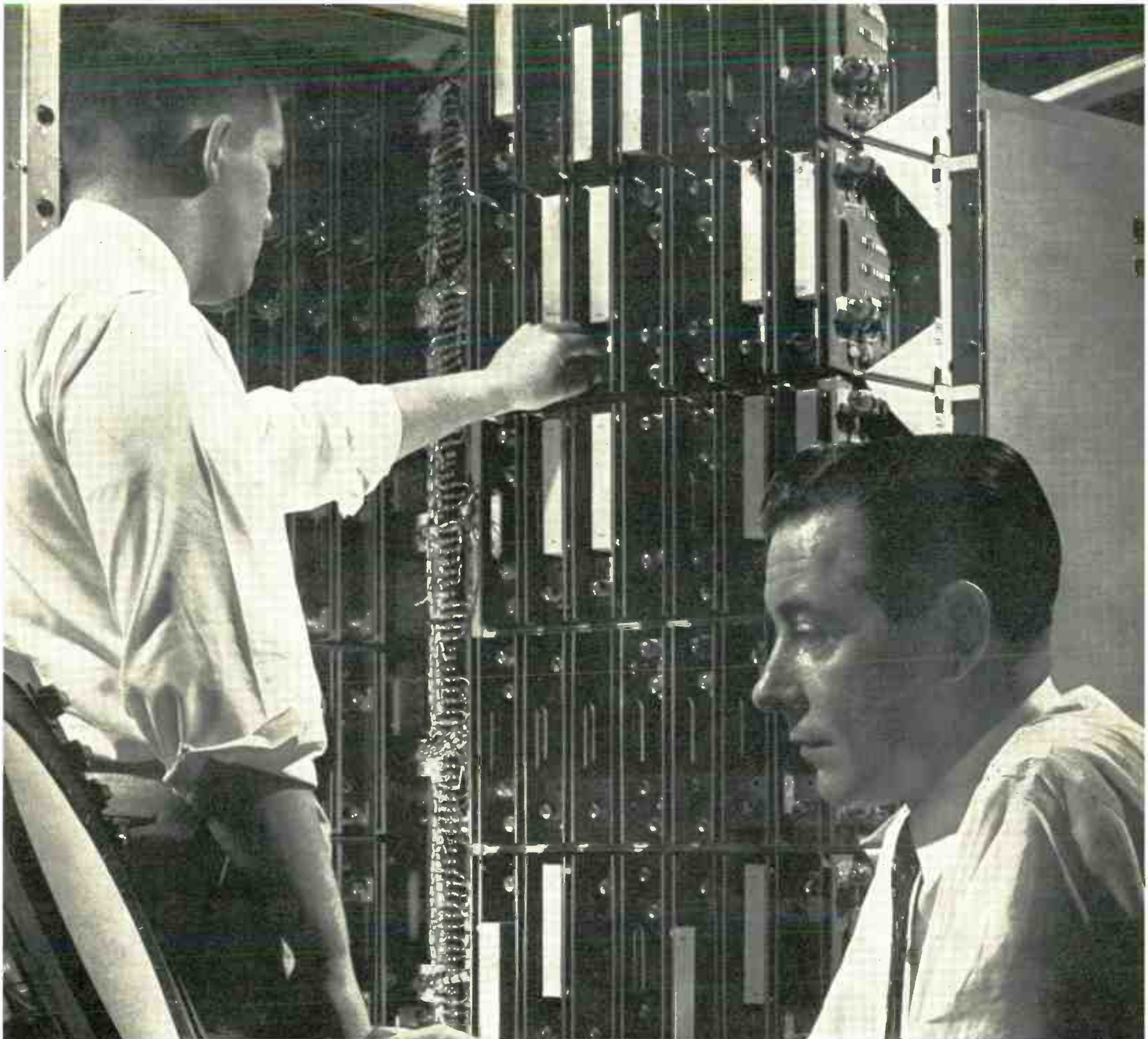

AN ACHIEVEMENT IN DEFENSE ELECTRONICS

AN/FSA-12--First to detect and process 3-D radar data automatically

The first equipment to successfully automate the processing of three-dimensional data direct from a working radar, the AN/FSA-12 (XW-1) has operated since 1958. This detector tracker has enabled General Electric to develop many improved radar techniques and equipment.

New concepts in correlation and smoothing in the track-while-scan method have been demonstrated. Delay lines applied to digital techniques and plug-in wiring boards have been improved. New ideas in data storage and digital circuitry have been applied.

This experimental model continues to be a proving ground in research and development of advanced military electronics. A completely solid state production version of the AN/FSA-12 will soon be available for many of our nation's air defense radar sites. 176-04

Progress Is Our Most Important Product

DEFENSE ELECTRONICS DIVISION
HEAVY MILITARY ELECTRONICS DEPARTMENT • SYRACUSE, NEW YORK

GENERAL ELECTRIC

IRE People

(Continued from page 40A)

receiving the B. A. degree in physics, and has done graduate work at the University of California and at UCLA.

❖

Ferdinand P. Diemer (S'46–A'49–M'55) of Los Angeles has been appointed vice president and director of engineering for the Defense Products Group of Daystrom, Incorporated, according to an announcement by Charles D. Manhart, group president.

F. P. DIEMER

Mr. Diemer will coordinate all engineering activities being carried on by the Defense Products Group's four divisions and will assist in organizing a systems development team for the Military Electronics Division at Archbald, Pa., in support of Daystrom's expanding defense program.

Mr. Diemer has devoted his entire professional career to electronics and defense systems. In joining Daystrom, he moves from the post of projects manager on the advance planning staff of the Hughes Aircraft Company's laboratories in Culver City, California.

Earlier he was director of engineering for Caltronics Corporation of Los Angeles. From 1954 to 1957 he was technical adviser to the president and manager of the Applied Physics Group of G. M. Giannini and Company, Pasadena.

A native of New York City, Mr. Diemer holds a bachelor's degree in electrical engineering from Cooper Union, New York, and a master's degree from New York University, N. Y. He has taken advance work towards his doctorate degree at New York University, Polytechnic Institute of Brooklyn, Massachusetts Institute of Technology, University of Southern California and the University of California at Los Angeles.

The new Daystrom executive spent two years in the Army and Signal Corps during World War II, serving in the European and Pacific theaters.

Mr. Diemer is a member of the American Institute of Electrical Engineers, Instrument Society of America, Industrial Mathematics Society, Society for Industrial and Applied Mathematics, Institute of Computing Machines and the Institute of Environmental Engineers.

❖

In a move designed to intensify and expand development work in several areas of electronics, Daystrom, Incorporated has named **Roswell W. Gilbert** (M'46–F'60) as director of corporate research.

R. W. GILBERT

Thomas Roy Jones, the firm's president, announced his promotion; for the last two years he has been vice president of research and development for Daystrom's Industrial Products Group, Newark.

In discussing the program, Mr. Gilbert reported that his group will concentrate on specific areas of intensified research in electrical measurements, semi-conductors, metallurgy, data systems and control systems. Its members will have the guidance and assistance of Daystrom's Technical Advisory Committee, which was named last fall. The committee is unique in industry. It is made up of five key professors or deans of engineering schools, who specialize in one or more areas that occupy the company's divisions.

After attending Lehigh University, Mr. Gilbert joined Weston Electrical Instruments Corporation, Newark, in 1934. He served as development engineer until 1938 when he became chief of the company's aircraft engineering division, a position that he held for four years. During th following four years, he directed Weston's Rockaway Valley Laboratory in Boonton and then became the company's director of Research. After Daystrom acquired Weston, he was made director of research and development for the Industrial Products Group.

He is a member of the American Insti-

(Continued on page 44A)

Testing insertion characteristics of X-band filter with Alfred Swept Generator. It consists of Alfred Microwave Oscillator and Alfred Microwave Leveler. This combination electronically sweeps frequency linearly with respect to time while maintaining RF power virtually constant across the band.

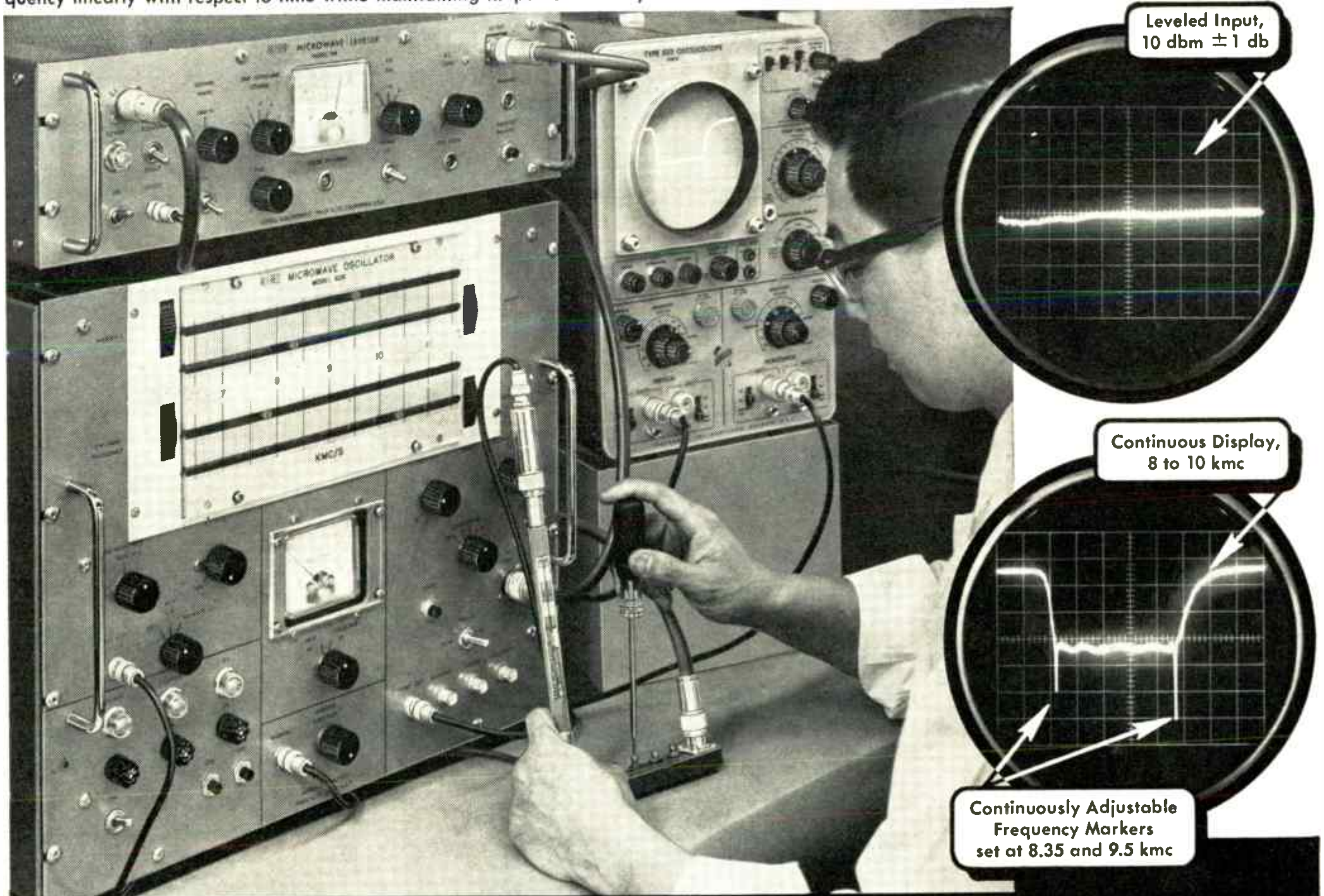

Save Test Time, Assure Test Accuracy

with ALFRED'S new SWEPT Microwave Generator..........

The scope patterns tell the story. Top pattern shows constant power input from Alfred Swept Generator to component (filter) under test. With known input, variation in output is due to filter characteristics. Lower pattern is especially significant, showing continuous, flicker-free display, 8 to 10 kmc. Any changes in stubs or irises are immediately reflected. Measurement accuracy is assured *at every frequency,* not just at selected points.

THIS TECHNIQUE CAN BE USED FOR MOST PRESENTLY KNOWN MICROWAVE TESTING APPLICATIONS. HERE'S WHY IT'S FASTER THAN CONVENTIONAL SIGNAL GENERATORS:

✱ *Continuous Display* allows immediate measurements—no plotting needed. Trace can be recorded if desired.

✱ *Sweep Technique* eliminates time-consuming "point-to-point" frequency and power setting methods of conventional signal generators. Sweep range is continuously adjustable with 1% accurate Direct Reading Slide Rule Dial.

✱ *"Quick Look Readout"* eliminates calculations in setting sweep range.

✱ *Adjustable Frequency Markers* allow rapid, broadband calibration of scope or recorder trace.

SOME MORE FACTS YOU SHOULD KNOW

✱ *Frequency Ranges.* The Swept Generator is available in five ranges to 12.4 kmc—1 to 2, 2 to 4, 4 to 8, 7 to 11, 8.2 to 12.4.

✱ *Stability.* At any single frequency, stability of the Swept Generator equals that of a conventional signal generator. Spurious modulation is low.

✱ *Power Output.* Greater than a signal generator: 10 milliwatts as compared to 1 milliwatt.

FUNCTION OF THE LEVELER It holds power output constant to ±1 db over standard frequency ranges, and better than ±1 db over narrower ranges. The Leveler serves as a broadband attenuator with up to 20 db dynamic range control, providing constant output over a wide range. It can be used as a general purpose instrument for a wide variety of oscillators and amplifiers.

For more details on the Alfred Swept Generator—please contact your Alfred sales engineering representative, or write direct.

Key specifications for Signal Generators available for coverage from 1 to 12.4 kmc

Frequency—Controls: Continuously adjustable with direct calibrated dial. Calibration accuracy: 1%. Stability: ±0.02%/hr. Residual FM: ±0.0025%. **Power Output** (Minimum): 10 mw ±1 db. Continuously adjustable from zero to maximum. **Attenuation Range:** Up to 20 db. **Sweep**—Selector: Recurrent Sweep, Single Sweep, Single Frequency, and External on panel switch. Time: 100 to .01 seconds, continuously adjustable. **Monitor Output**—Sweep Out: Positive linear sawtooth, 45 volts peak. Panel BNC connector. **Amplitude Modulation**—Internal Square Wave: RF output is alternately 0 and unmodulated CW value. Frequency 800 to 1200 cps, adjustable by panel control.

See us at Wescon, Booth 630

ALFRED ELECTRONICS
897 COMMERCIAL STREET
PALO ALTO, CALIFORNIA

7

IRE People

(Continued from page 42A)

tute of Electrical Engineers, Scientific Apparatus Makers Association and the American Association for the Advancement of Science.

❖

Richard W. Hodgson, president of Arnoux Corporation, West Los Angeles, designers and manufacturers of telemetry systems and other electronic products, has announced the appointment of **Dr. Donald J. Gimpel** (S'49–A'53–M'58) to the position of vice president in charge of engineering. Prior to this, Dr. Gimpel was director of engineering.

Dr. Gimpel, in this new position, will be directly responsible for all of Arnoux's research and development programs, including those being conducted by any of Arnoux's operating divisions, Astra Technical Instrument Corporation, Automation Electronics, Inc., and Astrometrics, Inc.

Prior to joining Arnoux in 1958, Dr. Gimpel was associated with Panellit, Inc., as the Director of the Computer Systems Department. Previous to this appointment, he was associated with Armour Research Foundation in research work involving analog, digital and other computer problems.

In 1956, he was awarded a prize for an outstanding contribution to industrial electronics. He is a member of AIEE, Tau Beta Pi, Eta Kappa Nu, Sigma Xi, American Rocket Society, American Ordnance Association, and other societies.

❖

William H. Gray (M'56) has recently been appointed manager of field operations for Silicon Transistor Corp., Carle Place, N. Y., manufacturers of medium and high power silicon transistors and silicon glass diodes. He will have his headquarters in Los Angeles, Calif., and will be responsible for national field operations. He will have responsibility for customer relations and field sales and engineering activity and will be working in close conjunction with STC's sales representatives on the West Coast as well as with those throughout the rest of the nation. He has just completed an intensive briefing on STC's over-all operation at its plant at Carle Place.

W. H. Gray

Mr. Gray received the B.S. degree in electrical engineering from Newark College of Engineering Newark N. J. In 1953 he joined Hughes Aircraft Co., Newark N. J. Division as sales engineer. He then moved through various positions until his appointment as sales manager two years ago. Prior to joining Hughes Aircraft he was employed by Bendix Aviation, Red Bank,

(Continued on page 46A)

IRE People

(*Continued from page 44A*)

N. J. in their marketing Division. Previous to that he was with I.B.M. as a customer engineer.

Mr. Gray is a member of the American Management Association, the American Institute of Management, and the Sales Executive Club of New York, N. Y.

❖

Appointment of a new director for its West Coast office, has been announced by the Crosley Division, Avco Corporation. He is **Maurice E. Heidbrink** (M'56) who succeeds Bert W. Marshall. Mr. Marshall recently was named West Coast Office Director for the Avco Corporation.

Prior to his association with Crosley, Mr. Heidbrink was western regional manager for the Government Electronics Division, Emerson Radio and Phonograph Corporation, a position he held from November, 1956 until his appointment with Crosley. Before joining Emerson, he was manager of West Coast operations for the Diamond Ordnance Fuze Laboratories for four years. From 1945 to 1952, he was manager of field operations for the Pacific Division, Bendix Aviation Corporation's Development Laboratories.

He is a native of Chatfield, Minnesota, and attended the University of Minnesota at Minneapolis. During his tour of duty with the U. S. Coast Guard, he attended the U. S. C. G. Service School at Groton, Connecticut. He is a member of the American Ordnance Association and the Instrument Society of America.

❖

Wilbur S. Hinman, Jr. (SM'54–F'57) has been awarded the Department of Defense Distinguished Civilian Service Award, the highest honor conferred on civilian employees by the Department of Defense. Technical Director of the Diamond Ordnance Fuze Laboratory, Department of the Army, Washington, D. C., he was presented the award for his scientific contributions in the use of radio-sonde for weather forecasting, the proximity fuze, and other military electronic advances, as well as his capable and enlightened leadership of the Laboratory.

❖

Jay H. Johnson (A'47–M'55), President of Erskine Precision Wire Corporation, has announced that the entire plant located in Emporium, Pa. will move all of its facilities to a new plant in Owensboro, Ky.

The company manufactures fine precision wire, round and flat wire parts for television, receiving, transmitting, and special purpose tubes, as well as other electronic devices. The move will be scheduled so that there will be no break in customer service. As soon as the move is completed, the company will maintain a New York City office.

❖

(*Continued on page 48A*)

Assure Reliability under Adverse Conditions...
in the Field and in your Plant

Typical field application of NF-105 in mobile Radio Interference Laboratory

SPECIFY EMPIRE'S COMPACT AND RUGGED
NOISE and FIELD INTENSITY METER
MODEL NF-105

- Measures 150 kilocycles to 1000 megacycles accurately and quickly with only one instrument.
- For measurements in accordance with Specifications: MIL-I-6181B, Class 1; MIL-S-10379A; MIL-I-11683B; MIL-I-11748B; MIL-I-12348A; MIL-I-13237; MIL-I-16910A; MIL-I-26600 (USAF), Category A; F.C.C. Specifications.
- Direct substitution measurements by means of broad-band impulse calibrator, without charts, assure repeatability.
- Economical...avoids duplication.
- True peak indication by direct meter reading or aural slideback.
- Four interchangeable plug-in tuning units, for extreme flexibility.
- Safeguards personnel...ALL antennas can be remotely located from the instrument without affecting performance.
- Self-calibrating, for reliability and speed of operation.
- Compact, built-in regulated "A" and "B" power supply, for stability.
- Minimum of maintenance required, proven by years of field experience.

DELIVERY FROM STOCK

The unique design of Model NF-105, with 4 plug-in tuning units, avoids costly repetition of circuitry and components common to all frequency ranges, at savings in size, weight and cost. Simple to operate, this instrument permits fast and accurate measurements of both broadband or CW signals. *Send for our Catalog*

Plan to attend our next seminar on interference instrumentation, details upon request.

edp

EMPIRE DEVICES PRODUCTS CORP.

AMSTERDAM, NEW YORK VICTOR 2-8400

MANUFACTURERS OF:

FIELD INTENSITY METERS • DISTORTION ANALYZERS • IMPULSE GENERATORS • COAXIAL ATTENUATORS • CRYSTAL MIXERS

IRE People

(Continued from page 46A)

Altec Lansing Corp. has announced the appointment of **William H. Johnson** (M'54) to manager of Engineering and Technical Information Dept.

W. H. Johnson

Prior to his transfer to the Altec Lansing plant in Anaheim, he was midwestern sales manager of the company with headquarters in Chicago, Ill. A graduate in electrical engineering from University of Wisconsin, Madison, in 1928 he worked as chief of communication engineering for Webster Electric Co. and was sound systems design consultant on special assignment with International Harvester.

❖

Armig G. Kandoian (S'35–A'36–SM'44–F'51) vice president of ITT Laboratories, has been named a vice president of ITT Federal Division.

He has been with ITT since 1935, following graduation from Harvard University with the B.S. and M.S. degrees in electrical communication engineering. He was named vice president and general manager of ITT Laboratories this year. Earlier, he was vice president-communication systems. Holder of more than 44 patents in the telecommunications field, Mr. Kandoian has served as chairman of the editorial board for *Reference Data for Radio Engineers*, a technical source book published by ITT.

❖

Walter A. Kirsch (SM'57) has joined Telechrome Manufacturing Corporation, Amityville, N. Y., as Defense Products Manager and Assistant to the vice president and director of sales, H. Charles Riker.

W. A. Kirsch

A sales engineer for the Servo Corporation of America for the past year, Mr. Kirsch previously was associated with Fairchild Camera and Instrument Company for three years as superintendent of electrical assembly and manufacture on the SAGE project.

Earlier, he spent a number of years in Research and Development with Bell Telephone Laboratories, Inc., Sylvania Electric Products, Inc., and other companies. He also served as plant manager for the Electronics and Instrument Co. and the New York Division of Allied Control Company.

Mr. Kirsch is a member of the Armed

(Continued on page 52A)

KCP SERIES

KT SERIES

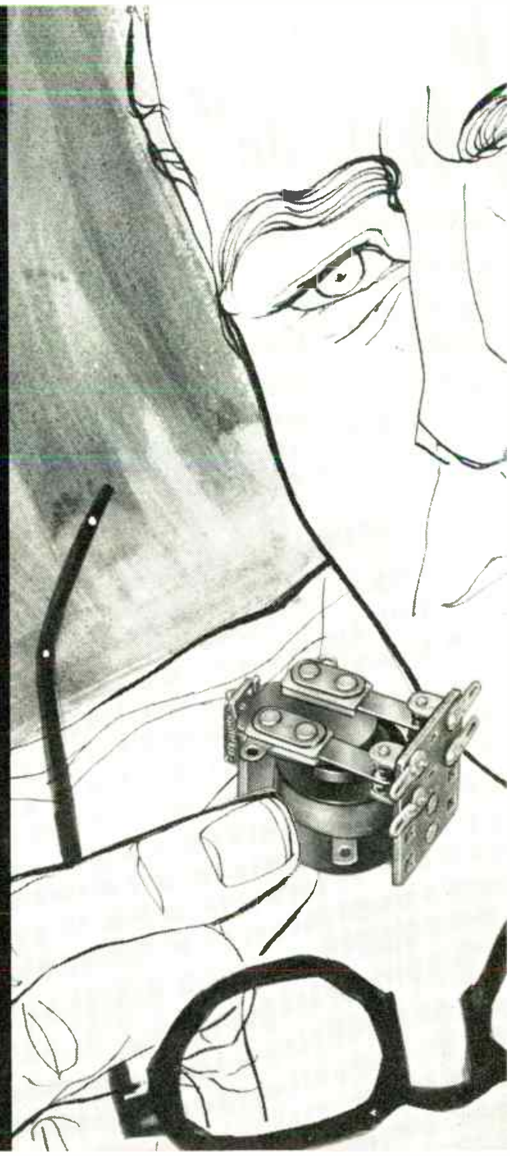

KR SERIES

three for dependability at low cost

MEET P&B's FAMILY OF "K SERIES" RELAYS

Here are only three of a large family of "K Series" relays by P&B. Blood brothers all, they are distinguished by fine craftsmanship and design maturity. Together they will handle a multitude of switching requirements.

Many design engineers find it saves time, saves money to integrate their circuits with *related* P&B relays. Makes sense, doesn't it?

KR—A small, lightweight relay used widely in communications and automation. Engineered for long life and dependability. 3PDT max. AC or DC. (See engineering data.)

KT—Designed for antenna switching. Capacitance: 0.5 mmfds between contacts. Terminal board is glass melamine and stack insulation is glass silicone for minimum RF losses to switch 300 ohm antenna line. 3 PDT max. AC or DC.

KC—Low cost plate circuit relay with sensitivity of 125 mw per pole. Factory adjusted to pull-in on specific current values. Available open, hermetically sealed or in clear plastic dust cover with standard octal-type plug. 3 PDT max. DC.

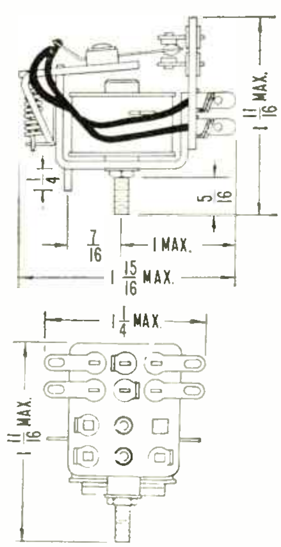

KR ENGINEERING DATA

GENERAL:
Breakdown Voltage: 500 volts rms minimum between all elements.

Temperature Range:
DC Coils—45°C to 85°C.
AC Coils—45°C to 70°C.

Terminals:
Pierced solder lugs standard. Octal 8 and 11 pin plug-in headers available.

Enclosures: Type K—Hermetically sealed. Type P clear cellulose acetate dust cover.

CONTACTS:
Arrangements: 3 Form C (3PDT) max.

Material: 1/8" dia. fine silver (gold plated). Other materials available to increase contact capacity.

Load: 5 amperes 115V 60 cycle resistive.

COILS:
Resistance: 16,500 ohms max. AC or DC.

Power: 1.1 watts minimum to 4 watts maximum for DC at 25°C ambient.

Duty: Continuous.
Insulation: Centrifically impregnated with insulating varnish.

P&B STANDARD RELAYS ARE AVAILABLE AT YOUR LOCAL ELECTRONIC PARTS DISTRIBUTOR

POTTER & BRUMFIELD

DIVISION OF AMERICAN MACHINE & FOUNDRY COMPANY, PRINCETON, INDIANA

IN CANADA: POTTER & BRUMFIELD CANADA LTD., GUELPH, ONTARIO

SELECT FROM INDUSTRY'S BROADEST LINE OF SILICON DIODES AND RECTIFIERS

HIGH CONDUCTANCE GENERAL PURPOSE SILICON DIODES

Type	Case Type	PIV	V_z	Min DC Fwd I @ 25°C ma @ 1v	Maximum LI_b @ 25°C μa	Maximum LI_b @ 100°C μa	P @ 25°C mw
1N645	N	225	275	400	0.2	15	600
1N645A	N	225	275	400	0.2 0.05@60v	15 10@125°C @ 60v	600
AF1N645	N	225	275	400	0.2	15	600
1N646	N	300	360	400	0.2	15	600
AF1N646	N	300	360	400	0.2	15	600
1N647	N	400	480	400	0.2	20	600
AF1N647	N	400	480	400	0.2	20	600
1N648	N	500	600	400	0.2	20	600
AF1N648	N	500	600	400	0.2	20	600
1N649	N	600	720	400	0.2	25	600
AF1N649	N	600	720	400	0.2	25	600

GENERAL PURPOSE SILICON DIODES

Type	Case Type	PIV	V_z	Min. DC Fwd I @ 25°C ma @ 1v	Maximum LI_b @ 25°C μa	Maximum LI_b @ 150°C μa	P @ 25°C mw
1N456	N	25	30	40	0.025	5	500
1N456A	N	25	30	100	0.025	5	500
1N457	N	60	70	20	0.025	5	500
1N457A	N	60	70	100	0.025	5	500
JAN 1N457	N	60	70	20	0.025	5	500
1N458	N	125	150	7	0.025	5	500
1N458A	N	125	150	100	0.025	5	500
JAN 1N458	N	125	150	7	0.025	5	500
1N459	N	175	200	3	0.025	5	500
1N459A	N	175	200	100	0.025	5	500
JAN 1N459	N	175	200	3	0.025	5	500
1N461	N	25	30	15	0.5	30	200
1N462	N	60	70	5	0.5	30	200
1N463	N	175	200	1	0.5	30	200
1N464	N	125	150	3	0.5	30	200
1N482	N	30	40	100*	0.25	30	500
1N482A	N	30	40	100	0.025	15	500
1N482B	N	30	40	100	0.025	5	500
1N483	N	60	80	100*	0.25	30	500
1N483A	N	60	80	100	0.025	15	500
1N483B	N	60	80	100	0.025	5	500
1N484	N	125	150	100*	0.25	30	500
1N484A	N	125	150	100	0.025	15	500
1N484B	N	125	150	100	0.025	5	500
1N485	N	175	200	100*	0.25	30	500
1N485A	N	175	200	100	0.025	15	500
1N485B	N	175	200	100	0.025	5	500
1N486	N	225	250	100*	0.25	50	500
1N486A	N	225	250	100	0.025	25	500
1N486B	N	225	250	100	0.05	10	500
1N487	N	300	330	100*	0.25	50	500
1N487A	N	300	330	100	0.025	25	500
1N488	N	380	420	100*	0.25	50	500
1N488A	N	380	420	100	0.025	25	500
600C	M	27	30	3	1 @ —10v	20 @ —10v**	150
601C	M	45	50	10	0.025@ —10v	40@ —10v	150
604C	M	4.7	5.5	60	0.1	40	150
606C	M	6.8	7.5	35	0.1	40	150
608C	M	10	11	25	0.1	40	150
610C	M	15	17	20	0.1	40	150
612C	M	22	25	20	0.1	40	150
614C	M	33	37	20	0.1	40	150
616C	M	47	52	10	0.2	40	150
618C	M	68	75	10	0.2	40	150
620C	M	100	110	10	0.2	40	150
622C	M	150	170	7	0.2	20**	150
624C	M	220	250	3	0.2	20**	150

* Measured at 1.1V
** At 100°C

GALLIUM ARSENIDE TUNNEL DIODES

Type	Case Type	I_P @ 25°C ma	I_P/I_V @ 25°C	Capacitance @ V_V @ 25°C μμf	V_F @ 25°C volts
1N650	U	10 (±10%)	> 15:1	30 (typ)	1.10 (±10%)
1N651	U	10 (± 2%)	> 10:1	30 (typ)	1.10 (± 5%)
1N652	U	5 (±10%)	> 5:1	40 (typ)	0.98 (±10%)
1N653	U	5 (±10%)	> 5:1	60 (typ)	0.98 (typ)

SILICON COMPUTER DIODES

Type	Case Type	PIV	V_z	Max. T_r @ 25°C μsec	Maximum LI_b @ PIV @ 25°C μa	Maximum LI_b @ PIV @ 100°C μa	Min Fwd Current @ 1 volt ma dc
1N625	N	20	30	1 †	1	30	4*
1N626	N	35	50	1 †	1	30	4*
1N627	N	75	100	1 †	1	30	4*
1N628	N	125	150	1 †	1	30	4*
1N629	N	175	200	1 †	1	30	4*
1N643	N	175	200	0.3**	0.025 @ 10v 1 @ 100v	10 @ 10v 15 @ 100v	10
1N658	N	50	120	0.3 ‡	0.05	25 @ 150°C	100
1N659	N	50	55	0.3 †	5	25	6
1N660	N	100	110	0.3 †	5	50	6
1N661	N	200	220	0.3 †	10	100	6
1N662	N	80	100	0.5 §	1 @ 10v 20 @ 50v	20 @ 10v 100 @ 50v	10
1N663	N	80	100	0.5**	5 @ 75v	50 @ 75v	100
1N914	N	75	100	0.0004#	5 @ 75 v 0.025 @ 20 v	50 @ 150°C @ 20v	10
1N916	N	75	100	0.0004#	5 @ 75v 0.025 @ 20v	50 @ 150°C @ 20v	10

* E_b equals 1.5v
† JAN 256 (30 ma forward, switched to —35 v reverse, recovery to 400 K ohms)
** JAN 256 (5 ma forward, switched to —40 v reverse, recovery to 200 K ohms)
‡ JAN 256 (5 ma forward, switched to —40 v reverse, recovery to 80 K ohms)
§ JAN 256 (5 ma forward, switched to —40 v reverse, recovery to 100 K ohms)
\# EGG Type 2236A (10 ma forward, switched to —6 volts reverse, recovery to 1 ma reverse)

HIGH VOLTAGE DIODE STACKS
(48 Standard Units)

Type	Case Type	PIV	V_F Max @ 250 ma @ + 25°C	Max Operating Freq. @ PIV (Sinusoidal)	Zener Min	Zener Max	No. of Diodes
1N2878 through 1N2925	GG	700	2	10 KC	800	1400	2
		6500	13	4.0 KC	7150	9100	13

VOLTAGE REGULATOR DIODES

Type	Case Type	Zener Voltage @ 25°C @ 5 ma I_z	Zener Voltage @ 25°C @ 20 ma I_z	Power Diss @ 25°C mw	Power Diss @ 150°C	Max. Z_z @ 25°C @ I_z Ohms	Typ Temp Coef %/°C
1N746†	N		3.3	400	100	28	—0.062
1N747†	N		3.6	400	100	24	—0.055
1N748†	N		3.9	400	100	23	—0.049
1N749†	N		4.3	400	100	22	—0.036
1N750†	N		4.7	400	100	19	—0.018
1N751†	N		5.1	400	100	17	—0.008
1N752†	N		5.6	400	100	11	+0.006
1N753†	N		6.2	400	100	7	+0.022
1N754†	N		6.8	400	100	5	+0.035
1N755†	N		7.5	400	100	6	+0.045
1N756†	N		8.2	400	100	8	+0.052
1N757†	N		9.1	400	100	10	+0.056
1N758†	N		10.0	400	100	17	+0.060
1N759†	N		12.0	400	100	30	+0.060
650C*	M	3.7 —4.5		150	40		
651C*	M	4.3 —5.4		150	40		
652C*	M	5.2 —6.4		150	40		
653C*	M	6.2 —8.0		150	40		
654C9*	M	8.5 —9.5		150	40		
655C9*	M	9.5 —10.5		150	40		

† Suffix A (±5% tolerance)
* (±5% or ±10% tolerance available)
Units 1N746 through 1N749 (A) meet Mil specification MIL-E-1/1258 (Navy) and are available with USN prefix.

most **advanced** line of diodes and rectifiers

silicon diodes and rectifiers

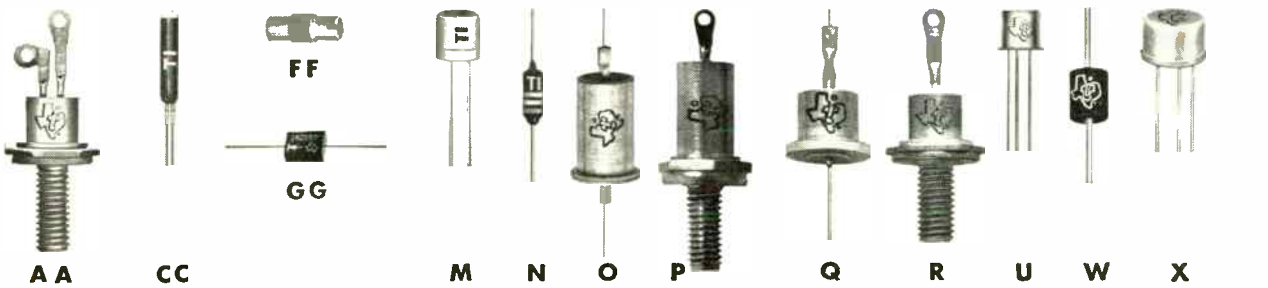

GALLIUM ARSENIDE VARACTOR

Type	Case Type	Min Breakdown Voltage—v	Junction Capacitance @ 0 volts bias $\mu\mu f$	Min Q @ 3 Kmc	Min Cut-off Frequency Kmc
XD-500	FF	−6	0.1 min 1.0 max	20 @ −2 volts 30 @ −6 volts	60 @ −2v

STABISTORS

Type	Case Type	I_F ma	PIV Volts	V_F Volts at 1 ma	V_F Volts at 100 ma	LI_b µa at −2v at 25°C
G 129	N	250	10	0.56±10%	1	0.1
G 130	N	150	6	0.64±10%	1	0.1

POWER REGULATORS AND DOUBLE ANODE CLIPPERS

Available with either anode or cathode to stud

Type	Case Type	Zener Voltage @ 25°C	I_z ma	Power Diss @ 50°C w	Reverse Current LI_b 25°C µa @ −5v	Reverse Current LI_b 25°C µa @ −10v	Max Z_z @ 25°C @ I_z Ohms	Typ Temp Coef %/°C
1N2498†	R	10	500	10	40	—	2	0.06
1N2499†	R	11	500	10	30	—	2	0.06
1N2500†	R	12	500	10	25	—	2	0.06
1N1816†	R	13	500	10	25	—	2	0.07
1N1817†	R	15	500	10	15	—	2	0.07
1N1818†	R	16	500	10	10	—	3	0.07
1N1819†	R	18	500	10	10	—	3	0.07
1N1820†	R	20	250	10	—	10	3	0.08
1N1821†	R	22	250	10	—	10	3	0.08
1N1822†	R	24	250	10	—	10	3	0.08
1N1823†	R	27	250	10	—	10	3	0.08
1N1824†	R	30	250	10	—	10	4	0.08
1N1825†	R	33	150	10	—	10	4	0.08
1N1826†	R	36	150	10	—	10	5	0.09
1N1827†	R	39	150	10	—	10	5	0.09
1N1828†	R	43	150	10	—	10	6	0.09
1N1829†	R	47	150	10	—	10	7	0.09
1N1830†	R	51	150	10	—	10	8	0.10
1N1831†	R	56	150	10	—	10	9	0.10
1N1832†	R	62	50	10	—	10	12	0.10
1N1833†	R	68	50	10	—	10	14	0.10
1N1834†	R	75	50	10	—	10	20	0.11
1N1835†	R	82	50	10	—	10	22	0.11
1N1836†	R	91	50	10	—	10	35	0.12
1N2008†	R	100	50	10	—	10	40	0.12
1N2009†	R	110	50	10	—	10	47	0.12
1N2010†	R	120	50	10	—	10	56	0.12
1N2011†	R	130	50	10	—	10	65	0.12
1N2012†	R	150	50	10	—	10	82	0.12

†Suffix A (± 5% Tolerance)

Units 1N1816 through 1N1836 (A & RA) meet Mil specification MIL-E-1/1259 (Navy) and are available with USN prefix.

SILICON RECTIFIERS—ECONOMY PACKAGE

Type	Case Type	PIV	I_o ma 25°C	I_o ma 100°C	Recurrent Peak Current @ 25°C a	DC Forward Voltage Drop @ 25°C v @ ma	Max Reverse Current @ 25°C µa @ v
1N2069	w	200	750	500	6	1.2 @ 500	10 @ 200
1N2070	w	400	750	500	6	1.2 @ 500	10 @ 400
1N2071	w	600	750	500	6	1.2 @ 500	10 @ 600

SILICON RECTIFIERS

Type	Case Type	Mounting	PIV v 25°C	PIV v 150°C	Io ma 25°C	Io ma 150°C	Recurrent Peak Current −65°C to +150°C ma	E_b @ 25°C v@a	LI_b @ PIV @ 25°C µa
1N588	O	Axial	1500	1000	25	10	150	10@10ma	50
1N589	D	Axial	1500	1000	50	25	250	8@50ma	50
1N1130	P	Cathode Stud	1500	1000	300	150	1 a	15@0.3	50
1N1131	P	Anode Stud	1500	1000	300	150	1 a	15@0.3	50
1N570	BB	plug in	1500	1000	37.5*	25*	1.2a@25°C*	10@50ma*	50
1N538	Q	Axial	200	200	750	250	2.5a@25°C	1@0.5	10
JAN 1N538	Q	Axial	200	200	750	250	2.5a@25°C	1@0.5	10
1N539	Q	Axial	300	300	750	250	2.5a@25°C	1@0.5	10
1N540	Q	Axial	400	400	750	250	2.5a@25°C	1@0.5	10
JAN 1N540	Q	Axial	400	400	750	250	2.5a@25°C	1@0.5	10
1N547	Q	Axial	600	600	750	250	2.5a@25°C	1@0.5	10
JAN 1N547	Q	Axial	600	600	750	250	2.5a@25°C	1@0.5	10
1N1095	Q	Axial	500	500	750	250	6a@25°C	1@0.5	10
1N1096	Q	Axial	600	600	750	250	6a@25°C	1@0.5	10
1N253†	R	Cathode Stud	100	100	3 a	1a@135°C	10a@50°C	1.1@1	10
JAN 1N253†	R	Cathode Stud	100	100	3 a	1a@135°C	10a@50°C	1.1@1	10
1N254†	R	Cathode Stud	200	200	3 a	0.4a@135°C	10a@50°C	1.1@1	10
JAN 1N254†	R	Cathode Stud	200	200	3 a	0.4a@135°C	10a@50°C	1.1@1	10
1N255†	R	Cathode Stud	400	200	3 a	0.4a@135°C	10a@50°C	1.1@1	10
JAN 1N255†	R	Cathode Stud	400	200	3 a	0.4a@135°C	10a@50°C	1.1@1	10
1N256†	R	Cathode Stud	600	200	3 a	0.2a@135°C	10a@50°C	1.1@1	10
JAN 1N256†	R	Cathode Stud	600	200	3 a	0.2a@135°C	10a@50°C	1.1@1	10
1N1124†	R	Cathode Stud	200	200	3 a	1 a	10a@50°C	1.1@1	10
1N1125†	R	Cathode Stud	300	300	3 a	1 a	10a@50°C	1.1@1	10
1N1126†	R	Cathode Stud	400	400	3 a	1 a	10a@50°C	1.1@1	10
1N1127†	R	Cathode Stud	500	500	3 a	1 a	10a@50°C	1.1@1	10
1N1128†	R	Cathode Stud	600	600	3 a	1 a	10a@50°C	1.1@1	10
1N1614†	R	Cathode Stud	200	200	15 a	5 a	50a@50°C	1.5@10	10
1N1615†	R	Cathode Stud	400	400	15 a	5 a	50a@50°C	1.5@10	10
1N1616†	R	Cathode Stud	600	600	15 a	5 a	50a@50°C	1.5@10	10

* For each half-wave section
† R Suffix denotes anode to stud configuration, i. e. 1N1124R

PHOTO DEVICE

Type	Case Type	Bias Voltage v max	Dark Current @ 25°C ±50v max µa	Dark Current @ 100°C ±50v max µa	*Typ Light Current @ 25°C @ ±10v µa	*Typ Sensitivity @ 10v µa/mw/cm²
1N2175	CC	50	0.5	100	200	22.3

* Light current measured in terms of radiation. Radiation = 9 mw/cm² in a frequency bandwidth of 0.7 to 1 micron.

SILICON CONTROLLED RECTIFIERS

Type	Case Type	At 80°C Case Temp: Av Rect Fwd Current Amps	At 80°C Case Temp: Recurrent Peak Current Amps	Non-Recurrent Surge Current 1 Cycle at 60 cps Amps	Min Fwd Off Voltage* v	PIV	Min Breakdown Voltage v	Max Case Temp °C	Max Fwd Gate Current ma	Gate to Cathode PIV v	max Fwd Voltage Drop @ Avg Rect. Fwd. Current @ 25°C Stud Temp v @ a	Gate Current Req to Fire ma Typ	Gate Current Req to Fire ma Max
2N1600	AA	3	10	25	50	50	60	150	100	5	2 @ 3 amps	1	10
2N1601	AA	3	10	25	100	100	120	150	100	5	2 @ 3 amps	1	10
2N1602	AA	3	10	25	200	200	240	150	100	5	2 @ 3 amps	1	10
2N1603	AA	3	10	25	300	300	360	150	100	5	2 @ 3 amps	1	10
2N1604	AA	3	10	25	400	400	480	150	100	5	2 @ 3 amps	1	10
2N1595	X	1	3	15	50	50	60	150	100	5	2 @ 1 amp	1	10
2N1596	X	1	3	15	100	100	120	150	100	5	2 @ 1 amp	1	10
2N1597	X	1	3	15	200	200	240	150	100	5	2 @ 1 amp	1	10
2N1598	X	1	3	15	300	300	360	150	100	5	2 @ 1 amp	1	10
2N1599	X	1	3	15	400	400	480	150	100	5	2 @ 1 amp	1	10
TI-010	X	1	3	15	50	50	60	150	100	5	See data sheet for switching information		
TI-025	X	1	3	15	50	50	60	150	100	5			
TI-050	X	1	3	15	50	50	60	150	100	5			

* Measured with 1K resistor gate to cathode

TEXAS INSTRUMENTS
INCORPORATED
SEMICONDUCTOR-COMPONENTS DIVISION
13500 N. CENTRAL EXPRESSWAY
POST OFFICE BOX 312
DALLAS, TEXAS

IRE People

(Continued from page 48A)

Forces Communications and Electronics Association and is a director of the New York Chapter.

❖

The appointment of **Victor Le Gendre** (M'53) as technical assistant to the division manager for the Electronic Tube Division of Allen B. Du Mont Laboratories, Inc. is announced by Joseph P. Gordon, general manager for the Division. Mr. Le Gendre will carry out special managerial assignments in research and production for industrial cathode-ray tubes, storage tubes, multiplier phototubes, and microwave tubes. His initial project will be the administration of an expansion program for direct-view storage tube production reporting to Dr. Albert E. Beckers, director of research and engineering, to fulfill mounting demand and sales of these Du Mont products.


V. LeGendre

Mr. Le Gendre comes to Du Mont from the post of chief engineer of storage cathode-ray tubes at the International Telephone and Telegraph Company, Components Division. He is a leading tube scientist and engineering administrator, having served as chief engineer of the Electronic Tube Division of Burroughs Corp prior to his position with IT&T. Previous posts were with Chatham Electronics, National Union Electric, Tung-Sol, and Western Electric.

Mr. Le Gendre has bachelors' degrees in Arts as well as Sciences and Philosophy and was a professor in Physics and Chemistry at Canadian colleges. He has been granted important electronic tube patents. During World War II he served as a captain in the Canadian Navy.

❖

Appointment of **Bertram Mintz** (M'57) as chief application engineer for the aircraft division of Hughes Tool Company, Culver City, Calif., has been announced by Rea E. Hopper, vice-president and general manager.

He most recently was with Marquardt Aircraft Company which he served for two and a-half years as eastern representative for research and development. His activities there covered application engineering in the fields of advanced propulsion, nuclear propulsion, advanced weapons systems and electronic support systems.

He previously served six years on the technical staff of the commanding general at Wright Air Development Center, and lectured for three years at Wittenberg College Extension School in mechanical engineering and industrial management.

(Continued on page 54A)

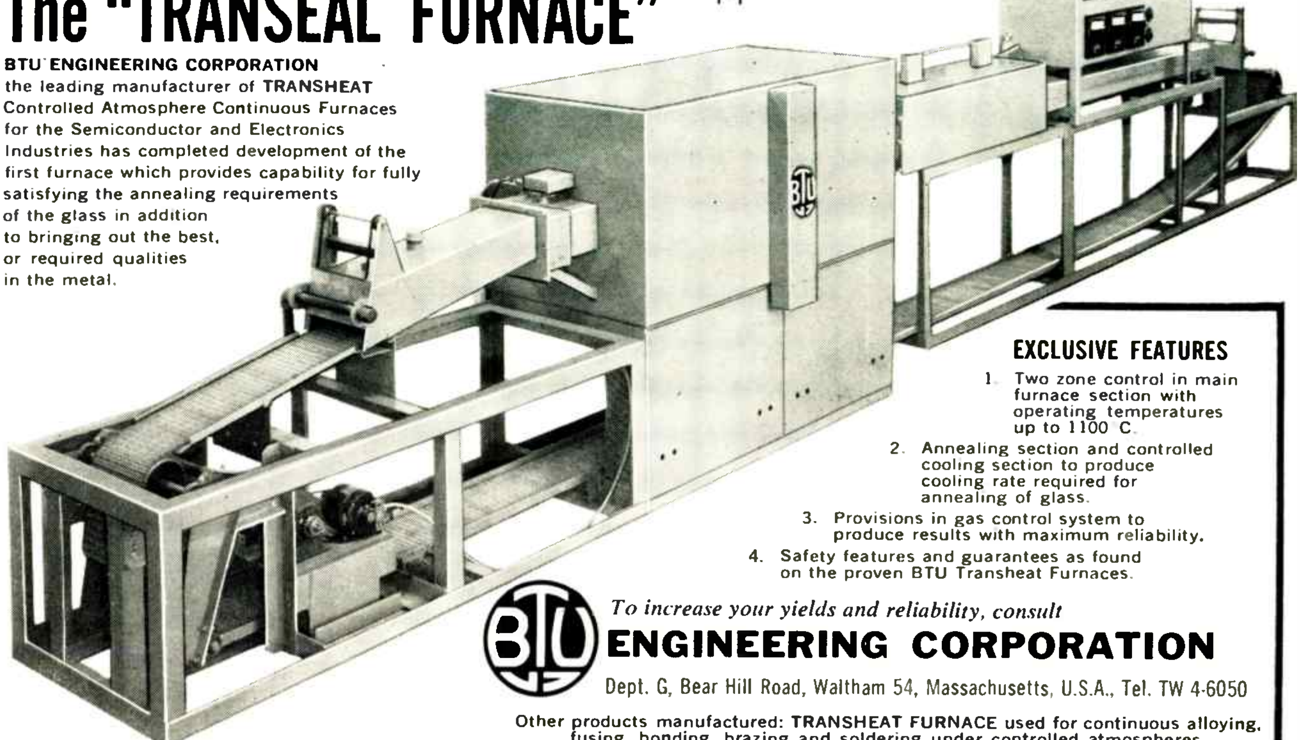

IRE People

(Continued from page 52A)

He holds B.S. and M.S. degrees in industrial engineering from Georgia Institute of Technology, and has performed graduate work in operations research and mathematics at Massachusetts Institute of Technology and in electronics at Ohio State University. He is a member of Alpha Pi Mu, Alpha Epsilon Pi and the American Rocket Society.

❖

On January 1, 1960, **N. A. Moerman** (M'46) assumed the presidency of Electronic Counters, Inc., an organization that, until recently, was an operating division of the Potter Instrument Company.

N. A. Moerman

He has been uniquely identified with the electronic counting technology for nearly twenty years. Graduating from the George Washington University with the B.S. degree in E.E., in 1938, he was appointed shortly thereafter by the Ballistic Research Laboratory of the Aberdeen Proving Grounds (Maryland) as its first electronic engineer.

Early in 1940 the General Engineering Laboratory of the General Electric Company completed a R&D program for the Proving Grounds resulting in the installation of the first Electronic Counter Chronograph, an innovation in the measurement field. As the government's engineer, Mr. Moerman was responsible for the maintenance and use of the equipment. He joined Potter Instrument Company after the War in late 1945.

Before assuming his present position, Mr. Moerman was for over ten years the Chief Engineer and a Vice President of the Potter Instrument Company.

❖

Dr. John J. Myers (S'43–A'45–M'47–SM'50) has been promoted by Hoffman Electronics Corporation to director of engineering of the company's Military Products Division in Los Angeles, Calif.

J. J. Myers

Since last August, he has been a senior scientist at the Hoffman Science Center in Santa Barbara, Calif., where he was responsible for studies in industrial electronics.

Previously he was a research assistant professor at the University of Illinois, Urbana. During 1956 and 1957 he was a member of the technical staff of the Electronics Division of Stewart-Warner Corporation, Chicago, Ill.

He also worked five years for Automatic Electric Company, Chicago, a subsidiary of General Telephone and Electronics Corporation. He was manager of microwave sales for Automatic Electric and later headed the electronics department of its Italian subsidiary in Milan.

Dr. Myers holds Ph.D. and M.S. degrees in electrical engineering from the University of Illinois and the B.S. degree in electrical engineering from Ohio State University. He is a member of Sigma Xi and Eta Kappa Nu, professional fraternities.

❖

The appointment of **Arthur P. Notthoff, Jr.** (S'45–A'49–M'55), to the position of Manager of Engineering of the Electronic Systems Division of Dalmo Victor Company has been announced by Vice President and Division Manager Glenn A. Walters.

In this position, Mr. Notthoff will be responsible for design engineering and management of all research and development projects for the Division.

For the past two years Mr. Notthoff has served as Manager of Servo Engineering in Dalmo Victor's Engineering Division. He joined the firm in 1949 as a research engineer after receiving the master's degree in electrical engineering from Massachusetts Institute of Technology, Cambridge. He completed his undergraduate work, also in electrical engineering, at the University of California, Berkeley.

❖

(Continued on page 56A)

Another New Acheivement from El-Menco

A New Smaller Size
Dipped Silvered
Mica Capacitor

El-Menco's
SUB-MINIATURE
DM-10
Mica Capacitor...

Approx. 5/16" long ...
1/4" wide ...
1/8" thick!
Smaller than a 1-carat diamond!

Sets New Standard in Miniature Reliability!

This sub-miniature DM-10 Mica Capacitor retains the same superior electrical characteristics of silvered mica capacitors as found in much larger sizes. It assures a high order of performance in extreme miniaturization applications — missiles, printed circuits and all compact electronic equipment. Parallel leads provide greater versatility. Tough phenolic casings protect against physical damage and penetration of moisture.

Capacity and Voltage Ranges

Working Voltage	Capacity Range
100 WVDC	1 MMF thru 360 MMF
300 WVDC	1 MMF thru 300 MMF
500 WVDC	1 MMF thru 250 MMF

Operating Temperature: *up to 150° C.*
Characteristics: *C, D, E and F, depending on capacitance value*
Leads: *#26 AWG (.0159") Copperweld wire*

EL-MENCO'S DM-10 MEETS ALL THE ELECTRICAL REQUIREMENTS OF MILITARY SPEC. #MIL-C-5B AND EIA SPECIFICATION RS-153

Other sizes also ideal for miniaturization applications —
DM-15 ... up to 820 mmf at 300 VDCW, up to 400 mmf at 500 VDCW.
DM-19 ... up to 5400 mmf at 300 VDCW, up to 4000 mmf at 500 VDCW.

WRITE FOR SAMPLES OF EL-MENCO DM-10 CAPACITORS and brochures describing El-Menco's complete line of capacitors.

EL-MENCO'S SUB-MIDGET DM-10 ... THE NEW SMALLER MINIATURE MICA CAPACITOR

El-Menco *Capacitors*

THE ELECTRO MOTIVE MFG. CO., INC.

Manufacturers of El-Menco Capacitors
WILLIMANTIC CONNECTICUT
• molded mica • dipped mica • mica trimmer • dipped paper
• tubular paper • ceramic • silvered mica films • ceramic discs

Arco Electronics, Inc., 64 White St., New York 13, N. Y.
Exclusive Supplier To Jobbers and Distributors in the U.S. and Canada

Improved Interference Filter Capacitors Have Excellent Environmental and Insertion Loss Characteristics

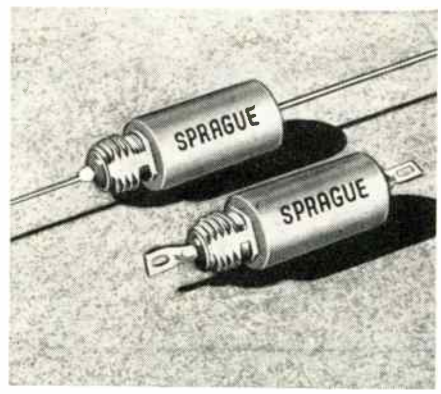

Recent technical data released by the Sprague Electric Company, North Adams, Massachusetts, reveals the unusual environmental and insertion loss characteristics of the company's subminiature Thru-Pass® Filter Capacitors. The performance of these capacitors is said to come closer to that of a theoretically ideal capacitor than any other type of paper capacitor ever made.

When properly installed, these capacitors reduce to a negligible value the effects of external cross coupling. They also provide a minimum length of path to ground for radio interference currents. Thru-Pass Capacitors are designed to meet all the electrical, mechanical, and environmental requirements of Military Specification MIL-C-11693.

Both Type 102P and Type 103P are impregnated with Vitamin Q, Sprague's exclusive inert synthetic impregnant, in order to achieve maximum insulation resistance and minimum capacitance change with temperature. Type 102P units are processed for −55 C to +85 C operation; Type 103P for −55 C to +125 C. Maximum feed-thru current for which both are rated is 5 amperes d-c continuous or equivalent.

For complete data on Thru-Pass Capacitors, write for Engineering Bulletin 8015 to Technical Literature Section, Sprague Electric Company, 235 Marshall Street, North Adams, Massachusetts.

IRE People

(*Continued from page 54A*)

Paul F. Pearce (S'49–A'52–M'57) has been appointed Manager, Systems Design, Information Technology Division, at Lockheed Electronics Company in Metuchen, N. J. He was formerly Manager of Project Engineering at the Lockheed Electronics and Avionics Division in Los Angeles, Calif., before that division's merger into the Lockheed Electronics Company. His group is concerned primarily with the research, design, and development of systems, including communications, navigation, air traffic control, and closed-circuit TV systems. Departments responsible for each of these systems have been established.

P. F. Pearce

He holds the B.S.E.E. and M.S.E.E. degrees from the Massachusetts Institute of Technology. He has taken additional graduate study in transistors and data processing at the University of California at Los Angeles, and in mathematical physics, mathematical statistics and information theory at the University of Southern California.

Previous to his position with Lockheed, he was head of strategic systems in the Communications Division of Hughes Aircraft from 1955 to 1959. He came to Hughes from Trans-Sonics, Inc., where he held the position of project engineer in the Research and Development Department. He also served as a research assistant at M.I.T.

Mr. Pearce is a member of Sigma Xi, and R.E.S.A.

❖

Victor L. Ronci (SM'51), former Director of Development of the Allentown Laboratory of Bell Telephone Laboratories, has been named Director of the Company's Pennsylvania Laboratories, effective June 1. In his new assignment, Mr. Ronci will be responsible for all development work on electron and semiconductor devices at both the Allentown and Laureldale, Pa., Laboratories.

V. L. Ronci

Mr. Ronci joined the Bell System in June, 1919 and had a wide variety of assignments until World War II, when he concentrated on the development of electron tubes for military applications. For his contribution to the war effort he received the Naval Ordnance Development

(*Continued on page 58A*)

PHILCO SILICON HIGH FREQUENCY TRANSISTORS

Philco SATs and SADTs have established the industry's greatest history of reliability in high frequency silicon transistors. They were the first of this type to be made available in production quantities and have been used extensively in thousands of critical military and commercial applications. Philco also has led the industry in the development of high-speed automatic production methods which have made possible a steady reduction of prices. This leadership in both reliability and low price results in the greatest performance per dollar in the high-frequency silicon field. For complete data, application information and prices on any of these silicon types, write Department IRE760.

SAT®... SILICON SURFACE ALLOY TRANSISTORS

	APPLICATIONS	FREQ. (MIN.)	SPECIAL PROPERTIES
2N495	Amplifier, Switch, Control	f_{max}-8 mc	V_{CE}=25v, TO-1 case
2N496	Switch	f_T-7.2 mc	very low V saturation, TO-1 case
2N1118	Amplifier, Switch, Control	f_{max}-8 mc	electrical equivalent of 2N495, TO-5 case
2N1118A	Amplifier, Switch, Control	f_{max}-8 mc	high beta version 2N1118
2N1119	Switch	f_T-7.2 mc	electrical equivalent of 2N496, TO-5 case
2N1428	Amplifier, Switch, Control	f_{max}-18 mc	low cost, high beta, TO-1 case
2N1429	Amplifier, Switch, Control	f_{max}-18 mc	low cost, high beta, TO-5 case

SADT®... SILICON SURFACE ALLOY DIFFUSED-BASE TRANSISTORS

(All TO-9 cases)

	APPLICATIONS	FREQ. (MIN.)	SPECIAL PROPERTIES
2N1199	Switch	f_T-75 mc	superior temperature stability
2N1267	Med. Frequency Amplifier	f_{max}-43 mc	low beta (video amplifier)
2N1268	Med. Frequency Amplifier	f_{max}-43 mc	medium beta
2N1269	Med. Frequency Amplifier	f_{max}-43 mc	high beta
2N1270	High Frequency Amplifier	f_{max}-125 mc	low beta (video amplifier)
2N1271	High Frequency Amplifier	f_{max}-125 mc	medium beta
2N1272	High Frequency Amplifier	f_{max}-125 mc	high beta
2N1472	Switch	f_T-75 mc	very low V saturation superior temperature stability
2N1663	Switch	f_T-100 mc	superior temp. stability . . . high beta

Immediately available in quantities 1-999 from your local Philco Industrial Semiconductor Distributor

PHILCO®

Famous for Quality the World Over

LANSDALE DIVISION • LANSDALE, PENNSYLVANIA

TRANSISTOR CENTER U.S.A.

IRE People

(*Continued from page 56A*)

Award in 1945. He holds more than 98 patents for his inventions in the electron tube and semiconductor device fields.

He is a member of the Semiconductor Device Council of the Joint Electron Device Engineering Councils.

❖

Francis M. Ryan (J'14–A'17–M'26–F'40), former head of the Radio Section of the Headquarters Organization of the American Telephone and Telegraph Co., has been elected Vice President and Director of Engineering at Page Communications Engineers, Inc.

F. M. Ryan

Announcement of Mr. Ryan's appointment was made by E. C. Page, President of the Washington-based firm which has planned and built advanced communications systems in more than 30 countries of the world. Mr. Ryan, who joined Page in March after 40 years with the Bell Telephone System, will be responsible for the engineering of the firm's world-wide projects.

From 1944 to 1960, Mr. Ryan was responsible for advising the Bell System Operating Organizations in the use of both domestic and overseas radio facilities. During this period the System undertook extensive use of microwave facilities for long distance telephone and television, and Mr. Ryan played an important part in shaping this program.

Assigned to the Bell Telephone Labs during World War II, he was in charge of a group developing underwater sound echo-ranging equipments for the U. S. Navy. He has represented the Bell System at a number of international conferences and most recently was a member of the U. S. Delegations to the Administrative Radio and Plenipotentiary Conferences held last year in Geneva.

An Engineering graduate of the University of Washington, Mr. Ryan is a Registered Professional Engineer in New York State. He is a Fellow of the AIEE.

❖

Herbert H. Schenck (SM'51), until recently Vice President and Director of Engineering at Page Communications Engineers, Inc., has been named Executive Vice President and General Manager of the newly-formed United States Underseas Cable Corporation.

H. H. Schenck

The new company, jointly organized by Phelps Dodge, Northrop, Page, and Felten and Guilleaume of West Germany, has been formed to provide one of the world's largest facilities for the design and construction of long distance underwater cable systems. Mr. Schenck's 24 years of experience in communications management and engineering embraces all phases of system planning, implementation and operation in the United States and in such diverse areas as Cuba, Brazil, the Philippines and Japan.

For seven years he was managing Director of the International Radio Company of Brazil, a subsidiary of International Telephone and Telegraph Corporation, and concurrently Vice President and Director of Standard Electric, an ITT manufacturing subsidiary, and a Director of the National Telephone Company of Brazil and the American Chamber of Commerce there. He spent several years with ITT's Havana subsidiaries, Radio Corporation of Cuba and Cuban Telephone Company, and as Vice President and General Plant Manager of the latter firm, he participated in the inauguration of the Florida-Cuba repeatered submarine telephone cable system, the prototype of the first North Atlantic System.

While serving as a Signal Officer with the U. S. Army from 1941 to 1946, his assignments included duty with GHQ Southwest Pacific Area involving the planning of wire and carrier systems in Australia and New Guinea and the supervision of Southwest Pacific Area radio operations in New Guinea, the Philippines and Japan. He left

(*Continued on page 60A*)

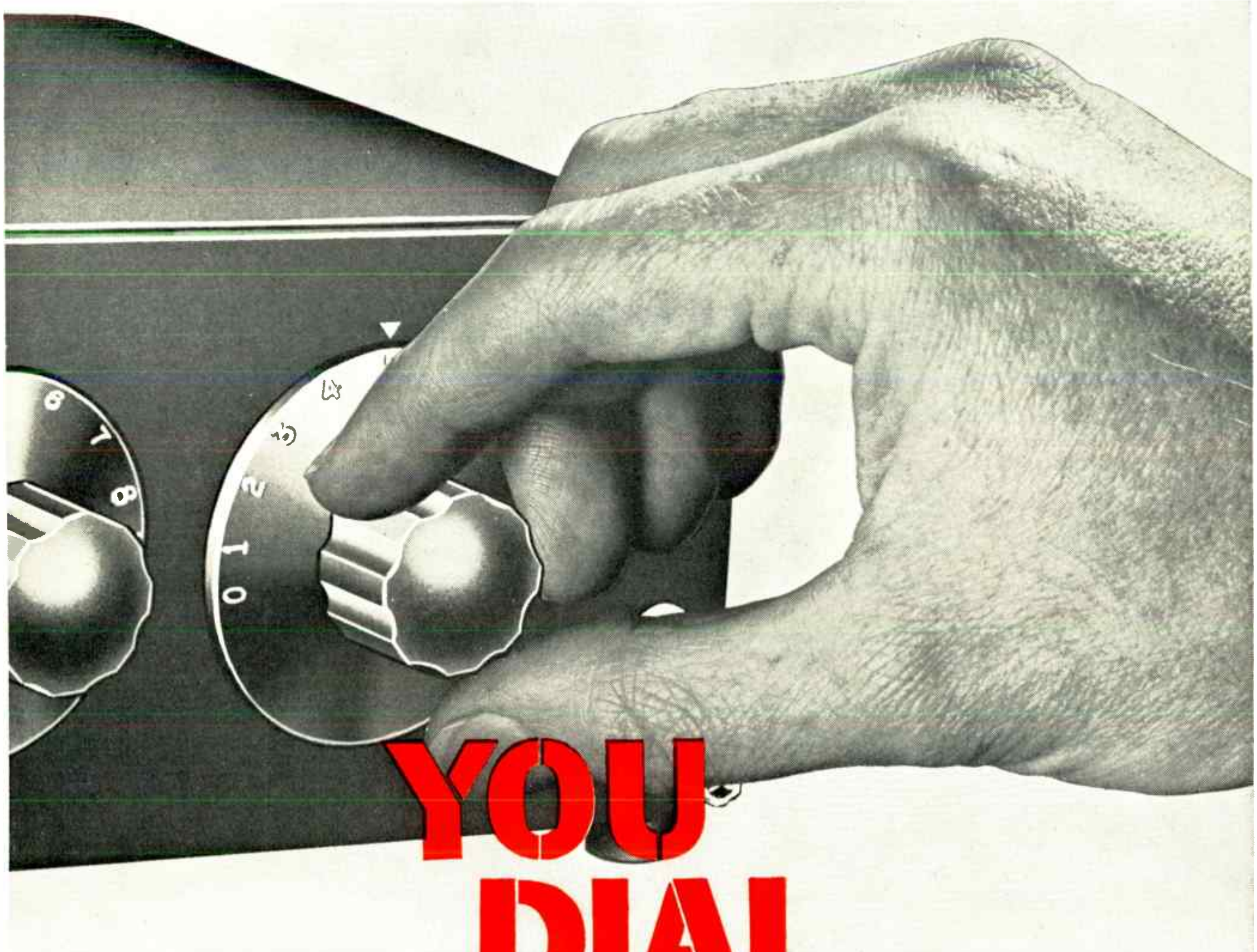

YOU DIAL THE DELAY TIME

with the New ESC **Direct Readout Variable Decade Delay Line**

Now you can make your own rapid selection of desired delay with the new Direct Readout Variable Decade Delay Line — the newest product developed and manufactured by ESC, America's leading manufacturer of custom-built and stock delay lines! Increments of 1/1,000 of the total delay may be selected by the turn of a dial. And there are three models:

Model 101 — a total delay of 9.99 usec.
Model 102 — a total delay of 99.9 usec.
Model 103 — a total delay of 999 usec.

There is a constant impedance of 1,000 ohms between input and output terminals for any delay increment. Delay/rise time ratio at maximum delay is 33:1. The ESC Direct Readout Variable Decade Delay Line is a passive delay network and will not introduce noise or jitter. Mechanical and electrical modifications available on special order.

ESC

WRITE TODAY FOR COMPLETE TECHNICAL DATA.

exceptional employment opportunities for engineers experienced in computer components... excellent profit-sharing plan.

ELECTRONICS CORP. 534 Bergen Boulevard, Palisades Park, New Jersey

Distributed constant delay lines • Lumped-constant delay lines • Variable delay networks • Continuously variable delay lines • Step variable delay lines • Shift registers • Video transformers • Filters of all types • Pulse-forming networks • Miniature plug-in encapsulated circuit assemblies

IRE People

(Continued from page 58A)

the service with the Legion of Merit and five battle stars.

Prior to military service, he was a transmission engineer with Southern Bell Telephone and Telegraph Company, and a communications and electronics engineer for the Tennessee Electric Power Company.

Mr. Schenck has the B.S. degree in electrical engineering from the University of Tennessee. He is a member of the American Institute of Electrical Engineers.

❖

Frederick J. Seufert (S'49–A'50–SM'57) has been promoted to director of the Systems Department in the Military Products Division of Hoffman Electronics Corporation, Los Angeles, Calif. The new Systems Department will include the Tall Tom and 480-L projects.

F. J. Seufert

With Hoffman since 1955, he is a former section manager and, most recently, has been assistant to the director of engineering.

He previously was with the Santa Barbara Research Center, Hughes Aircraft Co. and the Brookhaven National Laboratory.

He received the B.S. degree in electrical engineering from Rutgers University and the M.S. degree from the University of California at Los Angeles.

He is a member of Phi Beta Kappa and the Institute of Aeronautical Sciences.

❖

Appointment of **Dr. James E. Shepherd** (A'36–SM'44–F'48) as manager of the Sperry Rand Research Center, to be built this year in Sudbury, Mass., was announced today by the New York Corporation.

J. E. Shepherd

Dr. Shepherd, with a 25-year background in physics and electronics, was formerly manager of the electronic tube division, Sperry Gyroscope Company, at Great Neck, N. Y., where he directed research, development and production of microwave devices for radars and communications systems.

He joined Sperry in 1941 after six years on the science faculty at Harvard University and became heavily engaged in a wide range of scientific activities involving both highly theoretical and experimental

(Continued on page 62A)

Tung-Sol/Chatham CROWBAR Thyratrons

PROTECT HIGH-POWER CIRCUITS AGAINST DESTRUCTIVE ARCS

Any one of a host of causes can trigger internal arcs in high-power tubes with little or no warning . . . even if the tubes are well designed, operate in well-engineered circuits, and have conservative demands placed upon them. Cosmic rays, line-voltage transients, parasitic oscillations, spurious primary and secondary electrons and material whiskers are just a few of the potential sources of these highly destructive arcs.

But by engineering Tung-Sol/Chatham high reliability crowbar hydrogen thyratrons into your design, you can safeguard against costly arc-generated breakdowns. By short-circuiting destructive currents, these zero bias "arc-busters" extinguish the arcs before circuit elements can be damaged.

Instantaneous response and the ability to carry extremely large currents make these rugged thyratrons ideally suited for this purpose. Moreover, they are able to conduct these heavy surge currents even after having been idle for long periods. Each tube contains a hydrogen reservoir which promotes long life and permits optimum gas pressure adjustment for various operating conditions. Write for full technical details. Tung-Sol Electric Inc., Newark 4, N. J. TWX: NK193

Technical assistance is available through the following sales offices: Atlanta, Ga.; Columbus, Ohio; Culver City, Calif.; Dallas, Texas; Denver, Colo.; Detroit, Mich.; Irvington, N. J.; Melrose Park, Ill.; Newark, N. J.; Philadelphia, Pa.; Seattle, Wash. Canada: Toronto, Ont.

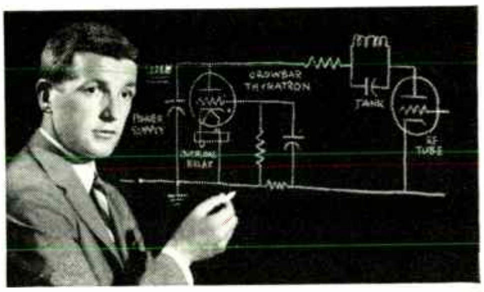

Typical application: *A crowbar thyratron is connected in series with a suitable impedance across the filter of the high voltage power supply for a high frequency amplifier tube. Whenever an arc occurs in the power tube, the rising current is used to deliver a suitable signal to the grid of the thyratron. The thyratron immediately conducts to short circuit the power supply, until the protective circuit breaker opens 0.1 second later.*

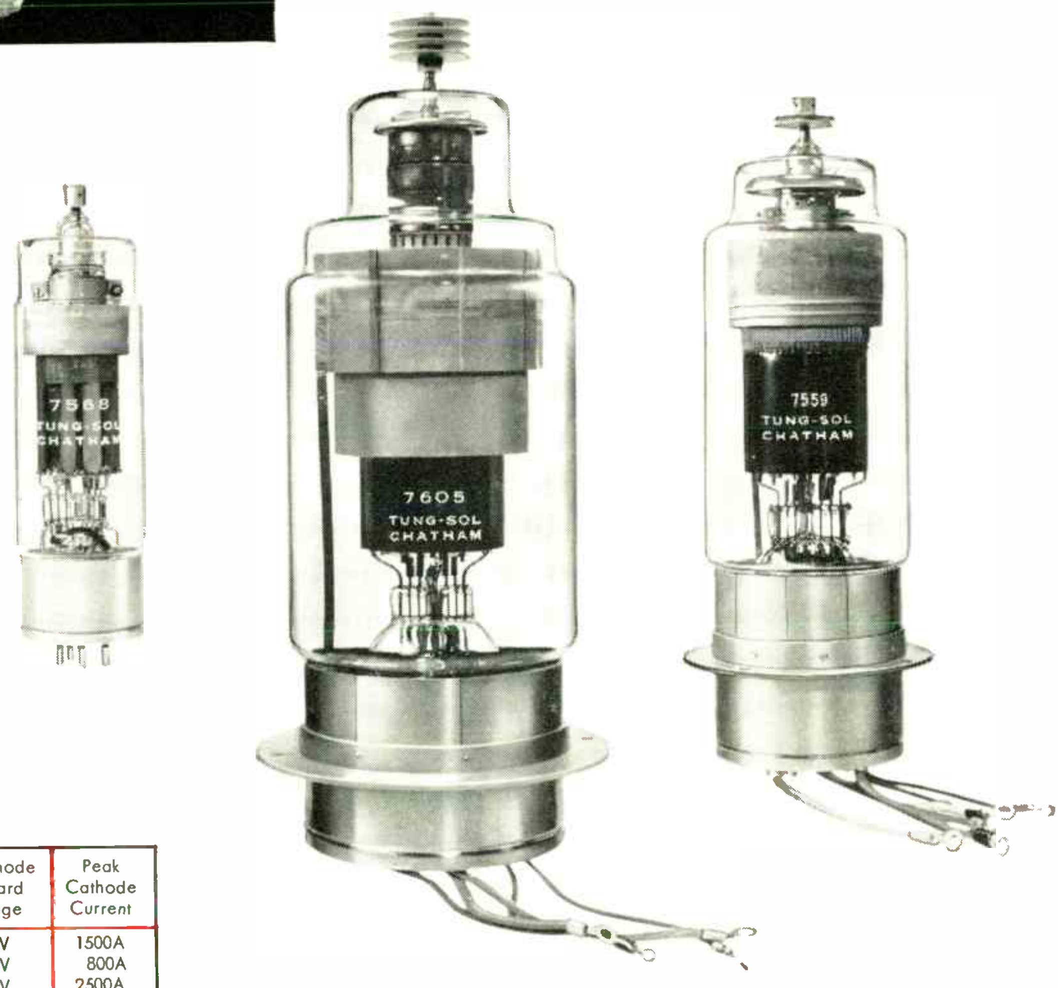

Type	DC. Anode Forward Voltage	Peak Cathode Current
7559	18KV	1500A
7568	25KV	800A
7605	25KV	2500A

TUNG-SOL®

IRE People

(Continued from page 60A)

work. Under his supervision rapid advances were achieved in both research and engineering which led to large scale production of advanced radar systems and microwave devices of all types.

The Sperry scientist received the B.A. degree in 1932 and the M.A. in physics and electrical engineering in 1933 at the University of Missouri, Columbia. At Harvard he earned the M.S. degree in 1935 and a Doctor of Science degree in 1940, both in communications engineering.

Dr. Shepherd holds 15 radar and electronic patents. He holds membership in Tau Beta Pi, Phi Beta Kappa, Eta Kappa Nu, Sigma Xi, and American Institute of Electrical Engineers.

❖

Dr. Sergei A. Schelkunoff (A'40–F'44), has been appointed professor of Electrical Engineering at Columbia University.

The appointment has been announced by Professor Ralph J. Schwarz, chairman of the Department of Electrical Engineering of the Columbia School of Engineering, who said that Dr. Schelkunoff will assume his duties at the University September 15. He has been an adjunct professor of Electrical Engineering at Columbia since 1958.

Dr. Schelkunoff was born in Russia, January 27, 1897. He received the Bachelor's degree from State College of Washington, Pullman, Wash., where he was awarded the Master's degree in mathematics in 1923. Columbia awarded him the Ph.D. degree in mathematics in 1928. He served in the engineering department of Western Electric Company in 1923–25, and in 1925–26 was a member of the technical staff of Bell Telephone Laboratories, Inc.

In 1926 27 he was an instructor in mathematics at State College, and served as an assistant professor of mathematics there from 1927 to 1929.

He returned to Bell Telephone Laboratories in 1929 as a member of the technical staff and became assistant director of mathematical research February 1, 1956. Since September 1, 1958, he has been assistant vice president of Bell Laboratories, at Murray Hill, N. J. He is the author of several scientific books and numerous scientific articles and papers.

Dr. Schelkunoff received the Liebmann Prize of the IRE in 1942 for mathematical contributions to the electromagnetic theory. In 1949 he was awarded the Ballantine Medal of the Franklin Institute for "outstanding research in communication and reconnaissance."

❖

Dr. Eric A. Walker (M'47), president of the Pennsylvania State University, University Park, is the new president of the American Society for Engineering Education. He will serve for the year beginning in July, 1960.

(Continued on page 64A)

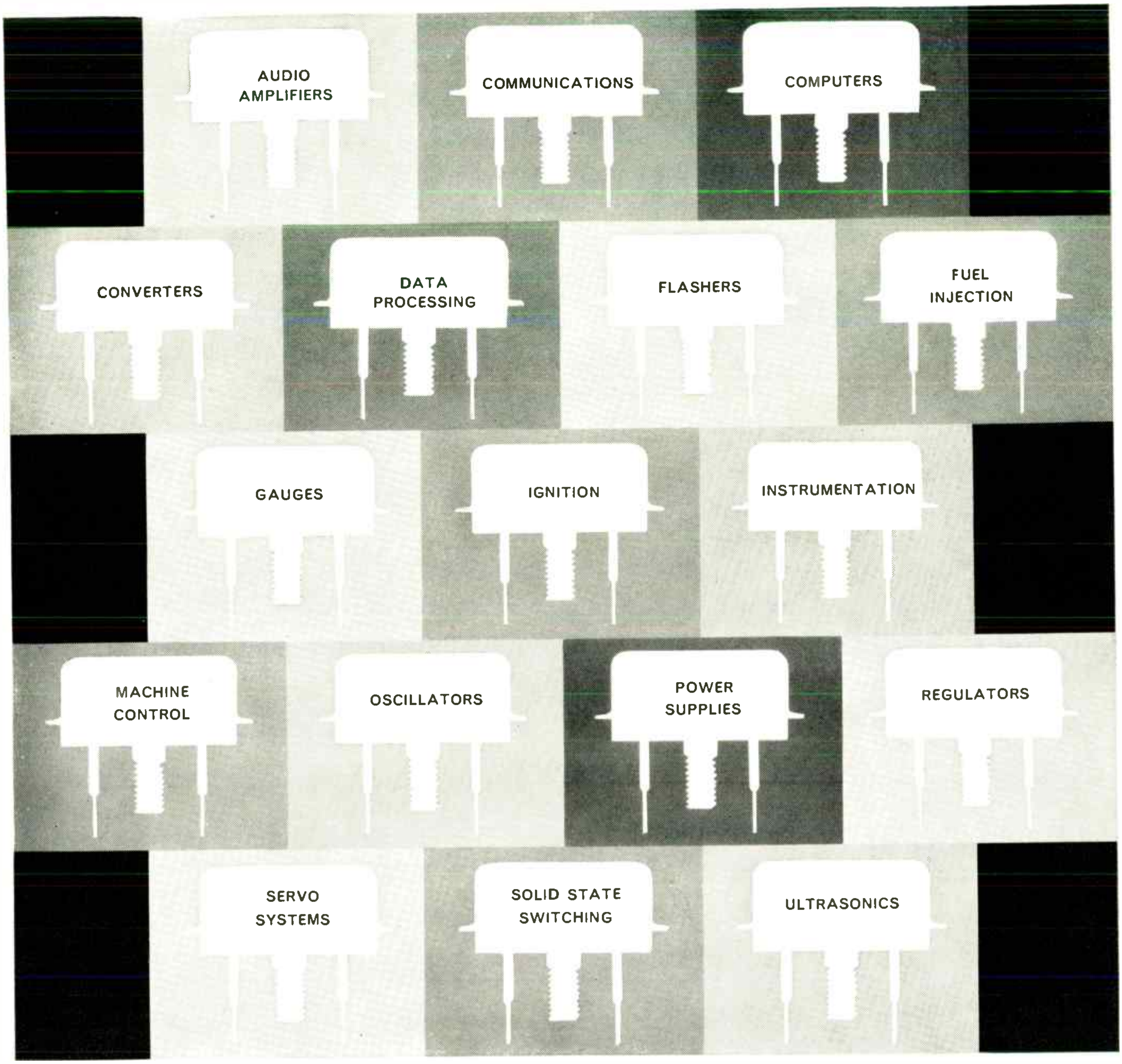

ONE TRANSISTOR— HUNDREDS OF USES

DELCO RADIO'S VERSATILE 2N174 For top performance in a wide, wide range of applications, depend on Delco Radio's 2N174. ■ This multi-purpose PNP germanium transistor is designed for general use with 28-volt power supplies, and for use with 12-volt power supplies where high reliability is desired despite the presence of voltage transients. ■ It has a high maximum emitter current of 15 amperes, a maximum collector diode rating of 80 volts and a thermal resistance below .8°C per watt. The maximum power dissipation at 71°C mounting base temperature is 30 watts. Low saturation resistance gives high efficiency in switching operations. ■ The 2N174 is versatile, rugged, reliable, stable and low priced. For more details or applications assistance on the 2N174 or other highly reliable Delco transistors, contact your nearest Delco Radio sales office.

DELCO RADIO

Dependability Reliability

Newark, New Jersey
1180 Raymond Boulevard
Tel.: Mitchell 2-6165

Santa Monica, California
726 Santa Monica Boulevard
Tel.: Exbrook 3-1465

Chicago, Illinois
5750 West 51st Street
Tel.: Portsmouth 7-3500

Detroit, Michigan
57 Harper Avenue
Tel.: Trinity 3-6560

Division of General Motors • Kokomo, Indiana

IRE People

(Continued from page 62A)

The selection was the result of a national mail balloting by the 9,300 members of the ASEE, the national professional organization of college and university teachers of engineers.

Dr. Walker has been a vice president of the Society and a member of its General Council and has been especially concerned with recent Society studies of engineering teaching. He came to Pennsylvania State University in 1945 after service at Tufts University, the University of Connecticut, and Harvard. He has been president of Penn State since 1956. An electrical engineer, he was executive secretary of the Department of Defense Research and Development Board in 1950–51 and is a consultant to many government agencies.

❖

Wilson R. Smith (M'46) has been named chief engineer, semiconductors, for CBS Electronics, manufacturing division of Columbia Broadcasting System, Inc., in an announcement by Robert G. Marchisio, vice-president and general manager of semiconductor operations. He will be responsible for development, pilot-line, and product engineering activities.

W. R. Smith

He joined CBS Electronics in 1958 as an engineering specialist, and was recently elevated to manager of engineering. He was graduated from Reed College with a degree in physics, and received the M.S.E.E. degree from Pennsylvania State College, where he was an assistant professor of electrical engineering from 1946 to 1951. From 1942 to 1946 he was a staff member of the M.I.T. Radiation Laboratory.

In 1951 he joined Hughes Aircraft Company as an engineering group leader. From 1953 to 1958, he was employed by Sylvania Electric Products, Inc., as an engineering specialist, product supervisor, and section head.

Mr. Smith is a member of Eta Kappa Nu.

❖

Astronautics, Inc. announced this week, through its Executive Committee, the appointment of **George W. Soderquist** (SM'59) as the President of the Corporation. Long associated with the AFMTC Range Contractor at Patrick Air Force Base, he is also a member of the Executive Committee and Board of Directors of the electronics firm.

As President, he will be the Chief Executive Officer and will direct the over-all business operations of the corporation.

(Continued on page 66A)

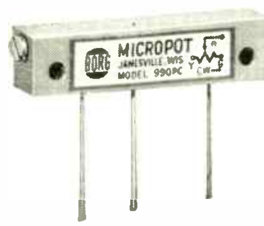

The size of things to come . . .

The advantages gained by miniaturization are numerous. Each segment of American industry, whether military or commercial, lists many such advantages. We hear a great deal of smaller missile packages, smaller payloads, smaller and lighter ground-support equipment . . . defense measures that are extremely important for military advantages today . . . for commercial advantages tomorrow. But what of the advantages of miniaturization we do not hear so much about . . . the advantages that are not front-page news? What of smaller, portable computers that will ease the burdens of paper work? What of shrinking automation equipment that will perform more reliably for and be available more economically to industry? What of the countless other designs on the drawing boards or in prototype form that will multiply in their efforts to reduce bottlenecks long a problem to productivity? If you are one of the many who are working on such projects, then you are also concerned with the availability of smaller, more reliable components such as Borg 990 and 991 Series Micropots (actual size above). These miniature potentiometers match, balance and adjust circuit variables in all sorts of electronic equipment. May we send you complete data? Ask for catalog sheets BED-A133 and BED-A134. Borg Equipment Division, Amphenol-Borg Electronics Corporation, 120 So. Main St., Janesville, Wisconsin.

BORG

Micropot Potentiometers • Turns-Counting Microdials • Sub-Fractional Horsepower Motors • Frequency and Time Standards

IRE People

(Continued from page 64A)

He received the B.S. degree from Alabama Polytechnic Institute, has been engaged in electronics research, development, and application engineering for approximately 10 years, and has held progressively responsible engineering and managerial positions in the missile instrumentation field since the inception of the Government's missile programs, and in military electronics prior to World War II. His most recent position prior to the formation of Astronautics, Inc. was in supervision of frequency control and analysis, underwater sound, and antenna design engineering activities at the Atlantic Missile Range.

❖

Appointment of **Philip A. Toll** (A'56) to the new position of director of building services for Sperry Gyroscope Company was announced by Edward M. Brown, vice president for administration.

P. A. Toll

Mr. Toll, formerly director of data processing, will be responsible for construction, plant engineering and other services at more than ten Sperry plant facilities. He joined Sperry in 1951 and served in various manufacturing posts.

In 1955 he was appointed manager of data processing and directed installation and operation of the company's central data processing facilities including the UNIVAC I and II large-scale electronic computers and a new UNIVAC high-speed, solid-state computer at the Sperry headquarters plant in Great Neck, L. I.

Mr. Toll received a degree in business administration at the University of Michigan, Ann Arbor, in 1951. He is also a graduate of the American Institute of Foreign Trade. His professional memberships include Institute of Management Sciences, Association for Computing Machinery, American Ordnance Association and the Delta Phi Epsilon professional fraternity.

A native of Detroit, Mr. Toll lives in Lloyd Harbor, L. I.

❖

Robert L. Trent (M'45–SM'57) has been appointed manager of the newly formed design engineering department by Fairchild Semiconductor Corporation, a wholly owned subsidiary of Fairchild Camera & Instrument Corporation, Syosset, L. I., N. Y.

R. L. Trent

In this capacity Trent will be responsible for engineering, instrumentation, tool design and tool fabrication.

A graduate of the Columbia School of Engineering, Trent received the BS and MS in Electrical Engineering (E.E.) in 1941 and 1946, respectively. He was at Bell Telephone Labs as a member of the Technical Staff from 1941 to 1957 doing systems development, transistor applications and transistor development. He comes to Fairchild from Texas Instruments where he has been since 1957, most recently as Manager, Germanium Development.

Fairchild Semiconductor Corporation is a manufacturer of high speed silicon transistors and diodes.

❖

Appointment of **John R. Whitford** (S'41–A'45–M'56) as manager of Sperry Gyroscope Company's Electronic Tube Division was announced by Arthur R. Weckel, Sperry vice president.

J. R. Whitford

Mr. Whitford joined Sperry in 1949 as a project engineer for microwave instruments and components and later advanced through a series of sales positions. During World War II, he served as a captain, U. S. Army Signal Corps, in the Pacific Theatre.

(Continued on page 70A)

ELECTRON TUBE NEWS
...from SYLVANIA

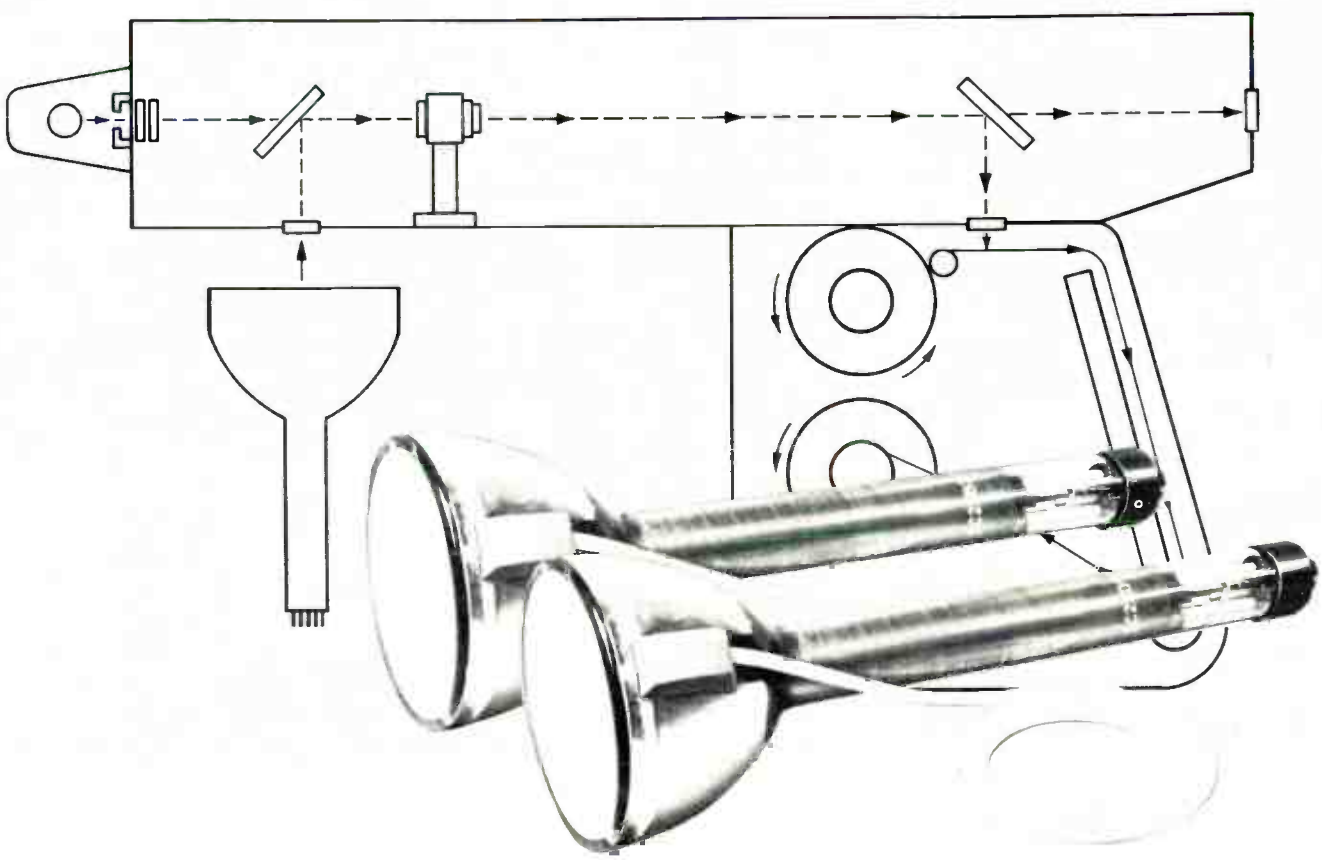

• HIGH RESOLUTION
• SIMPLIFIED CIRCUITRY
• IMAGE BRILLIANCE

with 2 new Sylvania C.R.T.'s for photo-recording applications

Sylvania SC-2809, SC-2782 utilize precision guns, fine grain P11 phosphor, aluminized screens, clear nonbrowning optical faceplates. Result: remarkably high resolution and excellent brilliance. SC-2809 has a line width of .0008", a resolution of 6000 lines. SC-2782 has a .001" line width and a 3000-line resolution. Both tube types feature conventional magnetic focusing and deflection, simple beam-centering magnets, no ion traps. They simplify external circuitry requirements, offer potential savings in equipment costs. Minimum useful screen area is 4¼". Deflection angle is 50°. Use of an integral encapsulated high-voltage connector minimizes possibility of corona at high altitudes. Screens other than P11 are available if desired. For further information and complete technical data, contact the Sylvania Field Office nearest you.

KEY CHARACTERISTICS	SC-2809	SC-2782
Anode Voltage	25,000 Volts dc*	25,000 Volts dc*
Anode Current (E_{G1}=0)	3 μA dc*	
Grid No. 2 Voltage	2,500 Volts dc*	2,500 Volts dc*
Grid No. 2 Current (E_{G1}=0)	2,000 μA dc*	
Screen Current	2 μA dc	5 μA dc
Line Width	0.0008"	0.001"
Face Diameter	5"	5"
Over-all Length	16⅜"	16"

*Absolute Max. Ratings

NEW SYLVANIA C.R.T.'s FEATURE

LOW HEATER POWER HIGH RELIABILITY "COOL" OPERATION

for battery-powered, portable 'scope applications

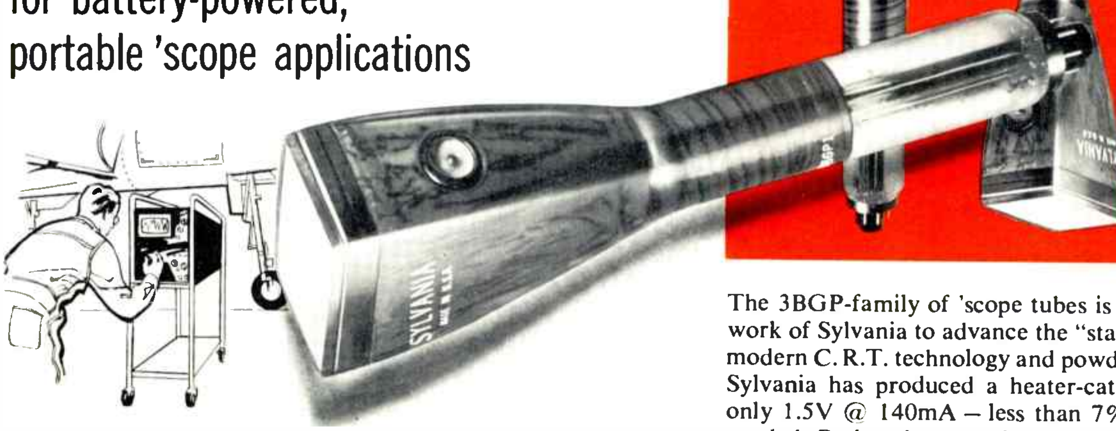

Sylvania 3BGP1, 3BGP2, 3BGP7, 3BGP11 . . . feature direct-view rectangular faces, electrostatic deflection and focus, high deflection sensitivity.

KEY CHARACTERISTICS	
Anode No. 2 Voltage	2,750 Volts dc*
Anode No. 2 Input	6 Watts*
Anode No. 1 Voltage (Focusing Electrode)	1,100 Volts dc*
Heater Ratings	1.5V/140mA
Line Width (Light output of 20 ft. Lamberts)	0.026"
Face Dimension	1½" x 3¾"
Useful Screen Area	1⅛" x 2¾"
Over-all Length	9¼"
*Absolute Max. Ratings	

The 3BGP-family of 'scope tubes is typical of the continuing work of Sylvania to advance the "state of the art." Combining modern C.R.T. technology and powder metallurgy techniques, Sylvania has produced a heater-cathode assembly requiring only 1.5V @ 140mA – less than 7% of the power normally needed. Reduced power demands result in much lower tube operating temperatures and low drain from battery or flyback heater supply. The heater-assembly has a relatively low mass which makes it virtually impervious to vibration of portable equipment. Clear, pressed faceplates are utilized for improved glass quality, greater uniformity of thickness resulting in minimized distortion. Complete information and technical data can be obtained from your local Sylvania Field Office.

The new Sylvania low power heater-cathode assembly holds vast promise for picture tubes for portable, battery-operated TV receivers. This concept is currently under investigation at Sylvania. Your inquiry is welcome.

4 NEW "BONDED SHIELD" TV PICTURE TUBES

all available with new reflection-diffusing, treated caps

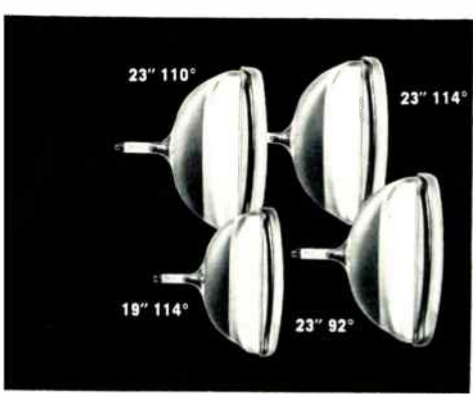

Sylvania continues its leadership in "Bonded Shield" picture tubes with an expanded line to help you meet the demand for squared-corner TV. Now, you can offer *broad-angle* and *low-reflection* viewing with the specially treated laminated cap. The treated surface of the tube cap can diffuse up to 70% of reflected light without appreciable loss in resolution—eliminating the old problem of mirror images.

Bonded Shield eliminates front-of-the-cabinet safety glass • Reduces front-to-back cabinet dimensions • Reduces danger of implosion • Reduces production-line rejects significantly • Offers squared-corner screen • Simplifies mounting with integral mounting lugs • Offers potential savings in set manufacture.

Sylvania pioneered the quantity production techniques of bonding cover panels to the face of a picture tube. These same techniques hold exciting possibilities for application in industrial and military cathode ray tubes. You may have a C.R.T. application that can benefit from Sylvania Bonded Shield "know-how." Sylvania Engineers will be pleased to work with you.

If your industrial or military design demands specialized Cathode Ray Tubes, call on the creative experience and production capabilities of Sylvania. Electronic Tubes Division, Sylvania Electric Products Inc., 1740 Broadway, New York 19, New York.

SYLVANIA

Subsidiary of **GENERAL TELEPHONE & ELECTRONICS**

IRE People

(Continued from page 66A)

He received the B.S. degree in electrical engineering from Northeastern University, Boston, in 1943, and the M.S. degree in electrical engineering from Massachusetts Institute of Technology in 1949. His professional memberships include the U. S. Army Association, Armed Forces Communications and Electronics Association and the Tau Beta Pi honorary fraternity.

❖

Pioneer Electronics Corporation, manufacturer of television picture tubes and special purpose tubes, announces the appointment of **Richard Zeh** (SM'57) as plant superintendent.

R. Zeh

Mr. Zeh moves to Pioneer Electronics from Hughes Aircraft, where he served as general superintendent of their Microwave Tube Department. Prior to that he was associated with Sylvania Electric Products, Inc. as an engineering section head.

Mr. Zeh received his training at Rensselaer Polytechnic Institute in Troy, New York and University of Southern California, Berkeley.

The addition of Mr. Zeh to Pioneer's staff is another step forward in its present program to broaden its production and development of cathode-ray tubes and related products.

❖

Dr. Louis Zitelli (S'47–A'51–M'56) has been named Manager, Klystron Development at Varian Associates, according to Dr. Richard Nelson, Manager, Research and Development, Palo Alto Tube Division.

Dr. Zitelli, who joined Varian in 1950 as a research engineer, will be responsible for advanced development of all Varian klystrons in his new post.

He received the B.S. degree from San Jose State College, and the M.S., E.E., and Ph.D. degrees from Stanford University.

A radar and electronics officer for the U. S. Navy during World War II, he received technical training at Columbia University, Harvard University, and Massachusetts Institute of Technology. He was a research assistant at Stanford's Electronics Research Laboratory for four years before joining Varian.

As Manager, Klystron Development, he takes over the post formerly held by Dr. Richard Nelson, who was recently appointed to his new position as head of Varian's Tube Division research and development at Palo Alto.

Dr. Zitelli is a member of Sigma Xi.

❖

Two new engineering advisory committees comprised of men from many parts of the country who are eminent in that field, have been appointed in the College of Engineering, University of Rochester, it was announced at a dinner meeting of the Corporate Relations Committee of the University's Board of Trustees.

Dr. John W. Graham Jr., dean of the College of Engineering, was the principal speaker, outlining the College's objectives and expanding programs of service. The meeting was designed to be of particular interest to Rochester-area business and industry.

The new committees are in mechanical and electrical engineering. Another committee, the Advisory Committee on Chemical Engineering, has been in existence for some years.

The Electrical Engineering Advisory Committee is composed of:

Dr. Howard S. Coleman, vice-president in charge of research and engineering, Bausch and Lomb Optical Co., Rochester; John S. Coleman, executive secretary, Division of Physical Sciences, National Academy of Sciences, National Research Council, Washington, D. C.; **Dr. Mervin J. Kelly** (M'25–F'38), research management consultant, New York City; **Dr. Ronald McFarlan** (SM'51), president, Institute of Radio Engineers, Chestnut Hills, Mass.; **Dr. George L. Haller** (A'28–M'36–SM'43–F'50), vice-president General Electric Company, Syracuse, N. Y., and **Dr. Royal Weller** (SM'57), vice-president for engineering, Stromberg Carlson Company, Rochester.

EIMAC CERAMIC TUBES DESIGNED FOR SPACE WITH RUGGED NEW 26.5 VOLT HEATERS

Three extremely sturdy Eimac ceramic tetrodes have been specially designed for missile telemetry and airborne military communication systems—with rugged new 26.5 volt heaters.

In actual missile systems and current key projects, these tubes have passed severe tests with flying colors. And have dramatically proved that they *can take it!*

For your space age needs, investigate the many advantages of these pioneering Eimac tubes: the X578G, X578H and X578J. Write for complete information.

EITEL-McCULLOUGH, INC.
San Carlos, California

GENERAL CHARACTERISTICS EIMAC 26.5 VOLT CERAMIC TUBES

Tube	Eimac Tube With Similar Characteristics	Length	Diameter	Frequency for Max. Ratings	Max. Plate-Diss. Rating	Heater Voltage
X578G	4CX300A	2.5"	1.65"	500 mc	300 watts	26.5
X578H	4CX125C	2.5"	1.25"	500 mc	125 watts	26.5
X578J	4CN15A	2.5"	0.9"	500 mc	15* watts	26.5

*A nominal rating. May be increased by employing a suitable heat sink or liquid immersion.

Industrial Engineering Notes*

Association Activities

The world of three-dimensional radio sound moved closer to reality with announcement by the Electronic Industries Association of target dates for installing and field-testing stereophonic radio broadcasting equipment. The announcement was made by J. D. Secrest, EIA Executive Vice President. Memorial Day, May 30, is equipment moving day. Testing is to begin the week of Sunday, June 5. The tests will start under the aegis of the Electronic Industries Association. They will be under the supervision of the Association's National Stereophonic Radio Committee and will constitute the committee's first official field-testing of stereo radio equipment on behalf of broadcasters, equipment manufacturers, and the Federal Communications Commission. The test broadcasts will be FM stereo, but will be compatible with present monophonic FM receivers. A number of receiver manufacturers are beginning experimentally to produce stereo sets. In addition, radio technicians may find it possible to adapt, for stereo reception, monophonic FM sets. So far as is now known, the only three-dimensional radio sound being transmitted by commercial stations is by simultaneous use of AM and FM transmitters. This means that the listener now has to tune an AM receiver to the Station's AM transmitter and an FM receiver to the FM transmitter. The National Stereophonic Radio Committee, to date, has selected one test site. This is a Pittsburgh FM station. Call letters of the station are among the most famous in the broadcast world. Millions will remember the magic sound of KDKA, Pittsburgh, Pa. The committee tentatively has selected two additional sites for the FM stereo system being studied. These are WCRB-FM and WBZ-FM. Both are in Boston, Mass. In direct charge of field-testing FM stereo are three subcommittees of Panel Five of the EIA National Stereophonic Radio Committee. The panel chairman is A. Prose Walker, Engineering Manager of the National Association of Broadcasters. Panel subcommittees bear the engineering designation of 5.1, 5.2, and 5.3. They are under the supervision of: A. C. Goodnow, Westinghouse Broadcasting Co., Chairman of Subcommittee 5.1 on Transmitting and Receiving Facilities; and R. L. Kaye, WCRB, Boston, Vice Chairman; W. J. Wintringham, Bell Telephone Laboratories, Chairman of Subcommittee 5.2 on Specifications and Measurements; R. N. Harmon, Westinghouse Broadcasting Co., and Daniel Recklinhausen, the H. H. Scott Co., Co-chairmen. Dr. M. R. Schroeder, Bell Telephone Laboratories, is in charge of preparing a test tape for qualitative, subjective evaluation of stereophonic broadcasting. . . . **Climaxing the 36th annual convention of EIA at the Pick-Congress Hotel in Chicago, L. Berkley Davis, Vice President of General Electric Company and General Manager of its Electronic Components Division, was elected President for 1960–61 following presentation of the EIA Medal of Honor to retiring President David R. Hull for his many contributions to the advancement of the electronics industry.** Eight new Directors, two new Vice Presidents, and three new Division Chairmen also were elected during the three-day industry conference. The eight new Directors elected by their respective Divisions are: *Consumer Products*—Chris J. Witting, Vice President of Westinghouse Electric Corp. *Military Products*—David F. Sanders, President, Lockheed Electronics Co. *Tube & Semiconductor*—Mark Shepherd, Jr., Vice Pres., Texas Instruments Inc. *Parts*—Allen W. Dawson, Mgr., Electronic Components Dept., Corning Glass Works, Allen K. Shenk, Vice Pres., Marketing, Erie Resistor Corp., and Walter W. Slocum, President, International Resistance Co. *Industrial Electronics*—Ben Adler, President, Adler Electronics, Inc. and Howard C. Briggs, Collins Radio Company. The two new Vice Presidents are William S. Parsons, President of Centralab Division of Globe-Union, Inc., representing the Parts Division, and Ben Adler, President of Adler Electronics, Inc., representing the Industrial Electronics Division. New Division Chairmen are: Edward R. Taylor, Executive Vice President, Consumer Products Division, Motorola Inc., Consumer Products Division; L. L. Waite, Senior Vice President, Engineering and Planning, North American Aviation, Inc., Military Products Division; and W. Myron Owen, President of Aerovox Corporation, Parts Division. . . . **The 1960 edition of the EIA Fact Book describes an electronics industry more than three and one-half times larger than it was at the beginning of the last decade.** The book attributes the industry's 10 years of lively growth to the "ever widening versatility of electronic techniques. The extensive range of tasks electronics can perform makes possible its application in every basic industrial and commercial activity. It has become the common denominator of weapons for defense. It continues to be an important increment of the consumer market, bringing more entertainment and labor-saving devices into the American home." The 1960 Fact Book, prepared and pub-

(*Continued on page 74A*)

* The data on which these NOTES are based were selected by permission from *Weekly Report* issues of April 4, 18, 25 and May 2, 16, and 23, 1960, published by the Electronic Industries Association, whose helpfulness is gratefully acknowledged.

For PROJECT MERCURY

Dresser-Ideco puts wings on tower construction ...completes 48 towers in 52 days!

Field assembly test of one of 48 antenna towers for the Man-In-Orbit program. This Dresser-Ideco contract included transmitting, receiving and boresight designs.

Space-age urgency set the pace for Dresser-Ideco in fulfilling its 48-tower contract for the National Aeronautics and Space Administration's Project Mercury. With the last of the complete shipment under way via exclusive truck and "special" train, the company had dispatched an average of one tower every nine working hours and shaved 12 days off the accelerated schedule! Soon these structures will be serving in a far flung instrumentation system, lifelining our astronauts' first venture into space.

Fabricating 560,000 pounds of precision antenna support components on a tight delivery schedule is typical of Dresser-Ideco's ability to assume unusual responsibilities. Outstanding structural facilities, and the knowledge and man-power to make them hum, have established Dresser-Ideco as a major source for antenna towers and antenna structures.

Find out how Dresser-Ideco can best serve *your* program. Consultation and cost estimates on structural requirements are available at no obligation.

Write for booklet: "Facilities for Defense Production." Dresser-Ideco Company, A Division of Dresser Industries, Inc., 875 Michigan Avenue, Columbus 15, Ohio.

DRESSER-IDECO COMPANY

DRESSER IDECO®

DRESSER INDUSTRIES INC.

ELECTRONIC • INDUSTRIAL
OIL • GAS • CHEMICAL

Industrial Engineering Notes

(Continued from page 72A)

lished by the EIA Marketing Data Department, will be mailed to all EIA member companies this week. Price to nonmembers and the general public is 75 cents. The publication, the sixth of an annual series, contains summary data of all statistical reports published by the Marketing Data Department and provides member companies—as well as libraries, schools, universities, research organizations and other institutions—with the most comprehensive review of the electronics industry available. The new edition is considerably expanded over previous ones, according to Executive Vice President James D. Secrest. A new feature is brief sketches of important historical, technological and market developments. The elusive industrial and military markets are described in greater detail than before, and estimated sales to major segments within these markets are provided.

Engineering

A summary index describing 1,400 research projects conducted by the Air Force Air Research and Development Command has been released to industry through the Office of Technical Services, U. S. Department of Commerce. Most of the scientific research projects described in the 342-page index are being conducted at leading U. S. colleges and universities. Other projects are the work of industrial laboratories, Government facilities, and private nonprofit research institutions. All work is listed under 24 subject categories which cover six technical program areas: electronics, propulsion, materials, geophysics, biosciences and aeromechanics. The publication is *Basic Research Resumes—A Survey of Basic Research Activities in the Air Research and Development Command*, Herner and Co., for ARDC, USAF, 342 pp. December 1959, (Order PB 161291 from OTS, U. S. Department of Commerce, Washington 25, D. C., $5.)

Industrial Marketing Data

Japan's monthly production of transistors reached 7,200,000 during December of last year, a total which, according to an article in a Japanese trade magazine, made that country "the world's top transistor-producing nation." The article said December production exceeded that in the United States by 1,700,000 units. Japanese output during December 1958 totaled one million transistors, according to the magazine. It attributed what it called the "transistor boom" to the increasing popularity of transistor radios. Sixty per cent of all Japanese transistors are manufactured by two firms, the magazine said. One, the Nippon Electric Co., ships 70 per cent of its output to the United States, according to the article. The other, Tokyo

(Continued on page 76A)

WHICH BENDIX TRANSISTOR IS BEST FOR THE JOB?

TYPICAL OPERATION AND MAXIMUM RATINGS OF BENDIX GERMANIUM PNP TRANSISTORS

Type Number	PRIMARY APPLICATIONS: Audio	Push-Pull	Switch	Power Supply	MAXIMUM RATINGS: Collector Voltage Vce (a)	Collector Current Ic	Thermal Resistance (b)	Junction Temp. Tj	TYPICAL OPERATION: Current Gain hFE —	Current Gain Ic Adc	Circuit Gain db	Power Output W
High Power Transistors (g)												
2N155	X				30 Vcb	3 Adc	3° C/W	85°C	40 (c)	0.5	33	2
2N176	X				40 Vcb	3	—	90	45 (c)	0.5	35	2
2N234A	X				30	3	2	90	25 (c)	0.5	30	2
2N235A, B	X				40	3	2	90	40, 60 (c)	0.5	33, 36	2
2N236A, B	X			X	40	3	2	95	40, 60 (c)	0.75	33, 36	4
2N242	X				45 Vcb	2	3	100	—	—	35	1
2N255	X	X			15 Vcb	3	3	85	40	0.5	22	1
2N256	X	X			30 Vcb	3	3	85	40	0.5	25	2
2N257	X				40	—	—	85	55 (c)	0.5	35	1
2N268, A	X		X		80 Vcb	—	—	85, 90	—, 40	—, 2.0	31, —	1, —
2N285A	X			X	40	3	2	95	150 (c)	0.5	40	2
2N297			X		60 Vcb	5	2	95	70	0.5	—	50 (d)
2N301, A	X				40, 60 Vcb	3	—	—	63 (c)	0.7	33	3
2N307, A	X				35 Vcb	1, 2	5, 3	75	80	0.2	—, 27	—, 1
2N399	X	X			40	3	2	90	40 (c)	0.75	33	8 (e)
2N400	X			X	40	3	2	95	50 (c)	1.0	36	6
2N401	X	X			40	3	2	90	40 (c)	0.5	30	5 (e)
2N418			X	X	80	5	2	100	50	4.0	—	100 (d)
2N419				X	45	3	2	95	60 (c)	0.5	—	5
2N420, A			X	X	40, 70	5	2	100	50	4.0	—	—
2N637, A, B	X		X	X	40, 70, 80	5	2	100	45	3.0	—	35, 70 (d)
2N638, A, B	X		X	X	40, 70, 80	5	2	100	30	3.0	—	35, 70 (d)
2N639, A, B	X		X	X	40, 70, 80	5	2	100	23	3.0	—	35, 70 (d)
2N677, A, B, C and 2N1029, A, B, C replaced by 2N1031, A, B, C												
2N678, A, B, C and 2N1030, A, B, C replaced by 2N1032, A, B, C												
2N1031, A, B, C	X		X	X	30, 40, 70, 80	15	1.5	100	40	10.0	—	75, 125, 250 (d)
2N1032, A, B, C	X		X	X	30, 40, 70, 80	15	1.5	100	75	10.0	—	75, 125, 250 (d)
2N1073, A, B (i)	X		X		40, 80, 120	10	2.0	100	40	5.0	—	100, 150, 200 (d)
2N1136, A, B	X		X	X	40, 70, 80	5	2.0	100	75	3.0	—	35, 70 (d)
2N1137, A, B	X		X	X	40, 70, 80	5	2.0	100	115	3.0	—	35, 70 (d)
2N1138, A, B	X		X	X	40, 70, 80	5	2.0	100	150	3.0	—	35, 70 (d)
B-177	X			X	30	3	2.2	90	150 (c)	0.5	39	2
B-178	X				30	3	2.2	90	40 (c)	0.5	33	2
B-179	X				40	3	2.2	90	25 (c)	0.5	28	2
Medium Power Transistors (h)												
2N1008, A, B	X	X	X		20, 40, 60	300mA	0.15°C/mW	85	95 (c)	10mA	—	400mW (f)
2N1176, A, B	X		X		20, 40, 60	300mA	0.20°C/mW	85	50 (c)	10mA	—	300mW (f)
Military Types												
2N297A (g)	X		X	X	50	5	2.0	95	70	0.5	—	35 (f)
2N331 (h)	X		X		30 Vcb	200mA	0.15°C/mW	85	50 (c)	1.0mA	—	400mW (f)
2N1011 (g)	X		X	X	70	5	2.0	95	55	3.0	—	70 (d)
2N1120 (g)	X		X	X	70	15	1.5	95	35	10.0	—	250 (d)

(a) Vce except where noted. Equivalent Vcb's are 20-50% higher. (b) Collector dissipation is the difference between the maximum junction temperature and the mounting base temperature divided by the thermal resistance. (c) hfe, AC current gain. (d) Square wave output power. (e) Push-pull output. (f) Pc—Maximum collector dissipation 25°C. (g) TO-3 package. (h) TO-9 package. (i) Diffused-Alloy-Power DAP transistor.

CHARACTERISTICS OF BENDIX SILICON RECTIFIERS

Type Number	Io Adc	PIV Vdc	LIb	Type Number	Io Adc	PIV Vdc	LIb	Type Number	Io Adc	PIV Vdc	LIb
1N536	0.75	50	10 uAdc (At 25°C)	1N1434	30	50	5 mAdc (At 150°C)	1N1612	5	50	1 mAdc (At 150°C)
1N537	0.75	100	10 uAdc	1N1435	30	100	5 mAdc	1N1613	5	100	1 mAdc
1N538	0.75	200	10 uAdc	1N1436	30	200	5 mAdc	1N1614	5	200	1 mAdc
1N539	0.75	300	10 uAdc	1N1437	30	400	5 mAdc	1N1615	5	400	1 mAdc
1N540	0.75	400	10 uAdc	1N1438	30	600	5 mAdc	1N1616	5	600	1 mAdc
1N547	0.75	600	10 uAdc								

Write Semiconductor Products

Red Bank Division

THE Bendix CORPORATION

LONG BRANCH, N. J.

West Coast Sales office: 117 E. Providencia Ave., Burbank, California • Midwest Sales office: 4104 N. Harlem Avenue, Chicago 34, Illinois
New England Sales office: 4 Lloyd Road, Tewksbury, Massachusetts • Export Sales office: Bendix International Division, 205 E. 42nd Street, New York 17, New York
Canadian Affiliate: Computing Devices of Canada, Ltd., P. O. Box 508, Ottawa 4, Ontario, Canada

Industrial Engineering Notes

(Continued from page 74A)

Shibaura Electric Co., exports 25 per cent of its transistors to this country. . . . **Japanese electronics output continued the strong upward trend in 1959 to set an all-time record, the Electronics Division, Business and Defense Services Administration, U. S. Department of Commerce, reported last week.** Production was valued at $936 million last year, compared with $498 million in 1958. The record level is attributed chiefly to the accelerated production of consumer electronic products, which rose to $531 million—exceeding the total 1958 output of all electronic products. Production of television receivers valued at $335 million (2.9 million units) continued to dominate the electronic industries output, followed by radio receivers at $157 million (10.0 million units). Other leading products were receiving tubes, $72 million (118.6 million units); television picture tubes, $59 million (3.2 million units); and transistors, $45 million (86.5 million units). Prospects for 1960 are for continued growth, as investments for industry expansion remain high. One Japanese industry source has estimated the country's total electronics output this year at a level about one-third above that of 1959. The production of transistors and other semiconductor devices probably will be at a substantially higher level in 1960. The increase in output of television and radio receivers may not be as great. At the end of 1959, more than 4 million television receivers were in use in Japan, and it is expected that the demand for receivers will tend to decrease after mid-1960. Also, in view of Japan's record output of 10 million radio receivers in 1959, it is not expected that domestic and foreign demand will increase sufficiently to permit the rapid rate of increase in production of recent years. . . . **There will be an increasingly better market in Japan for American-made data processing equipment, reports an executive of the International Business Machines Corp. now traveling with a Department of Commerce trade mission in Japan.** "As the economy of Japan continues to expand, the value and need for data-processing is bound to be recognized," reported Harry G. Eilers, Special Assistant to the Vice President of IBM. "There should be a good opportunity for American producers of such equipment to participate in the business which will result as Japan adopts modern equipment and methods," he continued. The U. S. Trade Mission to Japan, sponsored by the Commerce Department's Bureau of Foreign Commerce, is conducting an on-the-spot study of opportunities for expanded U. S.-Japanese trade, with particular emphasis on increasing sales of American products in that country. The group of six representatives of prominent U. S. business firms also reported that Japan's improved balance of payments and the over-all strength of its economy, coupled with its announced intention to reduce impediments to imports of American products, will result in a substantial increase in that market for U. S. capital goods. . . . **The Computing and Related Machines Industry did $1,117 million worth of business in 1958, an increase of 79 per cent in a four-year period.** Employment during the same period rose 45 per cent, to a total of 82.3 thousand workers. . . . **Electronics and communications firms received $473.2 million worth of business from the military services during the first quarter of fiscal year 1960.** The total includes $28.7 million in procurement from small business concerns, statistics accumulated by EIA's Marketing Data Department show.

Military Electronics

Chairman Overton Brooks (D) La. of the House Committee on Science and Astronautics has warned that if another world war broke out, it would be fought principally with man-monitored machines, with battles being directed by computing machines. The war would be fought so fast, he declared, that the President, if he could be found in time, would have ten minutes "to order retaliation or have our forces wiped out on the ground." The Louisiana Congressman emphasized the part science and technology would play in another world conflict, if one should occur, in an address at the state convention of the Louisiana Department of the Reserve Officers Association at Lake Charles, La. "Today," he stated, "our nation is looking at the scientist and engineer for survival in the future. . . . The next world war . . . may well be won during the preparation phase. The changing techniques of modern warfare will put us in a push-button type of war with electronics and weapons playing the most important roles. Men will provide the guidance and the pre-battle data, but the machine, monitored by man, will do the job. Warfare will be so fast that computers will be required for intelligence reports, force controls and battle direction," Rep. Brooks declared. . . . **Development of a rocket-borne radiosonde which electronically probes the atmosphere to an altitude of 40 miles—twice the ceiling for weather balloons—was disclosed by the Army.** The Army said the new radiosonde makes possible a more economical and flexible method than the complex rocket systems now used to collect data from levels above balloon ceilings. It will gather wind speed and temperature data. The six and one-half pound device contains a radio transmitter powered by silver-zinc batteries. The sensory and radio system is packed into the nose cone of a 77-pound ARCAS rocket. After release from the rocket, the radiosonde floats earthward on a 15-foot parachute. Wind speed and direction are plotted by an automatic ground tracker called a "rawin set," originally developed by the Army Signal Corps for monitoring balloon flights. The radiosonde was designed and built at the U. S. Army Signal Research and Development Laboratory. The Army said the device meets requirements of the military services, the National Aeronautics and Space Administration, and the U. S. Weather Bureau. . . . **Last week Aeronutronic Division of Ford Motor Company was selected by the**

(Continued on page 78A)

SEPTEMBER 19, 20, 21, 1960

1960 NATIONAL SYMPOSIUM SPACE ELECTRONICS AND TELEMETRY

Sponsored by

The Professional Group on Space Electronics and Telemetry

(PGSET)

of the Institute of Radio Engineers

EXHIBITS AND SESSIONS:
SHOREHAM HOTEL
WASHINGTON, D.C.

PROGRAM DETAILS UNDER
"IRE NEWS AND NOTES"
SECTION OF THIS ISSUE

Industrial Engineering Notes

(Continued from page 76A)

National Aeronautics and Space Administration for negotiation leading to construction of a 300-pound instrumented package to be impacted on the moon within the next two years. The package will contain a seismometer, temperature-recording devices and other instruments. After the crash landing, the instruments will radio data back to Earth for a month or longer. . . . A high-speed magnetic tape transmission system operating over standard telephone voice-type circuits has reduced to one hour an Army inventory control task which once took 13 hours. The system, developed by Collins Radio Co., is said by the Army to be the world's fastest for exchange of data between electronic computer centers. A system prototype now links the computer centers of the Army Signal Supply Agency at Philadelphia with the Lexington, Kentucky, Signal Depot. The agencies are 500 miles apart. The Army said it maintains proper inventory control by requiring daily reports from depots. Through use of relatively fast punched card data transmission, this operation had required about 13 hours of transmission daily. By using the new system, data on the entire inventory at Lexington can be transmitted to Philadelphia

(Continued on page 80A)

New Random Access Memory Package...

uses only 18.75″ IN STANDARD 19″ RACK

GENERAL CERAMICS, continuing its leadership in the memory packaging field, has made available double and triple bay random access memories with up to 4096 characters x 32 bits per character at cycle times up to 6 micro-seconds. Now you can get design economy since the basic G-C package requires only 18.75″ of standard rack space—a reduction of up to 80% over typical units requiring a full six feet.

General Ceramics offers space-saving random access memory designs with varying number of characters, word lengths and logic.

Optional design features include parity checking, test cycles, indicator lights and power supply locations.

Write on your company letterhead for additional information. Please mention your requirements; address inquiries to Section P.

DIVISION OF INDIANA GENERAL CORPORATION

APPLIED LOGIC DEPARTMENT

GENERAL CERAMICS

KEASBEY, NEW JERSEY, U.S.A.

TECHNICAL CERAMICS, FERRITE AND MEMORY PRODUCTS

Industrial Engineering Notes

(Continued from page 78A)

in about an hour. The system uses two compact, fully transistorized cabinet units at each end of the circuit. One cabinet transfers computer memory data to magnetic tape. The other converts taped data into electrical signals suitable for transmission over telephone lines. The same equipment receives and transmits data.

. . . **A single communications system, pulling into one agency all the long-haul requirements of the Department of Defense, will be established under two directives, the Department of Defense announced last week.** The documents, signed by Secretary Thomas S. Gates, Jr., authorized a new type of agency headed by an officer of general or flag rank with command responsibility direct from the Secretary of Defense through the Joint Chiefs of Staff. It resolves a problem that has been known to concern the Congress and the Pentagon for a long period. The two directives, designed to increase the effective use of long-line communications by centralizing their control, provide for a Defense Communications Agency and a Defense Communications System, both under the direction, authority and control of the Secretary of Defense. General responsibility for the operational control and supervision of the system will be assigned to the agency. The Defense Communications System will furnish facilities for command and control functions, intelligence, weather, logistics, and administration. Communications requirements which have been met by the three military services in support of the National Aeronautics and Space Administration will be furnished in the future by the agency. Implementation of the plan, with the assumption of operational control and full supervision of the system by the new agency, will be accomplished on a phased basis without disrupting essential communications during the transition period. This is expected to take about nine months from the date when the chief of the agency is appointed. The Defense Department said the single communications system is essential for the following reasons: a) To provide maximum communications for the dollar investment; b) To provide support for the more advanced weapons systems of the future through a centralized control; c) To provide maximum flexibility; d) to assure adequate dispersion with alternate routing capability; e) To eliminate duplication in the research and development field; and f) To provide for standardization of installation, operation, and maintenance to assure over-all system efficiency. The system does not include: Tactical communications which are self-contained within tactical organizations; self-contained information gathering, transmitting and/or processing facilities which are normally local in operation and use; weapons systems requirements which cannot be met through the facilities of the DCS; and land, ship or airborne terminal facilities of broadcast, ship-to-ship, ship-to-shore, and ground-air-ground systems.

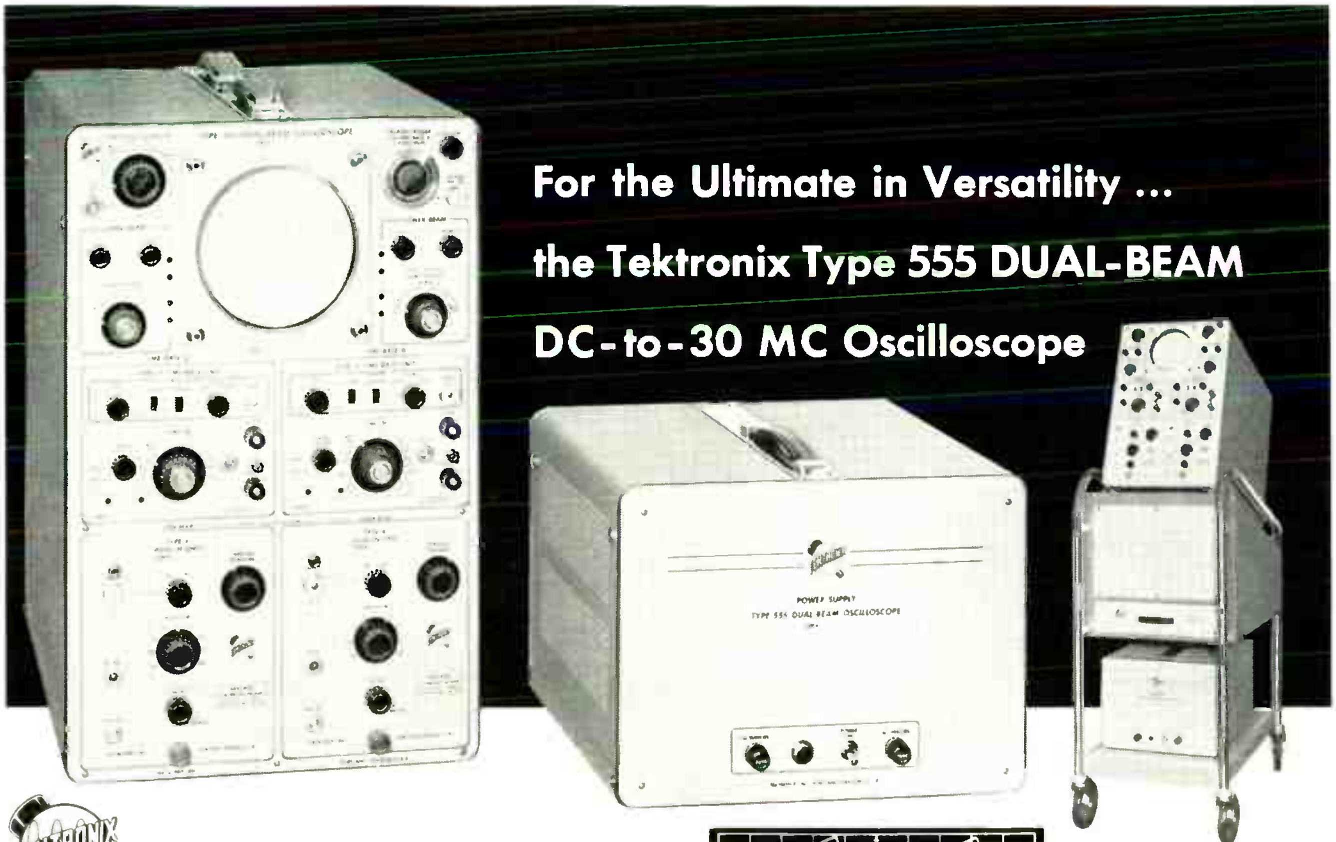

For the Ultimate in Versatility ... the Tektronix Type 555 DUAL-BEAM DC-to-30 MC Oscilloscope

The Type 555 writes with two independent electron beams. Each beam is controlled by its own separate horizontal and vertical deflection systems. Each vertical channel accepts all Tektronix Type A to Z Plug-In Units.

HORIZONTAL DEFLECTION—Either of the two time-base generators in the Type 555 can deflect either beam for single displays and for dual displays on different time bases, and either can deflect both beams for a dual display on the same time base. Time-base units are the plug-in type to facilitate instrument maintenance.

SWEEP DELAY—With one time-base generator functioning as a delay generator, the start of any sweep generated by the other can be held off for a selected time interval with a high degree of accuracy. Both the original display and the delayed display can be observed at the same time. The "triggered" feature can be used to obtain a jitter-free delayed display of signals with inherent jitter.

VERTICAL DEFLECTION—The availability of fifteen different plug-in units in the Tektronix Type A to Z Series provides for special and unique applications such as dual-beam pulse-sampling, transistor risetime testing, semiconductor diode-recovery-time measurements, strain gage and other transducer measurements, and differential comparator measurements as well as all general laboratory applications. In addition, three-channel or four-channel displays are available through use of the time-sharing characteristics of Tektronix Type C-A Dual-Trace Units in one or both channels.

Your Tektronix Field Engineer will be happy to arrange a demonstration in your application. Call him for complete details.

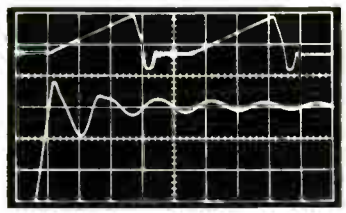

SWEEP DELAY
Same signal displayed simultaneously on slow sweep (upper beam) and fast sweep (lower beam) shows both coarse and fine structure of waveform.

CHARACTERISTICS

Independent Electron Beams
Separate vertical and horizontal deflection of both beams.

Fast-Rise Main Vertical Amplifiers
Passbands—dc-to-30 mc with Type K Units.
Risetimes—12 nanoseconds with Type K Units.
All Tektronix Plug-In Preamplifiers can be used in both vertical channels for signal-handling versatility.

Wide-Range Time-Base Generators
Either time-base generator can be used to deflect either or both beams.
Sweep Ranges—0.1 μsec/cm to 12 sec/cm. 5X magnifiers increase calibrated sweep rates to 0.02 μsec/cm.

Sweep Delay—Two Modes of Operation
Triggered—Delayed sweep started after the delay period by the signal under observation.
Conventional—Delayed sweep started at the end of the delay period by the delayed trigger.
Delay Range—0.5 μsec to 50 sec in 24 calibrated steps, with continuous calibrated adjustment between steps.

High Writing Rate
10-KV accelerating potential provides bright traces at low repetition rates and in one-shot application.

Separate Power Supply
All dc voltages electronically regulated.
Heater voltages also regulated.

PRICE, Type 555 without plug-in preamplifiers $2600
Includes Indicator Unit, Power Supply Unit, 2 Time-Base Units, 4 Probes, Time-Base Extension.

Type 500A Scope-Mobile (as shown with Type 555) $100

Type 500/53 Scope-Mobile (with supporting cradles for plug-in preamplifiers) $110

Prices f.o.b. factory

Tektronix, Inc.

P. O. Box 500 • Beaverton, Oregon
Phone MItchell 4-0161 • TWX—BEAV 311 • Cable: TEKTRONIX

TEKTRONIX FIELD OFFICES: Albuquerque, N. Mex. • Atlanta, Ga. • Baltimore (Towson, Md.) • Boston (Lexington, Mass.) • Buffalo, N.Y. • Chicago (Park Ridge, Ill.) • Cleveland, Ohio • Dallas, Texas • Dayton, Ohio • Denver, Colo. • Detroit (Lathrup Village, Mich.) • Endicott (Endwell, N.Y.) • Greensboro, N.C. • Houston, Texas • Kansas City (Mission, Kan.) • East Los Angeles, Calif. • West Los Angeles, Calif. • Minneapolis, Minn. • New York City Area (Albertson, L.I., N.Y. • Stamford, Conn. • Union, N.J.) • Orlando, Fla. • Philadelphia Pa. • Phoenix (Scottsdale, Ariz.) • Poughkeepsie, N.Y. • San Diego, Calif. • San Francisco (Palo Alto, Calif.) • St. Petersburg, Fla. • Syracuse, N.Y. • Toronto (Willowdale, Ont.) Canada • Washington, D.C. (Annandale, Va.)

TEKTRONIX ENGINEERING REPRESENTATIVES: Hawthorne Electronics; Portland, Oregon • Seattle, Washington. Tektronix is represented in twenty overseas countries by qualified engineering organizations.

In Europe please write Tektronix Inc., Victoria Ave., St. Sampsons, Guernsey C.I., for the address of the Tektronix Representative in your country.

Professional Group Meetings

Aeronautical and Navigational Electronics

Boston—May 5

"Air Collision Avoidance," Panel: F. M. McDermott, Air Traffic Control; J. A. Weber, Federal Aviation Agency; J. Lederer, Civil Aeronautics; H. E. Walls, Airline Pilots Association.

Metropolitan New York—October 8

"Current Status of Aircraft Collision Avoidance Systems and Proximity Warning Indicators," F. A. White, Air Transport Assn., Washington, D. C.

Metropolitan New York—November 12

"Guidance Considerations for Interplanetary Travel," P. E. Kendall, ITT Labs, Fort Wayne, Ind.

Metropolitan New York—December 10

"Automatic Landing Systems," D. Sheftell, Federal Aeronautics Assn.

Metropolitan New York—January 14

"Doppler-Inertial Navigation Systems," L. H. Dworetsky, General Precision Lab., Pleasantville, N. Y.

Metropolitan New York—February 11

"Man Machine Relationship in Jet Age Air Traffic Control," S. Saint, American Airlines.

Antennas and Propagation

Boston—March 16

"Lightning, Atmospherics and the Propagation of Long Radio Waves," E. T. Pierce, Avco Mfg. Co., Wilmington, Mass.

San Francisco—April 13

"The Structure of our Galaxy," Dr. M. Roberts, University of California, Berkeley.

San Francisco—April 20

"Radar Astronomy," Dr. A. M. Peterson, Stanford University and Stanford Research Institute.

(Continued on page 84A)

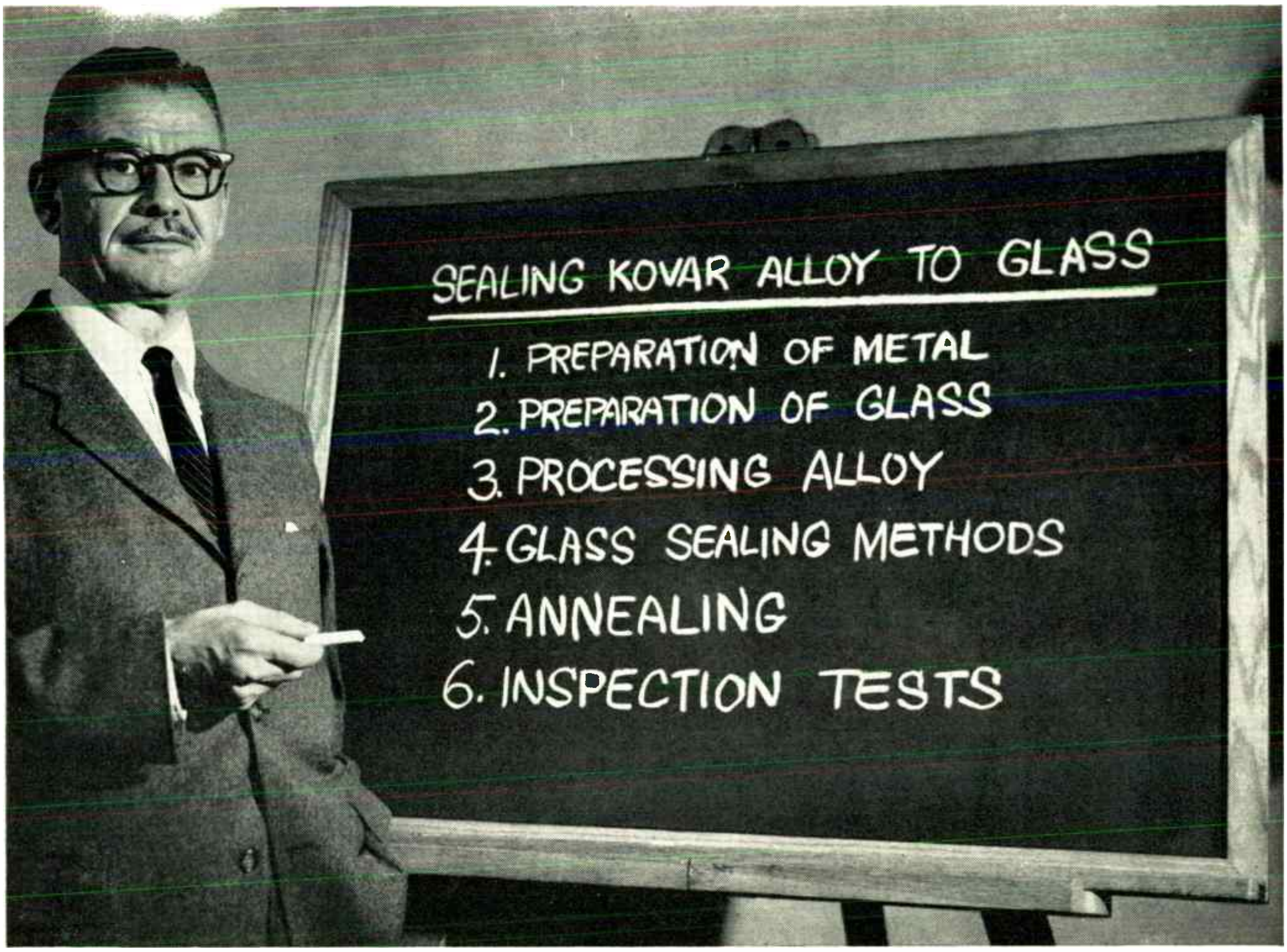

Engineering hints from Carborundum

6 steps to better glass-to-metal seals with KOVAR® Alloy

KOVAR® is the original iron-nickel-cobalt alloy with correct thermal expansion characteristics for making seals with several hard glasses. Procedures for obtaining a satisfactory seal—with optimum production yields—will vary according to the nature of the end product. This may range from large electron tubes to the smallest semi-conductor devices. The following hints typify recommendations for the more critical electron tubes; they can be modified for other products according to need.

1. KOVAR should be scratch-free. Polish with 180-grit aluminum oxide cloth, followed by 260-grit—never emery or carbide. Round edges of edge-type seals with a radius of about half metal thickness. Sand-blasted matt finish, using pure alumina, is preferable for butt type seals.
2. REMOVE DUST FROM GLASS with lint-free cloth. Rinse in 10% hydrofluoric acid solution, then in running tap water, finally in distilled water. Dip in methanol and hot air dry.
3. CLEAN KOVAR prior to sealing by trichlorethylene vapor degreasing, immersion in concentrated HCl, followed by rinses in tap and distilled water. Methanol dip and hot air dry. Heat treat in wet hydrogen atmosphere.
4. SEALING EQUIPMENT includes gas-oxygen burner and glass lathe. Oxidize surfaces by heating metal and glass to 850° C in air. Bring parts together by pressure. For strong seal, glass edge should approach 90° angle where it meets KOVAR alloy.
5. ANNEAL SEAL using flame or furnace program, advancing to annealing temperature for 30 mins. Reduce to 50° C below strain point at 1° per minute, then 10° per minute to room temperature.
6. INSPECTION may include stress analysis by polariscope viewing or other method. Examination under 10x to 15x magnification should show that glass is free from excessive bubbles. Glass color should be grayish or mouse brown.

FIND OUT ABOUT KOVAR—WHERE IT IS USED AND WHY
Bulletin 5134 gives data on composition, properties and applications of KOVAR Alloy. For data on sealing procedures, ask also for Technical Data Bulletin 100-EB6. Write Dept. P-70, Latrobe Plant, Carborundum Co., Latrobe, Pa.

For permanent vacuum and pressure-tight sealing . . . count on

CARBORUNDUM®

Professional Group Meetings

(Continued from page 82A)

Washington—April 25

"The Hourglass Scanner—A New Rapid Scan, Large Aperture Antenna," M. Fullilove, Melpar, Inc., Falls Church, Va.

Antennas and Propagation/ Microwave Theory & Techniques

Columbus—April 12

"On Interconnecting Two Equipments with a Slight Frequency Separation to a Single Antenna," Dr. W. B. Tilston, Sinclair Radio Labs, Toronto, Canada.

Columbus—May 6

"8-Millimeter Radiometry," Prof. S. Silver, University of California, Berkeley.

Orange Belt—April 12

"Tunnel Diode Symposium," Dr. C. Carter, Space Tech. Labs.; G. Messenger, Hughes Semiconductor Div.

Philadelphia—April 19, 1960

"Physics of Space Communication," C. T. McCoy, Philco, Corp., Philadelphia, Pa.

Audio

Albuquerque-Los Alamos—April 12

"FM Broadcasting," A. Koerner, D. Annett, Station KHFM, Albuquerque, N. M.

Albuquerque-Los Alamos—March 14

"Four Track Tape Recorder Standards," A. W. Fite, Sandia Corp., Albuquerque, N. M.

Baltimore—March 24

"High Intensity Sound," Dr. J. K. Hilliard, Ling Altec Research.

Boston—April 28

"The Loud Speaker—Can we improve it?" S. J. White, Audax, Inc.

Automatic Control

Fort Worth—May 9

"The Molecular Approach to Electronic Computer and Automatic Control Components," R. Biesele, Jr., Shockley Transistor Corp., Palo Alto, Calif.

Los Angeles—April 12

"Theory and Practice of Booster Rocket Control," Dr. J. Aseltine, Space Technology Lab., Los Angeles, Calif.

"Booster Rocket Control System Inflight Problems and their Solutions," F. H. Kaufman, Space Technology Lab., Los Angeles, Calif.

Milwaukee—May 10

"Feedback Theory Applied to Production and Inventory Control," Dr. G. J. Murphy, Northwestern University, Evanston, Ill.

Bio-Medical Electronics

Boston—December 8

"Computer Study of the Nervous System," W. Clark, MIT Lincoln Lab., Lexington, Mass.

Boston—April 26

"Biomedical Electronics as a Career," A. M. Grass, Grass Instruments; A. Miller, Sanborn Co.; S. Aronow, Mass. General Hospital; W. T. Peake, M.I.T.

Los Angeles—April 21

"Visualizing Soft Tissue Structure by Ultrasound," D. H. Howry, M.D., University of Colorado School of Medicine, Denver, Colo.

Montreal—February 29

"Electronics—Its Effect on Physiological Teachings and Research," C. Pinsky, G. Mandl, G. Smith, McGill University, Montreal, Canada.

New York—December 17

"Non-thermal Biologic Effects of Electromagnetic Fields," J. H. Heller, M.D., New England Institute for Medical Research.

New York—January 21

"The Physiologic and Clinical Significance of the Electroencephalogram," C. Wells, M.D., Cornell University Medical College, Ithaca, N. Y.; "Analysis of the Electroencephalogram," T. F. Weiss, M.I.T., Lexington, Mass.

New York—February 18

"Problems encountered in the use of infra-red imaging devices for penetration of ocular capacities," J. Friedman, D.D.S.

"Can the wave forms of the electrocardiograph be measured automatically?" C. A. Caceres, M.D., George Washington University Hospital.

"Is it possible to track the passage of a telemetering capsule through the gastrointestinal tract?" John T. Farrar, M.D., New York Veterans Administration Hospital.

Portland—April 28, 1960

"Electronics in Cardiovascular Radiology," C. Dotter, Univ. of Oregon Medical School, Portland.

"Magnetic Recording of Medical Data," L. Park, Park Electronics, Aloha, Ore.

San Francisco—October 27

"The Nervous System and Automatic Control," Panel: G. F. Franklin, Ph.D., Stanford E. E. Dept.; E. Callaway, M.D., Langley Porter Clinic and K. H. Pribrum, M.D., Stanford University.

(Continued on page 86A)

THE UNIVERSAL DIODE

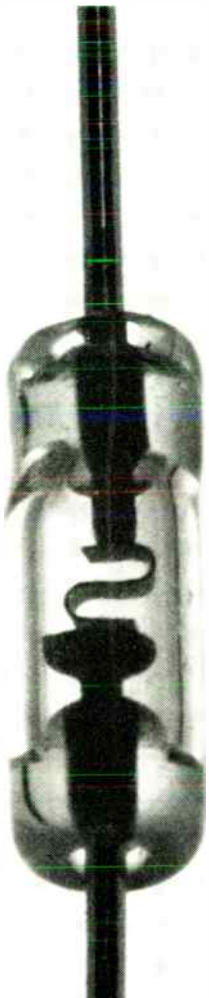

Fairchild FD200, actual size

High Conductance, Ultra Fast Silicon Planar Diode

. . . satisfies all of today's diode requirements and forestalls obsolescence by fulfilling foreseeable future demands for logic, switching and general-purpose applications with these advanced specifications:

- Over 100 mA forward conductance at 1.0 V
- Less than 50 mμsec reverse recovery time
- Capacitance under 5 μμf at 0 V
- 200 V minimum breakdown voltage

RELIABILITY is significantly advanced by the introduction of Fairchild's latest semiconductor state-of-the-art development—the Planar Structure.

UNIFORM CHARACTERISTICS and minimal parameter spreads give unvarying results and consistent performance from every FD200 diode.

IMMEDIATE AVAILABILITY—Call your local distributor or sales office. Complete listing attached. Complete line of Fairchild 1N-types to current specifications complement the FD200.

MAXIMUM RATINGS (25°C)—(Note 1)

WIV	Working Inverse Voltage	150 V
I_o	Average Rectified Current	100 mA
I_F	Forward Current Steady State D.C.	150 mA
i_f	Recurrent Peak Forward Current	300 mA
i_f (surge)	Peak Forward Surge Current Pulse Width of 1 sec.	500 mA
i_f (surge)	Peak Forward Surge Current Pulse Width of 1 μsec.	2000 mA
P	Power Dissipation	250 mW
P	Power Dissipation	100 mW @ 125°C
T_A	Operating Temperature	−65 to +175°C
T_{stg}	Storage Temperature, ambient	−65 to +200°C

ELECTRICAL SPECIFICATIONS (25°C unless noted)

SYMBOL	CHARACTERISTICS	MIN.	TYPICAL	MAX.	TEST CONDITIONS
V_F	Forward Voltage			1.0 V	I_F = 100 mA
I_R	Reverse Current			0.1 μA	V_R = −150 V
I_R	Reverse Current (150°C)			100 μA	V_R = −150 V
BV	Breakdown Voltage	200 V			I_R = 100 μA
t_{rr} (Note 2)	Reverse Recovery Time			50 mμsec	I_f = 30 mA I_r = 30 mA R_L = 150 Ohms
C_o (Note 3)	Capacitance			5.0 μμf	V_R = 0 V f = 1 mc
RE (Note 4)	Rectification Efficiency	35%			f = 100 mc
	Forward Voltage Temperature Coefficient		−1.8 mV/°C		

NOTES:

(1) Maximum ratings are limiting values above which life or satisfactory performance may be impaired

(2) Recovery to 1.0 mA

(3) Capacitance as measured on Boonton Electronic Corporation Model No. 75A-S8 Capacitance Bridge or equivalent

(4) Rectification Efficiency is defined as the ratio of D.C. load voltage to peak rf input voltage to the detector circuit, measured with 2.0 V r.m.s. input to the circuit. Load resistance 5 K ohms, load capacitance 20 μμf.

A wholly owned subsidiary of Fairchild Camera and Instrument Corporation

FAIRCHILD SEMICONDUCTOR CORPORATION

4300 Redwood Highway, San Rafael, California · GLenwood 6-1130 · TWX: SRF 26

Professional Group Meetings

(Continued from page 84A)

San Francisco—November 24

"The Nervous Systems Components vs. Computer Components," Panel: A. S. Hoagland, Ph.D., IBM; Dr. K. Killam, Stanford Medical School; Dr. C. Rosen, Stanford Research Institute.

San Francisco—January 19

"The Micro-Instrumentation of Nerve Cells," Panel: Dr. R. Grant, Stanford University; J. A. Patterson, Palo Alto Medical Research Foundation; K. Gardner, Stanford Research Institute.

San Francisco—February 24

"Linear Electron Accelerator and Cancer Therapy (Electronic Aspects)," Panel: M. A. Bagshaw, M.D., Stanford Medical School and M. Weissbluth, Ph.D., Stanford Medical School.

San Francisco—March 22

"Physiological Effects of Microwave and Ultrasonics," Panel: Dr. S. F. Thomas, Palo Alto Medical Clinic; T. Jaski and D. Lord, University of California.

San Francisco—April 19

"Studies on Use of Computers in Medical Practice and Research," Panel: C. J. Roach, MEDIC System Development Corp.

Circuit Theory

Los Angeles—April 19

"Synthesis of Group-Delay Functions and Group-Delay Correction Networks," Dr. T. R. O'Meara, Hughes Aircraft Co., Culver City, Calif.

Communication Systems

Los Angeles—April 13

"A Summer of Love in the Phase Plane," A. Viterbi, Jet Propulsion Labs., Pasadena, Calif.

Component Parts

Buffalo-Niagara—February 25

"Application of Tunnel Diode," E. Gottlieb, General Electric Co.

Philadelphia—March 29

"Tantalum Capacitors," G. Iaggi, Fansteel Metallurgical Co., No. Chicago, Ill.

Los Angeles—April 11

"Environmental Specs. for the 'Abe' Series of Space Vehicles," S. C. Morrison, Space Technology Labs.

Electron Devices

Boston—April 13

"Molecular Electronics," P. Pitman, Westinghouse Electric Co., Pittsburgh, Pa.

(Continued on page 89A)

Microwave Component News from SYLVANIA

Millimeter devices now available in six product lines

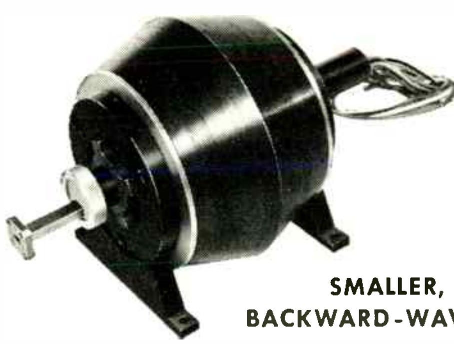

SMALLER, LIGHTER BACKWARD-WAVE OSCILLATOR

Type BW-1757 delivers up to 15 mw from 26.5-41 kmc in a streamlined new package. Also available are types from 18 to 26.5 and 40 to 75 kmc. BWO's above 75-100 kmc are in development.

FERRITE CIRCULATORS AND ISOLATORS

In production at Sylvania are Tee circulators and waveguide isolators in the 18 to 26 kilomegacycle range. Development programs are under way for devices above 26 kmc.

MAGNETRONS DELIVERING UP TO 100 KILOWATTS

Sylvania's line of rugged Ka-band magnetrons have output powers from 20 to 100 kw. K-band type M-4154 delivers 55 kw. Samples are available of new, rugged Ka-band type M-4218, weighing only 4½ pounds. Techniques are available for development of types to 100 kilomegacycles.

NEW WAVEGUIDE WINDOWS AVAILABLE

Sylvania is now producing two new waveguide windows in K and Ka bands, with flanged mica windows:

Type WG-4224	18 to 26 KMC
Type WG-4223	26 to 40 KMC

SYLVANIA TR AND ATR TUBES

Sylvania-developed TR and ATR tubes for Ka-band operation are available with power handling capability up to 100 kw.

IN THE DEVELOPMENTAL STAGE:

Sylvania has proved research and development capability for O and M type devices. One of the important projects now programmed at Sylvania's Bayside Physics Laboratory is a harmonic generator in the 200 to 400 kmc range which takes advantage of the non-linear conductivity characteristics of Germanium. And the Bayside labs are at work on the Tornadotron, with which 0.1 MM will be reached; millimeter amplifiers are also in development.

For further information write Sylvania Special Tube Operations, 500 Evelyn Ave., Mountain View, California, indicating the product lines in which you are interested.

SYLVANIA

Subsidiary of **GENERAL TELEPHONE & ELECTRONICS**

GENERAL SYSTEM

SUPRAMICA® 560 ceramoplastic

from the family of the world's most nearly perfect insulation

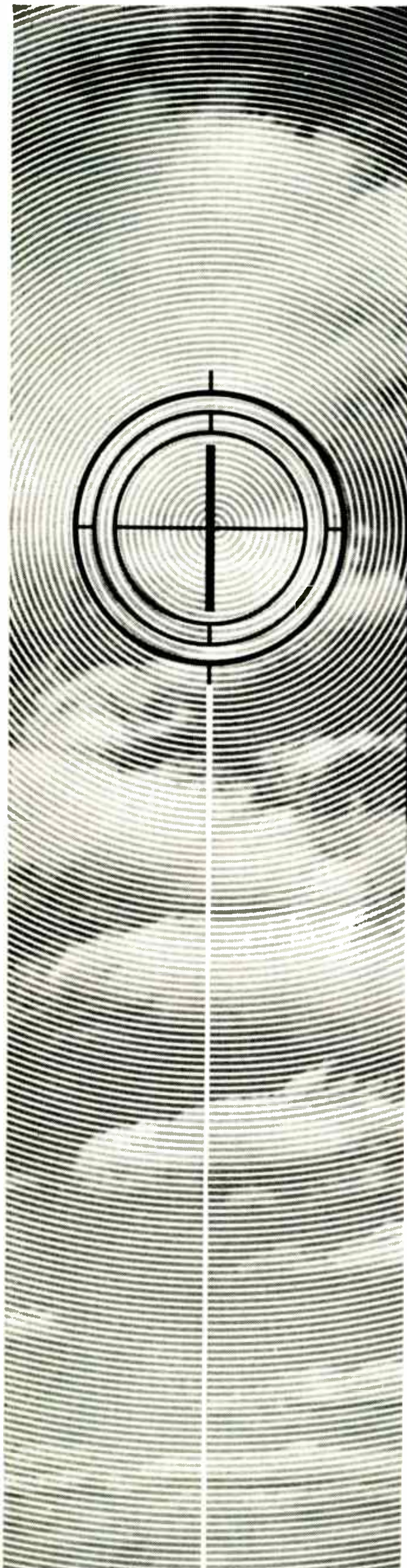

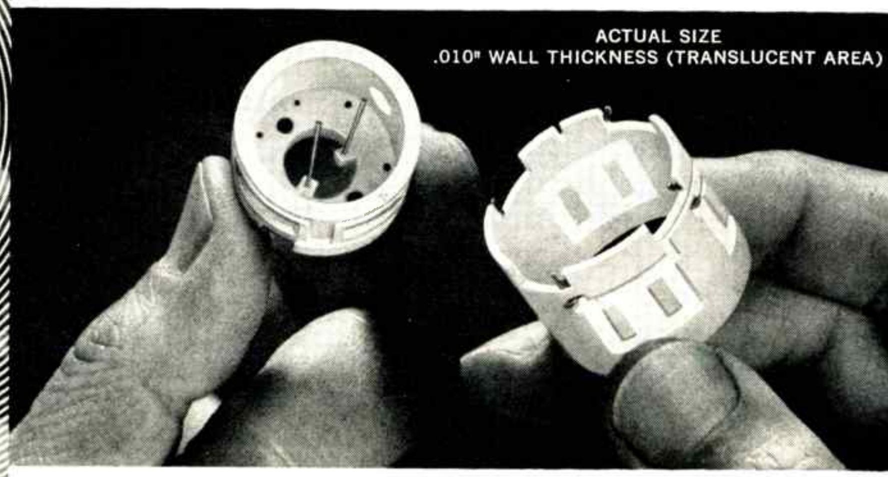

helps to maintain peak gyro efficiency

Leading gyro producers design parts made of precision-molded SUPRAMICA 560 ceramoplastic, an *exclusive formulation of* MYCALEX CORPORATION OF AMERICA capable of retaining absolute dimensional stability at a maximum temperature endurance up to +932°F (unstressed) . . . in complex but lightweight designs. These small parts function as vital components of miniature gyros . . . critical applications where the highest standards for precision accuracy must be met.

SUPRAMICA 560 ceramoplastic having the same thermal expansion coefficient of many insert metals, can tightly bond and permanently anchor gold leads, stainless steel contacts and stainless steel threaded inserts . . . in parts with wall thicknesses of only .010".

SUPRAMICA 560 ceramoplastic offers premium insulating properties with excellent economy in production scale runs. SUPRAMICA 560 ceramoplastic is but one of a family of versatile electrical and electronic insulating materials produced by MYCALEX CORPORATION OF AMERICA . . .

- MYCALEX® glass-bonded mica,
  maximum temperature endurance (unstressed)—up to +700°F
  heat distortion temperature * —up to +850°F
- SUPRAMICA® ceramoplastic,
  maximum temperature endurance (unstressed)—up to +1550°F
  heat distortion temperature * —up to +1360°F
- SYNTHAMICA® synthetic mica,
  maximum temperature endurance (unstressed)—up to +2000°F

* ASTM test method D 648 (modified) at stress of 264 psi.

Write for technical information today.

SYNTHAMICA® SYNTHETIC MICA · SINCE 1919 MYCALEX® THE INSULATOR · SUPRAMICA® CERAMOPLASTIC

MYCALEX
CORPORATION OF AMERICA

General Offices and Plant: 126 Clifton Blvd., Clifton, N. J.
Executive Offices: 30 Rockefeller Plaza, New York 20, N. Y.

World's largest manufacturer of glass-bonded mica, ceramoplastic and synthetic mica products

Professional Group Meetings

(Continued from page 86A)

New York—December 3

"Tunnel Diodes," Dr. I. A. Lesk, General Electric Company, Syracuse, N. Y.

New York—February 25

"Microwave Power Generation by Beam Plasma Interaction," J. E. Hopson, Sperry Gyroscope Co., Sunnyvale, Calif.

Washington, D. C.—March 28

"Dendritic Ribbon Crystal Growth of Semiconductors and Its Exploitations," Dr. R. L. Longini, Westinghouse Research Labs., Pittsburgh, Pa.

Electronic Computers

Binghamton—March 31

"The Vanishing Computer," C. F. King, Space Technology Lab., Los Angeles, Calif.

Binghamton—April 18

"Tunnel Diodes," Dr. L. A. Lesk and J. J. Suran, General Electric Co., Syracuse, N. Y.

Long Island—April 13

"Switching Circuit Design Based on Matrix Logic," E. J. Schubert, Monitor Systems, Inc.

Los Angeles—April 21

"Data Processing Equipment for Air Traffic Control," C. Lekven, Librascope, Inc., Glendale, Calif.

Philadelphia—April 12

"Impact of New Solid State Devices on Computer Systems Design," L. Burns, RCA Labs., Princeton, N. J.

Washington, DC—April 21

"Computer Applications of Tunnel Diodes," R. K. Lockhart, RCA, Camden, N. J., and M. M. Kaufman, RCA, Camden, N. J.

Engineering Management

Boston—April 14

"Weapons System Contracting," Dr. J. Sterling Livingston, Harvard Business School, Cambridge, Mass.

San Francisco—April 12, 1960

"Planning for an Expanding Organization," Dr. R. N. Noyce, Fairchild Semiconductor Corp., Mountain View, Calif.

Industrial Electronics

Cleveland—March 31

"Infrared Sensors and Optical Systems," Dr. W. H. Haynie, Eastman Kodak Co.

Information Theory

Boston—December 14

"Frog Vision," J. Letuinn and H. Maturana, MIT, Lexington, Mass.

Boston—February 9

"A New Language for Algorithm Representation," K. Iverson, Harvard Univ., Cambridge, Mass.

Los Angeles—April 26

"An Inductive Probability Criterion for Receiving Systems," L. S. Schwartz, New York Univ. and Adelphi College, New York, N. Y.

Instrumentation

Long Island—April 19

"Beam Observation and Control in the Brookhaven Alternating Gradient Synchrotron," E. C. Raka, Brookhaven Natl. Labs.

Los Angeles—April 14

"Cross Sectional Pictures of Soft Tissue in the Body by Ultrasound," Dr. D. H. Hoary, University of Colorado Medical Center, Denver, Colo.

Los Angeles—May 4

"Basics of Electronic Metal Detection," H. L. Eggleston, Jr., Goldak Co., Inc., Glendale, Calif.

Washington—May 9

"Microwave Power Standards and Comparison Techniques," G. F. Engen, Boulder Labs., NBS.

Microwave Theory and Techniques

Albuquerque-Los Alamos—February 23

"Measurement Accuracy Criteria—30 Mc through 12.4 Kmc," B. O. Weinschel, Weinschel Engineering, Kensington, Md.

Albuquerque-Los Alamos—February 29

"Engineering Problems Relative to Tektronix 519, Design and Application," C. Moulton, Tektronix, Inc., Portland, Ore.

Baltimore—April 6

"Microwave Optics," Dr. R. C. Spencer, The Martin Co., Baltimore, Md.

Los Angeles—April 14

"Magnetic Domains," Dr. M. Weiss, Hughes Aircraft Co., Los Angeles, Calif.

Washington—May 10

"Infrared Theory and Techniques," R. Grove, The Martin Co., Baltimore.

Military Electronics

Boston—October 8

"Reliability Management," M. M. Tall, RCA.

(Continued on page 90A)

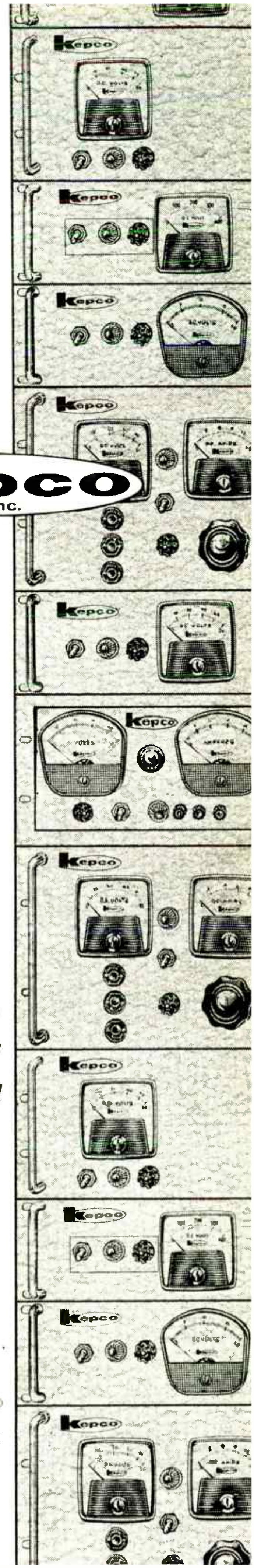

Professional Group Meetings

(*Continued from page 89A*)

Boston—April 21

"Design Reviews,"—all day session.

Boston—May 5

"Air Collision Avoidance," Panel: F. M. McDermott, Air Traffic Control; J. A. Weber, Federal Aviation Agency; J. Lederer, Civil Aeronautics; H. E. Walls, Airline Pilots Association.

Indianapolis—March 31

"Aspects of Flight Simulation," Mr. McIllnay, McDonnell Aircraft Corp., St. Louis, Mo.

Long Island—March 1

"Communications via Satellites" Dr. W. La Berge, Philco Western Development Labs., Palo Alto, Calif.

Long Island—April 26

"Research Problems in Undersea Warfare," F. A. Parker, Ass't. Dir. of Defense, Research and Engineering for Undersea Warfare.

Los Angeles—March 23

"Thermonuclear War—What the Engineer Should Know," H. Kahn, Rand Corp., Santa Monica, Calif.

Northwest Florida—March 29

"Theory and Application of Digital Encoders," D. Griffen, Norden Div. United Aircraft Corp., Milford, Conn.

Philadelphia—March 15

"The Military Field Use of Digital Systems and Human Factors Considerations," Capt. W. Leubert, Signal Corps, Ft. Monmouth, N. J., and Dr. Lucier, Univ. of Pennsylvania, Philadelphia.

Philadelphia—April 26

"The Nature of USAF Command and Control Systems," W. J. Sen, Wright-Patterson AFB, Ohio.

Nuclear Science

Oak Ridge—April 21

"Transistor Application at Southern Bell" L. N. Howell, Jr., Southern Bell Tel & Tel Co., Knoxville, Tenn.

Production Techniques

Boston—April 26

"Work Simplification," H. Schreiber, Jr., MIT, Lexington, Mass.

(*Continued on page 92A*)

electrical tests

mechanical tests

shock tests

centrifuge tests

vibration tests

humidity tests

storage life tests

Approved "MEG-A-LIFE" units

MOTOROLA "MEG-A-LIFE" INDUSTRIAL POWER TRANSISTORS

Only Motorola power transistors offer 90 watts power dissipation, 0.8°C/W maximum thermal resistance and 100°C junction operating temperature.

5 AMP

h_{FE} ($V_{CE}=2V$, $I_C=3A$)	BV_{CBO} 40V	60V	80V	100V
75 - 150	2N1544A	2N1545A	2N1546A	2N1547A
50 - 100	2N1539A	2N1540A	2N1541A	2N1542A
35 - 70	2N1534A	2N1535A	2N1536A	2N1537A
20 - 40	2N1529A	2N1530A	2N1531A	2N1532A

15 AMP

h_{FE} ($V_{CE}=2V$, $I_C=10A$)	BV_{CBO} 40V	60V	80V	100V
50 - 100	2N1557A	2N1558A	2N1559A	2N1560A
30 - 60	2N1553A	2N1554A	2N1555A	2N1556A
10 - 30	2N1549A	2N1550A	2N1551A	2N1552A

25 AMP

h_{FE} ($V_{CE}=1V$, $I_C=25A$)	BV_{CBO} 50V	80V	100V
15 - 65	2N1162A	2N1164A	2N1166A
15 - 65	2N1163A	2N1165A	2N1167A

Motorola "MEG-A-LIFE" program extended

NOW CERTIFIED RELIABILITY FOR INDUSTRIAL POWER TRANSISTORS

46 types in 3 current ranges provide military reliability for industrial applications

Now you can have the same assurance of reliability for your critical industrial power transistor applications as you do when using military-approved types for military applications. Motorola, in its "Meg-A-Life" quality assurance program (with written certification) now offers 46 "military-quality" industrial power transistors in three current ratings with voltages of 40 to 100 and betas to 150.

When you use Motorola "Meg-A-Life" industrial power transistors, you can be sure they have successfully passed electrical, mechanical and environmental tests (including shock, centrifuge, vibration, humidity and temperature tests) and 1000-hour storage life tests at 100°C in accordance with MIL-S-19500. You can be sure because written certification of compliance to "Meg-A-Life" reliability requirements is available to you. Only Motorola offers such documentation of quality. Approved "Meg-A-Life" units are stored and shipped to you from a bonded area.

Since all tests represent the most adverse conditions for which these devices are designed, Motorola's "Meg-A-Life" program provides you with an assurance of reliability not previously available in industrial units.

FOR COMPLETE "MEG-A-LIFE" BROCHURE and specification sheets on new Motorola "Meg-A-Life" power transistors, contact your Motorola district office:

BOSTON 385 Concord Ave., Belmont 78, Mass. .... IVanhoe 4-5070
CHICAGO 39, 5234 West Diversey Avenue .... AVenue 2-4300
DETROIT 27, 13131 Lyndon Avenue .... BRoadway 3-7171
LOS ANGELES 1741 Ivar Avenue, Hollywood 28, Calif. .... HOllywood 2-0821
MINNEAPOLIS 27, 7731 6th Avenue North .... LIberty 5-2198
NEW YORK 1051 Bloomfield Ave., Clifton, N.J. .... GRegory 2-5300
from New York .... WIsconsin 7-2980
SAN FRANCISCO 1299 Bayshore Highway, Burlingame, Calif. .... DIamond 2-3228
SYRACUSE 101 South Salina .... GRanite 4-3321
WASHINGTON 8605 Cameron St., Silver Spring, Md. .... JUniper 5-4485

MOTOROLA
Semiconductor Products Inc.
A SUBSIDIARY OF MOTOROLA, INC

Professional Group Meetings

(Continued from page 90A)

Radio Frequency Interference

Washington—April 19

"Measurement of Radio Frequency Spectrum Characteristics of Electronic Equipments," L. W. Thomas, Bureau of Ships, USN.

Reliability and Quality Control

Boston—October 8

"Reliability Management," M. M. Tall, RCA.

Boston—December 10

"Component Part Reliability," M. P. Feyerherm, RCA.

Boston—April 21

"Design Reviews,"—all day session E. Dertinger, Raytheon Mfg. Co.; Capt. H. Bernstein, EIA; H. Wuerffel, RCA; W. Saunders, Sylvania Electric Corp.; D. Simonton, RCA; E. Bersinger, Admiral Corp.

Florida West Coast—April 28

"An Approach to Reliability Development Methology," J. Chamberlain, Boeing Airplane Co., Seattle, Wash.

Los Angeles—February 15

"Agree Task Force Three Test of Talcan Equipment," Dr. A. Romig, Hoffman Labs.

Metropolitan New York—March 15

"Availability," S. R. Calabro, Internatl. Electric Corp.

Metropolitan New York—January 25

"Company Organization for Reliability Effectiveness," C. M. Ryerson, RCA; "Company Organization for Reliability Effectiveness," W. J. Masser, General Electric Company.

Philadelphia—April 12

"Value Engineering," S. Robinson, RCA, Moorestown, N. J.

"The Relationship between the QC and the Reliability Organizations," W. J. Bonner, General Electric, Philadelphia, Pa.

"Testing to Demonstrate Compliance with a Reliability Specification," M. J. Mozenter, Teledynamics Div., American Bosch Arma, Philadelphia, Pa.

San Francisco—April 19

"Transistor Reliability," J. Hilman, Fairchild Semiconductor Corp.

Space Electronics and Telemetry

Central Florida—April 28

"A Conceptional Hybrid Telemetry System—PACM," Dr. M. G. Pawley, Naval Ordnance Lab., Corona, Calif.

Detroit—March 23

Three movies were shown—"Man and the Moon," "Man in Space," and "The Biography of a Missile."

Vehicular Communications

Detroit—April 27

"Selective Signalling Techniques," O. Thompson, Secode Corp., San Francisco, Calif.

Los Angeles—April 21

"Integrated Radio Traffic Control System," C. J. Schultz, Motorola, Inc.

Section Meetings

Akron

"Masers—Some Problems and Advantages," R. H. Kingston, Lincoln Labs., Section Executive Comm. Meeting. 2/16/60.

"Fundamental Principles of Numerical Control," H. W. Mergler, Case Inst. of Technology, Annual Joint Cleveland-Akron Section Meeting—Nomination of officers. 4/21/60.

Alamogordo-Holloman

"Meteor Burst Influence on 15 mc Signal," H. T. Castillo, Aero Med. Lab. 4/18/60.

"Analog and Digital Computer Equipment," C. L. Johnson, AFMDC. 5/16/60.

Albuquerque-Los Alamos

"IRE and Its Role in Medical Electronics," Dr. R. L. McFarlan, President of the IRE. 4/18/60.

"Aspects of the Atomic Energy Program," C. P. Anderson, US Senator from N. M., Election of Officers. 5/11/60.

Anchorage

"Semiconductor Physical Structures and Circuit Applications," R. P. Merritt, Univ. of Alaska. 4/4/60.

Atlanta

"The Development of an Instrument Product Line," G. P. Robinson, Scientific-Atlanta. 4/29/60.

Bay of Quinte

"Nuclear Power Developments," L. G. McConnell, Hydro Elec. Power Comm. of Ont. 4/20/60.

Beaumont-Port Arthur

"Essentials of Stereo Records," G. W. Saylor

(Continued on page 94A)

HOW TO GENERATE 100-ma PULSES AT 10 mc

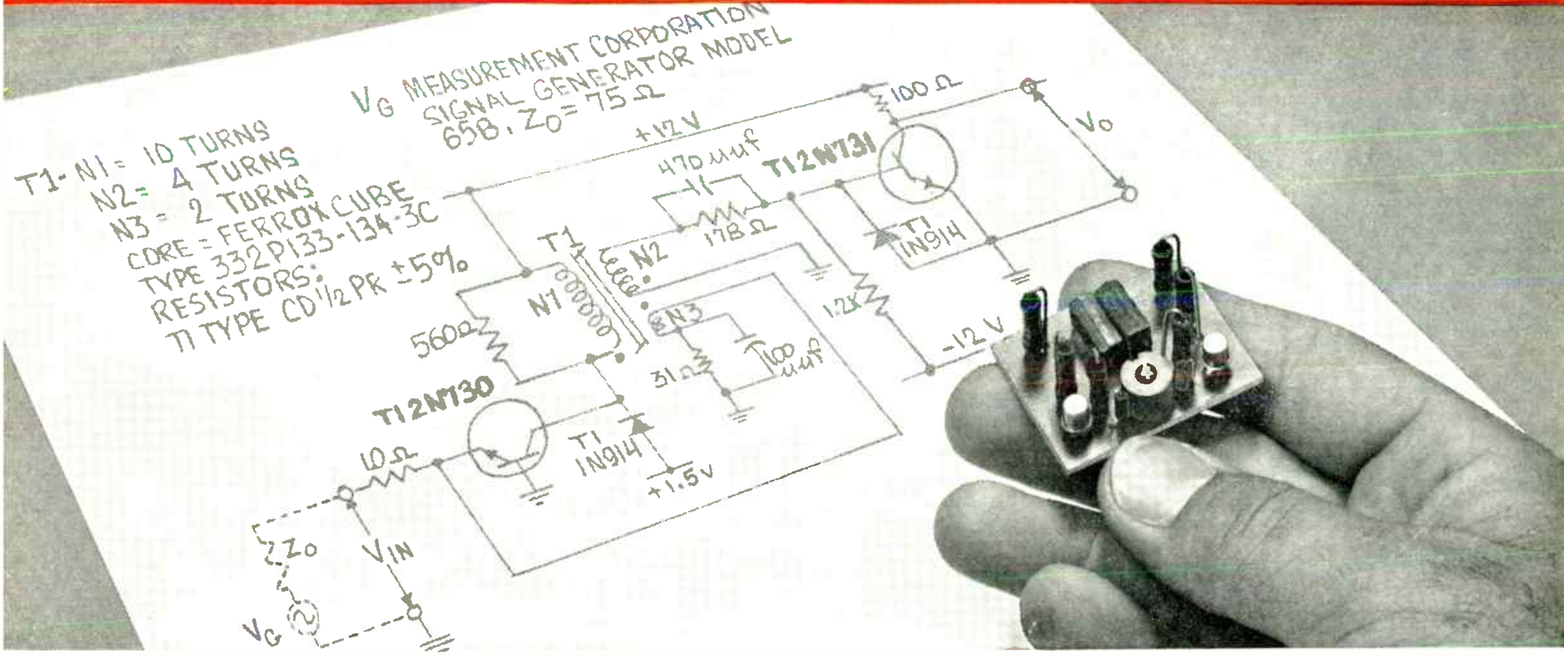

. . . WITH TI 2N730 and 2N731 SILICON MESA TRANSISTORS

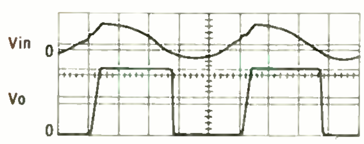

1 Megacycle
VERT.—5v /cm
HORIZ.—.2 μsec /cm
T_A—25°C

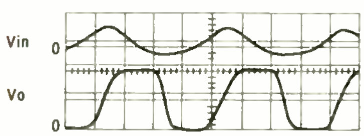

5 Megacycles
VERT.—5v /cm
HORIZ.—50 mμsec /cm
T_A—25°C

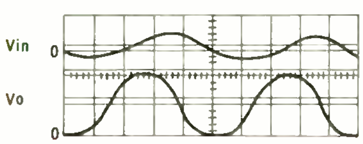

10 Megacycles
VERT.—5v /cm
HORIZ.—20 mμsec /cm
T_A—25°C


ACTUAL SIZE

See how these performance-proved characteristics apply to your high-current, high-speed switching circuits . . .

High-current loads — Switch *100 ma* at 10-mc rates using TI 2N730 and 2N731 transistors (see applications circuit) • *Fast switching* — Note *20 millimicrosecond* rise and fall times on the waveforms illustrated • *Size and weight* — Save *both* size and weight with the subminiature TO-18 packaging of the TI 2N730 and 2N731 'mesas' • *Dissipation* — Get a full *500 mw* ($T_A = 25°C$) or *1.5w* ($T_C = 25°C$) with beta spreads of 20-60 (2N730) and 40-120 (2N731) • *Reliability* — TI Quality Assurance *guarantees* you performance to specifications • *Applications* — Use the TI 2N730 and 2N731 guaranteed performance in your digital computer clock pulse generators and similar high-load, high-speed, high-reliability circuits. Check these specifications:

electrical characteristics at 25°C ambient (unless otherwise noted)

	PARAMETER	TEST CONDITIONS		2N730 min	2N730 max	2N731 min	2N731 max	unit
I_{CBO}	Collector Reverse Current	$V_{CB} = 30v$	$I_E = 0$	—	1.0	—	1.0	μa
I_{CBO}	Collector Reverse Current at 150°C	$V_{CB} = 30v$	$I_E = 0$	—	100	—	100	μa
BV_{CBO}	Collector-Base Breakdown Voltage	$I_C = 100\mu a$	$I_E = 0$	60	—	60	—	v
BV_{CER}	Collector-Emitter Breakdown Voltage	$I_{CER} = 100ma$ $R_{BE} = 10$ ohms		40	—	40	—	v
BV_{EBO}	Emitter-Base Breakdown Voltage	$I_E = 100\ \mu a$	$I_C = 0$	5	—	5	—	v
h_{FE}	DC Forward Current Transfer Ratio	$I_C = 150ma$	$V_{CE} = 10v$	20	60	40	120	
$V_{BE}(sat)$	Base-Emitter Voltage	$I_C = 150ma$	$I_B = 15ma$	—	1.3	—	1.3	v
$V_{CE}(sat)$	Collector-Emitter Saturation Voltage	$I_C = 150ma$	$I_B = 15ma$	—	1.5	—	1.5	v
h_{fe}	AC Common Emitter Forward Current Transfer Ratio	$I_C = 50ma$ f = 20mc	$V_{CE} = 10v$	2.0	—	2.5		
C_{ob}	Common-Base Output Capacitance	$I_E = 0$ f = 1mc	$V_{CB} = 10v$	—	35	—	35	$\mu\mu f$

*Pulse conditions: Length = 300μs, duty cycle < 2%

Collector-Base Voltage	60v
Collector-Emitter Voltage	40v
Emitter-Base Voltage	5v
Total Device Dissipation	0.5w
Total Device Dissipation at Case Temperature 25°C	1.5w
Storage Temperature Range	−65°C to +175°C

CALL YOUR TI SALES OFFICE OR LOCAL AUTHORIZED TI DISTRIBUTOR FOR PRICE, DELIVERY AND COMPLETE TECHNICAL DATA.

the FIRST silicon transistor manufacturer

TEXAS INSTRUMENTS
INCORPORATED
SEMICONDUCTOR-COMPONENTS DIVISION
13500 N. CENTRAL EXPRESSWAY
POST OFFICE BOX 312 • DALLAS, TEXAS

Section Meetings

(Continued from page 92A)

Philco Corp., Demonstration of modern stereo equipment. 12/15/59.

"Present Status and Future Developmental Trends in Transistors and other Semi-Conductor Devices," M. E. Jones, Texas Instruments. Joint Student-Section meeting. 1/26/60.

"Exploration Geophysics, Seismograph Instrumentation," A. C. Winterhalder, Sun Oil Co., "Exploration Geophysics, Gravity," George McCalpin, Sun Oil Co. 2/18/60.

"Electronic Control for Color Processing," Roy Gibbs, Majestic Photo., Tour of Majestic Photo Color Processing Plant. 3/29/60.

"Single Sideband Theory and Application, and Mechanical Filters for Transmitters and Receivers," J. F. Beckerich, Collins Radio Co., "Citizen's Band Radio" (Technical Brief), E. D. Coburn, Federal Communications Commission. 4/26/60.

Benelux

"The Layers of the Ionosphere," J. A. Ratcliffe, Vice-Pres. of the IRE. 4/25/60.

Binghamton

"Parametric Amplifiers: Historical Background," W. W. Mumford, Bell Telephone Labs.; "Parametric Amplifiers: Recent Results with T.W. Amplifiers," R. S. Engelbrecht, Bell Telephone Labs. 4/14/60.

Boston

"Undersea Explorations," H. E. Edgerton; Presentation of awards to new Fellows. 3/14/60.

"Air Collision Avoidance," -Panel Discussion: B. S. Kelsey, Moderator, F. M. McDermott, Air Traffic Control Assoc. J. A Weber, Federal Aviation Agency, Jerome Lederer, Civil Aeronautics, H. E. Walls, Engineering and Safety Dept., Air Line Pilots Assoc. Election of Section officers. 5/5/60.

Central Florida

"Human Errors and Accidents in Missile Operations," J. J. Rosa, U.S. Air Force. 4/21/60.

Cleveland

"Fundamental Principles of Numerical Control," H. W. Mergler, Case Inst. of Technology. Executive Board Meeting. 4/21/60.

"The IRE and Its Role in Medical Electronics," Dr. R. L. McFarlan, President of the IRE. Executive Comm. Meeting. 5/6/60.

Columbus

"Micro-electronics," E. B. Richter, USAF, Molecular Electronics Branch. 4/21/60.

"The Use of Microwaves for Power," Dr. R. L. McFarlan, President of the IRE. Presentation of Student Award. 5/4/60.

Dallas

"Wireless Transmission of Microwave Power to Maintain a High Platform," Dr. R. L. McFarlan, President of the IRE. 4/26/60.

"Radio Traffic Control for Vehicles," Charles Willyard, Motorola. 5/17/60.

Detroit

"The Evolution of the Klystron," Maurice Chodorow, Stanford Univ., Joint Meeting with Henry Ford Museum. 4/15/60.

Erie

Electronics in Brewing Industry and Plant Tour. 11/17/59.

Panel Discussion Trends in Communications, Robert Gray—Moderator, Erie Resistor Corp. 11/24/59.

Tour of Station WICU-TV. 4/20/60.

(Continued on page 98A)

AT LAST!

The EI Model 800 True Rms Digital Voltmeter

A TRUE RMS DIGITAL VOLTMETER

This revolutionary instrument incorporates a unique temperature stabilized diode network, operating on the square law principle, to yield a true rms voltage reading, regardless of the AC wave form or DC. No hot wire elements of any kind are used.

SPECIFICATIONS

- **All-electronic, totally-transistorized**
- **0.1% accuracy for crest factors up to two**
- **0.1% response from 50 cps through 5KC and at DC**
- **Higher frequency response (at least 10KC) at reduced accuracy and for certain waveforms**
- **3 second balance time, typical**
- **Calibration accuracy held for minimum of 30 days—typically much longer**
- **Automatic ranging**

Ask your nearest EI sales office or representative for complete information today!

Accuracy: Within the range and frequency capability of the instrument, RMS value of crest factor not exceeding two will be indicated to ±0.1% of reading or two digits, whichever is greater.

The instrument accurately accounts for:

Harmonic components	50 cps to 5KC	0.1% or 2 digits
Sinusoidal response	50 cps to 5KC	0.1% or 2 digits
Square wave	50 cps to 1KC	0.1% or 2 digits
Triangular wave	50 cps to 1KC	0.1% or 2 digits
DC (no polarity sense)		

Accuracy maintained 30 days without calibration adjustment. Above accuracies after 45 min. warm-up time.

Range: Automatic ranging. 1 volt to 999.9 volts with manually selected 0.1 volt to 1 volt range.

Balance time: Typically less than 3 seconds. Maximum 5 seconds per range.

Temperature: 0° to 50°C.

Power: 60 cps, single phase, 125 watts

Dimensions: 19" wide x 8¾" high x 20" deep.

Engineers: Many challenging positions are now open. For details contact Mr. Carl Sebelius.

Electro Instruments, Inc. 3540 AERO COURT SAN DIEGO 11, CALIF.

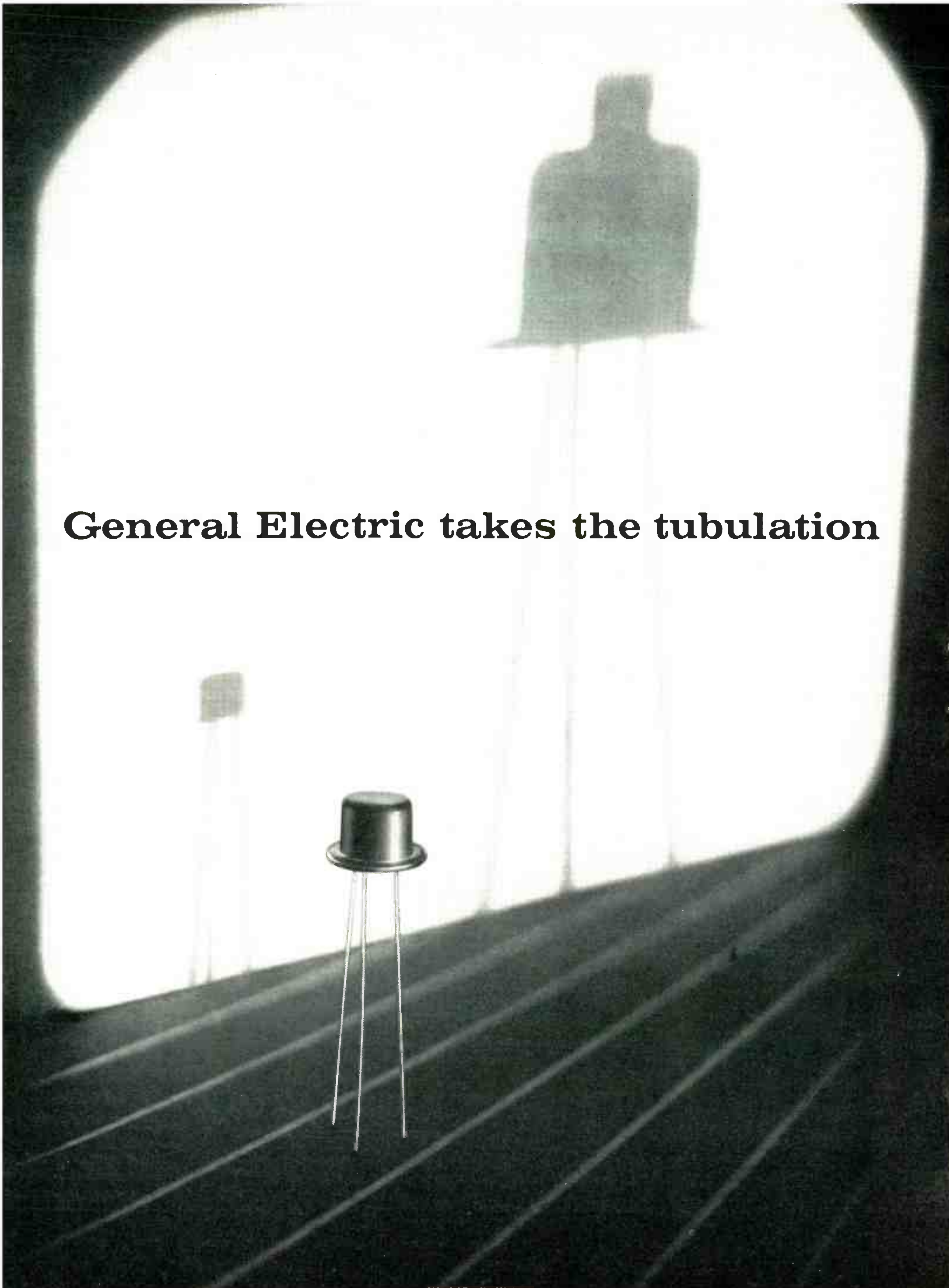
General Electric takes the tubulation

General Electric transistors hold the record in rate-grown reliability

General Electric has manufactured millions of rate-grown transistors in the past seven years. As a result of this experience, G.E.'s parameters are exceptionally stable and a vast amount of reliability data has been accumulated, some of which is shown here. These curves cover 29 lots of General Electric 2N167, tested to MIL-T-19500/11.

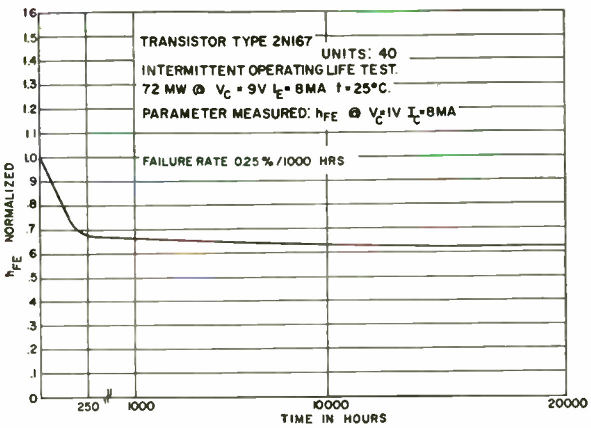

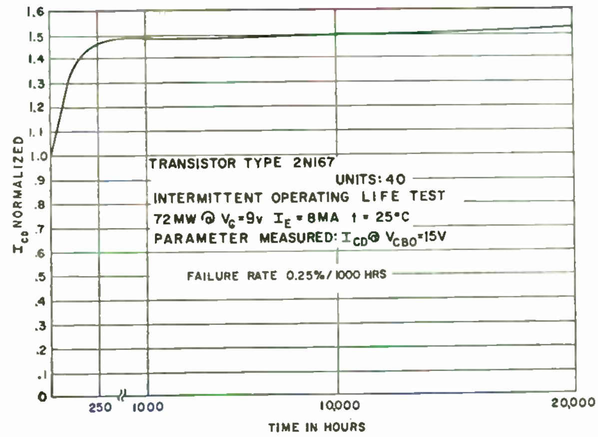

The rate-grown process produces a small, clean junction which exhibits almost no drift or deterioration at high voltages and offers the user low I_{CO} and I_{EO}. Two new types, the 2N1510 and 2N1217, will be useful for low-level switch and neon indicator applications. Both the 2N1217 and 2N167 operate at extremely low current and leakage levels, making them ideal for starvation circuits of 2 ma or less.

off rate-grown NPN transistors!

Remove the tubulation (pinch-off) from rate-grown transistors without sacrificing reliability? General Electric has done just that and even improved reliability with stabilized beta and collector cutoff current. Prices have been reduced on some types up to 20%.

Removal of the tubulation was made possible by adding a sieve or getter. Improved beta and collector cutoff current results from a 125-hour 85°C bake, which also improves the paint's resistance to solvents and chipping. Pellet, pellet mount and processing are identical to the previous process before encapsulation. Then a sieve is added rather than evacuation and subsequent pinch-off. The sieve is the same used and proved for years on G.E.'s PNP low-frequency 2N525 and PNP high-frequency 2N396 lines.

The high-reliability 2N78A and 2N167A have guaranteed 71°C I_{CO} and tight AQL's. The 2N78A also features a 20 volt BV_{CEO} rating compared with the 2N78's 15 volts. The 2N167A, in addition to 71°C I_{CO}, has a lower I_{EO}. For more information, see your G-E Semiconductor Sales Representative or Authorized Distributor. General Electric Company, Semiconductor Products Dept., Electronics Park, Syracuse, N. Y.

ADVANTAGES TO YOU: 40% lower height • Reduced prices • Stabilized I_{CO} and h_{FE}. All units baked 125 hours at 85°C • Greater resistance of paint to solvents, chipping, and salt spray • Improved low-temperature performance and reliability.

Type No.	Maximum Ratings				Electrical Parameters					
	$P_C$mw @ 25°C	BV_{CE} BV_{CB}	I_C ma	T_J°C	MIN h_{FE}	@ I_C ma	MIN f_{ab}mc	MIN $G_e$db	MAX I_{CO} (μa)	@ V_{CB}
2N78	65	15	20	85	45	1	5	27	3	15
2N78A	65	20	20	85	45	1	5	29	3	15
2N78A (Cert)	65	20	20	85	45	1	5	29	3	15
2N167	65	30	75	85	17	8	5	—	1.5	15
2N167A	65	30	75	85	17	8	5	—	1.5	15
USAF2N167A (per MIL-S-19500/11)	65	30	75	85	17	8	5	—	1.5	15
2N169A	65	15	20	85	34	1	—	27	5	15
2N1198	65	25	75	85	17	8	5	—	1.5	15
2N1217	65	20	20	85	40	2	5	—	1.5	15
2N1510	75	75	20	85	8	1	—	—	5	75

IN STOCK FOR FAST DELIVERY FROM YOUR AUTHORIZED GENERAL ELECTRIC DISTRIBUTOR

GENERAL ELECTRIC

Section Meetings

(Continued from page 94A)

Evansville-Owensboro

"The Conversion of Heat to Electricity by the Utilization of Thermionic Emission," J. E. Beggs, G.E. Research Lab. 4/20/60.

"Science in Space," R. W. Porter, G.E. Co.; Election of Officers. 5/18/60.

Florida West Coast

"Gravity and Dia-gravity," Charles Benfield, Honeywell Inertial Guidance Center. 4/20/60.

Fort Huachuca

Panel Discussion of Electromagnetic Environmental Test Facility at Fort Huachuca, J. Homsy, USAEPG, R. Gramling, PanAm, and J. L. Dunn, Bell Aircraft. 4/25/60.

Fort Worth

"Wireless Transmission of Microwave Power to Maintain a High Platform," Dr. R. L. McFarlan, President of the IRE. 4/26/60.

Gainesville

"The Magnetic Field of a Knotted Toroidal Inductor," John Kronsbein. 5/11/60.

Hamilton

"The Canadian Radio Technical Planning Board & the IRE," F. H. R. Pounsett, Philips Electronics Ltd., Election of Officers. 4/25/60.

Huntsville

"Current Problems in Infrared Physics & Technology," S. S. Ballard, Univ. of Florida. 4/29/60.

"The Radiation Belt," J. A. Van Allen, State Univ. of Iowa. 5/2/60.

Ithaca

"Thermoelectricity," A. C. Sheckler, Carrier Corp. 4/7/60.

Kansas City

"The Importance of Materials in Engineering," N. M. Bashara, Univ. of Neb.; Presentation of Student Award; Election of Officers. 5/9/60.

Las Vegas

Organizational Meeting. 2/16/60.

Organizational Meeting, Election of Officers. 3/15/60.

"Use of Microwave Power to Support a High Altitude Platform," Dr. R. L. McFarlan, President of the IRE. 4/15/60.

Little Rock

"Single Side Band Exciter Circuits using a New Beam Deflection Tube," H. C. Vance, Jr., RCA. 5/6/60.

London (Canada)

"The Problems of Manning Space Vehicles," R. A. Stubs, R.C.A.F., Inst. of Aviation Medicine. 4/12/60.

"The R.C.A. Canadian Video Tape Recorder," Philip Golden, Station C.F.P.L.-TV. 5/10/60.

Long Island

"Matter and Anti-Matter," C. E. Falk, Brookhaven Nat. Labs.; Movie: "High Energy Particle Accelerators"; Election of Officers. 4/12/60.

"ASTRON High Current Electron Accelerator," Nicholas Christofilos, Univ. of Calif. Radiation Lab. 5/3/60.

(Continued on page 102A)

FIRST SILICON MESA IN THE TO-36 CASE BROADENS THE COVERAGE OF THIS COORDINATED SILICON LINE

Similar to JEDEC TO-3 Case

2N1487
2N1488
2N1489
2N1490

JEDEC TO-8 Case

2N1483
2N1484
2N1485
2N1486

JEDEC TO-5 Case

2N1479
2N1480
2N1481
2N1482

RCA 2N1511, 2N1512, 2N1513, 2N1514, in JEDEC TO-36 Case

RCA Announces Four New Silicon Mesa Power Transistors in the Popular TO-36 Case

Available immediately in quantity...four new NPN Diffused-Junction Types... 2N1511, 2N1512, 2N1513, 2N1514 • electrically equivalent to 2N1487, 1488, 1489, 1490 respectively • utilize the industry-preferred JEDEC TO-36 single ended stud package with cold-weld seal • Designed for a wide variety of military and industrial applications

With RCA's new Silicon Mesa Power Transistors in the JEDEC TO-36 case, you gain all of these design advantages:

- **More positive heat sink contact** and excellent high-temperature performance up to 175°C plus the greater application flexibility of JEDEC TO-36 stud mounted case.
- **Low saturation-resistance** characteristics with high collector-current and voltage ratings.
- **Wider application** in military and industrial equipment—in power switching circuits, oscillator, regulator and pulse-amplifier circuits.
- **The dependability** of the cold-weld seal, proved by RCA through years of experience.
- **Coordinated line of 16 RCA Silicon Power Transistors.** These four new RCA transistors together with the 12 RCA Silicon Power Transistors shown in the accompanying table provide the designer of Industrial and Military equipment with a comprehensive selection of types to fit his specific needs.

ELECTRICAL CHARACTERISTICS
Minimum and Maximum Values at Case Temperature = 25°C

RCA Type	Min. V_{CEX} (volts)	Min V_{CEO}* (volts)	Max. I_C (amp)	Max I_{CBO} (μa)	Max Saturation Resistance ohms	h_{FE}	Max. Dissipation Watts 25°C Case	Max. Dissipation Watts 100°C Case
				V_{CB}=30v	I_C=1.5 amp	I_C=1.5 amp		
2N1514	100	55	6	25	0.67	25-75	60	30
2N1513	60	40	6	25	0.67	25-75	60	30
2N1512	100	55	6	25	2.00	10-50	60	30
2N1511	60	40	6	25	2.00	10-50	60	30
				V_{CB}=30v	I_C=1.5 amp	I_C=1.5 amp		
2N1490	100	55	6	25	0.67	25-75	60	30
2N1489	60	40	6	25	0.67	25-75	60	30
2N1488	100	55	6	25	2.00	10-50	60	30
2N1487	60	40	6	25	2.00	10-50	60	30
				V_{CB}=30v	I_C=0.75 amp	I_C=0.75 amp		
2N1486	100	55	3	15	1.00	35-100	15	7.5
2N1485	60	40	3	15	1.00	35-100	15	7.5
2N1484	100	55	3	15	2.67	15-75	15	7.5
2N1483	60	40	3	15	2.67	15-75	15	7.5
				V_{CB}=30v	I_C=0.2 amp	I_C=0.2 amp		
2N1482	100	55	1.5	10	7	35-100	4	2
2N1481	60	40	1.5	10	7	35-100	4	2
2N1480	100	55	1.5	10	7	15-75	4	2
2N1479	60	40	1.5	10	7	15-75	4	2

*sustaining volts

Call your RCA representative today for complete information. For additional technical data write to RCA Semiconductor and Materials Division, Commercial Engineering, Section G-35-NN, Somerville, N. J.

RCA SEMICONDUCTOR AND MATERIALS DIVISION SALES OFFICES

EAST: 744 Broad Street, Newark 2, N. J., HUmboldt 5-3900 • **NORTHEAST:** 64 "A" Street, Needham Heights 94, Mass., Hillcrest 4-7200 • **EAST CENTRAL:** 714 New Center Bldg., Detroit 2, Mich., TRinity 5-5600 • **CENTRAL:** Suite 1154, Merchandise Mart Plaza, Chicago 54, Ill., WHitehall 4-2900 • **WEST:** 6355 E. Washington Blvd., Los Angeles 22, Calif., RAymond 3-8361 • **SOUTHWEST:** 7905 Empire Freeway, Dallas 7, Texas, FLeetwood 7-8167 • **GOV'T:** 224 N. Wilkinson St., Dayton 2, Ohio, BAldwin 6-2366; 1725 "K" Street, N.W., Washington 6, D.C., FEderal 7-8500 AVAILABLE, TOO, THROUGH YOUR RCA DISTRIBUTOR

The Most Trusted Name in Electronics
RADIO CORPORATION OF AMERICA

July, 1960
Vol. 48 No. 7
Proceedings of the IRE

Poles and Zeros

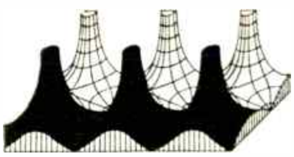

PGAP-SOET: The Professional Group on Antennas and Propagation has performed a valuable service by publishing the papers presented at the Symposium On Electromagnetic Theory. The Symposium was held at Toronto, Canada in June, 1959. It dealt with problems of diffraction and scattering theory, radio telescopes, surface waves, boundary value problems, the propagation of waves through various media, and antennas. The subjects treated are of great importance, bearing upon the various fields of radio from propagation through the atmosphere to the use of satellites as communication vehicles.

The Symposium papers were published as a Special Supplement to the December, 1959 issue of the PGAP Transactions. This 480 page document, for financial reasons, has not been distributed free of charge. Members of the PGAP may obtain copies for $8.00, other IRE members for $12.00. Why not order your copy from Headquarters now?

Correspondence. In 1959, 209 letters to the Editor were published in the correspondence columns of the PROCEEDINGS, requiring 166 pages. By the end of 1959, a backlog of letters had developed and the advantage of timeliness, an important function of the correspondence columns, had been impaired. This problem has been faced by the Editorial Board. After a careful study of the 1959 columns, a decision has been reached to establish a limit on the length of letters to be accepted for publication.

After July 15, the length of letters to the Editor will be limited to four double-spaced typewritten pages of manuscript. Illustrations, if any, will be counted as the equivalent of one-half page of manuscript. This will provide a limit on letters amounting to about two-thirds of a page. If such a limitation had been imposed in 1959, it would have been possible to have published approximately twenty per cent more letters. Undesirable publication delay would also have been avoided. Correspondents are urged to cooperate in the spirit of the intent of the limitation being imposed.

Houston and SWIRECO. The Executive Committee and the Board of Directors met in Houston last April in connection with SWIRECO. As usual when the Board meets outside of New York City, all were impressed with the hospitality and vitality of the IRE grass roots. The President had the honor of receiving the distinguishing mark of Texas, a glorious Stetson (5 or 10 gallon?). In addition, he was made an honorary citizen, in appropriate ceremonies.

On the more serious side, the Board received the reports of the Regional Directors, approved the formation of the Las Vegas Section as number 106, and passed a resolution honoring the memory of Past-President J. W. McRae, whose untimely death was reported in the PROCEEDINGS in March. The resolution was engrossed, and has been presented to Mrs. McRae by President McFarlan.

Student Quarterly. As the academic year has ended, and the Editor has given thought to the problems of IRE and education (see advertisement below), the accomplishments of the STUDENT QUARTERLY appear to be outstanding. This publication, which has grown in stature from year to year, deserves the attention of all members of the IRE. Many are subscribers and many more should be for their own edification. The issue of the STUDENT QUARTERLY for May, 1960 is an excellent example of the quality of this IRE product.

The May issue featured the following articles: "Electron Tubes Meet the Challenge of Modern Technology," by J. E. Beggs; "High Fidelity Sound Reproduction," by H. F. Olson; "Radio Waves from the Sun," by M. H. Cohen; "Why Is a Teacher," by R. G. Fellers; "Cryogenics—A Survey," by A. Juster and P. A. Shizume; and "Ferroelectric Capacitors in a Frequency Modulated VFO," by C. S. Rockafellow.

With no intent of slighting any of the authors of these excellent articles, and singling out one paper for comment, the Editor takes the liberty of recommending the Olson article for reading by every member of the IRE who is interested in hi-fi and stereo. Some will certainly contend that this article is an excellent candidate for reprinting as a review article in the PROCEEDINGS. The Editor will contend that this article and its companions provide excellent reasons for members to have their own copies of the STUDENT QUARTERLY. Subscriptions may be sent to IRE Headquarters. The STUDENT QUARTERLY is published in September, December, February, and May; send in your $3.00 for the 1960–1961 academic year now.

Advertisement. At a recent meeting of the Executive Committee, the Editor, as part of his report on editorial matters, stated that it was his intention to write an article for Poles and Zeros about IRE and education. One member of the Executive Committee declared that this was much too important a matter "to be buried in Poles and Zeros." After a deep swallow of pride at this unflattering, and perhaps truthful, remark about the arduous monthly labors of the Editor, and with the concurrence of the other members of the Executive Committee, the Editor bowed before so much accumulated wisdom and set forth to tell the story for IRE members and posterity. The result appears in this issue; after reading "An Aspect of the IRE," you may decide that it would have been better to have "buried" it. ADVERTISEMENT.—F. H., Jr.

C. W. Carnahan

Director, 1960–1961

C. Wesley Carnahan (A'34–SM'45–F'52) is Director of Planning, Central Research, at Varian Associates, Palo Alto, Calif., where he has been a member of the staff since 1953.

In his Varian post he assists Edward W. Herold, Vice President, Research, with the planning and administration of The Central Research Department, which was organized to allow the company to enter new fields of scientific investigation not within the scope of the research and development groups of Varian's operating divisions.

He was born July 4, 1907, in Berkeley, Calif., and received both the B.A. and M.A. degrees in physics from Stanford University, Stanford, Calif.

He served as instructor in physical sciences at Fresno State College from 1927 to 1930. After completing work for the M.A. degree in 1931, he joined Farnsworth Television, where he was employed in the field of television transmission and reception.

In 1933 he joined Hygrade Sylvania Corporation, where he worked for four years in the development of special tubes and lamps at the Salem, Mass., laboratory, and for three years at the St. Marys, Pa., laboratory, on design and testing of cathode ray tubes for television.

He then went to Zenith Radio Corporation as a research engineer in 1940. There he was involved in the dedevelopment of frequency modulation and television receivers, and, during World War II, on radar systems. From 1947 to 1948 he was senior engineer at Submarine Signal Company, in charge of the circuit development of submarine fire control radar.

In 1948 he joined Sandia Corporation as manager of the Electronics Research Department, engaged in the development of classified electronics devices. He was with Sandia until 1953.

Mr. Carnahan was awarded the degree of Fellow by the IRE "for original contributions in the field of frequency modulation, television, and electronics systems engineering." He was a member of the Paper Reviews Committee from 1945 to 1948, and served on the Board of Editors from 1948 to 1954. He was chairman of the first Seventh Region IRE Conference.

He holds six patents in the field of frequency modulation and television, and is the author of several papers in these fields.

Scanning the Issue

An Aspect of the IRE (Hamburger, p. 1216)—As noted on the Poles and Zeros page of this issue, the Executive Committee has prevailed upon the Editor of the IRE to describe an important area of IRE activity with which most members have all too little familiarity—the IRE student program. The grade of Student is now the second largest grade of membership in the IRE, accounting for 21 per cent of the total membership. The IRE STUDENT QUARTERLY, now entering its seventh year of publication, ranks second in circulation among IRE's 30 periodicals. As the author traces the threads of service which make up the fabric of the student program, the reader will find them woven into every segment of the IRE structure.

Low-Noise Parametric Amplifier (Knechtli and Weglein, p. 1218)—This paper should interest everyone with either a theoretical or practical interest in parametric amplifiers for low-noise receiving systems. The authors derive expressions which make it possible to relate the noise figure and pump power of a parametric amplifier directly to the actual parameters of the nonlinear reactance and associated circuits. Of particular interest are the discussions of the ultimate lower noise limit, the effects of cooling various circuit elements, and optimum pump frequency.

Theory of Single-Resonance Parametric Amplifiers (Fisher, p. 1227)—The author proposes a parametric amplifier in which the tuned circuit at the signal frequency is eliminated, leaving a tuned circuit just at the idler frequency. With only one circuit to tune, the fixed-tuned operation of parametric amplifiers, which is now almost mandatory, is no longer necessary. This simplification thus makes a continuously tunable parametric receiver much more pratical.

The Persistor—A Superconducting Memory Element (Crittenden, *et al.*, p. 1233)—The development of the cryotron in 1956 ushered in a new class of circuit component which made use of the superconductive properties of certain materials at extremely low temperatures. The cryotron was in essence a tiny bi-stable element which could be switched from a superconducting state to a resistive state by applying a magnetic field. Although the switching speed of the cryotron was too slow to make it attractive for computer applications, its development spurred an intensive search for new and improved forms of superconducting computer components. One such component has now emerged. The Persistor is a configuration of superconducting thin films which can store current pulses. It is very fast, with a switching time of 15 millimicroseconds or less, as compared to a millisecond for the cryotron. It is also very compact. Densities of a million units per cubic foot are possible. The Persistor represents an important step toward the eventual development of microminiature very-high-speed large-capacity computers.

Limitations and Possibilities for Improvement of Photovoltaic Solar Energy Converters (Wolf, p. 1246)—Last March, the following two events took place within a week of one another: (a) an electric car with an array of solar cells mounted on its roof spent a sunny afternoon riding around Central Park in New York City; (b) Pioneer V began sending signals from space by means of a 5-watt transmitter powered by 4800 solar cells. Ten weeks and 10 million miles later, the signals were still coming in. These events are indicative of the rapid strides that have been made in the development of practical solar energy converters in the last six years. This progress, in turn, foretells of further substantial progress in the next six years. The broad survey and evaluation of various conversion devices presented here provide a valuable guide to the many engineers interested in energy conversion and in avenues for further advances in materials and devices.

A New Class of Switching Devices and Logic Elements (McIsaac and Itzkan, p. 1264)—This paper adds a sturdy strand to the growing bond between microwave techniques and computer technology which, it is expected, will lead to enormous increases in computer speeds. By employing electron beams and circuit elements closely related to those used in microwave tubes, the authors have developed a variety of devices that are capable of performing switching and logic at clock time intervals of one millimicrosecond, an improvement of about 10^3 over conventional computers.

Skin Effect in Semiconductors (Frei and Strutt, p. 1272)—The well-known skin effect formulas for metallic conductors have now been extended to semiconductor materials. In the light of the recent increased activity in the use of semiconductors at microwave frequencies, this work becomes a quite general interest.

A Microwave Meacham Bridge Oscillator (Sooy, *et al.*, p. 1297)—The Meacham bridge oscillator has long been used as a low-frequency standard of exceptional stability. Placing a resonant element in the feedback path will increase the stability of an oscillator. In the Meacham circuit, the stability is further enhanced by placing the resonant element in one arm of a bridge in the feedback loop. The authors have built a microwave version of the Meacham bridge oscillator and have found it has a very high short-term stability, potentially about 2 parts in 10^{n}, a fact which will interest many radar and other microwave systems engineers. If the resonant element takes the form of a very-high-Q molecular resonator, unprecedented short-term stabilities become possible.

Unidirectional Paramagnetic Amplifier Design (Strandberg, p. 1307)—This paper presents a thorough discussion of the design considerations for a cavity-type solid-state maser which utilizes circularly polarized fields to achieve unidirectional and nonreciprocal gain. Many design matters are discussed which have not been treated before. The unidirectional characteristic is especially interesting because it minimizes the necessity for using a circulator to isolate the input from the output. Eliminating the circulator would reduce the noise figure by an order of magnitude, an improvement of particular significance to radio astronomy.

Excitation of Piezoelectric Plates by Use of a Parallel Field with Particular Reference to Thickness Modes of Quartz (Beckmann, p. 1278)—The author discusses the excitation of a piezoelectric plate by a field parallel to the major surface rather than the usually used method of a field perpendicular to the surface. His experimental results show that this gives a higher inductance and Q, a result that will be of considerable interest in the precise control of oscillators.

Transient Behavior of Aperture Antennas (Polk, p. 1281)—This paper explores how long it takes for the steady-state beam pattern to form after an antenna is switched on. This transient interval is a function of antenna size. It also presents a limitation as to how rapidly electronic scanning can be accomplished without degrading system performance. With antennas of ever-increasing size being built and the growing use of rapid scanning radar systems, the transient behavior of antennas is becoming a matter of growing pertinence in systems engineering as well as antenna design.

Radar Target Classification by Polarization Properties (Copeland, p. 1290)—The subject of this paper is one of general interest to the whole radar field because of urgent requirements for improved methods of target identification. The author contributes to the subject by developing a mathematical model for representing the polarization transforming properties of radar targets which enables a better understanding of polarization phenomena and facilitates the radar measurements of polarization properties.

Scanning the Transactions appears on page 1351.

An Aspect of the IRE*

FERDINAND HAMBURGER, JR.†, FELLOW, IRE

Summary—**This paper presents a discussion of activities of the IRE as they are related to education. It considers the several aspects of the IRE contribution to education in terms of student membership, student branches, IRE representatives, the PROCEEDINGS, the STUDENT QUARTERLY, several committees, the Professional Group on Education, and the local Sections.**

THE IRE Constitution states, "Its objects shall be scientific, literary, and educational." Thus one of the fundamental concepts of the IRE is participation and activity in "education." The gathering and impartation of knowledge, both basic to the educational process, are involved in all activities of an IRE member including those of reading, or writing for the PROCEEDINGS or TRANSACTIONS, or attending meetings and symposia as spectator or participant.

With increasing frequency the members of the IRE have been raising the question as to what is being done by the IRE in the area of education. The question is asked, however, in a much more restricted sense; what is really being asked is what is the IRE doing for students. To provide information for those members of the IRE who are not fully aware of its activities in this field, and to set forth the background from which additional activities may stem, are the purposes of this paper.

The core of the IRE program is in the provision for students to become members of this professional society. Pupils studying in regular programs in schools of recognized standing are accepted into the grade of "Student," and those following programs of study in a technical institute or other school approved by the Executive Committee of the IRE are accepted into the grade of "Student Associate." Where groups of not less than fifteen students are associated, in a given institution, branches may be formed; these branches are called Student Branches or Student Associate Branches. The 183 Student Branches presently in operation in the United States and Canada will undoubtedly soon be increased by branches in countries outside North America in which IRE Sections now exist.

All student branches are sponsored by IRE Representatives who are IRE members and who teach at the institution at which the branch is formed. Each IRE Representative is charged with promoting the welfare of the IRE at his school, particularly in matters relating to student membership. To aid the IRE Representative in effectively carrying out his responsibilities, the IRE provides assistance in several forms; these will be discussed later.

To implement its program for both students and branches, the IRE provides substantial subsidies. Undoubtedly the most significant subsidy is that provided to the student, as an individual, in the form of the publications made available to him. All Students and Student Associates receive the PROCEEDINGS and the STUDENT QUARTERLY as a part of their membership privilege. In addition, each student may join and participate in the activities of a Professional Group of his choice, for the nominal additional fee of one dollar. This provides an automatic subscription to the TRANSACTIONS of that Professional Group; about one-half of the students presently take advantage of this opportunity. The student, like any other IRE member, may join as many other Professional Groups as he desires, at the regular Group rate.

The program of Special Issues of the PROCEEDINGS has made a particular contribution to the educational aspect of the IRE. In fact, members of the IRE are recognizing these Special Issues as "textbooks" in their own right; so also do professors and students. Issues on Color Television, Transistors, Computers, Scatter Propagation, Infrared and many others, have been of especial value for their timely availability.

The STUDENT QUARTERLY is a particularly outstanding contribution to the IRE program for students. This magazine, published four times per year, is specifically designed for students. It contains articles written especially for them by outstanding members of the IRE and other contributors. For example, in the most recent issues will be found articles authored by such famous names as James A. Van Allen, F. E. Terman, Archie W. Straiton, J. R. Weisner, and Ronald L. McFarlan. The caliber of the STUDENT QUARTERLY is of such stature that many IRE members are regular subscribers, and the number continually increases.

That this program constitutes a substantial subsidy to student members is emphasized by the fact that the student membership fee is actually less than one-half the cost to the IRE of printing and mailing the PROCEEDINGS. In addition to the subscription to the STUDENT QUARTERLY, another component of the subsidy, each student may receive, upon request, a student pin. Book covers, embossed with the IRE emblem, are also available.

The student activity is also supported by the IRE program of financial allowances to the student branches. For both Student Branches and Student Associate

* Received by the IRE, April 14, 1960.
† The Johns Hopkins University, Baltimore 18, Md.

Branches, per capita rebates are provided, based on student branch membership. Additionally, an allotment for branch operation is made available. Each branch is entitled to a charter certificate and the IRE even helps defray the cost of framing. Free stationery is provided for branches, and in the case of branches that operate jointly with those of another professional society, an allowance for printing is available in lieu of stationery.

The program outlined above, dealing directly with students, is supplemented throughout the entire organizational structure of IRE. From the Board of Directors and its Executive Committee, through the several echelons to the local Sections of the IRE, consideration is continually given to educational and student matters. There is seldom a meeting of either the Board of Directors or the Executive Committee that does not devote some portion of its time to these areas.

The IRE By-laws provide for an Education Committee as one of the Standing Committees. The Education Committee is charged with advising the Executive Committee and the Board of Directors in the field of education. It is the intent that this committee consider matters relating to electronic engineering education in all areas, including the high schools, the technical institutes, and both undergraduate and graduate education in the universities and colleges.

The Professional Group structure, as mentioned above, contains the Professional Group on Education, providing another mechanism for attention to educational matters. This Group serves as a forum on education by providing seminars and publications for the discussion of educational philosophy, problems, and methods. Promotion of discussion of technical education and educational methods at all levels, and cooperation with other organizations in the interest of electronics in education, are the principal objectives of the Group.

In the eight Regions of the IRE, the emphasis on education continues. Each Region has established a Regional Education Committee which is responsible for handling all educational problems of the Region. This includes Student Member and Student Branch operations, supervision of student paper contests, and similar activities held on a Regional basis. All IRE Representatives in colleges and technical institutes in a Region are members of the Regional Education Committee. The IRE provides funds to pay the expenses of the Representative to one meeting per year of the Regional Education Committee, held within the Region.

The Professional Groups have demonstrated their interest in education and in students in one very tangible manner. At a number of specialized conferences and symposia, the Groups have arranged special sessions organized and planned in the interest of students. As examples, the Professional Group on Aeronautical and Navigational Electronics has on several occasions sponsored student sessions in connection with the annual East Coast Conference on Aeronautical and Navigational Electronics; the Professional Group on Instrumentation has held a student session in connection with the annual IRE Instrumentation Conference.

The 105 IRE Sections are all well aware of the importance of the educational activities that are significant adjuncts to the functions of the local Sections. Each Section appoints a Student Coordinator who serves as a member of the Section Executive Committee and is responsible for assisting the Student Branches within the local Section area. To list or discuss all of the varied types of student interest functions of local Sections is impractical. The most common might be mentioned. Student Nights are arranged by many Sections to provide an opportunity for students to mingle with and meet practicing members of the profession. Student prizes of several different types are offered by Sections usually in such form as to stimulate the embryonic engineer in written and oral presentation of scientific and engineering material. Many Sections do not confine their interest in educational problems to the university and college or technical institute level; increasingly the sections are taking an interest in the problem of guidance of the high-school student. To this end they plan and organize meetings and discussions to aid these students in the difficult problems surrounding decisions on the proper ultimate occupation.

Through these various methods of participation in student matters, the IRE is making a substantial contribution to education and is simultaneously fulfilling one of its basic objectives. It is the intention of the IRE to continue its present program and to modify or extend its activities as additional opportunities for service to the cause of education are recognized.

Low-Noise Parametric Amplifier*

R. C. KNECHTLI†, MEMBER, IRE, AND R. D. WEGLEIN†, SENIOR MEMBER, IRE

Summary—**The theory of the parametric amplifier has been reformulated to permit the prediction of noise temperature and pump power in terms of the physical parameters of the nonlinear element and circuit. The results of this analysis are supported by careful experiments at S-band using a gold-bonded germanium semiconductor diode. They can be summarized as follows.**

1) **Performance of a parametric amplifier using semiconductor diodes with respect to noise temperature and pump power can be accurately predicted, once the diode and circuit parameters have been measured.**
2) **It is shown that the ultimate limitation on noise temperature depends simply on the product of the diode cutoff frequency and the normalized capacitance swing.**
3) **The derived figure of merit for the diode can serve as a basis for optimum design of the semiconductor parameters.**

I. Introduction

Although expressions for the gain, bandwidth and noise figure of parametric amplifiers have been derived in rather general terms,[1-3] it is still difficult to find from these expressions the effects of the actual parameters of the circuits and of the nonlinear reactance on the performance of a given amplifier.[4] It is the purpose of this paper to express the noise figure and the pump power of a parametric amplifier in terms of physical parameters directly measurable, even at microwave frequencies. A further purpose is to show how the Q, the law of reactance variation of the nonlinear element, and its temperature impose an ultimate limit on the minimum noise figure attainable with a parametric amplifier and how this limit scales with frequency. For the present purpose, the nonlinear reactance is assumed to be a semiconductor diode operated in the reverse-bias region as a voltage-dependent capacitance. The relations that follow can, however, be readily modified to apply to other types of nonlinear reactances as well.

II. Basic Relations

The relations needed in this paper are those for the gain and the noise figure of a parametric amplifier. Because the variable reactance is to be a variable capacitance, it is convenient to derive these expressions for the equivalent circuit in Fig. 1 where the susceptances B_s, B_i, and B_p represent parallel L-C tank circuits resonant respectively at the signal frequency f_s, the idler frequency f_i, and the pump frequency f_p. At this point, it is important to make the following remarks.

1) For minimum noise figure, it is desirable to use a circulator[5] to separate the input conductance G_g from the load conductance G_L. When a circulator is used, the signal circuit sees *only* the load G_L; hence, the total conductance seen by this circuit does *not* include the input conductance G_g. From the standpoint of noise, only that originating in the generator conductance enters the amplifier; therefore it sees only the generator conductance and does *not* see the load conductance. Because, in the present considerations, $G_L=G_g$, the notation "G_g" will be used indiscriminately to represent either G_g or G_L.

2) In this equivalent circuit, the diode losses are represented by a conductance G_d. In fact, the significant measure of diode losses is the quality factor Q_d of the diode at the frequency considered; G_d is then obtained from Q_d by the relation $G_d=\omega C_d/Q_d$ where Q_d is measured at the frequency ω. If the losses were represented by a series resistance R_s, the relation between G_d and R_s would be given by

$$Q_d = \omega C_d/G_d = 1/\omega C_d R_s; \qquad G_d = R_s(\omega C_d)^2.$$

The representation of these losses by a parallel conductance G_d in the circuit in Fig. 1 is purely for mathematical convenience and will not affect the results,

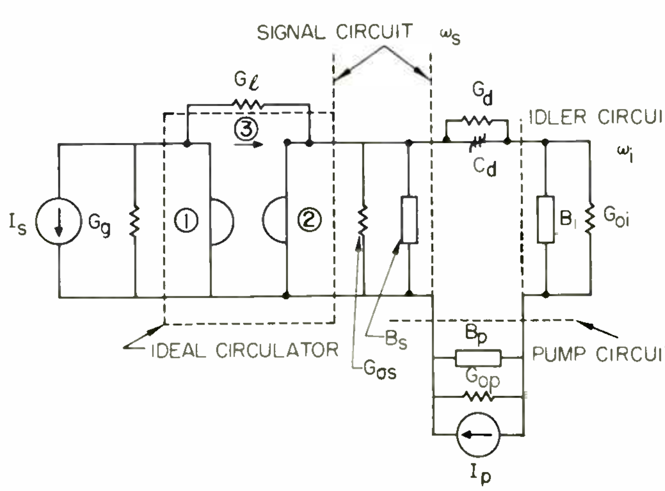

Fig. 1—Lumped-circuit model with circulator.

* Received by the IRE, October 15, 1959; revised manuscript received, February 26, 1960.
† Research Labs., Hughes Aircraft Co., Malibu, Calif.

[1] S. Bloom and K. K. N. Chang, "Theory of parametric amplification using nonlinear reactances," *RCA Rev.*, vol. 18, pp. 578–596; December, 1957.

[2] H. E. Rowe, "Some general properties of nonlinear elements. II. Small signal theory," Proc. IRE, vol. 46, pp. 850–860; May, 1958.

[3] H. Heffner and G. Wade, "Gain, band width and noise characteristics of the variable parameter amplifier," *J. Appl. Phys.*, vol. 29, pp. 1321–1331; September, 1958.

[4] M. Uenohara, "Noise consideration of the variable capacitance parametric amplifier," Proc. IRE, vol. 48, pp. 169–179; February, 1960. Uenohara's paper, which was published after the present paper had been submitted for publication, comes closest to relating physical circuit and diode parameters to amplifier characteristics, insofar as Uenohara's motives seemed to coincide with those of the present authors.

[5] This is true as long as the coupling of the load (output) to the signal circuit is not kept much smaller than the coupling of the signal generator (input) to the signal circuit. Because, for maximum gain-bandwidth product, it is desirable to have about the same coupling of both in- and out-put to the signal circuit, it is then desirable, for minimum noise as well as for stability, to use a circulator.

since in the final expressions, Q_d rather than G_d will be used. It should, however, be pointed out that in this representation G_d will, in general, be frequency dependent. Hence the G_d will be characterized by an additional index s, i, or p, respectively, to indicate that the value of G_d corresponding to signal, idler, or pump frequency is to be taken [*e.g.*, $G_{ds}=R_s(\omega_s C_d)^2=$ value of G_d at signal frequency]. It should also be pointed out that this analysis, C_d represents the actual capacitance of the semiconductor junction and Q_d the quality factor associated with the capacitance C_d only (excluding the reactances of the series inductance and shunt capacitance of the diode package).

3) In a parametric amplifier, in particular at microwave frequencies, the various circuits and the diode are not directly coupled. For this reason, the conductances and susceptances shown in Fig. 1 are not the actual values corresponding to each element but rather those seen at a given common reference plane. In the final expressions, only *ratios* of conductances seen at this plane will appear; these ratios will be found to be equal to ratios of quality factors Q and independent of the choice of the reference plane. For this reason, the equivalent circuit in Fig. 1 still remains useful for the present considerations, without any need for specifying further the common reference plane.

The derivation of the gain and noise-figure expressions for the amplifier represented in Fig. 1 is, in many respects, a dual of that given by Bloom and Chang;[1] the circuit in Fig. 1 is itself a dual of the circuit proposed by these authors. The two significant differences in our dual are the assumed circulator and the inclusion of the lossy part of the nonlinear element; these somewhat modify the final expressions but do not alter the steps in deriving them. For this reason, the details of the analysis are omitted, and the results are given. If a law of variation of C_d given by (1) is assumed,

$$C_d = C + \mathcal{C}V, \tag{1}$$

where

$C=$ diode capacitance in the absence of RF voltage,
$V=$ instantaneous RF pump voltage,

then one obtains for the power gain A (on the assumption of an ideal circulator)

$$A = \left|\frac{G_{gs} - Y_s}{G_{gs} + Y_s}\right|^2 \tag{I}$$

where

$$Y_s = G_s - |G| + j\left[B_s - |G|\frac{B_i}{G_{ti}}\right]$$

$$|G| \simeq \alpha G_{ts}\left|1 + j\frac{B_i}{G_{ti}}\right|^{-2}$$

$$\alpha = \frac{\omega_s\omega_i\Delta C^2}{4G_{ts}G_{ti}} \tag{2}$$

$$\Delta C = C_{\max} - C_{\min} \cong 2\mathcal{C}\hat{V}_p \text{ [from (1)]}$$

$$\hat{V}_p = \text{pump voltage amplitude.} \tag{3}$$

Further definitions useful in this derivation are

$G_{ts} = G_{os} + G_{gs} + G_{ds}$
$G_s = G_{os} + G_{ds}$
$G_{ti} = G_{oi} + G_{gi} + G_{di}$
$G_p = G_{op} + G_{dp}$
$B_s =$ total signal circuit susceptance
$B_i =$ total idler circuit susceptance

G_{os}, G_{oi}, G_{op} = conductances corresponding to losses in unloaded signal, idler, and pump resonant circuits, respectively

G_{gs}, G_{gi} = effective generator conductances as seen by signal and idler circuits, respectively.

If it is assumed that the signal circuit and the diode have temperatures T_s and T_d, respectively, and that the idler circuit has an effective temperature $T_{i,\,\mathrm{eff}}$ (these three temperatures are not necessarily all the same), then the following expression is obtained for the noise figure F[6] under the condition of high gain ($\alpha\to 1$):

$$F \cong 1 + \frac{T_s}{T_o}\left(\frac{G_{os}}{G_{gs}}\right) + \frac{T_d}{T_o}\left(\frac{G_{ds}}{G_{gs}}\right) + \frac{T_{i,\mathrm{eff}}}{T_o}\left(\alpha\frac{\omega_s}{\omega_i}\right)\left(1 + \frac{G_s}{G_{gs}}\right) \tag{II}$$

where T_o is the reference temperature for which the noise figure F is defined.

Eqs. (I) and (II) are the basic relations on which the subsequent derivation will be based.

III. Pumping Power

A. Definition of Critical Pump Power P_{cr}

The critical pump power is defined as the pump power at which oscillation starts when signal, idler, and pump circuits are tuned to resonance ($B_s=B_i=0$). According to this definition and (I), the critical pump power is the pump power needed to make $\alpha=1$. The actual pump power corresponding to $\alpha<1$ (finite gain) is related to P_{cr} according to the definition of α by

$$P_{\mathrm{pump}} = \alpha P_{cr}. \tag{4}$$

Indeed,

$$\alpha \propto \Delta C^2 \propto \hat{V}_p^2 \propto P_{\mathrm{pump}}.$$

B. Evaluation of Critical Pump Power P_{cr}

To find P_{cr} by using (2), the condition $\alpha=1$ is written

$$\frac{\omega_s\omega_i\Delta C^2}{4G_{ti}G_{ts}} = 1. \tag{5}$$

[6] The relation between $T_{i,\,\mathrm{eff}}$ and the actual temperature of the idler circuit will be derived later (see Appendix I).

The pump power is introduced into (5) by substituting, according to (1) and (3),

$$\Delta C^2 = (2\mathcal{C}\hat{V}_p)^2 = 8\mathcal{C}^2\left(\frac{P_{cr}}{G_p}\right). \tag{6}$$

From (5) and (6)

$$P_{cr} = \frac{G_{ts}G_{ti}G_p}{2\omega_s\omega_i\mathcal{C}^2}. \tag{7}$$

Eq. (7) may be written as follows, according to the definitions of G_{ts}, G_{ti}, and G_p:

$$P_{cr} = \frac{\omega_s C}{2}\left(\frac{G_{os}G_{oi}G_{op}}{\omega_s\omega_i\omega_p C^3}\right)\left(\frac{\omega_p}{\omega_s}\right)\left(\frac{C}{\mathcal{C}}\right)^2\left(1 + \frac{G_{gs}}{G_{os}} + \frac{G_{ds}}{G_{os}}\right) \cdot\left(1 + \frac{G_{gi}}{G_{oi}} + \frac{G_{di}}{G_{oi}}\right)\left(1 + \frac{G_{dp}}{G_{op}}\right). \tag{8}$$

It is now useful to define the following quality factors and ratios of quality factors:

Q_{os}, Q_{oi}, Q_{op} = unloaded Q of signal, idler, and pump circuit, respectively.

Q_{ds}, Q_{di}, Q_{dp} = external Q of signal, idler, and pump circuit, respectively, when circuit is loaded by diode only. (Q_{ds}, Q_{di}, $Q_{dp} \not\equiv Q_d$ at frequencies w_s, w_i, w_p, respectively.)

Q_{gs}, Q_{gi} = external Q of signal and idler circuits, respectively, when loaded only by generator conductances G_{gs} and G_{gi}, respectively.

Q_d = actual diode Q at signal frequency.

Further, let

$$k_{ds} = \frac{Q_{os}}{Q_{ds}} \equiv \frac{G_{ds}}{G_{os}}. \tag{9}$$

Similar relations defining k_{di} and k_{dp} can be written for the idler and pump circuits.

$$\mu_s = \frac{Q_{ds}}{Q_{gs}} = \frac{G_{gs}}{G_{ds}}; \qquad \mu_i = \frac{Q_{di}}{Q_{gi}} = \frac{G_{gi}}{G_{di}}. \tag{9a}$$

With (9) and (9a), (8) becomes

$$P_{cr} = \frac{\omega_s C}{2}\left(\frac{C}{\mathcal{C}}\right)^2\left(\frac{G_{ds}}{\omega_s C}\right)\left(\frac{G_{di}}{\omega_i C}\right)\left(\frac{G_{dp}}{\omega_p C}\right)\left(\frac{\omega_p}{\omega_s}\right) \cdot\left(1 + \mu_s + \frac{1}{k_{ds}}\right)\left(1 + \mu_i + \frac{1}{k_{di}}\right)\left(1 + \frac{1}{k_{dp}}\right). \tag{8a}$$

Note that in the absence of idler load, $\mu_i = 0$.

A good microwave diode has a quality factor practically inversely proportional to frequency.[7]

Hence

$$\frac{\omega_s C}{G_{ds}} = Q_D; \quad \frac{\omega_i C}{G_{di}} = \frac{\omega_s}{\omega_i}\cdot Q_D; \quad \frac{\omega_p C}{G_{dp}} = \frac{\omega_s}{\omega_p}\cdot Q_D.$$

[7] This corresponds to the frequency-independent "series resistance" of the diode.

Eq. (8a) then becomes

$$P_{cr} = \frac{\omega_s C}{2Q_D^3}\left(\frac{C}{\mathcal{C}}\right)^2\left(\frac{\omega_i}{\omega_s}\right)\left(\frac{\omega_p}{\omega_s}\right)^2\left(1 + \mu_s + \frac{1}{k_{ds}}\right) \cdot\left(1 + \mu_i + \frac{1}{d_{di}}\right)\left(1 + \frac{1}{k_{dp}}\right). \tag{III}$$

The expression for the pump power is interesting because it is given in terms of directly measurable diode parameters. The k's and μ's are ratios of Q's and therefore measurable by standard techniques, even at microwave frequencies.

In addition to this, one observes the following from (III).[8]

1) The pump power increases with diode losses as $1/Q_D^3$.
2) For given ratios of ω_i/ω_s and ω_p/ω_s, the pump power increases with the fourth power of the signal frequency.
3) The pump power decreases with increasing diode nonlinearity as $(C/\mathcal{C})^2$.

IV. Noise Temperature

A. Definitions

The excess noise temperature T_n of an amplifier whose power gain is G and bandwidth Δf is defined by the relation

$$kT_n\Delta f = N/G$$

where N is the noise power generated in the amplifier and available at the output. Hence

$$T_n = \frac{N}{kG\Delta f}. \tag{10}$$

Because the excess noise temperature (which will be simply called "noise temperature" in this paper) is a more fundamental quantity than the noise figure, noise temperatures rather than noise figures will be considered henceforth. The relation between both is

$$F = 1 + \frac{T_n}{T_o}, \tag{11}$$

where T_o is the reference temperature for which the noise figure is defined.

In a parametric amplifier, it is important to observe that there are in general two channels of amplification: the signal channel and the idler channel, of respective bandwidths Δf_s and Δf_i. (In general, $\Delta f_s = \Delta f_i$ even though $f_s \neq f_i$.) In a conventional system, input signals are provided to the signal channel only, so that for this case $\Delta f = \Delta f_s$ in (10). The noise temperature corresponding to this conventional case will be called the "single-channel noise temperature," and its corresponding noise figure, the "single-channel noise figure."

[8] The first two of the following remarks are valid only when the diode Q is inversely proportional to frequency and when μ_s and μ_i are kept constant (constant diode contribution to noise temperature, as shown in Section IV).

B. Single-Channel Noise Temperature T_{n1}

From (11), the following expression is found for the single-channel noise temperature T_{n1} of a parametric amplifier:

$$T_{n1} = \frac{1}{k_{gs}} T_s + \frac{1}{\mu_s} T_d + \alpha \frac{\omega_s}{\omega_i}\left(1 + \frac{1}{k_{gs}} + \frac{1}{\mu_s}\right)(T_{i,\text{eff}}) \qquad (12)$$

where

$$k_{gs} = \frac{Q_{os}}{Q_{gs}} = \frac{G_{gs}}{G_{os}}.$$

At this point, the significance of the effective idler-circuit temperature $T_{i,\text{eff}}$ must be scrutinized. In the most general case, the idler circuit, which itself is at temperature T_{oi}, can be coupled to a diode of temperature T_d and to an external load of temperature T_{li}. Part of the Johnson noise at the idler frequency is then generated at temperature T_{oi}, part at temperature T_d, and part at T_{li}. From these considerations, an expression for $T_{i,\text{eff}}$ is derived in Appendix I. Introducing this into (12) yields

$$T_{n1} = \frac{1}{k_{gs}} T_s + \frac{1}{\mu_s} T_d + \alpha \frac{\omega_s}{\omega_i}\left\{\frac{1 + \frac{1}{k_{gs}} + \frac{1}{\mu_s}}{1 + \frac{1}{kl_i} + \frac{1}{\mu_i}}\right\} \cdot \left(T_{li} + \frac{1}{\mu_i} T_d + \frac{1}{k_{li}} T_{oi}\right) \qquad \text{(IV)}$$

where

$$k_{li} = \frac{Q_{oi}}{Q_{li}} = \frac{G_{li}}{G_{oi}}.$$

Eq. (IV) is the general expression for the single-channel noise temperature of a parametric amplifier. A few special cases of particular interest may now be pointed out.

1) *No Idler Load:* In this case, $G_{li}=0$, hence $k_{li}=\mu_i=0$. (However, $k_{li}/\mu_i=k_{di}\neq 0$!) Further, let the circuit losses be relatively small so that k_{gs} and $k_{di}\gg 1$. Then from (IV)

$$T_{n1} \cong \frac{1}{k_{gs}} T_s + \left(\frac{1}{\mu_s} + \alpha \frac{\omega_s}{\omega_i}\right) T_d + \alpha \frac{\omega_s}{\omega_i} \cdot \frac{1}{k_{di}} \cdot T_{oi}. \qquad \text{(IVa)}$$

It is interesting to observe that here the contributions of the idler-circuit temperature T_{oi} to the amplifier noise temperature T_n becomes negligible if $k_{di} \gg T_{oi}/T_d$. This is explained by the fact that most of the noise at the idler frequency then is generated in the diode at a temperature T_d rather than in the rest of the idler circuit. This condition is also particularly favorable for the reduction of amplifier noise temperature T_n by cooling of the diode (reduction of T_d). Because the diode itself is quite small, cooling it to a low temperature is a rather simple process which could be carried out, *e.g.*, thermoelectrically at little expense of power or weight. It is important to realize that to gain this advantage, it is *not* necessary to cool the *whole* circuit.

2) *Heavy Idler Load:* Consider an external load of temperature T_{li} strongly coupled to the idler circuit. Let

$$k_{li},\ k_{gs},\ \mu_s, \quad \text{and} \quad \mu_i \gg 1.$$

Then[9]

$$T_{n1} = \frac{1}{k_{gs}} \cdot T_s + \left(\frac{1}{\mu_s} + \alpha \frac{\omega_s}{\omega_i} \frac{1}{\mu_i}\right) \cdot T_d + \alpha \frac{\omega_s}{\omega_i} T_{li} + \alpha \frac{\omega_s}{\omega_i} \cdot \frac{T_{oi}}{k_{li}}. \qquad \text{(IVb)}$$

It is seen that reducing the idler-load temperature T_{li} (*e.g.*, by coupling to an antenna looking at the cold sky) may make the contribution of the idler noise to the single-channel noise temperature rather negligible.

It should, of course, be observed that making $\mu_i \gg 1$ so as to operate under conditions where (IVb) is valid can be done only at the expense of increased pump power. This conclusion follows directly from (III).

C. Double-Channel Noise Temperature T_{n2}

It is also of interest to consider the case where both signal and idler channels are effectively used. Here, there is one input at the signal frequency (bandwidth Δf_s) and another at the idler frequency (bandwidth Δf_i). If the two channels do not overlap, the total useful bandwidth is $\Delta f = \Delta f_s + \Delta f_i$. The noise temperature corresponding to this mode of operation will be called the "double-channel noise temperature" T_{n2} and is derived in Appendix II. In the special case where generator, load, and diode couplings to the signal circuit equal the corresponding couplings to the idler circuit, the double-channel noise temperature is found to be

$$T_{n2} \cong \frac{1}{k_{gs}} T_s + \frac{1}{\mu_s} T_d. \qquad \text{(IVc)}$$

It is assumed in (IVc) that the signal and idler circuits have the same temperature ($T_{oi}=T_s$), although the diode temperature T_d may still differ from T_s. Eq. (IVc) also applies in the quasi-degenerate case where signal and idler have approximately the same frequency and are both supported by the same circuit.

A few comments about the significance of the double-channel noise temperature as given, *e.g.*, by (IVc), are now in order.

1) The double-channel noise temperature represents the inherent noise generated in the amplifier itself, independently of external circuitry.

[9] The limits to the maximum values of μ_s and μ_i, which are interdependent, are discussed in Section VI.

2) The double-channel noise temperature can be measured directly by means of a broad-band noise source supplying white noise at the signal and idler frequencies.
3) As a consequence of 1) above, the double-channel noise temperature is closely related to the minimum single-channel noise temperature.

This latter remark is borne out; *e.g.*, in the case of a parametric amplifier with a heavy idler load whose temperature tends to zero; then (IVb) tends to the form given by (IVc) when T_{li} approaches absolute zero.

V. Noise Temperature and Pump Power with Low-Loss Circuits

Parametric amplifier circuits are termed "low-loss" when the unloaded Q greatly exceeds the loaded Q. According to this definition and (9), all factors k in (III) and (IV) are much greater than 1. Hence, with low circuit losses, (III) and (IV) may be simplified as follows:

$$P_{cr} \cong \frac{\omega_s C}{2Q_D^3}\left(\frac{C}{\mathcal{C}}\right)^2\left(\frac{\omega_p}{\omega_s}\right)^2\left(\frac{\omega_i}{\omega_s}\right)(1+\mu_s)(1+\mu_i). \tag{13}$$

With idler load:

$$T_{n1} \cong \frac{1}{\mu_s} T_d + \alpha\frac{\omega_s}{\omega_i}\left[\frac{1+\dfrac{1}{\mu_s}}{1+\dfrac{1}{\mu_i}}\right]\left(T_{li} + \frac{1}{\mu_i} T_d\right). \tag{14}$$

Without idler load:

$$T_n = \left(\frac{1}{\mu_s} + \alpha\frac{\omega_s}{\omega_i}\right)T_d. \tag{15}$$

Double-channel noise temperature:

$$T_{n2} \cong \frac{1}{\mu_s} T_d. \tag{15a}$$

It is clear from these relations that the amplifier noise temperature can be reduced at the expense of increased pump power by making μ_s larger. The physical explanation is that increasing μ_s and μ_i is accomplished by reducing the coupling of the diode to the signal and idler circuits. By this process, the amount of Johnson noise power coupled from the diode to the signal input is reduced, which in turn reduces the amplifier noise temperature. At the same time, however, the ratio between the transformed change of capacitance seen by the signal and idler resonant circuits and the actual change of diode capacitance is reduced. To keep the gain constant, the transformed change of capacitance must remain constant. Hence, as the diode coupling is reduced, the actual diode capacitance swing has to increase; this means an increase in pump power. The process, however, is limited to the maximum permissible swing in the capacitance. The maximum capacitance corresponds to incipient forward conduction; the minimum capacitance corresponds to incipient reverse breakdown. To what minimum noise temperature this limit corresponds will be shown in the next section.

VI. Minimization of Noise Temperature

A. External Idler Load

The first step toward minimizing the noise temperature of a parametric amplifier is obviously to minimize circuit losses. This follows directly from (IV) and leads to (14) or (15), depending upon the presence or absence of an external idler load.

The general case where μ_i is different from zero (external idler load) will now be considered. It is seen from (13) that to increase μ_s and μ_i, one must increase P_{cr}. The maximum tolerable value of P_{cr} corresponds to the diode voltage swings between incipient breakdown in the reverse direction and conduction in the forward direction. If V_B is the diode breakdown voltage, this condition corresponds approximately to $\hat{V}_{p\max} \cong \frac{1}{2}|V_B|$. Then from (13)

$$P_{cr} = \frac{\hat{V}_{p\max}^2 G_p}{2}$$

$$\geq \frac{\omega_s C}{2Q_D^3}\left(\frac{C}{\mathcal{C}}\right)^2\left(\frac{\omega_p}{\omega_s}\right)^2\left(\frac{\omega_i}{\omega_s}\right)(\mu_s+1)(\mu_i+1) \tag{16}$$

$$(\mu_s+1)(\mu_i+1) \leq \left(\frac{\hat{V}_{p\max}\mathcal{C}}{C}\right)^2\left(\frac{G_p}{\omega_s C}\right)(Q_D^3)\left(\frac{\omega_s}{\omega_p}\right)^2\left(\frac{\omega_s}{\omega_i}\right). \tag{17}$$

Let

$$\Delta C|_{\max} = |C_{\max} - C_{\min}|_{\max} = 2\hat{V}_{p\max}\mathcal{C}$$

and observe that with low circuit losses

$$G_p \cong G_{dp} = \left(\frac{\omega_p}{\omega_s}\right)^2 G_{ds}$$

$$\frac{G_{dp}}{\omega_s C} = \left(\frac{\omega_p}{\omega_s}\right)^2\left(\frac{1}{Q_D}\right).$$

Further, let the diode cutoff frequency f_c be defined by $f_c = Q_D f_s$. Then

$$(\mu_s+1)(\mu_i+1) \leq \frac{1}{4}\left(\frac{\Delta C_{\max}}{C}\right)^2\left(\frac{f_c}{f_s}\right)^2\left(\frac{f_s}{f_i}\right). \tag{18}$$

Eq. (18) together with (14) shows that minimum noise temperature is obtained by maximizing the product $(\Delta C_{\max}/C)\,(f_c/f_s)$.

B. No Idler Load

In the absence of an external idler load, $\mu_i = 0$ in (13). Hence, instead of (18), we have

$$(\mu_s+1) < \frac{1}{4}\left(\frac{\Delta C_{\max}}{C}\right)^2\left(\frac{f_c}{f_s}\right)^2\left(\frac{f_s}{f_i}\right) \tag{19}$$

$$T_{n1} \cong \left(\frac{1}{\mu_s} + \alpha\frac{f_s}{f_i}\right)T_d. \tag{20}$$

It is interesting to observe from (19) and (20) that in the present case *the minimum noise temperature is in principle not obtained for the highest possible idler frequency.*[10] Further, it should be remembered [see (13)] that increasing the idler frequency leads to a higher pump frequency; this in turn, together with the higher idler frequency, soon leads to excessive pump power from the standpoint of generating this power and dissipating it in the diode.

C. Quasi-Degenerate Case

In this case, signal and idler are supported by the same circuit ($f_p \cong 2f_s$; $f_i \cong f_s$). Both signal and idler are coupled through the same coupling elements to the signal generator (input) and to the load. Then $\mu_s = \mu_i = \mu$, from (18), (14) and (15a). With T_g = noise temperature of generator impedance:

$$(\mu + 1)^2 \leq \frac{1}{4}\left(\frac{\Delta C_{\max}}{C}\right)^2\left(\frac{f_c}{f_s}\right)^2 \tag{21}$$

$$T_{n1} = \frac{1}{\mu}(1 + \alpha)\cdot T_d + \alpha T_g \tag{22}$$

$$T_{n2} \cong \frac{1}{\mu} T_d. \tag{23}$$

Here again, it is apparent that minimum noise temperature is obtained by maximizing the product

$$\left(\frac{\Delta C_{\max}}{C}\right)\left(\frac{f_c}{f_s}\right).$$

D. Cooling of Diode

It is clear from (14), (15) and (15a) that with low-loss circuits, the amplifier noise temperature can be greatly reduced by cooling the diode. This implies, of course, that the diode performance is not degraded by cooling.[11] For germanium, *e.g.*, the cutoff frequency and $\Delta C_{\max}/C$ at liquid-nitrogen temperature can even be made larger than at room temperature.[10] It will be shown in Section VIII that the possibility of reducing the amplifier noise by cooling a germanium diode has been very well verified experimentally.

VII. Optimum Design of Semiconductor Diode

From (18) to (23), it is seen that minimum noise temperature is obtained when the product of cutoff frequency f_c times the relative capacitance swing $\Delta C_{\max}/C$ is made as large as possible. This condition is entirely determined by the diode parameters. The value of $\Delta C_{\max}/C$ is determined by the maximum permissible voltage swing (between breakdown and forward conduction). When the conductivity of the semiconductor is increased to make f_c larger, the breakdown voltage V_B decreases in magnitude. For small values of V_B, in the limit,

$$\left.\frac{\Delta C}{C}\right|_{\max} \cong \Delta V \left.\frac{1}{C(V)}\frac{dC(V)}{dV}\right|_{C\simeq\bar{C}} \tag{24}$$

The normalized derivative depends on the type of semiconductor junction (abrupt or graded) and is given by

$$\frac{\mathcal{C}}{C} = \left(\frac{1}{C}\right)\left(\frac{dC}{dV}\right) = \frac{m}{B + |V|} \tag{25}$$

where

$C = A(B + |V|)^{-m}$,
$m \cong 0.50$ for the abrupt junction,
$m \cong 0.33$ for the graded junction.

Hence, to minimize the amplifier noise temperature, the quantity to maximize, in the limit of small breakdown voltages, is

$$f_c\left(\frac{m}{B + |\bar{V}|}\right)V_B \tag{26}$$

where $\bar{V}$ = bias voltage for which maximum capacitance swing is obtained.

To effect this, it is desirable:

1) to make m as large as possible, and
2) to make $f_c \cdot |V_B|$ as large as possible.

While making m large points toward an abrupt rather than a graded junction, the possibility of making $f_c \cdot |V_B|$ larger with a graded junction may overshadow this advantage.

The value of the product f_c times $|V_B|$ is essentially determined by the donor and acceptor levels on either side of the semiconductor junction; maximizing this product defines an optimim value for these levels.

VIII. Experimental Verification

The present theory of low-noise parametric amplifiers has been experimentally verified by means of a 3.1-kmc waveguide cavity amplifier with a pump power equal to about twice the signal frequency. This amplifier used an early developmental version of the Hughes gold-bonded germanium diode of the type HPA2800. A waveguide four-port circulator was used with isolation in excess of 30 db and forward loss of 0.25 db per port. In addition, isolators were used at input and output (0.6 db forward loss and greater than 25 db isolation) to increase the precision with which noise temperature could be measured. Signal and idler frequencies were supported by the same lossless S-band cavity ($k_{os} \gg 1$) although these frequencies were clearly separated on a spectrum analyzer. Typical gain and bandwidth were

[10] This limitation is considered in more detail in a paper by R. D. Weglein, to be submitted for publication in the near future. A brief derivation for the optimum idler frequency is given in Appendix III. A similar result also is given in a private communication by H. A. Haus and P. Penfield, Jr., from M.I.T.

[11] If the cutoff frequency f_c were, *e.g.*, to decrease with decreasing temperature as a consequence of the reduction of the number of ionized charge carriers, (18) to (21) show that reducing the diode temperature would be futile.

measured to be 20 db and 12 mc, respectively, yielding a voltage gain-bandwidth product of 120 mc, which was found relatively constant over a wide range of gain. To evaluate the noise temperature accurately, the insertion loss between the noise lamp and the input to the signal-idler cavity was measured to an accuracy of 0.1 db and properly subtracted from the measured noise figures. In addition to these precautions, the effect on gain of any residual changes in the VSWR of the noise lamp (argon discharge lamp in waveguide holder) was checked and found to be nonexistent. Two second harmonic filters reduced the pump power level in the signal waveguide by more than 80 db. The double-channel noise temperature was measured and verified using two independent techniques. First, the noise temperature was optimized using the noise lamp in the stated arrangement with a commercial automatic noise figure meter. Because these measured values were low, they could be checked by resorting to an absolute method. In this latter technique, two matched terminations (VSWR ≤ 1.02) were used, one at room temperature and one at liquid nitrogen (78°K). At fixed amplifier gain, the noise power output of the amplifier was measured on a linear power detector when the input was alternately connected to each of these terminations. The results of these absolute measurements agreed within 0.1 db with the noise lamp measurements.

The theoretical relations to be verified by this experiment are obtained from (III) and (IVc) with $\mu_i = \mu_s$ and $1/k_{gs} \cong 1/k_{ds} \cong 0$. They are:

$$T_{n2} \cong \frac{1}{\mu_s} T_d \tag{27}$$

$$P_{cr} = P_0\left(1 + \frac{T_d}{T_{n2}}\right)^2 \tag{28}$$

$$P_0 = \frac{2\omega_s C}{Q_D^3}\left(\frac{C}{\mathcal{C}}\right)^2. \tag{29}$$

The lower theoretical limit for T_{n2} is determined by (21):

$$\mu_s \big|_{\max} = \frac{1}{2}\left(\frac{\Delta C_{\max}}{C}\right)\left(\frac{f_c}{f_s}\right) - 1. \tag{30}$$

It may be observed that except for the signal frequency ω_s, all the parameters in (27) to (30) are diode parameters. Inasmuch as this theory assumes a linear capacitance-voltage variation, while the behavior for the abrupt junction is closely approximated by a square-root relation, some arbitrariness is necessarily involved in choosing the operating point on the diode capacitance-voltage characteristic.[12] Some plausible arguments can be given in support of the procedure followed in this paper. For establishing the admittance level of the diode, the mean capacitance seems a reasonable choice. Thus

$$C = \bar{C} = 1/2(C_{\max} + C_{\min}) \tag{31}$$

is used in (29). For establishing the value of $\mathcal{C}/C$ in (29), the slope of the C-V curve of the diode is taken at the point determined by the bias voltage. Optimum bias voltage corresponds to maximum capacitance swing (maximum attainable μ_s and minimum noise temperature) and is obtained for

$$V = \bar{V} = 1/2(V_{\text{conduction}} + |V|_{\text{breakdown}}). \tag{31a}$$

Hence in (29)

$$\frac{\mathcal{C}}{C} = \frac{m}{B + |V|}\bigg|_{V=\bar{V}}. \tag{32}$$

The value of Q_D and f_c to be introduced in (27) and (29) also corresponds to the value of C given in (31).

With the above definitions, the measured parameters pertinent to this experiment are listed in Table I.

TABLE I

Measured		Derived	
$C_{\max}$	2.4 $\mu\mu$f	$\bar{C}$	1.5 $\mu\mu$f
$C_{\min}$	0.6 $\mu\mu$f	$\mathcal{C}/C$	0.131 volt^{-1}
R_s	4 ohms	f_c	26.5 kmc
V	3.0 volts	Q_D	8.6
B	0.3 volt	f_s	3.1 kmc
m	0.44		

Substituting the above values into (30) and (31) shows that to first order, $\mu_s|_{\max} = 4.1$.

The experimental verification of (28)–(30) (noise temperature vs pump power) is shown in Fig. 2. The theoretical curve of Fig. 2 is fitted to $P_0 = 7$ milliwatts and $\mu_s|_{\max} \simeq 2.4$, which is not at an unreasonable variance with the theoretical value $\mu_s|_{\max} = 4.1$ found above. (The actual value of μ_s could have been measured from the reflection coefficient of the "cold cavity," but this had not been recognized at the time when the data were taken.)

The experimental verification of (27) and (30) (noise temperature vs diode temperature) is shown in Fig. 3. To obtain the data shown on Fig. 3, the diode was cooled by conduction using a highly-polished silver plated copper rod which was placed in liquid nitrogen. The lowest diode body temperature T_d achieved in this way was 150°K, as determined by thermocouple measurements. The second-stage noise figure of 7 db never contributed more than 15°K to the noise temperature at the gain level used in the experiment (>20 db) but was *not* subtracted from the measured values. On cooling the diode to 150°K constant gain was maintained by decreasing the pump power about 25 per cent, indicating an increase in Q_D by about 11 per cent. The diode capacitance was not appreciably changed, so that no retuning was necessary. The measured curve of noise temperature vs diode temperature is compared on Fig. 3 to the theoretical curves corresponding to the two

[12] The quantity $\Delta C_{\max}/C$ can be determined in closed form. See S. Sensiper and R. D. Weglein, "Capacitance and charge coefficients for parametric diode devices," to be published. Proc. IRE, Correspondence section.

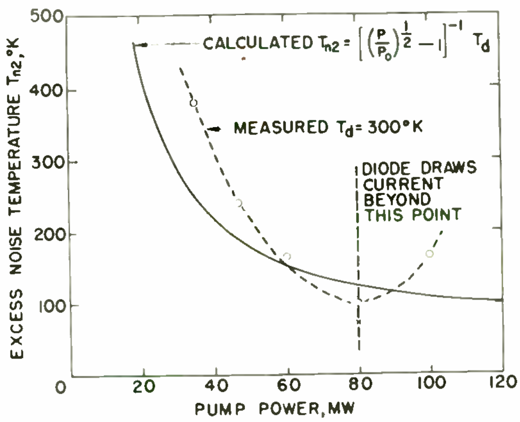

Fig. 2—Double-channel noise temperature vs pump power.

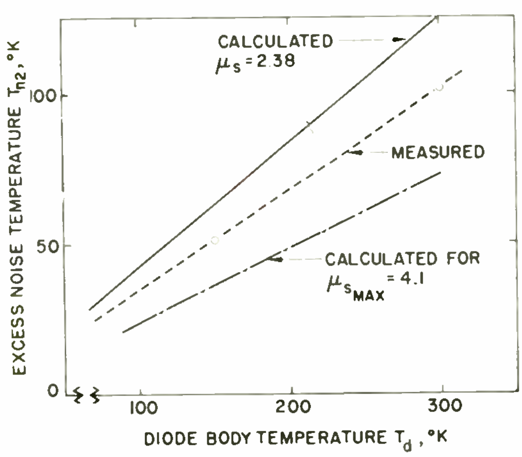

Fig. 3—Double-channel noise temperature vs diode temperature.

values of $\mu_s|_{\max}=4.1$ (calculated from diode parameters) and $\mu_s|_{\max}\cong 2.4$ (corresponding to best fit for data of Fig. 2). The agreement between theory and experiment is seen to be about as good as could be expected under the simplifying assumptions on which the theory is based. In particular, the fact that a linear capacitance vs voltage characteristic is assumed in the theory while the actual curve is not linear could well explain the major part of the moderate discrepancy observed between theory and experiment in Figs. 2 and 3.

IX. Conclusions

Expressions for the pump power and the noise temperature of parametric amplifiers have been derived in terms of directly measurable microwave circuit and diode parameters. Experimental verfication has been found to be adequate.

In the noise-temperature expressions, the effect of the temperature of the various elements on the amplifier noise temperature has been explicitly considered. The possibility of reducing the single-channel noise temperature by coupling the idler circuit to an external cold load has been pointed out. Further, the possibility of substantially reducing the amplifier noise by cooling the diode alone has been shown theoretically and experimentally.

The ultimate lower limit imposed by the diode parameters on the amplifier noise has been found to be a function of the product $(\Delta C/C)$ times f_c; this demonstrates that a large capacitance swing is as important as a high diode cutoff frequency.

The implication of this condition on the optimum design of a semiconductor diode is that the nonlinearity of the diode capacitance characteristic as well as the cutoff frequency should be maximized.

Appendix I

Effective Idler-Circuit Temperature

In line with the remarks in Section IV-B, the following expressions for the mean-square idler-noise current are applicable:

$$\frac{\overline{i^2}_{\text{idler}}}{4K\Delta f} = T_{i,\text{eff}}(G_{oi}+G_{li}+G_{di}) = T_{oi}G_{oi}+T_{li}G_{li}+T_dG_{di}.$$

Hence,

$$T_{i,\text{eff}} = \frac{T_{li} + \frac{1}{\mu_i}T_d + \frac{1}{k_{li}}T_{oi}}{1+\frac{1}{\mu_i}+\frac{1}{k_{li}}} \tag{33}$$

where k_{li} is defined by

$$k_{li} = \frac{Q_{oi}}{Q_{li}} = \frac{G_{li}}{G_{oi}}.$$

Appendix II

Double-Channel Noise Temperature

In this computation of the double-channel noise temperature T_{n2} of a parametric amplifier, it is assumed that if an output is also taken from the idler channel, the idler input and output are separated by a circulator in the same way as the input and output of the signal channel. Further, account is taken of the fact that an input signal fed to one channel is amplified by and provides useful output power in both channels. Let N_2 be the noise power generated within the amplifier and available at the output over the bandwidth Δf_s, where f_s is the center of this frequency band. Let G_{ss} be the power gain for a signal of input and output frequency f_s; let G_{is} be the power gain for a signal of input frequency f_i and output frequency f_s. Then, according to (10) and with $\Delta f_i=\Delta f_s$, the double-channel noise temperature at the output frequency f_s is

$$T_{n2} = \frac{N_2}{K\Delta f_s(G_{ss}+G_{is})}. \tag{34}$$

With coupling for maximum gain-bandwidth product,

$$G_{is} = \left(\frac{\omega_s}{\omega_i}\right)G_{ss}. \tag{35}$$

Further, because in the double-channel case the idler circuit is coupled to an input rather than to an external load, the noise-power output corresponding to the amplified noise coming from this idler input is *not* part of the noise N_2 generated in the amplifier itself. Hence,

$$N_2 = N_1 - KT_{li}G_{is}\Delta f_s \tag{36}$$

where

$$N_1 = KT_{n1}G_{ss}\Delta f_s \tag{37}$$

and

$$\Delta f_i = \Delta f_s.$$

Then, from (34)–(37),

$$T_{n2} = \frac{1}{1 + \frac{\omega_s}{\omega_i}}\left(T_{n1} - \frac{\omega_s}{\omega} T_{li}\right), \tag{38}$$

where $T_{li} \equiv T_g =$ temperature of the conductance of the input signal generator. (The idler "load" here is the input signal generator.) Let

$$\mu_i \gg 1, \quad k_{li} \gg 1, \quad \text{and} \quad \alpha\left(1 + \frac{1}{k_{ls}} + \frac{1}{\mu_s}\right) \cong 1.$$

Then, from (IV), (38), and with the assumption that $T_{oi} = T_s$ (signal and idler circuits at same temperature),

$$T_{n2} \cong \left[\frac{\frac{1}{k_{ls}} + \frac{\omega_s}{\omega_i}\frac{1}{k_{li}}}{1 + \frac{\omega_s}{\omega_i}}\right] T_s + \left[\frac{\frac{1}{\mu_s} + \frac{\omega_s}{\omega_i}\frac{1}{\mu_i}}{1 + \frac{\omega_s}{\omega_i}}\right] T_d. \tag{39}$$

In this particular case where couplings to the signal and idler circuit are equal, $k_{li} = k_{ls} = k_{gs}$ and $\mu_i = \mu_s$. Then,

$$T_{n2} \cong \frac{1}{k_{gs}} T_s + \frac{1}{\mu_s} T_d. \tag{IVc}$$

Appendix III

Optimum Idler Frequency and Effect of Idler Load on Amplifier Noise Temperature

In the limit of low circuit losses, high gain, and under the assumption of a perfect circulator, the single channel noise temperature of a parametric amplifier is given from (14) (with $\alpha \to 1$) by:

$$t_{n1} = \frac{T_{n1}}{T_d} = \frac{1}{\mu_s}\left[1 + \alpha\Omega\frac{1 + \mu_i t_i}{1 + \mu_i}\right] + \alpha\Omega\frac{1 + \mu_i t_i}{1 + \mu_i} \tag{40}$$

where

$$\Omega = \omega_s/\omega_i$$

$$t_i = T_{li}/T_d.$$

It is clear from (40) that to minimize t_{n1}, μ_s has to be minimized. With (18), this leads to the condition:

$$\mu_s + 1 = \frac{\Omega K^2}{1 + \mu_i} \tag{41}$$

where

$$K = \frac{Q_D}{2} \cdot \frac{\Delta C}{C}.$$

To minimize, t_{n1}, Ω and μ_i have to be optimized in (40), taking (41) into account. This leads to the following optimum values for Ω and μ_i, under the assumption of high gain ($\alpha \to 1$):

$$\left.\begin{aligned} \mu_i\big|_{\text{opt}} &= 0 && (42)\\ \Omega_{\text{opt}} &= \frac{1}{\sqrt{1 + K^2} - 1} && (43)\end{aligned}\right\}.$$

This result leads to the interesting conclusions that for minimum single-channel noise temperature with low-loss circuits:

1) there exists a definite optimum idler frequency;
2) the idler circuit should not be coupled to any external load.

In practice, the optimum idler frequency may be often found rather high. It may then be desirable, at the sacrifice of some deterioration of the noise temperature t_{n1}, to operate at an idler frequency lower than the optimum. Under these conditions, Ω is no more a parameter but rather is prescribed, and μ_i alone can be optimized. The optimum value of μ_i for given value of Ω is then found from (40) with the constraint (41) to be different from zero, and the corresponding noise temperature t_{n1} can be reduced by use of an idler load cooler than the diode ($t_i < 1$; $\mu_i > 0$). A practical situation where $\Omega < \Omega_{\text{opt}}$ and where a substantial reduction of t_{n1} is obtained by having a cold idler load could be that of a quasi-degenerate parametric amplifier where both signal and ilder frequencies are supported by a same circuit coupled to an antenna looking at a cold sky.

Theory of Single-Resonance Parametric Amplifiers*

SYDNEY T. FISHER†, MEMBER, IRE

Summary—A parametric amplifier that supports a resonance at the idler frequency only is capable of unlimited gain when operated either as a straight-through amplifier or as a lower-sideband up-converter. In the latter case, the idler frequency becomes the output frequency.

The analysis of the single-resonance parametric amplifier consists of determining the stability criteria and power gains associated with a nonlinear capacitance that is incorporated in a network producing a resonance at the idler frequency but not at the signal frequency. The admittance matrix of the network is first established; and then from this matrix the input admittances and the power-gain expressions for straight-through amplification and lower-sideband up-conversion are derived.

The single-resonance parametric amplifier, as contrasted with one which is tuned at both the signal frequency and the idler frequency, is, in principle, easy to adjust because there is only one resonance. For this reason, the feasibility of continuously tunable parametric receivers becomes immediately evident.

Introduction

During the past year or two, various experimenters have developed parametric amplifiers that exhibited large gains and low noise figures. A major characteristic of these amplifiers is their double tuning, having tuned circuits at both the signal frequency and at the idler frequency. (In a lower-sideband up-converter, the idler frequency becomes the output frequency.) Because of this double-tuned characteristic, adjustment of these amplifiers is a tricky and tedious procedure; consequently, with the present state-of-the-art, fixed-tuned operation is almost mandatory.

As demonstrated below, the tuned circuit at the signal frequency may be eliminated, allowing the design of a simple-to-adjust, *tunable* parametric amplifier. If a resonance is maintained at the idler frequency, the amplifier can be tuned to any signal frequency (within a reasonable range) simply by tuning the pump. Tuning the parametric amplifier, therefore, becomes analogous to tuning an ordinary superheterodyne receiver. The following analysis concerns both straight-through amplification and lower-sideband up-conversion.

Theory of Straight-Through Amplifier Operation

Admittance Matrix of a Nonlinear Capacitance

Suppose a nonlinear capacitance is pumped at a frequency ω_p, and that a *small* signal at a frequency $\omega_1 < \omega_p/2$ is impressed upon the nonlinear element; and further suppose that a voltage at the difference frequency, $\omega_2 = \omega_p - \omega_1$, is allowed to exist across the terminals of the capacitance, but that the sum frequency, $\omega_p + \omega_1$, is suppressed. Under these conditions the voltages across and the currents through the nonlinear capacitor are given by the matrix equation[1]

$$\begin{bmatrix} I_1 \\ I_2^* \end{bmatrix} = \begin{bmatrix} j\omega_1 C_0 & j\omega_1 C_1 \\ -j\omega_2 C_1 & -j\omega_2 C_0 \end{bmatrix} \begin{bmatrix} E_1 \\ E_2^* \end{bmatrix}, \qquad (1)$$

where

I_1 and E_1 are the current and voltage at ω_1,
I_2 and E_2 are the current and voltage at ω_2 (I_2^* indicates a complex conjugate), and
C_0 and C_1 are defined by

$$C(t) = C_0 + 2C_1 \cos \omega_p t + 2C_2 \cos 2\omega_p t + \cdots.$$

Suppose that the time-varying capacitance is connected in parallel with a two-terminal passive network whose admittance at the frequency ω_1 is given by

$$Y_{10} = G_{1T} + j(B_1 - \omega_1 C_0), \qquad (2)$$

and whose admittance at ω_2 is given by

$$Y_{20} = G_{2T} + j(B_2 - \omega_2 C_0). \qquad (3)$$

This situation is shown in Fig. 1.

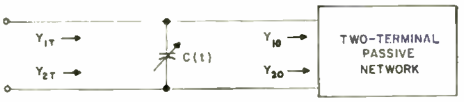

Fig. 1—Nonlinear capacitance connected in parallel with two-terminal passive network.

The voltages across and currents through the parallel combination of $C(t)$ and the network are related by the matrix equation

$$\begin{bmatrix} I_1 \\ I_2^* \end{bmatrix} = \begin{bmatrix} G_{1T}\left(1 + j\dfrac{B_1}{G_{1T}}\right) & +j\omega_1 C_1 \\ -j\omega_2 C_1 & G_{2T}\left(1 - j\dfrac{B_2}{G_{2T}}\right) \end{bmatrix} \begin{bmatrix} E_1 \\ E_2^* \end{bmatrix}. \qquad (4)$$

* Received by the IRE, October 8, 1959; revised manuscript received January 29, 1960.
† Research Division, Philco Corporation, 4700 Wissahickon Ave., Philadelphia, Pa.

[1] H. E. Rowe, "Some general properties of nonlinear elements. II. Small signal theory," Proc. IRE, vol. 46, pp. 851–860; May, 1958.

From (4) we find that the admittance Y_{1T} of the parallel combination at ω_1 is

$$Y_{1T} = G_{1T}\left[1 + j\frac{B_1}{G_{1T}} - \frac{\alpha}{1 - j\dfrac{B_2}{G_{2T}}}\right]$$

$$= G_{1T}\left\{1 - \frac{\alpha}{1 + \left(\dfrac{B_2}{G_{2T}}\right)^2} + j\left[\frac{B_1}{G_{1T}} - \alpha\frac{B_2/G_{2T}}{1 + \left(\dfrac{B_2}{G_{2T}}\right)^2}\right]\right\} \quad (5)$$

where

$$\alpha = \frac{\omega_1\omega_2 C_1^2}{G_{1T}G_{2T}}. \quad (6)$$

The admittance of the parallel combination of $C(t)$ and the passive network at ω_2 is

$$Y_{2T} = G_{2T}\left\{1 + j\frac{B_2}{G_{2T}} - \frac{\alpha}{1 - j\dfrac{B_1}{G_{1T}}}\right\}$$

$$= G_{2T}\left\{1 - \frac{\alpha}{1 + \left(\dfrac{B_1}{G_{1T}}\right)^2} + j\left[\frac{B_2}{G_{2T}} - \alpha\frac{B_1/G_{1T}}{1 + \left(\dfrac{B_1}{G_{1T}}\right)^2}\right]\right\}. \quad (7)$$

Eqs. (5) and (7) show that the parameter α introduces negative conductance at both frequencies, so that the real parts of the admittances decrease as α increases. If α becomes large enough, the device will become unstable. If the real part of the total admittance at either frequency is negative when the imaginary part is zero, instability occurs.

Effect of Single Resonance

Let the passive circuit be so arranged that, when it is placed in parallel with C_0, a resonance occurs at some $\omega_2 = \omega_{20}$; so that, by using the narrow band approximation $\omega_2 - \omega_{20} \ll \omega_{20}$,

$$B_2 = G_{2T}2Q\frac{\omega_2 - \omega_{20}}{\omega_{20}} \quad (8)$$

where Q is the Q of the resonant circuit formed by C_0 in parallel with the passive network. Let it further be stipulated that at the signal frequency, ω_1, the passive network in parallel with C_0 gives a total susceptance B_1, which is nearly constant for small changes of frequency about the frequency

$$\omega_{10} = \omega_p - \omega_{20},$$

where ω_p is the pump frequency.

Let

$$k = \frac{B_1}{G_{1T}} \quad (9)$$

and

$$x = \frac{B_2}{G_{2T}} = 2Q\frac{\omega_2 - \omega_{20}}{\omega_{20}} \quad (10)$$

where k is assumed to be constant over a small frequency range near ω_{10}. The variable x is the number of half-bandwidths of the idler tank by which ω_2 deviates from ω_{20}. The idler tank bandwidth is, of course, the ratio of the center frequency, ω_{20}, to the Q of the idler tank.

The admittance expressions now become

$$Y_{1T} = G_{1T}\left[1 - \frac{\alpha}{1 + x^2} + j\left(k - \frac{\alpha x}{1 + x^2}\right)\right] \quad (11)$$

and

$$Y_{2T} = G_{2T}\left[1 - \frac{\alpha}{1 + k^2} + j\left(x - \frac{\alpha k}{1 + k^2}\right)\right]. \quad (12)$$

Instability occurs if there exist one or more real values of x and k for which the real part of either admittance is negative and the imaginary part is zero. If $\alpha < 1 + k^2$, there is no (real) value of x for which the real part of either admittance is negative at the same time that the imaginary part is zero. When $\alpha = 1 + k^2$, the real and the imaginary parts of *both* Y_{1T} and Y_{2T} vanish for $x = k$, and marginal stability occurs. The device is unstable when $\alpha > 1 + k^2$.

Power Gain

The following example shows how the negative admittance characteristic of the pumped variable reactance device may be used as an amplifier. Consider the circuit of Fig. 2, in which it is assumed that

$$i(t) = |I_1| \cos(\omega_1 t - \phi_1)$$

$$G_{1T} = 2G + g$$

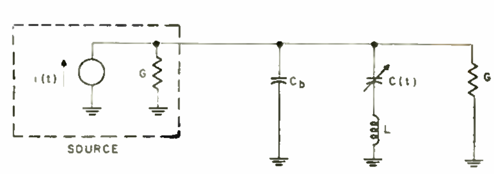

Fig. 2—Theoretical model of a single-resonance straight-through parametric amplifier.

where g represents circuit and diode losses at ω_1,

$$B_1 \approx \omega_1(C_b + C_0),$$

$$\omega_1 L \ll 1/\omega_1 C_0,$$

$$\omega_{20} \approx \frac{1}{\sqrt{LC_0}},$$

and G_{2T} is arbitrary. In this circuit, G_{2T} would consist of diode losses at ω_2 and the effect of $2G$ in parallel with the bypass capacitor, C_b. It is also assumed that

$$\omega_1 = \omega_{10} + \Delta\omega_1 = \omega_{10} - \Delta\omega_2$$

where

$$\omega_{10} = \omega_p - \omega_{20},$$

$$\Delta\omega_2 = \omega_2 - \omega_{20},$$

and ω_p is the pump frequency. The mechanism for pumping the variable capacitor is not shown here.

A study of the circuit of Fig. 2 shows that the effect of the bypass capacitor C_b, and of the idler tank consisting of $C(t)$ and L, is to place the admittance Y_{1T} across the current source. The power gain is defined as the power delivered to the load G divided by the power available from the source. The gain is given by

$$G_p = 4\frac{G^2}{|Y_{1T}|^2}$$

$$= \frac{4G^2}{G_{1T}^2} \frac{1}{\left(1 - \frac{\alpha}{1+x^2}\right)^2 + \left(k - \frac{\alpha x}{1+x^2}\right)^2}. \qquad (13)$$

If $G_{1T} = 2G + g$, and if $g \ll G$, (13) may be rewritten as

$$G_p = \frac{1}{1 + \frac{g}{G}} F(k, \alpha, x) \qquad (14)$$

where

$$F(k, \alpha, x) = \frac{1}{\left(1 - \frac{\alpha}{1+x^2}\right)^2 + \left(k - \frac{\alpha x}{1+x^2}\right)^2} \qquad (15)$$

in which

$$\alpha = \frac{\omega_1\omega_2 C_1{}^2}{G_{1T}G_{2T}} \approx \frac{\omega_{10}\omega_{20} C_1{}^2}{G_{1T}G_{2T}},$$

$$k = \frac{B_1}{G_{1T}} \approx \text{constant},$$

$$x = \frac{B_2}{G_{2T}} = 2Q\frac{\omega_2 - \omega_{20}}{\omega_{20}},$$

and Q is the Q of the idler tank.

Maximum Gain and Frequency Response

The gain function, $F(k, \alpha, x)$, contains all of the information required to analyze the single-tuned parametric amplifier. The gain becomes infinite when $x = k$ and $\alpha = 1 + k^2$. For values of α less than this critical value the gain is finite, and the value of x_0, that value of x for which the gain is maximum, approaches k as the gain approaches infinity.

The expression for $F(k, \alpha, x)$ is too complex to allow expression of the gain and bandwidth of the amplifier in closed form. The results shown in the following figures were obtained by means of a digital computer which was programmed to calculate F for various values of the variables k, α, and x.

Fig. 3 shows the plot obtained directly from the computed results for $k = 0.4$. Similar plots were obtained for other values of k. As the figure shows, the frequency response is not symmetrical about the point of maximum gain; however, for large gains, symmetry holds approximately over the amplifier bandwidth. For $k = 0$, symmetry holds for all values of gain.

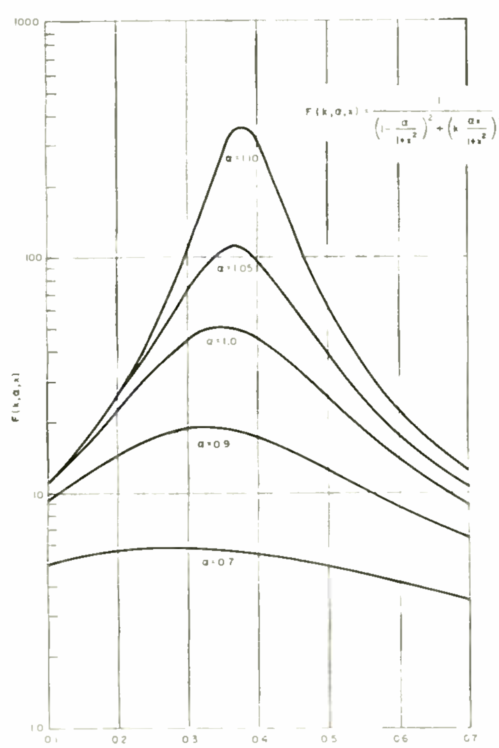

Fig. 3—Regenerative gain of straight-through amplifier as a function of the normalized idler frequency and of the stability parameter α for $k = 0.4$, where k denotes the normalized input susceptance.

Fig. 4 shows the value of α (solid curves) needed to give a particular value of midband ($x=x_0$) gain, and the value of $x=x_0$ (dashed curves) at which this gain occurs. Fig. 5 is a plot of bandwidth vs maximum gain. Since the frequency responses are not symmetrical, the quantity Δx is the average value of the change in x giving a 3-db reduction in gain from the maximum value, for constant k and α. It turned out that the bandwidth-vs-gain curves are so nearly independent of the constant k that a single curve is sufficient. From Fig. 5 it is evident that, to good approximation, the single-tank straight-through parametric amplifier obeys the law

$$(G_p)^{1/2}\Delta x = 1.$$

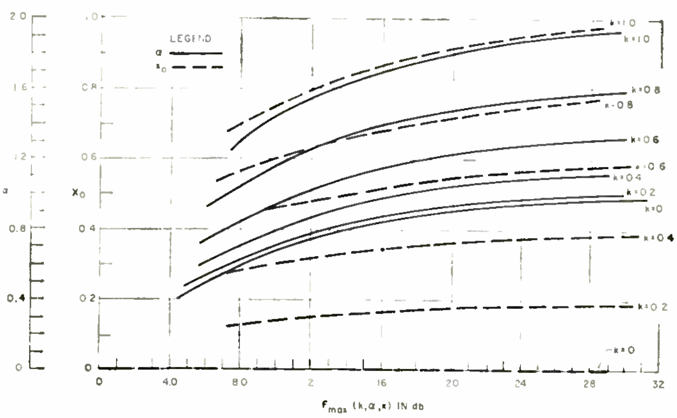

Fig. 4—Curves of a and x_0 as a function of maximum gain and of susceptance constant, k, where a is the stability factor and x_0 is the normalized idler frequency at which maximum gain occurs.

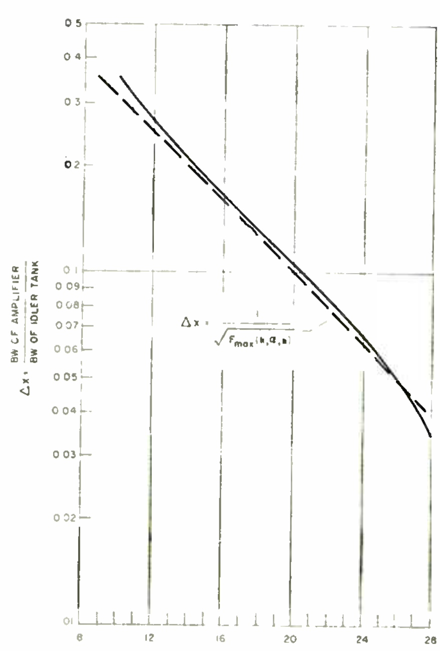

Fig. 5—Relative bandwidth of single-tank straight-through parametric amplifier as a function of regenerative gain. Dashed line represents a device having a constant voltage gain-bandwidth product equal to the bandwidth of the idler tank.

The double-tuned amplifier (gain)$^{1/2}$-bandwidth product approaches half this value as the gain approaches infinity.[1]

As a result of the above analysis, the following simple rule may be stated: *The voltage gain-bandwidth product of a straight-through parametric amplifier, resonant at the idler frequency only, is approximately equal to the bandwidth of the idler tank.*

Theory of Lower-Sideband Up-Converter Operation

Lower-sideband up-conversion can also be used for amplification. Consider again the matrix equation of the nonlinear capacitance in parallel with the passive network of Fig. 1:

$$\begin{bmatrix} I_1 \\ I_2^* \end{bmatrix} = \begin{bmatrix} G_{1T}\left(1+j\dfrac{B_1}{G_{1T}}\right) & j\omega_1 C_1 \\ -j\omega_2 C_1 & G_{2T}\left(1-j\dfrac{B_2}{G_{2T}}\right) \end{bmatrix} \begin{bmatrix} E_1 \\ E_2^* \end{bmatrix}. \tag{16}$$

Let G_{1T} consist of the source conductance G_1, in parallel with g_1, the total losses associated with the input frequency ω_1. Similarly, let G_{2T} consist of the load conductance G_2 in parallel with g_2, the losses associated with ω_2, the output frequency. The power delivered to G_2 is given by

$$P_{out} = \tfrac{1}{2}G_2|E_2|^2 = \tfrac{1}{2}G_2|E_2^*|^2. \tag{17}$$

The power available from the source is

$$P_{avail.} = \frac{1}{8}\frac{|I_1|^2}{G_1}. \tag{18}$$

Combining (17) and (18) gives

$$G_{p12} = 4G_1G_2\left|\frac{E_2^*}{I_1}\right|^2, \tag{19}$$

where E_2^*/I_1 is the transfer impedance relating voltages at ω_2 to currents at ω_1. From (16),

$$G_{p12} = 4G_1G_2\frac{\omega_2^2C_1^2}{\left|G_{1T}G_{2T}\left(1+j\dfrac{B_1}{G_{1T}}\right)\left(1-j\dfrac{B_2}{G_{2T}}\right)-\omega_1\omega_2C_1^2\right|^2}$$

$$= \frac{G_1}{G_{1T}}\frac{G_2}{G_{2T}}\frac{\omega_2}{\omega_1}\frac{4\alpha}{\left|\left(1+j\dfrac{B_1}{G_{1T}}\right)\left(1-j\dfrac{B_2}{G_{2T}}\right)-\alpha\right|^2} \tag{20}$$

where

$$\alpha = \frac{\omega_1\omega_2C_1^2}{G_{1T}G_{2T}}.$$

In accordance with the notation used above, let

$$x = \frac{B_2}{G_{2T}} = 2Q\frac{\omega_2 - \omega_{20}}{\omega_{20}}$$

and

$$k = \frac{B_1}{G_{1T}}$$

where k is approximately constant over a small range of frequencies,

$$\omega_1 = \omega_{10} + \Delta\omega_1$$

and

$$\omega_{10} + \omega_{20} = \omega_p,$$

ω_p being the pump frequency. Eq. (20) becomes

$$G_{p12} = \frac{G_1}{G_{1T}}\frac{G_2}{G_{2T}}\frac{\omega_2}{\omega_1}G(k, \alpha, x) \tag{21}$$

where $G(k, \alpha, x)$, the regenerative gain, is given by

$$\begin{aligned} G(k, \alpha, x) &= \frac{4\alpha}{(1 - \alpha + kx)^2 + (k - x)^2} \\ &= \frac{4\alpha}{(1 - \alpha)^2 + k^2 - 2\alpha kx + (1 + k^2)x^2}. \end{aligned} \tag{22}$$

This expression is less complex than that of $F(k, \alpha, x)$ of the previous section, and the entire frequency response may be plotted as a single curve, provided the right variables are chosen. The denominator of $G(k, \alpha, x)$ is minimum when

$$x = x_0 = \frac{k\alpha}{1 + k^2}.$$

In (22) putting

$$x = \frac{k\alpha}{1 + k^2} + (x - x_0)$$

gives

$G(k, \alpha, x)$

$$= \frac{4\alpha}{(1 - \alpha)^2 + k^2\left(1 - \frac{\alpha^2}{1 + k^2}\right) + (1 + k^2)(x - x_0)^2}. \tag{23}$$

We recall that the device becomes marginally stable when

$$\alpha = 1 + k^2.$$

Let a new variable, a, be defined

$$a = \frac{\alpha}{1 + k^2}$$

so that

$$\alpha = a(1 + k^2).$$

In terms of a and $(x - x_0)$, the gain expression becomes

$$G_{p12} = \frac{G_1}{G_{1T}}\frac{G_2}{G_{2T}}\frac{\omega_2}{\omega_1}H(a, x)$$

where

$$\begin{aligned} H(a, x) &= \frac{4a}{(1 - a)^2 + (x - x_0)^2} \\ &= \frac{4a}{(1 - a)^2}\frac{1}{1 + \left(\frac{x - x_0}{1 - a}\right)^2} \end{aligned} \tag{24}$$

in which

$$x_0 = \frac{k\alpha}{1 + k^2} = ka.$$

Fig. 6 is a plot of the frequency response of an up-converter whose single resonance is near the output frequency, ω_2. The value of $x - x_0$ for which $H(a, x)$ becomes half its maximum value, $H(a, x_0)$ is given by

$$x_1 - x_0 = 1 - a. \tag{25}$$

Double-tuned lower-sideband up-converters have approximately half this bandwidth.[1]

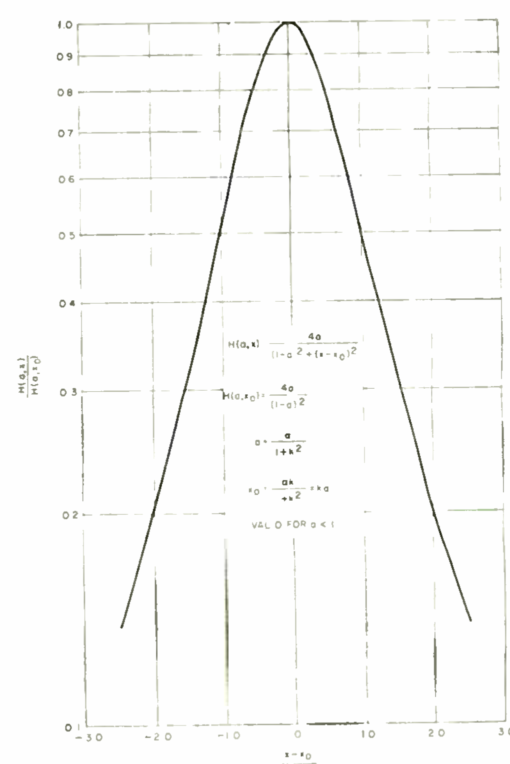

Fig. 6—Normalized frequency response of single-resonance parametric up-converter with resonance near the output frequency.

The relative (gain)$^{1/2}$-bandwidth product for the up-converter is given by

$$(G_p)^{1/2}\left| x_1 - x_0 \right| = \left(\frac{G_1}{G_{1T}}\frac{G_2}{G_{2T}}\right)^{1/2}\left(\frac{\omega_2}{\omega_1}\right)^{1/2} 2\sqrt{a}. \tag{26}$$

For the lossless case, where $G_1 = G_{1T}$ and $G_2 = G_{2T}$, this reduces to

$$(G_p)^{1/2}\left| x_1 - x_0 \right| = 2\sqrt{a\frac{\omega_2}{\omega_1}}\,. \tag{27}$$

The actual (gain)$^{1/2}$-bandwidth product in cycles per second is

$$(G_p)^{1/2}BW = 2\sqrt{a\frac{\omega_2}{\omega_1}}\,BW_0 \tag{28}$$

where BW_0 is the bandwidth of the output tank circuit.

$$BW_0 = \frac{1}{2\pi}\frac{\omega_{20}}{Q}\,. \tag{29}$$

It can therefore be stated that, for the lossless case and for large gains, *the voltage gain-bandwidth product of a parametric up-converter, resonant at the output frequency only, is approximately twice the bandwidth of the output tank circuit times the square root of the frequency ratio.*

Discussion

The single-resonance parametric amplifier, with the resonance occurring at the idler (or output) frequency, is theoretically capable of unlimited gain.

The main advantage of the single-resonance amplifier, compared to the more conventional parametric amplifier which supports a resonance at both the signal and the idler (or output) frequencies, lies in its relative ease of tuning. This ease of tuning, stemming from the fact that there is only one resonance instead of two, results in the feasibility of a continuously tunable parametric amplifier. If a single-resonance parametric up-converter were followed by a fixed-tuned, conventional receiver, the entire low-noise receiving system would be tuned simply by adjusting the pump frequency and then carefully adjusting the pump power to give the desired gain. If a straight-through parametric amplifier were used, the following receiver as well as the parametric amplifier itself would have to be tuned to the signal frequency.

The main drawback of the single-resonance parametric amplifier, compared to the double-tuned amplifier, is the extra capacitance swing, and therefore pump power, required to give adequate gain. The extra pump power is required because of the lack of a transformation network to provide a high source impedance at the diode. Such a transformation network would behave as a resonant circuit at the signal frequency and is therefore unacceptable from the standpoint of this treatment.

Another drawback is the unsymmetrical frequency response of the straight-through amplifier. This might, in some applications, lead to difficulties involving distortion of coherent signals. This difficulty would not manifest itself in the single-resonance parametric up-converter, which has a symmetrical frequency response.

Correction

Keith W. Henderson, author of "Nomographs for Designing Elliptic-Function Filters," which appeared on pages 1860–1864 of the November, 1958, issue of Proceedings, has requested that the following correction be made to his paper.

In (7) on page 1861, the first bracket should precede the minus sign, *i.e.*,

$$q(k) = \exp\left[-\pi\frac{K(k')}{K(k)}\right].$$

The "Persistor"—A Superconducting Memory Element*

E. C. CRITTENDEN, JR.†, J. N. COOPER†, AND F. W. SCHMIDLIN‡

Summary—The basic components of a Persistor memory element are a superconducting inductor in parallel with a switch element which is normally superconducting, but which becomes resistive when the current exceeds a critical value. When a suitable current pulse is applied to a Persistor memory element, a persistent circulating current is stored. A second pulse in the same direction as the first makes no change, but a pulse in the opposite direction reverses the circulating current and produces a voltage across the element. By mutual inductance coupling to two or more driving circuits, these memory elements can be made to operate in matrices similar to those employed with ferromagnetic cores. Persistor memory elements utilizing lead inductors and thin tin or indium films have performed typical memory unit functions for pulses of 15-mμsec duration and a repetition rate of 15 mc. Performance at higher speeds is possible. The limiting speed is determined by the thickness of the thin film switch element and can be made as fast as is useful for the other parts of the associated circuits. The elements are well suited to compact printed circuit production, with densities of a million per cubic foot possible.

Introduction

A MEANS OF utilizing transitions between the resistive and superconducting states in the operation of a computer component has been proposed by Buck, who developed a circuit element called the cryotron.[1] Buck's cryotrons were made of fine wires which had switching times of the order of a millisecond—too long to be attractive for computer applications. A different manner of utilizing superconductivity in the operation of computer components[2] has been devised for the purpose of obtaining a high speed and compact memory. The primary circuit element, called the Persistor memory element, involves the use of superconducting thin films to form a loop in which circulating currents persist until a new signal pulse arrives. This memory element has been operated with read-in or read-out times down to 15 mμsec with shorter times possible. The underlying principles and experimental data on the behavior of Persistor memory elements are described in the following sections.

* Received by the IRE, November 3, 1959; revised manuscript received, February 23, 1960. This work was supported in part by the General Research Provision of contract between the Air Force and Space Technology Labs., Inc., and in part by the Office of Naval Research.

† Dept. of Physics, U. S. Naval Postgraduate School, Monterey, Calif., and Space Technology Labs., Inc., Los Angeles, Calif.

‡ Space Technology Labs., Inc., Los Angeles, Calif.

[1] D. A. Buck, "The cryotron-superconductive computer component," PROC. IRE, vol. 44, pp. 482–493; April, 1956.

[2] E. C. Crittenden, Jr., "A computer memory element employing superconducting persistent currents," *Proc. of the Fifth Internatl. Conf. on Low Temp. Phys. and Chem.*, Madison, Wis.; August 26–30, 1957.

Superconductivity

In 1911, Kammerlingh-Onnes discovered that the resistance of mercury falls abruptly to zero at 4.12°K (indicated by the solid curve in Fig. 1); however, if the mercury is cooled in a magnetic field, the temperature for transition to superconducting behavior is lower (indicated by the dashed curve).

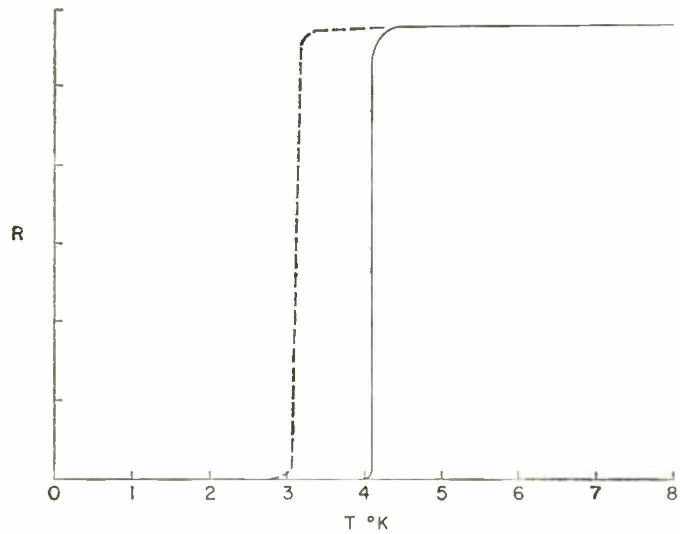

Fig. 1—Variation of resistance with temperature for a superconductor.

When the critical magnetic induction B is plotted as a function of the temperature at which a material becomes superconductive, the curves of Fig. 2 are obtained for several metals which become superconducting. The intercept on the abscissa for each metal is the transition temperature for that metal in the absence of a magnetic field. The curves are roughly parabolic in shape.

The magnetic induction can also be supplied internally by passing a current through the specimen. For a cylindrical conductor the magnetic induction at the surface is readily calculated and a curve of critical current I_c required to produce transition as a function of temperature would have the same shape as the appropriate curve of Fig. 2 for any given metal. For specimens of other cross sections the problem is more complicated, but there is still a definite critical current for each temperature which switches the specimen from superconducting to resistive.

The Persistor Memory Element

For purposes of discussion, an idealized Persistor memory element consists (Fig. 3) of an inductor L made of a superconductor with a high transition temperature in parallel with a resistance R constructed of a metal having a superconducting transition temperature slightly above the temperature at which the device is to operate. In practice, the inductor L has been made of lead and the switching element R has been an evaporated film of indium or tin, but other choices might be made. The component R is normally superconducting, becoming resistive only for a short interval when storing a bit of information.

In operation, a current pulse is applied through the leads I of Fig. 3. Let the magnitude of this pulse be $2\,I_c$, where I_c is the critical current for R. Both the inductor L and the switch element R are initially superconducting. For purposes of discussion, it will be assumed at first that R has negligible inductance compared to L. Hence, the initial current change occurs almost entirely through the element R. The current I_R rises rapidly until the current becomes great enough to produce a transition to the resistive state when $I_R=I_c$, the critical current. A potential drop then appears across R. The current in the inductor L increases, while the current in the resistor decays to approximately the critical current I_c. If the pulse is terminated at a time when the current I_R has fallen approximately to I_c, the current through R drops rapidly and the element develops superconducting behavior. During this time, the currents through R and L change by the same magnitudes as their initial changes but in the opposite sense. Thus, a current equal in magnitude to the increase in current through the inductor while R was resistive now returns through R leaving a closed loop persisting current. Under favorable circumstances a current of as much as I_c can thus be stored. The current pulse and the corresponding currents through R and L are shown in the left portion of Fig. 4.

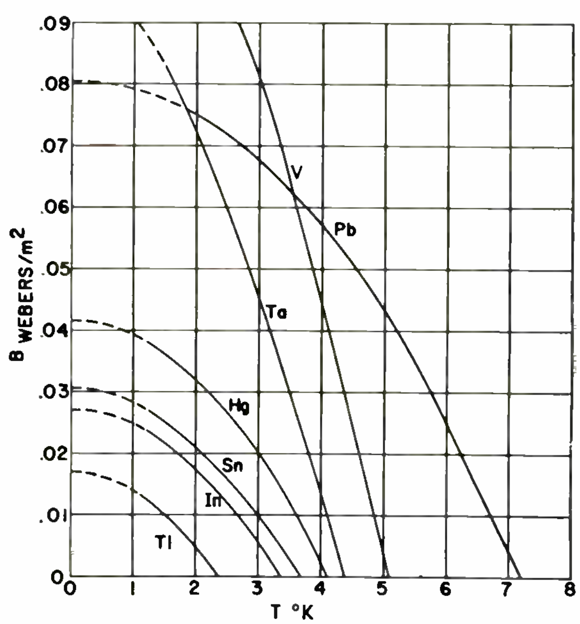

Fig. 2—Critical magnetic induction B for cessation of superconductivity as a function of temperature for several superconductors.

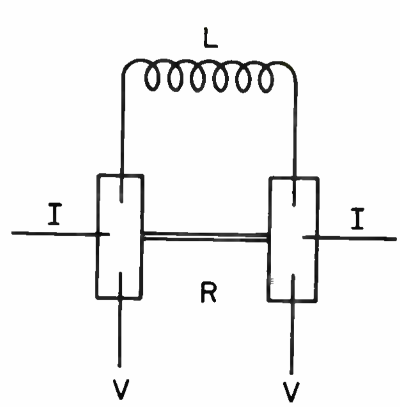

Fig. 3—Idealized Persistor memory element.

The bottom trace of Fig. 4 shows the potential difference V_R across the element. The dashed curves represent a "derivative signal," which arises from the fact that the switch element R has a small inductance across which an electromotive force proportional to the time rate of change of current is developed. Such a derivative signal acts as a spurious pulse, but it can be eliminated by doubling back one of the leads for measuring voltage (Fig. 5) in such a way that an equal counter electromotive force is induced in this voltage lead. Such back-coupling was done in the experimental tests, but in some cases complete cancellation was not quite achieved and a small derivative signal remained.

The first pulse applied to a Persistor memory element establishes a circulating current which continues until another pulse arrives. The response to a new pulse depends not only on its magnitude but also on its direction.

Consider a second pulse of magnitude $2I_c$ opposite to the pulse which established the circulating current. This pulse and its effects are indicated in the central part of Fig. 4. In this case the current through R is driven from $-I_c$ downward toward $-3I_c$. The element R becomes resistive and I_R decays back toward $-I_c$. At the same time, a negative current builds up in the inductor L. If the pulse is terminated at the appropriate time, the current in R goes through zero to $+I_c$. Now the Persistor memory element stores a current $+I_c$ in R and $-I_c$ in L. Meantime the voltage pulse V has appeared across the Persistor memory element as indicated in the fourth line of Fig. 4.

On the other hand, if a pulse of magnitude $2I_c$ is applied in the same direction as the preceding pulse, the behavior is as shown in the right portion of Fig. 4. In this case the current in R is changed from $+I_c$ to $-I_c$. Since it does not exceed the magnitude of I_c, the element R does not become resistive and no current decay occurs. Hence, upon removal of the pulse the current in R reverts to I_c, and the previously existing circulating current is restored. In this case, no voltage pulse appears across the element. The element thus has a memory represented by the direction of a circulating persistent current. Interrogation is accomplished by observing the presence or absence of a voltage pulse on application of a current pulse to the memory element. If the interrogating signal evokes a response, the memory current is reversed.

Returning to the first pulse, it should be pointed out that the response of an element to the first pulse differs from its response to later pulses because no memory current has yet been established. The pulse shown in the figure for the first pulse is shorter in time than later pulses. Pulses of the same length as later pulses can be employed, but in this case the element requires several alternating polarity pulses when first used before the ideal behavior is achieved.

The separation of the circuit into a pure inductance and a pure "resistance" is not necessary for the operation of the memory element. In practice, the switch element R has inductance, but significantly less than that of the inductive component L. The memory functions equally well under these circumstances.

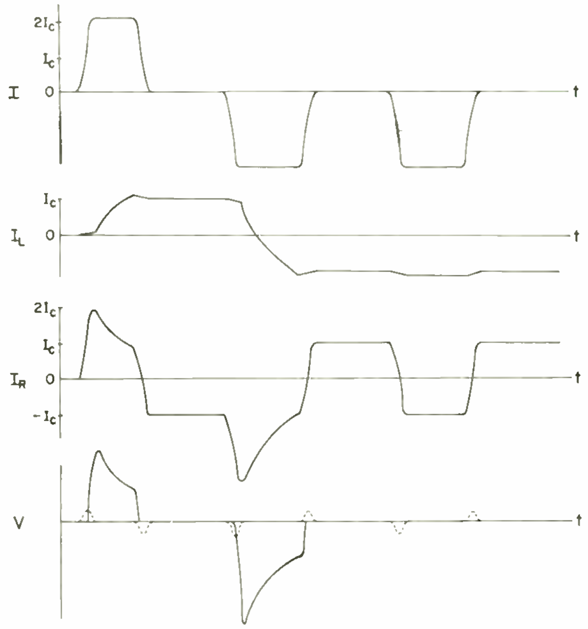

Fig. 4—Behavior of current and voltage as a function of time for an idealized Persistor memory element operated singly (not in an array).

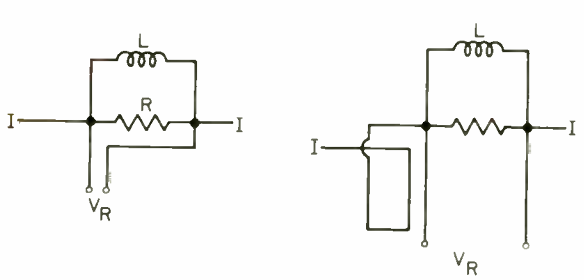

Fig. 5—Two forms of back coupling to eliminate $L(dI/dt)$ or derivative signal in the switch element R.

Two early working memory elements are shown in Fig. 6. The unit at the left has an inductor of roughly 4.5 turns of lead wire with an inductance of about 0.2 μh. The unit at the right, made by printed circuit techniques, consists of six turns of plated lead conductor and also has an inductance of 0.2 μh. In each case the switch element is an evaporated tin film about 0.7 μ thick. The switch element on the left was deposited on mica, the one on the right on the plastic backing of the printed circuit. The rather large thickness of the switch elements restricted operation to the microsecond range and required the large coils shown. Present elements are made by evaporating tin or indium onto optically polished glass. Fig. 7 is a photograph of such an element, although it has a greater width than usually used. The elements usually are of the order of 5 mm long, 60 μ wide, and 0.10 μ thick with resistance of 1 to 5 ohms when resistive at low temperature. The enlarged ends of the element are provided to avoid contact difficulties. Bulk indium has been soldered to the glass in these areas before deposition of the thin film. A Persistor memory element is made by combining such a switch element with a small loop as an inductor. Fig. 8 is a photograph of 2×2 array of Persistors and coupling coils for memory array operation, the entire circuit produced by evaporation in high vacuum. The results to be described in this paper are the properties of single Persistor memory elements, and the manner in which these relate to single operation or operation within arrays.

Fig. 9 shows the response of a Persistor memory element to pulses of 140-mμsec duration. These slow pulses have been used to make the details of operation visible. Both current and voltage traces are shown, with the voltage traces inverted for visibility. The current pulse is the upward pulse in the left side of the picture in each case. For the upper half of Fig. 9 current pulses of alternating sign have been applied. Clearly, each time a full pulse of opposite sign is imposed upon the memory element, the switch element becomes temporarily resistive and a circulating current is established in the opposite sense. The circulating current remains until an opposite pulse is applied. A period as long as two hours has elapsed between pulses with no evidence of any decay. Although no longer tests have been made on Persistor memory elements to show that the superconductor currents can persist indefinitely, it is known that persistent currents have existed in closed superconducting circuits for years with no observable diminution.

In the lower half of Fig. 9 there is a repeated current pulse always in the same sense. In this case, the switch element never undergoes a transition to the resistive

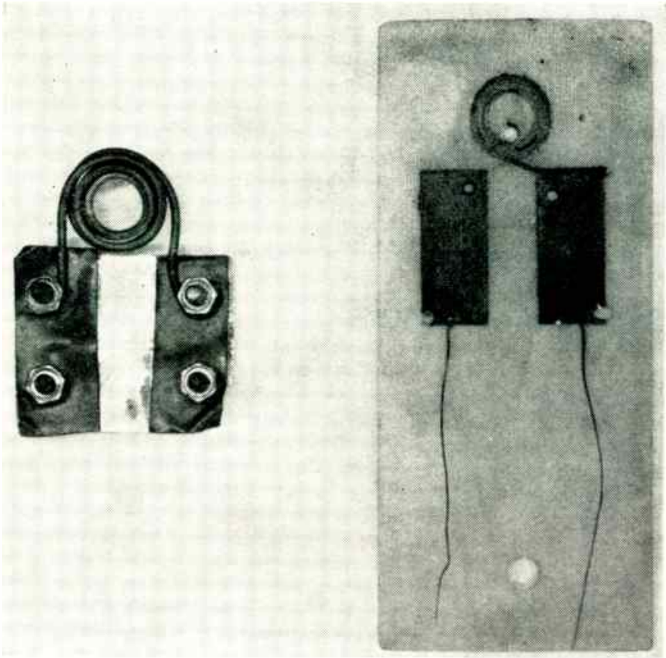

Fig. 6—Early Persistor memory elements.

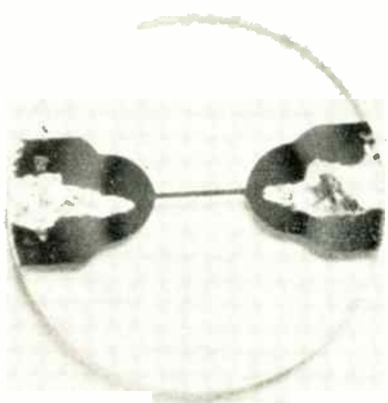

Fig. 7—Switch element deposited on one-inch diameter optically polished glass disk.

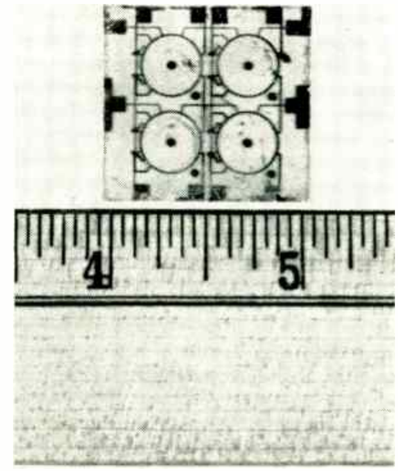

Fig. 8—A 2×2 Persistor array produced by vapor deposition.

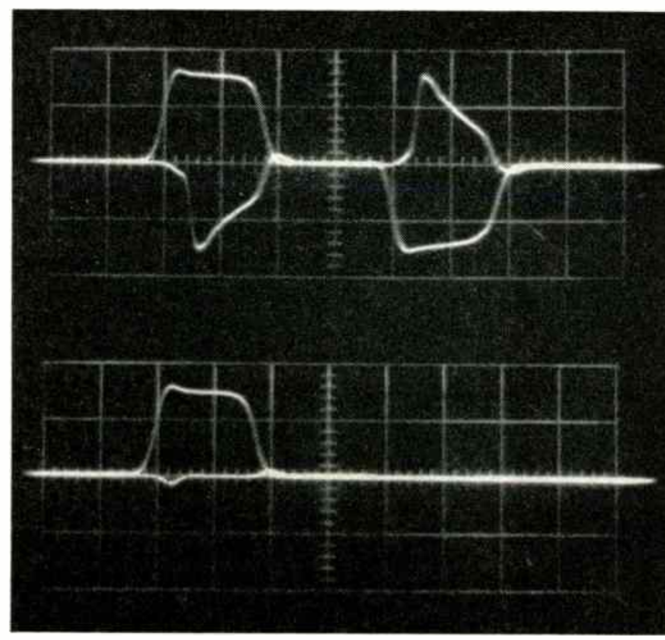

Fig. 9—Response of Persistor adjusted for slow pulses to show detail. (Time scale: 0.1 μsec per large division.)

phase, and therefore the memory element gives no significant output pulse. The small pips are derivative signals which were not quite cancelled by the back-coupling described above.

The switching which occurs after the current exceeds I_c, of course, is not instantaneous. In practice, for single memory elements (not operated in multi-dimensional arrays) the pertinent switch time is that which occurs on application of a pulse of magnitude $3I_c$. As will be shown later, this switch time depends on switch element thickness and can be made to be in the range 1 to 10 mμsec. Memory elements can be made to optimize the performance for any specific pulse length by choosing the proper L/R ratio. In general, the sum of the switch time and L/R should be set equal to the pulse length, and the switch time should be less than half of L/R.

The behavior of a single memory element operating with a pulse length of 15 mμsec (at half maximum) is shown in Fig. 10. This pulse is about the minimum resolvable by the Tektronix 517A oscilloscope employed. The upper trace shows the voltage response to a current pulse as shown in the lower trace after a preceding current pulse of opposite polarity. The middle trace shows the null response to a current pulse of the same height but preceded by a current pulse of the same polarity. The small signal results from incomplete cancellation of the derivative pulse. The switch element was a tin film 0.06 μ thick and 60 μ wide.

Phase Transition in Thin Films

The potential usefulness of the Persistor as a computer component depends greatly on the speed with which it can perform the required switching operations.

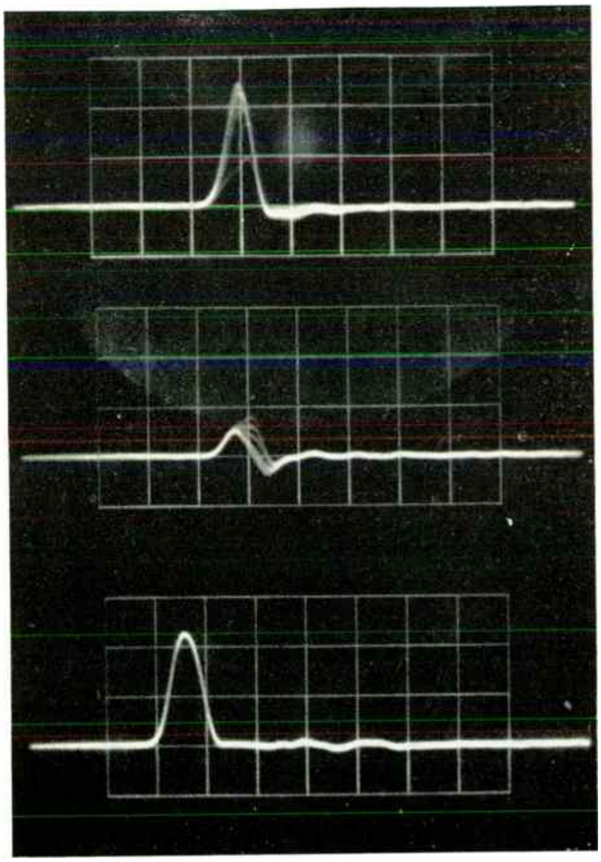

Fig. 10—Response of Persistor adjusted for use with 15-mμsec pulses. (Time scale: 20 mμsec per large division.)

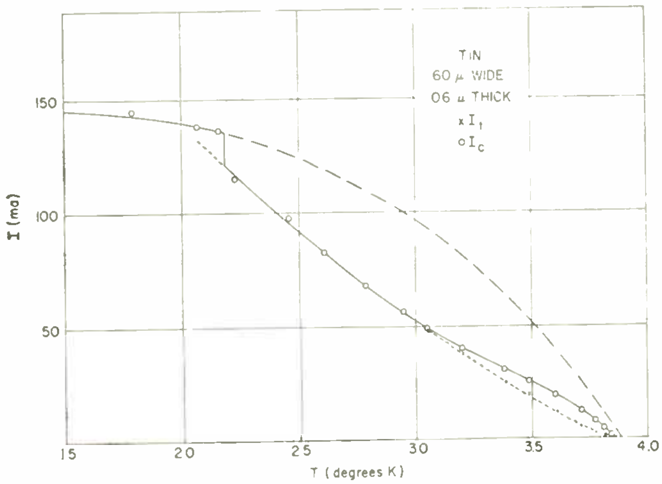

Fig. 11—Critical current as a function of temperature.

A fundamental part of this memory device is the switch element R which must become resistive when the current in it exceeds a critical current and must promptly return to the superconducting phase when the current falls below this critical value. The transitions from superconducting to normal and return are very similar to changes in metallurgical phase. Thus, the thermodynamic properties of a superconductor resemble those of alloys having an order-disorder transition; in the normal or resistive phase the conduction electrons are in the disordered state, while in the superconducting phase they are highly ordered.

The behavior of critical current is somewhat more complicated than has been implied up to this point. A typical curve of dc critical current I_c as a function of temperature is shown as the solid curve of Fig. 11. The specimen was a film of tin 5 mm long, 60 μ wide, and 0.06 μ thick deposited on optically polished glass, as shown in Fig. 7. The specimen had a resistance of 6 ohms when resistive at low temperature. The dc critical current required to cause switching was measured with the help of a circuit which slowly increases the current until the specimen switches, then drops the current to zero within a microsecond. This circuit permits measurement under conditions where I^2R heating, if sustained, would destroy the specimen.

The vertical discontinuity in the curve of Fig. 11 occurs at the helium lambda point (2.186°K) where the thermal conductivity of liquid helium abruptly becomes exceedingly high. This large change in thermal conductivity is a valuable tool in separating thermal and magnetic effects. Below the lambda point, the tendency of helium II to creep along the surfaces of the cryostat results in a more rapid loss of helium, but this is not troublesome.

The dc critical current below the lambda point is approximately fitted by the function $I_c/I_{co}=1-(T/T_c)^4$. This function, extrapolated to the critical temperature, is shown as the dashed curve in Fig. 11. It will be useful later to relate pulse heights employed in switch speed measurements to the values of current given by this equation. Such current values will be termed the extrapolated dc critical current I_e.

The discontinuity in I_c at the lambda point shows that the dc switch behavior at temperatures above the lambda point is not ideal magnetic switching. Instead, the specimen appears to initiate its switch in the vicinity of some small imperfection. Joule heating then develops, raises the temperature locally and causes the normal region to grow, sweeping toward the two ends of the specimen. An oscillograph photograph of voltage as a function of time is shown in Fig. 12 for a specimen held at 2.26°K. A long pulse of current amplitude equal to dc critical was used. It appears as the rectangular pulse in Fig. 12. The first, and steeper, of the two sloping regions of the voltage curve corresponds to the rate of rise of resistance as both ends of the normal region sweep along the specimen. Since the imperfection responsible was not in the center of the specimen, one of the boundaries reaches one end of the specimen first. After this, the slope is reduced to approximately half its previous value as the other boundary sweeps toward the other end of the specimen. Similar behavior has been observed by Bremer and Newhouse[3] after trig-

[3] J. W. Bremer and V. L. Newhouse, "Thermal propagation effects in thin superconducting films," *Phys. Rev. Letts.*, vol. 1, p. 282; October, 1958.

gering a specimen with an external applied local field. The magnitudes of switch times observed at the dc critical current for temperatures above the lambda point are of the order of one millisecond per centimeter of length.

Although a large rise in thermal conductivity of the liquid helium occurs on lowering the temperature below the lambda point, the switching behavior on application of the dc critical current is similar to that above the lambda point temperature. Fig. 13 shows a specimen switching at dc critical current at a temperature of 1.74°K.

If the current through the specimen is increased slowly from zero, for some specimens in certain temperature ranges, the voltage across the specimen does not remain zero right up to the dc critical current. The current at which any detectable voltage appears will be termed the threshold current I_t. The dotted curve of Fig. 11 represents the threshold current I_t as a function of temperature for that specimen. The threshold current was measured by displaying voltage vs current on a Tektronix 545 oscilloscope and sweeping the current from zero to dc critical in about 0.05 second. This permitted use of an ac preamplifier unit with a vertical sensitivity of 50 μv/cm. At each temperature, curves were recorded photographically for two vertical sensitivities, one millivolt per large division and 50 μv per large division, the latter trace displaced upward on the oscilloscope screen for clarity. These traces permitted approximate extrapolation to the current at which the voltage drop was zero. A representative pair of such traces is shown in Fig. 14. The onset of voltage drop in this element was estimated to occur at 6.7 divisions. The curve of threhold current in Fig. 11 differs from the dc critical in two regions, near the transition temperature and at temperatures below the lambda point. In both temperature ranges an imperfection is presumably able to concentrate the current locally to a sufficient extent to cause local magnetically induced transition. As this transformed region further concentrates the current, a small width band of normal metal must form across the specimen, and this causes a small resistance to appear. If the current is small enough or the heat transfer good enough, the boundaries of this region may be stable and not sweep along the specimen until higher current is reached. This is the case near the critical temperature T_c. At lower temperature the threshold curve joins the critical curve because the local heating is great enough to cause the boundaries to move at the current at which initial magnetic transition occurs. For temperatures below the lambda point the great increase in thermal conductivity of the liquid helium causes the boundaries of any small transformed region to be stable again.

As a means of characterizing curves such as Fig. 11, the critical current below the lambda point extrapolated to absolute zero, I_{co}, is useful. I_c varies with temperature approximately according to $I_c/I_{co}=1-(T/T_c)^4$. For

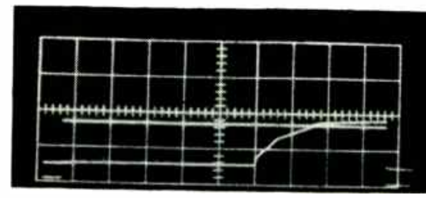

Fig. 12—Indium at 2.26°K. Voltage vs time for switching at dc critical current at temperature above the helium lambda point. (Time scale: 100 μsec per large division.)

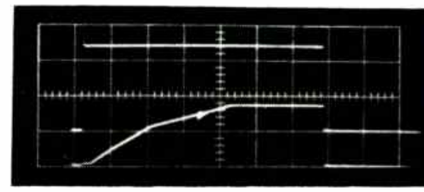

Fig. 13—Indium at 1.74°K. Voltage vs time for switching at dc critical current at temperatures below the helium lambda point. (Time scale: 2 μsec per large division.)

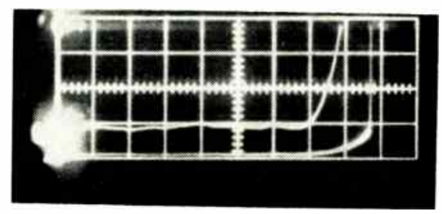

Fig. 14—Voltage-current curves to establish the threshold current I_t. Upper and lower traces—50 μv and 1 mv per large division, respectively.

very thin films, less than 0.03 μ, I_c varies less rapidly than this function indicates. The fourth power function above has still been used for extrapolation for lack of a better function, but the curve has been fitted at 2.0°K when deviation is appreciable.

Values of I_{co} are plotted as a function of width in Fig. 15 for indium films 0.06 μ thick. The value of I_{co} is essentially linear with width. The variation of I_{co} with thickness is shown in Fig. 16 for indium films 60 μ wide. As thickness increases, the slope of this curve decreases and the element becomes less and less sensitive to thickness.

For tin the value of I_{co} for elements 60 μ wide and 0.06 μ thick is 150 ma as compared with 135 ma for indium for this same width and thickness.

Switch Times

In order to make numerical measurement of the switch delay time, a time τ has been defined as the time for the resistance to rise to one half its full value after the application of a rapidly rising current pulse. In practice, current pulses having rise time of about one mμsec were used. The oscilloscopes employed were a Tektronix 545 with a rise time of 12 mμsec and a Tektronix 517A with a rise time of 7 mμsec. The rise time of the current pulses employed was established as being about 1 mμsec by means of an Edgerton, Germeshausen and Grier oscilloscope having a rise time of 10^{-10} seconds. Unfortunately, no preamplifier was available to

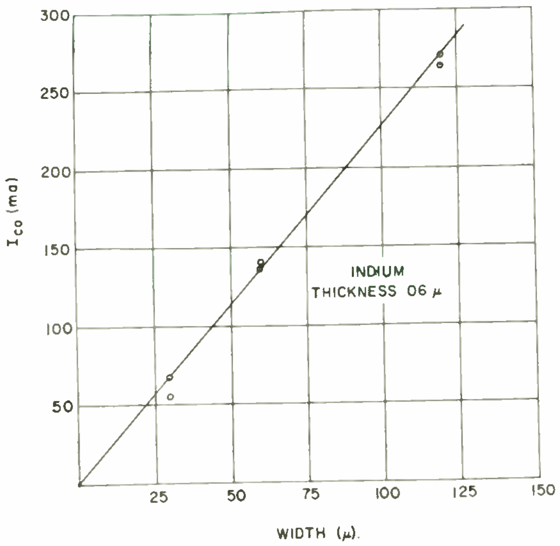

Fig. 15—Values of dc critical current extrapolated to 0°K as a function of width for 0.06 μ thick indium specimens.

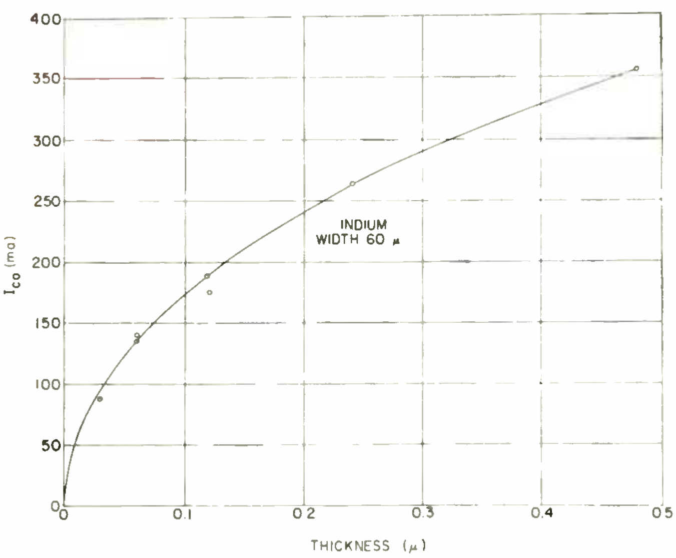

Fig. 16—Values of dc critical current extrapolated to 0°K as a function of thickness for 60 μ wide indium specimens.

take advantage of this oscilloscope for the low level signals sometimes encountered in the superconducting switch time measurements. The switch times reported are the delay between the half-rise points for the current and for the voltage traces as observed with oscilloscopes having rise times of either 7 or 12 mμsec. Delay resulting from the time-of-flight in the cables is observed by raising the temperature of the specimen above the critical temperature so that it behaves as a normal ohmic resistance. Such cable delays were usually of the order of 20 to 30 mμsec, and were subtracted from the observed delay to obtain τ.

The observed switch delay time is a sensitive function of the pulse current. If a given switch time is selected and the pulse current required to produce this switch time is measured as a function of temperature, the pulse current falls on curves as shown in Fig. 17. The curves having no discontinuity in this figure are found to be fitted by the function $I_p/I_{po}=1-(T/T_c)^4$, where I_{po} is the pulse current extrapolated to absolute zero of temperature. Pulses just slightly higher than dc critical have a discontinuity at the lambda point as shown by the dashed curve of Fig. 17.

As the pulse current is increased above the dc critical, switching proceeds by more and more rapid motion of boundaries toward the ends of the specimen. The switching also begins to initiate at a number of points along the specimen, so that the voltage first rises rather abruptly after an initial delay, after which there is a slower rise corresponding to the boundary motion. At a rather definite current value the initial rise becomes the full switch. Under this condition the specimen is presumably undergoing a magnetically initiated switch simultaneously all along its length. This current will be termed the simultaneous switch current I_s. This pulse current is the minimum for a fast full switch, *i.e.*, lower pulses require a considerably longer time to reach full switch because of the gradual rise following the initial switch. For good quality specimens, I_s at any temperature is approximately 1.25 times I_e, the dc critical current extrapolated to that temperature from below the lambda-point temperature (given by the dashed curve of Fig. 11). The switch delay times τ associated with pulse currents I_s are found to be constant, independent of temperature. A curve of I_s vs T follows the function $I_s/I_{so}=1-(T/T_c)^4$ (Fig. 17).

For the purpose of plotting switch time vs current at a given temperature, it is convenient to use the ratio of pulse current to the extrapolated dc critical current I_e. Switch times as a function of I/I_e are shown in Fig. 18 for an indium specimen 5 mm long, 60 μ wide, and 0.15 μ thick. This curve shows two regions having distinctly different slope. These regions correspond to different switching mechanisms. For pulse heights in the region of steeper slope, *i.e.*, smaller I/I_e, measurement of voltage as a function of time during the switching process yields traces such as shown in Fig. 12. The switching here proceeds by a localized transition near an imperfection, followed by motion of boundaries of the transformed region toward the two ends of the specimen. The region of smaller slope, corresponding to higher I/I_e, is the region of fast switch. The break in the curve occurs at a pulse current which causes the initial fast switch to develop one-half of the normal resistance of the specimen; the remainder of the resistance develops slowly. This interpretation is supported by Fig. 19 which shows the voltage vs time behavior of a 0.06-μ tin specimen for three different pulse currents. Both current and voltage traces are shown, with the voltage delayed after the current due to both the switch delay time and a cable delay of 28 mμsec. The voltage sensitivity has been adjusted to give a full response exactly reaching the height of the current trace. The sensitivities are constant in all three pictures so that the relative size of the current pulses can be estimated from the scale. The lowest trace does not reach full switch in the picture, the next reaches full switch after a final gradual rise, and the top trace is the switch for a pulse current I_s, just critical for a fast switch. Because of this behavior, fast response in a Persistor memory element requires a current pulse I_s or greater.

The switch delay time associated with the curve of I_s vs T is found to depend on specimen thickness, but not on width or length. The switch delay time as a function of thickness is shown in Fig. 20 for indium. As the thickness increases, the switch time increases smoothly up to a thickness of about 0.25 μ. At this thickness, the switching behavior becomes more complicated, and it is no longer possible to set a definite current pulse height at which the initial rapid rise of voltage proceeds completely to a value corresponding to full switch. Appar-

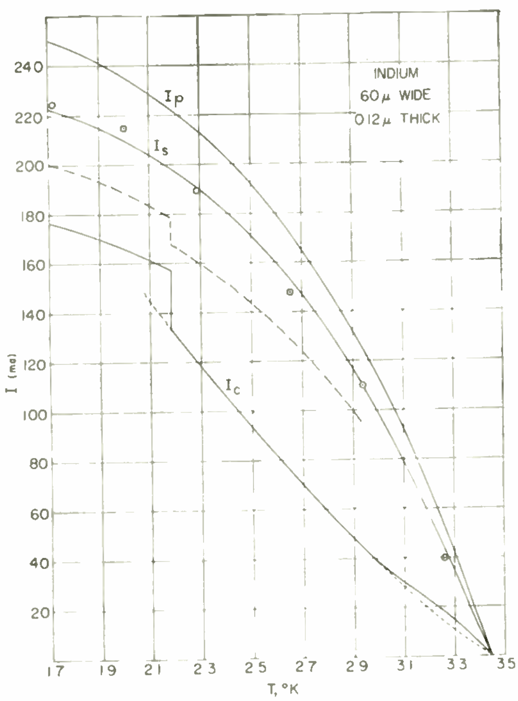

Fig. 17—Values of critical current for simultaneous switch along the specimen I_s as a function of temperature.

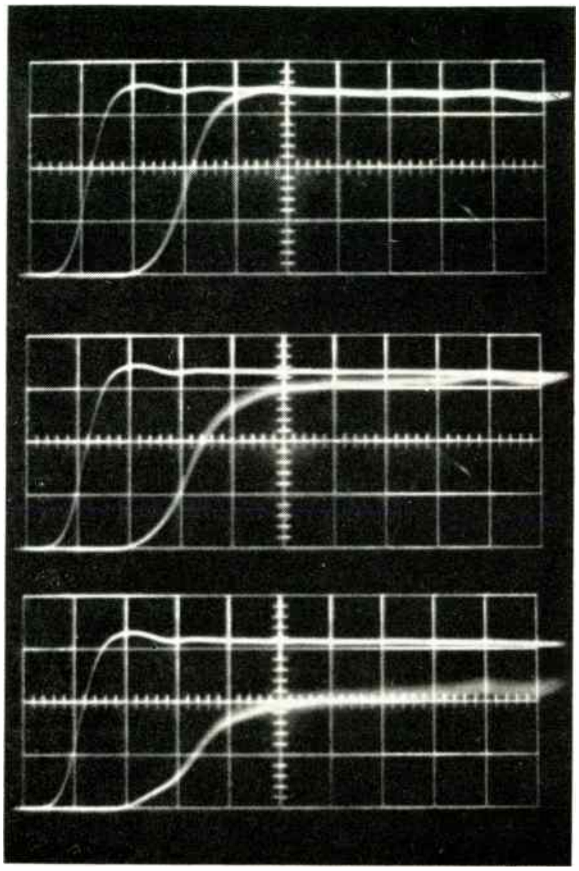

Fig. 19—Switching behavior for currents approaching I_s at $T=2.56°$K. (Time scale: 20 mμsec per large division.)

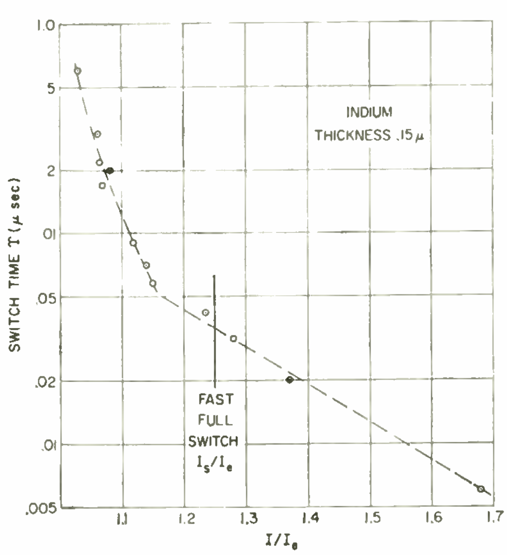

Fig. 18—Switch time τ as a function of pulse current, expressed as I/I_e.

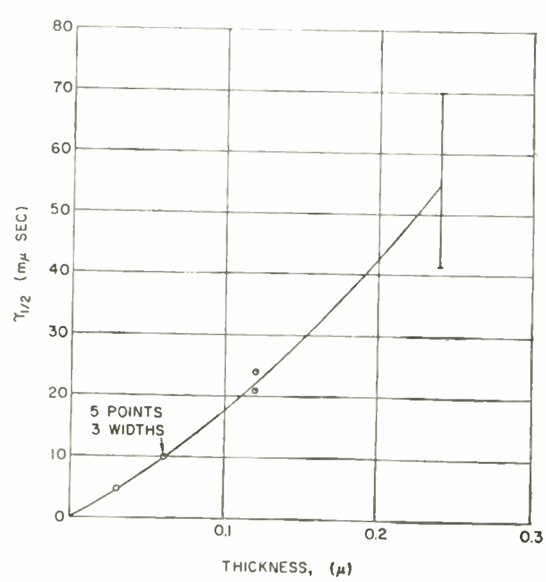

Fig. 20—Switch time for pulses of amplitude I_s as a function of specimen thickness for indium.

ently a more complicated mode of switching becomes possible at thicknesses greater than this.

The fast switch behavior of tin is similar to that of indium, but with slightly higher pulse currents required at a given temperature as would be expected. The delay time for pulses of height I_s is 10 mμsec for films 60 μ wide and 0.06 μ thick, identical with that for indium.

Dependable elements have been produced at a thickness of 0.03 μ of both tin and indium. Probably elements can be produced down to about 0.01 μ, limited at the lower end of this range by imperfection problems. Referring to Fig. 20, the switch time for 0.01-μ films for pulses of height I_s is estimated to be 1 to 2 mμsec.

In pulse operation of a switch element such as in a Persistor memory element, it is also of interest to know the pulse critical current, *i.e.*, the size of a pulse that will just fail to initiate any switching. Unfortunately, current pulses of height equal to or slightly greater than the threshold current I_t prove to cause threshold switching. The time delay of this switching is of the order of a few millimicroseconds. Only a tiny fraction of the full switch occurs, but this is sufficient to cause degradation of memory current, if permitted. In temperature regions where the dc critical and threshold current coincide, the same type of threshold switching occurs at the dc critical. Thus the pulse critical current must be taken as the threshold current.

Recovery Time

The time required for a switch element to switch back from normal to superconducting, hereafter called the recovery time or n–s transition time, is as important as the transition time for the superconducting-to-normal (s–n) transformation previously called the switch delay time. Measurements of the recovery time show that it is of the same order of magnitude as the s–n transition time for properly chosen pulses. Possibly, the short recovery time is associated with the existence of many isolated superconductive domains trapped by the current pulses in the generally resistive switch element. A specimen in such a condition is described as being in the intermediate state—a state which occurs for many other situations[4] throughout the field of superconductivity. The presence of superconducting nuclei throughout the switch element may well be required for short recovery times, since it is known that the nucleation of superconducting domains is a slow process.

Multidimensional Arrays

In the experiments described above, the memory element was driven by direct application of a current pulse. Memory elements have been driven by inductive coupling as shown in Fig. 21. Here, two mutual inductance coils M_1 and M_2 were coupled to the inductance L of the Persistor. The amplitudes of the pulses in coils M_1 and M_2 were made equal and of sufficient magnitude so that coincident pulses from the two coils caused reversal of the memory current, while individual pulses from either coil had no effect on the memory current.

Mutual inductance drive could be used for an array such as that of Fig. 22 in which a memory unit lies at each intersection of vertical and horizontal lines. Each horizontal wire feeds the coils M_1 of the memory units in one row and, similarly, each vertical wire drives the coils M_2 of one column. The diagonal lead in the diagram would connect in series the output from the switch elements R of each memory unit. Thus, a given memory unit could be selected from this array by pulsing simultaneously the horizontal and vertical wires intersecting at that unit. The reversal of the memory current in this element would be detected by the presence of a voltage output in the diagonal lead. The operation would be similar to that of the matrix array system used for small ferromagnetic cores.

Three, or even more, dimensional operation may be possible so far as the operation of individual Persistors is concerned. For three or more dimensional arrays, the number of leads into the cryostat and the number of pulsing circuits would be greatly reduced. If N is the number of Persistors in the cryostat, only $3\sqrt[3]{N}+1$ leads are needed for three-dimensional operation, while $2\sqrt{N}+1$ leads are required for two-dimensional opera-

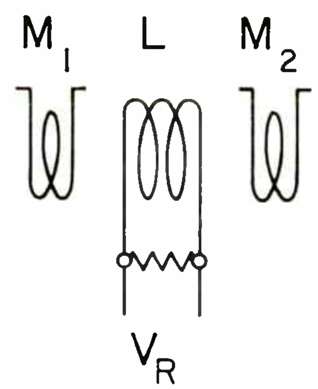

Fig. 21—Schematic diagram of mutual inductance drive for a Persistor memory element.

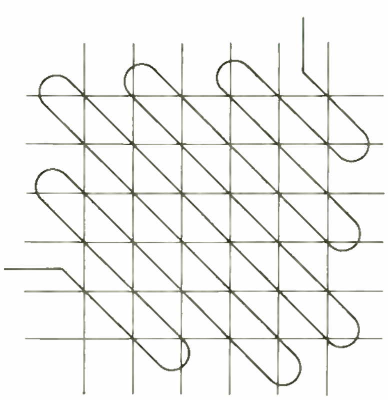

Fig. 22—Schematic memory array.

[4] D. Shoenberg, "Superconductivity," Cambridge University Press, Cambridge, Eng., pp. 21–25, 103–110; 1952.

tion. Thus, for a million Persistor memory, 301 leads are required in a three-dimensional array, while 2001 are needed in a two-dimensional net. Difficulty with interconnections between layers of Persistors seems a problem for three-dimensional operation, although an interesting feature of superconductivity may give some help.[5] No resistance is reported to appear if a pair of superconducting metals are separated by a nonsuperconducting layer as thick as 0.02 μ. Thus, relatively poor contacts can presumably be tolerated.

Operation of Two-Dimensional Arrays

In the operation of a Persistor memory bank, it is important to choose pulse currents which give optimum performance and which give some leeway for minor variations in pulse size and switch element characteristics. Some insight to a sound choice of pulse current can be obtained from a consideration of the conditions which must be satisfied for a two-dimensional array. First, the simultaneous arrival of two pulses in the same direction must produce fast switching for which a total pulse current of I_s is needed. Second, a single pulse superimposed on the memory current must not produce switching. Third, two simultaneous pulses in the direction opposite to that of the memory current must not produce switching. These conditions may be represented by the inequalities

$$2P + M > I_s \tag{1}$$

$$P + M < I_t \tag{2}$$

$$2P - M < I_t \tag{3}$$

where M represents the memory current, P the magnitude of the external pulse fed to either a row or a column of the matrix, and I_t is the threshold current.

For simplicity, let $m = M/I_s$, $p = P/I_s$ and $\alpha = I_t/I_s$. Then, after dividing through by I_s, the inequalities may be rewritten:

$$2p + m > 1 \tag{4}$$

$$p + m < \alpha \tag{5}$$

$$2p - m < \alpha. \tag{6}$$

These three conditions restrict operation to the triangle bounded by the lines $2p+m=1$, $p+m=\alpha$, and $2p-m=\alpha$ shown in Fig. 23. The practical operating region is thus the triangle shown shaded in Fig. 23.

The uppermost lines of Fig. 23 have been drawn for the case of $\alpha = 0.7$. Inspection of this diagram will show that reducing α corresponds to sliding the two lines $2p-m=\alpha$ and $p+m=\alpha$ downward, keeping their directions constant and changing their intercepts on the vertical axis to the new values of α and $\alpha/2$, respectively. The smallest possible useful value of α corresponds to the case in which all three lines intersect at a point. Solving for this condition, one finds $\alpha = \frac{3}{5}$ as the minimum value. Under these conditions $p = \frac{2}{5}$ and $m = \frac{1}{5}$, or $P = 2I_s/5$ and $M = I_s/5$. It would normally be advisable to operate under conditions giving a finite operating area rather than a point to allow for uncertainties in pulse height and switch element characteristics.

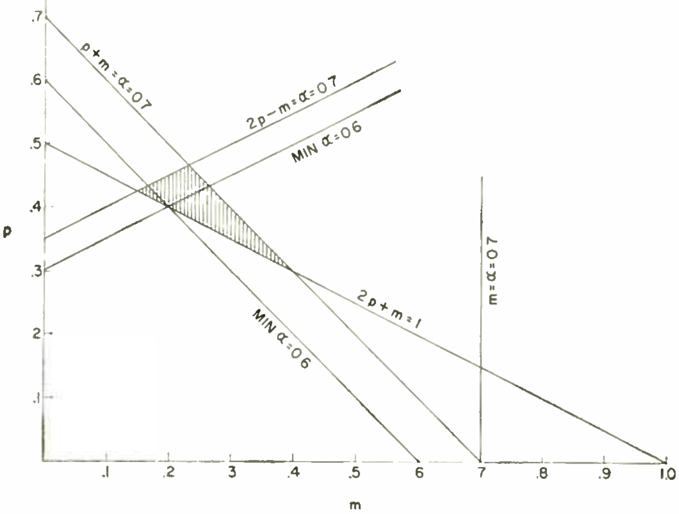

Fig. 23—Diagram delineating permissible operating range for a two-dimensional array.

The requirement that α be $\frac{3}{5}$ or more can be met for real switch elements, but the requirement is a stringent one. Fig. 24 shows values of α as a function of temperature for specimens of indium and tin 60 μ wide and 0.1 μ thick. The values have been calculated from data similar to that of Fig. 11 and Fig. 17. It can be seen that α is $\frac{3}{5}$ or greater for the indium only for temperatures less than about 2.4°K. For tin this is true only for temperatures less than about 2.6°K.

Fig. 25 shows oscillograph traces for operation of an indium element with values of α as in Fig. 24 at 2.2°K under conditions satisfying the requirements for two-dimensional matrix operation. Primarily, this means a choice of pulse length relative to L/R for the element such that the current in the switch element will decay from I_s to 0.6 I_s during the pulse. This comes about because the decay must be twice the memory current, which in turn is $I_s/5$. The switching current in the element is initially $2P+M=I_s$. The time constant thus must satisfy $0.6 = e^{-Rt/L}$, giving $L/R = 2.0t$. To make the details of operation clear a long L/R of 420 mμsec was chosen. The pulse length used was then 210 mμsec (at full amplitude). The current and voltage traces are superposed on alternate sweeps with an electron switch circuit, but with the voltage trace inverted for visibility. The current pulses are the more rectangular pulses. The upper set of traces shows the behavior with alternating polarity but equal height current pulses (each $2P$). The middle set of traces shows the behavior with the second current pulse reduced to half height (P). The lower set of traces shows the response with the sec-

[5] H. Meissner, "Measurements on superconducting contacts," *Phys. Rev.*, vol. 109, p. 686; February, 1958.

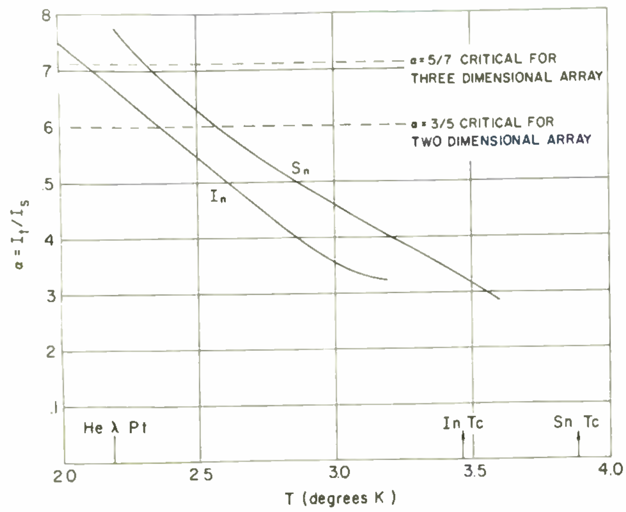

Fig. 24—Values of (I_t/I_s) as a function of temperature for tin and indium.

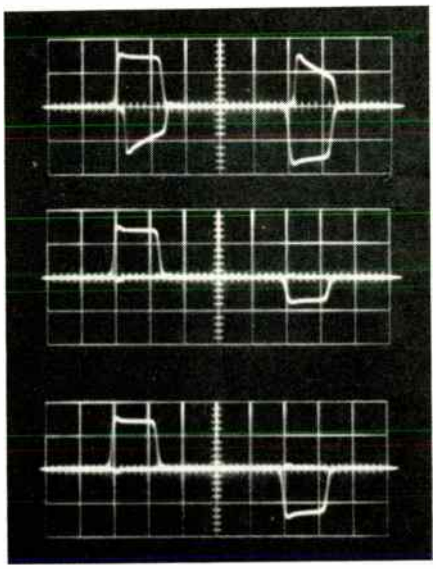

Fig. 25—Oscillograph traces for Persistor memory element operated under conditions required by two-dimensional array, adjusted for slow speed to show detail.

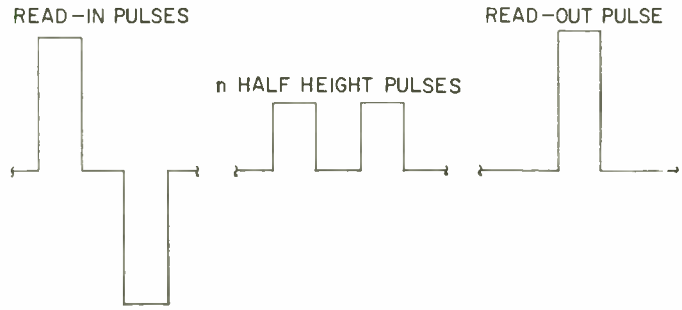

Fig. 26—Pulse pattern employed to test for degradation by threshold switching.

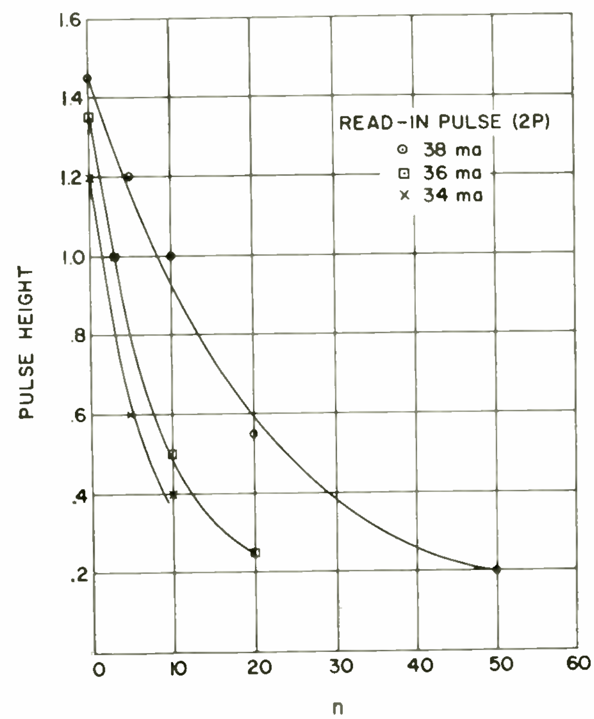

Fig. 27—Response on interrogation at end of text pattern of Fig. 26 as a function of the number n of half-height pulses.

ond current pulse increased to the highest value which will not produce a signal. This latter pulse height, however, is large enough to produce degradation if repeated many times. The specimen has a 4.0°K resistance of 1.6 ohms. Its value of I_s at the operating temperature of 2.2°K is 190 ma. The applied current pulse $(2P)$ is 150 ma. The peak voltage signal is 0.28 volt as compared with the ideal value of $I_s = R = 0.30$ volt.

Operation of a two-dimensional matrix with values of alpha below $\frac{3}{5}$ is possible but degradation of the memory current is produced by the half-select pulses for other elements in the row and column of an interrogated element. This behavior can be illustrated by a test pulse pattern such as indicated in Fig. 26.

After a number of full-height alternating forward and reverse pulses a sequence of n half-select forward pulses is applied. The voltage response V on interrogation with a full-height forward pulse is then observed as a function of n. Fig. 27 shows curves of V as a function of n for several different full-height pulse magnitudes for the same indium specimen as in Fig. 24 operated at 3.27°K. As can be seen, serious degradation of response occurs due to threshold switching. Another consequence of this degradation of the memory current is that a full-height reverse pulse begins to produce a response. A large computer could not tolerate either of these effects. These tests applied to the same element, but at 2.2°K where $\alpha = 0.67$, gave no degradation and no reverse response signal for any number of pulses, tested up to $n = 300{,}000$.

Operation of Three-Dimensional Arrays

The extension to N dimensional arrays is straightforward. For a diagram similar to Fig. 23, operation is restricted to a triangle bounded by the lines $Np+m=1$, $(N-1)p+m=\alpha$, and $Np-m=\alpha$. The critical condition for operation, *i.e.*, with operating triangle shrunk to a point, yields a minimum value of $\alpha=(2N-1)/(2N+1)$; correspondingly $p=2/(2N+1)$ and $m=1/(2N+1)$. Applying the above to the case of a three-dimensional array, the critical conditions are $\alpha=5/7$, $p=2/7$, and $m=1/7$. For the films for which data are plotted in Fig. 24, $\alpha=5/7$ can be realized for temperatures below 2.0°K for indium or below 2.3°K for tin.

Heating Limitations

Since a small amount of Joule heating occurs during the time that a memory element has its switch element in the resistive state, repetitive pulsing of any one element with pulses of alternating sign will presumably be limited by the rate at which the substrate and the liquid helium can remove heat. The tests on a Persistor memory element employing an indium switch element 60 μ wide and 0.06 μ thick showed no measurable heat loading for a 15-mc repetition rate for alternating pulses of 30-mμsec duration. This was the highest possible repetition rate with the equipment available.

Choice of Materials

There are nine pure superconducting metals which might be considered for use in switch elements for Persistors. Most of the data reported in this paper relate to indium ($T_c=3.43$°K). Some data are included for tin (3.74°K), which behaves much like indium. The other materials have disadvantages of varying degree. Beginning with the materials of higher transition temperature, lead (7.22°K), although easy to evaporate, requires large magnetic fields to produce transition, as well as having a high T_c. This is reflected in large critical currents at working temperatures (2° to 5°K), and large heat evolution occurs in the normal state. This leads to long recovery times determined by thermal relaxation and tends to make lead unsuitable for Persistor switch elements. Niobium (8.8°K) and vanadium (4.89°K) have this same difficulty. They, as well as tantalum (4.38°K), are transition metals and are likely to be hard superconductors, especially if not well annealed. That is, their transitions may not be sharp. They also have high boiling points and are consequently difficult to evaporate for film production.

Lanthanum has a transition temperature near 5.0°K in its hexagonal close-packed structure and a transition temperature of 5.95°K for its face-centered cubic structure. Ordinary specimens of lanthanum have a broad transition region which would make them unsuitable for switch elements. Mercury (4.16°K) is unsuitable because of its low melting point. Thallium (2.39°K) has almost too low a transition temperature to be useful, unless working below the lambda point of liquid helium (2.186°K) were desired to permit high heat dissipation. There are no other pure metals that are superconductors except at lower temperatures. There are alloys (actually intermetallic compounds) that have T_c in the useful range, but they tend to have broad transitions and also would be difficult to produce by evaporation.

Returning to the elements indium and tin, their superconductlng behavior is very similar. The slightly higher critical temperature of tin permits operation of superconducting devices at slightly higher temperature than for indium. As shown previously, multidimensional operation of Persistors can also be carried out at slightly higher temperature for tin than for indium. This makes the cooling system slightly easier to operate. Tin films of good quality can also be produced at slightly higher substrate temperature than indium. Tin has another crystal phase, grey tin, to which it can transform at temperatures below 18°C. Transition is relatively unlikely because of the low self-diffusion rate at 18°C and below; however, transition can occur and is most likely in the general vicinity of −50°C. Once a transition is started it spreads rapidly. The transition changes metallic tin to a powder and would destroy the switch elements. Since a memory bank would be cooled or warmed through the dangerous range occasionally, there is some risk involved. The transition to grey tin is reported to be almost completely suppressed by addition of a few tenths of a per cent of bismuth so that this problem is probably not serious. Evaporation of such an alloy requires different but well-known source techniques, such as feeding prealloyed powder onto a hot boat. These considerations suggest that tin is somewhat preferable to indium as a switch-element material.

For parts of the circuits other than the switch elements, lead is well suited. It can be evaporated easily in large thicknesses on substrates at room temperature. Surface coating is desirable since the lead oxidizes on exposure to the atmosphere. The high transition temperature and relatively high magnetic field required to extinguish superconductivity ($B_o=0.0805$ weber/m^2) permit it to remain superconducting even when carrying relatively large currents.

Switch Element Design Parameters

The dc switch current of an element can be described by quoting I_{co}, the dc critical current extrapolated to absolute zero of temperature. As shown previously this depends linearly on width and nonlinearly on thickness of the element. The fast-switch critical pulse height I_{so} varies in a similar manner. The resistance of an element in the normal state depends on its width, thickness, and length. The speed of an element for pulses of height I_s, just sufficient to reach fast-switch behavior, is dependent on thickness only, as previously shown. Thus, by appropriate choices of length, width, and thickness, it is possible to produce switch elements with a wide range of fast-switch speed, sensitivity, and resistance.

Specimen Preparation

The switch elements of indium and tin were produced by vacuum evaporation at a pressure of 5×10^{-7} mm of mercury or less and at a deposition rate of about 0.01 μ/sec. A low pressure and a high deposition rate are needed in order to reduce impurities codeposited from the residual gas.

Deposition of neither indium nor tin is satisfactory with glass substrates at room temperature. The problem seems to be the nucleation of an insufficient surface density of initial metal crystals on the surface. At lower temperatures a larger surface density of crystals is nucleated and thus a flatter film is produced. The indium specimens reported here were deposited on substrates held at $-120°$C by cementing to a surface which could be cooled. The tin specimens were deposited at $-50°$C.

The test specimens employed were all similar to the specimen shown in Fig. 7. The edges were defined by Gillette thin razor blades with the ends of the razor blades ground to provide the widened terminal regions. The specimens were pressed directly against the razor blades. The blades are 0.004 inch thick and have a double bevel, so that the defining edges were 0.002 inch from the glass substrate.

The vapor source was a tantalum boat 10 cm from the specimen. The drop of molten indium or tin was about 3 mm wide at the maximum. Some surface creep of the evaporating metal occurs on the tantalum so that the source is usually wider than the drop width. A penumbra shadow width of about 2 μ occurs at the edge of the specimen, in which the metal tapers toward zero thickness. At the outer edge of this shadow, the metal usually terminates in a scalloped region with the period of the scallop about one micron. This scallop seems related to the nucleation process of formation of the film. Attempts to use knife edges with a single bevel to reduce the penumbra width met with failure due to scratches invariably introduced on removal of the knife edges.

Reproducibility of specimen width from one set of knife edges to another could be held to the limit of straightness of the knife edges (± 2 μ) for specimen lengths of 5 mm.

The thickness of the specimens is controlled by placing a known mass of metal in the boat and evaporating to completion. If the boat is nearly flat and both the specimen and the boat are perpendicular to the line between them, the thickness is given by mass/(πr^2)(density). The thickness was also calibrated by interferometric measurements in the results reported.

Size of Elements

The Persistor memory element requires a relatively small volume. It is estimated that sheets of Persistors having the order of magnitude of 10,000 units per square foot can be produced by printed circuit techniques and that at least 100 sheets could be stacked together per linear foot. Thus, a cubic foot might hold a million Persistors. It would be necessary to achieve very complete shielding between sheets, but this should be readily accomplished by use of thin lead foils between sheets. The lead would be superconducting at operating temperatures and magnetic flux cannot pass through a superconductor. This phenomenon, known as the Meissner effect after its discoverer, is expected to eliminate interactions between adjacent sheets.

Low Temperatures

The achievement of the low temperature needed for a superconducting memory bank should not be a major problem. Fig. 28 shows a typical cryostat used in the measurements described above. The cryostat proper is the set of glass containers appearing in the center of the photograph. These consist of an inner Dewar flask suspended from a plate at the top and an outer Dewar flask containing liquid nitrogen as a heat shield. The latter has been lowered to expose the inner Dewar in the photograph. The inner Dewar flask is sealed to the plate with a rubber gasket, filled with liquid helium to a

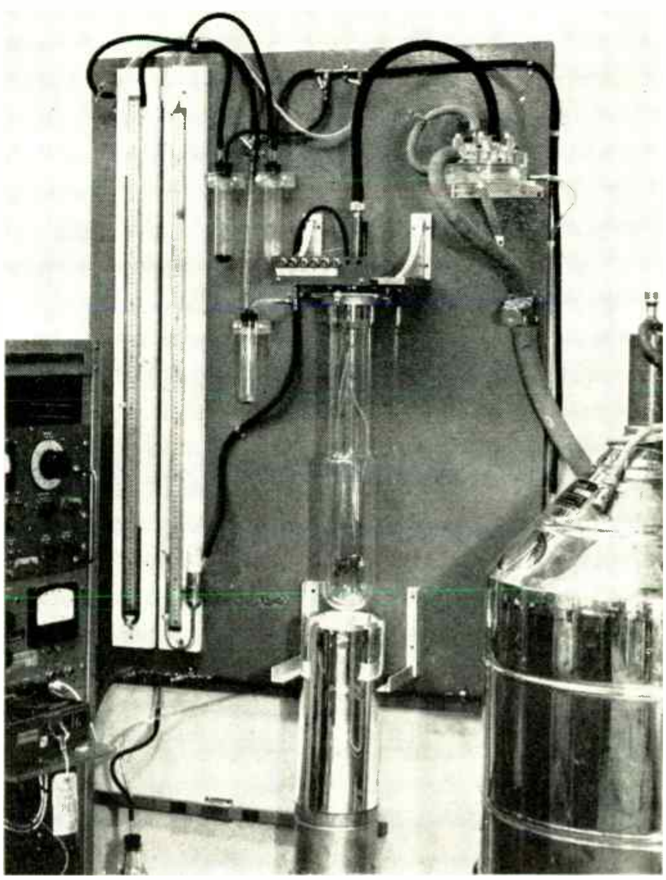

Fig. 28—Cryostat used in experimental program.

depth of about eight inches, and pumped to a pressure of about half an atmosphere by a mechanical pump not shown in the photograph. Control of the temperature is provided by regulating the pressure with the regulator shown in the upper right of the photograph. On the left are mercury and oil manometers for reading the pressure. On the right is a liquid helium storage tank. Electrical leads are carried through the vacuum seals in the top plate. Small coaxial cables then extend to a specimen jig at the bottom of the inner Dewar flask. A computer memory consisting of a large number of memory elements would presumably be refrigerated in a similar cryostat of larger dimensions. For a large computer a continuous cooling system could be provided, rather than one in which the cryostat must be recharged with liquid helium.

Conclusion

Individual Persistor memory elements with switching times from a few to several hundred millimicroseconds have been produced and tested. Before such elements can be incorporated into a memory, appropriate gates, drive circuits and sensing circuits must be developed. An active program to develop superconducting devices to perform the several functions required by a computer is currently in progress.

Acknowledgment

The authors wish to thank C. Marinoff of Space Technology Labs., Inc., Los Angeles, Calif., and K. C. Smith of the U. S. Naval Postgraduate School, Monterey, Calif., for their enthusiastic help with the experimental program throughout the course of the work.

Limitations and Possibilities for Improvement of Photovoltaic Solar Energy Converters*

Part I: Considerations for Earth's Surface Operation

M. WOLF†, SENIOR MEMBER, IRE

Summary—Seven factors limiting the performance of photovoltaic solar energy converters are listed and explained. They can be classified into basic and technology determined limitations. Possibilities for improvement on technology determined limitations are investigated for the silicon solar cell. Such possibilities are: heavier *p*-layer doping; change of geometry, possibly by application of grid structures; improvement of the material constants; and utilization of drift fields for improved collection. Discussed are materials other than silicon in regard to their potential for better performance than that obtainable from the silicon solar cell; and finally, new methods of approach, such as the multilayer and the multiple transition solar cell. Both of these methods yield theoretically large improvements, but realization depends on further advances in compound semiconductor technology and in knowledge about localized centers in the forbidden gap. Limit conversion efficiencies of 38.2 per cent for a 3-layer cell and of 51 per cent for a 3-transition cell, compared to 23.6 per cent for a single *p-n* junction, single transition cell, are obtained. Also discussed are the possible merits of the application of the graded energy gap to photovoltaic energy converters, and potential improvement in collection efficiency is found for certain cases.

I. Introduction

FIVE years have passed since the first solar energy converters utilizing a *p-n* junction in silicon were made by Chapin, Fuller and Pearson in 1954.[1] Continued research efforts during these years have led to a considerable improvement in the performance of this device as well as to a deeper understanding of its operation.[2,3] It can be expected that continued developmental efforts will lead to a saturation of the performance of this device within the next few years. Since the silicon solar cell has created a vast interest it appears necessary to survey the different possibilities for improvement of photovoltaic solar energy converters in order to point the directions for future fruitful development efforts. This discussion concerns itself with an evaluation of the following devices: silicon solar cells,

* Received by the IRE, August 19, 1959; revised manuscript received, January 11, 1960. A part of the work reported in Section II-D was carried out in partial fulfillment of the requirements for the Ph.D. degree at the Illinois Institute of Technology, Chicago, Ill.

The following paper, partially paralleling this one, has been published after the submission of this manuscript: P. Rappaport, "The photovoltaic effect and its utilization," *RCA Rev.*, vol. 20, pp. 373–296; September, 1959.

† Semiconductor Division, Hoffman Electronics Corp., El Monte, Calif.

[1] D. M. Chapin, C. S. Fuller, and G. L. Pearson, "A new silicon *p-n* junction photocell for converting solar radiation into electrical power," *J. Appl. Phys.*, vol. 25, pp. 676–677; May, 1954.

[2] M. B. Prince, "Silicon solar energy converters," *J. Appl. Phys.*, vol. 26, pp. 534–540; May, 1955.

[3] M. Wolf and M. B. Prince, "New Developments in Silicon Photovoltaic Devices and Their Application in Electronics," Congress for Solid State Physics and its Applications in Electronics and Communications, Brussels, June, 1958; Proceedings to be published by Academic Press, Inc., New York, N. Y. M. B. Prince and M. Wolf, "New developments in silicon photovoltaic devices," *J. Brit. IRE*, vol. 18, pp. 583–595; October, 1958.

single p-n junction solar cells with constant energy gap, single p-n junction devices with graded energy gap, multiple p-n junction devices with different energy gaps, and solar cells using multiple photon transition possibilities.

Since the device under consideration is a solar energy converter and not a light converter in general, the nature of the sun's radiation and its spectral distribution in particular are of essence in these considerations. The more refined and sophisticated a solar energy converter will be, the better it will be matched to the sun's spectrum, and a deviation in the input spectrum will affect the performance more severely. It will, therefore, be important to consider different cases for the optimization of solar energy converters separately. This part of the paper will concern itself with a solar energy converter utilizing the sun's radiation as it is received on a clear day at the earth's surface, and is based on the general assumption that the energy converter can be kept at 25°C or in a relatively small range about this temperature. The second part of this paper will consider the case of solar radiation in free space outside the earth's atmosphere, as well as the effect of variation of operating temperature of the photovoltaic solar energy converter.

The basic equations describing the characteristics of photovoltaic solar energy converters and the corresponding equivalent circuit were given in previous papers.[2-4]

II. The Factors Limiting Photovoltaic Solar Energy Converter Performance

In this section all the limitations on the conversion efficiency of photovoltaic solar energy converters will be listed and their nature, their importance on the converter performance, and possibilities for their improvement will be discussed.

The limitations on the efficiency of photovoltaic solar energy converters can be broken down into the following major factors:

1) Reflection losses on the surface;
2) Incomplete absorption;
3) Utilization of only a part of the photon energy for the creation of electron-hole pairs;
4) Incomplete collection of the electron-hole pairs by diffusion to the p-n junction;
5) A voltage factor given by the ratio of open circuit voltage to energy gap potential difference;
6) A curve factor given by the ratio of maximum power point voltage times maximum power point current to open-circuit voltage times short-circuit current for an ideal p-n junction;
7) Additional degradation of the curve due to internal series resistance.

Losses due to refraction in the semiconducting material are not known to occur in any of the systems considered. Internal and surface leakage are also not considered as loss factors since it has been established that, on normal photovoltaic solar energy converters prepared with present techniques, such leakage is small enough to be neglected in view of the relatively high injection level in the operation of these devices. It is expected that these losses can also be held small in future systems.

Factors 1), 2) and 4) can be combined and called "over-all collection efficiency" as has been done previously.[3] This is reasonable to do since all 3 factors are controlled by the absorption characteristic of the material. Factors 1) through 4) together determine the amount of short-circuit current available from the device, while points 5) and 6) can also be considered together as losses due to the V-I characteristic.

Some of the seven factors governing the obtainable efficiency of photovoltaic solar energy converters are basic limiting factors while others are mainly determined by techniques, and improvement on these may be possible up to near elimination of their influence. The factors listed under numbers 1), 4), and 7) belong to this latter category while the factors listed under numbers 2), 3), 5), and 6) have absolute physical limitations beyond which improvement is not possible. It should be noted that these factors having basic limitations are also technique influenced to some extent, and that, in general, better choices of parameters and improvements in techniques can be made in regard to these factors in order to approach the basic limits more closely. It has also to be stated that, in order to make estimates of some of the basic limits, parameters have to be introduced into the calculations which are partially technique influenced, such as minority carrier lifetime and mobility. Here values will be introduced which appear reasonable by present day knowledge, but which may have to be revised at a later date.

A. Reflection Losses

The reflection losses given by the reflection coefficient $r(\lambda)$ are extremely small on present silicon solar cells.[3] This low reflection has been achieved by high impurity concentration obtained under proper diffusion conditions. It can be hoped that with a change to other materials a similar effect can be achieved in the process of formation of the p-n junction. If this should not be the case, special films for the reduction of reflection losses may have to be applied.

B. Incomplete Absorption

Fig. 1 shows the energy spectrum of sunlight on a bright clear day on the earth surface at sea level as given by P. Moon.[5] The same figure also shows curves of the maximum amount of energy utilized in the generation of electron-hole pairs in semiconductors with dif-

[4] J. J. Loferski, "Theoretical considerations governing the choice of the optimum semiconductor for photovoltaic solar energy conversion," *J. Appl. Phys.*, vol. 27, pp. 777–784; July, 1956.

[5] P. Moon, "Proposed standard solar-radiation curves for engineering use," *J. Franklin Inst.*, vol. 230, pp. 583–617; November, 1940.

ferent energy gaps. It is seen that for every value of the energy gap a cutoff line is obtained beyond which the photon energy is not sufficient to create electron-hole pairs. It is also observable that the smaller the energy gap of the material, the larger a portion of the energy spectrum of the sun can be utilized.

The result of this cutoff is a rapid change in absorption coefficient for photons having energies close to the amount of the energy gap. The dependence of the absorption coefficient $\alpha(\lambda)$ on wavelength λ near the absorption edge, shown in Fig. 2 for silicon,[3] is similar for most semiconductors investigated so far. Such a curve

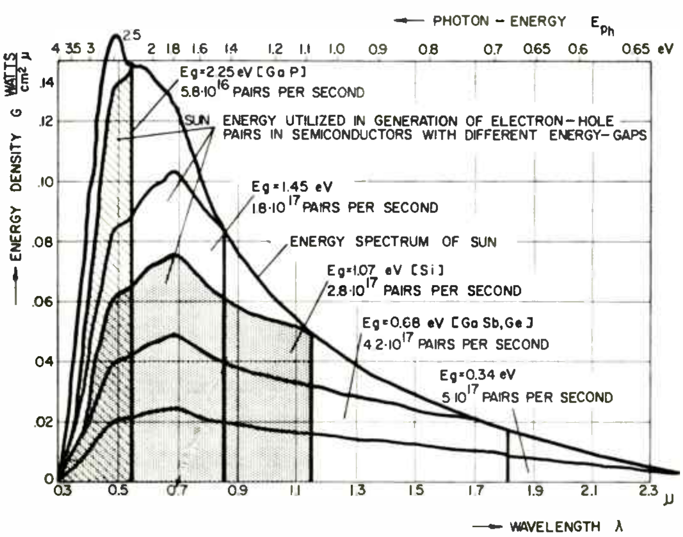

Fig. 1—The energy spectrum of the sun on a bright, clear day at sea level, and the parts of this spectrum utilizable in the generation of electron-hole pairs in semiconductors with energy gaps of 2.25, 1.45, 1.07, 0.68 and 0.34 ev, respectively. Listed for each of these cases is the number of electron-hole pairs generated, obtained under the assumption of the existence of an abrupt absorption edge with complete absorption and zero reflection on its high energy side.

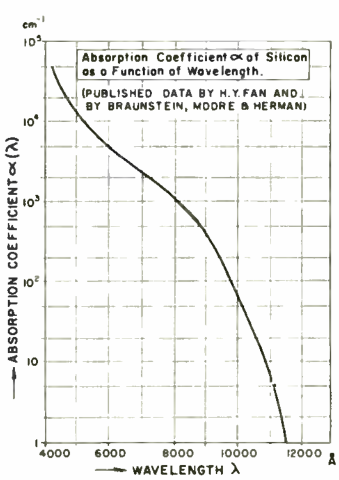

Fig. 2—Absorption coefficient α vs wavelength λ for silicon in the range of interest for solar energy conversion. (Published data by H. Y. Fan, M. L. Shepherd and W. Spitzer, "Intra-Red Absorption and Energy-Band Structure of Germanium and Silicon," John Wiley and Sons, Inc., New York, N. Y.; 1956, and by R. Braunstein, A. R. Moore and F. Herman, "Intrinsic optical absorption in germanium-silicon alloys," *Phys. Rev.*, vol. 109, p. 695; February 1, 1958.)

is largely determined in magnitude and form by the shape of the energy bands of the semiconductor, but can also be affected by lattice imperfections.[6] A small absorption coefficient means deep penetration of the photons and eventually transmission through the material due to insufficient photon-electron interactions. The power P_{Tr}, lost due to such transmission, is given by

$$P_{Tr} = \int_0^\infty P_{In}(\lambda) \exp(-\alpha(\lambda)d)d\lambda \qquad (1)$$

where d is the thickness of the semiconducting wafer. It should be noted that this expression is only appropriate if the absorption coefficient is small in the whole region on the long wavelength side of the absorption edge; this means that no essential free carrier or impurity absorption takes place. There will be no possibility of decreasing these absorption losses except by application of multiple layers of different energy gap material or by modification of the absorption pattern by introducing levels inside the forbidden gap.

C. Partial Utilization of the Photon Energy

A large number of the photons absorbed have more energy than necessary for the generation of an electron-hole pair. The energy needed for this photon-electron interaction is equal to the energy difference between the bottom of the conduction band and the top of the valence band, called the energy gap. The excess energy of the photons contributes to lattice vibrations, meaning that it is dissipated in heat.

Fig. 1 takes this energy loss into consideration by showing the actual part of the sun spectrum used for the generation of electron-hole pairs for different energy gap materials. The smaller the energy gap, the more power is wasted near the peak of the sun spectrum. This energy loss is expressed through the introduction of a factor hc/λ with h being Planck's constant and c the velocity of light [see (7)].

Fig. 3 presents a curve showing that portion of the sun energy which is utilized in the generation of electron-hole pairs as a function of energy gap under the assumption that all photons with sufficient energy to create electron-hole pairs are actually absorbed. This curve combines the effect of the loss factors 2) and 3), and is obtained by numerical evaluation of the spectral distribution of the sunlight (Fig. 1). One can see that the maximum is near 46 per cent of the total impinging energy at an energy gap of 0.9 ev.

Fig. 4 gives the maximum possible number of electron-hole pairs generated by sunlight per cm² of exposed area per second and the corresponding maximum light generated current density, $j_{L_{max}}$, both as a function of energy gap of the semiconductor used. Figs. 3 and 4 give basic limits of the corresponding quantities which

[6] T. S. Moss, "Optical Properties of Semiconductors," Academic Press, Inc., New York, N. Y., pp. 34–52; 1959.

are completely independent of technique factors, and about which no assumptions about certain parameters had to be made for their evaluation.

D. Collection Losses

Most of the electron-hole pairs created by photon absorption are not generated within the space charge region of the p-n junction. Therefore, on the average, only those electron-hole pairs will be collected which are within a diffusion length from the junction. The majority of pairs generated in greater distances from the junction will recombine, causing the collection efficiency to fall below 100 per cent. This collection efficiency is defined as the ratio of electron-hole pairs separated by the electric field of the p-n junction to the total number of electron-hole pairs generated, and is here designated as η_{coll}. The collection process is determined by material constants: the location of the pair generated by the absorption mechanism and the diffusion and recombination by mobility and minority carrier lifetime.

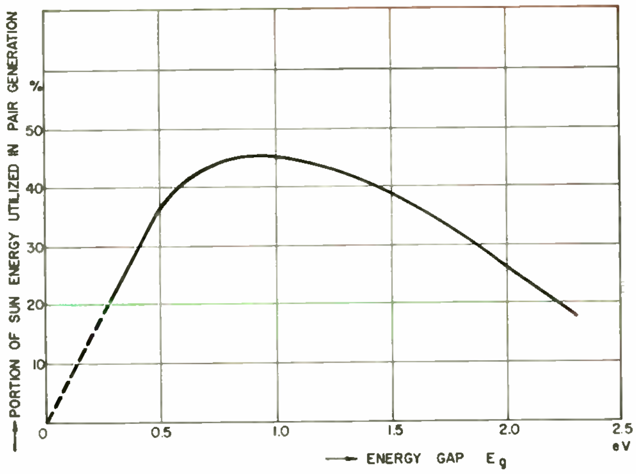

Fig. 3—The portion of the sun energy which can be utilized in electron-hole pair generation as a function of the width of the energy gap of the semiconductor.

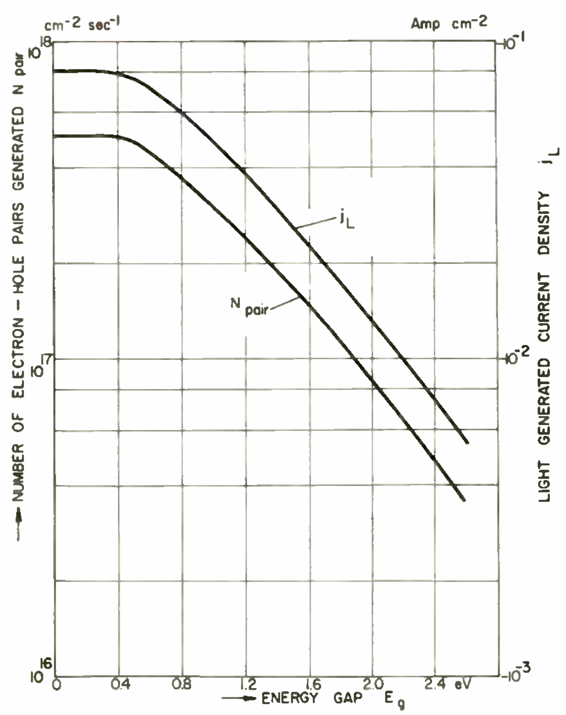

Fig. 4—The number of electron-hole pairs generated and the corresponding maximum theoretically possible light generated current vs energy gap.

The collection process can be analytically evaluated, as was done by Wolf and Prince.[3] A diffusion differential equation for the steady state was set up and solved under the appropriate boundary conditions, resulting in the electron distribution $n(x)$ in the p-layer, which is exposed to a flux of $N(\lambda)$ photons entering the semiconductor per cm² per second in the wavelength range $d\lambda$ around λ (see Appendix I):

$$n(x_n', \lambda) = \alpha(\lambda)\tau_n N(\lambda) \left\{ \frac{1}{b_n^2 - 1} e^{-x_n'} \left[e^{(1-b_n)y_n} - e^{(1-b_n)x_n'} \right] + \left[\frac{a_n + 1}{b_n^2 - 1} (e^{(1-b_n)y_n} - 1) - \frac{1}{b_n + 1} \right] \cdot \frac{\sinh (x_n' - y_n)}{\cosh y_n + a_n \sinh y_n} \right\} \quad \text{for} \quad b_n \neq 1 \tag{2}$$

with the notations

$$x_n' = \frac{x}{L_n}; \quad y_n = \frac{x_j}{L_n}; \quad a_n = \frac{s_n L_n}{D_n}; \quad b_n = \alpha(\lambda) L_n.$$

The hole distribution $p(x)$ in the n-layer is:

$$p(x_p', \lambda) = \alpha(\lambda)\tau_p N(\lambda) \left\{ \frac{1}{b_p^2 - 1} e^{-x_p'} \left[e^{(1-b_p)y_p} - e^{(1-b_p)x_p'} \right] + \left[\frac{a_p + 1}{b_p^2 - 1} (e^{(b_p-1)(z-y_p)} - 1) - \frac{1}{b_p + 1} \right] \cdot \frac{e^{-b_p z} \sinh (x_p' - y_p)}{\cosh (z - y_p) - a_p \sinh (z - y_p)} \right\} \quad \text{for} \quad b_p \neq 1 \tag{3}$$

with

$$x_p' = \frac{x}{L_p}; \quad y_p = \frac{x_j}{L_p}; \quad z = \frac{d}{L_p}; \quad a_p = \frac{s_p L_p}{D_p};$$

and

$$b_p = \alpha(\lambda) L_p.$$

Here τ_n and τ_p are the lifetimes and D_n and D_p the diffusion coefficients for minority carriers in the p- and n-layer respectively, $L_n = \sqrt{D_n \tau_n}$, $L_p = \sqrt{D_p \tau_p}$ the diffusion lengths, and s_n, s_p the surface recombination velocities on the p- and the n-type surfaces. x is the distance from the light-exposed p-type surface and x_j the distance from the surface to the p-n junction, which is assumed to be infinitesimally thin.

Since (2) and (3) are indeterminate for the case $b = 1$, their forms for this case have to be given:

$$n(x_n', \lambda)_{b_n=1} = \tfrac{1}{2}\alpha(\lambda)\tau_n N(\lambda) \left\{ -(y_n - x_n')e^{-x_n'} + [(a_n+1)y_n + 1] \frac{\sinh (y_n - x_n')}{\cosh y_n + a_n \sinh y_n} \right\} \quad (2a)$$

and

$$p(x_p', \lambda)_{b_p=1} = \tfrac{1}{2}\alpha(\lambda)\tau_p N(\lambda) \left\{ (x_p' - y_p)e^{-x_p'} - [(a_p+1)(z - y_p) + 1] \cdot \frac{e^{-z} \sinh (x_p' - y_p)}{\cosh (z - y_p) - a_p \sinh (z - y_p)} \right\}. \quad (3a)$$

Eqs. (2) and (3) can be evaluated after the material constants and dimensions are determined, which can be readily done on prepared solar cells for all of these quantities except τ_n. This quantity can be found, however, by matching the short wavelength part of the calculated spectral response to the actually measured curve. Fig. 5 shows the minority carrier distributions obtained in this manner at two different wavelengths,[3] corresponding to a large and a smaller absorption coefficient. The surface recombination velocity on the p-layer was assumed to be 10^3 cm second^{-1}. τ_n was determined as 10^{-8} second, while τ_p was directly measured as 4.10^{-6} second.

Due to the extremely wide variation of the absorption coefficient with wavelength in the range of interest, practically all electron-hole pairs are created in an extremely thin layer adjacent to the solar cell surface in certain parts of the spectrum, while in others a large portion of the pairs are generated deep inside the material. Due to this and the limited diffusion lengths, the junction has to be placed at such a distance from the light exposed surface that a maximum number of minority carriers will be collected from both sides of the junction. Calculation shows that optimum collection efficiency will be obtained if the layer between the light exposed surface and the p-n junction is as thin as possible, and if at the same time the minority carrier diffusion length in the layer of opposite impurity type is as large as possible.

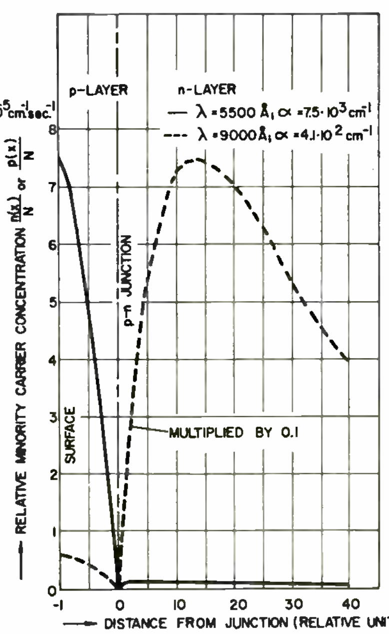

Fig. 5—Relative minority carrier distributions in the p- and n-layer at 2 different wavelengths of incident radiation: $\lambda = 5500$ Å, solid line; and $\lambda = 9000$ Å, dashed line. The distance from the surface to the p-n junction was chosen as the unit for the abscissa. Note the change of scale on the abscissa at the p-n junction, as well as the compression by a factor of 10 of the hole-distribution in the n-layer for $\lambda = 5500$ Å. The distributions were calculated for cell #3-329, which had the following parameters: $x_j = 2.8 \cdot 10^{-4}$ cm; $d = 5 \cdot 10^{-2}$ cm; $\tau_p = 4.2 \cdot 10^{-6}$ second; $\tau_n = 10^{-8}$ second; $\mu_p = 500$ cm^2/volt sec; $\mu_n = 80$ cm^2/voltsec; $s = 10^3$ cm second^{-1}.

The gradient of the minority carrier distribution near the junction due to the photon absorption gives rise to a current flow across the junction. The magnitude of these currents can be obtained from (2) and (3),[3] and is, for the electron current density $j_n(\lambda)$ from the p-layer,

$$j_n(\lambda) = qN(\lambda)b_n \left\{ \frac{1}{b_n+1} e^{-b_n y_n} + \frac{1}{b_n^2 - 1} \cdot \frac{e^{(1-b_n)y_n} - b_n + a_n(e^{(1-b_n)y_n} - 1)}{\cosh y_n + a_n \sinh y_n} \right\} \quad \text{for } b_n \neq 1 \quad (4)$$

and

$$j_n(\lambda)_{b_n=1} = \tfrac{1}{2} qN(\lambda) \left\{ e^{-y_n} - \frac{1 + (1+a_n)y_n}{\cosh y_n + a_n \sinh y_n} \right\} \quad \text{for } b_n = 1. \quad (4a)$$

The corresponding hole current density $j_n(\lambda)$ from the n-layer is

$$j_p(\lambda) = -qN(\lambda)b_p \left\{ \frac{1}{b_p+1} e^{-b_p y_p} + \frac{e^{-b_p z}}{b_p^2 - 1} \cdot \frac{e^{-(1-b_p)(z-y_p)} - b_p + a_p(e^{-(1-b_p)(z-y_p)} - 1)}{\cosh (z - y_p) - a_p \sinh (z - y_p)} \right\} \quad \text{for } b_p \neq 1 \quad (5)$$

and

$$j_p(\lambda)_{b_p=1} = -\tfrac{1}{2} qN(\lambda) \cdot \left\{ e^{-y_p} - e^{-z} \frac{1 - (1+a_p)(z - y_p)}{\cosh (z - y_p) - a_p \sinh (z - y_p)} \right\} \quad \text{for } b_p = 1. \quad (5a)$$

Eqs. (5) and (5a) reduce for the case of an ohmic contact covering the back surface of the wafer ($s_p \to \infty$) to

$$j_p(\lambda)_{a_p \to \infty} = -qN(\lambda)b_p \left\{ \frac{1}{b_p+1} e^{-b_p y_p} - \frac{e^{-b_p z}}{b_p^2 - 1} \cdot \frac{e^{-(1-b_p)(z-y_p)} - 1}{\sinh (z - y_p)} \right\} \quad \text{for } b_p \neq 1 \quad (6)$$

and

$$j_p(\lambda)_{a\to\infty,b_p=1} = -\tfrac{1}{2}N(\lambda)\left\{e^{-y_p} - e^{-z}\frac{z-y_p}{\sinh(z-y_p)}\right\} \quad \text{for } b_p = 1. \tag{6a}$$

The total light generated current density j_L is then

$$j_L = \int_0^\infty [j_n(\lambda) + j_p(\lambda)]d\lambda. \tag{7}$$

The collection efficiency $\eta_{\text{coll}}(\lambda)$ is given by

$$\eta_{\text{coll}}(\lambda) = \frac{j_n(\lambda) + j_p(\lambda)}{qN(\lambda)(1 - e^{-\alpha(\lambda)d})} \tag{8}$$

where the term in parenthesis in the denominator takes account of the fraction of photons transmitted through the wafer. The relationship between the photon flux in the light beam $N_{\text{inc}}(\lambda)$ and that actually entering the semiconductor is determined by the reflection coefficient

$$N(\lambda) = N_{\text{inc}}(\lambda)(1 - r(\lambda)) \tag{9}$$

so that one finally arrives at the over-all collection efficiency $\gamma(\lambda)$:

$$\gamma(\lambda) = (1 - r(\lambda))(1 - e^{-\alpha(\lambda)d})\cdot\eta_{\text{coll}}(\lambda). \tag{10}$$

A collection efficiency curve as a function of wavelength (Fig. 6) was obtained for a sample cell in extension of the calculations discussed in relation to Fig. 5.[3]

This over-all collection efficiency curve can be readily converted into a constant-intensity spectral response-curve by division through the factor hc/λ as explained in Section II-C. Such a curve was shown by Wolf and Prince[3] together with the actually measured points.

Improvement in collection efficiency for any given material can be obtained by increasing the minority carrier lifetime in the p- and n-materials, or by using materials with higher electron and hole mobilities. It also would be desirable to find materials with somewhat smaller absorption coefficients in the peak region of the solar spectrum. Collection efficiencies of around 80 per cent in the major part of the response spectrum of silicon are normally obtained in present solar cells (Fig. 6).

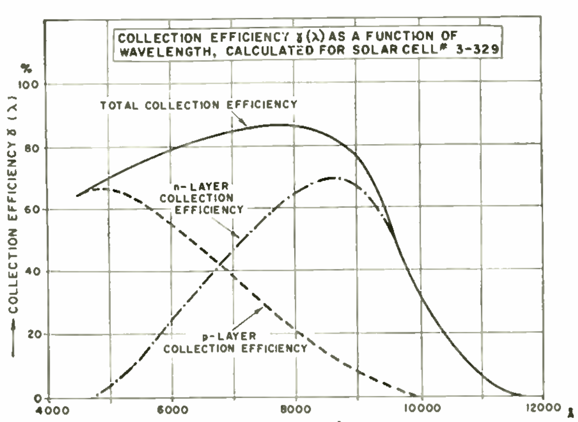

Fig. 6—Collection efficiency vs wavelength for cell #3-329 from Fig. 5. Collection efficiency from the p-layer alone (dashed), from the n-layer alone (dashed-dotted) and from the sum of both (solid) are shown.

E. The Voltage Factor

The amount of energy utilized in the generation of electron-hole pairs is equal to the potential difference between the top of the valence band and the bottom of the conduction band. The largest recoverable voltage, however, is the open-circuit voltage, which is always smaller than the above mentioned energy gap. The reason for this is twofold:

1) The barrier height, which is equal to the maximum applicable forward voltage on a p-n junction, is determined by the difference in Fermi levels in the n- and the p-type material on both sides of the junction. These Fermi levels are a function of impurity concentration and temperature in any given semiconductor, and are normally located inside the forbidden gap, so that the barrier height is less than the energy gap;
2) A voltage equal to the barrier height will only be obtained at extremely high injection levels which can never be reached by photon absorption from direct sunlight.

These two reasons cause the open-circuit voltage to be essentially less than the energy gap potential difference. The magnitude of this open-circuit voltage V_0 can be determined from a transformation of (1) of Wolf and Prince[3] by setting the terminal current $I=0$ and neglecting the term V/R_{sh}, which is permissible for most silicon solar cells at high light level applications (such as direct sunlight):

$$V_0 = \frac{AkT}{q}\ln\left(\frac{I_L}{I_0} + 1\right). \tag{11}$$

Then the ratio of open-circuit voltage to energy gap E_g, called "Voltage Factor" (V.F.), becomes

$$(\text{V.F.}) = \frac{V_0}{E_g} = \frac{AkT}{qE_g}\ln\left(\frac{I_L}{I_0} + 1\right). \tag{12}$$

The quantities determining the open-circuit voltage are the light generated current I_L (equal to the short-circuit current), the saturation current I_0 and the "constant" A. The magnitude of I_L is obtainable from (7). A plot of the maximum limits of I_L per unit exposed area as a function of energy gap was given in Fig. 3. These values will be used here for the evaluation of V_0.

The saturation current I_0 and the constant A are determined by material properties and junction configurations. The diffusion theory of p-n junctions (W. Shockley[7]) results in $A=1$ and

$$I_0 = 1.6\cdot 10^{19}\exp(-39\cdot E_g) \cdot\left(\sqrt{\frac{\mu_p}{\tau_p}}\frac{1}{N_d} + \sqrt{\frac{\mu_n}{\tau_n}}\frac{1}{N_a}\right) \tag{13}$$

[7] W. Shockley, "Electrons and Holes in Semiconductors," D. Van Nostrand Co., Inc., New York, N. Y., pp. 309–315; 1954.

at 25°C, where

μ_p = hole mobility in the n-type region,
μ_n = electron mobility in the p-type region,
N_d = density of ionized excess donor atoms in the n-region,
N_a = density of ionized excess acceptor atoms in the p-region.

One recognizes that the saturation current is determined exclusively by material constants, some of which can be modified by doping or special treatments.

Fig. 7 shows the saturation current as a function of energy gap, calculated with the assumption:

$$\mu_p = 400 \text{ cm}^2 \text{ volt}^{-1} \text{ second}^{-1},$$
$$\tau_p = 10^{-5} \text{ second},$$
$$N_d = 10^{17} \text{ cm}^{-3},$$
$$N_a = 10^{19} \text{ cm}^{-3},$$
$$\mu_n = 10^3 \text{ cm}^2 \text{ volt}^{-1} \text{ second}^{-1},$$
$$\tau_n = 10^{-7} \text{ second},$$
$$T = 25°\text{C}.$$

There is a newer theory on p-n junction behavior which takes account of the generation and recombination of charge carriers in the space charge region of the p-n junction.[8,9]

According to this theory, saturation current and constant A are dependent upon the density and location of energy levels of recombination centers in the forbidden energy gap, besides being dependent on the quantities entering into the diffusion theory. This theory generally results in higher saturation currents than the diffusion theory, and constants A between 1 and 2 are obtained.

Finally, there is a third, not explicitly expressed theory on p-n junction behavior which takes account of internal field emission taking place in extremely narrow space charge regions in p-n junctions.[10] The results are values of the constant A as high as 6 and essentially higher saturation currents than compatible with the two above mentioned theories. It has been shown that the observed behavior of p-n junctions obtained in the preparation of silicon solar cells can best be explained by this third theory.[11] It is fortunate that, in their application to silicon solar cells, the effect of the different theories is rather small. The differences in j_0, although of many orders of magnitude, are compensated to a large extent by simultaneous changes in the constant A for higher injection levels. Therefore, it is justifiable in most cases, and especially in a preliminary survey of photovoltaic energy converters, to assume that the diffusion theory is applicable. This assumption will be made throughout this paper.

The voltage factor has been calculated in accordance with this discussion and the results of this calculation are shown in Fig. 8 as a function of energy gap. One can see that better voltage factors are obtained for larger energy gap semiconductors.

F. The Curve Factor

The maximum power can be extracted from a photovoltaic device at that point for which the largest rectangle can be inscribed into the current-voltage characteristic (Fig. 1 of a previous work[3]). This point is given by the voltage and current values V_{max} and I_{max}. The ratio of the products $V_{max} \cdot I_{max}$ to $V_0 \cdot I_L$ is called here

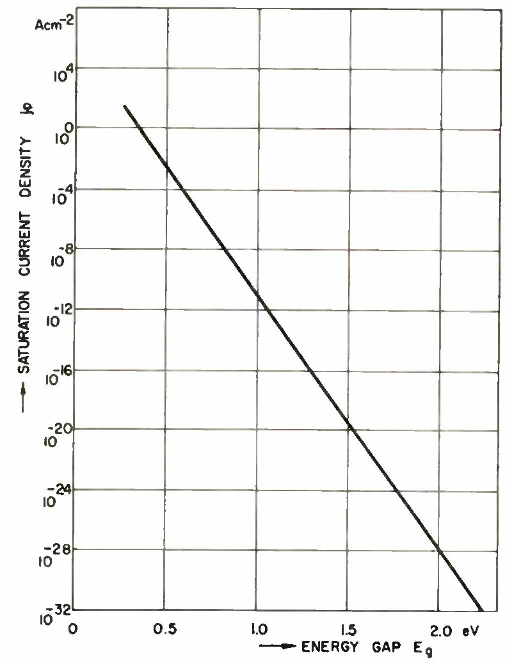

Fig. 7—Saturation current density vs width of energy gap.

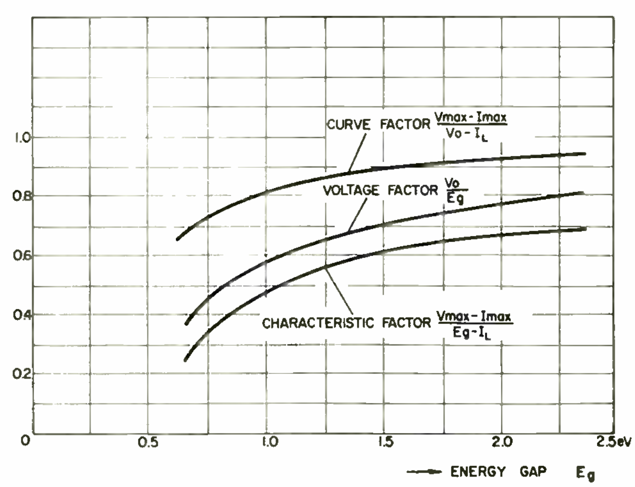

Fig. 8—Voltage factor, curve factor, and characteristic factor vs width of energy gap, calculated with the saturation currents from Fig. 7.

[8] H. S. Veloric and M. B. Prince, "High voltage conductivity—modulated silicon rectifier," *Bell Syst. Tech. J.*, vol. 36, pp. 975–1004; July, 1957.
[9] C. J. Sah, R. N. Noyce and W. Shockley, "Carrier generation and recombination in p-n junctions and p-n junction characteristics," PROC. IRE, vol. 45, pp. 1228–1243; September, 1957.
[10] A. G. Chynoweth, and K. G. McKay, "Internal field emission in silicon p-n junctions," *Phys. Rev.*, vol. 106, pp. 418–426; May 1, 1957.
[11] M. Wolf, "Design of silicon photovoltaic cells for special applications," presented at the AIEE-IRE Semiconductor Devices Conference, Boulder, Colo.; July 15–17, 1957.

the curve factor (C.F.):

$$(\text{C.F.}) = \frac{V_{max}\cdot I_{max}}{V_0\cdot I_0} = \left[1 - \frac{AkT}{qV_0}\ln\left(1+\frac{qV_{max}}{AkT}\right)\right] \cdot\left[1 - \frac{I_0}{I_L}\exp\left(\frac{qV_{max}}{AkT}-1\right)\right] \quad (14)$$

with V_0 given by (11) and V_{max} determined by

$$\left(1+\frac{qV_{max}}{AkT}\right)\exp\left(\frac{qV_{max}}{AkT}\right) = \frac{I_L}{I_0}+1 = \exp\frac{qV_0}{AkT}. \quad (15)$$

The curve factor as well as the voltage factor are determined by the saturation current I_0. This means that the same considerations as given in the previous section are applied here. As in the case of the voltage factor, better values of the curve factor are obtained at larger energy gaps, as is evident from Fig. 8. The product of the curve factor and the voltage factor is here called the "characteristic factor," which is also displayed in the same figure as a function of energy gap.

Not very much can be done for the improvement of the characteristic factor other than proper choice of materials with suitable energy gap and the selection of proper doping levels.

G. Series Resistance Losses

It has been found that in actual silicon solar cells, the internal series resistance is large enough so that it causes a deviation of the current-voltage characteristic from its ideal curve. The best presently known methods do not yield sufficiently high impurity concentrations of the diffused *p*-layer so as to keep its contribution to the total series resistance within tolerable limits, if the *p*-layer thickness would be reduced to values as are necessary for obtaining highest collection efficiency. In the present silicon solar cell a compromise is obtained between *p*-layer thickness (1 to 2 microns) and *p*-layer series resistance (order of 5 ohms) in order to obtain the highest possible over-all efficiency.[2]

A small additional series resistance is experienced in the ohmic contacts of the silicon solar cells, but this contact resistance has been reduced to a negligible value by application of proper techniques.

The output current from a solar cell with series resistance is

$$I_R = I_0(e^{B(V-IR_s)}-1) - I_L, \quad \text{with} \quad B = \frac{q}{AkT}. \quad (16)$$

For sufficiently small series resistance, in order that

$$BIR_s \leq 1, \quad (17)$$

a first order approximation may be introduced for the exponential term without causing excessively large errors, leading to the relationship

$$I_R = \frac{I}{1 + I_0BR_se^{BV}} \quad (18)$$

where

$$I = I_R(R_s = 0) = I_0(e^{BV}-1) - I_L. \quad (19)$$

Following Prince,[2] one can express the power obtainable from a solar cell as

$$P = I_RV = I_RB\ln\left(\frac{I_L+I_R}{I_0}+1\right) + I_R^2R_s \quad (20)$$

where the last term represents the power dissipated in the series resistance. One should observe, in the use of this and other similar formulas, that the current I is a negative quantity for photovoltaic operation, making the first and determining term of (20) negative, as is appropriate for a power generator.

Eq. (20) shows that a power loss as the result of the series resistance is obtained not only from direct dissipation in the series resistance, but also from a change in the first term of (20), caused by the variation of the current-voltage curve due to the series resistance (18).

The total power loss due to this series resistance shall be called P_{R_s}. Possibilities for the reduction of series resistance through the development of improved techniques are good.

H. Conversion Efficiency and Limit Conversion Efficiency

Combining all the loss factors discussed above, one obtains the following expression for the conversion efficiency of a photovoltaic solar energy converter:

$$\eta = \frac{P_{out}}{P_{in}} = (\text{V.F.})(\text{C.F.})(1-P_{R_s})\cdot\frac{q}{hc}\int_0^\infty[1-r(\lambda)] \cdot[1-\exp(-\alpha(\lambda)d)]\eta_{coll}(\lambda)P_{in}(\lambda)\lambda d\lambda \cdot\left[\int_0^\infty P_{in}(\lambda)d\lambda\right]^{-1} \quad (21)$$

where $P_{in}(\lambda)$ is the light power incident on the solar cell surface in a narrow range $d\lambda$ around the wavelength λ, and all other quantities are as previously explained. The first integral together with the factor q/hc describes the short-circuit current density j_L, the second integral, the total light input. The factor $(1-P_{R_s})$ could be considered a modification of the curve factor but is kept separate for reasons of discussion.

The limit conversion efficiency describes an efficiency which is dictated solely by basic physical phenomena, and which is not affected by technique factors on which improvement may or may not be possible. It is an idealized efficiency, which most probably will never be reached, but which is a good tool for the evaluation of different materials or approaches. The concept of the limit conversion efficiency is somewhat analogous to the theoretical efficiencies of thermodynamics. The limit conversion efficiency can be expressed as

$$\eta_{\lim} = (\text{V.F.})(\text{C.F.}) \frac{q}{hc} \int_0^{\text{cutoff}} P_{\text{in}}(\lambda)\lambda d\lambda \cdot \left[\int_0^{\infty} P_{\text{in}}(\lambda) d\lambda \right]^{-1}. \quad (14)$$

The assumptions are: zero reflection losses, complete absorption on the short-wavelength side of the absorption edge, 100 per cent collection of electron-hole pairs, and no series resistance losses. It should be noted that the voltage factor and the curve factor cannot be evaluated without introducing quantities which are somewhat technique affected, as minority carrier lifetime and mobility are, but the dependence of the value of the factors on these not always well-determined quantities is not a very strong one. In order to keep the evaluations consistent, the same lifetimes, mobilities, impurity concentrations and temperature as for the preparation of Fig. 7 have been used throughout. This may be justified with the assumption, that, with further advances of the art, other materials may be brought to properties similar to those now obtainable in silicon.

III. Possibilities for the Improvement of Photovoltaic Solar Energy Converters

The first part of this section will be concerned with solar cells having a single *p-n* junction, and made of a single material of constant energy gap, while the second part will be devoted to an investigation of newer methods of designing photovoltaic solar energy converters, such as graded energy gap, multilayer, and multiple transition solar cells. All paragraphs except the first are chiefly concerned with a study of the basic limitations of new materials and methods, and it can be assumed that technique refinements as discussed in the first paragraph will be applicable in a similar manner to most of the other methods and materials discussed.

A. *Single P-N Junction, Constant Energy Gap Solar Cell*

1) *The Improvement of Silicon Solar Cells:* The limit conversion efficiency for silicon solar cells is 21.6 per cent as first calculated by Prince.[2] The best conversion efficiency achieved on silicon solar cells to date is 14 per cent, while normally efficiencies of 8 to 12 per cent are obtained, depending on the geometry of the cells prepared. It does not seem reasonable to try to improve on the reflection losses since they are already extremely small. Losses due to incomplete absorption or insufficient utilization of the photon energy are also not open to improvement on devices of this type since they are determined by basic physical phenomena. The largest loss experienced on silicon solar cells is due to incomplete collection of the electron-hole pairs. The plot of the over-all collection efficiency $\gamma(\lambda)$ (Fig. 6) indicates that improvements might be expected in the short wavelength region from an increase of the *p*-layer collection efficiency, and towards the long wavelength cutoff by improvement of the *n*-layer collection efficiency.

A high collection efficiency would require an extremely small *p*-layer thickness and a large value of electron mobility and of electron lifetime in the *p*-layer. The latter two could be most easily obtained by low impurity concentration of the *p*-layer. All these requirements would lead to intolerably high *p*-layer sheet resistances. It may be possible to increase the impurity density in the *p*-layer although surface concentrations of about 10^{21} impurity atoms per cubic centimeter are used already. Such an increase in the impurity concentration should lead to an improved collection efficiency after a reduction of the *p*-layer thickness, together with an improvement due to simultaneously decreased series resistance. But even if techniques can be developed which allow a substantial increase in the impurity density, it may be found that this increase results in a simultaneous reduction of carrier mobility and minority carrier lifetime of sufficient magnitude to offset any gains.

While these *p*-layer problems are under study, quicker improvements can be expected from a change in the geometry of the cell. Such a geometry change can be verified either by a change of the cell dimensions, in particular the length-to-width ratio, or by the application of a contact grid structure. It has been known for some time that the $\frac{1}{2}\times 2$ cm silicon solar cells have consistent conversion efficiencies about 20 per cent higher than those obtained in the 1×2 cm size. The reason for this effect is that, with the smaller width of the cell, equivalent to a shorter mean path for the hole current and a lower current density in the *p*-layer, higher values of sheet resistance can be tolerated while still obtaining satisfactory values of series resistance. Thus, a reduction in the *p*-layer thickness can be made while simultaneously obtaining a decrease in the series resistance. A proposed step in this direction was a change of the over-all dimensions. An example was the change from the 1×2 cm cell, which is the most widely accepted type at the present time, to an 0.55×4 cm cell, which has the same active area as the previously mentioned cell but gives better conversion efficiencies.

A second and better approach is the application of contact grids. Recently developed techniques allow the application of such grids consisting of fine metal strips in contact with the *p*-layer placed at suitable distances from each other (Fig. 9). Again, one is confronted with two conflicting requirements: wide grid lines have low resistance, but decrease the active to exposed area ratio. Knowing the terminal voltage V near the maximum power point and other data of the solar cell without grid structure, one can calculate the optimum spacing S and width T of the grid lines (see Appendix II)·

$$T = 2^{5/4} \frac{\rho_T^{3/4}}{\rho_p^{1/2}} (BCj_0 e^{BV})^{1/4} W^{-3/2}, \quad (15)$$

$$S = \sqrt[3]{\frac{2T}{BC\rho_p j_0 e^{BV}}} - \frac{2T}{3} \quad (16)$$

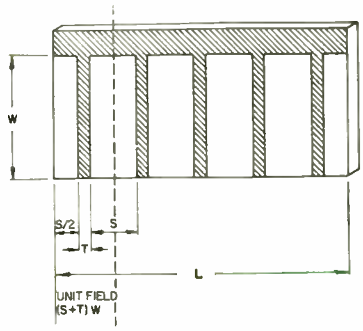

Fig. 9—Configuration of a contact grid structure.

where ρ_T is the sheet resistance of the contact strip, ρ_p is the sheet resistance of the p-layer, j_0 is the saturation current density, and

$$C = 1 - \frac{I_0}{I_L}(e^{BV} - 1). \tag{17}$$

Such an optimum grid for the 1×2 cm cell should have 5 lines with a spacing of 0.4 cm and a line width of 6×10^{-3} cm. This grid reduces the series resistance of the p-layer by a factor of 5.10^{-2}.

Another very desirable feature obtained with the application of grid structures is freedom for the over-all dimensions of the cells. Proper contact grids make it feasible to prepare solar cells in as large a size as crystal growing and cutting techniques permit. 1×2 cm silicon solar cells with contact grids have been prepared showing an average efficiency increase by a factor of 1.15, compared to nongridded, but otherwise identical cells, and 2×7.5 cm cells were made with the same efficiencies as the smaller cells.

One might also consider the application of a thin metal film over the whole p-layer as a means of reducing the p-layer sheet resistance. Investigations have shown, however, that it is not possible to obtain sufficiently low sheet resistances simultaneously with good optical transmission properties on such metal films.

Besides reduction of the p-layer thickness, the collection efficiency can also be improved by increasing the diffusion length of minority carriers. This is equivalent to an improvement in minority carrier lifetimes, which may be achieved through a reduction in the density of unwanted impurities and of dislocation centers in the crystals which both could act as recombination centers. This means that methods for better purification of the raw silicon and better methods for the growing of silicon crystals have to be developed.

While the improvement of collection efficiency due to better minority carrier lifetimes is a long-range goal, speedier results may be obtained by a shift from the reliance on the diffusion process for the collection of minority carriers to the introduction of a drift process by means of built-in fields. Such drift fields can be obtained by proper impurity grading which leads to a varying position of the Fermi level with regard to the band edges (Fig. 10). Such drift fields are applied in some transistors and diodes in order to improve their performance. It should be possible to use near intrinsic silicon and diffuse the n- and p-type impurities from both sides with proper parameters so as to obtain a junction in the desired distance below the surface and simultaneously obtain desired impurity gradings.[12]

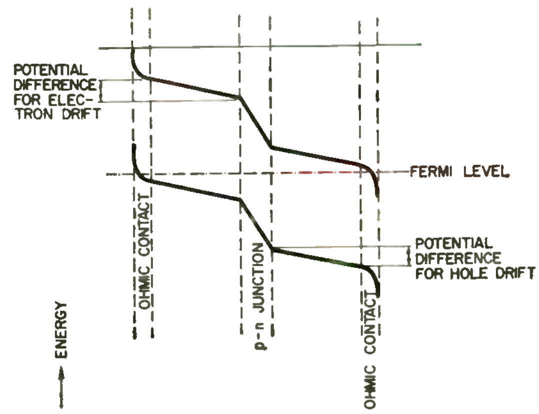

Fig. 10—Energy level diagram for a solar cell utilizing drift fields for improved collection efficiency.

It is expected that after realization of the improvements mentioned here, the achievement of conversion efficiencies of 15 to 16 per cent on silicon solar cells can be expected.

2) Single P-N Junction, Constant Energy Gap Solar Cells of Materials Other than Silicon: While the previous discussions about improvement of photovoltaic solar energy converters dealt exclusively with technique problems, the possibilities of improvement by use of materials other than silicon have to be considered also. Fig. 8 shows that the voltage factor and the curve factor both increase towards larger energy gap materials, while Fig. 3 shows that the percentage of sun energy utilized in the generation of electron-hole pairs decreases with increasing energy gap. The combination of both figures leads to the limit conversion efficiency as a function of energy gap E_g, plotted in Fig. 11, which is in agreement with similar curves published by Prince[2] and Loferski.[4] This figure shows a broad maximum reached by semiconductors with a 1.25- to 1.5-ev energy gap with a maximum conversion efficiency of 23.6 per cent. Several semiconducting compounds are known in this range: for example, indium phosphide, gallium arsenide, cadmium telluride, aluminum antimonide and stibnite.[13,14]

[12] As an example, data for a drift field in the p-layer are cited. A drift field of 200 volts cm^{-1} in a 2-micron thick p-layer requires a difference in Fermi-level across the p-layer of only 0.04 ev. Such a difference in Fermi-level is achievable by a change in acceptor concentration by one order of magnitude even at high acceptor concentrations (about 10^{20} cm^{-3}). A drift field of such magnitude causes an average drift velocity of the electrons in the p-layer of 10^6 cm second^{-1}, which is two orders of magnitude larger than the surface recombination velocity, and twice as large as the average diffusion velocity. This results in an average drift length of 5 times the thickness of the p-layer.

[13] Abraham Coblenz, "Semiconductor compounds open new horizons," *Electronics*, vol. 30, pp. 144–149; November, 1957.

[14] D. A. Jenny, "The stratus of transistor research in compound semiconductors," Proc. IRE, vol. 46, pp. 959–968; June, 1958.

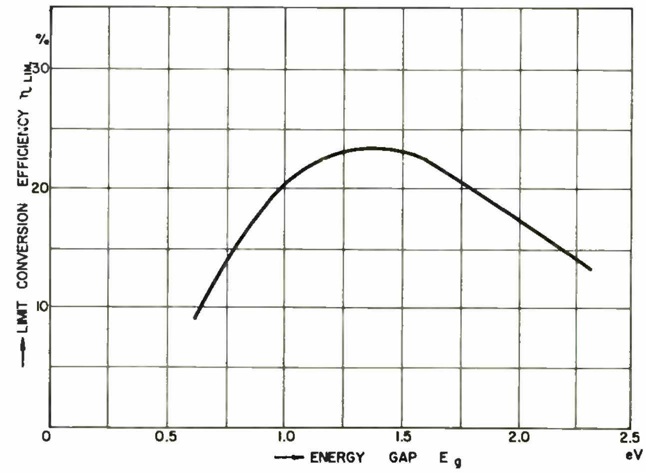

Fig. 11—The limit conversion efficiency as a function of the width of the energy gap for single p-n junction, direct transition solar cells.

Gallium arsenide would appear to be the most promising material for solar energy conversion at the earth's surface for two reasons: first, its energy gap is closest to the maximum of the curve of Fig. 11, and second, the electron mobility is similar to that of silicon. If minority carrier lifetimes nearly as large as those obtained in silicon could be achieved in this material, and if its absorption coefficients could be of a magnitude similar to that of silicon in the range of interest, then this material should yield conversion efficiencies several per cent higher than those ultimately obtainable with silicon solar cells. There is, however, disagreement among different workers in the field on these two points, although definite information about absorption coefficients and minority carrier lifetimes obtained recently in this material are not available. One should expect that gallium arsenide materials with lifetimes much better than 10 mμsec, as frequently quoted now, will ultimately become available, and that reliable data about absorption coefficients will be published. At that time, a final assessment of the usefulness of this material for photovoltaic solar energy converters can be made. In the meantime, conversion efficiencies of 7 per cent have been announced for gallium arsenide solar cells.[15]

Another material of high interest, since it also has high mobilities, is indium phosphide, but even less is published about this material, probably because it is more difficult to prepare than gallium arsenide.[16]

Cadmium telluride, aluminum antimonide and stibnite all have low mobilities, which would suggest that it will be difficult to obtain good collection efficiencies in these materials. But since these materials have not been investigated thoroughly, there is a chance that at a later time essentially higher mobilities may be reported moving these materials closer into the range of interest. It should be noted that any photovoltaic solar energy converter with a single p-n junction utilizing only direct transition photon-electron interaction cannot be expected to yield large increases in conversion efficiencies above those ultimately obtainable in silicon solar cells, no matter what the energy gap or the other properties of the material may be.

B. New Methods

1) *The Multi-Layer Solar Cell:* Since very large improvements cannot be expected from either technique improvements or new materials for single p-n junction constant energy gap solar cells, the viewpoint has to shift to radically different methods of preparing solar cells. A critical investigation of Fig. 1 suggests one method of approach. As the radiation on the long wavelength side of the absorption edge is transmitted through the semiconducting material, it may be absorbed and utilized in a solar cell made from a semiconductor with smaller energy gap placed behind the first cell. Thus, a larger part of the energy of the sun's spectrum can be utilized than possible with a single cell. In doing this one matches the photovoltaic energy converter more closely to the energy spectrum of the sun. This method can easily be expanded to more than two layers, theoretically up to infinitely many. This approach has first been mentioned by Jackson[17] who calculated the case of a 3-layer solar energy converter using semiconducting materials of 1.91-, 1.3- and 0.94-ev energy gap. He found that 69 per cent of the sun energy could be utilized in the generation of electron-hole pairs in this device. This value compares very favorably with the maximum of 46 per cent for the single p-n junction uniform energy gap solar cell shown in Fig. 3.

The idea of this method is to reduce the losses due to incomplete absorption and partial energy utilization in the generation of electron-hole pairs by splitting the solar spectrum into several different bands using the semiconducting material most suitable for each individual band. No consideration is given to the voltage and the curve factors. In fact, both factors decrease not only with energy gap but also with a decrease in light generated current I_L. By splitting the solar spectrum into different bands, the current I_L for the individual layer is reduced with every decrease of the width of its corresponding band of light energy. Therefore, one should expect the existence of an optimum number of layers to yield highest conversion efficiency. If this optimum number is exceeded, the increase in losses due to the voltage and curve factors outweighs the decrease in losses obtained from a better match to the sun spec-

[15] J. J. Loferski, P. Rappaport and J. J. Wysocki, "Recent Solar Converter Research," Thirteenth Annual Power Sources Conference, Atlantic City, N. J.; April 28–30, 1959.

[16] H. T. Minden, "Intermetallic Semiconductors," *Semiconductor Products*, vol. 2, pp. 30–42; February, 1959.

[17] E. D. Jackson, "Areas for improvement of the semiconductor solar energy converter," *Trans. Conf. on the Use of Solar Energy, Tucson, 1955*, University of Arizona Press, Tucson, vol. 5, pp. 122–126; 1958.

trum. For practical purposes, however, one may not even want to apply such a large number of different layers. Three layers appear to be a good number for practical purposes as well as for good conversion efficiency.

It appears necessary to discuss how a useful device can be prepared utilizing several layers of semiconducting material with different energy gap. This can be easily done by viewing Fig. 12 which shows three possible configurations of a two-layer cell. Fig. 12(a) shows the energy level diagram for a *p-n-p-n* arrangement of two such layers. In this arrangement the transition region between the two semiconducting materials is a *p-n* junction. The electric field in this *p-n* junction is directed so as to impede the flow of light generated current from one layer to the other, thus destroying the usefulness of the device. Fig. 12(b) shows a *p-n-n-p* arrangement of the two layers. In this case the transition between the two different energy gap materials is an *n-n* transition. The polarity of the two *p-n* junctions in the different layers is so, however, that the two light generated currents oppose each other, again destroying the usefulness of the arrangement. Fig. 12(c) finally shows a workable arrangement. The two layers of different semiconducting materials are joined together through ohmic contacts, so that current flow from one cell to the other is facilitated without a blocking barrier. In this arrangement optical reasons prohibit covering the back side of the cells with a metal contact layer as is now done on most solar cells. The different layers may be joined together through matching contact grids which cover a minimum of the exposed area, or the back surfaces of the individual layers may be equipped with an extremely low resistivity diffused surface leading to contacts on the outside of the cell.

Normally, it will not be desirable to use the individual layers in separate circuits. Since each layer will have a different voltage because of its energy gap, the only possibility for single circuit operation is a series connection to the individual layers. In this case the same current has to flow through all the layers. It is advisable to design a multilayer cell in such a way that each layer conducts the same current at its maximum power point. This means that each layer has to absorb the same number of photons from the sun spectrum. This condition dictates the choice of the energy gap for each of the individual layers. A three-layer model was calculated in a numerical evaluation of Fig. 1, meeting these conditions. Energy gaps of 1.82, 1.24, 0.68 ev were found suitable. The first layer absorbs $1.11 \cdot 10^{17}$ photons cm^2 second^{-1}, the second $1.37 \cdot 10^{17}$, and the third $1.75 \cdot 10^{17}$. This choice has been made in order to compensate for the deterioration of the curve-factor with decreasing energy gap. Calculating the maximum power point for the layer adjacent to the light exposed surface, and calculating the voltage contributions from the next two layers for the same current as obtained from the first layer, an over-all voltage of 2.25 volts at a current of 17.4 ma per square cm was obtained. This corresponds to a limit conversion efficiency of 36.4 per cent, with 73 per cent of the sun energy utilized in the generation of electron-hole pairs. It is assumed that these values can be exceeded by better choice of all parameters for a three-layer cell, and that still higher limit conversion efficiencies can be obtained for cells with more than three layers.

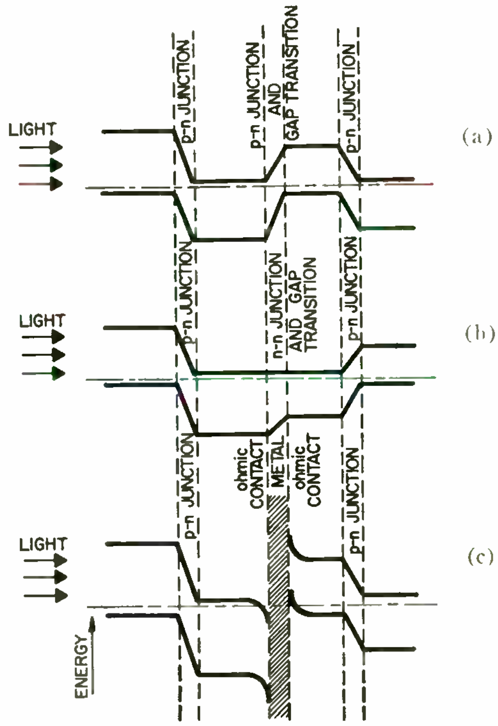

Fig. 12—Energy level diagrams for 3 possible 2-layer arrangements: (a) *p-n-p-n* arrangement (barrier for electron and hole flow); (b) *p-n-n-p* arrangement (light currents in both junctions opposing each other); (c) *p-n*-ohmic contact-metal-ohmic contact-*p-n* arrangement.

It should not be overlooked that the realization of the multilayer cell depends on material problems similar to those discussed in Section III-A-2). In particular, it will be necessary to use ternary compounds in order to fulfill the energy gap requirements. By present day knowledge, it appears that ternary compounds have greatly reduced carrier mobilities, especially in compositions farther removed from the apices of the phase diagram. The achievement of good multilayer solar cells depends mainly on advances in the material technology, and a final evaluation of the merits of this type of cell can only be made after much more information on compound semiconductors is available. In the meantime, a few Si-Ge two-layer solar cells have been prepared proving the principle of operation. These cells have to be used in two-circuit operation since the energy gaps of the two materials are such that the two layers cannot have the same current flow at their maximum power points.

2) *Graded Energy Gap Solar Cells:* From the discussion of the multilayer solar cell and of the improvement of the utilization factor by matching more closely to the

sun spectrum, an intriguing idea emerges. By using a semiconductor with varying width of the energy gap and selecting it so that a perfect fit to the sun energy spectrum is obtained, an energy utilization of 100 per cent can be achieved for electron-hole pair generation.

The preparation of semiconducting materials with graded energy gaps is now technically possible, but their application to photovoltaic cells does not appear to be very useful. It was shown in the discussion of Fig. 12 that a multiplicity of *p-n* junctions in a single piece of semiconductor material is ineffectual. If one has to separate the junctions by ohmic contacts one automatically arrives at a multilayer cell. Thus, only a single *p-n* junction could be applied to a graded energy gap solar cell. Fig. 13 shows examples of each of the principal configurations of graded energy gap single junction solar cells. The configuration of Fig. 13(a) would appear as a desirable one. The grading of the energy gap is combined with varying doping levels in such a way that a drift field will aid the collection normally carried by diffusion of the photon-generated electron-hole pairs. The disadvantage of the system is, however, that the barrier height V_p for hole current flow corresponds to a junction in that portion of the semiconductor which contains the smallest energy gap.

The barrier height determines the current-voltage characteristic of the *p-n* junction. If the barrier height of holes V_p is lower than that for electrons V_n, then a hole current corresponding to V_p and a smaller electron current corresponding to V_n will flow across the junction in forward bias condition. If V_p is much smaller than V_n, then the current across the junction is predominantly a hole current, and its magnitude is approximately one-half of the total current flow that crosses a symmetrical junction, where the barrier height for electron flow would be equal to V_p. This means that the *I-V* characteristic of such an unsymmetrical junction is in the same order of magnitude as that of a conventional junction with the lower of the two barrier heights. A discussion of such junctions has been carried out by Kroemer.[18] Fig. 13(b) shows an arrangement where the grading in the energy gap extends only over the *n*-side. The grading and impurity concentration on the *n*-side has been applied here in such a way that the bottom of the conduction band is affected. In this case, no drift assistance in the collection can be obtained from the graded energy gap. The barrier height corresponds to a junction in that part of the semiconductor which contains the smallest energy gap.

Fig. 13(c) shows a system in which the grading of the energy gap extends only over the *p*-side, which can be obtained by heavy acceptor doping. In this way, the grading of the energy gap affects mainly the bottom of the conduction band, resulting in a drift field for the electrons on the *p*-side. Again the barrier height corresponds to the material with the smallest energy gap involved. Fig. 13(d) presents a configuration in which the energy gap gradient is confined to the space charge region. No drift fields are obtained in this case, and again the barrier height corresponds to the smaller energy gap material. Fig. 13(e) finally shows an arrangement in which the graded energy gap is again placed exclusively on the *n*-side, but is combined with a high donor concentration so that the potential barrier V_p of the *p-n* junction corresponds to a junction in that part of the semiconductor which contains the largest energy gap. Although the large barrier height is a desirable feature, it is obtained only by sacrificing any hole collection

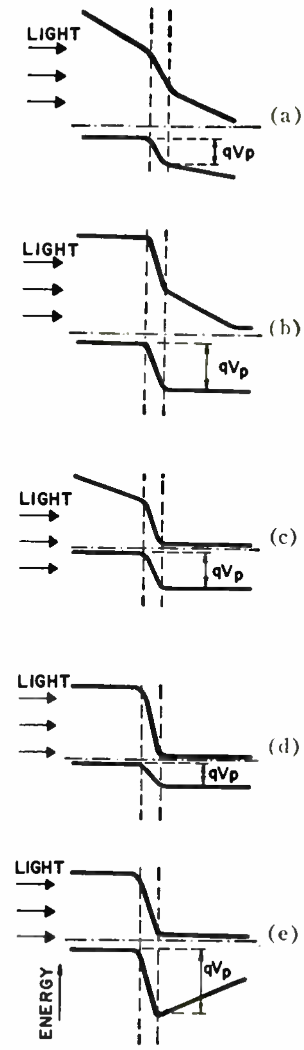

Fig. 13—The major possibilities for application of a graded energy gap to a solar cell: (a) Continuously graded energy gap. Desirable: drift fields for electrons on *p*-side and for holes on *n*-side. Undesirable: barrier height V_p corresponding to narrowest gap material. (b) Grading of energy gap only on *n*-side, affecting only bottom of conduction band. Desirable: nothing. Undesirable: barrier height corresponding to small energy-gap material. (c) Graded energy gap only on *p*-side, heavy acceptor doping. Desirable: drift field for electrons on *p*-side. Undesirable: same as (b). (d) Grading of energy gap only in space charge region of the *p-n* junction. Desirable: same as (b). Undesirable: same as (b). (e) Graded energy gap only on *n*-side, heavy donor doping. Desirable: large barrier height. Undesirable; no collection from *n*-side possible due to internal field.

[18] H. Kroemer, "Theory of a wide-gap emitter for transistors," Proc. IRE, vol. 45, pp. 1535–1537; November, 1957.

from the *n*-side. The reason is that the top of the conduction band forms a potential barrier against hole flow towards the *p-n* junction. This fact makes the arrangement under discussion useless.

It becomes evident from the discussion of Fig. 13 that a large basic advantage cannot be obtained from the application of the graded energy gap to a photovoltaic solar energy converter. Although utilization factors of 100 per cent may be obtainable with proper grading, this energy gain is completely lost in a lower voltage factor which corresponds to a device with the smallest energy gap present. This fact follows also from energy considerations which would make it impossible for an electron-hole pair of small energy to be separated by a junction with wider energy gap unless electron-electron interactions would be possible so that some of the excess energy of certain electrons could be transferred to the low energy electrons, making a configuration as shown in Fig. 13(e) possible. The probability for such interactions to take place is extremely small.

Fig. 13(c), however, suggests an application which may lead to an improvement in collection efficiency in certain cases. If extremely large absorption coefficients and large surface recombination velocities should not be simultaneously avoidable, then the absorption coefficient near the surface may be decreased by the application of a larger energy gap material in this location. The drift field would also assist in the collection of minority carriers. This means that a graded energy gap solar cell cannot yield improvements above the basic limitations of a single *p-n* junction constant energy gap solar cell, but that this method may constitute a technique improvement for the collection efficiency. It should be noted that in most instances drift fields of sufficient magnitude in order to overcome the effect of large surface recombination velocities should be obtainable through proper impurity density grading [see Section III-A-1)]. One should also note that (2) to (5) are not applicable in the cases of graded energy gaps and of drift fields, so that a theoretical evaluation of these cases is not immediately possible.

3) *The Multitransition Solar Cell:* A newer method of design for a photovoltaic solar energy converter may yield conversion efficiencies essentially higher than possible with other single *p-n* junction devices. This method utilizes energy levels in the forbidden gap in order to facilitate transitions from photons with insufficient energy to cause direct transitions from the valence to the conduction band. As an example, it shall be assumed that a very slow trap level can be inserted 1.20 ev above the top of the valence band in a semiconductor with an energy gap of 1.88 ev. These values for energy gap and location of the trap level have been chosen for a sample calculation only. A slow trap level will be preferred to a fast one for this mechanism since electrons shall stay long enough in this level so that another photon can interact with the electron while it is still trapped. It shall be further assumed that this trap level modifies the absorption characteristic of the material sufficiently so that high absorption is obtained for all photons above 0.68 ev of energy, the energy difference between the bottom of the conduction band and the trap level. It shall be further assumed that the probabilities for transitions from the valence band to an empty trap level and from a filled trap level to the conduction band are unity as are those for transitions from the valence band directly to the conduction band, under the condition that corresponding photon-electron interactions take place. The sun spectrum has $1.66 \cdot 10^{17}$ photons per cm^2 per second available for transitions from the valence band to the assumed trap level, and $1.55 \cdot 10^{17}$ photons per cm^2 per second for transitions from this trap level to the conduction band. Under the above conditions this would correspond to $1.55 \cdot 10^{17}$ direct transitions from the valence band to the conduction band per cm^2 per second. In addition to this, the sun spectrum has $1.01 \cdot 10^{17}$ photons per cm^2 per second available for direct transitions from the valence band to the conduction band, giving a total of $2.56 \cdot 10^{17}$ transitions to the conduction band per cm^2 per second. This corresponds to a light generated current of 41 ma cm^2. This large light generated current is obtained in a semiconductor of 1.88-ev energy-gap, which both give rise to a very good characteristic factor. The result is a maximum power point voltage $V_{max} = 1.31$ volts at a current of 40.2 ma cm^{-2}. The corresponding conversion efficiency is 48.7 per cent while the utilization factor of photon energy in the generation of electron-hole pairs is 73.2 per cent.

Introduction of a single trap level results in three possibilities for photon transitions from the valence to the conduction band while two different energy levels yield already six different transition possibilities (Fig. 15). This corresponds to a closer match to the sun energy spectrum resulting in a better utilization factor. Fig. 14 shows the percentage of sun energy utilizable in the generation of electron-hole pairs in semiconducting materials with two, one and no levels in the forbidden gap. The assumptions made in the calculation leading to Fig. 14 are that the density of trapping centers is such that high absorption is obtained, and that under irradiation the number of filled and the number of empty traps are of the same order of magnitude. Under the assumption that the cross section for photon-electron interaction equals the atomic cross section, and with the requirement that most of the absorption takes place within a diffusion length from the *p-n* junction, one arrives at a necessary trap density of 10^{18} to 10^{19} cm^{-3}. Making the assumption that a sufficiently high absorption coefficient can be obtained for transitions between the trap centers and both bands, one can calculate the most suitable location of the trap level for a material of given energy gap by imposing the requirement that the number of photons available for transition from the valence band to the trap level shall equal the number of photons available for transitions from the trap level to the con-

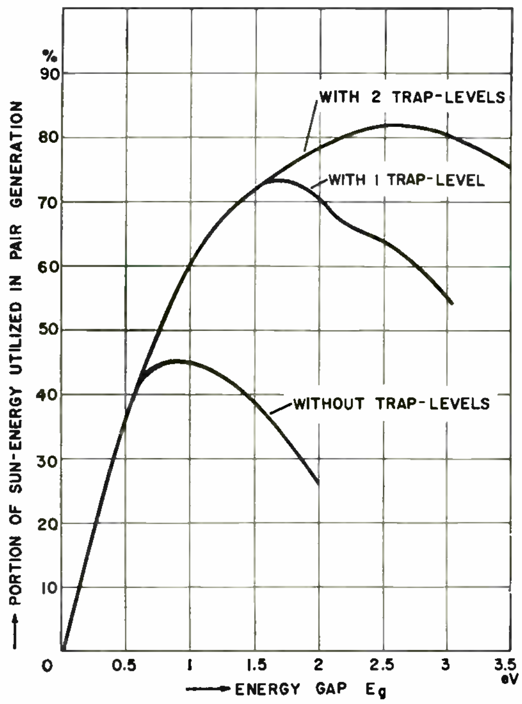

Fig. 14—The portion of the sun-energy utilizable in single *p-n* junction solar cells without, with one and with two trap levels in the forbidden gap, as a function of the width of the energy gap.

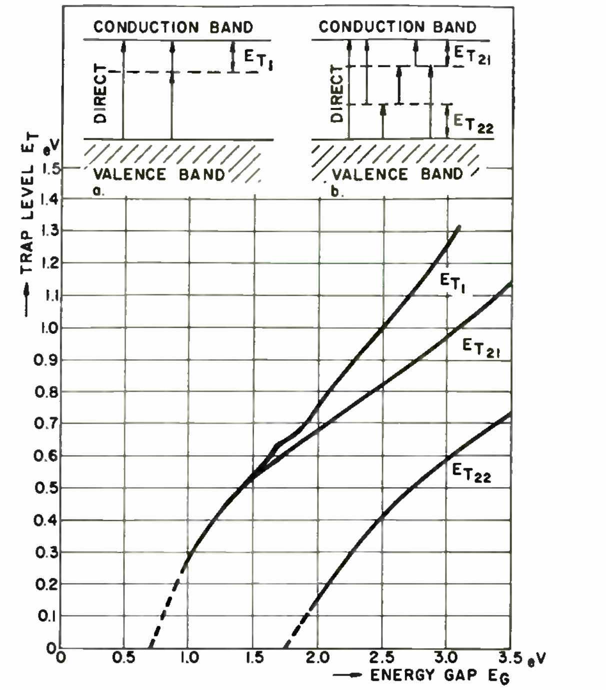

Fig. 15—The trap levels leading to optimum utilization of the sun-energy as a function of the width of the energy gap: (a) energy level diagram with one trap-level; (b) energy level diagram with two trap-levels in the forbidden gap, showing all transition possibilities.

duction band. These are the conditions which lead to Fig. 14, and the energies for the trap levels obtained in this manner are displayed in Fig. 15. Once the generation rate of electron-hole pairs is obtained in this manner the same considerations as for the single *p-n* junction cell apply. In particular, the voltage and curve factors from Fig. 8 can be used. This leads to Fig. 16 showing the limit conversion efficiency obtainable from cells with two, one and no trap levels.

One should note that this method affords a good match to the sun's energy spectrum as well as a large "characteristic factor" due to large energy gaps of the materials usable here, so that this method would appear to be the most ideal one.

Rather little is known yet about the physical properties of trap levels as needed here. Moss[6] discusses absorption by localized impurity centers but puts main emphasis on levels near to the band edges. An extension of the photoconductivity of cadmium sulfide with silver or copper impurities beyond the absorption edge into the red region has been reported by Bube,[19] while Reynolds and Czyzak[20] attributed a photovoltaic response in the red in cadmium sulfide to an intermediate band in the forbidden gap. The recent achievement of 7 per cent conversion efficiency in the cadmium sulfide solar cell

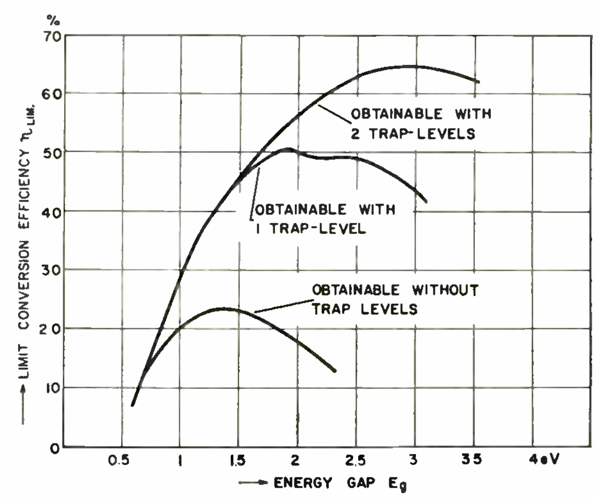

Fig. 16—The limit conversion efficiency obtainable without, with one and with two trap-levels in the forbidden gap, shown as a function of the width of the energy gap.

has to be attributed also to the existence of such multiple transitions.[21]

With the introduction of levels in the forbidden gap with such high density as required here, one has to be very concerned about the recombination properties of these levels. The statistics of trapping and recombination processes have been investigated by Shockley[22] in

[19] R. H. Bube, "Photoconductivity of the sulfide, selenide, and telluride of zinc or cadmium," Proc. IRE, vol. 43, pp. 1837–1850; December, 1955.

[20] D. C. Reynolds and S. J. Czyzak, "Mechanism for photovoltaic and photoconductivity effects in activated CdS crystals," *Phys. Rev.*, vol. 96, p. 1705; December, 1954.

[21] D. A. Hammon and F. A. Shirland, "A Cadmium Sulfide Solar Energy Generator for Space Vehicles," 1959 Electronic Components Conference, Philadelphia, Pa.; May 7–8, 1959.

[22] W. Shockley, "Electrons, holes, and traps," Proc. IRE, vol. 46, pp. 973–990; June, 1958.

general and by Rose[23] specifically for cadmium sulfide. In general it will be necessary to obtain small capture coefficients for holes and for electrons in both p- and n-type materials, and simultaneously large emission coefficients.

The ratios of emission coefficient e_n, e_p to capture coefficient c_n, c_p for the electrons and the holes respectively are determined as soon as the trap level E_t is chosen.[22] They are given by

$$\frac{e_n}{c_n} = n_1 = n_i \exp\left(\frac{E_t - E_i}{kT}\right) \tag{22}$$

and

$$\frac{e_p}{c_p} = p_1 = \frac{n_i^2}{n_1} \tag{23}$$

where E_i is the intrinsic level, while the ratios e_n/e_p and c_n/c_p are determined by choice of the equality level. Only the ratios of the four coefficients are described by these energy levels while the magnitude of the capture coefficients is proportional to the trap density and to the effective capture cross section[24] of the traps. The limiting lifetimes, by which the minority carrier lifetimes in the device are largely determined, are the inverse of the corresponding capture coefficients:

$$\tau_{n0} = \frac{1}{c_n}; \qquad \tau_{p0} = \frac{1}{c_p}. \tag{24}$$

To what extents desirable recombination properties will be realizable for high trap densities with predetermined trap levels is hard to foresee at this time. The trapping and recombination problems are the crucial ones determining the ultimate performance of a cell utilizing multiple transitions. Although the assumptions made here are quite severe, the large improvements which appear theoretically possible will make further investigations quite rewarding. These investigations will have to be directed to a large extent towards better knowledge of impurities or dislocations in the various materials which are of interest for cells of this type. Such knowledge will have to be available before the value of this method of approach to photovoltaic energy conversion can finally be assessed.

Conclusion

In studying the limitations affecting the performance of solar cells, it was found there are two groups: basic limitations and technology determined limitations. Possibilities for the improvement of technology determined limitations were discussed for silicon solar cells, although these techniques may be similarly applicable to cells of other materials or methods. The possibilities of the application of new materials were studied, and the improvement on basic limitations by the application of new methods was investigated. It was found that while technology improvements on silicon solar cells may be carried out quite readily, an essentially larger amount of information will have to be accumulated in regard to the properties of compound semiconductors and of levels inside the forbidden gap before either essential progress or a final verdict can be obtained in regard to any one of these types of photovoltaic solar energy converters.

Appendix I

Minority Carrier Distribution and Current Across the Junction Due to Photon Absorption

From Lambert's law of absorption, one obtains the number of photons absorbed per unit time in a unit area of a layer of thickness dx at a distance x below the surface:

$$g(x)dx = \alpha N e^{-\alpha x} dx. \tag{25}$$

This number is equal to the number of electron-hole pairs generated. The continuity equation for excess holes (above the equilibrium density) in n-type material is then

$$\frac{\partial p}{\partial t} = -\frac{p}{\tau} + D_p \frac{\partial^2 p}{\partial x^2} + \alpha N e^{-\alpha x} \tag{26}$$

where the first term on the right hand side denotes the recombination rate of minority carriers in excess of the equilibrium density p_n, the second term, the diffusion rate into or out of the layer under consideration, and the last term, the above mentioned generation rate. Such a one-dimensional model is very satisfactory for the case of a solar cell since the length and width dimensions are extremely large compared to a diffusion length for minority carriers, so that surface effects on the edges of the cell can be neglected, and since one is justified in assuming that such a cell is sufficiently uniform over its whole area.

Eq. (26) is valid even in the case of high injection due to photon absorption, since detailed balancing of charges is always preserved due to the generation of pairs of electrons and holes and the absence of electric fields. Only the steady-state case is of interest for solar energy conversion. Thus, one obtains

$$\frac{d^2 p}{dx^2} - \frac{1}{L_p^2} p + \frac{\alpha N}{D_p} e^{-\alpha x} = 0. \tag{27}$$

The general solution of this inhomogeneous differential equation is

$$p = p_1 e^{x/L_p} + p_2 e^{-x/L_p} - \frac{N}{\alpha D_p \left(1 - \frac{1}{\alpha^2 L_p^2}\right)} e^{-\alpha x} \tag{28}$$

[23] A. Rose, "Performance of photoconductors," Proc. IRE, vol. 43, pp. 1850–1869; December, 1955. Also, "Progress in Semiconductors," John Wiley and Sons, Inc., New York, N. Y., vol. 2, pp. 109–136; 1957.

[24] W. Shockley and W. T. Read, Jr., "Statistics of the recombination of holes and electrons," *Phys. Rev.*, vol. 87, pp. 835–842; September 1, 1952.

and an equivalent equation exists for electrons in p-type materials:

$$n = n_1 e^{x/L_n} + n_2 e^{-x/L_n} - \frac{N}{\alpha D_n\left(1 - \frac{1}{\alpha^2 L_n^2}\right)} e^{-\alpha x} \quad (29)$$

The constants p_1, p_2 and n_1, n_2, can be determined from the following set of boundary conditions:

1) At $x=0$, surface recombination takes place which is given by

$$D_n\left(\frac{dn}{dx}\right)_{x=0} = s_n n(0). \quad (30)$$

2) At $x=x_j$ is a p-n junction which is kept in the zero-bias condition (leading to short-circuit current) so that a perfect sink for minority carriers exists:

$$n(x_j) = p(x_j) = 0. \quad (31)$$

Operation under different bias conditions does not have to be considered here because of the voltage independence of the light generated current and its linear superposition with the current flow across the p-n junction in the opposite direction due to different terminal voltages [see (16)].

3) Surface recombination also takes place at the back surface at $x=d$:

$$D_p\left(\frac{\partial p}{\partial x}\right)_{x=d} = s_p p(d). \quad (32)$$

Frequently ohmic contacts are applied to this surface so that in these cases $s_p \to \infty$.

Application of these boundary conditions results in two systems of two linear equations each, the solution of which leads directly to (2) and (3) for αL_n and $\alpha L_p \neq 1$. The limits $\lim_{\alpha L_n \to 1} n(x)$ and $\lim_{\alpha L_p \to 1} p(x)$ are given in (2a) and (3a) respectively.

The current densities into the p-n junction are then determined by the minority carrier gradients on both sides of this junction:

$$j_n = qD_n\left(\frac{dn}{dx}\right)_{x=x_j} \quad (33)$$

and

$$j_p = -qD_p\left(\frac{dp}{dx}\right)_{x=x_j} \quad (34)$$

which lead to (4) through (6a) for the different cases.

Appendix II

Calculation of Optimum Contact Grid Structure

The resistance of one contact strip (Fig. 9) is

$$R_T = \rho_T \frac{W}{2T} \quad (35)$$

where ρ_T is the sheet resistance of the metal layer. The factor $\frac{1}{2}$ arises because of the uniform density of the current from the p-layer to the contact strip. Current flow from the p-layer directly to the big contact strip extending parallel to the long dimension of the wafer has been neglected for reasons of simplicity of the analysis.

The resistance of one half unit field of the p-layer is

$$R_p = \rho_p \frac{S}{4W} \quad (36)$$

where ρ_p is the sheet resistance of the p-layer. A factor $\frac{1}{2}$ is caused by the uniform distribution of current sources over the whole p-layer.

Then the total series resistance of a unit field with two p-layer half unit fields in parallel connection is

$$R_s^1 = \rho_T \frac{W}{2T} + \rho_p \frac{S}{8W}. \quad (37)$$

Minimization of (37) gives the optimum cell width for given S and T

$$W = \tfrac{1}{2}\sqrt{\frac{\rho_p}{\rho_T}}\sqrt{ST} \quad (38)$$

and the corresponding minimum series resistance

$$R_{s_{\min}}' = \tfrac{1}{2}\sqrt{\rho_p\rho_T}\sqrt{\frac{S}{T}}. \quad (39)$$

The light generated current in the whole cell is

$$I_L = j_L \cdot nWS \quad (40)$$

where n the number of fields on the cell:

$$n = \frac{L}{S+T}. \quad (41)$$

The total saturation current, neglecting the area under the big contact strip, is simply

$$I_0 = j_0 WL. \quad (42)$$

Then the output current density from the total cell becomes (16)

$$j_R = j_0\left[e^{B(V - I_R R_s)} - 1\right] - \frac{S}{S+T} j_L \quad (43)$$

with

$$j_R = \frac{I_R}{WL}.$$

Introducing the symbol

$$C = 1 - \frac{I_0}{I_L}(e^{BV} - 1) \quad (44)$$

for a given set of I_L and V, one can write

$$I = I_0(e^{BV} - 1) - I_L = -CI_L. \quad (45)$$

If $I_R R_s \ll V$, I may be substituted for I_R in the exponent of (43) without introducing large errors and one may write

$$j_R = j_0\left[\exp B\left(V + \tfrac{1}{2}Cj_L\sqrt{\rho_p\rho_T}\,\frac{WS^{3/2}}{T^{1/2}}\right) - 1\right] - \frac{S}{S+T}i_L \qquad (46)$$

where

$$R_s = \frac{S+T}{L}R_{s_{\min}}'$$

was used.

Doing this, and making an approximation for the exponential term in (43) for the case $BIR_s \leq 1$, which is usually fulfilled, further substituting for W according to (38) and using

$$R_s = \frac{S+T}{L}R_{s_{\min}}'$$

together with (39) one obtains

$$j = j_0\{(1 + \tfrac{1}{4}BCj_L\rho_p S^2)e^{BV} - 1\} - \frac{S}{S+T}j_L. \qquad (47)$$

The maximum of the current density from (47) is obtained for

$$S \approx \sqrt[3]{\frac{2T}{BC\rho_p j_0 e^{BV}}} - \frac{2T}{3}. \qquad (48)$$

This is a good approximation for $2/27T^2BC\rho_p j_0 e^{BV} \ll 1$, which is normally the case.

Substituting (48) into (38), one finally gets

$$T = 2^{5/4}\frac{\rho_T^{3/4}}{\rho_p^{1/2}}(BCj_0e^{BV})^{1/4}W^{3/2}. \qquad (48)$$

Thus, one obtained a set of self-consistent parameters for the optimum grid structure.

Acknowledgment

The author wants to express his special appreciation to M. B. Prince for stimulating discussions and valuable suggestions.

List of Symbols

- λ = Wavelength (cm);
- α = Absorption coefficient (cm^{-1});
- γ = Reflection coefficient;
- n, p = Excess minority carrier density in p- and n-layer, respectively (cm^{-3});
- τ_n, τ_p = Minority carrier lifetime in p- and n-layer, respectively (second);
- D_n, D_p = Diffusion coefficient for electrons and holes, respectively (cm^2 second^{-1});
- s_n, s_p = Surface recombination velocity for electrons and holes, respectively (cm second^{-1});
- e_n, e_p = Emission coefficient from a trap for electrons and holes, respectively;
- c_n, c_p = Capture coefficient for a trap for electrons and holes, respectively;
- N_d, N_a = Density of ionized excess donors and acceptors, respectively (cm^{-3});
- N_{inc} = Incident photon flux outside the semiconductors (cm^{-2} second^{-1});
- $N(\lambda)$ = Monochromatic photon flux entering wafer (cm^{-2} second^{-1} μ^{-1});
- x = Distance from light exposed surface (cm);
- x_j = Distance from light exposed surface to p-n junction (cm);
- d = Thickness of wafer (cm);
- I_0, j_0 = Saturation current, total and density, respectively, (ampere) and (ampere cm^{-2}), respectively;
- I_L, j_L = Light generated current, total and density, respectively, (ampere) and (ampere cm^{-2}), respectively;
- I, I_R = Terminal current without and with series resistance, respectively (ampere);
- V = Terminal voltage (volt);
- V_0 = Open-circuit voltage (volt);
- V_n, V_p = Barrier height for electron and hole flow, respectively (volt);
- E_g = Width of energy gap (ev);
- E_T = Distance of trap level from nearest band edge (ev);
- R_s = Total cell series resistance (ohms);
- ρ_p = P-layer sheet resistance (ohms);
- ρ_T = Contact strip sheet resistance (ohms).

A New Class of Switching Devices and Logic Elements*

P. R. McISAAC†, ASSOCIATE MEMBER, IRE, AND I. ITZKAN‡, MEMBER, IRE

Summary—With a new class of switching devices employing microwave tube elements, appropriate combinations of particular components can create a variety of devices that are capable of performing switching and logic at extremely high speeds (one operation per mμsec or less). Such speeds represent a large step forward in the computer art. A preliminary device described herein demonstrated the ability of a microwave signal to control a dc current. The goal of operating a computer with pulse trains dictated a choice of components that would provide large bandwidth with gain; therefore, an experimental traveling-wave interaction type tube was built which demonstrated the ability of one microwave signal to control another.

I. Introduction

PRESENT DAY commercially available high-speed digital computers operate with clock time intervals on the order of one μsec. The efforts of computer engineers are directed at increasing these speeds by a factor of 10 or even 100 by refining and improving techniques and components now in use, and these efforts are meeting with reasonable success. If, however, computers could be made which utilize microwave frequencies, then clock times comparable to the period of these frequencies may be attainable, *i.e.*, as short as one mμsec or even 0.1 mμsec.

These enormous increases in speed would open up new computational areas. Computers capable of solving extremely complex problems in short intervals would be feasible. They could solve in a reasonable period problems that are not now undertaken because of the length of time required and expense involved.

This paper describes a new class of devices that perform switching and logic at microwave frequencies and employ electron beams and circuit elements closely related to those used in modern microwave tube technique.[1,2] Experimental results are also presented, and their initial success holds great promise for the future of these devices. In addition to computer applications, the use of the devices in the measurement and detection of high-speed scientific phenomena is also a possibility.

* Received by the IRE, October 26, 1959; revised manuscript received, January 14, 1960. Presented in part before the 17th Annual Conference on Electron Tube Research, Mexico City, Mexico, June, 1959. This work was sponsored by the Bureau of Ships, Dept. of the Navy, Washington, D. C.

† Cornell University, Ithaca, N. Y. Formerly of Sperry Gyroscope Co., Great Neck, N. Y.

‡ Sperry Gyroscope Co., Great Neck, N. Y.

[1] A. H. W. Beck, "Thermionic Valves," Cambridge University Press, Cambridge, Eng.; 1953.

[2] J. R. Pierce, "Traveling Wave Tubes," D. Van Nostrand Co., Inc., New York, N. Y.; 1950.

II. Description

A. The device consists of (see Fig. 1):

1) A modulating circuit,
2) a discriminator,
3) a controlled amplifier circuit,
4) an electron beam which couples all three of the above in the order shown, and
5) an electron gun, collector, and focusing system.

a) The modulating circuit impresses information on the electron beam. Generally, this information amounts to the presence or absence of a signal on the modulating circuit; that is, if an RF signal is present on the modulating circuit, the beam in passing through this section is significantly changed in some way relative to the beam which passes through the section if no signal is present on the modulating circuit.

b) The discriminator is a device which distinguishes between the arrival of a modulated beam and an unmodulated beam. It admits only one of these to the next section and rejects the other.

c) The controlled amplifier circuit has gain in the presence of a beam, attenuation in the absence of a beam, and a sizeable difference in signal level between the two states. Therefore, this section either amplifies or attenuates a microwave signal depending or whether another microwave signal exists on the modulating circuit.

In the device built to demonstrate this principle, the discriminator was of the type that rejected the modulated beam. Thus a signal appeared at the output of the amplifier only if there was a signal at the amplifier input (called input "B") and no signal at the modulator input (called input "A"). Such a device is a logic element which performs the logical operation "A-not, B" (symbolized $\bar{A}B$). It can be proven that the ability to build elements with this type of logic is sufficient to build a computer. See, for example, any standard text on computer logic.

B. Types of Modulating Circuits

Two types of modulation that can be applied to an electron beam are pertinent for our purposes. The first is transverse velocity modulation in which the electrons are given a velocity in a direction perpendicular to the axis of the beam, causing a transverse deflection of the beam. The second is longitudinal velocity modulation in which the axial electron velocity is varied away from the initial velocity of the beam. This produces longitudinal bunching of the beam with alternating regions of high- and low-charge density.

The most common methods of longitudinal modulation are a gap and resonant cavity as used in klystrons and a helix or other type of periodic slow-wave structure, such as the interdigital line, used in traveling-wave tubes. These methods are well known in the literature.[1,2] Schemes of transverse modulation are discussed in the literature by Pierce and others[3–5] in reference to use in traveling-wave oscilloscopes.

C. Types of Discriminators

The simplest transverse-modulation discriminator is essentially a mask with an opening in it placed perpendicular to the axis of the beam. The opening is located at the place where the modulated beam would strike the mask if one wants to use the unmodulated beam in the subsequent amplifier. Or the opening can be placed in a position to intercept the unmodulated beam for the converse type of operation.

A longitudinal-modulation discriminator is a device which sorts velocities, passing those electrons which have velocities within a certain band and rejecting all others. Devices which have pass bands for electrons of particular velocities have been described in the literature,[6,7] and a particularly useful velocity discriminator has been developed for these particular tubes and is described below.

D. Types of Amplifiers

The most obvious devices which come to mind for the amplifier section (that is, meet the requirement of having amplification only in the presence of a beam) are klystrons and traveling-wave tubes with a helix or some other slow-wave structure. However, it is also possible that for some purposes another type of microwave-beam operated amplifier, such as a crossed-field amplifier, would have advantages.

A particular combination of modulator, discriminator, and amplifier was chosen so that one RF signal can control another (see Fig. 1). 1) The modulator was a conventional traveling-wave-tube helix operating just below saturation. It has been shown[8] that the beam emerging from such a device when a high-level RF signal is present has most of its electrons slowed down. 2) The discriminator was a velocity sorter developed for this device which passed only those electrons having a velocity greater than a certain value. This value was set just below the value of the velocity of the dc beam. Therefore, the slowed electrons in the modulated beam were rejected and the unmodulated beam was transmitted. 3) A conventional traveling-wave-tube helix amplifier was chosen for the amplifier section. The choice of a helix for the interaction circuit was dictated by the large bandwidth required for narrow pulse-type operation, as is discussed in Section III.

Three devices were built: 1) The first device shown schematically in Fig. 2 consisted of an electron gun, velocity sorter, and an electrically isolated collector to measure the dc characteristics of the velocity discriminator; this was called a velocity-discriminator tester. 2) The second device shown schematically in Fig. 3 consisted of an electron gun, modulating helix, velocity dis-

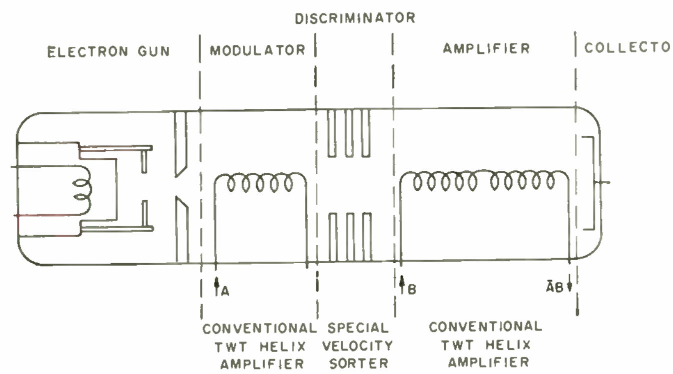

Fig. 1—Elements of switching device (LVST).

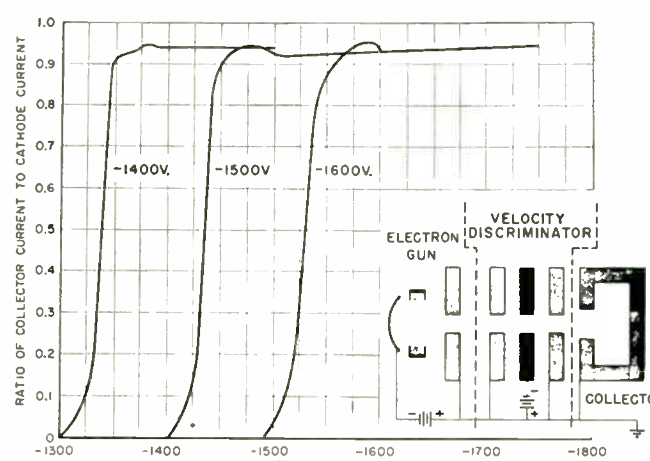

Fig. 2—Cutoff characteristics of velocity discriminator for various values of discriminator potential, and schematic of device used to determine characteristics (VDT).

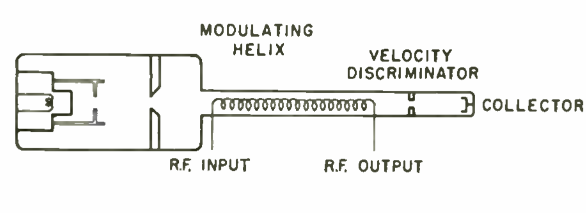

Fig. 3—Schematic of RF switch (RFS).

[3] J. R. Pierce, "Traveling wave oscilloscope," *Electronics*, vol. 22, pp. 97–99; November, 1949.

[4] A. V. Haeff, U. S. Patent No. 2,064,469; December, 1936.

[5] K. J. Germeshausen, S. Goldberg, and D. F. McDonald, "A high-sensibility cathode-ray tube for millimicrosecond transients," IRE Trans. on Electron Devices, vol. ED-4, pp. 152–158; April, 1957.

[6] A. C. Hughes and V. Rojansky, "On the analysis of electronic velocities by electrostatic means," *Phys. Rev.*, vol. 34, p. 284; July, 1929.

[7] G. A. Harrower, "Measurement at electron energies by deflection in a uniform electric field," *Rev. Sci. Instr.*, vol. 26, p. 9; September, 1955.

[8] C. C. Cutler, "The nature of power saturation in traveling wave tubes," *Bell Sys. Tech. J.*, vol. 35, pp. 841–876; July, 1956.

criminator, and an isolated collector to measure the switching action of the front end; it was called an RF switch. 3) The third device, a full tube, consisted of an electron gun, modulating helix, velocity discriminator, and an amplifying helix; it was called a longitudinal-velocity sorter tube (LVST). (See Fig. 1.)

III. Mode of Operation

The use of elements capable of operating in the microwave range implies that millimicrosecond computer operation may be feasible if the bandwidths of the devices are sufficiently broad. For example, a computer capable of handling 10^9 pulses per second would probably require a bandwidth of the order of 5×10^9 cps. At the present time, logic elements with operating bands extending from zero to 5 kmc do not exist. However, some devices (*e.g.*, traveling-wave tubes) which operate in the neighborhood of 10 kmc do have bandwidths of the order of 5 kmc. Thus, by operating with a carrier frequency of about 10 kmc, it is feasible to perform logical operations at a 1-kmc rate.

The generation of millimicrosecond pulses with a carrier frequency of the order of 10 kmc is well within the present state of technology. For example, a generator[9] has been proposed which is capable of forming millimicrosecond pulses on a repetitive basis. In addition, the recent advances in fast-switching semiconductor diodes[10] enable these to be used to generate millimicrosecond pulses of RF.

For the type of switching element described in this paper, there are several kinds of distortion, or pulse degradation, that might occur. In one category is the distortion caused by the finite bandwidth and nonideal phase shift of the amplifying section of the LVST.[11] Traveling-wave tubes with helix circuits (these correspond to the amplifying section) have gain vs frequency curves which are roughly parabolic in shape when the gain is expressed in db. The phase-shift vs frequency curves are nearly straight but have a slight upward concavity (see Fig. 4). The finite bandwidth which is a consequence of the parabolic-gain curve will cause the pulse width to increase somewhat in the amplifier. For example, if a Gaussian-envelope RF pulse is used which is one mμsec wide between points where the envelope is down 40 db from the maximum (0.275 mμsec at the 3-db points), then Fourier analysis of the signal transmitted through the amplifier shows that the pulse lengthening produced by a gain curve with a 4-kmc, 3-db bandwidth is about 10 per cent (see Fig. 5). The main effect of the phase shift through the amplifier is to delay the output pulse relative to the input. This delay will depend on the total phase shift and for fairly high gains may be of the order of several millimicroseconds (see Fig. 6). The curvature of the phase-shift vs frequency-characteristic curve has several minor results. First it makes the time delay and pulse lengthening depend somewhat on the relative values of the input-pulse RF carrier frequency and the frequency at which the amplifier has maximum gain (see Figs. 7 and 5). Second, it causes a certain amount of frequency modulation so that the instantane-

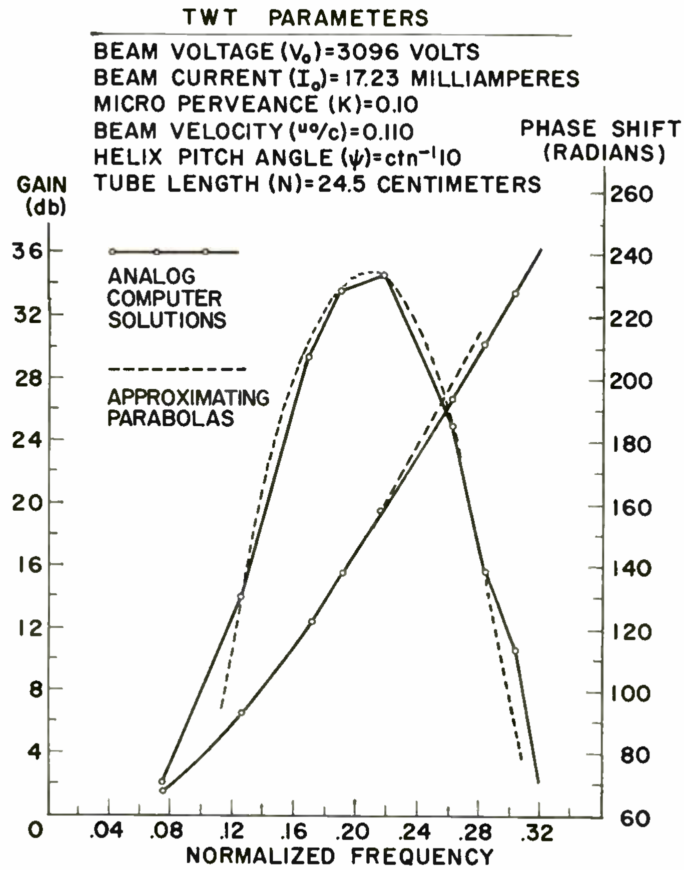

Fig. 4—Gain and phase shift vs normalized frequency for TWT amplifier.

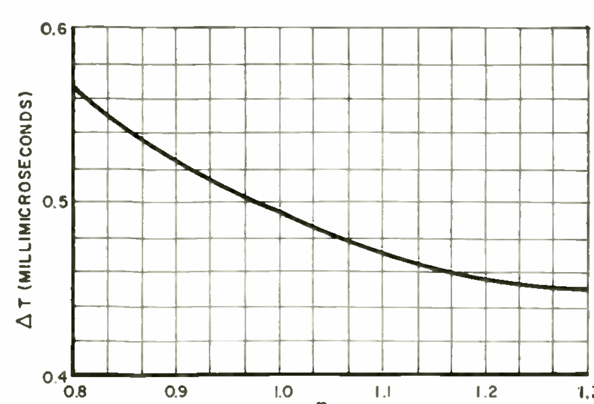

Fig. 5—Output pulse width vs η for TWT amplifier.

[9] C. C. Cutler, "The regenerative pulse generator," Proc. IRE, vol. 43, pp. 140–148; February, 1955.

[10] R. V. Carver, E. G. Spencer, and R. C. LeCraw, "High speed switching at semiconductors," *J. Appl. Phys.*, vol. 28, p. 1336; November, 1957.

[11] The pulse response of a traveling-wave tube using Fourier integral analysis is presented in the Appendix.

ous frequency of the output pulse is not equal to the carrier frequency of the input pulse (see Fig. 8). These are relatively minor effects, however.

There are several other possible sources of pulse degradation. One is the production of "echoes" by reflections from nonideal matches into and out of the modulator and amplifier sections. In all measurements so far, there has been no sign of such echoes, and this is not believed to be a serious problem if reasonable care is taken with the matches.

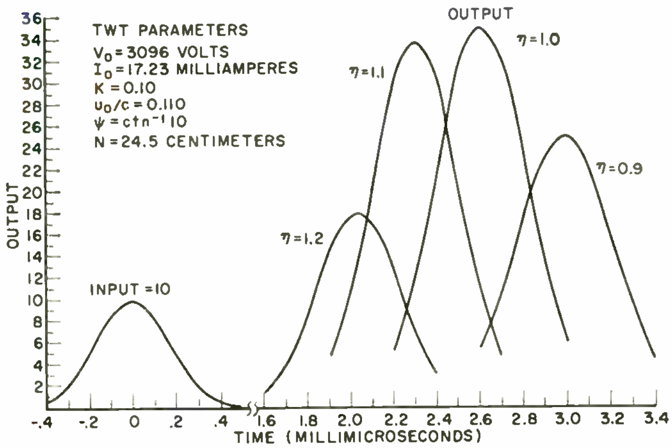

Fig. 6—TWT response for Gaussian input pulse.

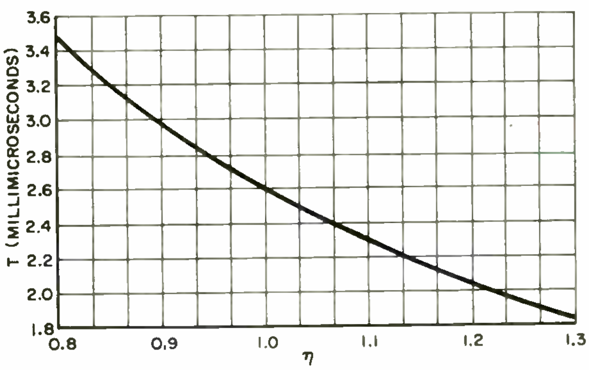

Fig. 7—Time delay of output pulse vs η for TWT amplifier.

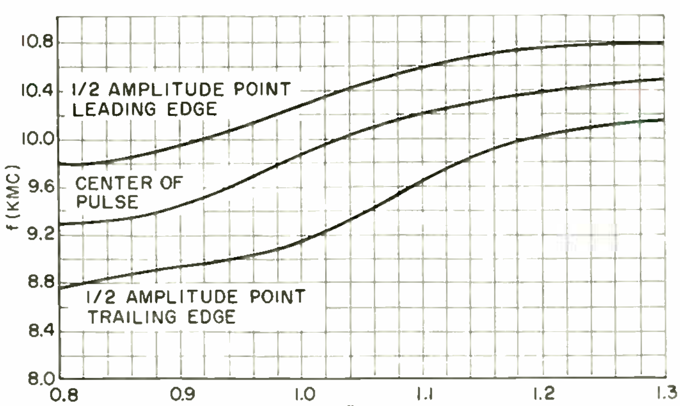

Fig. 8—Frequency modulation of a Gaussian pulse vs η for a TWT amplifier.

Another possible source of trouble is the shock excitation of relatively low-frequency oscillations on the helix structure by the short pulses of electrons in the tube.[12] These oscillations are most likely to occur at low frequencies where the helix is in the neighborhood of a half wavelength long because the added attenuation on the helices become less effective at low frequencies. The main problem that this oscillation may cause is modulation of the effective beam voltage, thus altering electron velocity sufficiently to reduce the interaction with the helix. This problem may be eliminated by care in providing sufficient helix attenuation at low frequencies. No such effects have been observed on the LVST's so far.

The final effect which can cause distortion is the dispersion of the millimicrosecond pulses of electrons in the modulator section. The pulses will tend to spread as they move through the helix because of space-charge forces. This effect is hard to evaluate quantitatively,[12] but it is estimated to be relatively small for millimicrosecond pulses.

Using this device, which performs "$\bar{A}B$" logic as pointed out above, any logical operation may be synthesized by using the proper combinations of these switching devices together with passive microwave components. As an example, a schematic diagram is shown in Fig. 9 for a serial-adder circuit utilizing LVST's and magic Tee's. This circuit is not the optimum in speed for a serial adder using LVST's but is presented to illustrate a possible application. Faster logical operations may be synthesized by more sophisticated circuitry which will in general require more LVST's.

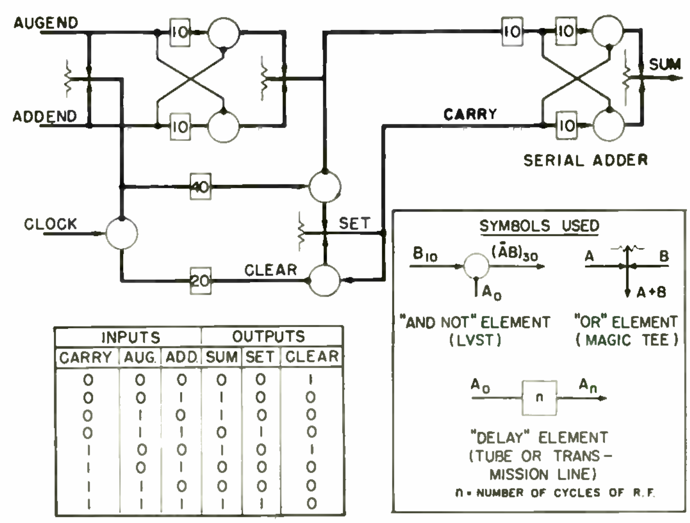

INPUTS			OUTPUTS		
CARRY	AUG.	ADD.	SUM	SET	CLEAR
0	0	0	0	0	1
0	0	1	1	0	0
0	1	0	1	0	0
0	1	1	0	1	0
1	0	0	1	0	1
1	0	1	0	0	0
1	1	0	0	0	0
1	1	1	1	1	0

Fig. 9—Example of computer application of an LVST taking delay times into account ("and not" element) with an inherent delay of 30 cycles of RF.

[12] A. V. Brown, "Transient Phenomena in Traveling Wave Tubes," Stanford Electronics Lab., Stanford, Calif., Tech. Rept. No. 6; July 30, 1956.

IV. Experimental Results

A. Velocity Discriminator Tube

The geometry of the velocity-discriminator tube is shown schematically in Fig. 2 and the dc characteristics of the particular geometry which was finally used are shown in the same figure. The "−1500-volt center aperture potential" curve goes from 10 per cent transmission to 90 per cent transmission when the potential through which the incoming electrons have been accelerated goes from 1425 volts to 1450 volts. Thus, if we are operating at the 90 per cent point on this curve, a decrease of 1 per cent in electron velocity will cause the transmitted current to drop to one-tenth of its original value and a decrease of 2 per cent will cause the current to drop to zero.

B. RF Switch

The RF switch, whose geometry is shown schematically in Fig. 3 is a conventional traveling-wave tube with the end of the tube cut off and replaced by the velocity discriminator and collector section shown. The tube was operated pulsed (50 μsec pulse width, 60 pulses per second), and switching action was looked for towards the center of the "on" portion of the cycle. The collector current was measured with an oscilloscope by passing the current through a viewing resistor to ground. For a particular combination of operating parameters, Fig. 10 shows the collector current when a 10-μsec RF pulse was introduced towards the center of the tube pulse. An expanded view of the leading edge of the RF pulse showed that its rise time was that of the oscilloscope amplifier. This photograph shows the RF pulse depressing the collector current to 50 per cent of its "no signal" value.

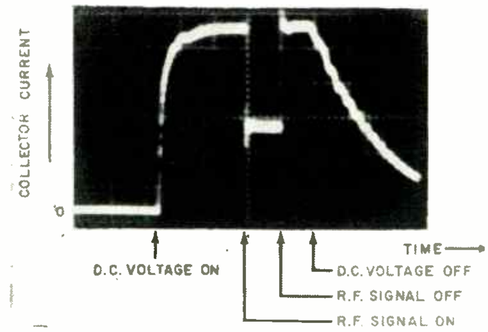

Fig. 10—DC collector current vs time for the RFS; scale: 10 μsec/div.

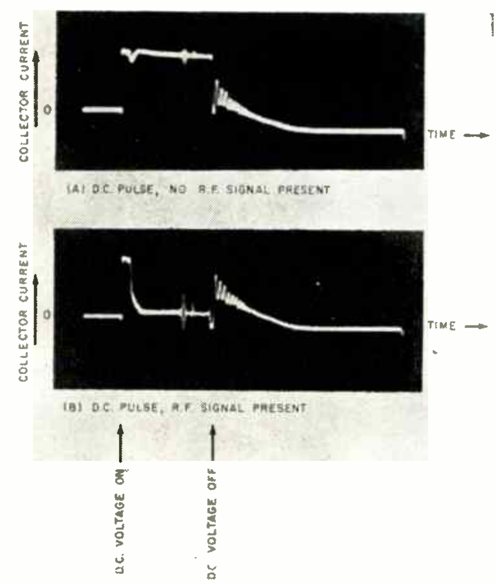

Fig. 11—DC collector current vs time for RFS showing almost complete cutoff by RF signal.

By suitable adjustment of the accelerating voltage, cutoff electrode voltage, frequency of operation, and focusing magnet current, it was possible to obtain almost complete cutoff. Fig. 11(a) is a photograph of the entire dc pulse. This shows some ringing and hash at the beginning and end of each pulse, which are effects caused by turning the traveling-wave tube on and off, but also shows an essentially flat portion. The slight oscillations which appear at about 30 μsec may be plasma oscillations caused by some sort of ion buildup. Fig. 11(b) shows the same pulse, with a 9-kmc RF signal applied to the input throughout the entire trace length. The collector current is now depressed almost to zero during the flat part of the pulse.

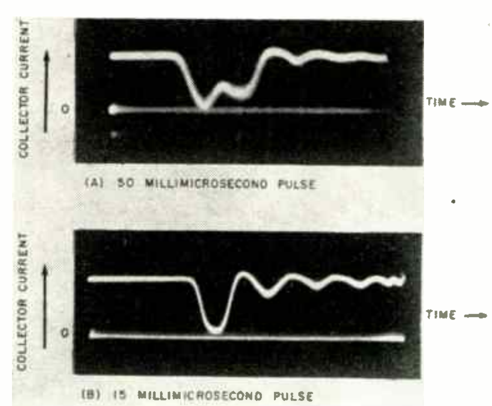

Fig. 12—Collector current vs time for RFS with short RF pulses; scale: mμsec/div.

Fig. 12(a) shows the results of using a 50-mμsec pulse as an envelope for the RF signal generated by a fast rise-time pulse generator and diode switch, and Fig. 12(b) shows a 15-mμsec pulse. The flat trace represents the zero level of collector current. Again, the depression is almost to zero, and the rise time is that of the oscilloscope amplifier: 7 mμsec.

Fig. 13 is a curve of relative collector current vs RF drive power for the pulse of Fig. 12(b). Readings were taken at the peak of each pulse, and the peaks actually go to negative current values. This is undoubtedly because of a capacitive overshoot, and the difference between the maximum negative value and zero gives an estimate of the ac portions of the pulse, or about 10 per

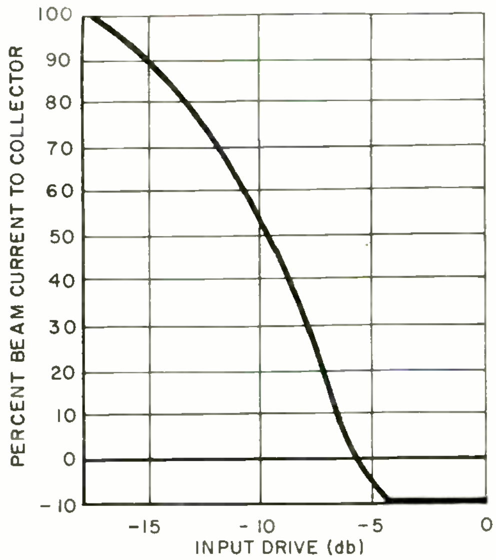

Fig. 13—Percentage of beam transmitted to collector vs input drive level for RF switch.

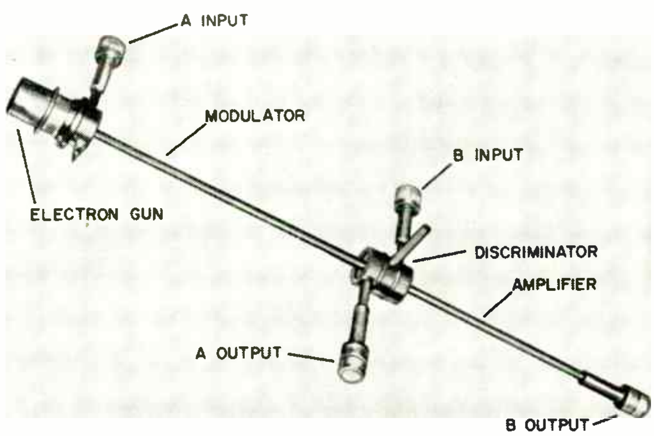

Fig. 14—Longitudinal velocity sorting tube (LVST).

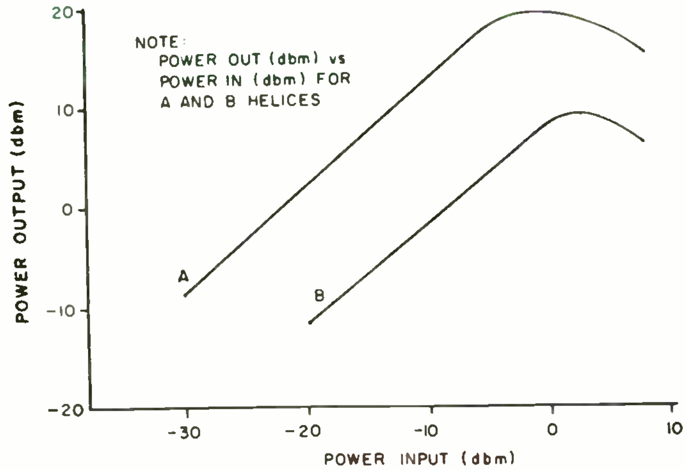

Fig. 15—Drive curves for longitudinal velocity sorting tube.

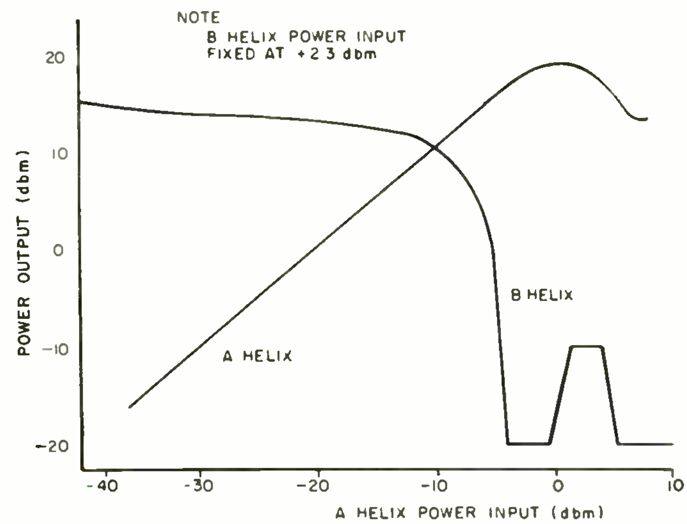

Fig. 16—A and B helices power output vs A-helix input power.

cent. Thus, the feasibility of switching a dc beam by this technique was successfully demonstrated by the performance of this tube.

C. Longitudinal Velocity Sorting Tube (LVST)

A photograph of the LVST is shown in Fig. 14. The first tube built was designed to have a 20-db small signal gain in the modulating section or "A" helix, and a 36-db small signal gain in the amplifier section or "B" helix. However, the necessity for having three output connections at the center of the tube—the modulating-helix output, the amplifying-helix input, and the potential lead for the velocity discriminator—required some modifications in the velocity-discriminator design. These modifications decreased beam transmission to the amplifying helix with attendant decrease in amplifying-helix gain. Experimentally, a small signal gain of 21 db in the modulating section and 9 db in the amplifying section were measured. The gain curves are shown in Fig. 15.

In spite of the low-power output of the amplifier, it was still possible to demonstrate switching action. Fig. 16 shows the output of both helices as a function of helix drive power with the constant input to the "B" helix being that which gave maximum output with no "A" input.

Several characteristics of the curves in Fig. 15 are of interest. Over much of the small signal range of helix "A," the output power of helix "B" falls off slowly. Then, at an "A" helix drive about 6 db below the saturation drive power, the power output of the "B" helix drops to a minimum. These effects are predicted by Cutler[8] wherein it is shown that at first only a few of the electrons are slowed down. The number slowed increases gradually with increasing drive, then increases rapidly until just before saturation almost all the electrons have velocities below that of the dc beam and hence should be stopped by the discriminator. As the drive is increased to saturation, the "B" output increases. This again is explainable by Cutler[8] where it is shown that, at saturation, there exist groups of fast electrons which actually have velocities greater than the dc beam and hence should get through the discriminator. It is interesting also to note the sharpness of the cutoff. A 10-db change in drive power on the "A" helix from −14 db to −4 db is sufficient to cause a decrease in the "B" helix output of 30 db.

A final experiment with the LVST was designed to demonstrate mμsec switching. A pulse of RF, one mμsec wide, was generated by means of an SKL fast-rise time pulse generator and the semiconductor technique of Carver.[10] The pulse was split into two pulses, one of which drove helix "A" and the other passed through a variable delay line to the input of helix "B." The output of the "B" helix was viewed through a crystal detector on an E.G. and G. traveling-wave oscilloscope. When the delay was adjusted so that the two pulses could not interact within the LVST, an output pulse was observed at the output of the "B" helix. Varying the delay to bring the two pulses into synchronism caused the output to disappear. A variation of delay time of one-half mμsec was needed to bring the output pulse from full-pulse height to zero-pulse height.

V. Applications

In addition to the computer applications outlined in Section III, a number of other uses for these devices come to mind. Some of these are outlined below:

1) Pulse generator:

If a continuous signal is put into the "B" helix and a portion of the output is fed back to the "A" helix through a delay element, then the LVST will act as a pulse generator, putting out pulses of RF whose envelope is a square wave with a period equal to twice the total delay around the feedback loop. Pulses of several mμsec pulse width could be generated in this manner.

2) Frequency converter:

If the device were designed so that one of the helices operated at a different frequency from the other, signals of one frequency could control signals of another frequency.

3) Coincidence and anticoincidence detectors:

If nuclear events are converted to RF pulses (a system which might have some advantages in the measurement of very short time separations), various combinations of coincidence and anticoincidence circuits can be devised using LVST's.

VI. Evaluation

These devices have two serious drawbacks when considered for computer applications. The first is the time delay in a signal passing through a unit. The time delay in each helix is of the order of three mμsec, and the delay in the discriminator is of the order of one mμsec. If we consider an application where the amplifier of one tube drives the modulator of a second tube, then, in order for two pulses to interact in the second tube, one pulse must enter the amplifier of the second tube seven mμsec later than the other pulse enters the amplifier of the first tube. If the computer is of the type which must perform its operations sequentially, the delays soon add up to outweigh the increase in speed. If, however, during the waiting time the elements can be employed on other portions of the same problem or other problems, then the time delay only means a delay in receiving the final answers and the enormous increase in information-handling ability would be well worth the additional complications necessary to design such a computer.

The second drawback is the expense and size of traveling-wave tubes and their associated power supplies. This is probably a present day limitation which will soon be removed. Since these tubes need only to transmit information and not to amplify power, they can be small and light in weight. Electrostatic focusing can remove the need for bulky magnets and power supplies, and mass production techniques should reduce the cost to reasonable values for use in large numbers. Also, 9 kmc is not even the present-day limit in the state of the art, and the use of higher frequencies should lead to both faster switching and smaller structures.

We have demonstrated a class of devices which use microwave signals to control other microwave signals and can be combined to perform computer logic. These devices have the advantage of inherent amplification and high-speed switching and should find numerous applications in future work done in the fields of computation and control.

Appendix

Traveling-Wave Tube Pulse Response

The response of a traveling-wave tube to pulse of RF can be conveniently determined by a Fourier integral analysis for signal levels in the linear range of the tube. After determining that both theoretically and experimentally the gain curve (in db) for a traveling-wave tube is approximately a parabola, then, for a set of typical operating data, the gain and phase-shift curves were determined by an analog computer and approximated by parabolas, as shown in Fig. 4. The set of typical parameters chosen is listed in Table I.

TABLE I

Traveling-Wave Tube Parameters Chosen

Beam voltage	$V_0 = 3096$ volts
Beam current	$I_0 = 17.23$ ma
Microperveance	$K = 0.10$
Ratio of electron velocity to velocity of light	$\mu_0/c = 0.110$
Interaction circuit is a sheath helix with radius a and pitch angle ψ	$\cot \psi = 10$
Active tube length at maximum gain point	24.5 wavelengths at maximum

The basic Fourier transform pair was chosen as:

$$G(\omega) = \int_{-\infty}^{\infty} g(t)e^{-j\omega t}dt$$

$$g(t) = \frac{1}{2\pi}\int_{-\infty}^{\infty} G(\omega)e^{j\omega t}d\omega. \tag{1}$$

The input pulse has a Gaussian envelope:

$$f(t) = e^{-bt^2}e^{j\omega_0 t}$$

$$F(\omega) = \sqrt{\frac{\pi}{b}}\, e^{-\frac{(\omega-\omega_0)^2}{4b}}. \tag{2}$$

The carrier frequency of the input pulse $\omega_0/2\pi$ is taken to be 10 kmc per second. The value of b is chosen so that the pulse envelope is one mμsec wide between the 1-per cent amplitude points, $b = 18.4 \times 10^{18}$ sec^{-2}. If the transfer function for the traveling-wave tube is

$$H(\omega) = |H(\omega)|\, e^{-j\theta(\omega)}, \tag{3}$$

then

$$g(t) = \frac{1}{2\pi}\int_{-\infty}^{\infty} H(\omega)F(\omega)e^{j\omega t}d\omega. \tag{4}$$

From the date of Fig. 4, the gain and phase shift curves may be expressed as

$$\begin{aligned} \text{gain} &= 20\log|H(\omega)| \\ &= 34.8 - 3340(ka - 0.206)^2\,\text{db}. \\ \text{Phase shift} &= \theta(\omega) \\ &= -41.4 + 820(ka + 0.278)^2\ \text{radians}. \end{aligned} \tag{5}$$

Here ka is a normalized frequency and is equal to $\omega a/c$. Denoting the frequency for maximum gain as ω_1, then

$$a = \frac{0.206}{\omega_1}\, c.$$

One of the parameters of interest is the ratio of the frequency for maximum gain to the carrier frequency of the input pulse, $\omega_1/\omega_0 = \eta$. After substituting (5) into (4) and evaluating, the output pulse is given by

$$g(T) = \text{Re}\left\{\left[\frac{163\sqrt{\pi}}{\sqrt{\frac{16.3}{\eta^2} + 53.6 + \frac{j34.8}{\eta^2}}}\right]e^{(P+jQ)}\right\} \tag{6}$$

where

$$P + jQ = 69.9 + j22.02 - \left[\frac{\left(\frac{32.6}{\eta} + 107.2 - j\frac{94.0}{\eta} + j20\pi T\right)^2}{4\left(\frac{16.3}{\eta^2} + 53.6 + j\frac{34.8}{\eta^2}\right)}\right]. \tag{7}$$

Here T is the time measured in mμsec.

The results of this computation for various values of η are shown in Figs. 5–8. Fig. 6 shows the time delay and relative amplitude for the envelope of the output pulse. The input-pulse envelope, multiplied by a factor of ten, is also shown for comparison. It is seen that the value of η affects the time delay and the pulse-envelope amplitude and width. Fig. 7 shows explicitly how the time delay depends on η and Fig. 5 shows the dependence of the pulse width ΔT (measured at the half-amplitude points) on η. If the instantaneous frequency is defined to be the time rate of change of the phase divided by 2π,

$$f = \frac{1}{2\pi}\frac{dQ}{dt},$$

then Fig. 8 gives this instantaneous frequency as a function of η at various points in the output pulse. It is seen that the traveling-wave tube does introduce some frequency modulation into the pulse.

VII. Acknowledgment

The authors are deeply indebted to Dr. C. C. Wang, Department Head for Research and Development, Sperry Gyroscope Co., Great Neck, N. Y., for his encouragement, suggestions, and helpful discussions. We would like to thank W. Gehlich and Miss A. Fredricks for their work on the velocity-discriminator tube and RF switch, H. Dagavarian, Mrs. K. White, and B. Onken for their work on the LVST; and W. Lyons who took the data. Also, the experiment in which millimicrosecond pulses were actually switched by the LVST was designed and run by D. Abraham and G. Young.

Skin Effect in Semiconductors*

A. H. FREI†, MEMBER, IRE AND M. J. O. STRUTT‡, FELLOW, IRE

Summary—This paper deals with the theory of skin effect in semiconductor materials including the effect of displacement currents, which are generally neglected in the skin-effect theory for metallic conductors. In the case of flat plates, formulas are derived for the field distribution, the impedance and the eddy-current power losses, considering symmetrical electric as well as magnetic fields. Impedance as a function of frequency is measured for germanium in the microwave cm-range. The measured values agree with the theoretical results. The equivalent depth of penetration is calculated and compared with the skin depth for metals. All theoretical results are represented in graphs for different values of the ratio γ, *i.e.*, the displacement current divided by the conduction current. The formulas are extended to the case of complex permeability, corresponding to hysteresis.

I. Introduction

In many practical applications, slabs of semiconductors are being subjected to alternating electric fields. Similarly to the analogous case of conductor slabs, skin effect will occur in many cases. It is the aim of this paper to extend the well-known skin-effect formulas for conducting slabs to semiconducting ones. Simple as this extension is, the corresponding formulas and curves seem to be absent in previous papers.

Of predominant importance is the ratio of displacement to conduction current in a semiconductor. This ratio is:

$$\gamma = \frac{\omega\epsilon_0\epsilon_r}{\sigma}, \qquad \omega = 2\pi f, \tag{1}$$

where

$$\epsilon_0 = (4\pi\, 9\, 10^9)^{-1}\left(\frac{A\sec}{Vm}\right),$$

ϵ_r is the relative dielectric constant of the semiconductor, σ is its conductivity, and f is the frequency of the alternating field under consideration. As an example, consider germanium of $\sigma = 10$ mho/m and $\epsilon_r = 16$ at $f = 10^{10}$ cps. Then, $\gamma = 0.89$.

Skin-effect theory starts from Maxwell's equations (Giorgi MKS-units) for isotropic media:

$$\text{curl } \boldsymbol{H} = \boldsymbol{i} + \frac{\partial \boldsymbol{D}}{\partial t}; \qquad \boldsymbol{i} = \sigma \boldsymbol{E},$$

$$\text{div } \boldsymbol{B} = 0; \qquad (\boldsymbol{B} = \mu_0\mu_r\boldsymbol{H}),$$

$$\text{curl } \boldsymbol{E} = -\frac{\partial \boldsymbol{B}}{\partial t},$$

$$\text{div } \boldsymbol{D} = 0; \qquad \boldsymbol{D} = \epsilon_0\epsilon_r\boldsymbol{E},$$

where $\boldsymbol{E}$ is the electric and $\boldsymbol{H}$ the magnetic-field strength, $\boldsymbol{i}$ is the electric conduction current density, and $\boldsymbol{B}$ is the magnetic and $\boldsymbol{D}$ the electric flux density. Further,

$$\mu_0 = 4\pi 10^{-7}\left(\frac{V\sec}{Am}\right),$$

and μ_r is the relative magnetic permeability. From the above equations, we obtain:

$$\text{curl curl } \boldsymbol{E} = -\text{curl}\frac{\partial \boldsymbol{B}}{\partial t} = -\mu_0\mu_r\left(\frac{\partial \boldsymbol{i}}{\partial t} + \frac{\partial^2 \boldsymbol{D}}{\partial t^2}\right);$$

$$\nabla(\text{div } \boldsymbol{E}) - \text{div}(\nabla \boldsymbol{E}) = -\mu_0\mu_r\left(\frac{\partial \boldsymbol{i}}{\partial t} + \frac{\partial^2 \boldsymbol{D}}{\partial t^2}\right).$$

Assuming all vectors to be proportional to exp $(j\omega t)$, where $j = \sqrt{-1}$, we obtain for homogeneous semiconductors:

$$\Delta \boldsymbol{E} = \mu_0\mu_r(\sigma j\omega - \epsilon_0\epsilon_r\omega^2)\boldsymbol{E}. \tag{2}$$

This differential equation has to be solved for the particular problem in hand.[1]

II. Symmetrical E-Field

The first case under consideration is shown in Fig. 1.

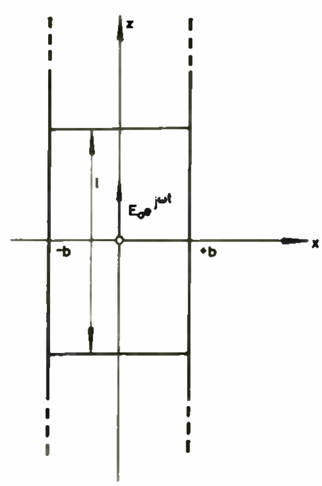

Fig. 1—Semiconducting slab with coordinates, dimensions, and indication of electrical-field strength.

* Received by the IRE, August 17, 1959; revised manuscript received, December 4, 1959. This work was supported by the Swiss National Fund for Scientific Research.
† David Sarnoff Research Center, RCA Labs., Princeton, N. J.
‡ Dept. of Electrical Engrg., Swiss Federal Institute of Technology, Zürich, Switzerland.

[1] Sir J. Jeans, "The Mathematical Theory of Electricity and Magnetism," Cambridge University Press, New York, N. Y.; 1951.

The electrical field is parallel to z and the slab is bounded by the two planes $x = \pm b$. The length along z of the slab is l. Then

$$E = E(x) \exp(j\omega t),$$

$$\frac{d^2E(x)}{dx^2} = \omega\sigma\mu_0\mu_r(j - \gamma)E(x). \qquad (3)$$

Here, the following the abbreviations are introduced:

$$\left\{\begin{aligned} K^2 &= \omega\sigma\mu_0\mu_r(j - \gamma), \\ d_0{}^2 &= \frac{2}{\omega\sigma\mu_0\mu_r}, \\ K^2 &= \frac{2}{d_0{}^2}(j - \gamma). \end{aligned}\right. \qquad (4)$$

The quantity d_0 is equal to the depth of penetration of an alternating electric field into a conductor of plane boundary at a frequency $\omega/2\pi$, a conductivity σ, and a relative permeability μ_r.[2]

Assuming the electric field to be symmetrical with respect to $x=0$ (Fig. 1), the solution of (3) is:

$$E = E_0 \text{ ch } (Kx) \exp(j\omega t).$$

Obviously, E_0 is the field strength at $x=0$. The function ch (Kx) is shown as dependent on x/d_0 at different values of γ in Figs. 2 and 3.

We proceed to evaluate the impedance, Z, of a slab of length l, of width $2b$, and of breadth a.

The alternating current, I, flowing through the slab is

$$I = \int_{-b}^{+b} dx \int_0^a dy(\sigma + j\omega\epsilon_0\epsilon_r)E_0 \text{ ch } (Kx) \exp(j\omega t),$$

$$I = \frac{2a(\sigma + j\omega\epsilon_0\epsilon_r)E_0 \text{ sh } (Kb) \exp(j\omega t)}{K}.$$

The alternating voltage, U, along the slab's surface is

$$U = E_0 l \text{ ch } (Kb) \exp(j\omega t).$$

Hence, the impedance $Z = U/I$ is

$$\frac{Z}{R_0} = \frac{\frac{b}{d_0}\sqrt{2}\sqrt{j-\gamma}\,\text{cth}\,(Kb)}{1 + j\gamma}, \qquad (5)$$

where R_0 indicates the slab's dc resistance:

$$R_0 = \frac{l}{2ab\sigma}.$$

[2] M. J. O. Strutt, "Ultra- and Extreme-Short Wave Reception," D. Van Nostrand Co., Inc., Princeton, N. J., p. 21; 1947.

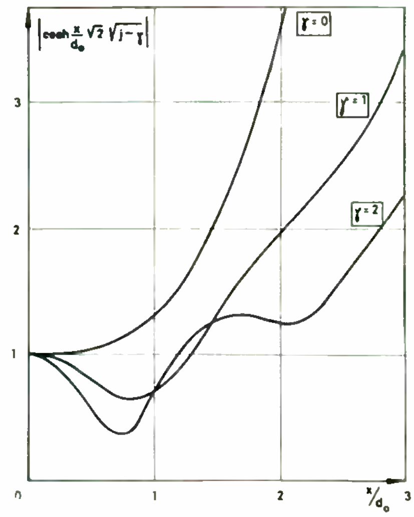

Fig. 2—Absolute amount of the function ch (Kx) as dependent on x/d_0 at three different values of γ.

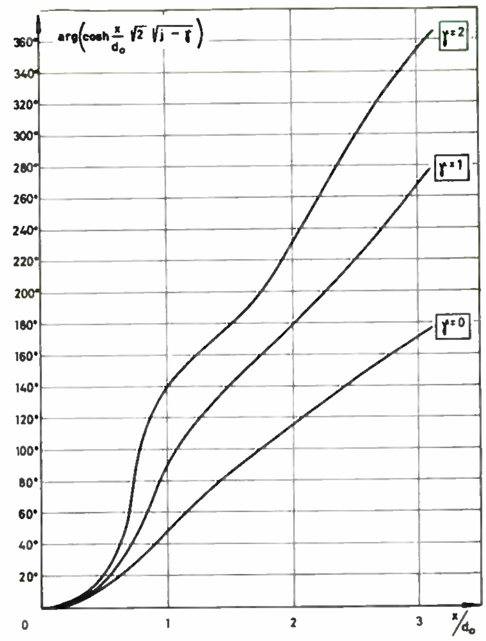

Fig. 3—Phase angle of the function ch (Kx) as dependent on x/d_0 at three different values of γ.

The ratio Z/R_0 is dependent on the ratio of the width, $2b$, to the depth, d_0, of penetration, and on the ratio, γ. The ratio, Z/R_0, is shown in Figs. 4 and 5. The curves for the absolute amount of Z/R_0 (Fig. 4) start from the points of the vertical axis:

$$\lim_{b/d_0 \to 0} \left|\frac{Z}{R_0}\right| = \frac{1}{\sqrt{1+\gamma^2}}.$$

The tangents of the curves at these points are horizontal. The phase angles of Z/R_0 at $b/d_0 \to 0$ are given by $-$arc tg γ. These curves (Fig. 5) have also horizontal tangents at these points.

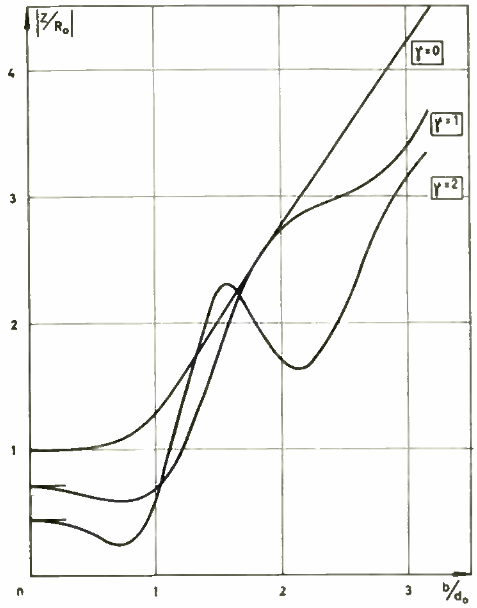

Fig. 4—Absolute amount of the ratio Z/R_0 as dependent on b/d_0 at three different values of γ.

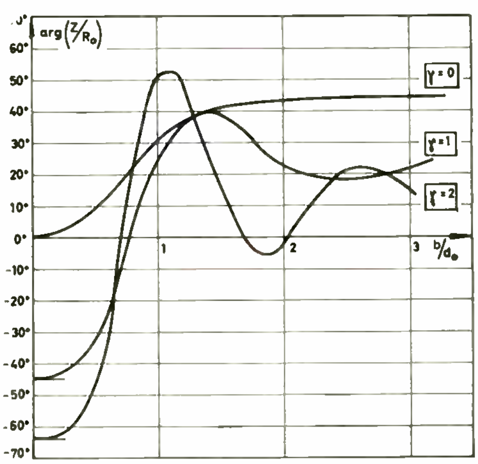

Fig. 5—Phase angle of the ratio Z/R_0 as dependent on b/d_0 at three different values of γ. The impedance becomes resistive at certain frequencies for semiconductors, which might be of practical interest.

It is interesting to consider a purely dielectric slab ($\sigma = 0$) as a frontier case. Evaluating Z for $\sigma = 0$ and for

$$b \ll \frac{\lambda}{2\pi\sqrt{\epsilon_r}},$$

where $\lambda = c/f$, c being the velocity of propagation in vacuum, we obtain

$$1/Z = j\omega \frac{2ab\epsilon_0\epsilon_r}{l} = j\omega C,$$

$$C = \frac{2ab\epsilon_0\epsilon_r}{l},$$

which is the electrostatic capacitance.

We evaluate the eddy-current losses in the slab per unit of volume:

$$P_w = \frac{1}{2b}\int_{-b} \left| \sigma E_e \right| \cdot \left| E_e \right| dx.$$

Here, E_e is the effective value of the electric-field strength. The integral yields:

$$P_w = \sigma E_{0e}^2\left(\frac{\text{sh } 2\alpha b}{4\alpha b} + \frac{\sin 2\beta b}{4\beta b}\right). \tag{6}$$

Here, E_{0e} is the effective field strength at the slab's center, $\alpha = \text{Re }(K)$, and $\beta = \text{Im }(K)$. The quantity in brackets contains the skin-effect part of P_w. It is shown in Fig. 6 as dependent on b/d_0 and on γ.

III. Experimental Confirmation

The experimental setup is shown schematically in Fig. 7. A cylindrical slab of germanium is arranged in a coaxial line, which is short-circuited at a distance $\lambda/4$ from the slab's surface. The radii of this line are $r_1 = 1.5$ mm and $r_2 = 3.5$ mm. The slab's width is $b = 1.44$ mm. The coaxial line is connected to a generator of frequencies between 4 and 7 kmc, the electrical field being radial and the magnetic field circular. The electric field is measured in the usual way by means of a suitable probe, which slides along the coaxial line. The impedance of the slab is obtained from the displacement of the minimum electric-field point and from the width of the field curve as dependent on the probe's displacement. This procedure is well known.[3,4]

At the slab's boundary, corresponding to $x = 0$ in Fig. 7, the electric-field strength, E, is different from zero, and dE/dx, which is proportional to the magnetic-field strength, is zero. Hence, the electric-field strength in the slab is given by $E = E_0 \text{ ch } (Kx) \exp (j\omega t)$. This corresponds to the theory of Section II, the slab of Fig. 7 having exactly half of the width of the slab in Fig. 1.

Considering a circular ring of inner radius r, of radial thickness dr, and of width b, its impedance is:

$$dZ_r = \left(\frac{Z}{R_0}\right)\frac{dr}{2\pi r b\sigma},$$

where the ratio Z/R_0 is the same as was calculated in Section II (Figs. 4 and 5). The total impedance, Z_r, of the slab is obtained by integration of the above expression between r_1 and r_2:

[3] P. Ramer, "Experimental Investigation of the Dispersion of Conductivity of Single Crystals of Germanium, Caused by Plasma Oscillation," Ph.D. dissertation, Swiss Federal Institute of Technology, Zürich, No. 2875, pp. 34–43; 1959. (In German.)

[4] K. S. Knol and M. J. O. Strutt, "On a method for measuring complex impedances in the decimeter wave range," *Physica*, vol. 9, pp. 577–590; June, 1942.

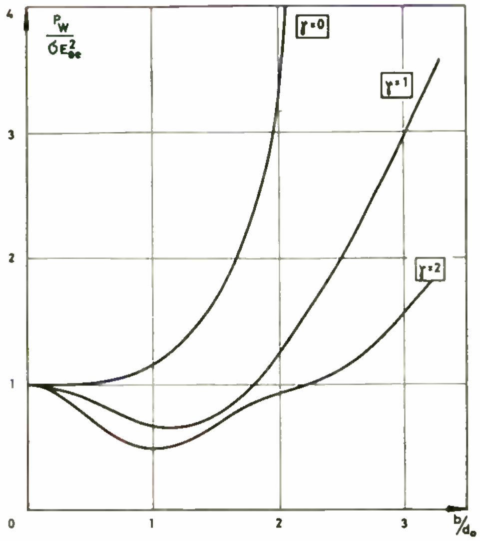

Fig. 6—Power loss P_w per unit volume divided by σE_{0r}^2 (see Fig. 1) as dependent on b/d_0 at three different values of γ.

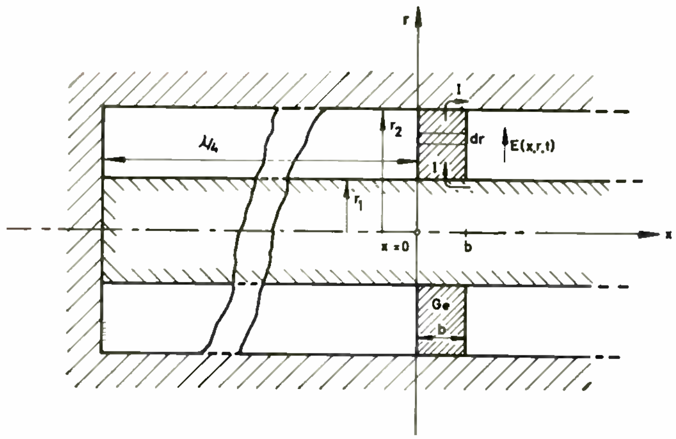

Fig. 7—Schematic picture of the coaxial-line arrangement for measuring the impedance of a cylindrical semiconductor slab in the cm-wave range.

$$Z_r = \left(\frac{Z}{R_0}\right) R_r, \qquad R_r = \int_{r_1}^{r_2} \frac{dr}{2\pi r b \sigma}.$$

Obviously, R_r is the dc resistance of the slab. The conductivity, σ, of the germanium being 3.28 mho/m, we obtain $R_r = 28.6$ ohms.

In previous work on lossy dielectrics,[5] the fact that the field *distribution* may be altered by the conductivity was not taken into account, as this effect was probably small in the cases considered.

The impedance $Z_r = R + jX$ was measured as a function of frequency between 4 and 7 kmc. The results are shown in Figs. 8 and 9. The values marked by circles were obtained while the contact between the slab and the coaxial line was not tight but included a small air

[5] S. Roberts and A. van Hippel, "A new method for measuring dielectric constant and loss in the range of centimeter waves," *J. Appl. Phys.*, vol. 17, pp. 610–616; July, 1946.

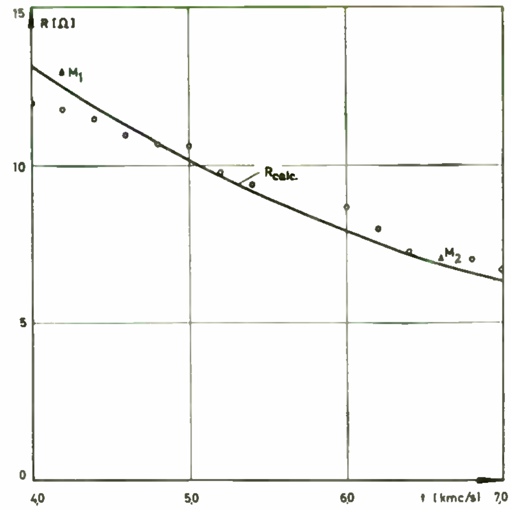

Fig. 8—Real part of the impedance of the semiconductor slab of Fig. 7 as dependent on frequency. Curve calculated; circles measured with a relatively small air gap; triangles measured without air gap.

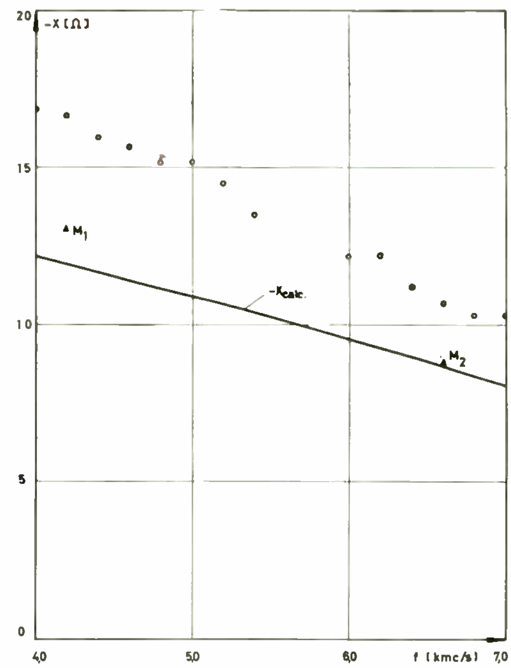

Fig. 9—Imaginary part of the impedance of the semiconductor slab of Fig. 7 as dependent on frequency. Curve calculated; circles and triangles measured as in Fig. 8.

gap. The values M_1 and M_2 were obtained with tight contacts between the slab and the coaxial line, the gaps being filled with silver paste.

The maximum errors of the measured points were about five per cent for the real part R of Z_r and about ten per cent for the imaginary part X of Z_r.

In the case of the circles, a difference, exceeding experimental errors, exists between calculated and measured values of X. This may be due to the air gap, which was present in these measurements.

The triangular experimental points show coincidence with the calculated curves within the said experimental errors.

We may conclude from Figs. 8 and 9 that the conductivity σ of the germanium in question does not show any dispersion in the frequency range under consideration. The results of further measurements on this question will be published later. Figs. 8 and 9 show results for germanium of $\sigma = 3.28$ mho/m. If σ is different, the curves corresponding to those of Figs. 8 and 9 may be obtained from Figs. 4 and 5.

IV. Skin Effect at a Symmetrical Magnetic Field

In this case, the value $E_0 \exp(j\omega t)$ at the center of the slab of Fig. 1 is replaced by $H_0 \exp(j\omega t)$, the field strength H being a symmetrical function of x:

$$H = H_0 \operatorname{ch}(Kx) \exp(j\omega t).$$

The complex hyperbolic function ch (Kx) is shown in Figs. 2 and 3.

We shall determine the magnetic impedance of a slab of length l, width $2b$ and breadth a. The magnetic flux ϕ through the crossection $2ab$ is:

$$\phi = \int_{-b}^{b} dx \int_{0}^{a} dy \cdot \mu_0 \mu_r H_0 \operatorname{ch}(Kx) \exp(j\omega t),$$

$$\phi = \frac{2\mu_0\mu_r H_0 a}{K} \operatorname{sh}(Kb) \exp(j\omega t).$$

At the slab's surface we have:

$$\theta = \int_0^l dl \cdot H_0 \operatorname{ch}(Kx) \exp(j\omega t),$$

$$\theta = l H_0 \operatorname{ch}(Kx) \exp(j\omega t).$$

Hence, the magnetic impedance $R_M = \theta/\phi$ is given by:

$$\frac{R_M}{R_{M0}} = \frac{b}{d_0} \sqrt{2}\sqrt{j - \gamma} \operatorname{cth}\left(\frac{b}{d_0}\sqrt{2}\sqrt{j-\gamma}\right). \tag{7}$$

The value R_{M0} is the magnetic impedance at dc: $R_{M0} = l/2\ \mu_0\mu_r ab$. The absolute value and the phase angle of the ratio R_M/R_{M0} are shown in Figs. 10 and 11. All the curves of Fig. 10 start from 1 at $b/d_0 = 0$ with a horizontal tangent. The phase-angle curves of Fig. 11 tend to assume fixed values, if b/d_0 becomes large with respect to unity. These fixed values are marked in the figure.

Finally, we evaluate the eddy-current losses in the slab per unit of volume:

$$P_W = \frac{\sigma}{2b} \int_{-b}^{b} |E_e^2|\, dx.$$

The electric-field strength E_e (effective value), in the present case, is:

$$E_e = -\frac{j\omega\mu_0\mu_r H_0}{K} \operatorname{sh}(Kx) \exp(j\omega t).$$

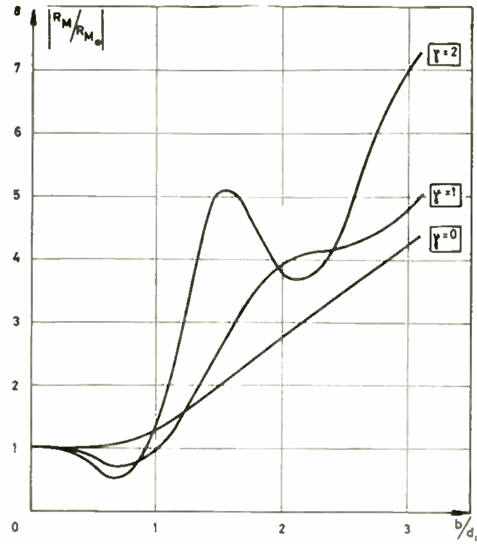

Fig. 10—Absolute amount of the magnetic impedance R_M of a slab according to Fig. 1 at a symmetrical magnetic field over its value R_{M0} at dc, as dependent on b/d_0 at three different values of γ.

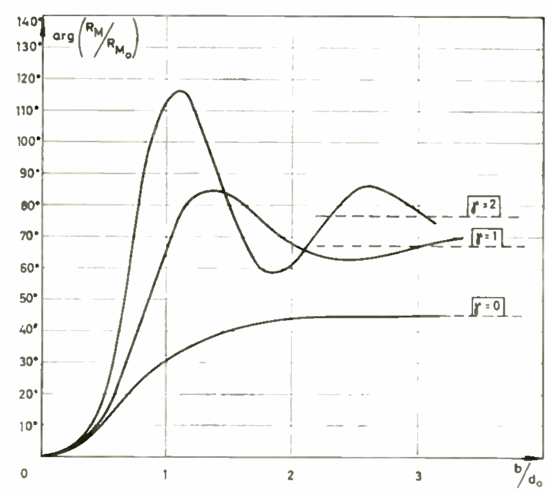

Fig. 11—Phase angle of the ratio R_M/R_{M0} as dependent on b/d_0 at three different values of γ.

From this we obtain

$$P_W = \sigma(\omega\mu_0\mu_r H_0 b)^2 \left(\frac{\dfrac{\operatorname{sh}(2\alpha b)}{2\alpha b} - \dfrac{\sin(2\beta b)}{2\beta b}}{2\alpha^2 b^2 + 2\beta^2 b^2} \right). \tag{8}$$

The expression in brackets is shown in Fig. 12 as a function of b/d_0 at $\gamma = 0$, 1 and 2. All these curves start from $\frac{1}{3}$ at $b/d_0 = 0$.

V. Depths of Penetration of Alternating Fields

In the calculation of this depth of penetration, we refer to Fig. 13, which depicts the plane boundary of a semiconductor and the adjacent vacuum. We assume:

$$\text{at } x = 0: \qquad E = E_0 \exp(i\omega t)$$

$$\text{at } x = \infty: \qquad E = 0.$$

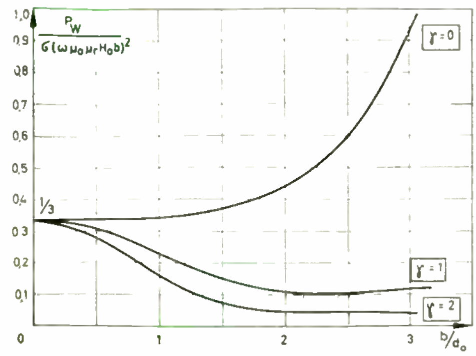

Fig. 12—Losses per unit volume (P_w) over $\sigma(\omega\mu_0\mu_r H_0 b)^2$ as dependent on b/d_0 at three different values of γ.

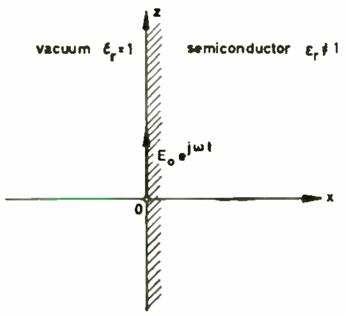

Fig. 13—Coordinate system for the calculation of the depth of penetration.

Then,

$$E = E_0[\text{ch } (Kx) - \text{sh } (Kx)] \exp (j\omega t).$$

The depth, d_1, of penetration is defined as the distance, x, from the boundary, at which the absolute amount of the field strength has dropped to $1/e$ of its value at the boundary, e being the basis of Napierian logarithms:

$$\left| \frac{E(d_1)}{E_0} \right| = \frac{1}{e}.$$

Some calculation yields

$$\frac{d_0}{d_1} = [(1+\gamma^2)^{1/2} - \gamma]^{1/2}, \tag{9}$$

where $d_0^2 = 2/\omega\sigma\mu_0\mu_r$. As already mentioned in Section I, the value d_0 corresponds to the depth of penetration in a conductor of conductivity σ and relative permeability μ_r.

The ratio d_1/d_0 is plotted in Fig. 14. At values $\gamma \ll 1$, we have approximately

$$d_1 \approx d_0\left(1 + \frac{\gamma}{2}\right).$$

As is to be expected, d_1 is always greater than d_0. Skin effect at a metal-semiconductor contact has been considered previously,[6] neglecting, however, the influence of displacement currents.

[6] H. C. Torrey and C. A. Whitmer, "Crystal Rectifiers," McGraw-Hill Book Co., Inc., New York, N. Y., p. 421; 1948.

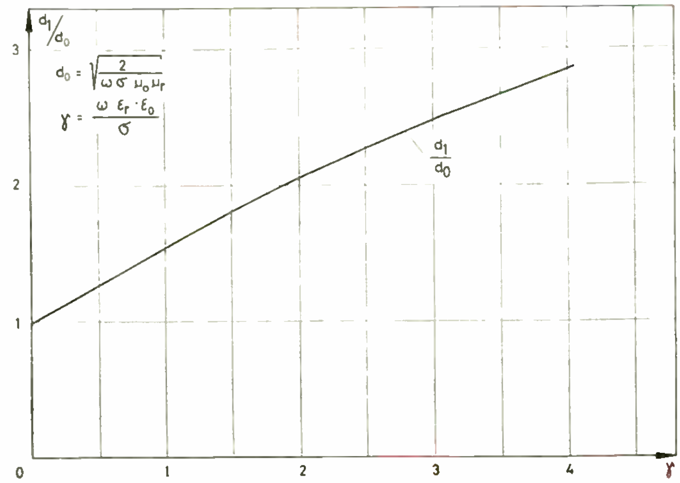

Fig. 14—Depth of penetration d_1 in a semiconductor, over its value d_0 at $\gamma=0$, as dependent on γ.

VI. Extension to Include Hysteresis (Complex Permeability)

If we approximate the hysteresis loop by an ellipse, the linear relation between B and H being preserved, this hysteresis loop may be accounted for by the introduction of a complex permeability $\mu_r = \mu_{r1} - j\mu_{r2}$. In this case, (2) must be replaced by

$$\Delta E = [j\mu_0(\omega\sigma\mu_{r1} + \epsilon_0\epsilon_r\omega^2\mu_{r2}) + \mu_0(\omega\sigma\mu_{r2} - \epsilon_0\epsilon_r\omega^2\mu_{r1})]E.$$

Hence, we obtain, instead of K^2, a quantity K_1^2, given by the right-hand expression in square brackets. The quantity γ must be replaced by γ_1, which is given by

$$\gamma_1 = \frac{\epsilon_0\epsilon_r\omega - \sigma\dfrac{\mu_{r2}}{\mu_{r1}}}{\sigma + \epsilon_0\epsilon_r\omega\dfrac{\mu_{r2}}{\mu_{r1}}},$$

whereas the quantity d_0 must be replaced by δ_0:

$$\delta_0^2 = \frac{2}{\omega\sigma\mu_0\mu_{r1} + \epsilon_0\epsilon_r\omega^2\mu_0\mu_{r2}}.$$

We may then use the curves of Figs. 2–6, 10–12, and 14 also in the present case, using γ_1 instead of γ and δ_0 instead of d_0.

Obviously, in the case of ferroelectric materials, their hysteresis curves may also be approximated by ellipses, corresponding to a complex dielectric constant, $\epsilon_r = \epsilon_{r1} - j\epsilon_{r2}$. The changes to be applied to the above formulas are simple to work out and need not be detailed here.

Acknowledgment

The authors take pleasure in thanking Dr. P. Ramer and F. K. Reinhart, of this department, for their aid in obtaining the experimental data of Section III.

Excitation of Piezoelectric Plates by Use of a Parallel Field with Particular Reference to Thickness Modes of Quartz*

R. BECHMANN†, FELLOW, IRE

Summary—The parallel field excitation of piezoelectric plates, particularly of plates vibrating in thickness modes, and their resulting piezoelectric stress constants in general and of various quartz cuts are considered. Quartz AT-cut crystals excited by a parallel field are of practical interest for high precision frequency control and the data of the equivalent electric circuit of a 1000-kc AT quartz oscillator excited by a parallel field are given.

I. Introduction

Piezoelectric oscillators having the form of plates or bars, vibrating in various modes of motion, *e.g.*, thickness modes, contour modes or extensional modes, generally can be excited by an electric field perpendicular or by a field parallel to the major surfaces of the plate. Fig. 1 schematically shows the excitation by a field perpendicular to the thickness of the plate; Fig. 2 shows the excitation by a parallel field. In Fig. 1, two electrodes are arranged on either side of the crystal plate, normal to the thickness direction. In Fig. 2, the electrodes are arranged so that each covers part of both major surfaces leaving a gap g parallel to the major surfaces of the plate. Atanasoff and Hart[1] excited thickness modes of quartz plates by a parallel field for the purpose of determining some of the elastic stiffnesses. The excitation of various contour modes of differently oriented square and rectangular quartz plates was thoroughly investigated[2] and the general expression for parallel field excitation of thickness modes was given by R. Bechmann.[3] Excitation by a parallel field of the various contour and thickness modes of plates of the orientation $(yxl)\theta$,[4] specified for the various crystal classes for determination of the elastic stiffnesses and the piezoelectric stress constants, are discussed by Bechmann and Ayers;[5] this excitation has been used particularly for the determination of the elastic stiffnesses of some water soluble crystals. For plates of the orientation $(yxl)\theta$, vibrating in thickness modes, the formula for the parallel field excitation was shown previously.[6] However, the application of parallel field excitation of AT-type crystals is of interest particularly for application to high precision frequency control. Such crystals have a much higher value for the impedance. It has been found that the values for Q are higher in the case of parallel field excitation. Some experimental results concerning parallel field excitation are given in Section IV.

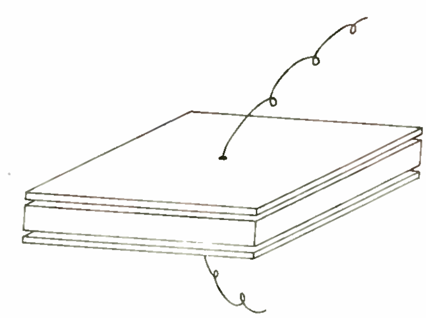

Fig. 1—Electrode arrangement for piezoelectric excitation using a field perpendicular to a plate.

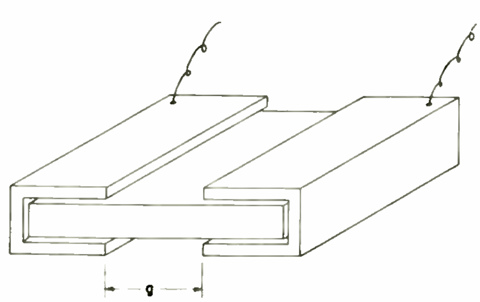

Fig. 2—Electrode arrangement for piezoelectric excitation using a field parallel to a plate.

II. Excitation of Thickness Modes of Plates

The theory of thickness modes of infinitely extended plates of anisotropic media is well known[7] and the formulas need not be repeated. In the general case when

* Received by the IRE, November 17, 1959; revised manuscript received, January 6, 1960.
† U. S. Army Signal Res. and Dev. Lab., Fort Monmouth, N. J.

[1] J. V. Atanasoff and P. J. Hart, "Dynamical determination of the elastic constants and their temperature coefficients for quartz," *Phys. Rev.*, vol. 59, pp. 85–96; January, 1941.

[2] R. Bechmann, "Längsschwingungen quadratischer Quarzplatten," *Z. Phys.*, vol. 118, pp. 515–538; February, 1942.

[3] R. Bechmann, "Über Dickenschwingungen piezoelektrischer Kristallplatten," *Arch. elekt. Übertragung*, vol. 6, pp. 361–368; September, 1952; Addendum, vol. 7, pp. 354–356, July, 1953.

[4] Throughout this paper, the IRE "Rotational Symbol" is used. (To be found in "Standards on piezoelectric crystals, 1949," Proc. IRE, vol. 37, pp. 1378–1395; December, 1949.) From this the appropriate transformation can easily be derived. (See R. Bechmann, "Zur Festlegung der Orientierung von Kristallplatten und die zugehörige Koordinatentransformation," *Arch. elekt. Übertragung*, vol. 7, pp. 305–307; June, 1953.)

[5] R. Bechmann and S. Ayers, "Theory of dynamical determination of elastic and piezoelectric constants," in "Piezoelectricity," Post Office Research Station, Her Majesty's Stationery Office, London, 1957.

[6] R. Bechmann, "Filterquarze im Bereich 7 bis 30 MHz," *Archiv. elektr. Übertragung*, vol. 13, pp. 90–93; February, 1959.

[7] W. G. Cady, "Piezoelectricity," McGraw-Hill Book Co., Inc., New York, N. Y.; 1946.

the direction of the electric field $s_f(l_f, m_f, n_f)$ and the direction of the propagation $s(l, m, n)$, that is the normal of the plate, form an arbitrary angle, the resulting piezoelectric stress constant can be written as[3]

$$e = p\Xi_1^{(f)} + q\Xi_2^{(f)} + r\Xi_3^{(f)} \tag{1}$$

where p, q and r are the direction cosines of the motion of the mode. These direction cosines are solutions of the third-order secular equations for the thickness modes and the three sets of direction cosines p_i, q_i, r_i $(i=1, 2, 3)$ solutions of the two shear modes and the extensional mode. In an anisotropic medium, these direction cosines are neither parallel nor perpendicular to the direction of propagation so that in general the modes corresponding to the three displacements are not purely extensional or shear. The constants $\Xi_i^{(f)}$ $(i=1, 2, 3)$ for the most general case—the triclinic crystal having 18 different piezoelectric stress constants $e_{l\mu}(l=1, 2, 3; \mu=1, 2 \cdots 6)$—are given by

	l_fl	m_fm	n_fn	m_fn	n_fm	n_fl	l_fn	l_fm	m_fl	
$\Xi_1^{(f)}$	e_{11}	e_{26}	e_{35}	e_{25}	e_{36}	e_{31}	e_{15}	e_{16}	e_{21}	
$\Xi_2^{(f)}$	e_{16}	e_{22}	e_{34}	e_{24}	e_{32}	e_{36}	e_{14}	e_{12}	e_{26}	(2)
$\Xi_3^{(f)}$	e_{15}	e_{24}	e_{33}	e_{23}	e_{34}	e_{35}	e_{13}	e_{14}	e_{25}	

where the piezoelectric moduli $\Xi_i^{(f)}$ are obtained as sums of the products of the corresponding e's and the direction cosines expressions listed at the top of this equation; *e.g.*,

$$\Xi_1^{(f)} = e_{11}l_fl + e_{26}m_fm + e_{35}n_fn + e_{25}m_fn + e_{36}n_fm + e_{31}n_fl + e_{15}l_fn + e_{16}l_fm + e_{21}m_fl.$$

For a field parallel to the plane of the plate, the condition of orthogonality,

$$l_fl + m_fm + n_fn = 0, \tag{3}$$

must be fulfilled.

When the direction of the electric field s_f coincides with the normal of the plate, $l_f=l$, $m_f=m$, $n_f=n$, the expressions $\Xi_i^{(f)}$ reduce to those for the usual excitation perpendicular to the plate Ξ_i

	l^2	m^2	n^2	mn	nl	lm	
Ξ_1	e_{11}	e_{26}	e_{35}	$e_{25}+e_{36}$	$e_{31}+e_{15}$	$e_{16}+e_{21}$	(4)
Ξ_2	e_{16}	e_{22}	e_{34}	$e_{24}+e_{32}$	$e_{36}+e_{14}$	$e_{12}+e_{26}$	
Ξ_3	e_{15}	e_{24}	e_{33}	$e_{23}+e_{34}$	$e_{35}+e_{13}$	$e_{14}+e_{25}$.	

Two quartz cuts are considered: 1) a rotated Y-cut, a plate of the orientation $(yxlt)\theta\psi$, with the angle θ describing the orientation of the plate and the second angle ψ, describing the direction of the electric field in the plane of the plate and 2) a rotated X-cut, having an orientation $(xylt)\theta\psi$.

1) For the rotated Y-cut, $(yxlt)\theta\psi$, the transformation matrix is given by the product of two rotational matrices; *i.e.*, the rotation for the plate and the direction of the field and is

	x	y	z	
x'	$\cos\psi$	$\sin\theta\sin\psi$	$-\cos\theta\sin\psi$	
y'	0	$\cos\theta$	$\sin\theta$	
z'	$\sin\psi$	$-\sin\theta\cos\psi$	$\cos\theta\cos\psi$.	(5)

The direction cosines for the normal of the plate and the field in the plane of the plate are

$$l = 0, \qquad m = \cos\theta, \qquad n = \sin\theta$$
$$l_f = \cos\psi, \qquad m_f = \sin\theta\sin\psi, \qquad n_f = -\cos\theta\sin\psi,$$

where the angle ψ is measured between s_f and the X-axis. Thus, for excitation by a field perpendicular to the plate $E_\perp$ in accordance with (4),

$$e_1 = -p_i(e_{11}\cos^2\theta + e_{14}\cos\theta\sin\theta), \quad e_2 = 0, e_3 = 0, \tag{6}$$

and for a field parallel to the plate $E_\parallel$ according to (2),

$$\begin{aligned} e_{i\psi} = &-p_i(e_{11}\cos\theta\sin\theta + e_{14}\sin^2\theta)\sin\psi \\ &-q_i(e_{11}\cos\theta - e_{14}\sin\theta)\cos\psi \\ &+r_ie_{14}\cos\theta\cos\psi. \end{aligned} \tag{7}$$

Considering an AT quartz plate with an orientation $\theta=35°15'$, we obtain the following values which solve the third-order secular equation mentioned:

i	Mode	Elastic Stiffness c_i^{D}* $10^9 N\,m^{-2}$	p_i	q_i	r_i
1	Shear Mode I	29.37	1	0	0
2	Shear Mode II	38.41	0	0.6244	−0.7811
3	Extensional Mode	130.67	0	0.7811	0.6244.

* c_i^D denotes the elastic stiffness at constant electric displacement.

The values for the piezoelectric stress constants in $C\,m^{-2}$ using $e_{11}=0.171$ and $e_{14}=-0.0406$ are as follows:

Field perpendicular, $E_\perp$

$$e_1 = 0.0953, \qquad e_2 = 0, \qquad e_3 = 0,$$

Field parallel, $E_\parallel$

$$e_{1\psi} = 0.0673\sin\psi, \quad e_{2\psi} = 0.128\cos\psi, \quad e_{3\psi} = 0.107\cos\psi.$$

By application of a field $E_\perp$, Shear Mode I only can be excited. By application of a field $E_\parallel$, generally all three thickness modes are excitable except for $\psi=0$, the direction of the X-axis, where Shear Mode II and the Extensional Mode only can be excited and for $\psi=90°$ where Shear Mode I only can be excited.

2) The transformation matrix for a rotated X-cut, $(xylt)\theta$, is

	x	y	z	
x'	$\cos\theta$	0	$-\sin\theta$	
y'	$\sin\theta\sin\psi$	$\cos\psi$	$\cos\theta\sin\psi$	(8)
z'	$\sin\theta\cos\psi$	$-\sin\psi$	$\cos\theta\cos\psi$.	

The direction cosines for the normal of the plate and the field in the plane of the plate are

$$l = \cos\theta, \qquad m = 0, \qquad n = -\sin\theta$$
$$l_f = \sin\theta\sin\psi, \qquad m_f = \cos\psi, \qquad n_f = \cos\theta\sin\psi,$$

where the angle ψ is measured between s_f and the Y-axis. Excitation by a field perpendicular to the plate $E_\perp$, is expressed by

$$e_i = p_ie_{11}\cos^2\theta - q_ie_{11}\cos\theta\sin\theta, \tag{9}$$

and excitation by a field parallel to the plate $E_\parallel$, by

$$e_{i\psi} = (p_i e_{11} \cos\theta \sin\theta - q_i e_{14} \sin^2\theta) \sin\psi + [p_i e_{14} \sin\theta - (q_i e_{11} + r_i e_{14}) \cos\theta] \cos\psi. \quad (10)$$

For each mode there exists an angle ψ_0 giving the direction for maximum excitation by a parallel field in the plate. The general expression for the optimum angle $\psi_0^{(i)}$ of the plate $(xylt)\theta\psi_0^{(i)}$ is given by the expression

$$\tan\psi_0^{(i)} = \frac{p_i e_{11} \cos\theta \sin\theta - q_i e_{14} \sin^2\theta}{p_i e_{14} \sin\theta - (q_i e_{11} + r_i e_{14}) \cos\theta}. \quad (11)$$

Similar but more complicated expressions hold for thickness modes of double rotated plates which, for the sake of brevity, will not be given here. Considering an X-cut (xy), $(\theta = 0)$, we obtain the following values:

i	Mode	Elastic Stiffness c_i^D $10^9 N\,m^{-2}$	p_i	q_i	r_i
1	Shear Mode I	29.26	0	−0.8460	−0.5331
2	Shear Mode II	69.32	0	−0.5311	0.8460
3	Extensional Mode	82.48	1	0	0

The values for the piezoelectric stress constants in $C\,m^{-2}$ are as follows:

Field perpendicular to the plate $E_\perp$

$$e_1 = 0, \qquad e_2 = 0, \qquad e_3 = 0.171.$$

Field parallel to the plate $E_\parallel$

$$e_{1\psi} = 0.145 \cos\psi, \qquad e_{2\psi} = 0.091 \cos\psi, \qquad e_{3\psi} = 0.$$

The optimum excitation for both shear modes using the parallel field excitation coincides with the Y-axis.

Another example is the rotated X-cut, $(xylt)30°\psi$, Shear Mode I, having a small temperature coefficient of frequency. For this cut, we obtain

i	Mode	Elastic Stiffness c_i^D $10^9 N\,m^{-2}$	p_i	q_i	r_i
1	Shear Mode I	38.58	0.2071	0.9553	0.2109
2	Shear Mode II	44.53	−0.6549	−0.0278	0.7553
3	Extensional Mode	112.22	0.7273	−0.2943	0.6200,

giving the piezoelectric stress constants in $C\,m^{-2}$ for a field perpendicular to the plate $E_\perp$

$$e_1 = 0.010, \qquad e_2 = 0.084, \qquad e_3 = 0.099,$$

and for a field parallel to the plate $E_\parallel$

$$\begin{aligned} e_{1\psi} &= 0.025 \sin\psi - 0.139 \cos\psi \\ e_{2\psi} &= -0.049 \sin\psi + 0.044 \cos\psi \\ e_{3\psi} &= 0.051 \sin\psi + 0.051 \cos\psi. \end{aligned} \quad (12)$$

The angles for maximum excitation of this plate are given by

$$\psi_0^{(1)} = -10°14'; \quad \psi_0^{(2)} = -48°12'; \quad \psi_0^{(3)} = +45°12'.$$

These optimum angles, of course, are functions of the mode considered and the orientation of the plate.

III. Equivalent Electric Circuit of Thickness Modes by Use of Parallel Field Excitation

The data for the elements of the equivalent electric circuit of a plate vibrating in one of the thickness modes, when excited by a parallel field and the electrodes plated on the surface of the plate, are dependent on the width of the gap between the two pairs of electrodes. An example for the variation of the inductance as function of the width of the gap for an AT-type crystal oscillating at 750 kc, was shown previously.[8] The expressions for the data of the equivalent electric circuit following from consideration of the potential distribution will be discussed in a forthcoming paper.

IV. Experimental Results on AT-Type Crystals

The application of parallel field excitation to AT-type crystals is of interest, particularly for application to high precision frequency control. A sample of an AT-type high precision quartz crystal for 1000 kc excited by a parallel field has been manufactured by Bliley Electric Co.[9] The contoured blank of this unit is identical with blanks used for perpendicular field excitation in Bliley BG9A high precision oscillators for 1000 kc having a diameter of one inch. The crystal was evacuated. The measured data of this experimental model excited by a parallel field are shown in the third line of Table I. The gap between the electrodes is 0.040 inch. For comparison, the data of the crystal type Bliley BG9A, 1000.000 kc vibrating in the fundamental mode, and the crystal type Bliley BG61A-5, high precision 5 mc vibrating in the fifth overtone, are summarized in the first and second line of Table 1. The frequency using parallel field excitation in the example given in Table I is about $4 \cdot 10^{-4}$ higher than for perpendicular field excitation and depends on the width of the electrode gap. The very high value of the inductance L_1 for parallel field excitation is remarkable and can further be increased by a wider gap width.

TABLE I

	f kc	n	C_1 10^{-4} pF	L_1 H	R_1 Ω	C_0 pF	Q 10^6
⊥ *Field Excitation*							
Bliley BG9A	1000.000	1	177	1.43	5	12	1.8
Bliley BG61A-5	5000.000	5	1.15	8.8	125	4.5	2.2
‖ *Field Excitation* Experimental Model	1000.381	1	3.35	75.5	180	3.3	2.6

[8] R. Bechmann, "Improved high precision quartz oscillators using parallel field excitation," Proc. IRE, vol. 48, pp. 367–368; March, 1960.
[9] Erie, Pa.

Transient Behavior of Aperture Antennas*

CHARLES POLK†

Summary—The transient behavior of aperture antennas is analyzed. For an antenna which is illuminated by a field of uniform phase and either uniform or cosine tapered amplitude, it is shown that the steady-state main lobe is established within $(\tau/2+R/c)$ seconds after the aperture is energized. τ is the period of the carrier frequency, R is the distance from the center of the aperture to the point where the field is evaluated, and c is the velocity of light. The time required for the establishment of the steady-state pattern at all angles between 0° and 90° is $(\tau/2\theta_0+R/c)$ where $2\theta_0$ radians is the beamwidth between first nulls of the steady-state pattern $(\theta_0 \ll 1)$. An antenna may be useful, however, before $(\tau/2\theta_0+R/c)$ seconds, because the maxima of the transient sidelobes are not higher than the maxima of the steady-state sidelobes.

The requirement that the steady-state pattern be established at all angles between 0° and 90° leads to a limitation on range discrimination ΔR and angular discrimination $\Delta\theta$ for a pulse radar $\Delta R \Delta\theta = \lambda$, where λ is the wavelength of the carrier frequency.

For a scanning antenna employing linear phase variation over the aperture, it is shown that the main lobe, located at an angle $\theta_{\max}$, is established within a time $(\tau/2+R/c+a \sin\theta_{\max}/2c)$ measured from the instant at which one edge of the aperture is first energized. The quantity a is the dimension of the aperture in the plane in which the field is evaluated.

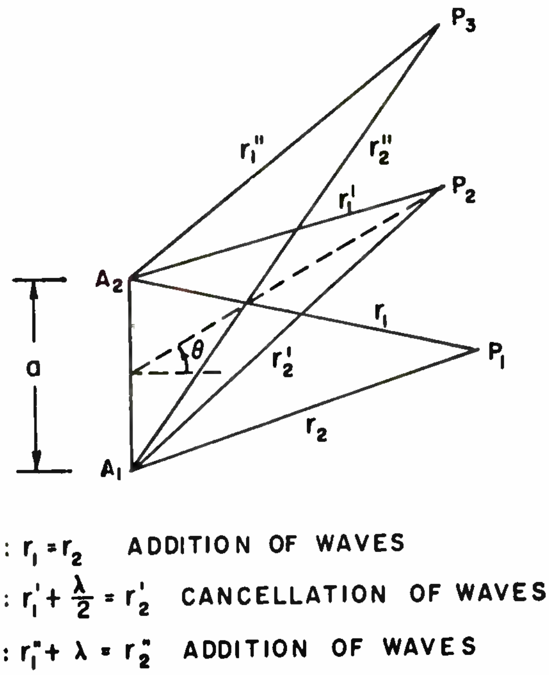

Fig. 1—Pattern formation.

Introduction

THE simplest physical picture which can be used to explain how the radiation pattern of a large antenna is formed employs Huygens' principle. As illustrated by Fig. 1, the pattern is due to the fact that waves which originate at different points on the aperture reinforce each other at some points in space and cancel each other at other points. This picture employs, of course, steady-state concepts. It refers to a single frequency and well-defined phase fronts. Nevertheless, it suggests what might happen in the transient case. At point P_2 in Fig. 1, for example, energy which has to travel the distance r_2' will arrive later than energy which only has to travel over r_1'. Thus, during a short time interval after the antenna is switched on, waves from A_1 and A_2 will not cancel at P_2. How long this transient effect lasts clearly depends upon how far the points A_1 and A_2 are separated. One would thus expect that the transient behavior of the antenna will at least depend upon the size of the antenna and in particular upon the size of the antenna as related to the velocity of electromagnetic energy in free space (c). If a/c is small, one would expect a transient effect of very short duration. As a/c is increased, the transient effect should become more important.

In recent years, antennas of ever-increasing size have been built and the use of the moon or of planets as reflectors has been considered. At the same time, the use of very short pulses for the accurate location of objects and the rapid scanning of antenna beams has become important. Thus applications exist, or are at least under investigation, where the transient behavior of large antennas may impose essential limitations upon over-all system performance.

In the present paper a rigorous, detailed solution of the boundary value problem involving a vector wave equation is not attempted. Instead, an approximate method (developed in Appendix I) employing Fourier Integrals and the Kirchhoff solution of the scalar diffraction problem is used. It has the advantage of being relatively simple, and it permits the direct application of a vast amount of results which have been obtained during the past two decades for aperture antennas in the steady state [1]. The limitations of the method are those of scalar diffraction theory: the signals applied to the antenna must be such that most of their energy is contained in a frequency spectrum over which the antenna is large in terms of wavelengths; simple linear polarization is assumed and only points outside the near-field (further than several wavelengths from the antenna) can be considered. Not inherent in the method, but used to obtain the results given below, is the further restriction to Fraunhofer radiation patterns; that is, to points farther than about a^2/λ from the antenna.

* Received by the IRE, July 16, 1959; revised manuscript received, January 12, 1960.

† University of Rhode Island, Kingston, R. I. This work was completed while the author was at RCA Labs., Princeton, N. J.

Basic Equations

The signal applied to the antenna is an arbitrary function of time $f(t)$. If $F(\omega)$ is its Fourier mate defined by

$$F(\omega) = \frac{1}{\sqrt{2\pi}} \int_{-\infty}^{\infty} f(t) e^{-i\omega t} dt, \tag{1}$$

then

$$f(t) = \frac{1}{\sqrt{2\pi}} \int_{-\infty}^{\infty} F(\omega) e^{i\omega t} d\omega. \tag{2}$$

Let ω be the radian frequency, let the vector $\bar{r}$ locate the position of a point in space, let r, θ, and ϕ be spherical coordinates, and let ξ and η be the coordinates in the plane of the aperture A. Then, if $P_0(\bar{r}) = K_0(\bar{r}) g(\bar{r}, \omega) = K_0(\xi, \eta) g(\xi, \eta, \omega)$ is the field distribution over a specified plane aperture (where K_0 is the amplitude and g the phase distribution) it can be shown [1] that the steady-state Fraunhofer field $R(\bar{r}, \omega)$ is given by

$$R(\bar{r}, \omega) \approx \frac{i}{\lambda r} e^{i(\omega t - kr)} (\cos\theta + \bar{\imath}_z \cdot \bar{s})$$

$$\cdot \int_A P_0(\xi, \eta) \exp ik \sin\theta(\xi\cos\phi + \eta\sin\phi) d\xi d\eta, \tag{3}$$

where k is the phase constant (2π/wavelength). The unit vector $\bar{\imath}_z$ is normal to the aperture plane, and the unit vector $\bar{s}$ is normal to the incident phase front. When writing $\bar{\imath}_z \cdot \bar{s}$ outside the integral sign, one assumes that the phase front incident upon the aperture is plane; however, its orientation does not have to coincide with the aperture plane (in that case, $\bar{\imath}_z \cdot \bar{s}$ would be equal to unity). Results obtained by (3) are given for many types of aperture illumination by Silver [1].

In Appendix I it is shown that, subject to the limitations enumerated in the introduction, the radiation field is given as a function of time by

$$\psi(\bar{r}, t) = \frac{1}{\sqrt{2\pi}} \int_{-\infty}^{\infty} F(\omega) R(\bar{r}, \omega) e^{i\omega t} d\omega. \tag{4}$$

Results obtained by (4) are given below for various signals $f(t)$ and various aperture distributions $K_0(\bar{r})$. Rectangular apertures and aperture distributions which are separable in rectangular coordinates will be assumed. Under these circumstances, the radiation pattern can be written as a product of two functions, each corresponding to the aperture distribution along one of the axes (ξ or η). As far as transient behavior is concerned, all significant results become apparent if radiation patterns in one of the principal planes such as the x-z plane (where $\phi = 0$) are considered [2]. Consequently, only the transient fields in that plane are evaluated below.

Response to Step Function

A step function which is superimposed upon a carrier can be written as

$$\begin{aligned} f(t) &= 0 \qquad & t < 0 \\ f(t) &= \sin\omega_1 t \qquad & t \geq 0. \end{aligned} \tag{5}$$

Its frequency spectrum can be obtained by (1) and is given by

$$F(\omega) = \frac{1}{\sqrt{2\pi}} \frac{1}{\omega_1^2 - \omega^2}. \tag{6}$$

The steady-state radiation field of a uniformly illuminated aperture (*i.e.*, one with constant amplitude and phase) can be obtained by (3). In the $\phi = 0$ plane the result, as given by Silver [2], is

$$R(\bar{r}, \omega) = \frac{iAe^{-i(\omega R/c)} \sin\omega x}{4\pi c R x}, \tag{7}$$

where A is the area of the aperture, R the distance of the point where the field is evaluated from the center of the aperture, c the velocity of light, and x is given by

$$x = \frac{a}{2c} \sin\theta. \tag{8}$$

The quantity a is the length of the aperture in the plane $\phi = 0$.

The radiation field ψ as a function of time is obtained by (4). The result is conveniently expressed in terms of the variable q which is the time measured from the instant when the signal is switched on, less the time which it takes electromagnetic energy to travel the distance R in free space, as follows:

$$q = t - \frac{R}{c}. \tag{9}$$

We also employ the constant

$$M = \frac{A\omega_1}{4\pi c R}. \tag{10}$$

The radiation field is then given by

$$\psi_0 = M \frac{\cos x\omega_1}{x\omega_1} \sin q\omega_1 \qquad 0 \leq q \leq x, \tag{11}$$

$$\psi_0 = M \frac{\sin x\omega_1}{x\omega_1} \cos q\omega_1 \qquad q \geq x. \tag{12}$$

The result expressed by (12) clearly corresponds to the steady-state antenna pattern $\sin x\omega_1 / x\omega_1$. However, it is apparent that a time interval t larger than R/c is required before this steady-state pattern is established. This interval is determined by the critical value of q,

$$q_1 = x = \frac{a}{2c} \sin\theta. \tag{13}$$

Thus on a line normal to the center of the antenna ($\theta = 0$), the steady-state value of the field is established at $q = 0$ while for larger values of θ, the delay q becomes larger.

It is interesting to determine the value of q required for establishment of the steady-state pattern in the region of the main beam only. The location of the first null in the $\sin x\omega_1/x\omega_1$ pattern is given by $x\omega_1=\pi$ or $\sin\theta=(\lambda/a)$. Substitution into (13) gives

$$q_1' = \frac{a}{2c}\,\frac{\lambda}{a} = \frac{\tau}{2}, \tag{14}$$

where τ is the period of the carrier frequency. On the other hand, establishment of the steady-state pattern at all angles between 0° and 90° requires $q_1=a/2c$, and for an antenna of specified beamwidth (between first nulls)

$$2\theta_0 \approx 2\sin\theta_0 = 2\frac{\lambda}{a} \tag{15}$$

one may also write, in view of (13),

$$q_{1,\max} = \frac{a}{2c} = \frac{\lambda}{\theta_0 2c} = \frac{\tau}{2\theta_0}\,. \tag{16}$$

Thus for a beamwidth $2\theta_0$ of 0.01 radian, the delay $q_{1,\max}$ is equal to 100 periods of the carrier frequency.

Several transient patterns are shown for the neighborhood of the main lobe in Fig. 2. Each curve corresponds to (11) for $q<x$ and to (12) for $q>x$. Both equations give the same numerical result at $q=x$.

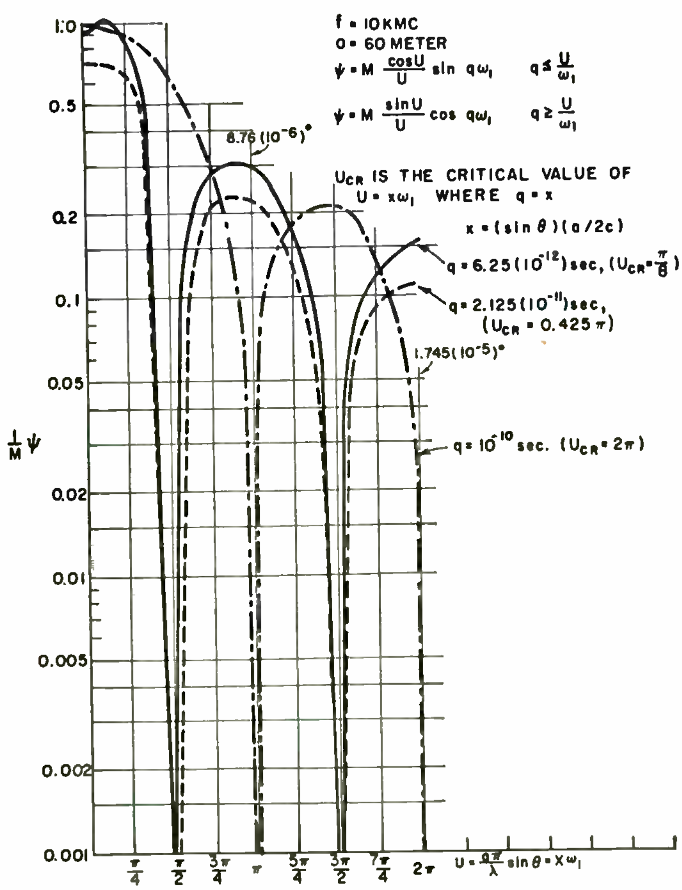

Fig. 2—Transient patterns of uniformly illuminated aperture.

It is very important to notice that for a fixed antenna beam, the significant limitations as far as applications are concerned are expressed more realistically by (14) than by (16). The reason is that beyond the main lobe region, the only transient effect is that the sidelobes shift in position without changing amplitude. This is clearly apparent from examination of (11) and (12). Beyond the second null of the steady-state pattern ($x\omega_1\geq 2\pi$), for example, relation (12) gives

$$\frac{\sin x\omega_1}{x\omega_1} \leq \frac{1}{2\pi}, \tag{17}$$

while (11) gives

$$\frac{\cos x\omega_1}{x\omega_1} \leq \frac{1}{2\pi}\,. \tag{18}$$

The results expressed by (11) and (12) are those for an aperture illuminated by a constant-amplitude, constant-phase field. Corresponding results for a tapered illumination are the following:

$$K_0(\xi) = \cos\frac{\pi\xi}{2} \qquad |\xi| < 1 \quad \text{(cosine illumination)}, \tag{19}$$

$$R(\bar{r},\omega) = \frac{i4Ae^{-i(\omega R/c)}}{\lambda R}\,\frac{\cos\omega x}{\pi^2 - 4\omega^2x^2}, \tag{20}$$

$$M' = \frac{A\omega_1}{\pi c R}, \tag{21}$$

$$\psi_1 = M'\frac{1}{\pi^2 - 4\omega_1^2x^2}\left(\sin\frac{\pi}{2}\,\frac{q}{x} - \sin x\omega_1 \sin q\omega_1\right) \qquad 0 \leq q \leq x, \tag{22}$$

$$\psi_1 = M'\left(\frac{\cos x\omega_1}{\pi^2 - 4\omega_1^2x^2}\right)\cos q\omega_1 \qquad q \geq x. \tag{23}$$

The steady-state pattern is given by (23) and the limiting condition is again (13). The location of the first null in the steady-state pattern is given by $x\omega_1=(3/2)\pi$ or $\sin\theta=(3/2)(\lambda/a)$, and the critical time required for establishment of the steady-state pattern in the region between first nulls is

$$q_1'' = \frac{a}{2c}\,\frac{3}{2}\,\frac{\lambda}{a} = \frac{3}{4}\tau, \tag{24}$$

which is of the same order of magnitude as (14).

Response to Rectangular Pulse and Limitations on Radar Resolution

We consider a rectangular pulse of duration w superimposed upon a carrier frequency ω_1:

$$\begin{aligned} f(t) &= 0 & t &< 0 \\ f(t) &= \sin\omega_1 t & 0 &\leq t \leq w \\ f(t) &= 0 & t &> w. \end{aligned} \tag{25}$$

This pulse is applied to the uniformly illuminated aperture whose steady-state radiation pattern is given by (7). One may consider this pulse as the addition of two step functions, one of positive sign applied at $t=0$ and one of negative sign applied at $t=w$. It is necessary, however, to allow for the condition that $\sin \omega_1 t$ is not necessarily equal to zero at $t=w$, while it is of course equal to zero at $t=0$. The frequency spectrum of (25) is

$$F(\omega) = \frac{1}{\sqrt{2\pi}} \frac{1}{\omega_1^2 - \omega^2} \cdot \left[\omega_1 - e^{-i\omega w}(\omega_1 \cos \omega_1 w + i\omega \sin \omega_1 w)\right]. \quad (26)$$

By the application of (4) and (7), one obtains the radiation field

$$\bar{\psi} = \psi_0 - \psi_2. \quad (27)$$

ψ_0 is given by (11) and (12), and ψ_2 is given by

$$\psi_2 = M \frac{\cos x\omega_1}{x\omega_1} \sin q\omega_1 \qquad 0 \leq (q - w) \leq x, \quad (28)$$

$$\psi_2 = M \frac{\sin x\omega_1}{x\omega_1} \cos q\omega_1 \qquad (q - w) \geq x. \quad (29)$$

At the beginning of the pulse the time q_1, given by (13), is required for the establishment of the steady-state pattern, and all considerations embodied in (14) to (18) also apply.

If the pulse is long enough ($w \geq x$) so that the steady-state condition expressed by (12) can be established, it follows from (27) and (29) that the signal subsides to zero when $q \geq (x+w)$. From (27) and (28), it is clear that a transient pattern will exist at the end of the pulse during the interval $w \leq q \leq (x+w)$.

In view of (11) and (27), the steady-state pattern is never established when $w < x$. If we substitute w for q_1' in (14), we obtain the minimum pulse length required for establishment of the steady-state radiation pattern over the main-lobe region of that pattern,

$$w_1 = \frac{\tau}{2} \cdot \quad (30)$$

If we assume that the best range resolution ΔR_0 which can be obtained from a radar which emits such a pulse is $\Delta R_0 = w_1 c$, then it follows from (30) that

$$\Delta R_0 = \frac{\lambda}{2} \cdot \quad (31)$$

If a criterion corresponding to (16) is used; that is, if one requires a pulse of sufficient duration for establishment of the steady-state radiation pattern at all angles between 0° and 90°, which implies that

$$w_1 \geq x_{\max} \quad \text{or} \quad w_1 \geq \frac{a}{2c}, \quad (32)$$

one obtains in terms of the beamwidth $2\theta_0$ between first nulls,

$$w 2\theta_0 \geq \frac{\lambda}{c}, \quad (33)$$

or

$$\Delta R(2\theta_0) \geq \lambda. \quad (34)$$

If $2\theta_0$ is a measure of the best possible angular resolution, this equation gives a limit for the product of angular and range resolution. In view of what has been said, however, in the discussion of (16) and (17), the relation (34) does not necessarily constitute a limitation in most applications of antennas. If the radiation pattern only in the vicinity of the main lobe is of interest, (31) expresses adequately the limitations on radar resolution which result from the transient behavior of the antenna.

Scanning Antennas—Linear Phase Variation

An application where the transient behavior of aperture antennas is particularly important is that of electronic scanning. Clearly one cannot move a beam of prescribed shape at a rate which does not allow sufficient time for the formation of the desired beam.

The simplest aperture distribution which will give a main lobe in a direction other than $\theta=0$ is that of constant amplitude and linear phase:

$$P_0(\xi, \eta) = 1e^{-ip\xi\omega}. \quad (35)$$

From (3) it follows that the steady-state field in this case is given by

$$R(\bar{r}, \omega) = \frac{iAe^{-\omega(R/c)}(\cos\theta + \sqrt{1 - p^2c^2})}{2\pi cR} \cdot \frac{\sin \omega\left(x - \frac{pa}{2}\right)}{\omega\left(x - \frac{pa}{2}\right)} \cdot \quad (36)$$

The direction of the peak field intensity is, as a consequence of (36), determined by

$$\sin \theta_{\max} = pc. \quad (37)$$

To analyze the transient behavior, we assume a step function

$$f(t - p\xi) = 0 \qquad t \leq p\xi$$
$$f(t - p\xi) = \sin \omega_1(t - p\xi) \qquad t > p\xi. \quad (38)$$

This time function implies that the aperture $-a/2 \leq \xi \leq a/2$ is first energized at $t = -pa/2$ along the line $\xi = -a/2$. Thereafter, the signal appears successively at larger values of ξ. The center of the aperture, $\xi=0$, is energized at $t=0$. This corresponds to the physical situation in a scanning antenna which is fed by an RF delay network.

Substitution of (36) into (4)—a procedure which is justified in Appendix I [(61) to (66)]—and use of the Fourier transform (6) of the step function gives results very similar to (11) and (12):

$$q = t - \frac{R}{c}, \tag{9}$$

$$M'' = \frac{A\omega_1}{4\pi c R}(\cos\theta + \sqrt{1 - p^2c^2}), \tag{39}$$

$$\psi = M'' \frac{\cos\omega_1\left(x - \frac{pa}{2}\right)}{\omega_1\left(x - \frac{pa}{2}\right)} \sin q\omega_1$$

$$0 \le q \le \left(x - \frac{pa}{2}\right), \tag{40}$$

$$\psi = M'' \frac{\sin\omega_1\left(x - \frac{pa}{2}\right)}{\omega_1\left(x - \frac{pa}{2}\right)} \cos q\omega_1 \quad q \ge \left(x - \frac{pa}{2}\right). \tag{41}$$

The time interval $\bar{q}_1$ beyond the delay R/c which is required for establishment of the steady-state field is

$$\bar{q}_1 = x - \frac{pa}{2} = \frac{a}{2c}\sin\theta - \frac{pa}{2}. \tag{42}$$

At the location of the pattern maximum, given by (37) the value of $\bar{q}_1$ is zero just like the value of q_1 given by (13) was zero for $\theta=0$. One should notice here, however, that in view of (38) the power was applied at least to one point (or one line) in the aperture at $t=-pa/2$. If we therefore measure time (delayed by R/c) from the instant when the power was first turned on, we must consider

$$Q = t - \frac{R}{c} + pa/2. \tag{43}$$

The criterion for existence of the steady-state field is then

$$Q \ge x, \tag{44}$$

and the maximum of the steady-state pattern will be established at the location given by (37) when

$$Q_1 = \frac{ap}{2}. \tag{45}$$

For example, for $\theta_{\max}$ to be located at 45°, $p=2.357$ (10^{-9}) from (37), and if a 200-meter antenna is employed, the delay Q_1 is 0.2357 μsec beyond R/c.

The time beyond R/c necessary for establishment of the steady-state pattern over the region between first nulls is

$$Q_1' = \frac{\tau}{2} + \frac{pa}{2}. \tag{46}$$

Finally, the time necessary for establishment of the steady-state pattern at all angles between 0° and 90°, is in view of (44), given by $Q=a/2c$. Like (16), this can be written in terms of the beamwidth between first nulls. Neglecting the factor $\cos\theta+\sqrt{1-p^2c^2}$ in (36), one obtains

$$Q_{1,\max} = \frac{\tau}{2\theta}. \tag{47}$$

Conclusions

It has been shown that the transient behavior of aperture antennas can be analyzed, within the limitations outlined in the Introduction, by a combination of scalar diffraction theory and the application of the Fourier Integral theorem. The results are as follows.

1) In all situations which were analyzed, the critical parameter $(\sin\theta)a/2c$ appears, indicating that the transient behavior of the antenna depends upon its size as related to the velocity of light, and that transient conditions in the radiation pattern depend upon the angle from the normal to the antenna.

2) The steady-state main lobe of an antenna illuminated by a field of uniform phase and uniform amplitude is established within $(\tau/2+R/c)$ seconds[1] after the aperture is energized.

3) For the same aperture, the time required for the establishment of the steady-state pattern at all angles between 0° and 90° is $(\tau/2\theta_0+R/c)$. $\tau/2\theta_0$ is in general much longer than $\tau/2$, because θ_0 measured in terms of radians is usually very much less than unity. An antenna may be useful, however, before the period $(\tau/2\theta_0+R/c)$, because the maxima of the transient sidelobes are not higher than the maxima of the steady-state sidelobes.

4) The requirement that the steady-state pattern be established at all angles between 0° and 90° leads to a limitation on range discrimination and angular discrimination of a pulse radar as defined by (30) to (34). $\Delta R\Delta\theta \ge \lambda$.

[1] $3\tau/4+R/c$ seconds for cosine distribution.

5) For an antenna with uniform amplitude and linearly varying phase—which could be used as a simple scanning antenna—it has been shown that the main lobe of the steady-state pattern, in the direction of $\theta_{\max}$, is established within a time $(\tau/2+R/c+a\sin\theta_{\max}/2c)$ measured from the instant at which one edge of the aperture is first energized [(37), (43), and (46)].

Appendix I
Details of Mathematical Method

Derivation of (4)

The problem is to find a solution of the homogeneous wave equation

$$\nabla^2\psi(\bar{r}, t) - \frac{1}{c^2}\frac{\partial^2\psi(\bar{r}, t)}{\partial t^2} = 0, \qquad (48)$$

subject to the boundary condition that on some closed surface S,

$$\psi(\bar{r}, t) = f(t)K_0(\bar{r}). \qquad (49)$$

The function $f(t)$ is the pulse applied to the antenna and $K(\bar{r})$ is the aperture distribution. $K(\bar{r})$ is neither a function of time nor of the frequency ω, which will be introduced later.

Let us assume that (48), subject to the boundary condition (49), has the solution

$$\psi(\bar{r}, t) = \frac{1}{\sqrt{2\pi}}\int_{-\infty}^{\infty} F(\omega)R(\bar{r}, \omega)e^{i\omega t}d\omega. \qquad (50)$$

Substitution of (50) into (48) gives

$$\frac{1}{\sqrt{2\pi}}\int_{-\infty}^{\infty} F(\omega)\left[\nabla^2R(\bar{r}, \omega) + \frac{\omega^2}{c^2}R(\bar{r}, \omega)\right]e^{i\omega t}d\omega = 0. \qquad (51)$$

Hence (50) is the desired solution, provided that

$$\nabla^2R(\bar{r}, \omega) + k^2R(\bar{r}, \omega) = 0 \qquad \text{outside } \bar{S}, \qquad (52)$$

and

$$\psi = \frac{1}{\sqrt{2\pi}}\int_{-\infty}^{\infty} F(\omega)K_0(\bar{r})e^{i\omega t}d\omega \qquad \text{on } S, \qquad (53)$$

where

$$K_0(\bar{r}) = R(\bar{r}, \omega) \qquad \text{on } S. \qquad (54)$$

From (49) and (53), it follows that

$$f(t) = \frac{1}{\sqrt{2\pi}}\int_{-\infty}^{\infty} F(\omega)e^{i\omega t}d\omega, \qquad (55)$$

and therefore $F(\omega)$ is the Fourier mate of $f(t)$, as follows:

$$F(\omega) = \frac{1}{\sqrt{2\pi}}\int_{-\infty}^{\infty} f(t)e^{i\omega t}dt. \qquad (56)$$

Eq. (50) in conjunction with (53) constitutes a solution of (48) and (49).

If the aperture is large in terms of wavelengths and if the aperture field is linearly polarized, it can be shown [1] that a good approximation to the vector diffraction problem is obtained by the solution of the scalar problem. Furthermore, (52) and (54) can be solved, subject to the usual approximations applicable for the Fraunhofer field, by the Kirchhoff diffraction formula [1], *provided that for all frequencies the illuminated aperture is large in terms of wavelengths* and the distance r from the aperture to the point where the field is evaluated is large ($r \geq a^2/\lambda$, where a is the largest linear dimension of the aperture, for validity of the Fraunhofer approximation).

Background of Method

The solution (50) is suggested by the fact [3] that "homogeneous differential equations with nonhomogeneous boundary conditions (*i.e.*, boundary conditions such that $\psi \neq 0$ over some part of the boundary) are essentially equivalent to nonhomogeneous differential equations with homogeneous boundary conditions."

The nonhomogeneous equation corresponding to (48) is

$$\nabla^2\psi(\bar{r}, t) - \frac{1}{c^2}\frac{\partial^2\psi(\bar{r}, t)}{\partial t^2} = f_1(t), \qquad (57)$$

which has the following solution [4] as a consequence of the Fourier Integral theorem [5] and the superposition principle

$$\psi(\bar{r}, t) = \frac{1}{\sqrt{2\pi}}\int_{-\infty}^{\infty} F(\omega)R(\bar{r}, \omega)e^{i\omega t}d\omega, \qquad (58)$$

where

$$F(\omega) = \frac{1}{\sqrt{2\pi}}\int_{-\infty}^{\infty} f_1(t)e^{-i\omega t}dt. \qquad (59)$$

Eqs. (58) and (50) are of the same form.

Generalization to Case where Aperture Distribution is a Function of Frequency

We consider again the homogeneous equation (48). However, the boundary condition is now

$$\left.\begin{aligned}\psi(\bar{r}, t) &= f(t - p\xi)K_0(\bar{r})\\ f(t - p\xi) &= 0 \qquad \text{when } t \leq p\end{aligned}\right\}\ \text{on } S. \qquad (60)$$

If S has a plane aperture which extends from $-a/2$ to $+a/2$ in the ξ direction, (60) implies that the line $\xi = -a/2$ is first energized at $t = -pa/2$. Thereafter, the signal appears successively at larger values of ξ. The center of the aperture, $\xi = 0$, is energized at $t = 0$. This corresponds to the physical situation existing in a scanning antenna which is fed by a phasing (delay) network. If $f(t-p\xi)$ contains a carrier frequency, the notation used implies that the phase of the sinusoidal carrier will vary over the aperture plane as $\sin(t-p\xi)$. Thus, (60) corresponds to a linear phase variation along ξ in the steady state.

We assume again that (48), subject to (60), has the solution (50). If $F(\omega)$ is not a function of position, $R(\bar{r}, \omega)$ is again a solution of (52).

Let the value of $R(\bar{r}, \omega)$ on S be given by

$$R(\bar{r}, \omega) = K_0(\bar{r})g(\xi, \omega) \qquad \text{on } S, \tag{61}$$

where $K_0(\bar{r})$ is the amplitude distribution prescribed by (60) and is independent of the frequency ω. The function $g(\xi, \omega)$ is as yet unknown.

By (50) and (62) the value of $\psi(\bar{r}, t)$ on S must be

$$\psi = \frac{1}{\sqrt{2\pi}}\int_{-\infty}^{\infty} F(\omega)K_0(\bar{r})g(\xi, \omega)e^{i\omega t}d\omega, \tag{62}$$

which must be identical with (60). Equating (60) to (62), one obtains

$$f(t - p\xi) = \frac{1}{\sqrt{2\pi}}\int_{-\infty}^{\infty} F(\omega)g(\xi, \omega)e^{ip\xi\omega}e^{i(t-p\xi)\omega}d\omega. \tag{63}$$

From the Fourier Integral theorem, it follows that

$$F(\omega)g(\xi, \omega)e^{ip\xi\omega} = \frac{1}{\sqrt{2\pi}}\int_{-\infty}^{\infty} f(v)e^{-i\omega v}dv.$$

If we let $v = t - p\xi$ in the time function prescribed by (60), or simply by (55) and (56), we have

$$F(\omega) = \frac{1}{\sqrt{2\pi}}\int_{-\infty}^{\infty} f(v)e^{-i\omega v}dv. \tag{64}$$

Consequently

$$g(\xi, \omega) = e^{-ip\xi\omega}. \tag{65}$$

Using (61) and (65), one can obtain again the solution of (52) by the Kirchhoff diffraction formula. The boundary condition (61) is now that of linear phase variation over the aperture. $F(\omega)$ is given by (64) and the solution of the problem can be obtained by (50).

Appendix II

Mathematical Symbols

t = time.
ω = radian frequency $= 2\pi f$.
ω_1 = carrier frequency of applied signal $= 2\pi f_1$.
c = velocity of light in free space.
$f(t)$ = time function (signal) applied to the antenna.
$F(\omega)$ = Fourier transform of $f(t)$.
$\bar{r}$ = radius vector locating the position of a point in space.
r, θ, ϕ = spherical coordinates.
$2\theta_0$ = angular width of steady-state radiation pattern between first nulls (θ_0 = angle between pattern maximum and first null).
θ_{max} = direction of peak field intensity, in the steady state, due to an aperture with linear phase variation.
ξ, η = rectangular coordinates in the plane of the aperture.
$P_0(r)$ = field distribution over plane aperture $= K_0(\bar{r})\ g(\bar{r}, \omega) = P_0(\xi, \eta) = K_0(\xi, \eta)\ g(\xi, \eta, \omega)$.
$K_0(\bar{r})$ = amplitude distribution $= K_0(\xi, \eta)$.
$g(\bar{r}, \omega)$ = phase distribution $= g(\xi, \eta, \omega)$.
$R(\bar{r}, \omega)$ = steady-state Fraunhofer (far) field of the aperture.
λ = wavelength of em wave in free space.
k = phase constant $= 2\pi/\lambda$.
$\bar{\imath}_Z$ = unit vector normal to aperture.
$\bar{s}$ = unit vector normal to phase front.
$\psi(\bar{r}, t)$ = far field of the aperture as a function of time.
ψ_0 = far field, as a function of time, of aperture with constant amplitude and phase, energized by step-function superimposed upon sinusoidal carrier.
ψ_1 = far field, as a function of time, of aperture with cosine amplitude distribution and constant phase, energized by step function superimposed upon sinusoidal carrier.
$\bar{\psi}$ = far field, as a function of time, of aperture with uniform amplitude and phase energized by a rectangular pulse of width w, superimposed upon a sinusoidal carrier $= \psi_0 - \psi_2$.
R = distance of a point where field is evaluated from center of aperture.
a = length of aperture in plane $\phi = 0$.
$x = (a \sin \theta/2c)$.
$q = t - R/c$ = time beyond the delay R/c; the antenna is first energized at $t = 0$ (q_1, q_1', q_1'' and $\bar{q}_1$ are critical values of q).
A = area of aperture.
$M = A\omega_1/4\pi cR$.
$M' = A\omega_1/\pi cR$.
M'' = given by (39).
τ = period of carrier frequency $= 1/f_1$.
w = width of rectangular pulse.
ΔR_0 = range resolution of radar.
p = parameter used to specify a linear phase distribution (35); p has the dimensions of seconds per meter.
$Q = t - R/C + pa/2$ = time beyond the delay R/c; one edge of the antenna is first energized at $t = -pa/2$ (Q_1, Q_1' and $Q_{1,max}$ are critical value of Q).
$v = t - p\xi$.

ACKNOWLEDGMENT

The author wishes to acknowledge the help which was extended to him in the preparation of this report by R. W. Madden of RCA, Burlington, Mass., who first suggested the analysis of the problem, and who proposed (34). The author's former colleagues at RCA Laboratories, Princeton, N. J., particularly Dr. R. W. Klopfenstein, Dr. R. H. Parmenter, J. Epstein, J. B. Rankin, and O. M. Woodward all helped by discussing the problem. Mathematically exact solutions of related problems have been published by F. Oberhettinger [6], H. E. Moses [7], V. M. Papadopoulos [8], and Gardner and Keller [9]. H. J. Schmitt [10] at Harvard University and G. G. Weill [11] at the California Institute of Technology have considered transients in linear antennas.

BIBLIOGRAPHY

[1] S. Silver, "Microwave Antenna Theory and Design," M.I.T. Rad. Lab. Ser., McGraw-Hill Book Co., New York, N. Y., vol. 12, pp. 164–167, 169–174, 187; 1949.
[2] *Ibid.*, pp. 180, 187.
[3] R. Courant and D. Hilbert, "Methods of Mathematical Physics," Interscience Publishers, New York, N. Y., vol. I, p. 277; 1953.
[4] C. Page, Physical Mathematics," D. Van Nostrand, Inc., Princeton, N. J., p. 194; 1955.
[5] P. M. Morse and H. Feshbach, "Methods of Theoretical Physics," McGraw-Hill Book Co., New York, N. Y., pt. 1, p. 453; pt. 2, pp. 1361, 1933; 1953.
[6] F. Oberhettinger, "On the diffraction and reflection of waves and pulses by wedges and corners," *J. Res. NBS*, vol. 61, pp. 343–365; November, 1958.
[7] H. E. Moses, "The Solution of Maxwell's Equations in Terms of a Spinor Notation. Part I: The Initial Value Problem in Terms of Field Strengths and the Inverse Problem," Div. of Electromagnetic Res., Inst. of Math. Sciences, New York Univ., New York, N. Y., Res. Rept. No. EM-114; June, 1958.
[8] V. M. Papadopoulos, "Diffraction and Refraction of Plane Electromagnetic Pulses," presented at the URSI Symp. on Electromagnetic Theory, Toronto, Canada; June 15–20, 1959.
[9] C. S. Gardner and J. B. Keller, "The Field of a Pulsed Dipole in an Interface," presented at the URSI Symp. on Electromagnetic Theory, Toronto, Canada; June 15–20, 1959.
[10] H. J. Schmitt, "Transients in Cylindrical Antenna," Cruft Lab., Harvard University, Cambridge, Mass., Tech. Rept. No. 296; January 5, 1959.
[11] G. G. Weill, "Transients on a Linear Antenna," California Institute of Technology, Pasadena, Antenna Lab., Tech. Rept. No. 20; August, 1959.

CORRECTION

In "Space Telemetry Systems," by W. E. Williams, Jr., which appeared on pages 685–690 of the April, 1960, issue of PROCEEDINGS, the final printing of Table I (page 687) had some of the horizontal columns not in proper alignment. The Table, correctly reproduced, appears opposite.

TABLE I

Name	Frequency (mc)	Transmitter Power	Type Modulation	Amount of Carrier Modulation	Antenna Type	Radiation Polarization	Subcarrier Bands‡ (If IRIG FM/FM)	Approximate Transmitter Life	Type Power Supply	Weight of Batteries (pounds)	Apogee (miles)	Perigee (miles)	Launch Vehicle
Explorer I	108.00	10–20 mw	FM/PM	0.7 radian (rms)	Dipole	Linear	2, 3, 4, 5	3½ months	Mercury batteries	2.2	1,573	224	Jupiter C
	108.03	50–100 mw	FM/AM	50 per cent	Turnstile	Circular	2, 3, 4, 5	½ month		2.1			
Explorer III	108.00	10 mw	FM/PM	0.7 radian (rms)	Dipole	Linear	2, 3, 4, 5	2½ months	Mercury batteries	2.2	1,746	121	Jupiter C
	108.03	*60 mw	FM/AM	50 per cent	Dipole	Linear		1½ months		3.1			
Explorer IV	108.00	10 mw	FM/PM	0.3 radian (rms)	Dipole	Linear	1, 2, 3, 4, 5	1¾ months	Mercury batteries		1,380	163	Jupiter C
	108.03	30 mw	FM/AM	100 per cent	Dipole	Linear	1, 2, 3, 4, 5	2¼ months					
Explorer VI (Paddlewheel)	108.06	*10 mw	FM/FM		Two monopoles	Linear	1, 2, 3, 4, 5, 8	1 month	Solar cells and chemical batteries	17	26,000	156	Thor-Able
	108.09	*60 mw	FM/FM		Two monopoles	Linear	1, 2, 3, 4, 5, 6						
	378.00	* 5 watts	PCM/PM		Two monopoles	Linear							
Vanguard I	108.00	10 mw	FM	Approx. 6 kc	Turnstile	Circular		19 days	Mercury batteries	10.5 ounces	2,453	407	Vanguard
	108.03	5 mw	FM	Approx. 6 kc	Dipole	Linear		Years	Solar cells				
Vanguard II	108.00	10 mw	FM	Approx. 6 kc	Turnstile	Circular		27 days	Mercury batteries	10.5 ounces	2,061	350	Vanguard
	108.03	* 1 watt	AM/AM	60 per cent				18 days		8½			
Vanguard III	108.00	30 mw	PDM-FM/AM	100 per cent	Turnstile	Circular		90 days Predicted	Silver—zinc	22.35†	2,330	318	Vanguard
	108.03	*80 mw	AM	100 per cent	Turnstile	Circular							
Pioneer I	108.06	300 mw	FM/PM	1.0 radian	Dipole	Linear	1, 2, 3, 4, 5, 6	43 hours	Mercury batteries		Altitude 70,700	Space probe. Did not orbit	Thor-Able
	108.09	100 mw	FM/PM	1.0 radian	Dipole	Linear	1, 2, 3, 4, 5, 6	Life of probe					
Pioneer II	108.06	300 mw	FM/PM	1.0 radian	Dipole	Linear	1, 2, 3, 4, 5, 6	Life of probe	Mercury batteries		Altitude 963	Space probe. Did not orbit	Thor-Able
	108.09	100 mw	FM/PM	1.0 radian	Dipole	Linear	1, 2, 3, 4, 5, 6						
Pioneer III	960.05	180 mw	FM/PM	0.79 radian (peak)	Conical payload served as the antenna	Linear	1, 2, 3	38 hours	Mercury batteries	6.6	Altitude 63,580	Space probe. Did not orbit	Juno II
Pioneer IV	960.05	180 mw	FM/PM	0.79 radian (peak)	Conical payload served as the antenna	Linear	1, 2, 3	90 hours	Mercury batteries	6.6	In orbit around the sun. TM data and tracking were continuous to 400,000 miles.		Juno II

* Transmitters have command features.
† This battery weight includes power for the magnetometer polarizing field.
‡ IRIG FM/FM Subcarrier Bands (cps) (in part): 1) 400, 2) 560, 3) 730, 4) 960, 5) 1,300, 6) 1,700, 7) 2,300, 8) 3,000.

Radar Target Classification by Polarization Properties*

J. R. COPELAND†, MEMBER, IRE

Summary—**The polarization properties of radar targets are studied as a parameter related to, but quite distinct from, echo area. It is found that targets are divided into several different classes. The polarization properties may be measured by rotating a linearly polarized radar antenna around the line of sight, and measuring the complex voltage presented at the receiving antenna terminals.**

It is shown that the polarization properties of any target so measured can be represented by a 3-parameter model (excluding echo area), and the parameters of such a model can be used as the basis for discriminating between targets of the same or different classes.

Introduction

It has been shown by Sinclair[1] and by Kennaugh[2] how a radar target acts as a polarization transformer, *i.e.*, how the polarization of a backscattered electromagnetic wave will differ, in general, from the polarization of the wave incident upon a radar target. Sinclair expressed this transformation as a matrix which could be incorporated into the radar range equation.[1] Kennaugh treated the power received by a radar of arbitrary polarization, extending geometrical significance to the transformation by using the Poincaré polarization sphere.[2]

The Poincaré sphere is a useful mapping of polarization states onto the surface of a sphere. The two parameters necessary to describe an elliptical polarization state are the orientation angle θ (the position in space coordinates of the major axis of the polarization ellipse), and the axial ratio r (the ratio of minor to major diameters of the polarization ellipse). An algebraic sign is frequently attached to the axial ratio to indicate the "sense" of the elliptical polarization, with a positive (+) sign indicating right-hand ellipitical polarization and a negative (−) sign indicating left-hand elliptical polarization.

$$|r| = \frac{\text{minor axis}}{\text{major axis}}; \qquad -1 \leq r \leq +1. \tag{1}$$

Then, according to Deschamps,[3] defining an ellipticity angle α by $\tan \alpha = r$ permits plotting polarization states on the sphere by using 2α for latitude and 2θ (orientation angle) for longitude. Thus, the equator of the sphere contains all linear polarizations, and the poles of the sphere are opposite-sense circular polarizations. There is a 1:1 correspondence between polarization states and points on the sphere, and orthogonal polarizations map into points diametrically opposite on the sphere.

Kennaugh showed that the polarization transforming properties of any target are characterized by two null polarizations; *i.e.*, two radar polarization states exist for which the backscattered wave is polarized orthogonally to the radar antenna. In such a case the radar would be blind to that target.

Kennaugh further suggested that radar targets be classified according to their polarization transforming properties, apart from their effective echoing areas (radar cross sections). Several classes of targets are recognized to exist:[2]

1) *Linear Target*—The linear target's null polarizations coincide at a single point on the polarization sphere. The polarization of the reflected wave is independent of radar polarization, but the reflected power is not. A thin straight wire would be an example of a linear target.

2) *Isotropic Target*—The isotropic target has two orthogonal null polarizations. On the polarization sphere they would appear at opposite ends of some diameter. The power in the reflected wave is independent of radar polarization, but the reflected wave polarization is not. A homogeneous sphere would be the simplest example of an isotropic target.

3) *Symmetrical Target*—The symmetrical target has two null polarizations located anywhere along parallels of latitude which are equidistant from the equator of linear polarizations. (One axial ratio is the negative of the other.) It has no sense preference for elliptical polarizations. Any target with a plane of symmetry containing the radar line of sight is a symmetrical target.

4) *General Target*—The general target has two distinct null polarizations not located on a common diameter of the polarization sphere. Both power and polarization of the backscattered wave are functions of radar polarization.

* Received by the IRE, August 26, 1959; revised manuscript received, December 21, 1959. The research in this paper was sponsored in part by Air Res. and Dev. Command, Wright Air Dev. Center, Wright-Patterson Air Force Base, Dayton, Ohio, under Contract AF 33(616)-5078.

† Antenna Lab., Ohio State University, Columbus, Ohio.

[1] G. Sinclair, "Modification of the Radar Range Equation for Arbitrary Targets and Arbitrary Polarization," Antenna Lab., The Ohio State University Res. Foundation, Columbus, Rept. No. 302-19, September 25, 1948; prepared under Contract W 36-039-sc-33634, Evans Signal Lab., Belmar, N. J.

[2] E. M. Kennaugh, "Polarization Properties of Radar Reflections," Antenna Lab., The Ohio State University Res. Foundation, Columbus, Rept. No. 389-12, March, 1952; prepared under Contract AF 28(099)-90, Rome Air Dev. Center, Griffiss Air Force Base, Rome, N. Y.

[3] G. A. Deschamps, "Geometrical representation of the polarization of a plane electromagnetic wave," Proc. IRE, vol. 39, pp. 540–544; May, 1951.

Types 1 and 2 are mutually exclusive classes, while type 3 is a very large class containing all isotropic and some linear targets. Practically all simple target shapes have planes of symmetry and fall into this third class. A symmetrical target might be described as a general target having no sense preference.

Idealized Target Model

In the following development, it will be convenient to replace the radar target by a mathematical model. It should be stressed that the model represents the target's polarization properties only at a specific frequency and a fixed aspect, and is used only to formulate the polarization state of the scattered wave. The analysis is restricted to monostatic, or backscattered echo.

The idealized model will consist of two fictional antennas of different elliptical polarizations, so coupled together that all energy received by either antenna is retransmitted by the other back toward the radar (see Fig. 1).

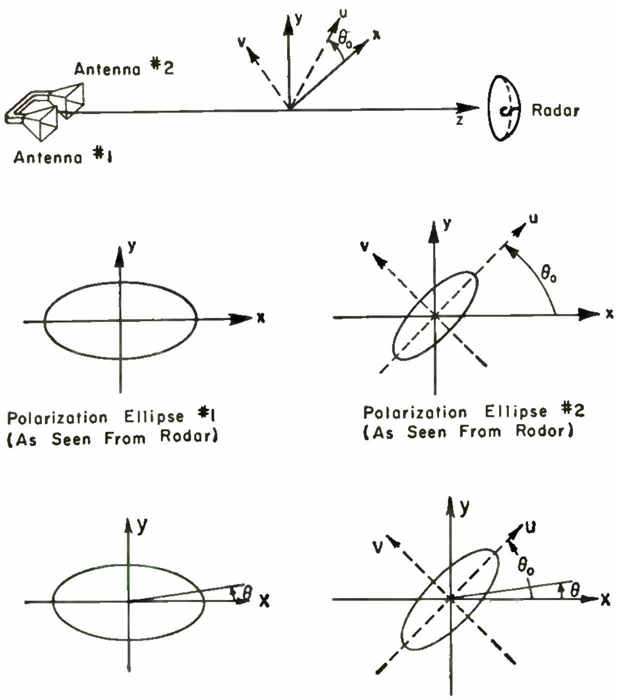

Fig. 1.

It is necessary to assume that all energy in the matched polarization state incident upon either of these fictional antennas is received by it, and that no scattering occurs from the hypothetical structure, which would have to be considered in addition to the reradiation from the opposite antenna.

Reciprocity also must be assumed for these antennas. Each antenna must have the same vector height in transmitting as in receiving.

Vector Height

The vector height (or length) of a receiving antenna may be defined as the vector whose dot product with the incident electric field of a plane wave yields the open circuit voltage at the antenna terminals.[4]

$$V = h \cdot E.$$

In the case of elliptically polarized antennas and waves, the principal components of both h and E (*e.g.*, x and y components) will be, in general, complex numbers representing magnitudes and phase angles.[5] The resulting dot product is then a phasor voltage and is handled by the usual complex number techniques of ac circuits.

In the analysis to be carried out here, the actual rms magnitude of this voltage is not important, so it is convenient to normalize the vector heights to unity.

$$\sqrt{|h|^2} = 1.$$

The vector height components are mathematically equivalent to the electric components of a plane wave. A plane wave is said to have a polarization state which can be plotted on the polarization sphere, so the vector height may be treated in the same fashion. The polarization state of a receiving antenna is the same as that of the wave which it best receives (the "matched polarization").

In applying this to the fictional antennas of the target model, it is necessary to know the two null polarizations shown to exist by Kennaugh. The two model antennas must be polarized so as to match incident waves of polarization orthogonal to the two null polarizations, respectively.

Thus, if the radar were polarized to either of the null polarizations, the antenna model would be invisible to the radar, just as the original radar target is invisible.

Justification of Target Model

It is necessary to demonstrate that the stated combination of two idealized antennas simulates the target's polarization properties. The scattering matrix relates the components of a plane wave incident on a target (E^t) to the reflected plane wave (E^r) as follows:

$$E^r = \begin{bmatrix} E_x^r \\ E_y^r \end{bmatrix} = \begin{bmatrix} a_{11} & a_{12} \\ a_{21} & a_{22} \end{bmatrix} \begin{bmatrix} E_x^t \\ E_y^t \end{bmatrix} \cdot \frac{1}{\sqrt{4\pi r^2}}, \qquad (2)$$

where the matrix

$$A = \begin{bmatrix} a_{11} & a_{12} \\ a_{21} & a_{22} \end{bmatrix} \qquad (3)$$

[4] H. G. Booker, "Introduction to techniques for handling elliptically polarized waves with special reference to antennas," Proc. IRE, vol. 39, pp. 533–534; May, 1951.

[5] J. D. Kraus, "Antennas," McGraw-Hill Book Co., Inc., New York, N. Y., p. 466; 1950.

is Sinclair's scattering matrix, describing the polarization transforming properties of the target at a specific frequency and in a specific direction.

Now if the target were replaced by the postulated antenna system, the open circuit voltages received by the two respective antennas may be written in terms of the incident electric field and the vector heights.

In antenna No. 1,

$$V_1 = E_x^t \cdot h_x^{(1)} + E_y^t \cdot h_y^{(1)}, \tag{4a}$$

and in antenna No. 2,

$$V_2 = E_x^t \cdot h_x^{(2)} + E_y^t \cdot h_y^{(2)}. \tag{4b}$$

Now it may be assumed, because these antennas are only mathematical fiction, that the open circuit voltages are exchanged to the opposite antennas giving rise to radiated fields of the form,

$$E^r = h \cdot V,$$

where, for simplicity, the factor $1/\sqrt{4\pi r^2}$ will be implied but not expressed.

Hence, for both antennas reradiating,

$$E^r = \begin{bmatrix} E_x^r \\ E_y^r \end{bmatrix} = \begin{bmatrix} h_x^{(1)} & h_x^{(2)} \\ h_y^{(1)} & h_y^{(2)} \end{bmatrix} \begin{bmatrix} V_2 \\ V_1 \end{bmatrix}. \tag{5}$$

But from (4)

$$\begin{bmatrix} V_2 \\ V_1 \end{bmatrix} = \begin{bmatrix} h_x^{(2)} & h_y^{(2)} \\ h_x^{(1)} & h_y^{(1)} \end{bmatrix} \begin{bmatrix} E_x^t \\ E_y^t \end{bmatrix}, \tag{6}$$

$$E^r = \begin{bmatrix} E_x^r \\ E_y^r \end{bmatrix}$$
$$= \begin{bmatrix} 2h_x^{(1)} \cdot h_x^{(2)} & h_x^{(1)} \cdot h_y^{(2)} + h_y^{(1)} \cdot h_x^{(2)} \\ h_x^{(1)} \cdot h_y^{(2)} + h_y^{(1)} \cdot h_x^{(2)} & 2h_y^{(1)} \cdot h_y^{(2)} \end{bmatrix}$$
$$\cdot \begin{bmatrix} E_x^t \\ E_y^t \end{bmatrix}. \tag{7}$$

This equation is now in the same form as the scattering matrix equation, and it follows that

$$\begin{aligned} a_{11} &= 2h_x^{(1)} \cdot h_x^{(2)} \\ a_{12} = a_{21} &= h_x^{(1)} \cdot h_y^{(2)} \cdot h_y^{(1)} \cdot h_x^{(2)}. \\ a_{22} &= 2h_y^{(1)} \cdot h_y^{(2)}. \end{aligned} \tag{8}$$

The vector heights of the fictitious antennas are specifically related to the scattering matrix of the target which they replace. They are such that the two antennas receive (and retransmit) best the polarizations orthogonal to the two null polarizations of the radar target.

As mentioned before, a right elliptically-polarized antenna will be said to have a positive axial ratio, and a left elliptically-polarized antenna to have a negative axial ratio.

In the coordinate system shown in Fig. 1, the polarization ellipses of both antennas are viewed from the position of the radar. The x-y plane has been rotated so that the x axis coincides with the major axis of one of the polarization ellipses; the major axis of the other is inclined by an angle θ_0 to the x axis. A u-v coordinate system is similarly impressed upon this second polarization ellipse.

Analysis of the polarization-transforming properties of a target involves radar measurements using a number of different radar polarizations. In theory, these polarizations could lie on nearly any arbitrary path around the polarization sphere; but, in practice, the most easily obtainable path is the locus of linear polarizations. For this reason the present development will be applied to use of rotating linear radar polarization.

The frequency and propagation factor $e^{j(\omega t \pm \beta z)}$ will be suppressed, and only the polarization terms will be considered.

Using the definition of vector heights previously advanced, it is seen that the two model antennas are described by the relations of Fig. 2.

For Antenna No. 1

$$\begin{cases} h_x^{(1)} = \sqrt{\dfrac{1}{1 + r_1^2}} \\ h_y^{(1)} = -jr_1 \sqrt{\dfrac{1}{1 + r_1^2}} \end{cases}$$

For Antenna No. 2

$$\begin{cases} h_u^{(2)} = \sqrt{\dfrac{1}{1 + r_2^2}} \\ h_v^{(2)} = -jr_2 \sqrt{\dfrac{1}{1 + r_2^2}} \end{cases}$$

Fig. 2.

The vector heights have been normalized to unity. If the parameter of echo area (or radar cross section) were to be considered, then they would be normalized to some other value to alter the magnitude of the backscattered wave.

Note the existence of the negative sign in $h_y^{(1)}$ and in $h_v^{(2)}$. They occur here because of the choice of coordinates, with the observer looking toward the receiving antenna.

Reflection from the Target Model

Consider now a radar with transmitting vector height h^t and receiving vector h^r. The field radiated from the transmitter is proportional to h^t, and will be denoted by E^t. Since the transmitted wave may be subject to normalization, the transmitting vector height may be chosen so that

$$E^t = h^t,$$

and

$$\sqrt{|h_x|^2 + |h_y|^2} = 1.$$

The complex voltage measured at the radar receiver antenna terminals will be found by a three-step procedure:

1) Find the voltages, both magnitude and phase, induced in the respective model antennas.

2) Exchange the voltages between the two antennas and calculate the reradiated fields.
3) Sum the fields from the two antennas, and calculate the component which would be returned to the linearly polarized radar.

Following the outline,

1) Into Antenna 1:

$$V^{(1)}(\theta) = h^{(1)}\cdot E^t = h^{(1)}\cdot h^t. \tag{9a}$$

Into Antenna 2:

$$V^{(2)}(\theta) = h^{(2)}\cdot E^t = h^{(2)}\cdot h^t. \tag{9b}$$

Now denoting the field reradiated back toward the radar by E^r;

2) Reradiated from Antenna no. 1:

$$E^{1r} = h^{(1)}\cdot V^{(2)}(\theta) = h^{(1)}\cdot(h^{(2)}\cdot h^t). \tag{10a}$$

Reradiated from Antenna No. 2:

$$E^{2r} = h^{(2)}\cdot V^{(1)}(\theta) = h^{(2)}(h^{(1)}\cdot h^t). \tag{10b}$$

The total reradiated field is the sum of these two components. Step 3) gives the voltage in the radar receiver:

$$\begin{aligned} V(\theta) &= h^r\cdot E^r = h^r\cdot E^{1r} + h^r\cdot E^{2r} \\ &= h^r\cdot h^{(1)}(h^{(2)}\cdot h^t) + h^r\cdot h^2(h^{(1)}\cdot h^t). \end{aligned} \tag{11}$$

However, since the dot product of vectors is a commutative operation, it is permissible to rewrite this phasor voltage in a simplified form:

$$V(\theta) = 2h^{(1)}\cdot h^{(2)}(h^t\cdot h^r). \tag{12}$$

Still suppressing the frequency and propagation factor, this is the most general expression of the phasor voltage at the radar receiver antenna terminals as a function of transmitter and receiver polarizations. For the present case, as already indicated, the transmitter and receiver will be taken as identical, or the same linearly polarized antenna. Then the received phasor voltage may be written

$$\begin{aligned} V(\theta) &= 2(h^{(1)}\cdot h^t)(h^{(2)}\cdot h^t) \\ &= 2V^{(1)}(\theta)V^{(2)}(\theta) \qquad \text{for } h^t = h^r. \end{aligned} \tag{13}$$

This last expression says that the voltage in the radar receiver may be written immediately from the results of step 1, without performing the remaining steps in the outline.

Rotating Linear Radar Polarization

Then, for a linearly polarized radar, polarized at angle θ with respect to the x axis (see Fig. 2).

$$\begin{cases} h_x^t = \cos\theta \\ h_y^t = \sin\theta \end{cases} \qquad \begin{cases} h_u^t = \cos(\theta-\theta_0) \\ h_v^t = \sin(\theta-\theta_0). \end{cases}$$

Performing step 1,

$$\begin{cases} V^{(1)}(\theta) = \sqrt{\dfrac{1}{1+r_1^2}}\cos\theta - jr_1\sqrt{\dfrac{1}{1+r_1^2}}\sin\theta \\ V^{(2)}(\theta) = \sqrt{\dfrac{1}{1+r_2^2}}\cos(\theta-\theta_0) \\ \qquad - jr_2\sqrt{\dfrac{1}{1+r_2^2}}\sin(\theta-\theta_0). \end{cases} \tag{14}$$

Then

$$V(\theta) = 2V^{(1)}(\theta)V^{(2)}(\theta) = \frac{2}{\sqrt{(1+r_1^2)(1+r_2^2)}} \cdot \left\{ \begin{array}{l} \cos\theta\cos(\theta-\theta_0) - r_1r_2\sin\theta\sin(\theta-\theta_0) \\ -j[r_1\sin\theta\cos(\theta-\theta_0) + r_2\cos\theta\sin(\theta-\theta_0)] \end{array} \right\}. \tag{15}$$

Expanding and collecting terms,

$$V(\theta) = \sqrt{\frac{1}{(1+r_1^2)(1+r_2^2)}} \cdot \left\{ \begin{array}{l} 2\cos\theta_0\cos^2\theta - 2r_1r_2\cos\theta_0\sin^2\theta \\ +2(1+r_1r_2)\sin\theta_0\sin\theta\cos\theta \\ -j\left[\begin{array}{l} -2r_2\sin\theta_0\cos^2\theta + 2r_1\sin\theta_0\sin^2\theta \\ +2(r_1+r_2)\cos\theta_0\sin\theta\cos\theta \end{array}\right] \end{array} \right\}, \tag{16}$$

from which,

$$V(\theta) = \sqrt{\frac{1}{(1+r_1^2)(1+r_2^2)}} \cdot \left\{ \begin{array}{l} (1-r_1r_2)\cos\theta_0 \\ +(1+r_1r_2)\cos\theta_0\cos 2\theta \\ +(1+r_1r_2)\sin\theta_0\sin 2\theta \\ -j\left[\begin{array}{l} (r_1-r_2)\sin\theta_0 \\ -(r_1+r_2)\sin\theta_0\cos 2\theta \\ +(r_1+r_2)\cos\theta_0\sin 2\theta \end{array}\right] \end{array} \right\}, \tag{17}$$

and using the difference-angle formulas,

$$V(\theta) = \sqrt{\frac{1}{(1+r_1^2)(1+r_2^2)}} \cdot \left\{ \begin{array}{l} (1-r_1r_2)\cos\theta_0 \\ +(1+r_1r_2)\cos(\theta_0-2\theta) \\ -j\left[\begin{array}{l} (r_1+r_2)\sin\theta_0 \\ -(r_1+r_2)\sin(\theta_0-2\theta) \end{array}\right] \end{array} \right\}. \tag{18}$$

$V(\theta)$ is the complex voltage received by a rotating linearly polarized radar from an arbitrary target at a fixed aspect.

Special Targets

Applying this relationship to several different radar targets yields the results shown in Table I. The sketches accompanying each entry are plots of $V(\theta)$ in the complex plane. The ability to discriminate among these plots is the key to target classification.

Inspection of the general expression for $V(\theta)$ reveals that it has the form of an ellipse displaced from the origin in the complex plane. Its major and minor axes lie respectively parallel to the real and imaginary coordinate axes.

It is recalled that one degree of freedom was removed from the system at the beginning; θ was chosen zero along the positive x axis, in the direction of one of the major axes of the target's polarization ellipses. This restriction may be eliminated by replacing θ everwhere by $\theta' = \theta + \theta_1$. θ_1 is then an arbitrary angle of rotation between a new reference axis (horizontal, for example) and the positive x axis.

Clearly this change will not alter the form of $V(\theta)$. The same ellipse will still be traced out in the complex plane, and introduction of θ_1 only serves to push the zero point around the ellipse somewhat. This is to say that an arbitrary rotation of the target about the line of sight does not affect the validity of this solution.

The General Target

An example of $V(\theta)$ is shown in Fig. 3. This example was calculated by arbitrarily choosing the parameters as follows:

$$r_1 = 0.75,$$

$$r_2 = 0.25,$$

$$\theta_0 = 60°.$$

θ is measured from the positive x axis as originally prescribed. The numbers listed around the perimeter of the ellipse indicate the angles θ for which the various phasor voltages occur.

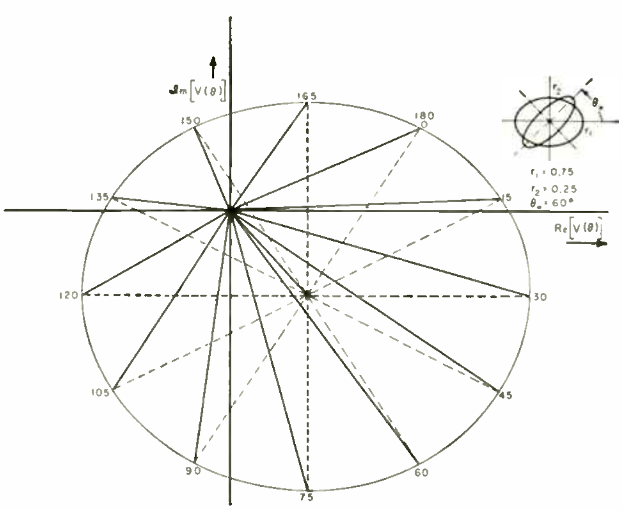

Fig. 3—Complex voltage received by radar.

It will be shown that any target may be represented by a combination of a linear reflector and a sphere, using only the size and shape of the ellipse, and the phasor from the origin to the center of the ellipse. It should be remarked that the phase measurement at the radar will contain an arbitrary zero setting because of the unknown (but fixed) range to the target. This causes the complex voltage pattern to be rotated about the origin in the complex plane by an arbitrary angle. However, inasmuch as the absolute phase of the reflection is unimportant, the coordinates of the complex plane may be rotated so that the real and imaginary axes lie respectively parallel to the major and minor axes of the ellipse, with the center of the ellipse somewhere in the right half-plane. See Fig. 3, for example.

Minimum Number of Measurements

Geometrically speaking, the voltage variation is merely an ellipse translated from the origin and rotated in the complex plane, so it could be determined by a minimum of four measurements. Two of these should be taken with linear polarizations separated by 90° in space so that the resulting points would lie diametrically opposite on the ellipse. The center of the ellipse would then be the midpoint of the line joining those two points. The two remaining measurements could be spaced at convenience to determine uniquely the size and shape of the ellipse.

Practically speaking, however, it is recognized that reliance upon the minimum number of measurements is likely to lead to undesirably large errors, especially in the cases where the ellipse collapses toward a straight line. It is preferable to assume that a sufficiently large number of measurements is taken to determine the ellipse precisely, or even that the radar is equipped to trace out a continuous recording of the complex voltage as the polarization rotates. Under these circumstances the reduction into a sphere component plus a linear component can be accomplished directly.

Reduction to Elementary Component Targets

Table I shows that the complex received voltage from the unit linear scatterer has the form,

$$V^{\text{Lin}}(\theta) = \frac{1 - r^2}{1 + r^2} + \cos 2\theta - j\frac{2r}{1 + r^2}\sin 2\theta, \qquad (19)$$

in which the cosine term has unit magnitude, and r is the axial ratio of the polarization ellipse of the linear component. Clearly, if the measured ellipse is traced out clockwise with increasing θ, as in Fig. 3, r is a positive number; if traced counter-clockwise, r is negative.

The axial ratio of the measured ellipse may be denoted r_{eff}. Then, if the measured ellipse is to be fitted to the ellipse which would result from the unit linear target, two conditions must be satisfied:

1) The size of the measured ellipse must be adjusted so that its semimajor axis is one unit long, and

TABLE I

Object	r_1	r_2	θ_0	$V(\theta)$	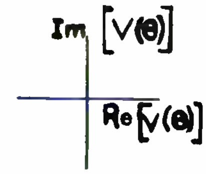
Sphere*	$+1$	-1	0	1	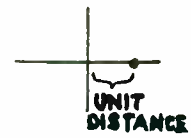
Thin wire	0	0	0	$1+\cos 2\theta$	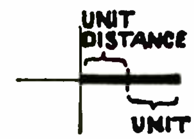
Dihedral corner	0	0	$\pi/2$	$\sin 2\theta$	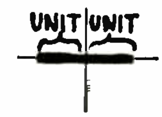
RCP reflector*	1	1	0	$\cos 2\theta - j \sin 2\theta$	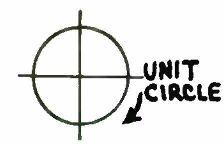
LCP reflector*	-1	-1	0	$\cos 2\theta + j \sin 2\theta$	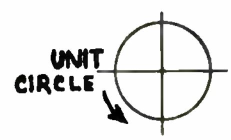
Isotropic reflector	r	$-r$	$\pi/2$	$\frac{1-r^2}{1+r^2} \sin 2\theta - j \frac{2r}{1+r^2}$	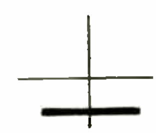
Linear reflector	r	r	0	$\frac{1-r^2}{1+r^2} + \cos 2\theta - j \frac{2r}{1+r^2} \sin 2\theta$	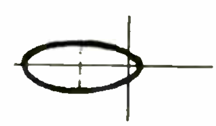
Symmetrical reflector	r	$-r$	θ_0	$\cos\theta_0 + \frac{1-r^2}{1+r^2}\cos(\theta_0 - 2\theta) - j\frac{2r}{1+r^2}\sin\theta_0$	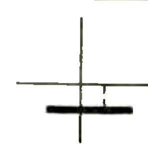

* For the sphere, θ_0 may be chosen as convenient, affecting only an associated phase angle. Choosing $\theta_0 = 0$ makes the phase angle become zero. Similar arguments apply to both the right and left circularly polarized reflectors.

2)

$$r_{\text{eff}} = \frac{2r}{1+r^2}, \tag{20}$$

where r_{eff} (and consequently r also) is a positive number if the measured ellipse is traced clockwise.

The quadratic equation (20) may be solved for r in terms of r_{eff}, and is plotted in Fig. 4.

Knowing r permits calculation of the fixed real portion due to the linear reflector, $(1-r^2)/(1+r^2)$. This is shown in Fig. 4 also, and turns out to be a circular arc when plotted as a function of r_{eff}.

Now the sphere component is obtained from a vector triangle, where the sum of the sphere component and the fixed portion of the linear component, $(1-r^2)/(1+r^2)$, is the fixed line from the origin to the center of the ellipse. See Fig. 5.

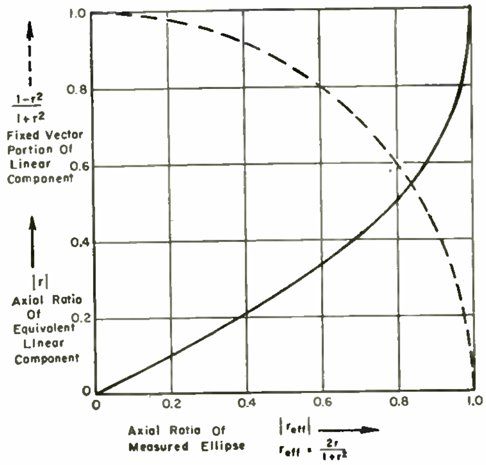

Fig. 4— $|r|$ and $\dfrac{1-r^2}{1+r^2}$ vs $|r_{eff}|$.

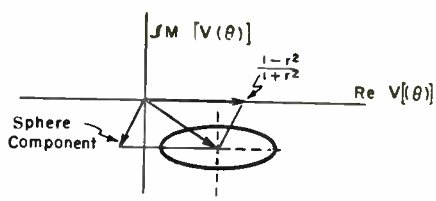

Fig. 5.

The sphere component thus has a magnitude and a phase angle relative to the linear component. The relative magnitude of this voltage is proportional to the square root of echo area, and hence directly proportional to the diameter of the sphere. The phase angle may be interpreted as displacement from the linear scatterer along the line of sight by a fraction of a quarter-wavelength. Displacement toward the radar implies a positive, or leading phase angle with respect to the linear target, while displacement away from the radar implies a negative, or lagging phase angle.

General Example

The example of Fig. 3 will be analyzed for its sphere and linear components as an illustration.

1) Adjusting the scale of Fig. 3 to give the semimajor axis unit magnitude yields

$$V(\theta) + [0.342 - j\,0.365] + [\cos(60° - 2\theta) + j\,0.842 \sin(60° - 2\theta)].$$

The fixed angle $\theta_0 = 60°$ is not significant here, because the target could be rotated about the line of sight, changing that figure arbitrarily.

2) $r_{eff} = 0.842$, and the ellipse is traced clockwise, so r_{eff} and r are both positive.
3) From Fig. 4, $r = 0.55$ and $(1-r^2)/(1+r^2) = 0.536$.
4) Subtracting $(1-r^2)/(1+r^2)$ from the fixed phasor to the ellipse center, the sphere component $V^{sph} = 0.342 - 0.536 - j\,0.365 = -0.194 - j\,0.365$.

Expressing the sphere term in polar coordinates,

$$V^{sph} = 0.414\underline{/-118°}.$$

These results may be interpreted as a unit linear scatterer of axial ratio $r = 0.55$ plus a sphere of relative size 0.414 placed $(118°/180°)\cdot(\lambda/4) = 0.164\,\lambda$ closer to the radar.

Conclusion

For the purpose of describing the polarization transforming properties of a radar target, the target may be replaced by a mathematical model based upon the scattering matrix. This model facilitates computation of the complex voltage received by the monostatic radar antenna. The received voltage is derived for a rotating linearly polarized radar antenna, and is shown to take on characteristic forms for certain classes of targets. The analysis is based upon a complex plot of this voltage.

It is shown that the polarization-transforming properties of any target may be represented by a sphere and a so-called linear target, of which a thin wire would be a degenerate example. In the case where the target has a plane of symmetry containing the line of sight, the linear component becomes a thin wire. Curves are given to assist in this solution for the target properties.

This analysis facilitates the radar measurement of polarization properties, a parameter which is frequently treated lightly in echo studies. A method is given for classification and possible identification of targets by these radar mesurements.

Because a sequence of phase measurements is necessary, it has been assumed that the target is held at a fixed range, as in laboratory measurements. However, a change in range involves only a rotation of coordinates in the complex voltage plot, so it is assumed this analysis could be made to yield useful results in a dynamic situation with targets moving radially toward or from the radar.

Acknowledgment

Dr. E. M. Kennaugh of The Ohio State University Antenna Laboratory contributed many helpful suggestions to this investigation.

A Microwave Meacham Bridge Oscillator*

W. R. SOOY†, F. L. VERNON†, MEMBER, IRE, AND J. MUNUSHIAN†, ASSOCIATE MEMBER, IRE

Summary—A microwave analog of the low-frequency Meacham bridge oscillator, long known for its exceptional stability, is described. The incorporation of the resonant element of a feedback oscillator into an appropriate bridge circuit effectively multiplies the Q of the element and consequently the stability of the oscillator. The performance and design of an X-band oscillator consisting of a traveling-wave tube amplifier, a cavity, a microwave Wheatstone bridge, and a bolometer element are described, and experimental results are compared with theory. The application of the principle to ultrastable systems utilizing very high-Q molecular resonators and low-noise amplifiers is also discussed.

Introduction

The oscillator circuit which has been most widely used for radio frequency standard oscillators is the Meacham bridge oscillator.[1-3] This type of oscillator utilizes a bridge-type feedback circuit in which the resonant element is used in a bridge to increase the sensitivity of the frequency control circuit. Because of its stability, this oscillator is used in many frequency standards at frequencies characteristic of quartz crystals which serve as the resonant elements. The need for oscillators with a high degree of stability at microwave frequencies has suggested the possibility of developing a microwave analog to the low-frequency Meacham bridge oscillator (MBO).

A simple feedback circuit consisting of an amplifier, discriminator, and limiter in a closed loop will sustain oscillations if 1) the loop gain is unity and 2) the total phase shift around the loop is $2n\pi$ where n is an integer. The frequency stability of the oscillations is directly proportional to the rate of change of loop phase-shift with frequency. The main source of short-term frequency variations are the fluctuations in the phase shift through the amplifier. The amplifier is the only active element in the loop and is capable of short-term variations of gain and phase. The second condition for oscillation requires that the variations in amplifier phase shift must be compensated by an equal and opposite phase variation in the external feedback loop. The required phase variation in the passive elements of the loop can be obtained only by a change in frequency. Thus frequency changes or frequency instability accompanies phase variations in the amplifier. The degree of frequency instability may be minimized by increasing $d\phi/df$ where ϕ is the phase shift around the loop and f is the frequency.

A resonant element placed directly in the feedback loop to serve as the frequency-determining circuit has, very near resonance, a rate of change of phase with frequency, $d\phi/df$, related to its quality factor Q by the relation $d\phi = 2Q(df/f)$. The unique feature of the Meacham oscillator is the placement of the resonant element in one arm of an otherwise resistive bridge and the use of the bridge as the resonant element of the feedback loop.

A schematic diagram of the low-frequency MBO is shown in Fig. 1. Two of the bridge arms are ordinary

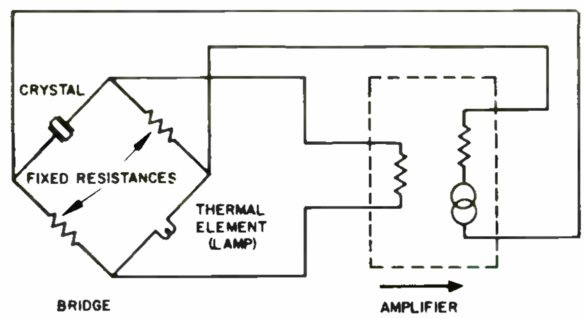

Fig. 1—Low-frequency Meacham bridge quartz-crystal oscillator.

fixed resistances, a third arm is a power sensitive resistor, and the fourth is the resonant element, a crystal in this case. The circuit is designed for operation in the vicinity of bridge balance since it is in this region that the bridge has the highest $d\phi/df$ and, correspondingly, the highest stability. The bridge can approach balance only at the resonant frequency of the crystal where this element becomes resistive, and at a power level which gives the third arm the proper resistance. It may be shown[4] that for an equal arm bridge at resonance,

$$d\phi_{\text{bridge}} = 2Q \frac{df}{f} \frac{G}{4}$$

at the operating point where G is the gain of the amplifier. It is apparent, therefore, that the stabilization action of the frequency-controlling feedback element is increased by a factor of $G/4$ when the resonant element is used in a bridge rather than placed directly in the feedback loop. The action of the bridge is, in effect, a Q-multiplication.

* Received by the IRE, July 16, 1959; revised manuscript received, January 25, 1960. This paper was published in the 1959 IRE National Convention Record, pt. 3, pp. 68–78.

† Microwave Lab., Hughes Aircraft Co., Culver City, Calif.

[1] L. A. Meacham, "The bridge stabilized oscillator," *Bell Sys. Tech. J.*, vol. 17, pp. 574–591; October, 1938.

[2] W. A. Edson, "Vacuum-Tube Oscillators," John Wiley and Sons, Inc., New York, N. Y., p. 192; 1953.

[3] F. D. Lewis, "Frequency and time standards," Proc. IRE, vol. 43, pp. 1046–1068; September, 1955.

[4] L. B. Arguimbau, "Vacuum-Tube Circuits," John Wiley and Sons, Inc., New York N. Y., p. 321; 1948.

When a power sensitive, rather than a linear, resistor is used in the bridge, the bridge does the limiting instead of the amplifier, as is usually the case. Because of its thermal inertia, the power sensitive element has an essentially constant resistance during an oscillation period. It therefore acts like a linear adjustable resistor, and the bridge is linear. Also, since limiting occurs in the bridge, the amplifier operates in the linear region, and intermodulation, which is a source of frequency instability, is virtually eliminated. Furthermore, since the linear region of the amplifier is usually the region of highest gain, such operation enhances the frequency stability.

Simple microwave feedback oscillators in which the resonant element is placed directly in the feedback path have been investigated by Price and Anderson[5] and by Hetland.[6] These feedback oscillators utilize a traveling-wave tube amplifier with a cavity as the resonant feedback element. Using a commercially available tube and its associated power supplies and a cavity with a Q of 4500, Price and Anderson obtained short-term stabilities of one part in 10^6 at X band. Hetland, by using exceptionally well-regulated power supplies and a cavity with a Q of 20,000, obtained a short-term stability of one part in 10^8 at S band.

With the high stability offered by the traveling-wave tube oscillator to serve as a starting point, it is attractive to explore the possibility of obtaining a further increase in stability by means of the principle of Q-multiplication. It should be emphasized, before progressing further, that the type of bridge oscillator that will be described in this work is different from Meacham's original oscillator. Meacham's oscillator had excellent long-term stability because a crystal was used as the resonator. The oscillator which will be described here uses a cavity as a resonator, and the resulting oscillator has only short-term stability. By application of Meacham's bridge-stabilization principle, a high order of short-term stability is achieved. Such an oscillator is, of course, still useful since many applications such as radar require that the frequency of an oscillator be stable to a specified degree only over a time interval of milliseconds or even microseconds. Therefore, although the microwave bridge oscillator to be described here does not possess the type of stability exhibited by the original Meacham bridge oscillator, it will illustrate the principle of Q-multiplication of the resonator and the consequent increase in the basic stability of the oscillator. The principles which are verified here can easily be adapted to microwave oscillators utilizing resonators which have long-term stability, such as gas cells or molecular standards.

It is believed that the work reported here is the first comprehensive study of the extension of the Meacham bridge method to the microwave region. Some preliminary work has been reported by Lyons[7] who used gas absorption cells as resonators, but no results have been published.

The Microwave Meacham Bridge Oscillator

The basic low-frequency Meacham bridge oscillator (MBO) has been studied for many years in considerable detail and is well understood. The development of a microwave MBO logically involves the substitution of microwave equivalents for the various components of the low-frequency MBO. Specifically, the crystal, the lamp, the Wheatstone bridge, and the amplifier of the low-frequency oscillator correspond, respectively, in the microwave analog, to a microwave resonant element such as a resonant cavity or molecular standard, a thermally sensitive microwave element such as a bolometer, a waveguide junction which has the properties of a Wheatstone bridge and, finally, a traveling-wave tube amplifier. The combination of traveling-wave tube and cavity is, as previously mentioned, the basic microwave feedback oscillator to which the principle of bridge stabilization was applied in this work. Although it appears superficially that the microwave analog of the MBO is straightforward and involves merely the substitution of components, there are significant differences between the low-frequency and microwave devices; these differences will become apparent in later sections.

A microwave Wheatstone bridge, first suggested by R. Dicke, is described by Chodorow, Ginzton, and Kane[8] and is shown in Fig. 2(a). It is made by joining six sections of waveguide at a symmetrical junction. Each waveguide represents an arm of the bridge, the input terminals or the output terminals. Note that opposite arms, such as 1 and 4 or 2 and 3, are rotated 90° with respect to one another so that direct coupling is prevented. When arms 1 through 4 are terminated in impedances, it can be shown analytically that Fig. 2(b) is the equivalent circuit of the junction. Because of the fringing fields at the center of the junction, a shunting reactance jb exists across each of the bridge arms. As in simpler junctions, the value of this reactance is frequency dependent. Furthermore, because of asymmetries in construction, the values of the various shunting reactances are not equal. The appearance of these unequal reactances prevents perfect balancing of the bridge unless resonating tuning screws are used. The tuning of the bridge will be described in greater detail in a later section. A magic tee could also be used in the oscillator, but the Wheatstone bridge allows more free-

[5] V. G. Price and C. T. Anderson, "X-band traveling-wave tube feedback oscillator," 1957 IRE National Convention Record, pt. 3, pp. 57–65.

[6] G. Hetland, "The Effect of Noise on Oscillator Stability," Appl. Electronics Lab., Stanford University, Stanford, Calif., Tech. Rept. No. 40; August 1, 1955.

[7] H. Lyons, "Spectral lines as frequency standards," *Ann. N. Y. Acad. Sciences*, vol. 55, pp. 831–837; November, 1952.

[8] M. Chodorow, E. L. Ginzton, and F. Kane, "A microwave impedance bridge," Proc. IRE, vol. 37, pp. 634–639; June, 1949.

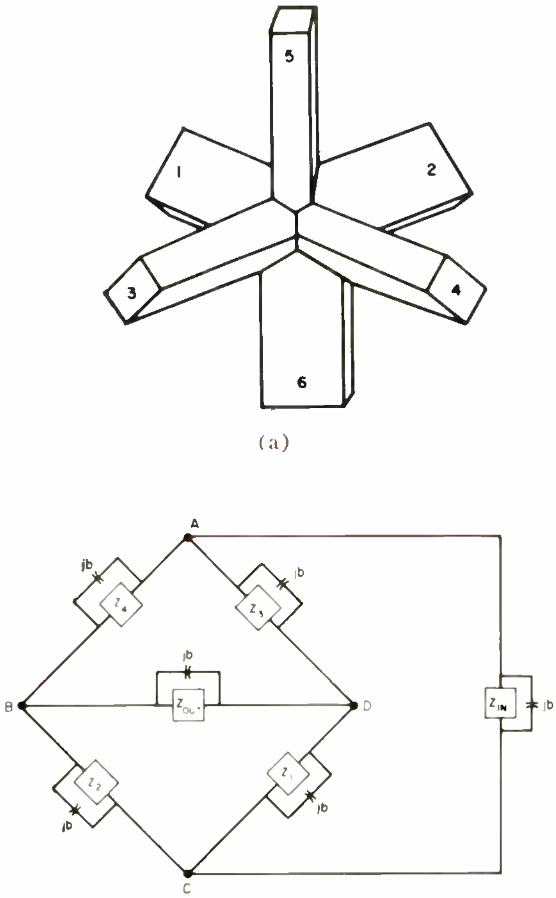

(a)

(b)

Fig. 2—Microwave Wheatstone bridge. (a) The waveguide junction. (b) Equivalent circuit.

dom in choosing impedance levels, since impedance matching can be achieved by adjustment of the ratio arms.

The microwave equivalent of a resistor whose resistance changes with power level is a waveguide load or termination whose impedance varies with incident power. Crystals and bolometers possess this property to a certain degree. The crystal, however, is not slow-acting; it does not have the thermal inertia required for quasi-linear operation and consequently is excluded from consideration. Bolometers (thermistors and barretters) have the required thermal characteristics; however, the rate of change of impedance with power level is relatively small. Despite this shortcoming, a thermistor bolometer was used in the experimental bridge oscillator and functioned well enough to provide the oscillator with satisfactory stability.

The resonant arm of the bridge was a cavity termination of the arm opposite the thermal arm. No particular care was taken with this cavity; it was a commercially available high-Q cavity and it was only necessary to tune out the mismatch at resonance. A commercial X-band traveling-wave tube with associated power supplies provided the gain for the system.

The list of components is not yet complete; one additional element is needed in the microwave MBO which does not exist in the low-frequency oscillator. This component is a filter cavity. The feedback path of the low-frequency oscillator is electrically short and the bandwidth of the amplifier is not sufficiently broad to support oscillations at frequencies other than the design frequency; that is, oscillations for which the total loop phase shift is 2π, 4π, 6π, etc., are not possible. In the experimental microwave oscillator, however, because of the physical size of the various components (including an electrically long traveling-wave tube) the line length was several hundred wavelengths long at X band, and if the filter cavity were not used, the phase condition could be met at a large number of frequencies in the vicinity of the desired mode. It can be shown[9] that for the configuration used, *i.e.*, long line, filter cavity and bridge in series, such resonances will be present at approximately

$$f_0, f_0 \pm \frac{1}{4}\frac{f_0}{n_0}\cdot f_0 \pm \left(\frac{f_0}{4n_0}+\frac{f_0}{n_0}\right)$$

where f_0 is the resonant frequency of the filter and the bridge (the desired mode), n_0 is l/λ_0, and l is the electrical length of the loop. A filter cavity with a Q of 6000 was used to introduce sufficient attenuation at $f_0 \pm \frac{1}{4}f_0/n_0$ to prevent oscillation at other than the desired frequency.

The basic microwave circuit in its final experimental form is shown in Fig. 3. The filter cavity is shown isolated from the bridge by a ferrite device to prevent complicated interactions caused by reflections between the two resonant elements.

Analysis of the Microwave Meacham Bridge Oscillator

The analysis of the microwave MBO is obviously more complex than that of its low-frequency counterpart. The analysis presented in this section is based on the use of transmission matrices.[10,11] The amplitude and phase characteristics of the bridge may conveniently be separated. The former will not appear in the analysis; it will simply be assumed that the bridge is almost balanced and is limiting properly, and therefore the system is linear.

A block diagram of the microwave circuit is shown in Fig. 4(a). Under conditions of oscillation, the input and output of the traveling-wave tube are connected as shown by the dotted line. The open-loop transmission characteristics of the complete circuit are used to find

[9] W. R. Sooy, F. L. Vernon, and J. Munushian, "A Microwave Meacham Bridge Oscillator," Hughes Aircraft Co., Culver City, Calif., Tech. Memo. No. 586; September, 1958.

[10] S. Ramo and J. R. Whinnery, "Fields and Waves in Modern Radio," John Wiley and Sons, Inc., New York, N. Y., 2nd ed., p. 461; 1953.

[11] J. R. Whinnery, "Some Notes on Oscillators Utilizing Wave Type Tubes," Hughes Aircraft Co., Culver City, Calif., Tech. Memo. No. 279; February 28, 1952.

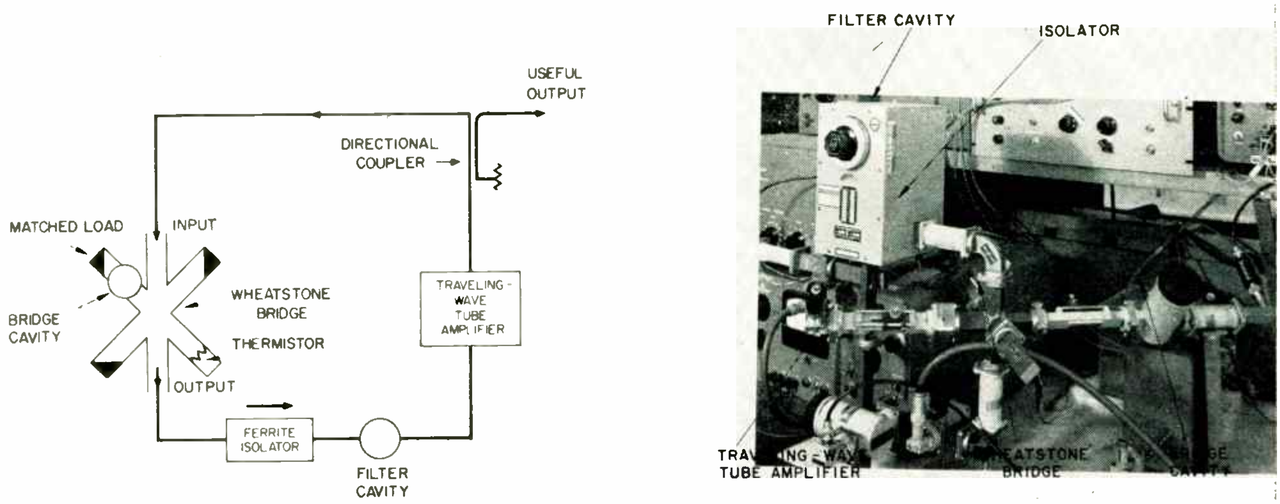

(a) (b)

Fig. 3—Microwave Meacham bridge oscillator. (a) Basic schematic diagram. (b) Photograph of the experimental oscillator.

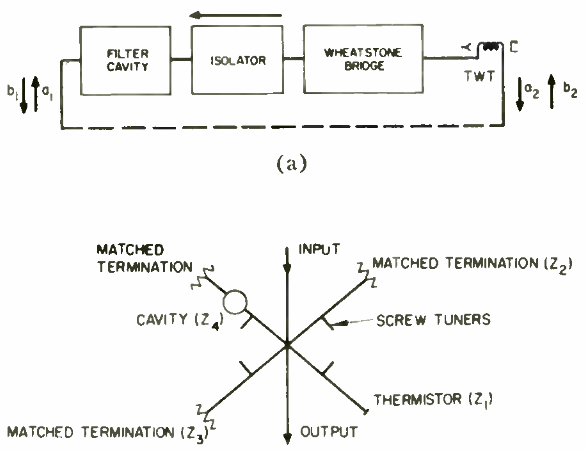

(a)

(b)

Fig. 4—Microwave Meacham bridge circuit representation used in the analysis. (a) Incident and reflected wave representation. (b) Details of microwave bridge.

the necessary conditions for oscillation. Symbolically the input and output waves, (a_1, b_1) and (a_2, b_2), may be related by means of the transmission matrices of the individual networks in the loop. Thus

$$\begin{pmatrix} a_2 \\ b_2 \end{pmatrix} = (\text{TWT})\begin{pmatrix}\text{Wheatstone}\\ \text{bridge}\end{pmatrix}(\text{isolator})\begin{pmatrix}\text{filter}\\ \text{cavity}\end{pmatrix}\begin{pmatrix} a_1 \\ b_1 \end{pmatrix}, \tag{1}$$

where a and b represent incident and reflected waves as shown in Fig. 4(a) and the quantities in parentheses represent the transmission matrices of the indicated elements. The transmission matrices of the traveling-wave tube, isolator, and filter cavity are easily computed[10] so that (1) becomes

$$\begin{pmatrix} a_2 \\ b_2 \end{pmatrix} = \begin{bmatrix} 0 & 0 \\ 0 & \dfrac{e^{j\beta l}}{G} \end{bmatrix} \begin{pmatrix} T_{11} & T_{12} \\ T_{21} & T_{22} \end{pmatrix} \begin{pmatrix} 0 & 0 \\ 0 & 1 \end{pmatrix} \begin{bmatrix} \left\{1 - \dfrac{Q_L'}{2Q_u} - j\dfrac{Q_L'x}{2}\right\} & \left\{\dfrac{Q_L'}{2Q_u} + j\dfrac{Q_L'x}{2}\right\} \\ \left\{-\dfrac{Q_L'}{2Q_u} - j\dfrac{Q_L'x}{2}\right\} & \left\{1 + \dfrac{Q_L'}{2Q_u} + j\dfrac{Q_L'x}{2}\right\} \end{bmatrix} \begin{pmatrix} a_1 \\ b_1 \end{pmatrix}$$

$$= \begin{bmatrix} 0 & 0 \\ -\left\{\dfrac{Q_L'}{2Q_u} + j\dfrac{Q_L'x}{2}\right\}\dfrac{e^{j\beta l}}{G}T_{22} & \left\{1 + \dfrac{Q_L'}{2Q_u} + j\dfrac{Q_L'x}{2}\right\}\dfrac{e^{j\beta l}}{G}T_{22} \end{bmatrix} \begin{pmatrix} a_1 \\ b_1 \end{pmatrix}, \tag{2}$$

where

G = voltage gain of the traveling-wave tube,
βl = phase shift of the traveling-wave tube and connecting lines,
Q_L' = Q of a lossless symmetrical filter cavity loaded on one side by Z_0,
Q_u = unloaded Q of the filter cavity,
x = a detuning parameter $(\omega/\omega_0 - \omega_0/\omega)$.

The condition for oscillation is found by placing $a_1 = a_2$ and $b_1 = b_2$. The previous equation then becomes

$$\begin{bmatrix} 1 & 0 \\ \left\{\left(\frac{Q_L'}{2Q_u} + j\frac{Q_L'x}{2}\right)\frac{e^{j\beta l}}{G} T_{22}\right\} & \left\{1 - \left(1 + \frac{Q_L'}{2Q_u} + j\frac{Q_L'x}{2}\right)\frac{e^{j\beta l}}{G} T_{22}\right\} \end{bmatrix} \begin{pmatrix} a_1 \\ b_1 \end{pmatrix} = 0. \tag{3}$$

In order for this equation to be consistent, the determinant of the coefficients must vanish. Therefore the oscillation condition becomes

$$\left\{1 + \frac{Q_L'}{2Q_u} + j\frac{Q_L'x}{2}\right\}\frac{e^{j\beta l}}{G} T_{22} = 1. \tag{4}$$

As indicated, (4) is valid when a general four-terminal network, represented by the matrix T_1, is used in the feedback line. For the particular case under consideration, this network is a bridge and it can be shown that its transmission coefficients are

$$T_{11} = 0, \qquad T_{21} = -1,$$

$$T_{12} = 1, \qquad T_{22} = \frac{2(Z_1 + 1)(Z_4 + 1)}{Z_1 Z_4 - 1}, \tag{5}$$

where Z_1, Z_2, Z_3, and Z_4 are the impedances at the equivalent planes in arms 1 through 4 of the bridge shown in Fig. 4(b). The equivalent planes, of course, are those specific planes in the various arms of the waveguide bridge at which the various impedances obey the balance laws characteristic of a Wheatstone bridge. The impedances Z_2 and Z_3 represent matched terminations and are equal to unity on a normalized basis. As may be seen from (4), only the component T_{22} of the matrix of the bridge is needed in the calculation of the oscillation condition. Since Z_1 (the impedance of the thermal element) is to be resistive and since Z_4 is a resonant cavity, then

$$Z_1 = R_1,$$

$$Z_4 = 1 + jQ_4 x,$$

where Q_4 is the Q of the bridge cavity loaded on one side by Z_0 and its internal loss. Thus,

$$T_{22} = \frac{2(1 + R_1)(2 + jQ_4 x)}{(R_1 - 1) + jR_1 Q_4 x}. \tag{6}$$

The value for T_{22} is inserted and the condition for oscillation expressed by (4) becomes

$$\left\{1 + \frac{Q_L'}{2Q_u} + j\frac{Q_L'x}{2}\right\}\left\{\frac{2 + jQ_4 x}{(R_1 - 1) + jR_1 Q_4 x}\right\} \cdot \frac{2(1 + R_1)}{G} e^{j\beta l} = 1. \tag{7}$$

At the frequency of operation of the system, both the filter and bridge cavities are assumed to be resonant; therefore $x = 0$. Then (7) can be used to determine relationships which must hold between the gain of the tube, the unbalance of the bridge, and the other circuit parameters for oscillation at bridge resonance. In particular $e^{j\beta l}$ must be either $+1$ or -1, corresponding to a phase shift $\beta l = 2n\pi$ or $\beta l = (2n+1)\pi$, so that the oscillation condition is satisfied at resonance. If $e^{j\beta l} = \pm 1$, then at resonance, (7) becomes

$$\frac{4}{G}\left\{1 + \frac{Q_L'}{2Q_u}\right\}\left\{\frac{R_1 + 1}{R_1 - 1}\right\} = \pm 1$$

or

$$R_1 = \frac{1 \pm \frac{4}{G}\left\{1 + \frac{Q_L'}{2Q_u}\right\}}{1 \mp \frac{4}{G}\left\{1 + \frac{Q_L'}{2Q_u}\right\}}. \tag{8}$$

The doubled-valued nature of (8) indicates that, unlike the situation in the low-frequency MBO, the microwave oscillator will oscillate for two different values of resistance of the thermal arm. Only one of these values corresponds to the condition of stable oscillation desired. The double-valued nature of R_1 must be borne in mind when the bridge is adjusted for proper operation. In order to determine whether the plus or the minus sign represents the desired condition, the stability at resonance must be determined. A convenient figure of merit for the stability of the oscillator is the factor $d\phi/d\omega$ where ϕ is the open-loop phase shift of the complete system and ω is the operating frequency. For the open loop, the input wave is related to the output wave through (2) as

$$b_1 = \left\{\left[1 + \frac{Q_L'}{2Q_u} + j\frac{Q_L'x}{2}\right]\frac{e^{j\beta l}}{G}T_{22}\right\}^{-1} b_2$$

$$b_1 = \frac{1}{|T_{22}|_{\text{system}}} e^{-j\phi}b_2, \tag{9}$$

where

$$\frac{1}{|T_{22}|_{\text{system}}} = \left\{\left[\left(1 + \frac{Q_L'}{2Q_u}\right)^2 + \frac{Q_L'^2x^2}{4}\right]^{1/2}\frac{2(1+R_1)}{G} \cdot \left[\frac{4 + Q_4^2x^2}{(R_1-1)^2 + R_1^2Q_4^2x^2}\right]^{1/2}\right\}^{-1}. \tag{10}$$

The term $|T_{22}|_{\text{system}}$ refers to the indicated transmission matrix coefficient of the entire open loop of the system. The phase angle ϕ in (9) is given by

$$\phi = \beta l + \tan^{-1}\left\{\frac{Q_L'x}{2 + \frac{Q_L'}{Q_u}}\right\} + \tan^{-1}\left(\frac{Q_4x}{2}\right) - \tan^{-1}\left(\frac{R_1Q_4x}{R_1 - 1}\right). \tag{11}$$

This last expression may be simplified if it is noted that

$$\frac{Q_L'x}{2 + \frac{Q_L'}{Q_u}} = \frac{x}{\frac{2}{Q_L'} + \frac{1}{Q_u}} = \frac{x}{\frac{1}{Q_L}} = xQ_L, \tag{12}$$

where Q_L is the loaded Q of the filter cavity. Therefore,

$$\phi = \beta l + \tan^{-1}Q_Lx + \tan^{-1}\frac{Q_4x}{2} - \tan^{-1}\left(\frac{R_1Q_4x}{R_1-1}\right). \tag{13}$$

The rate of change of phase shift with frequency is given by

$$\frac{\partial\phi}{\partial\omega} = \frac{l}{v} + \left\{\frac{Q_L}{1 + Q_L^2x^2} + \frac{2Q_4}{4 + Q_4^2x^2} - \frac{(R_1-1)R_1Q_4}{(R_1-1)^2 + R_1^2Q_4^2x^2}\right\}\left\{\frac{1}{\omega_0} + \frac{\omega_0}{\omega^2}\right\}. \tag{14}$$

At the resonance frequency $\omega = \omega_0$ and

$$\left.\frac{\partial\phi}{\partial\omega}\right|_{\omega_0} = \frac{1}{\omega_0}\left(\frac{\omega_0 l}{v}\right) + \left\{\frac{2Q_L}{\omega_0} - \frac{Q_4}{\omega_0}\left(\frac{R_1+1}{R_1-1}\right)\right\}. \tag{15}$$

For maximum stability, $(\partial\phi/\partial\omega)|_{\omega_0}$ should be a maximum. Therefore, R_1 must be less than unity. Thus $\beta l = (2n+1)\pi$ and the negative sign must be used in (8) yielding, for the condition for oscillation at resonance,

$$R_1 = \frac{1 - \frac{4}{G}\left(1 + \frac{Q_L'}{2Q_u}\right)}{1 + \frac{4}{G}\left(1 + \frac{Q_L'}{2Q_u}\right)}. \tag{16}$$

Substituting for R_1 in (15) gives

$$\left.\frac{\partial\phi}{\partial\omega}\right|_{\omega_0} = \frac{1}{\omega_0}\{\beta_0 l + 2Q_L\} + \frac{Q_4G}{4\omega_0\left(1 + \frac{Q_L'}{2Q_u}\right)}. \tag{17}$$

It is meaningful and customary to compare this stabilization factor at resonance with the value obtained when the bridge is replaced by a transmission cavity which has the same loaded Q as the stabilizing cavity in the bridge. When this is done,

$$\left(\frac{\partial\phi}{\partial\omega}\right)_{\text{cavity F.B.}} = \frac{\beta_0 l}{\omega_0} + \frac{2Q_L}{\omega_0} + \frac{2Q_{4L}}{\omega_0}, \tag{18}$$

where Q_{4L} is the loaded Q of the reference cavity.

It is necessary to consider the relationships between the quantities designated as Q_4 and Q_{4L}. The equivalent circuit of the cavity in the bridge is shown in Fig. 5(a). At resonance, the tuner is positioned so that the impedance of the cavity (with its internal loss) and of the load is matched to the characteristic impedance of the line feeding the tuner. The tuner and the input transformer may be replaced by an equivalent transformer whose turns ratio is n_1. This ratio is easily related to the turns ratio n shown in Fig. 5(a) yielding

$$n_1^2 = \frac{R_c + n^2Z_0}{Z_0}. \tag{19}$$

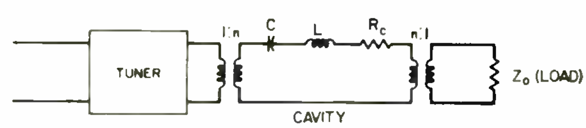

(a)

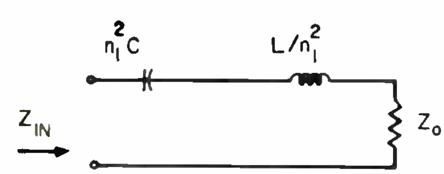

(b)

Fig. 5—(a) Equivalent circuit of cavity arm of bridge showing tuner and matched load. (b) Alternative equivalent circuit.

From appropriate terminals located to the left of the tuner, the equivalent circuit of the cavity is as shown in Fig. 5(b). The input impedance of this network may be written

$$Z_{\text{in}} = Z_4 = Z_0(1 + jQ_4x),$$

where

$$\frac{1}{Q_4} = \frac{1}{Q_{4L}'} + \frac{1}{Q_{4u}}. \tag{20}$$

The term $Q_{4L}'/2$ is the Q of the original symmetrical cavity loaded on both sides by Z_0 (excluding internal losses), and Q_{40} is the unloaded Q of the original cavity. In terms of the loaded $Q=Q_{4L}$, the following equation holds:

$$\frac{1}{Q_4} = \frac{1}{2Q_{4L}} + \frac{1}{2Q_{40}}. \tag{21}$$

The preceding equation together with the subsidiary relations,

$$Q_{40} = Q_{4L}(1 + 2\beta), \tag{22}$$

$$T(\omega_0) = \frac{4\beta^2}{(1 + 2\beta)^2} = \left(\frac{P_{\text{out}}}{P_{\text{in}}}\right)_{\text{cavity}} = \begin{array}{l}\text{transmission}\\ \text{at resonance,}\end{array}$$

serve to determine Q_4 and Q_{40} in terms of Q_{4L}.

The ratio of stabilization with the cavity in the bridge $(\partial\phi/\partial\omega)\big|_{\text{bridge F.B.}}$ to that obtained with the same cavity used as a transmission cavity (no bridge) is given by

$$\frac{\left(\frac{\partial\phi}{\partial\omega}\right)_{\text{bridge F.B.}}}{\left(\frac{\partial\phi}{\partial\omega}\right)_{\text{cavity F.B.}}} = \frac{\beta_0 l + 2Q_L + \dfrac{Q_4 G}{4\left(1 + \dfrac{Q_L'}{2Q_u}\right)}}{\beta_0 l + 2Q_L + 2Q_{4L}}. \tag{23}$$

In the low-frequency case, $\beta_0 l=0$ and $Q_L=0$, and the result is

$$\frac{\left(\frac{\partial\phi}{\partial\omega}\right)_{\text{bridge F.B.}}}{\left(\frac{\partial\phi}{\partial\omega}\right)_{\text{cavity F.B.}}} = \frac{G}{4}$$

in the limit of infinite Q_{40} where

$$Q_4 = 2Q_{4L}. \tag{24}$$

Thus, when the general analysis of the microwave system is specialized to correspond to the low-frequency MBO, the improvement of stability offered by the bridge circuit is one-fourth the amplifier gain; this agrees with the familiar result in the low-frequency MBO.

Discussion of Experimental Work

Experimental Procedures

The experimental oscillator utilized commercially available components except for the bridge, which was fabricated with considerable care to achieve a high degree of symmetry. The bridge cavity was not of exceptionally high Q (7500) since, as has been explained, it was merely desired to demonstrate a principle rather than to develop an ultrastable oscillator. The traveling-wave tube had a small signal gain of approximately 44 db; the exact value depended on the beam current. The tube was a packaged unit complete with power supplies, although well-regulated external supplies were used for improved stability. A fan used for cooling was disconnected because it contributed considerably to microphonically induced instability. The electrical length of the tube was unnecessarily long for the oscillator application because of the arrangement in the package of the input and output terminals. However, since the system parameters did not require an excessively high filter cavity Q, the tube package was not altered. The thermal element was a simple thermistor mounted in a matched coax-to-waveguide transition.

One of the most important parts of this study was the determination of a procedure for adjusting and tuning the microwave system to obtain bridge-limited stable oscillation. The adjustment proved to be very delicate, and certain relationships had to be established before stable operation was obtained. The bridge parameters must be adjusted so that 1) the minimum transmission occurs at the resonant frequency of the cavity arm, 2) the attenuation of the bridge at balance is greater than the gain of the amplifier, 3) bridge limiting occurs at a lower power level than amplifier limiting, 4) the change in phase shift through the bridge as the cavity arm is detuned is approximately π. This last step assures that the impedance of the thermal element is the value which provides the bridge with a transmission null corresponding to the stabilized mode of operation of the amplifier. It will be recalled from the analysis of the oscillator that oscillations are possible for two values of thermal arm resistance; only one of these provides the desired stabilized oscillation. The adjustment procedure is described in detail elsewhere.[9]

With the bridge adjusted for these conditions and the filter cavity tuned to the same frequency as the bridge, the system can be set into oscillation by adjusting the helix voltage of the traveling-wave tube. This brings the loop phase shift to $2n\pi$. The experimentally observed values of power level at various points in the loop are shown in Fig. 6; the saturation characteristics of the traveling-wave tube and the limiting action of the bridge are clearly displayed in this figure. The measurements were made with a matched load replacing the cavity arm of the bridge. This procedure separates, for convenience, the power behavior from the frequency behavior and the results correspond to bridge performance at resonance. The three curves in Fig. 6 show the input-output power relations (in a clockwise direction) of the various components of the oscillator loop. One curve shows the relation looking from B to A through the external loop and another gives the relation looking from A to B through the tube. The intersection of these curves defines the point where the attenuation of the external loop (bridge and cavity) equals the gain of the amplifier; this is the operating point. When these curves were taken, the output power was removed by a 20-db

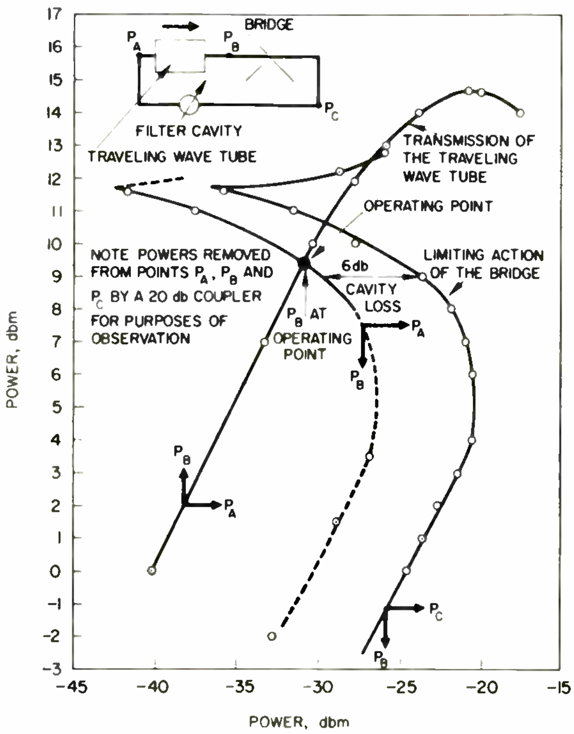

Fig. 6—Measured power characteristics of the oscillator at various points in the loop.

coupler so that this loss of power did not seriously affect the power balance.

The sensitivity of the oscillator to gain variations can be estimated from Fig. 6 by computing the variation of P_B caused by a given change in traveling-wave tube gain. Since the operating point of the system falls in the linear region of operation of the tube, a gain variation in the tube involves merely a horizontal translation of the tube characteristic. In the case depicted in the figure, the gain is 40.5 db, the operating power level P_B is 9.4 dbm. A change in gain of 1 db moves the point of operation to a level corresponding to a change of 0.25 dbm.

Stability Measurements

The frequency stability of the oscillator was measured by removing a portion of the output of the traveling-wave tube by means of a directional coupler and zero-beating this signal against a transfer oscillator. The frequency of the transfer oscillator was measured by two companion instruments, a counter and a frequency converter. Short-term frequency variations of a periodic or regular nature were observed by zero-beating the test signal with the transfer oscillator first at one extremity of the frequency deviation and then at the other. The frequency of the transfer oscillator was measured at both these points; the frequency deviation of the test signal was then obtained as the difference in the two readings. These measurement techniques are well known and are adequately described elsewhere.[12]

[12] *Hewlett-Packard J.*, vol. 6, no. 12; August, 1955.

With the use of bridge feedback, the frequency deviation of the experimental oscillator was less than that claimed for the transfer oscillator so that no conclusion could be made directly about short-term stability. However, frequency drift over appreciable time intervals could be measured, although even this was comparable to transfer oscillator uncertainty. The stability measurement system could not detect frequency variations of less than 1 kc at X band.

Since the available measurement system was not sufficiently stable to measure accurately the absolute short-term stability of the experimental oscillator, a measurement of relative stability was undertaken. A modulating voltage was impressed on the helix of the traveling-wave tube in order to produce a phase variation and a consequent frequency variation of sufficient magnitude to be observed easily with the transfer oscillator. With the use of bridge feedback in the oscillator, a measurement was made of deviation. This value was then compared with that obtained with the same modulating voltage on the helix but with only simple feedback through the filter cavity (bridge removed). The difference in the two measurements is attributable to the stabilization provided by the bridge circuit. The measurement was repeated again using a bridge but replacing the thermal arm with a matched load and tuning screw (nonlimiting bridge). The results are shown in Table I where it may be seen that the use of the bridge offers approximately an order of magnitude improvement in stability.

TABLE I
RESULTS OF STABILITY MEASUREMENTS

	Cavity Loop	Limiting Bridge	Nonlimiting Bridge
Mode of Operation	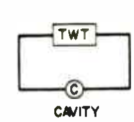	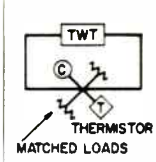	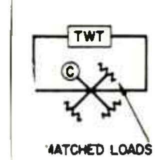
Short-Term Stability (1.7-volt Helix Modulation)	$\Delta f = 185$ kc	$\Delta f = 15$ kc	$\Delta f = 24$ kc
Long-Term Stability (Frequency Drift)	27 kc/minute	2 kc/minute	3 kc/minute

The measurements in Table I were made with 60-cycle sine wave modulation on the helix of the traveling-wave tube; the peak-to-peak voltage excursion was 1.7 volts. The rate of change of phase shift in the tube with respect to helix voltage is approximately the same in the linear and the saturated regions of operation; it is thus the same in the three modes of operation represented in the table. The phase shift vs voltage sensitivity was measured to be

$$\frac{\Delta\phi}{\Delta V_{\text{helix}}} = \frac{360°}{38 \text{ volts}},$$

so that

$$\Delta\phi_{\text{TWT}} = \frac{360°}{38 \text{ volts}} \times 1.7 \text{ volts} = 0.28 \text{ radian}.$$

This change in phase shift through the tube must, under oscillation conditions, be compensated by an equal and opposite phase change in the external loop. Thus for the simple cavity feedback system,

$$\left(\frac{\Delta\phi}{\Delta f}\right)_{\text{loop}} = \left(\frac{\Delta\phi}{\Delta f}\right)_{\text{line}} + \left(\frac{\Delta\phi}{\Delta f}\right)_{\text{cavity}}.$$

The Q_L of the cavity equals 6000. Inserting the values of the parameters used in the experimental oscillator,

$$\left(\frac{\Delta\phi}{\Delta f}\right)_{\text{line}} = \frac{360°}{40 \text{ mc}} = 0.157 \text{ rad/mc},$$

$$\left(\frac{\Delta\phi}{\Delta f}\right)_{\text{cavity}} = \frac{2Q_L}{f} = \frac{12 \times 10^3}{9 \times 10^3} = 1.33 \text{ rad/mc}.$$

Therefore,

$$\left(\frac{\Delta\phi}{\Delta f}\right)_{\text{loop}} \cong 0.16 + 1.33 = 1.49 \text{ rad/mc}.$$

The frequency variation produced by the above computed value of $(\Delta\phi/\Delta f)_{\text{loop}}$ is given by

$$\Delta f = \Delta\phi_{\text{TWT}}\left(\frac{\Delta f}{\Delta\phi}\right)_{\text{loop}} = 188 \text{ kc}.$$

This value is in close agreement with the measured value of 185 kc indicated in the first column of Table I.

The foregoing considerations involved the use of the filter cavity as the feedback element. If performance of the oscillator with a given cavity in the bridge is to be compared with the performance offered by that same cavity used as a feedback element without the bridge, it is necessary to estimate the frequency variation which would occur with both the filter and bridge cavities in series in the loop. For simplicity, the experimental work was done with only the filter cavity in the loop. However, the behavior of performance with the two cavities in series in the loop may easily be calculated.

$$\left(\frac{\Delta\phi}{\Delta f}\right)_{\text{loop}} = 1.49 \text{ rad/mc} + \frac{2Q_L}{f} = 1.49 \text{ rad/mc}$$

$$+ \frac{15 \times 10^3}{9 \times 10^3} \text{ rad/mc} = 3.15 \text{ rad/mc},$$

where Q_L is the loaded Q of the bridge cavity. Therefore,

$$\Delta f = \Delta\phi\left(\frac{\Delta f}{\Delta\phi}\right)_{\text{loop}} = 89 \text{ kc}.$$

In the case of limiting bridge stabilization (column 2, Table I),

$$\left(\frac{\Delta\phi}{\Delta f}\right)_{\text{loop}} = \left(\frac{\Delta\phi}{\Delta f}\right)_{\text{line}} + \left(\frac{\Delta\phi}{\Delta f}\right)_{\text{cavity}} + \left(\frac{\Delta\phi}{\Delta f}\right)_{\text{bridge}}.$$

Now, as shown in the analysis of the microwave MBO,

$$\left(\frac{\Delta\phi}{\Delta f}\right)_{\text{bridge}} = \frac{Q_4 G}{4 + \left(1 + \frac{Q_L'}{2Q_u}\right)}.$$

The tube was operated at 40 db gain or a voltage gain of 100; Q_4 was equal to 10,250. Since

$$\frac{Q_L'}{2Q_u} = 1,$$

then

$$\left(\frac{\Delta\phi}{\Delta f}\right)_{\text{bridge}} = \frac{10{,}250 \times 100}{4 \times 9 \times 10^3 \times 2} = 14.2 \text{ rad/mc},$$

$$\left(\frac{\Delta\phi}{\Delta f}\right)_{\text{loop}} = 1.5 + 14.2 = 15.7 \text{ rad/mc},$$

and

$$\Delta f = \Delta\phi\left(\frac{\Delta f}{\Delta\phi}\right)_{\text{loop}} = 17.8 \text{ kc}.$$

The computed value of Δf of 17.8 kc is in fair agreement with the measured value of 15 kc. With this order of magnitude of Δf, the measurement uncertainties prevented closer agreement. A similar calculation was made for the nonlimiting bridge mode of operation (column 3, Table I) in which operation at the peak of the traveling-wave tube input-output power characteristic was assumed. This resulted in $\Delta f = 26$ kc which was also in good agreement with the experiment. It may be readily appreciated that it would require a very high Q cavity used directly in the feedback line to obtain the same stabilization that is offered by the bridge. The term $(\Delta\phi/\Delta f)_{\text{bridge}}$ was equal to 14.2 rad/mc; a cavity would require a Q of 64,000 to give the same value of $d\phi/df$. Thus, a Q-multiplication of 8.5 is achieved by use of the bridge.

The performance of the system using a tube gain of 44 db was observed. This value of gain was slightly higher than the value at which modes adjacent to the desired frequency would just begin to oscillate when a filter cavity with a Q of 6000 is used. The adjacent modes were observed but could be removed by a slight adjustment of helix voltage.

The main source of long-term frequency drift was the temperature variations of the tube solenoid. These variations affected the gain and phase shift of the tube. The results of the drift measurements shown in Table I are only approximate because of instabilities in the transfer oscillator. However, the stabilizing effect of the bridge circuit is equally effective against either long- or short-term fluctuations.

The relative amplitude stability of the various systems shown in Table I was also observed. It was found that the limiting bridge circuit was only slightly more amplitude-stable than the other circuits. This is to be expected since the thermal arm was not very sensitive.

An estimate of the absolute short-term frequency deviation (without the modulating voltage) of the limiting-bridge oscillator was made in the following manner. The helix voltage ripple was measured and found to be 11.3 millivolts peak-to-peak. Under an impressed modulation voltage of 1.7 volts peak-to-peak, a 15-kc deviation was found. Since frequency deviation is approximately linearly related to the variation in helix voltage, a deviation of about 100 cps at the power-supply frequency is indicated. This corresponds to a short-term fluctuation of one part in 10^8. Although this same order of stability has been obtained[6] by use of a simple cavity feedback oscillator, it was achieved by use of extremely well-regulated power supplies with a ripple of only 20 microvolts. If these same power supplies were used with the microwave MBO, a short-term stability of two parts in 10^{11} is predicted if it is assumed that only voltage fluctuations limit the ultimate stability.

Stability Limitations

In the limiting case of completely noise-free and ripple-free power supplies, the short-term stability of the oscillator is determined by noise in the electron beam of the traveling-wave tube. In ultrastable systems, therefore, it is important to use low-noise traveling-wave tubes. The longer-term frequency drifts of the oscillator are caused by the drift of the power supply voltages of the tube, by temperature variations and by microphonic disturbances.

The stability of the microwave MBO can be improved by an increase in the gain of the amplifier. The gain of the amplifier can be extended by cascading traveling-wave tubes. However, increased amplifier gain will require a bridge with a comparable degree of balance. The limitation in gain and, therefore, stability is thus determined by the irreducible mechanical asymmetries in the bridge and the increased susceptibility to microphonics of a deep bridge null. The configuration of the waveguide Wheatstone bridge does not lend itself to a compact system and the problem of shock-mounting the various portions of the oscillator is difficult. It is therefore important to develop compact waveguide junctions with the required electrical characteristics.

The stability of the microwave MBO can also be improved by an increase in the Q of the bridge resonator. The resonator Q can be greatly increased over the values used in this work by the use of gas absorption cells or superconducting microwave cavities. Superconducting cavity-loaded Q's of more than 4 million have been observed at X band in this laboratory.

It was indicated earlier that the thermal arm (thermistor) of the bridge was not sufficiently sensitive to power variations. Stability can therefore also be improved by the development of thermistor elements at microwave frequencies in which the change in impedance with power change is greater than in existing elements.

Conclusions and Recommendations

The validity and realizability at microwave frequencies of the Meacham bridge principle of linear-bridge oscillator limiting and Q-multiplication has been theoretically and experimentally demonstrated. A microwave resonator such as a cavity or gas absorption cell of given Q can be made to provide an oscillator stability corresponding to a resonator of much greater Q. The increase in effectiveness of the resonator is proportional to the gain of the amplifier. The possibility of attaining unprecedented short-term stabilities by use of amplifiers with large gains and low-noise figures, resonators with high Q's and extremely well-regulated power supplies has also been pointed out.

The cavity-type microwave MBO which has been described in this work is very difficult to tune. It was necessary to adjust the tuning screws for each new operating frequency; in order to eliminate this inconvenience, a broad-band bridge with a deep null is required. Furthermore, for broad-band operation, the resonance mismatch of the bridge cavity and the impedance of the thermal arm must also be frequency insensitive. With sufficient effort, it may be possible to construct an easily tuned oscillator in which a single-knob control appropriately varies the frequencies of the bridge and filter cavities and the helix voltage of the traveling-wave tube. Such a system may serve as a substitute for an automatic frequency-controlled klystron. It would have greater ultimate stability and could be made more compact, particularly if permanent-magnet focused traveling-wave tubes are used. Except for the traveling-wave tube amplifier, no active components such as low-frequency electronic loops would be required.

Unidirectional Paramagnetic Amplifier Design*

M. W. P. STRANDBERG†, FELLOW, IRE

Summary—**The radio-frequency parameters and the quantum-mechanical parameters entering into the design of paramagnetic quantum-mechanical amplifiers are described and discussed. The physical and electrical limitations on such parameters as gain-bandwidth product, gain stability, and nonreciprocity are described analytically and with design curves. Two realizations of nonreciprocal amplifiers are described and discussed. In particular, operation of a nonreciprocal amplifier at 9 kmc is described. Explanations for the observed properties of previously reported amplifiers are given, and the steps necessary to achieve high gain-bandwidth product and nonreciprocity with paramagnetic amplifiers are described.**

Introduction

Of the many desirable characteristics of a solid-state amplifier, such as large gain-bandwidth product, low noise figure, and tunability,[1] one important quality is a unidirectional and nonreciprocal amplification characteristic. Although it has been pointed out[1] that these amplification characteristics are achievable by using circularly-polarized electromagnetic fields and the inherent Faraday effect of paramagnetic systems, little interest in development of amplifiers along these lines is apparent. This is difficult to understand because, for example, the application of paramagnetic amplifiers to L-band radioastronomy is hampered by the lack of a lossless L-band circulator. Furthermore, other methods of obtaining unidirectional gain—for example, through the use of a circulator (nonreciprocal) or through the use of a negative-resistance bridge—are incomparably more difficult to engineer for acceptable performance than is a circular-polarization amplifier. Probably the only other reason for the absence of interest in a circular-polarization amplifier arises from the fact that a concrete and detailed design does not exist. This paper offers a simple and easily realizable design for a circularly-polarized cavity amplifier. The basic idea upon which the amplifier rests is quite simple. It is that a two-port RF system can be made to absorb or to emit, coherently, energy in a unidirectional fashion if the RF fields comprising the system are resolvable into two orthogonal field systems. This system can also have nonreciprocal gain if the matter in which the fields exist exhibits a Faraday effect and the orthogonal modes are positive and negative circularly-polarized fields. The system need not exhibit a pure Faraday effect, however, and still have a nonreciprocity of gain which is sufficient to stabilize the amplifier against gain-fluctuation arising from variation of the reflection coefficient of the input or output ports.

Amplifier Structure

This discussion will be restricted to a regenerative or cavity paramagnetic amplifier. This is not a severe restriction; ample gain-bandwidth product is available from such structures, and they can be cascaded by any number of means to form an amplifying structure with over-all gain and bandwidth characteristics equal to those envisaged by present slow-wave structures. Whether one calls such a structure a cascade of low-loaded Q resonant systems or a slow-wave structure is a matter of semantics rather than of engineering. The relationship between the Q of the structure, the gain in decibels per free-space wavelength G', and the wave-slowing factor s, the ratio of the group velocity v_g, of the structure to the velocity of light c is,

$$Q = \frac{20\pi s \log(e)}{G'}. \tag{1}$$

The type of structure to be used is obviously dictated by the gain and bandwidth requirements for any particular application. For example, in the hydrogen-line radioastronomy studies at 1420 mc, a bandwidth of 300 mc with a gain of 20 db would be sufficient; but for ther-

* Original manuscript received by the IRE, June 26, 1959; revised manuscript received, January 12, 1960. This work was supported in part by the U. S. Army Signal Engineering Laboratories and in part by the U. S. Army (Signal Corps), the U. S. Air Force (Office of Scientific Research, Air Research and Development Command), and the U. S. Navy (Office of Naval Research).

† Res. Lab. of Electronics, Mass. Inst. Tech., Cambridge, Mass.

[1] M. W. P. Strandberg, "Quantum-mechanical amplifiers," Proc. IRE, vol. 45, pp. 92–93; January, 1957. As a matter of historical accuracy, it is necessary to point out that many of these ideas were developed in collaboration with H. R. Johnson in the summer of 1955. Pioneering work on ammonia beam experiments (see H. R. Johnson and M. W. P. Strandberg, "Beam system for reduction of Doppler broadening of a microwave absorption line," *Phys. Rev.*, vol. 85, pp. 503–504; February 1, 1952) had indicated the limitations on the use of ammonia beam masers as practical amplifiers. Discussions, which were held in Cambridge, Massachusetts, and in Culver City, California, established a firm scientific basis for confidence in the ultimate and tremendous usefulness of solid-state amplifiers. Simple though it sounds, the novel idea at that time was that paramagnetic materials presented the means by which one could make a practical quantum-mechanical amplifier with large gain-bandwidth product, low noise figure, tunability, and large dynamic range. In 1955, the state of development of quantum-mechanical amplifiers showed a lack of ability to achieve all of these qualities rather than lack of confidence in being able to build amplifiers, since all of the methods for obtaining negative resistance in gases and solids that are known today had been disclosed (and some demonstrated) at that time. General design problems were given further consideration by the writer and were discussed with various people. Some of these ideas were presented at a Physics Department Colloquium at M.I.T., in May, 1956. These discussions inspired interest in many quarters in most of the elements of paramagnetic-amplifier design and use, the outstanding exception being the realization of a circular-polarization cavity amplifier. A proper understanding of the noise figure of quantum-mechanical amplifiers was certainly not available before the analysis made by the writer and others in 1956 and, furthermore, the proper application of this theory in terms of observed circuit parameters was not well understood even after that. The actual translation of theory into application to actual devices is always difficult; this paper is merely intended, again, as a translation of theory into a concrete device. *Cf.* M. W. P. Strandberg, "Inherent noise of quantum-mechanical amplifiers," *Phys. Rev.*, vol. 106, pp. 617–620; May 15, 1957.

mal-source studies one would like to have a bandwidth of the order of the operating frequency and a gain of 20 db. For radar or communications applications, one would possibly have requirements for modest bandwidth of the order of a few tens of megacycles with gains of the order of 30 db. In some work there is also a requirement for high stability of gain of the device with changes in operating conditions. For example, in broadband radioastronomy, the thermal radiation is integrated in time in order to improve the sensitivity of the device. Here the requirement for the gain stability is high and has a high priority.

The traveling-wave amplifier has an exponential increase of gain with length as follows:

$$P_{\text{out}} = e^{\gamma l} P_{\text{in}} = G P_{\text{in}} \qquad (2)$$

where

$$\gamma = \frac{8\pi^2 f \eta}{v_g} \operatorname{Im}(\chi). \qquad (3)$$

Here f is the wave frequency, η is the filling factor, and a single resonant term in the complex susceptibility is[2]

$$\chi = -\chi_0 \frac{f}{(f - f_0) + i\dfrac{B_x}{2}} \qquad (4)$$

$$|r|^2 = G = \frac{16\Delta f^4 + 4\Delta f^2\left[B_e^2\left(1 - \dfrac{Q_e}{Q_0}\right)^2 + B_x^2 - 2\dfrac{Q_e}{Q_{x0}} B_e B_x\right] + B_e^2 B_x^2\left(1 - \dfrac{Q_e}{Q_0} - \dfrac{Q_e}{Q_{x0}}\right)^2}{16\Delta f^4 + 4\Delta f^2\left[B_e^2\left(1 + \dfrac{Q_e}{Q_0}\right)^2 + B_x^2 - 2\dfrac{Q_e}{Q_{x0}} B_e B_x\right] + B_e^2 B_x^2\left(1 + \dfrac{Q_e}{Q_0} + \dfrac{Q_e}{Q_{x0}}\right)^2}. \qquad (10)$$

with B_x the paramagnetic resonant linewidth. The gain thus exponentially follows the frequency variation of the susceptibility of the paramagnetic material both through the imaginary part of the susceptibility directly and through the real part of the susceptibility in its influence on the group velocity. If we neglect the latter effect, the 3-db bandwidth of a traveling-wave amplifier with a gain G, in decibels, is

$$B = B_x\left(\frac{3}{G_{\text{db}} - 3}\right)^{1/2}. \qquad (5)$$

A similar expression can be derived for a single regenerative cavity. Previously, the amplifiers envisaged were of sufficiently narrow bandwidth that the frequency variation of the susceptibility could be neglected. This is not true in general. The introduction of the frequency dependence of the complex susceptibility for the paramagnetic material modifies the magnetic Q, so that it has a frequency dependence that is the reciprocal of the frequency dependence of the susceptibility

$$\boldsymbol{Q}_x \to Q_{x0}\left(1 + i\frac{2(f - f_0)}{B_x}\right) = (4\pi\chi\eta)^{-1}. \qquad (6)$$

If a cavity containing this complex susceptibility terminates a transmission line having an admittance Y_0, it represents a load admittance, $Y = g + ib$, which is conventionally described in terms of the cavity unloaded Q, Q_0, the magnetic Q, $\boldsymbol{Q}_x$, the coupling Q, Q_e, and the frequency as:

$$\frac{g}{Y_0} = \frac{Q_e}{\boldsymbol{Q}_x} + \frac{Q_e}{Q_0} \qquad (7)$$

$$\frac{b}{Y_0} = 2Q_e\frac{(f - f_0)}{f_0} \equiv \frac{2\Delta f}{B_e}. \qquad (8)$$

Then the reflection coefficient (or voltage gain) is:

$$r = \frac{Y_0 - Y}{Y_0 + Y} = \frac{\left(1 - \dfrac{Q_e}{Q_0} - i\dfrac{2\Delta f}{B_e}\right)\left(1 + i\dfrac{2\Delta f}{B_x}\right) - \dfrac{Q_e}{Q_{x0}}}{\left(1 + \dfrac{Q_e}{Q_0} + i\dfrac{2\Delta f}{B_e}\right)\left(1 + i\dfrac{2\Delta f}{B_x}\right) + \dfrac{Q_e}{Q_{x0}}}. \qquad (9)$$

The bandwidth, B, of a single-tuned stage is defined as the frequency width between the points at which the magnitude of the reflection coefficient squared is reduced to half of its value at resonance.

Therefore,

$$B^2 = \frac{1}{2}\Bigg[\Bigg\{\left[1 + \left(\frac{Q_e}{Q_0}\right)^2\right]B_e^2 + B_x^2 - 2\frac{Q_e}{Q_{x0}}B_e B_x - 4\frac{Q_e}{Q_0}B_e^2\,\frac{3 + 2\left(\dfrac{Q_e}{Q_0} + \dfrac{Q_e}{Q_{x0}}\right) + 3\left(\dfrac{Q_e}{Q_0} + \dfrac{Q_e}{Q_{x0}}\right)^2}{1 + 6\left(\dfrac{Q_e}{Q_0} + \dfrac{Q_e}{Q_{x0}}\right) + \left(\dfrac{Q_e}{Q_0} + \dfrac{Q_e}{Q_{x0}}\right)^2}\Bigg\}^2 - \frac{4B_e B_x\left(1 - \left(\dfrac{Q_e}{Q_0} + \dfrac{Q_e}{Q_{x0}}\right)^2\right)^2}{1 + 6\left(\dfrac{Q_e}{Q_0} + \dfrac{Q_e}{Q_{x0}}\right) + \left(\dfrac{Q_e}{Q_0} + \dfrac{Q_e}{Q_{x0}}\right)^2}\Bigg]^{1/2}$$

$$- \frac{1}{2}\Bigg\{\left[1 + \left(\frac{Q_e}{Q_0}\right)^2\right]B_e^2 + B_x^2 - 2\frac{Q_e}{Q_{x0}}B_e B_x - 4\frac{Q_e}{Q_0}B_e^2\,\frac{3 + 2\left(\dfrac{Q_e}{Q_0} + \dfrac{Q_e}{Q_{x0}}\right) + 3\left(\dfrac{Q_e}{Q_0} + \dfrac{Q_e}{Q_{x0}}\right)^2}{1 + 6\left(\dfrac{Q_e}{Q_0} + \dfrac{Q_e}{Q_{x0}}\right) + \left(\dfrac{Q_e}{Q_0} + \dfrac{Q_0}{Q_{x0}}\right)^2}\Bigg\}. \qquad (11)$$

[2] M. W. P. Strandberg, "Microwave Spectroscopy," Methuen and Company, Ltd., London, p. 70; 1954.

For large gain, the gain-bandwidth product can be reduced to

$$\sqrt{GB} \approx \frac{2}{\dfrac{1}{B_z} + \dfrac{Q_{z0}}{f_0}}. \qquad (12)$$

Care must be exercised in using expressions (5) and (12) for B; for gains less than 3 db, a 3-db point does not exist.

If a series of these regenerative cavities is coupled in cascade, the gains of each stage will multiply and the frequency dependence of the gains will also multiply. The frequency dependence of the reflection coefficient may be crudely approximated by a curve of the form

$$|r|^2 = [1 + b^2]^{-1} |r|_{\max}^2. \qquad (13)$$

In this case one may show that the net gain-bandwidth product for N synchronously-tuned cascaded cavities, each having a gain-bandwidth product of B_1, is given as

$$G^{1/(2N)} B = (2^{1/N} - 1)^{1/2} B_1. \qquad (14)$$

These relationships are shown in Fig. 1 for N equals one, two, and eight, and infinity for the traveling-wave case.

There is also an interest in the variation of the gain with variation of the paramagnetic susceptibility. The logarithmic derivative of the total gain at resonance for N cascaded stages yields the following expression:[3]

$$\frac{dG}{G} = (G^{1/(2N)} - G^{-1/(2N)}) \frac{d\chi_0}{\chi_0}. \qquad (15)$$

These relationships are given in Fig. 2, again for a traveling-wave amplifier ($N = \infty$) and for a system of cascaded single-resonance circuits.

It is apparent from these relationships that only a few cascaded cavities can duplicate the behavior in gain-bandwidth and gain-sensitivity characteristics that a truly distributed traveling-wave amplifier would possess. The chief difference between the two configurations is tunability. A traveling-wave amplifier, as we have indicated above, is restricted in bandwidth only by the paramagnetic resonance line-shape, the RF bandwidth of the system presumably being many times this width. The bandwidth of the cavity structure is restricted not only by the paramagnetic line-shape but also by the tuning characteristic of the cavity. In the former case, one can tune electronically by changing the resonance frequency of the paramagnetic material through a change of magnetic field; in the latter case, a mechanical cavity tuning has to be made along with the magnetic tuning of the paramagnetic resonance.[4]

Both cavity and traveling-wave structures can be made unidirectional by the use of circular polarization.

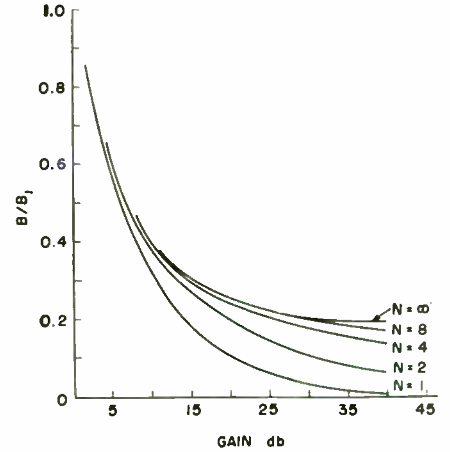

Fig. 1—Gain versus bandwidth curves as a function of the number of cascaded elements.

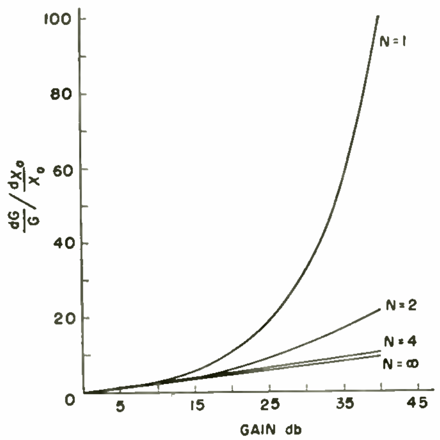

Fig. 2—Sensitivity of gain to variation of susceptibility as a function of the gain for varying numbers of cascaded elements.

This question has been discussed, and realizations for circuits have been given.[5] Here, we are mainly interested in suggesting an actual structure that is adaptable to a wide-frequency region; presumably, one that can utilize coaxial lines as transmission lines for the system.

The basic element of a circular-polarization system, as pointed out before,[5] is a cavity structure that has a degeneracy of modes arising from geometrical symmetry. The circular TE_{11n} mode has a degeneracy of two modes on axes 90° spatially separated, and hence this mode can be used to produce a circularly-polarized field. The field distributions of these cylindrical cavity fields are shown in Fig. 3(a). The corresponding fields in the square waveguide would be the TE_{01n} modes, which are shown in Fig. 3(b). If these two frequency-degenerate, spatially-orthogonal modes are driven $\pi/2$ radians out of phase with each other in time, a pure circularly-polarized magnetic field will be produced along the axis of the cavity. This field becomes more and more elliptical as the cylindrical walls of the cavity are approached.

[3] R. L. Kyhl provided this form of (15).

[4] R. W. DeGrasse, E. O. Schulz-DuBois, and H. E. D. Scovil, "The three-level solid state traveling-wave maser," *Bell Sys. Tech. J.*, vol. 38, pp. 305–334; March, 1959.

[5] See, for example, M. Tinkham and M. W. P. Strandberg, "The excitation of circular polarization in microwave cavities," Proc. IRE, vol. 43, pp. 734–738; June, 1955.

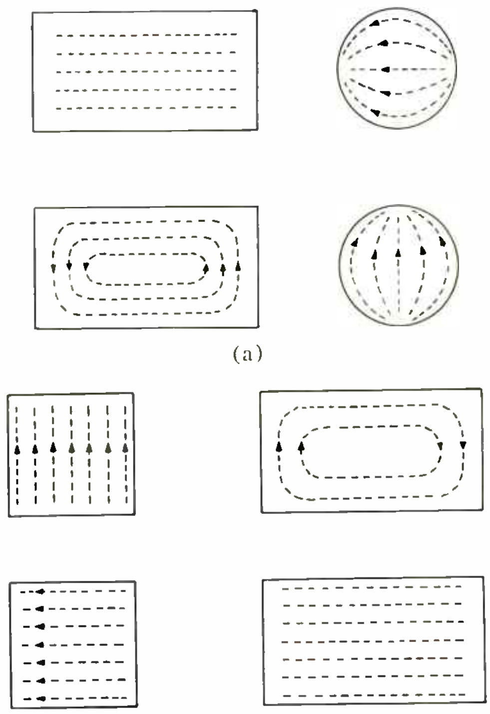

Fig. 3—(a) Radio-frequency magnetic-field configurations for the degenerate TE_{111} modes. (b) Radio-frequency magnetic-field configurations for the degenerate TE_{111} and TE_{101}, modes.

However, even for a cavity uniformly filled with a paramagnetic crystal, one finds that the average square of the right and left circularly-polarized and longitudinal fields divided by the average square of the total field are:

$$\eta_+ \max = 0.92(1 - \eta_z)$$
$$\eta_- \max = 0.079(1 - \eta_z)$$
$$\eta_z \max = \left[1 + 0.727\left(\frac{Dn}{l}\right)^2\right]^{-1} \tag{16}$$

with

$$\eta_{\pm,z} = \frac{\int_{\text{crystal}} H_{\pm,z}{}^2 dv}{\int_{\text{cavity}} H^2 dv} \tag{17}$$

where D is the cavity diameter, and l is the length. The basic problem of exciting the circular-polarization field, then, is to achieve equality of field amplitude for these two orthogonal modes of the cavity through variation of the coupling coefficient to the transmission line feeding them and to have them time-phased $\pm\pi/2$ radians.

Methods that use waveguides to achieve this coupling and phasing are rather abundant. A convenient method of obtaining such excitation with a cavity axis perpendicular to the feed waveguide has been given previously.[5] For frequencies lower than X-band frequencies, for example, it is convenient to use coaxial lines, especially for feedline structures which must be immersed in low-temperature dewars and inserted in magnetic fields. For this reason, we restrict our attention to excitation methods that can be achieved by using a coaxial line structure. It will be noted that each of these TE_{11n} modes can be fed by a separate coaxial line or waveguide, if a simple method of driving the two waveguides or coaxial line structures $\pi/2$ radians out of phase can be realized.

This coupling of the two feed lines so that they are $\pi/2$ radians out of phase with each other in time is readily accomplished by using a 3-db reactive or slot coupler. It is the property of a matched coupler that the two output fields which are established by the single input field must be 90° out of phase with each other in order to preserve the energy of the system. Therefore, if a 3-db, single-slot or multiple-slot matched coupler is used, the actual transmission line will be as shown in Fig. 4. The input coaxial line is coupled through a matched 3-db slot coupler into two feed transmission lines that are coupled directly into the two degenerate modes of the cavity. The energy reflected from the cavities, whether it is greater or less than the incident energy, will experience equal phase shift upon reflection from both cavity modes (we will indicate later how both modes can be made degenerate in their impedance characteristics so that this is so); hence, upon recombining in the 3-db coupler again the reflected energy goes entirely out the output line.

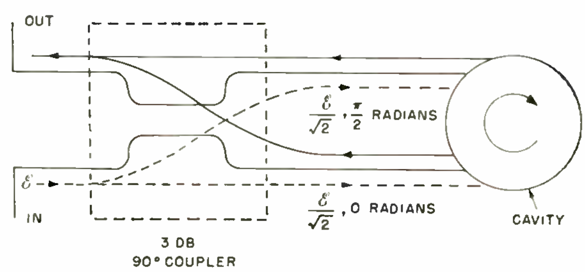

Fig. 4—Radio-frequency transmission line configuration for the 3-db coupler, circular-polarization excitor.

This structure is apparently reciprocal in the sense that energy coming in the output line is split in the 3-db coupler and sent down the two cavity transmission lines equally and with a $\pi/2$ radian time-lag to set up the necessary circular-polarization field in the cavities. It will be noted, however, that in this case the polarization direction will be the negative of the one set up when the radiation impinges on the cavity from the input line. This is an important observation and is useful, as we shall see later on, in providing nonreciprocal gain. In any case, the fields reflected from the cavity, whether they are greater or less than the incident fields, will be recombined again in the 3-db slot coupler so as to emerge in toto from the input line.

The degree of unidirectionality depends, of course, upon how well the impedances of the two linear cavity modes are matched. With the two modes sharing a single absorbing or emitting crystal, the crystal losses or gains will be identical in both systems to the degree that the geometrical configuration of both modes is the same. In order for the impedance characteristics of the two modes to be matched in frequency, they can be tuned to each other with small perturbing plugs which equalize the frequencies and Q's of the two modes. Variation of the frequency and Q's of the two degenerate modes with time will be identical because they are mutually inclusive structures. Thus, although a circular-polarization amplifier is in essence a bridge amplifier, since the amplifying cavities are mutually inclusive, the bothersome effects of drifts of gain characteristics are reduced to a minimum. An actual amplifier employing a ruby crystal is shown in Fig. 5.

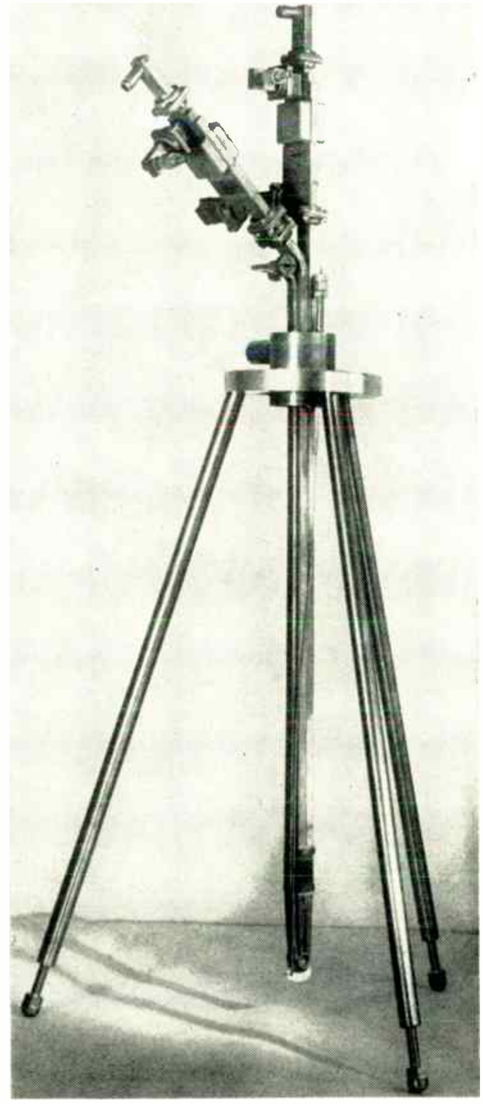

Fig. 5—An X-band circularly-polarized amplifier.

Tolerance

As we indicated above, it is impossible to have a perfect circular-polarization amplifier unless the active material is restricted to an infinitesimal volume on the axis of the cavity itself. In a filled cavity, however, the ratio of the average of the two circular polarizations is large enough so that one circular polarization is in sufficient predominance for most practical cases. The actual interaction between the electromagnetic field and the crystal is measured by the product of quantum-mechanical operators $|S_+|^2$, $|S_-|^2$, and $|S_z|^2$ for the spin transition that is involved and, respectively, the electromagnetic field operators, H^2, H_+^2 and H_z^2. The ratio of the magnetic Q for the signal circular-polarization direction, $(+)$, to the magnetic Q for the circular polarization of the opposite direction, $(-)$, is thus given by the fraction

$$\frac{(Q_{x0})_-}{(Q_{x0})_+} = \frac{(\langle H_-^2\rangle |S_+|^2 + \langle H_+^2\rangle |S_-|^2 + \langle H_z^2\rangle |S_z|^2)}{(\langle H_+^2\rangle |S_+|^2 + \langle H_-^2\rangle |S_-|^2 + \langle H_z^2\rangle |S_z|^2)} \tag{18}$$

where the symbol $\langle\ \rangle$ means an average over the crystal. Thus, using (16), with the cavity filled with a material exhibiting a perfect Faraday effect (*i.e.*, a material for which $S_-^2 = S_z^2 = 0$) we can obtain a nonreciprocity of active or passive magnetic Q of 10.6 db. The resonant gain, (10) with $\Delta f = 0$, for either polarization is written directly as

$$\sqrt{G_\pm} = \frac{\dfrac{1}{Q_e} - \dfrac{1}{Q_0} - \dfrac{1}{Q_{x0\pm}}}{\dfrac{1}{Q_e} + \dfrac{1}{Q_0} + \dfrac{1}{Q_{x0\pm}}}. \tag{19}$$

The gain equation can be manipulated into the form

$$\sqrt{G_-} = \frac{1 + \dfrac{Q_e}{Q_0}\left(\dfrac{Q_{x0-}}{Q_{x0+}} - 1\right) - \dfrac{Q_{x0-}}{Q_{x0+}}\left(\dfrac{1 - \sqrt{G_+}}{1 + \sqrt{G_+}}\right)}{1 - \dfrac{Q_e}{Q_0}\left(\dfrac{Q_{x0-}}{Q_{x0+}} - 1\right) + \dfrac{Q_{x0-}}{Q_{x0+}}\left(\dfrac{1 - \sqrt{G_+}}{1 + \sqrt{G_+}}\right)}. \tag{20}$$

For a backward gain of the 1, the ratio of the magnetic Q's in the forward and backward direction must be:

$$\frac{Q_{x0-}}{Q_{x0+}} = \frac{Q_0}{Q_e}\left(\frac{\sqrt{G_+} - 1}{\sqrt{G_+} + 1}\right) + 1. \tag{21}$$

This ratio of magnetic Q's for the variation of $\sqrt{G_+}$ from 1 to ∞ is from 1 to $1 + Q_0/Q_e$, the latter limit being a separately controllable factor through the ratio Q_0/Q_e.

Actually, then, we need not require that the active material exhibit a perfect Faraday effect because a ratio of the two magnetic Q's of 3 or 4 is sufficient to obtain, by (21), a gain nonreciprocity of $\sqrt{G_+}$. In fact, an X-band ruby amplifier designed with the magnetic field making an angle of 70° with the crystalline c axis and with the circular polarization vector itself and at a field of approximately 3.8 kilogauss operating between the two highest energy levels, as indicated in Fig. 6, will have a ratio $S_+:S_-:S_z = 0.78:-0.069:-0.65$. Thus, the ratio $(Q_{x0})_-/(Q_{x0})_+$ in a TE_{111} cavity is for $D/l = 2.58$,

$$\frac{Q_{x0-}}{Q_{x0+}} = \frac{(0.78)^2 0.76 + (-0.069)^2 0.066 + (-0.65)^2 0.172}{(0.78)^2(0.066) + (-0.069)^2 0.76 + (-0.65)^2 0.172} = 4.4 \tag{22}$$

and hence the reverse gain is one, or less, for a Q_0/Q_e ratio of 3.5, or less. At first sight it might seem that this arrangment would have very poor directional properties because the magnetic field makes such a large angle with the actual circular-polarization axis. That this is not the case is merely an indication that the quantum-mechanical mixing and transition probabilities are not intuitively evident.

The effect of reflection in the output line on the stability of the amplifier using this circular-polarization structure can be considered. It is evident that nonreciprocity is of tremendous assistance in reducing the effect of the reflections on the amplifier gain. If we call the reflection coefficient in the output and input arms r_o and r_i, the actual gain of the device is

$$\frac{G_+}{(1 - \sqrt{G_+G_-r_or_i})^2}. \tag{23}$$

A typical value of $\sqrt{G_+}$ is 10 (20-db gain) and of $\sqrt{G_-}$ is 1. This means that for a gain stability of ± 10 per cent for all phases of the reflection coefficients the magnitude of reflection coefficients in both the input arm and the output arm will be required to be less than 0.07. A reciprocal amplifier would, of course, require that the reflection coefficients in this case be less than 0.02. This improvement is more spectacular when stated in terms of VSWR: the nonreciprocal amplifier requires a VSWR of less than 1.14 in input and output arms, but the reciprocal amplifier (using an external isolator circulator) requires a VSWR of 1.04 or less with the same forward gain condition.

The further advantage of nonreciprocity in a unidirectional amplifier stems from its insensitivity to noise radiated from the output load. This noise is characterized by the temperature of the output load, which would be about 300°K. This temperature, T_L, is not to be confused with the effective noise temperature of the second stage, T_0, since this temperature, T_0, includes the effect of conversion losses in this stage. The noise from the output terminal characterized by T_L is amplified by the paramagnetic system to give G_-T_L at the input. Reflections in the input arm, r_i, then increase the apparent source noise temperature by $r_i^2G_-T_L$. For this to be only a few degrees Kelvin, with $G_- \approx 1$, $r_i \leq 0.1$. This means that the antenna or input VSWR must be less than 1.2, which is readily achieved. With a unidirectional reciprocal amplifier operating with a circulator, the same analysis yields $r_i \leq 0.1\sqrt{c/G_-}$, or $\text{VSWR} \leq 1 + (0.2\sqrt{c/G_-})$, where c is the reverse loss of the circulator.

Design Features

The design of a circular-polarization cavity requires that attention shall be paid to the cylindrical symmetry of the system. For example, since some paramagnetic crystals, such as ruby, are anisotropic in electric susceptibility, one must try to have a crystal with its c-axis as parallel to the cavity axis as possible. Even this is not a great restriction; with ruby, the difference in the index of refraction means essentially that if the crystal axis is 5° off the cylinder axis the two modes in the cavity will not be degenerate by approximately 100 mc. This can be of the order of magnitude of perturbations of other asymmetries in the system, so that one can readily align the crystal to the cavity axis sufficiently accurately. Small tuning plugs that change both frequency and cavity Q's (by introducing resistive loss into the one cavity selectively) can then be used to obtain balance of the two mode impedances.

An additional problem encountered in saturation paramagnetic amplifiers, is the introduction of the pumping power. This saturating power is introduced in our amplifier through a K-band waveguide, slot-coupled to the cavity midway between the two amplifier coupling irises. The slot is a large one, essentially resonant at the pumping frequency. At a symmetrical point, $\pi/2$ radians in space, a dummy coupling iris is introduced in order to compensate for the mode-splitting effect of the pumping iris.

In discussions of this type of amplifier, it seems not to be realized that the amplifier cavity need not be made resonant at any particular pump frequency, since tuning elements of the pump feed guide can be used to resonant the over-all structure, which comprises guide, coupling window, and amplifier cavity, to the pumping electromagnetic radiation. In the present amplifier, we do not need to be as sophisticated as this; there are many available K-band resonances. A glance at a cavity mode chart is convincing on this point. With an anisotropic dielectric constant, the usual cylindrical cavity mode chart is not directly applicable, but, between K and K_A bands, several dozen resonances are available. In this case, one need only arrange the static field and its angle with the crystal-axis to be proper for the amplifier and pump frequency cavity resonances to coincide with the spin system resonances. For example, using ruby, as shown in Fig. 6, for variation of the static field from 2 to 3.8 kg and the simultaneous variation of angle between the field and c axis from 55° to 70°, we find the amplifier resonances to be constant at 9 kmc, while the necessary pump varies from 23 kmc to 36 kmc. The ratio of forward to backward negative Q does not vary greatly with these changes in operating conditions.

There is also no need to restrict the active crystal to regions of high-pumping electromagnetic field. As has been pointed out in the literature, an inhomogeneous electromagnetic field can give rise to homogeneous polarization of the amplifier levels since several mechanisms exist to give energy transport within the crystal.[6] If this were not so, only a small filling factor could be obtained, because the paramagnetic crystal would have to be limited to those points in the amplifier at which

[6] R. J. Morris, R. L. Kyhl, and M. W. P. Strandberg, "A tunable maser amplifier with large bandwidth," Proc. IRE, vol. 47, p. 80; January, 1959.

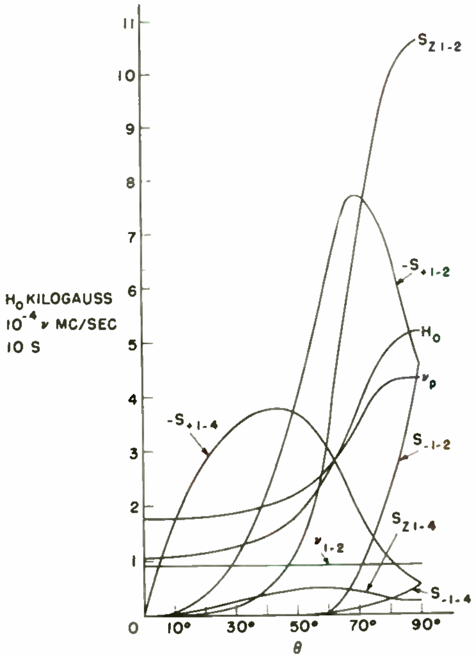

Fig. 6—Operating parameters curves for amplification on the two highest energy ruby levels, with pumping from the top to the bottom level.

the pumping field had a large amplitude. Thus, the possibility of phonon (or other) transport of pumping energy within the amplifying crystal tremendously simplifies the design of the pumping cavity mode. Any means of tuning the coupling waveguide, coupling iris, and cavity to match the pumping power into the crystal may be used, since the important factor is the actual power transfer to the crystal and not the mode configuration. This is not a reckless gesture with the pumping power, as so little power (hundreds of microwatts), matched into the crystal, is needed in a properly designed amplifier. Furthermore, the absence of a restriction on placing the active crystal on the vicinity of pumping-field nodes means that the whole cavity can be filled with a crystal. This gives a maximum filling-factor η and lowest magnetic Q and hence greatest gain-bandwidth product for the amplifier.

Quantum-Mechanical Design

In order to test the feasibility of these suggestions, two amplifiers were constructed embodying the principles involved. One operates at X band (3 cm), using a waveguide structure, and the other at L band, using coaxial lines. The L-band amplifier presents somewhat different problems from those of the X-band amplifier, most of which are simply problems of translating waveguide structures into coaxial line structures and have been solved at this point. The 3-db coupler, which was designed by using stripline techniques, presents no difficulty. Instead of using a circular TE_{111} cavity at L band as a mutually inclusive structure, it was decided to use two geometrically-orthogonal quarter-wave stripline cavities, as indicated in Fig. 7. These two orthogonal resonance structures share a common crystal. The filling factor achievable by this technique is about one-third, but this is sufficient to yield an amplifier for operation at the hydrogen line frequency which should have a bandwidth of 100 kc with a gain of 30 db. The possibility of operating such a device without a circulator is indeed exciting, especially for radioastronomy purposes. Circulators that are available in this frequency region have insertion losses of approximately 0.2 db.

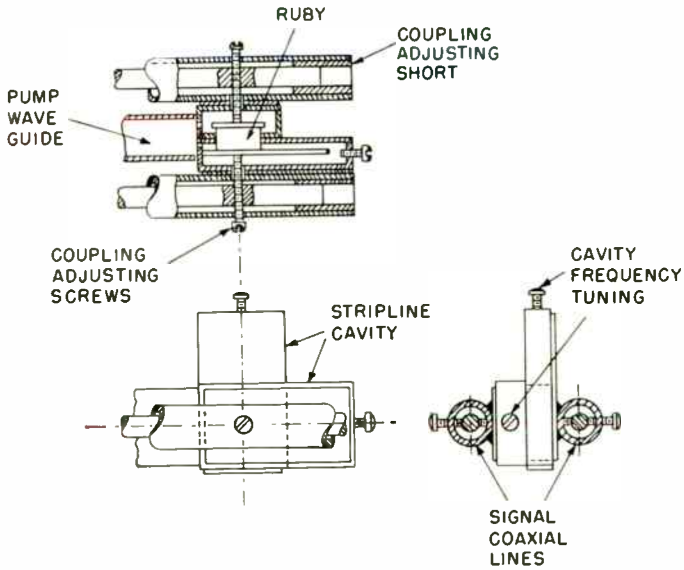

Fig. 7—Stripline, orthogonal-cavity, circularly-polarized amplifier for L-band.

This gives a limiting amplifier temperature of 14°K, an order of magnitude greater than the intrinsic temperature of the amplifier. Hence, one would expect an order of magnitude improvement in the sensitivity of a radio telescope equipped with such an intrinsically unidirectional amplifier over that obtainable with the reciprocal amplifier-lossy circulator combination. Since tests of this amplifier are not finished, the following description will be restricted to a discussion of the design and operation of the X-band amplifier.

It was decided at the start, to make the test amplifier in a structure with an intrinsic Q limited by dielectric Q of ruby at low temperature. It is our experience that this limiting ruby Q at helium temperatures and X band is around 3000. It will be seen later that such a Q is an order of magnitude greater than the achievable magnetic Q of ruby operated at this temperature. However, we felt that if a high-Q structure could be made to behave properly as a circularly-polarized amplifier, then it would be less work to eliminate the difficulties encountered with lower-Q systems. As it turned out, no difficulty was encountered in operating the device, even with a Q of several thousand, if a few relatively simple precautions were taken. The ruby c axis was aligned to within one degree of the cylinder axis by the method of

Mattuck and Strandberg.[7] It is our feeling that this is sufficiently accurate for the present purpose. The D/l ratio for the cavity was chosen large in order to minimize the contribution to the magnetic Q from the Z component of the spin-matrix elements. A commercial top-wall coupler was used for the 3-db coupler.

The design of a paramagnetic amplifier is almost entirely reducible to analytical expressions. The paramagnetic resonant frequencies for the ruby crystal as a function of magnetic field at various angles and the magnetic moment dipole matrix elements, the $S_{\pm,z}$, were computed by the method outlined by Davis and the present author.[8] One set of these calculations is given in Fig. 6, where the two energetically-highest levels in the ruby spectrum are used as amplifier levels. A similar set of design curves is given in Fig. 8, where the amplifier levels are the middle two levels of the ruby spectrum. The object of the game of designing an amplifier is to use these curves to select operating regions in which the spin-matrix elements for the amplifying levels are as nonreciprocal as possible and as large as possible, and at the same time to maintain reasonable strength in the possible saturating transition matrix elements.

There is a further qualification, however, in designing saturation amplifiers with four levels, and this is to select from among the possible amplifier and pumping transitions those which, in the presence of a saturating field, have the most favorable distribution of spin-lattice transition probabilities so as to allow, under equilibrium saturation conditions, the maximum polarization of the amplifier levels. These equations are a simple extension of the type of equation written for a three-level saturation amplifier.[9]

$$\frac{dn_i}{dt} = \sum_{\substack{j=1\\ j\neq i}}^{4} - n_i w_{ij} + n_j w_{ji} + (n_j - n_i) W_{ji}$$

$$N = \sum_{j=1}^{4} n_i \tag{24}$$

where n_i is the number of spins per cm³ in the level i, w_{ij} is the probability of the lattice inducing a spin transition from level i to level j, and $W_{ji} = W_{ij}$ is the probability that an applied RF field will cause a spin transition from level i to level j. The steady-state solution is obtained by setting the time rate of change of the level populations equal to zero. For small amplifier signals, it is sufficient to consider only the pump saturating W_{ji}.

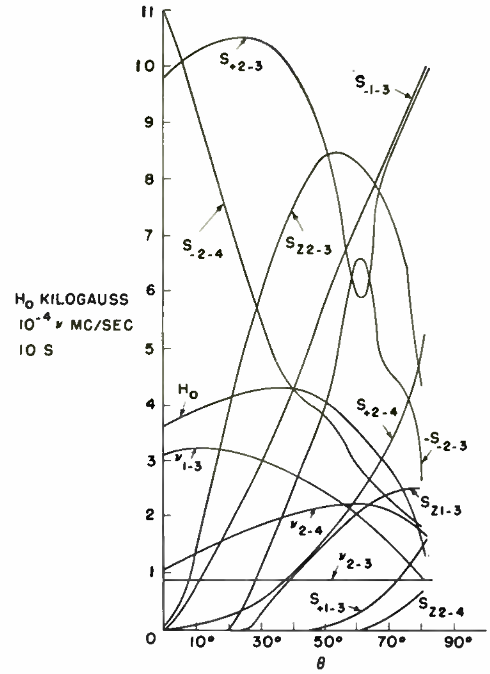

Fig. 8—Curves of the operating parameters for ruby with the two intermediate levels as amplifying levels.

With the assumption that the ratio of the energy differences divided by kT is much less than 1, solutions of the following form can be obtained. With only $W_{13} \to \infty$ and with E_i, the energy of the ith level, such that $E_1 > E_2 > E_3 > E_4$:

$$n_2 - n_3 = \frac{Nh}{4kT}\,\frac{f_{12}[w_{41}w_{42} + w_{21}(w_{41} + w_{42} + w_{43})] - f_{23}[w_{43}w_{42} + w_{32}(w_{41} + w_{42} + w_{43})]}{w_{42}(w_{41} + w_{43}) + (w_{41} + w_{42} + w_{43})(w_{21} + w_{32})}. \tag{25}$$

For a degeneracy of the possible saturating transitions (for example, at θ equals 55°, in Fig. 8) two pairs of levels are being saturated, and a different solution is obtained. If the pumping transitons are the $1\to 3$ and $2\to 4$ transitions and if the amplifying transition is the $2\to 3$ transition, these equations have the solution of the form

$$n_2 - n_3 = \frac{Nh}{4kT}\,\frac{w_{41}f_{41} + w_{43}f_{43} + w_{21}f_{21} - w_{32}f_{32}}{w_{21} + w_{32} + w_{43} + w_{41}} \tag{26}$$

with $W_{13} = W_{24} \to \infty$. This type of operation has been called push-pull pumping. Although it is apparent that nonreciprocal gain is available in this orientation, the unfavorable amplifier-transition probabilities make it a less interesting operating point for the present problem.[10]

[7] R. D. Mattuck and M. W. P. Strandberg, "Optical method for determining the c axis of ruby boules," *Rev. Sci. Instr.*, vol. 30, pp. 195–196; March, 1959.

[8] C. F. Davis, Jr. and M. W. P. Strandberg, "The paramagnetic resonance spectrum of ammonium chromium alum," *Phys. Rev.*, vol. 105, pp. 447–455; January 15, 1957.

[9] N. Bloembergen, "Proposal for a new type solid state maser," *Phys. Rev.*, vol. 104, pp. 324–327; October 15, 1956.

[10] Morris, Kyhl, and Strandberg, *op. cit.*, is probably the first published report of an amplifier with direct push-pull pumping. Note also G. Makhov, C. Kikuchi, J. Lambe, and R. W. Terhune, "Maser action in ruby," *Phys. Rev.*, vol. 109, pp. 1399–1400; February 15, 1958. Here, the operating point was 9.22 kmc and 24.2 as amplifier and saturation frequencies, with a magnetic field of 4230 gauss. It can be seen that the angle θ must have been somewhat less than 50° and that the $2\to 4$ transition was 500 mc off resonance. For push-pull pumping at 9.2 kmc, the pumping frequency would have to be 23.4 kmc and the magnetic field 3980 gauss.

Unfortunately, our present understanding of the spin-lattice transition matrix elements, the w's in the equations above, is based for the most part on theoretical considerations. The experiments that have been performed on paramagnetic systems such as ruby have measured a spin-lattice relaxation time that is essentially a measure of the net interaction due to all of these transition probabilities. It is sufficient to say that the major interaction of the lattice with the spin comes through the crystalline electric field.[11] The dominant spin-dependent term, in this case, yields w's that depend upon the square of the spin anticommutator:

$$w_{ij} \propto \left| S_\alpha S_\beta + S_\beta S_\alpha \right|_{ij}^2 \qquad \alpha, \beta = x, y, z. \tag{27}$$

For example, between the pure spin states of $S_z = \pm\frac{1}{2}$, this operator vanishes, and as a consequence these spin levels should have a small w_{ji}, or a long spin-lattice relaxation time. That the selection of operating point on the basis of most favorable spin-lattice relaxation ratios is an important consideration may be seen as follows. If our present understanding of the spin-lattice relaxation process is correct, one may introduce the following relationships which must exist in paramagnetic systems having nearly pure spin spatial quantization (*e.g.*, in ruby with a magnetic field parallel or nearly parallel with the c axis):

$$\begin{aligned} w_{41} &\approx 0 \approx w_{32} \\ w_{43} &\approx w_{21}. \end{aligned} \tag{28}$$

The minimum ratio of pump to amplifier frequency is then given by (25) as

$$\frac{f_{\text{pump}}}{f_{\text{amp}}} = \frac{2w_{21}w_{42} + w_{21}^2}{w_{21}w_{42} + w_{21}^2}. \tag{29}$$

We have not, as yet, computed the local normal lattice modes for chromium in ruby, but it is reasonable to think that the allowed transitions will have comparable magnitudes. With the spin-lattice relaxation time for the 42 levels approximately equal to that of the 21 levels, we are led to believe that a pump-to-amplifier frequency ratio of only 3/2 is necessary for operation near the region where the spin-projection quantum numbers S_z are reasonably good. They cannot be perfect quantum numbers, obviously, because this would mean that the pumping transition would not be allowed. On the other hand, the rate of growth of the spin-lattice relaxation probability, $w_{-1/2,\,+1/2}$, between the $+\frac{1}{2}$, $-\frac{1}{2}$ levels is identical with that of the coupling between the pumping field and the spin levels. This means that a convenient compromise between a small $w_{-1/2,\,+1/2}$ and a small pumping Q_{x0} can be arranged. For example, in ruby with the magnetic field of eight kilogauss at approximately 5° from the crystal axis, one should be able to operate an amplifier at $\nu_{23} = 22$ kmc with a pump at $\nu_{24} = 34$ kmc.

[11] R. D. Mattuck, "Phonon-Spin Absorption in Paramagnetic Crystals," Ph.D. Thesis, Department of Physics, M.I.T.; June 1959; also, R. D. Mattuck and M. W. P. Strandberg, "Quadrupole Selection Rule," *Phys. Rev. Letter 3*, p. 369; October 15, 1959; also R. D. Mattuck and M. W. P. Strandberg, "Spin-phonon interaction in paramagnetic crystals," *Phys. Rev.* (to be published).

For all of the reasons outlined above, the actual ruby amplifier operating point should be determined from Fig. 8, keeping in mind the desirability of a high pump-to-amplifier-frequency radio, large amplifier matrix elements, the greatest difference between the S_+ and S_- matrix elements for the amplifier transition, and the use of those amplifier levels most nearly characterized by the S_z quantum numbers of $\pm\frac{1}{2}$. The most appropriate operating point would be around $\theta = 20°$ with a pump at about 31 kmc. The actual tests of the amplifier structure were made at $\theta = 45°$ and $\theta = 55°$, since available pump oscillators were limited to the frequency region between 22 and 26 kmc.

Results

The circular polarization structure showed little fundamental difficulty in obtaining proper performance. There was some splitting of the modes on cooling (a few megacycles) but this was corrected by a rocking tuner arm that could be used to tune either one or the other mode to a lower frequency. As shown in Fig. 9, the device was arranged with circulators used in order to separate the incident and reflected signals. In operation at the 55° orientation the ratio of the magnetic Q's for the two directions of circular polarization is shown in Fig. 10. With the amplifier signal on the A terminal, the transmitted power detected at the a crystal is shown on the top trace of the oscilloscope picture; with the signal on the B terminal, the transmitted power is shown on the bottom trace. Of course, with the signal on the A

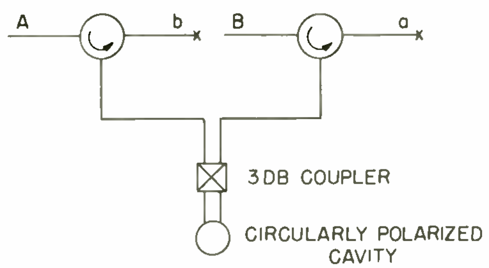

Fig. 9—Circularly-polarized amplifier test signal paths.

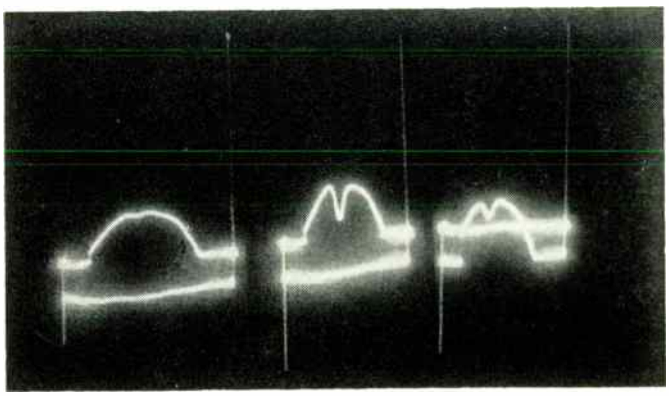

(a) (b) (c)

Fig. 10—Signal klystron mode curves. (b) the pumping klystron turned off and the paramagnetic transition resonance off cavity resonance; (a) the paramagnetic resonance on resonance and the signal on terminal A; (c) the signal on B. In each picture the upper trace of the double-trace presentation is from crystal a and the lower trace is from crystal b.

terminal, the b crystal (the lower trace) detects the reflected power. The ratio of the forward and backward magnetic Q's is obviously large. In the forward direction, the magnetic Q is much smaller than the off-resonant loaded Q of the cavity (3000); the reverse magnetic Q is of the order of 4000. Operation with the pump power on, led only to oscillation since the external Q was much larger than the magnetic Q of the crystal. In order to obtain amplifier action, it was necessary to operate the amplifier with a high signal input. This has the effect of increasing the magnitude of the magnetic Q by reducing a difference in populations of the amplifier levels. The effect of the large signal power is essentially to increase w_{23} in the denominator of (25) or (26) in proportion to the signal power. The operating characteristics of the amplifier can be seen from Fig. 11. With the signal introduced through the forward direction, the forward gain was large; with the signal introduced in the reverse direction, the reflection gain was large, while the forward gain was actually a loss. The directionality indicated is apparently even greater than the amplifier gain itself.

The magnetic Q can only be estimated from the signal saturation power, which was in the 10 μw region, and would indicate a negative magnetic Q of approximately 300. Since this is the order of the absorption Q at 4°K, the amplifier temperature must likewise be of the order of 4°K.

Conclusion

The physical parameters which enter into the design of paramagnetic quantum-mechanical amplifiers have been discussed. It has been shown that the most crucial elements in the amplifier design are reducible to analytical expressions. It has been especially demonstrated that regenerative cavity amplifiers can be made unidirectional, with obvious simplicity, and that a simple cascade of such amplifiers can give operational characteristics similar to those of traveling-wave devices. It has been indicated that unidirectional regenerative amplifiers can have noise figures an order of magnitude less than the noise figures of cavity amplifiers requiring circulators for isolation of input and output because the noise temperature for the amplifier increases with circulator loss at a rate of 7.2°K per 0.1-db loss in the circulator. The relaxed specification for input and output reflection coefficient should also yield more stable amplifier gain characteristics; even with a circulator, the reflection coefficients of the circulator must be reduced to a very low level when a reciprocal amplifier is being used, or the electrical-line length between amplifier and circulator must be very well stabilized. This is quite difficult to accomplish, especially in transmission lines filled with an amount of liquid helium, which varies with time.

The selection of the type of amplifier—a single-cavity regenerative amplifier, a cascade of cavity amplifiers, or a slow-wave structure—is to be determined by the end use of the amplifier. No single amplifier type is fitting for all applications. For uses requiring wide tunability and moderate gain-bandwidth product, the regenerative-cavity configuration is probably most effective. For wide-band high-gain purposes, cascaded cavities or a slow-wave structure will have to be used. The latter device requires more engineering development and is less conveniently tuned over a wide frequency region. It is most important to note that a single regenerative cavity can never have a gain-bandwidth product greater than twice the intrinsic paramagnetic linewidth. From this point of view, it seems futile to try to achieve magnetic Q's which are much smaller than the operating frequency divided by the paramagnetic linewidth. The linewidth can be increased if we increase the concentration of the paramagnetic ions with a rapid increase of other deleterious effects, such as the cross relaxation between the paramagnetic energy levels. This effect decreases the spin-lattice relaxation time and rapidly increases the required pumping power. Alternatively, the linewidth may be broadened by making the magnetic field inhomogeneous or by using more than one crystal in the structure, each crystal having a separate alignment with respect to the magnetic field. Unless these measures are consciously carried out, it would seem incredible that gain-bandwidth products in excess of 100 mc could be achieved at any foreseeable microwave frequency.

(a)

(b)

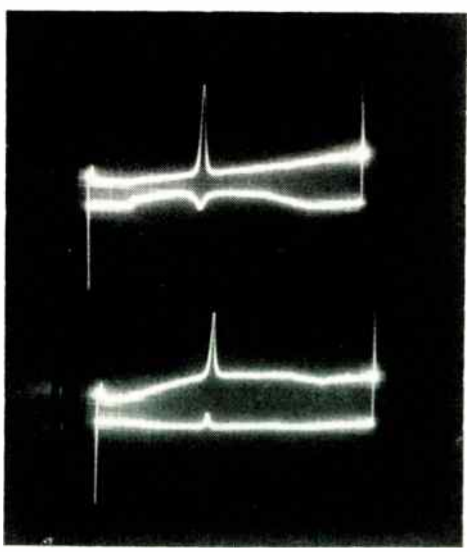

Fig. 11—Circularly-polarized amplifier in operation with pump radio-frequency turned on, and $\theta=55°$. The signal level is high so that the amplifier is operated at its saturation point in order to increase the magnitude of the paramagnetic Q to a value at which the amplifier does not oscillate. The two lower traces show the detected current at crystal a on (a), and crystal b on (b) for the signal on the A terminal. The two upper traces show the same crystal signals with the signal on the B terminal. The reflection that is being amplified arises from the thin teflon window at the amplifier output.

Analytical Appendix

The energy levels of a paramagnet are determined from a spin-Hamiltonian $\mathcal{H}$, which essentially expresses the three-dimensional rotational transformation properties of the spin system as defined by the symmetry of its crystalline environment. It may be expressed as a power-series expansion in the operators of the static field, $\boldsymbol{H}_0$, and the spin, $\boldsymbol{S}_x$, $\boldsymbol{S}_y$, and $\boldsymbol{S}_z$. The expansion is truncated at the spin term expressing the lowest symmetry of the system and with the field and spin terms first power in the field. The latter truncation is for simplicity and is a reasonable approximation in general. For ruby, with the Cr^{+++} ion in a crystal site having trigonal symmetry, the form this expansion takes is

$$(\mathcal{H}) = g_{\parallel}\beta_0 H_0 \cos\theta(S_z) + g_{\perp}\beta_0 H_0 \sin\theta(S_{x,y}) + D\left[(S_z^2) - \tfrac{1}{3}S(S+1)(I)\right] \tag{30}$$

where

- $g_{\parallel}$ = magneto-gyric conversion factor parallel to c axis
- $g_{\perp}$ = magneto-gyric conversion factor perpendicular to c axis
- β_0 = the Bohr magneton = $1.4\text{-}h$ mc/gauss, where h is Planck's constant
- H_0 = applied static-magnetic field magnitude in gauss
- θ = angle between $\boldsymbol{H}_0$ and c axis
- $2D$ = zero field crystalline splitting = $-11{,}470$ mc
- $S = 3/2$, the maximum spin-projection quantum number
- $(\boldsymbol{S}_{x,y})$ = either the $\boldsymbol{S}_x$ or $\boldsymbol{S}_y$ matrix

$$\boldsymbol{S}_z = \begin{vmatrix} \frac{3}{2} & 0 & 0 & 0 \\ 0 & \frac{1}{2} & 0 & 0 \\ 0 & 0 & -\frac{1}{2} & 0 \\ 0 & 0 & 0 & -\frac{3}{2} \end{vmatrix}$$

$$\boldsymbol{S}_x = \begin{vmatrix} 0 & \sqrt{\frac{3}{2}} & 0 & 0 \\ \sqrt{\frac{3}{2}} & 0 & 1 & 0 \\ 0 & 1 & 0 & \sqrt{\frac{3}{2}} \\ 0 & 0 & \sqrt{\frac{3}{2}} & 0 \end{vmatrix}$$

$$\boldsymbol{S}_y = \begin{vmatrix} 0 & i\sqrt{\frac{3}{2}} & 0 & 0 \\ -i\sqrt{\frac{3}{2}} & 0 & i & 0 \\ 0 & -i & 0 & i\sqrt{\frac{3}{2}} \\ 0 & 0 & -i\sqrt{\frac{3}{2}} & 0 \end{vmatrix}$$

$$\boldsymbol{I} = \begin{vmatrix} 1 & 0 & 0 & 0 \\ 0 & 1 & 0 & 0 \\ 0 & 0 & 1 & 0 \\ 0 & 0 & 0 & 1 \end{vmatrix}.$$

The characteristic energies of this matrix are those of its diagonal representation, or, explicitly, the energies that make the secular determinant formed from the Hamiltonian equal to zero. Symbolically,

$$\left| \mathcal{H}_{ij} - \delta_{ij}\lambda_{ij} \right| = 0, \qquad \text{with } \delta_{ij} = \begin{cases} 1, & i = j \\ 0, & i \neq j \end{cases}. \tag{31}$$

The process for solving the secular determinant may be considered the same as the process used in finding an orthogonalized transformation $\boldsymbol{T}$ such as the $\boldsymbol{T}\mathcal{H}\boldsymbol{T}^{-1} = \boldsymbol{\lambda}$, where $\boldsymbol{\lambda}$ is the diagonal matrix $|\delta_{ij}\lambda_{ij}|$. The methods for diagonalizing this form of matrix and for determining the transformation $\boldsymbol{T}$ have been given.[2] For convenience, the spin Hamiltonian is tabulated in terms of a natural, or crystalline, coordinate system, the static magnetic field $\boldsymbol{H}_0$ having any orientation with respect to these axes. In general, then, the transformation $\boldsymbol{T}$ will vary not only with the magnitude of $\boldsymbol{H}_0$ but also with its orientation with respect to the spin-Hamiltonian axes.

The interaction energy of a spin of a paramagnetic ion with an RF magnetic field is also given to first order in terms of the spin-magnetic moment $\boldsymbol{\mu}$ and the RF magnetic field $\boldsymbol{H}$ having a frequency f, as:

$$\mathcal{H}_{\text{interaction}} = -\boldsymbol{\mu}\cdot\boldsymbol{H}\cos 2\pi f t \tag{32}$$

with

$$-\boldsymbol{\mu}_{x,y,z} = g_{x,y,z}\beta_0 \boldsymbol{S}_{x,y,z}. \tag{33}$$

One may show that, in general, a system having a phase-memory time τ (spin-spin relaxation time) $= (\pi B_x)^{-1}$ has a magnetization when perturbed by $\mathrm{Re}(-\boldsymbol{\mu}\cdot\boldsymbol{H}e^{-i2\pi f t})$ of[2]

$$\boldsymbol{M}(t) = \sum_{ij} \boldsymbol{\mu}_{ij}(\boldsymbol{\mu}_{ji}\cdot\boldsymbol{H}e^{-i2\pi f t})\left[1 - \frac{f}{f - f_{ij} + i\dfrac{B_x}{2}}\right]\frac{N_i - N_j}{2hf_{ij}} + \sum_{ij} \boldsymbol{\mu}_{ji}(\boldsymbol{\mu}_{ij}\cdot\boldsymbol{H}e^{i2\pi f t})\left[1 - \frac{f}{f - f_{ij} - i\dfrac{B_x}{2}}\right]\frac{N_i - N_j}{2hf_{ij}} \tag{34}$$

where h is Planck's constant, B_x is the line frequency width, and N_i and N_j are the number of spins per cm^3 in levels i and j. We may neglect the second term on the right as a non-resonant high-frequency contribution to the susceptibility. Using Cartesian components of $\boldsymbol{\mu}$, it will be seen that M_x depends upon both H_x and H_y, yielding a non-diagonal tensor susceptibillty.

The $-\boldsymbol{\mu}_{\pm} = \beta_0(g_x S_x \pm i g_y S_y)/\sqrt{2}$, $H_{\pm} = (H_x \pm iH_y)/\sqrt{2}$ operators are convenient in that they simply exhibit the circular-polarization properties of the system, and incidentally yield a diagonal tensor susceptibility under some conditions. In general, the susceptibility tensor is not diagonal. However, since we are interested in the circuit averages of $\boldsymbol{H}\cdot d\boldsymbol{M}^*$, the off-diagonal terms average to zero by symmetry or design in cavity systems. Thus, one need use only the diagonal terms expressed as (since $(S_\pm)_{ij}(S_\mp)_{ji} = |S_\pm|_{ij}^2$):

$$\chi_{\pm,z} = \frac{M_{\pm,z}}{H_{\pm,z}^*} = g^2\beta_0^2 \sum_{ij} |S_{\pm,z}|_{ij}^2 \cdot \left(1 - \frac{f}{f - f_{ij} + i\frac{B_z}{2}}\right)\frac{N_i - N_j}{hf_{ij}}. \quad (35)$$

The factor 1 gives rise to the static susceptibility, which we neglect since it is 500 times smaller than the resonant factor at X-band frequencies.

If we are interested in the susceptibility arising from two levels of a system, say i and j, as the magnetic field changes magnitude and orientation, we must study the transformation properties of the spin angular-momentum components upon which the magnetic moment depends:

$$(S'_{\pm,z})_{ij} = \boldsymbol{T}\boldsymbol{S}_{\pm,z}\boldsymbol{T}^{-1}. \quad (36)$$

These elements have been given by Davis and Strandberg for the case $S=3/2$ with trigonal symmetry.[8] We merely note that the transformation properties of this electromagnetic coupling term may be studied for the general case in terms of the three-dimensional finite rotational properties of the spin Hamiltonian,[12] or by the simple expedient (if rapid-computing facilities are available) of computing the interaction operator for various magnetic-field magnitudes and orientations. Though the zero-interaction field angle (*i.e.*, the orientation angle for the RF field for no interaction with the quantum mechanical system) exists at a discrete angle, care must be taken to understand these coupling matrices to avoid this angle. We have indicated a splendid mistake of this kind in which the RF field was mistakenly oriented along the zero interaction angle.[13] The fact that the device operated almost as expected (the required pumping power was, in fact, too much) was due only to other fairly subtle and esoteric effects that are, as yet, not fully understood.

We may define a circuit, or effective, complex susceptibility, $\chi = \chi' - i\chi''$, and hence a complex magnetic $\boldsymbol{Q}_z$ in terms of the crystal susceptibility averaged over the whole circuit with a weighting factor of the square of the RF magnetic-field components (since energy loss and storage are proportional to the field squared):

$$\boldsymbol{Q}_z^{-1} = \frac{4\pi\left[\chi_+ \int_{\text{crystal}} H_-^2 dv + \chi_- \int_{\text{crystal}} H_+^2 dv + \chi_z \int_{\text{crystal}} H_z^2 dv\right]}{\int_{\text{cavity}} H^2 dv} = 4\pi[\chi_+\eta_+ + \chi_-\eta_- + \chi_z\eta_z] \quad (37)$$

where η = filling factor: in the denominator, we may neglect the effect of χ' on the stored energy because it is zero on resonance, the condition that we are investigating, and usually is negligible on off-resonance in paramagnetic materials.

For nonreciprocity, we want the factors contributing to $\chi_+\eta_+$ (or $\chi_-\eta_-$) to be large as compared to the other factors so that, as direction of propagation is reversed and $H_+ \rightarrow H_-$ (or $H_- \rightarrow H_+$), the RF coupling term is reduced by a large factor. Note that H_+, H_-, and H_z refer in our case to the natural crystal axes simply because we represented $\mathcal{H}$ in terms of these axes. Since we must use TE modes to obtain circular polarization in the method presented here, an H_z component must always exist. Thus, the breakdown of a pure Faraday effect, *i.e.*, $(-\boldsymbol{\mu}\cdot\boldsymbol{H}_{\text{RF}})$ not proportional to H_+, may not be due to a growth of interaction with the H_- component so much as to a growth of the interaction with the H_z component. Evidently, the polarization axis for the maximum ratio of the backward-to-forward interaction is not restricted to the crystalline-field axis for general static magnetic-field magnitude and orientation. The optimum axis is found by studying the effect of the three-dimensional finite rotation operators required to change the quantization axes to other than the crystalline magnetic axes.[12] We do not discuss this topic here because such an optimization of the nonreciprocity is experimentally difficult in an anisotropic crystal such as ruby. Establishing a circularly-polarized field off the crystal axis is very difficult in the presence of anisotropy. Since we can achieve our results without the extra effort of optimizing them, we have gratefully chosen expediency to elegance and polarized along the c axis.

For application of these results to amplifiers, we need to express the gain-bandwidth product, the pumping power, and the noise figures in terms of them. From (12) we have

$$\sqrt{G}B = \frac{2}{\frac{1}{B_z} + \frac{Q_{x0}}{f_0}}. \quad (38)$$

[12] M. W. P. Strandberg, "Cross-over Transitions," Ninth Quarterly Progress Report on Contract No. DA36-039-sc-74895, Research Laboratory of Electronics, M.I.T.; Aug. 15, 1959–Nov. 15, 1959.

[13] M. W. P. Strandberg, C. F. Davis, Jr., B. W. Faughnan, R. L. Kyhl, and G. J. Wolga, "Operation of a solid-state quantum-mechanical amplifier," *Phys. Rev.*, vol. 109, pp. 1988–1989; March 15, 1958.

The activation pumping power can be computed by noting that in steady state the power into the pumped levels of the crystal must be equal to the power which is transferred to the crystal lattice because of spin-lattice relaxation. The rate at which the spin returns to thermal equilibrium population is conventionally measured by a time τ_1, the spin-lattice-relaxation time. Without entering into a critical discussion of the meaningfulness of the parameter,[14] we note that the spin-lattice transition rate is defined as

$$\left[\frac{d(N_i - N_j)}{dt}\right] = -\frac{(N_i - N_j) - (N_i - N_j)_{\text{equilibrium}}}{2\tau_1}. \qquad (39)$$

When levels i and j are saturated, *i. e.*, when $N_i \approx N_j$, the energy is transferred at a rate

$$hf_0 V\left[\frac{d(N_i - N_j)}{dt}\right] = hf_0 \frac{V(N_i - N_j)_{\text{equilibrium}}}{2\tau_1} \qquad (40)$$

where V is the crystal volume. In terms of Q's and the total stored energy U, we have

$$P_{\text{in}} = \frac{2\pi f_0 U}{Q_0} + \frac{(N_i - N_j)_{\text{equilibrium}} hf_0 V}{2\tau_1}$$

$$= \frac{2\pi f_0 U}{Q_0} + \frac{2\pi f_0 U}{Q_{x0}}. \qquad (41)$$

In order to match most of the power into the spins rather than into the cavity walls, $Q_{x0\,\text{pump}}$ must be much less than Q_0 so that saturation will be reached when $Q_{x0} \approx Q_0$, *i.e.*, when half the pump power is absorbed by the cavity walls. Thus,

$$P_{\text{in}} \approx \frac{(N_i - N_j)_{\text{equilibrium}} hf_0 V}{\tau_1}. \qquad (42)$$

The spin temperature T_x is conveniently related to the gain-bandwidth product if we note that $Q_{x0}^{-1} \propto (N_i - N_j)$ and $T_x \propto (N_i - N_j)$. Thus,

$$T_x = \frac{|Q_{x0}|_{\text{amplification}}}{|Q_{x0}|_{\text{absorption}}} T_{\text{Lattice}}\,°\text{K}. \qquad (43)$$

But

$$|Q_{x0}|_{\text{amplification}} = f_0\left[\frac{2}{\sqrt{GB}} - \frac{1}{B_x}\right], \qquad (44)$$

the right-hand side of the equation being conveniently measurable.

The minimum matched-output noise figure, F, is then determined from the following:

$$F = \frac{(\text{noise power available at the output})}{G(\text{noise power available at antenna when matched to load at } 290°\text{K})}$$

$$F = \frac{1}{290°}\left[\frac{(\sqrt{G}+1)^2}{G}\left\{T_s + \frac{Q_e}{Q_0}\left[T_c + |T_x|\right] + \left(\frac{\sqrt{G}-1}{\sqrt{G}+1}\right)|T_x|\right\} + \frac{T_0}{G}\right] \qquad (45)$$

where T_s is the source or antenna temperature, T_c is the cavity temperature, and T_0 is the input noise temperature of the following amplifier.

For design calculations, using (25), (26), and (28), we can take

$$|Q_{x0}|_{\text{amplification}} \approx (Q_{x0})_{\text{absorption}}.$$

Thus, the curves given in Fig. 8 can be used to predict nonreciprocity, gain-bandwidth, and noise figure for the proposed amplifier.

For $\theta = 25°$, $H_0 = 4.2$ kilogauss, $T_{\text{bath}} = 4.2°\text{K}$, ruby with Cr:Al = 1:10^4, $B_x = 42$ mc.

$$|Q_{x0}|_{\text{amplification}+} = 210$$
$$|Q_{x0}|_{\text{amplification}-} = 1450$$
$$(Q_{x0})_{\text{pump}} = 1000$$
$$P_{\text{pump}} = 280\ \mu\text{watts}$$
$$\sqrt{GB} = 42\ \text{mc}$$

Calculations of this type not only point out the way for making the best amplifier with a given system, but also clearly point out the weakness of the given system. As favorable as these figures may seem to represent our nonreciprocal ruby amplifier, they can also be used to show how unsuitable ruby is for amplifier use. The source of the disadvantage of ruby material is the anomalously low ratio of spin density to linewidth which enters in (35). Our research on the reason for this low ratio is still in progress, but preliminary results indicate that it is not attributable to the aluminum nuclear magnetic moment, nor to inhomogeneities in crystalline splitting. It is quite possible that the effect is the result of clustering of Cr^{+++} in the crystal so that the effective Cr-Cr distance is much smaller than the distance that would be computed on the basis of a random distribution of Cr^{+++} ions. In effect, this "bunching" anomalously increases the linewidth for a given concentration of Cr^{+++} over the value computed from purely random distribution of Cr^{+++} impurity ions. It has been suggested that this peaking in Cr^{+++} density distribution could arise if

[14] M. W. P. Strandberg, "Spin-lattice relaxation," *Phys. Rev.*, vol. 110, pp. 65–69; April 1, 1958.

the Cr^{+++} ions preferentially go into the lattice along dislocations. We cannot discuss this problem at length here, but we can say that the magnetic Q for a ruby amplifier with a Cr^{+++}:Al ratio of 1:10,000 should be five times smaller. In other words, with a ruby with a Cr^{+++} concentration of $5:10^4$ truly randomly distributed, the magnetic Q should be approximately 40, and the linewidth should still be approximately 42 mc. Notice, however, that in the equation for the gain-bandwidth product a very low magnetic Q contributes little to that product, once the latter is limited by the intrinsic paramagnetic linewidth. Thus, even with a decrease of magnetic Q factor of 5, the gain-bandwidth product increases only to 72 mc. That this is indeed the case experimentally was demonstrated by research reported previously,[6] which describes an experiment in which the magnitude of the magnetic Q was decreased by reducing the operating temperature from 4.2°K to 1.5°K. The measured gain-bandwidth products at these two temperatures were 43 mc and 65 mc. If the magnetic Q at 4.2°K is computed from the observed gain-bandwidth product, it will be found to be 210. The magnetic Q at 1.5°K is then 1.5/4.2 times 210, or 75, and the gain-bandwidth product computed for this magnetic Q is 62 mc, in excellent agreement with the observed value. It is for this reason that we said in the main text that gain-bandwidth products in excess of 100 mc are rather incredible unless special precautions are taken in simple regenerative cavity amplifiers, to achieve that gain-bandwidth product. Note that this result is independent of the operating frequency, and this means that the limiting gain-bandwidth product at L- or S-band would also be of the order of 50 mc.

This limitation is not widely understood. Giordmaine *et al.*[15] report for a single amplifier a gain-bandwidth product of 50 mc, using a permanent magnet, and 100 mc, using a laboratory magnet. No physical explanation is given, but it is implied that increase in gain-bandwidth product with the laboratory magnet was due to the greater homogeneity of the static field of the laboratory magnet. Since the magnetic Q is not the limitation here, the inverse should be true, for an inhomogeneous field will make B_x artificially larger!

It is interesting to note that, in the face of these considerations, one is not obliged to sacrifice greatly in gain-bandwidth product when operating at temperatures higher than that of liquid helium. For example, if the $5:10^4$ ruby is operated under the conditions suggested above, a magnetic Q of approximately 40 at 4.2°K would be obtained. One can approach a temperature of 40°K by pumping on the vapor over liquid nitrogen. This means that a magnetic Q of 400 could be obtained with a liquid nitrogen refrigerant, and this would yield a gain-bandwidth product of approximately 31 mc. The gain-bandwidth product for this same amplifier at 4.2°K would be 72. Thus, though the temperature is increased by a factor of ten, the loss in gain-bandwidth product is only 2.3.

As we have pointed out before, this limitation of gain-bandwidth product is no real limitation. Circularly-polarized cavity configuration can be conveniently cascaded because the circularly-polarized fields provide unidirectional coupling. For example, a series of three or four ruby cavities could be driven in cascade by coupling them to the circularly-polarized field which exists on the broad wall of a rectangular waveguide. Stagger-tuning the paramagnetic resonance frequencies would then give bandwidths several times B_x.

Some of the remarks made in the paper have been made rather prematurely, it is admitted, but the points are intended to be as much salutary as scientific. Only through a sure analytical understanding of the operation of these devices can the ultimate amplifier be confidently demanded, and only when it is confidently demanded will it be rapidly produced.[16]

Note:

Most of this paper was written in the Fall of 1958. The experimental results came slowly in the Spring of 1959. During this time, reports of extreme gain-bandwidth product in amplifiers constructed elsewhere—as much as 1200 mc for a single-cavity amplifier—were perplexing and indicated that our gain-bandwidth criterion[1] was not totally satisfactory. Paramagnetic amplifiers that we have built seem to meet our analytical expectations. Since some amplifiers that were built elsewhere apparently exceeded values allowed by the analysis herein, writing this paper made the author realize that an understanding of how to *design* such large gain-bandwidth amplifiers is obviously very important. One clue to the solution came from realizing that the reason that the exponent of G in the gain-bandwidth expression is $\frac{1}{2}$ is that the derivation essentially assumes a response of the form $[1+x^2]^{-1}$. With a response curve of the form $[1+x^{2n}]^{-1}$, the gain-bandwidth expression is $G^{1/(2n)}B=\text{constant}$. Thus, as n increases, *i.e.*, the response curve flattens, the bandwidth becomes increasingly independent of gain. This situation has now been resolved; and Kyhl has been able to indicate how constant-bandwidth gain-independent amplifiers can be realized with active paramagnets.[12] Thus, more than a year after this paper was started, although we now understand *how* larger gain-bandwidth products, using the meaningless $\sqrt{G}B$ criterion, can occur, the implication of the paper that they must be consciously and cleverly designed for remains significant.

[15] J. A. Giordmaine, *et al.*, "A maser amplifier for radio astronomy at X-band," Proc. IRE, vol. 47, p. 1067; June, 1959.

[16] For a different presentation of some of these points, see P. N. Butcher, "Theory of three-level paramagnetic masers," *Proc. Inst. Elec. Engrs.* (*London*), vol. 105, Part B, Supplement no. 11, pp. 684–711; May, 1958.

Correspondence

Absolutely Stable Hybrid Coupled Tunnel-Diode Amplifier*

A hybrid coupled tunnel-diode amplifier has been constructed using two matched tunnel diodes and a quarter-wave stripline coupled hybrid. Preliminary tests show that it has reasonable gain, extremely wide bandwidth, low noise, and more significantly, it is both open- and short-circuit stable at the input without any nonreciprocal device.

The block diagram of the amplifier is shown in Fig. 1. By proper wave cancellation, the hybrid coupled amplifier is a reciprocal bilateral amplifier with matched positive input and output impedances under ideal circumstances.[1,2] These conditions are 1) ideal hybrid action, 2) matched negative resistances, and 3) matched source and load impedances. The condition for stability is

$$|S_{21}|^2 |\rho_i| |\rho_0| < 1 \qquad (1)$$

where $|S_{21}|^2$ is the transducer power gain and ρ_i, ρ_0 are the source and load voltage reflection coefficients, respectively. It can be seen from (1) that if the load match is perfect, *i.e.*, $\rho_0 = 0$, then any source impedance variation would not render the circuit unstable. The transducer power gain and the noise figure of the amplifier, including the effect of noise from the load conductance at $T_0 = 290°K$, are

$$|S_{21}|^2 = \frac{4 G_0^2}{(G_0 + G_1 - \eta G)^2} \qquad (2)$$

$$F = 1 + \frac{G_1}{G_0} + \frac{20 I_0}{G_0} \eta + \frac{|S_{22}|^2}{|S_{21}|^2} \qquad (3)$$

where

G_0 = characteristic conductance of the line
G_1 = effective circuit loss
I_0 = dc bias current of the diodes
η = coupling factor
G = magnitude of the diode negative conductance at low frequencies
$|S_{22}|^2$ = reflective gain at the output
$|S_{21}|^2$ = transducer gain.

Ideally, $|S_{22}| = 0$, and we see that the noise contribution from the load vanishes in (3).

Two GE germanium tunnel diodes (ZJ56) are used. The peak currents of the units are 1.1 ma, and the minimum low-frequency negative resistance is 115 ohms. The diodes have a resistive cutoff frequency of 2.1 kmc, much beyond the operating frequency of the amplifier.

The tunnel diodes and the bias circuits are mounted on type-N connectors. The bias circuit must be such that dc operating point is single-valued in the negative resistance region, the bias loading at ac should be negligible, and any relaxation oscillation must be avoided.

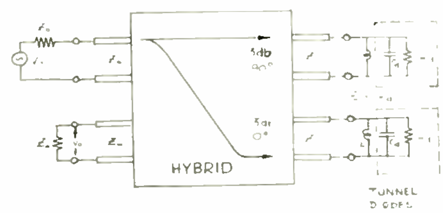

Fig. 1—Block diagram of hybrid coupled tunnel diode amplifier.

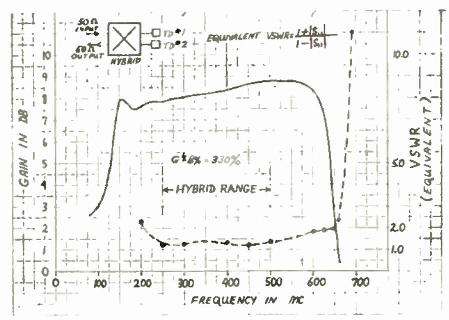

Fig. 2—Frequency response and equivalent input VSWR of hybrid coupled tunnel-diode amplifier.

Frequency Range	210 mc–625 mc
Gain	8.2 db ± 0.6 db
Noise Figure (@ 365 mc) a) Measured b) Calculated	 1.93 db ± 0.4 db* 1.5 db
Equivalent Input VSWR	<2.0
Gain ½ Percentage Bandwidth	330%
Dynamic Range a) ±1 db b) ±3 db c) Input level at −3 db deviation	 78 db 91 db −20 dbm (22 mv)
Input-Output Connections	50 Ω type N.
Tunnel Diodes	GE 1N 2939 (ZJ56)
Hybrid	SAGE 750
Stability with Input VSWR Variation	>100:1 (Load VSWR = 1.05)

* Limit of experimental accuracy.

Fig. 3—Experimental results of hybrid coupled tunnel-diode amplifier.

The equivalent input VSWR, calculated from the input reflective gain, is less than 2.0 from 210 mc to 625 mc. Over this frequency range, the gain is 8.2 db ± 0.6 db. The voltage gain percentage bandwidth product is 330 per cent. The noise figure was measured at 356 mc to be 1.9 db. The IF bandwidth used was 0.4 mc. There is no reason why the noise figure should vary at other frequencies since the noise isolation from the load is very good across the frequency band. The input saturation level for a −3 db deviation from linearity is −20 dbm. The circuit is absolutely stable with variation of bias circuit. For a load VSWR of 1.05, the circuit is absolutely stable for an input VSWR variation of greater than 50:1. The response shape and pertinent results are shown in Figs. 2, and Fig. 3.

The above results represent a usable low-noise regenerative amplifier with several orders of magnitude performance improvement over existing devices. The same principle can be used to extend this amplifier to higher frequencies as better tunnel diodes become available.

The author wishes to acknowledge the assistance of J. Kouzoujian in building the diode mounts and taking measurement data.

John J. Sie
Surface Communications Systems Lab.
RCA, Defense Electronics Products
75 Varick St.
New York 13, N. Y.

* Received by the IRE, March 14, 1960.

[1] J. Sie and S. Weisbaum, "Noise figure of receiver systems using parametric amplifiers," 1959 IRE National Convention Record, pt. 3, pp. 141–157.

[2] S. H. Autler, "Proposed for a maser amplifier without nonreciprocal elements," Proc. IRE, vol. 46, pp. 1880–1881; November, 1958.

Noise of Measure of Lossy Tunnel Diode Amplifiers*

An important question in tunnel diode amplifiers is how much the noise figure is deteriorated by circuit and device losses. It is the aim of this note to show that a very simple answer to this question becomes possible by using a series equivalent circuit of the junction.

The actual circuit under investigation is shown in Fig. 1(a). The device has a negative conductance $-g_d$ and a capacitance C_d in parallel and has a series resistance r. The device is tuned by means of a series inductor of inductance L_c and series resistance r_c. The source resistance R_s and the series resistances r_c and r should show thermal noise, and the junction itself should show full shot noise, that is

$$\overline{i_d^2} = 2eI_d\Delta f. \qquad (1)$$

In Fig. 1(b), the junction is represented by an equivalent circuit consisting of a resistance $-R$ and a reactance $-jX$ in series; obviously,

$$-R = -g_d/(g_d^2 + \omega^2 C_d^2). \qquad (2)$$

The noise of the junction is represented by an equivalent series noise emf e, given by

$$\overline{e^2} = 4kTR_n\Delta f, \qquad (3)$$

where R_n is the equivalent noise resistance of the junction. Bearing in mind that the exchangable noise power[1] of the junction is the same in the two representations, we get:

$$2eI_d\Delta f/g_d = 4kTR_n\Delta f/R,$$

or:

$$R_n/R = (e/2kT)(I_d/g_d). \qquad (4)$$

* Received by the IRE, April 11, 1960.

[1] H. A. Haus and R. B. Adler, "Optimum noise performance of linear amplifiers," Proc. IRE, vol. 46, pp. 1517–1533; August, 1958.

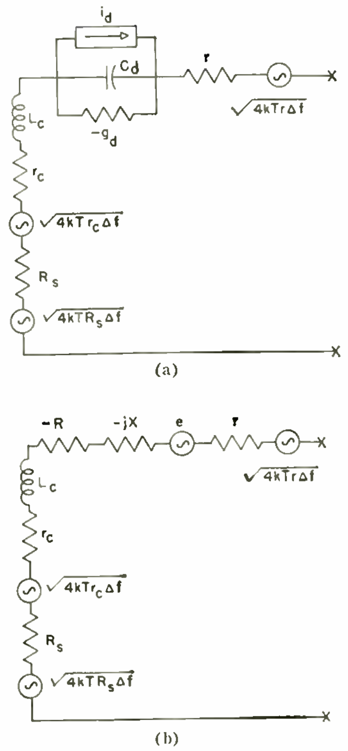

Fig. 1.

It is seen by inspection of Fig. 1(b) that the spot noise figure F at the tuning frequency of the circuit is given by

$$F = 1 + (R_n + r + r_c)/R_s, \quad (5)$$

whereas the available gain G_a is given by

$$G_a = R_s/(R_s - R + r + r_c). \quad (6)$$

The noise measure M of the circuit[1] is defined as

$$M = \frac{F-1}{1-1/G_a} = \frac{R_n + r + r_c}{R - r - r_c}$$
$$= \frac{M_0 + (r + r_c)/R}{1 - (r + r_c)/R}, \quad (7)$$

where M_0 is the noise measure for negligible losses:

$$M_0 = R_n/R = (e/2kT)(I_d/g_d). \quad (7a)$$

This factor is independent of frequency for all frequencies of practical interest.

Because of the term

$$(r + r_c)/R = (r + r_c)g_d(1 + \omega^2 C_d^2/g_d^2), \quad (7b)$$

the noise measure of the circuit increases with increasing frequency. This factor occurs twice: in the numerator and in the denominator. The factor in the numerator is caused by the thermal noise of the losses; the factor in the denominator is due to the deterioration of the available gain caused by these losses. The value of M becomes infinite at the frequency where $(r+r_c)/R=1$; at higher frequencies, the circuit ceases to operate as a negative resistance amplifier.

A. VAN DER ZIEL
Electrical Engrg. Dept.
University of Minnesota
Minneapolis 14, Minn.

A Parametric Subharmonic Oscillator Pumped at 34.3 KMC*

In a microwave-carrier computing system using subharmonic oscillators,[1-3] the ultimate limit of computing speed is determined by the rise time of the subharmonic oscillations. It can be shown[4] that this rise time is, in general, inversely proportional to the subharmonic frequency. This note describes a very high frequency parametric subharmonic oscillator using a specially packaged variable-capacitance germanium junction diode in a ridged waveguide circuit. This device requires less than 4 milliwatts of 34.3-kmc pump power to produce oscillations at the subharmonic frequency of 17.15 kmc, and has a maximum conversion efficiency of about seven per cent. It operates at considerably higher frequency and requires substantially less pump power than previously reported subharmonic oscillators.[5,6]

In the millimeter-wave region, coaxial and strip transmission-line circuits are not very useful because they are quite lossy; in addition, it is difficult to suppress higher-order modes in them. On the other hand, conventional waveguide circuits require complex cross-coupled structures because waveguides large enough to support the subharmonic frequency will propagate in higher modes at the pump frequency, and waveguides small enough to prevent these higher modes will be cut off to the subharmonic frequency. However, ridged waveguides may be designed to operate over very great bandwidths without propagating higher modes. A subharmonic oscillator may be constructed in which a single ridged waveguide will support both frequencies of interest in the same mode. Also, this ridged waveguide is smaller in size than the corresponding conventional rectangular waveguide having the same lower cutoff frequency.

Fig. 1 is a cutaway drawing of a subharmonic oscillator designed to be pumped by a klystron having a fixed frequency of 34.3 kmc. The oscillator consists of a length of RG-96 waveguide containing a single ridge centered on the wide wall, as shown. The lower cutoff frequency of rectangular waveguide of the same size is normally about 21 kmc. With the ridge inserted, however, this cutoff frequency is lowered to 15.4 kmc. The upper limit of operation before the TE_{20} mode occurs is 41.5 kmc.

The structure is designed so that a varactor diode, mounted in a special low-inductance encapsulation,[7] will nearly fill the cross-sectional area between the top of the

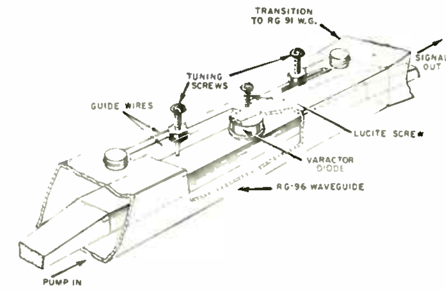

Fig. 1—Subharmonic oscillator for 34.3-kmc pump.

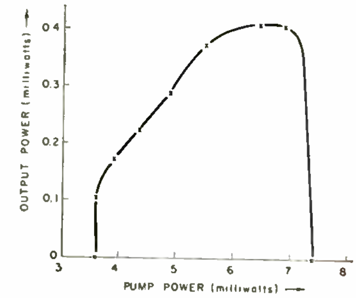

Fig. 2—Subharmonic power output vs incident pump power.

ridge and the upper waveguide wall. A characteristic of ridged waveguide is that the electric field is concentrated between the ridge and the waveguide wall above it. For a given power input, the electric-field intensity is much higher in this region than in any part of a conventional rectangular waveguide operating at the same frequency; hence, the diode in this structure occupies a most advantageous position. A lucite screw holds the diode in position and permits it to operate in a self-biased condition (there is no dc path between the diode and the upper waveguide wall). The circuit may be tuned to resonance at the subharmonic frequency by means of two sliding screws with adjustable penetration. The ridge is tapered at the input end so that pump power may be fed from standard RG-96 waveguide. At the output end there is a transition to RG-91 waveguide, which will propagate the subharmonic frequency. This transition consists of a growing taper of the waveguide walls and a diminishing taper of the ridge height.

Several variable-capacitance germanium junction diodes[7] were tested in this oscillator. These diodes, measured at a bias of −1.0 volt, ranged in cutoff frequency from 130 to 159 kmc, and in capacitance from 0.31 to 0.76 micromicrofarad. All the diodes were able to reproduce oscillations at the subharmonic frequency of 17.15 kmc.

Fig. 2 shows the subharmonic power output as a function of incident pump power for a diode having a Q of about 10 at the subharmonic frequency. Pump power of less than 4 milliwatts was required to start oscillations; maximum output was obtained with about 6 milliwatts. Maximum conversion efficiency was about seven per cent.

The oscillator may also be used as an amplifier if a signal is fed into the output end through a tee or a circulator. Although this type of operation was not thoroughly investigated, a preliminary test showed that power gain could be obtained in the vicinity of 17.15 kmc.

* Received by the IRE, March 28, 1960. The work reported here was supported by the Bureau of Ships under Contract No. NObsr 72717.

[1] J. Von Neumann, "Non-linear capacitance or inductance switching, amplifying, and memory organs," U. S. Patent No. 2,815,488; December 3, 1957.

[2] R. L. Wigington, "A new concept in computing," PROC. IRE, vol. 47, pp. 516–523; April, 1959.

[3] E. Goto, "The parametron, a digital computing element which utilizes parametric oscillations," PROC. IRE, vol. 47, pp. 1304–1316; August, 1959.

[4] J. Hilibrand and W. R. Beam, "Semiconductor diodes in parametric subharmonic oscillators," *RCA Rev.*, vol. 20, pp. 229–253; June, 1959.

[5] F. Sterzer, "Microwave parametric subharmonic oscillators for digital computing," PROC. IRE, vol. 47, pp. 1317–1324; August, 1959.

[6] B. C. De Loach and W. M. Sharpless, "An X-band parametric amplifier," PROC. IRE, vol. 47, pp. 1664–1665; September, 1959.

[7] J. Hilibrand, C. W. Mueller, C. F. Stocker, and R. D. Gold, "Semiconductor parametric diodes in microwave computers," IRE TRANS. ON ELECTRONIC COMPUTERS, vol. EC-8, pp. 287–297; September, 1959.

The authors thank Dr. J. A. Rajchman for encouraging this work, Dr. C. W. Mueller for supplying the variable-capacitance diodes, and H. C. Johnson for technical assistance.

A. H. Solomon
F. Sterzer
Radio Corp. of America
Electron Tube Div.
Princeton, N. J.

17.35 and 30-KMC Parametric Amplifiers*

Parametric amplifiers have previously been reported at frequencies as high as 11.55 kmc.[1,2] Point contact gallium arsenide diodes were used in these amplifiers. It was expected that these diodes would operate at considerably higher frequencies, and to demonstrate this capability degenerate amplifiers were built with first a 34.7-kmc pump frequency and second a 60.0-kmc pump frequency.

The 17.35-kmc amplifier (34.7-kmc pump frequency) employed the type I gallium arsenide diodes of footnote 2. Gain bandwidth measurements were not made on this amplifier but an upper limit on noise figure was obtained (Fig. 1) by means of a narrow-

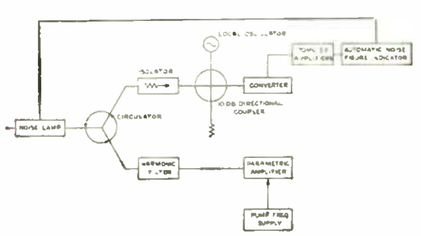

Fig. 1.

band converter and an automatic noise figure indicator employing an argon noise lamp. The noise figure of the converter employed was 18.5 db. With the parametric amplifier appropriately adjusted and preceding the converter the over-all system double-sideband noise figure was reduced to 7 db (±1 db). Since a loss of 1 db preceded the parametric amplifier itself (0.6-db harmonic filter loss and 0.4-db circulator loss) a double-sideband noise figure of less than 6 db is indicated for the amplifier. Due to the simplicity of the circuit employed, adjustments were quite difficult to make. However, amplification and oscillations also were obtained with type II gallium arsenide diodes[2] as well as with p-type and n-type silicon diodes.[3]

The 30-kmc amplifier tests utilized a new traveling-wave amplifier tube, built by the tube development department of these laboratories, to supply the 60-kmc pump power. Specially designed diodes were built into the waveguide circuit. Gain and subharmonic oscillations were obtained here also with gallium arsenide point contact diodes[1] and with p-type and n-type silicon[3] diodes. Subharmonic oscillations were obtained with as little as 28 milliwatts of pump power. It is believed that much higher frequency operation is possible with these diodes and that, as higher frequency pump sources are obtained, this operation will become a reality.

B. C. DeLoach
Bell Telephone Labs., Inc.
Holmdel, N. J.

* Received by the IRE, April 20, 1960.

[1] B. C. De Loach and W. M. Sharpless, "An X-band parametric amplifier," Proc. IRE, vol. 47, pp. 1664–1665; September, 1959.

[2] B. C. De Loach and W. M. Sharpless, "X-band parametric amplifier noise figures," Proc. IRE, vol. 47, p. 2115; December, 1959.

[3] Small area p-n junction diodes especially processed for this application by C. A. Burrus of Bell Telephone Labs., Inc., Holmdel, N. J. (To be published.)

[1] Special diodes provided by W. M. Sharpless of Bell Telephone Labs., Inc., Holmdel, N. J.

Single-Diode Parametric Up-Converter with Large Gain-Bandwidth Product*

A voltage gain-bandwidth product of 41.1 per cent has been obtained in a low-noise nondegenerate lower sideband up-converter using a single parametric diode. Gain-bandwidth products of 57 per cent were also obtained, but with noise figures greater than 3 db. It is felt that these initial experimental results represent a definite advancement in the parametric art and indicate the feasibility of single-diode broad-band regenerative amplifiers in the microwave region.

The frequency converter type of amplifier was operated at a signal frequency of 1000±65 mc with a pump centered at 10,295 mc. The difference frequency output was 9295±65 mc. The gain was 10 db, while the noise figure was 2.3 db[1]. Fig. 1 is a schematic representation of the physical structure. In order to keep the frequency sensitivity of the device as low as possible and, to enhance the independence of various tuning adjustments, the diode mount is simply a section of uniform X-band waveguide instead of the more common waveguide cross. A high-pass filter in the form of a short length of waveguide below cutoff is used to stop the idler frequency (9295 mc) while passing the pump at 10,295 mc. The other port of the diode mount faces a maximally-flat filter of 180 mc bandwidth, centered in the idler frequency. The location of this filter together with the position of the high-pass filter were adjusted so as to approximate a condition where the self-admittance Y_{22} of the diode is a part of the idler filter structure. An isolator is used in the idler circuit in order to present a constant output load impedance to the device at all times. It is not an essential circuit element. In the signal circuit, a coaxial monitor tee enables dc bias to be applied to the diode while the coaxial low-pass filter blocks the idler and the pump frequencies. No attempt was made to optimize the position of the low-pass filter. The three filters are also seen to perform three additional functions. First, the various frequencies are confined to their respective circuits and are not loaded down unnecessarily by losses from other parts of the device. Second, the filters help to provide mutually independent tuning adjustments, *i.e.*, adjusting the slide-screw tuner in the idler circuit, for example, does not affect the pump frequency tuning and vice versa. Third, the filters also act as frequency selective tuning plungers when their positions with respect to the diode are varied, since they act as short circuits only for frequencies in the stop band while appearing nearly transparent to those in the pass band. Experiments have shown that the positions of the two waveguide filters with respect to the diode are very much less critical than the positions of the tuning plungers in parametric structures utilizing crossed waveguides.

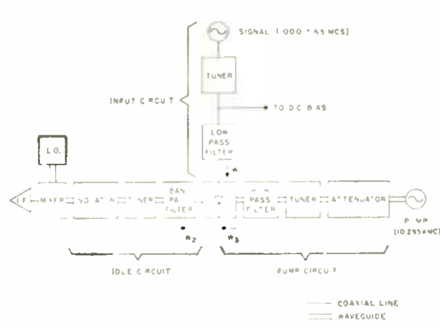

Fig. 1—Schematic representation of the parametric up-converter unit.

If the settings of various tuning devices influence all three frequencies, *i.e.*, signal, idler and pump, then a systematic experimental study of the up-converter becomes rather difficult because of the many uncontrollable interactions present. Therefore, the independence between the three circuits and their tuning elements is an essential requirement for good reproducibility of results and ease of tuning.

The up-converter just described exhibits the following characteristics:[1,2]

Gain	10 db,
Bandwidth	130 mc,
Noise figure	2.3 db,
Dynamic range[3] (±1 db deviation)	99.2 db,
Dynamic range[3] (±3 db deviation)	109.5 db,
3-db input saturation level	−4.5 dbm, and
Diode characteristics	$C_0=2.0\ \mu\mu f$, $F_c=52$ kmc (at C_{min}).

A photograph of the amplifier response is shown in Fig. 2.

For most work, pump powers of 30–85 mw and a negative bias of approximately −0.2 volt were used. Either low pump powers or some negative bias was found to be necessary in order to achieve a low noise figure. This is not unexpected, since too large a swing in pump voltage can carry the diode to a forward conducting region where high currents will rapidly degrade the noise figure. The measured noise figure of 2.3 db was constant within the pass band of the device.

Measurements of stability as a function of mismatch at the input generator (or an-

* Received by the IRE, March 14, 1960. This work was partially sponsored by Contract AF 30-602-2115 AICBM Radar Techniques.

[1] Noise figure measurement includes an output insertion loss of 0.5 db.

[2] These results were obtained concurrently.

[3] Postreceiver bandwidth equal to 0.6 mc.

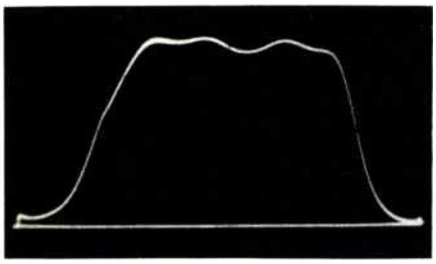

Fig. 2—Swept gain characteristic of the up-converter.

tenna) have shown that a VSWR of 1.8 can exist before the output characteristic is distorted by ±3 db. Fig. 3 shows the gain characteristic as a function of the incident pump power. For this experiment the up-converter was adjusted to a gain of 13 db. This type of up-converter could be made tunable over a wide frequency range by tracking the pump frequency with respect to the signal frequency in order to maintain a constant difference. The experimental device has also been operated at signal frequencies of 700 mc and 2000 mc, respectively, with slight adjustments in tuning.

The above encouraging results stem from an integration of experimental work and a theoretical analysis[1] which uses a more realistic model for the parametric diode (*i.e.*, includes the parasitic elements of the varactor diode such as the lead inductance L and the internal resistance R_S). The equivalent circuit of the diode is as shown in Fig. 4. If the Q of the diode is very high at the operating frequency, then the quantities shown in the figure become purely imaginary. Thus,

$$Y_{11} = \frac{j\omega_1 C_0}{D}\left[\beta_2 + \left(\frac{\omega_2}{\omega_0}\right)^2\left(\frac{\Delta C}{2}\right)^2\right], \quad (1)$$

$$Y_{12} = j\omega_1 \frac{\Delta C}{2D}, \quad (2)$$

$$Y_{21} = -j\omega_2 \frac{\Delta C}{2D}, \quad (3)$$

$$Y_{22} = -j\omega_2 \frac{C_0}{D}\left[\beta_1 + \left(\frac{\omega_1}{\omega_0}\right)^2\left(\frac{\Delta C}{2}\right)^2\right], \quad (4)$$

$$D = \beta_1\beta_2 - \frac{\omega_1^2\omega_2^2L^2\left(\frac{\Delta C}{2}\right)^2}{\beta_3^2},$$

$$\beta_n = 1 - \left(\frac{\omega_n}{\omega_0}\right)^2, \quad \text{and}$$

$$\omega_0 = \frac{1}{\sqrt{LC_0}}$$

= series resonance frequency of the diode.

C_0 = static capacitance of the diode at the bias point.

At resonance, the self-admittances of the diode, Y_{11} and Y_{22}, are tuned out by reactive elements in the input and output circuits. Under these conditions, the over-all circuit becomes that of Fig. 5, and the transducer gain G_T is obtained by applying conventional theory of four-terminal networks.

$$G_T = \frac{|v_2^*|^2 G_L}{\dfrac{|i_g|^2}{4G_g}} = \frac{4G_gG_L\omega_2G}{G_{T_2}[G_{T_1} - G]^2\omega_1} \quad (5)$$

[1] J. J. Sie, "Controlled Source Representation of a Parametric Diode," RCA Internal Rept.; December, 1959.

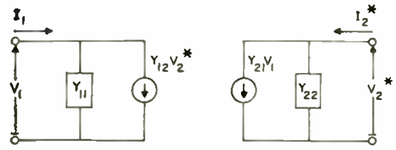

Fig. 3—Equivalent circuit of parametric diode.

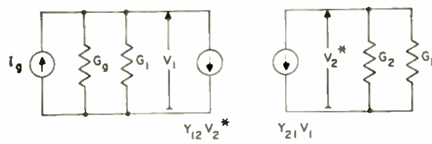

Fig. 4—Equivalent circuit of the up-converter at resonance.

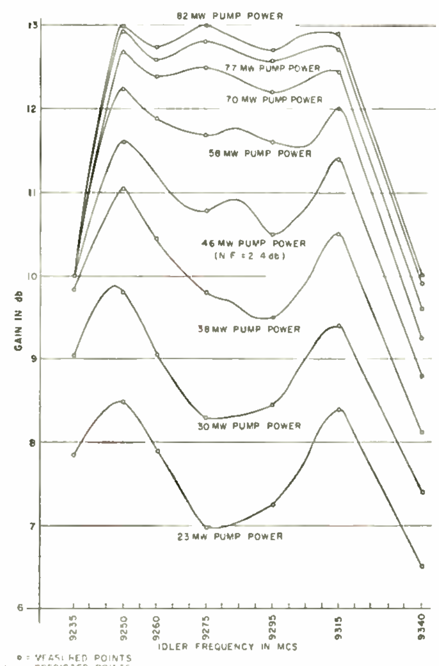

Fig. 5.

where

$$G_{T_1} = G_g + G_1,$$

$$G_{T_2} = G_L + G_2,$$

$$G = \frac{\omega_1\omega_2(\Delta C)^2}{4G_{T_2}D^2}, \quad (6)$$

and G_1, G_2 represent losses in the two circuits.

Off resonance, the sharp selectivity of single-cavity structures used to tune out Y_{11} and Y_{22} renders the gain low, and the gain-bandwidth product of the device is rather small. A further deterioration is caused by the presence of frequency sensitive parasitic elements in the diode [$D \neq 1$ in (1)–(4) and (6)]. These limitations can be alleviated by the use of multiple-cavity networks in which the self-admittances Y_{11} and Y_{22} at the input and output frequencies are incorporated as parts of a ladder structure. In this manner, the admittances seen at the diode, looking in either direction, can be kept real over a large band of frequencies and substantial gain-bandwidth products are possible. Because of the frequency sensitive terms in G [see (6)], the gain will not be altogether flat; yet the basic argument of obtaining broad bandwidth still holds.

An interesting aspect of (5) and (6) is that the gain is increased by decreasing either G_{T_1} or G_{T_2}. If standard size lines must be used, suitable transformers are necessary to adjust the admittances seen at the diode. By simply lowering G_{T_2} by a factor of four, we were able to increase the gain to 20 db at points throughout the amplifier pass band. These results indicate that a properly synthesized idler network will greatly increase the gain-bandwidth product. For a given diode and a given set of operating frequencies, the lowest safe limit for G_g and G_L is obviously determined by stability requirements. Thus, if the method of utilizing Y_{11} and Y_{22} as parts of a broadband ladder structure is coupled with broadband transformations of G_g and G_L, large gain-bandwidth products are possible.

The authors wish to thank J. Kouzoujian for helping with the experimental work and J. Sie for interesting discussions on the theoretical analysis.

R. PETTAI
B. BOSSARD
S. WEISBAUM
RCA-Defense Electronic Products
Surface Communications Systems Lab.
New York, N. Y.

Optimum Noise Performance of Parametric Amplifiers*

In the literature there exist various analyses for the noise performance of parametric amplifiers.[1–4] It has been shown, for example, there is a minimum noise figure for the ideal negative-resistance parametric amplifier at room temperature given by the ratio of pump to idle frequency,[3] while for the pure up-converter there is no such minimum.[4] When one begins to include the effects of various circuit losses, however, the expressions rapidly multiply into a maze of conductances, circuit Q's, and frequency ratios. The result is quite often one of confusion in trying to determine in practice just how low a noise figure one can expect. It is the purpose of this note to present in brief form the results of some analysis done in an attempt to answer this question. It is planned to submit the details of this analysis for publication at a later date.

The assumed amplifier model will consist of a semiconductor diode placed in a suitable resonant structure. It will be assumed that circuit loss is small compared to the diode loss. (The degree to which this condition is met in practice may be considered a measure of the quality of the circuit, for any such loss will increase the noise

* Received by the IRE, February 23, 1960; revised manuscript received, April 15, 1960.

[1] H. Heffner and G. Wade, "Gain, bandwidth and noise characteristics of the variable-parameter amplifier," *J. Appl. Phys.*, vol. 29, pp. 1321–1331; September, 1958.

[2] S. Bloom and K. K. N. Chang, "Theory of parametric amplification using nonlinear reactances," *RCA Rev.*, vol. 18, pp. 578–593; December, 1957.

[3] H. Heffner and G. Wade, "Minimum noise figure of a parametric amplifier," *J. Appl. Phys.*, vol. 29, p. 1262; August, 1958.

[4] D. Lennov, "Gain and noise figure of a variable capacitance up-converter," *Bell Sys. Tech. J.*, vol. 37, pp. 989–1008; July, 1958.

figure above that predicted by this analysis.) For the case of the negative-resistance amplifier, the additional assumptions will be made that the amplifier is operated at high gain with an ideal circulator, and that the idler circuit is resistively loaded only by the diode loss. Series circuit representations will be assumed, as shown in Fig. 1. The ideal filters are open circuits except at the indicated frequencies, at which point they become short circuits. In practice these filters might be approximated by high-Q series resonant circuits.

With these assumptions, the results turn out to be functions of two parameters of the diode: capacitance change and diode Q. We will define

$$\gamma = \frac{C_1}{2C_0} \qquad Q = \frac{1}{\omega_s C_0 R_s} \tag{1}$$

where in the small signal approximation we have a capacitance varying as $C = C_0 + C_1 \cos \omega_p t$ in series with a constant resistance R_s. The quantity γ is of course a function of pump power.

For the up-converter, analysis shows there exists an optimum load and source impedance to achieve a minimum noise figure with a given diode.[4] This minimum noise figure is given very closely by

$$F_{\min} = 1 + 2\frac{T_d}{T_0}\left[\frac{1}{\gamma Q} + \frac{1}{(\gamma Q)^2}\right] \tag{2}$$

where

T_d = temperature of diode resistance, °K
T_0 = 290°K.

The corresponding source and load resistances are

$$R_g = R_l = R_s\sqrt{1 + (\gamma Q)^2}. \tag{3}$$

It can also be shown that when the up-converter is optimized for maximum gain, instead of minimum noise figure, the expression for transducer power gain becomes

$$g = \frac{(\gamma Q)^2}{\left[1 + \sqrt{1 + \frac{\omega_{\text{in}}}{\omega_{\text{out}}}(\gamma Q)^2}\right]^2} \tag{4}$$

when

$$R_g = R_l = R_s\sqrt{1 + \frac{\omega_{\text{in}}}{\omega_{\text{out}}}(\gamma Q)^2}. \tag{5}$$

While the noise figure is somewhat higher in this case, the gain is also higher, the net result being little difference in over-all system noise figure.

By examining (4), we see that a practical up-converter should have a value of γQ of about ten or so. (It is interesting to note that the maximum possible gain for an up-converter is equal to $\frac{1}{4}(\gamma Q)^2$, and is independent of the frequency ratios involved.) The value of γ which one can obtain depends upon the diode capacitance-voltage characteristic as well as the amount of pump power available. An analysis of the Fourier coefficients of capacitance indicates that a reasonable value might be $\gamma = 0.3$. Assuming $\gamma = 0.3$, we see that a diode Q of 33 at signal frequency will be needed to give $\gamma Q = 10$. The minimum noise figure that one could hope to obtain with this diode would then be given by (2). At room temperature this minimum noise figure would be about 0.8 db.

Quite similar noise figure formulations can be obtained for the negative-resistance

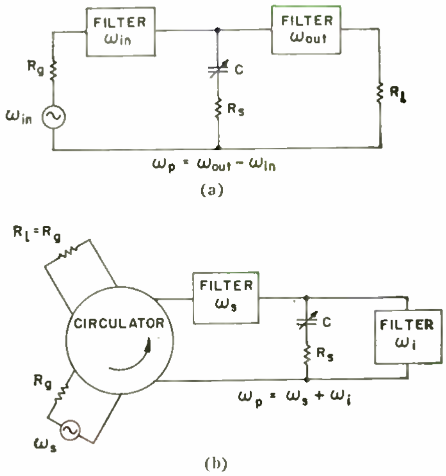

Fig. 1—Circuit models used in analysis of up-converter and negative-resistance amplifier. (a) Up-converter. (b) Negative-resistance amplifier.

parametric amplifier. With the assumptions previously mentioned, the minimum noise figure with the diode at room temperature can be written as

$$F_{\min} = \frac{1}{1 - \frac{\omega_s}{\omega_p}} \cdot \frac{(\gamma Q)^2}{(\gamma Q)^2 - \frac{\omega_p}{\omega_s} + 1}. \tag{6}$$

It is easily shown there exists an optimum ratio of pump to signal frequency for minimum noise figure. In a lossless amplifier, no such optimum frequency ratio exists, and the noise figure will always decrease as the pump frequency is increased. However, when a lossy diode is used, raising the pump frequency will not necessarily lower the noise figure because the diode Q at the idle frequency decreases with increasing pump frequency. The optimum frequency ratio is found by differentiation of (6). The result is

$$\left(\frac{\omega_p}{\omega_s}\right)_{\text{optimum}} = \sqrt{1 + (\gamma Q)^2}. \tag{7}$$

The noise figure at room temperature for this optimum condition is then closely given by

$$F_{\min} = 1 + 2\left[\frac{1}{\gamma Q} + \frac{1}{(\gamma Q)^2}\right] \tag{8}$$

which is identical to the result obtained for the up-converter. The source resistance which is needed to give this minimum noise figure is

$$R_g = R_s\sqrt{1 + (\gamma Q)^2} \tag{9}$$

Another point of interest is the comparison of the noise performance of a degenerate parametric amplifier with that of the optimum negative-resistance "three-frequency" amplifier just discussed. The minimum noise figure (single-sideband signal) for a degenerate parametric amplifier can be written as

$$F_d = 2 + 2\left[\frac{1}{\gamma Q} + \frac{1}{(\gamma Q)^2}\right]. \tag{10}$$

Note that this result *cannot* be obtained from (6) since the assumption of no excess idler loading was made in its derivation.

For comparison purposes, an operating noise temperature will be defined:

$$T_{\text{op}} = \frac{N_{\text{out}}}{gkB};$$

N_{out} = total noise power delivered to load
g = transducer gain
k = Boltzmann's constant
B = noise bandwidth. (11)

A simple rearrangement will show that

$$S_{\text{in}} = (S/N)_{\text{out}} KBT_{\text{op}},$$

where

S_{in} = input signal power
$(S/N)_{\text{out}}$ = output signal-to-noise ratio. (12)

When a minimum usable output signal-to-noise ratio is specified, (12) can be interpreted as an expression for receiver sensitivity. Operating noise temperature as defined here is directly related to operating noise figure as used by Strum[5] and others. The relation is simply

$$T_{\text{op}} = F_{\text{op}} T_0,$$

where

$$F_{\text{op}} = \text{operating noise figure}. \tag{13}$$

For amplifiers other than the degenerate parametric amplifier it is easily shown that

$$T_{\text{op}} = (F - 1)T_0 + T_A,$$

where

$$T_A = \text{antenna temperature}. \tag{14}$$

For the single-sideband degenerate parametric amplifier, the operating noise temperature is

$$(T_{\text{op}})_d = (F_d - 2)T_0 + 2T_a. \tag{15}$$

Substituting (8) and (10) into the appropriate expressions for operating noise temperature we obtain,

$$T_{\text{op}} = 2T_0\left[\frac{1}{\gamma Q} + \frac{1}{(\gamma Q)^2}\right] + T_A \tag{16}$$

for the optimum "three-frequency" amplifier at room temperature; and

$$(T_{\text{op}})_d = 2T_o\left[\frac{1}{\gamma Q} + \frac{1}{(\gamma Q)^2}\right] + 2T_A \tag{17}$$

for the optimum degenerate amplifier at room temperature. Therefore,

$$(T_{\text{op}})_d - T_{\text{op}} = T_A. \tag{18}$$

Hence, an optimum degenerate parametric amplifier in single-sideband operation will have a somewhat higher operating noise temperature than the corresponding optimum three-frequency amplifier. It is interesting to note that the difference is equal to the antenna temperature. For the special application where the signal is broad-band noise, as in radiometry, the so-called double-sideband noise figure of the degenerate amplifier is applicable, and the appropriate operating noise temperature is just one-half that given above for the single-sideband case. For this application the degenerate amplifier will have the lower operating noise temperature.

This work was done in the Apparatus Division of Texas Instruments, Inc., Dallas, Tex., whose support the author gratefully acknowledges.

K. L. Kotzebue
Watkins-Johnson Co.
Palo Alto, Calif.

[5] P. D. Strum, "A note on noise temperature," IRE Trans. on Microwave Theory and Techniques, vol. MTT-4, pp. 145–151; July, 1956.

WWV and WWVH Standard Frequency and Time Transmissions*

The frequencies of the National Bureau of Standards radio stations WWV and WWVH are kept in agreement with respect to each other and have been maintained as constant as possible with respect to an improved United States Frequency Standard (USFS) since December 1, 1957.

The nominal broadcast frequencies should, for the purpose of highly accurate scientific measurements, or of establishing high uniformity among frequencies, or for removing unavoidable variations in the broadcast frequencies, be corrected to the value of the USFS, as indicated in the table below.

The characteristics of the USFS, and its relation to time scales such as ET and UT2, have been described in a previous issue,[1] to which the reader is referred for a complete discussion.

The WWV and WWVH time signals are also kept in agreement with each other. Also they are locked to the nominal frequency of the transmissions and consequently may depart continuously from UT2. Corrections are determined and published by the U. S. Naval Observatory. The broadcast signals are maintained in close agreement with UT2 by properly offsetting the broadcast frequency from the USFS at the beginning of each year when necessary. This new system was commenced on January 1, 1960. The last time adjustment was a retardation adjustment of 0.02 s on December 16, 1959.

WWV FREQUENCY
WITH RESPECT TO U. S. FREQUENCY STANDARD

1960 April 1600 UT	Parts in 10^{10}†
1	−146
2	−146
3	−146
4	−146
5	−146
6	−146
7	−146
8	−146
9	−147
10	−147
11	−147
12	−147
13	−146
14	−146
15	−146
16	−146
17	−146
18	−146
19‡	−145
20	−146
21	−146
22	−146
23	−146
24	−146
25	−146
26	−146
27	−146
28	−146
29	−146
30	−146

† A minus sign indicates that the broadcast frequency was low.
‡ On April 19 the frequency was decreased 2×10^{-10}.

NATIONAL BUREAU OF STANDARDS
Boulder, Colo.

* Received by the IRE, May 23, 1960.

[1] "United States National Standards of Time and Frequency," PROC. IRE, vol. 48, pp. 105–106; January, 1960.

Millimeter Wave Generation by Parametric Methods*

One of the most dependable methods of generating coherent millimeter wave radiation has been the multiplication of some lower frequency by means of the nonlinear resistance of a semiconductor diode. This technique has been used successfully by many workers in the field of molecular spectroscopy. Some fairly typical results are those published by Johnson, Slager, and King[1] in which a conversion loss of −18 db was obtained for the second harmonic (6.25 mm) of a 24-kmc (12.5 mm) fundamental.

Manley and Rowe[2] have derived a power relation for three linear circuits which are resonant individually at frequencies ω_1, ω_2, and ω_3, and coupled by means of a nonlinear reactance. This power relation states that

$$\frac{P_{12}}{\omega_1+\omega_2} = -\frac{P_1}{\omega_1} = -\frac{P_2}{\omega_2}$$

where P_{12}, P_1, P_2 are the average powers flowing into the nonlinear reactor at the frequencies $\omega_1+\omega_2$, ω_1 and ω_2. The fact that power flows from the reactor at the lower frequencies ω_1 and ω_2, at the expense of the higher-frequency pumping power, is indicated by the minus signs. The above power relations can also be written as

$$\frac{-P_{12}}{\omega_1+\omega_2} = \frac{P_1}{\omega_1} = \frac{P_2}{\omega_2}.$$

This suggests that if the reactor is pumped at the two lower frequencies, power will flow from the reactor at the higher frequency $\omega_1+\omega_2$. It is obvious that the two lower-frequency pumps can have the same frequency, making harmonic generation possible from this scheme. Since the nonlinear reactance is essentially lossless, the conversion efficiency should be high compared to those obtained with nonlinear resistances.[3,4]

Using the nonlinear (voltage-dependent) capacitance of a back-biased semiconductor function diode in a coaxial circuit, Chang[5] has obtained a conversion efficiency of 21 per cent (−6.8 db) for doubling from 3300 to 6600 mc. The extension of this principle to the millimeter region is not an easy one. Indeed, the only published experimental result is that of Kita,[6] who obtained a minimum conversion loss of 15.8 db in doubling from 24,000 to 48,000 mc using a germanium point-contact diode. The main problems are those of obtaining materials suitable for operation in the millimeter region, and a microwave system capable of high performance at these frequencies. This note describes some recent experiments in the generation of millimeter waves using the nonlinear capacitance of a back-biased, point-contact gallium arsenide semiconductor diode.

EXPERIMENTAL METHODS

The experimental setup employed is shown schematically in Fig. 1. The modulated input signal was 24 kmc and the output of the harmonic generator was observed at 48 kmc. The harmonic generator consisted of a K-band fundamental guide (operating range, 18–26 kmc) crossed by an RG98U harmonic guide (operating range, 45–75 kmc). This is shown in Fig. 2. The harmonic guide acts as a high-pass filter which is below cutoff for the fundamental radiation. Thus, separation between input and output frequencies was obtained.

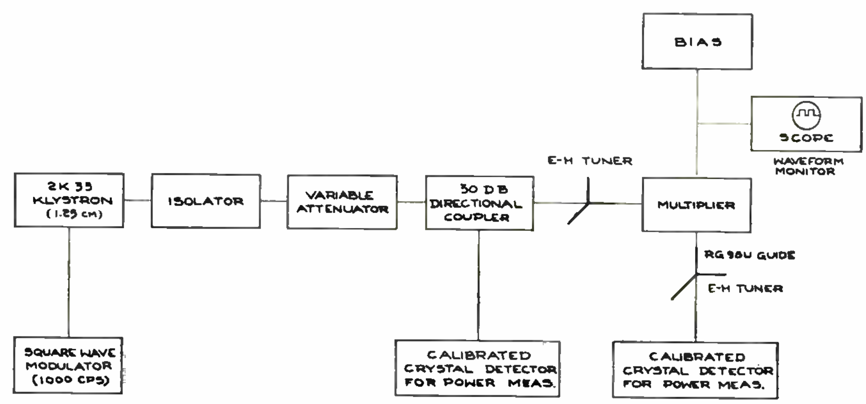

Fig. 1—Block diagram of measuring apparatus.

The crystal was mounted, flush with the bottom of the harmonic guide, at the junction of the two guides, and an RF by-pass is provided so that a dc bias can be employed. A differential screw mounted on the top of the guide with an effective pitch of 364 turns per inch permitted extremely low pressure contacts to be made to the crystals. Short-circuiting plungers were employed behind the crystal in both fundamental and harmonic guides for matching purposes.

EXPERIMENTAL RESULTS

The results obtained with gallium arsenide point-contact nonlinear capacitance

* Received by the IRE, December 21, 1959. This work was sponsored in part by the Air Res. and Dev. Command, AF Cambridge Res. Center, under Contract No. AF19(604)-4980.

[1] C. M. Johnson, D. M. Slager, and D. D. King, "Millimeter waves from harmonic generators," *Rev. Sci. Instr.*, vol. 25, pp. 213–217; March, 1954.
[2] J. M. Manley and H. E. Rowe, "Some general preoperties of nonlinear elements," PROC. IRE, vol. 44, pp. 904–913; July, 1956.
[3] A. Uhlir, "Potential of semiconductor diodes in high-frequency communications," PROC. IRE, vol. 46, pp. 1099–1115; June, 1958.
[4] D. Leenov and A. Uhler, "Generation of harmonics and subharmonics" at microwave frequencies with p-n junction diodes, PROC. IRE, vol. 47, pp. 1724–1729; October, 1959.
[5] K. K. N. Chang, "Harmonic generation with nonlinear reactances," *RCA Rev.*, vol. 19, pp. 455–464; September, 1958.
[6] S. Kita, "A harmonic generator by use of the nonlinear capacitance of germanium diode," PROC. IRE, vol. 46, p. 1307; June, 1958.

Fig. 2—Harmonic generator.

diodes are summarized below.

Fundamental frequency = 24,000 mc
Second harmonic = 48,000 mc
Conversion loss = 9 db
Bias = zero.

The gallium arsenide crystals employed in these experiments were n-type with a resistivity of 0.009 ohm-cm.

The superiority of point-contact gallium arsenide nonlinear capacitance diodes over the germanium variety can be explained as follows. The higher electron mobility of gallium arsenide gives rise to a lower spreading resistance. This, together with the lower capacitance due to a lower dielectric constant, yields a higher value of cutoff frequency than germanium or silicon units. In addition, the higher band gap of gallium arsenide gives rise to a voltage-current characteristic which increases more slowly in the forward direction than that for germanium. This permits wider voltage excursions into the forward direction, where the capacitance nonlinearity is greatest, before appreciable diode current is drawn and the Q deteriorates.

The author wishes to acknowledge many helpful discussions with Drs. K. K. N. Chang, W. Eckhardt, and B. Rosenblum. The gallium arsenide crystals were provided by C. F. Stocker.

George H. Heilmeier
David Sarnoff Res. Center
RCA Labs.
Princeton, N. J.

Effect of a Generator or Load Mismatch on the Operation of a Parametric Amplifier*

In order to minimize the contribution of the load to the noise figure of a parametric amplifier without a circulator, it may be desirable to make the effective generator conductance in the signal circuit much larger than the effective load conductance. In this analysis, it is found that for such a "mismatch," a condition of potential instability results. For a severe mismatch, a parametric amplifier is very likely to break into oscillation; for a slight mismatch, an amplifier remains stable. In what follows, it is assumed that the reader is acquainted with the referenced literature.[1-3]

* Received by the IRE, December 6, 1959.

In order to obtain a low noise figure with a parametric amplifier without any nonreciprocal devices, such as a circulator or isolator, it is desirable to make the generator conductance much larger than the sum of all other signal-circuit conductances. If "match" is defined as the condition where the generator conductance is equal to the sum of all other signal-circuit conductances (including load conductance), the condition for minimum noise figure then corresponds to that of maximum mismatch. It is the purpose of this analysis to show the effect of such a mismatch on amplifier gain and stability.

The equivalent circuit for a parametric amplifier without a circulator is shown in Fig. 1.

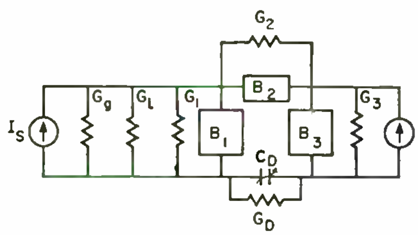

Fig. 1—Parametric amplifier equivalent circuit.

The equivalent circuit consists of signal, idler and pump resonant circuits, B_1, B_2, B_3, respectively, such that $\omega_3 = \omega_2 + \omega_1$.

Across the signal circuit there is a current source I_s, a generator conductance G_g, a load conductance G_L, and other loss conductances G_1. The idler circuit has a loss conductance G_2 across it, and the pump circuit has a loss conductance G_3 and a current source I_P across it. These circuits are all connected through a nonlinear capacitor C_D with a conductance G_D across it. The nonlinearity of the capacitor is given by $C_D = C_0 + \mathcal{C} V$, where V is the voltage across the nonlinear capacitor. The gain for this circuit at resonance is

$$A = \frac{4G_L G_g}{G_T^2(1-\alpha)^2}, \tag{1}$$

where

$$\alpha = \frac{\omega_1\omega_2(\Delta C)^2}{G_T G_2} \tag{2}$$

and

$$(\Delta C)^2 = \left(\frac{\mathcal{C} I_p}{G_3}\right)^2 \tag{3}$$

$$G_T = G_g + G_L + G_D + G_1. \tag{4}$$

[1] S. Bloom and K. K. N. Chang, "Theory of parametric amplification using nonlinear reactances," *RCA Rev.*, vol. 18, pp. 578–596; December, 1957.

[2] H. Heffner and G. Wade, "Gain bandwidth characteristics of the variable parametric amplifier," *J. Appl. Phys.*, vol. 29, pp. 1321–1331; September, 1958.

[3] R. C. Knechtli and R. D. Weglein, "Low noise parametric amplifier," Proc. IRE, vol. 47, pp. 584–585; April, 1959.

Let us define

$$G_0 = G_L + G_D + G_1. \tag{5}$$

Normally $G_1 \ll G_D \ll G_L$; hence, $G_0 \simeq G_L$ and $G_T \simeq G_g + G_L$.

The noise figure for an amplifier and load at a temperature T, with a generator at temperature T_0, may be expressed as

$$F = 1 + \frac{T}{T_0}\left(\frac{G_0}{G_g} + \alpha\frac{\omega_1}{\omega_2}\frac{G_T}{G_g}\right). \tag{6}$$

From the noise-figure expression, one may readily see that if we desire a low noise figure, we want $G_g \gg G_0$. Let us now see how such a mismatch affects the gain and stability of the amplifier.

It is convenient to represent the mismatch between the generator conductance and the rest of the signal circuit by considering that the generator has a conductance G_g and is connected to the signal circuit by a length l of transmission line having a characteristic admittance $Y_0 = G_0$. This permits one to express this mismatch in terms of a reflection coefficient ρ and a phase angle βl. The generator conductance seen by the signal circuit then is

$$G_{g_i} = \text{R.P. } Y_i \tag{7}$$

$$Y_i = Y_0\left[\frac{Y_g\cos\beta l + jY_0\sin\beta l}{Y_0\cos\beta l + jY_g\sin\beta l}\right], \tag{8}$$

where $\beta = 2\pi/\lambda_s$, $Y_0 = G_0$ and $Y_g = G_g$.

We may define a reflection coefficient ρ as

$$\rho = \frac{Y_g - Y_0}{Y_g + Y_0} = \frac{G_g - G_0}{G_g + G_0}. \tag{9}$$

Hence, we may write

$$Y_i = Y_0\left[\frac{1+\rho e^{-2j\beta l}}{1-\rho e^{-2j\beta l}}\right] = Y_0\xi'. \tag{10}$$

Now

$$G_{g_i} = \text{R.P. } Y_i = G_0 \text{ R.P. } \xi'. \tag{11}$$

For convenience, let R.P. $\xi' = \xi$ and $2\beta l = \phi$. We may now calculate ξ as

$$\xi = \frac{1-\rho^2}{1+\rho^2-2\rho\cos\phi}. \tag{12}$$

Our gain expression may be rewritten to include ξ as

$$A = \frac{4G_L\xi}{G_0(1+\xi)^2(1-\alpha)^2} \tag{13}$$

and

$$\alpha = \frac{\omega_1\omega_2(\Delta C)^2}{G_2G_0(1+\xi)}. \tag{14}$$

This may be simplified to give

$$A = \frac{4G_L\xi}{G_0(\xi-\gamma)^2}, \tag{15}$$

where

$$\gamma = \frac{\omega_1\omega_2(\Delta C)^2}{G_2G_0} - 1.$$

It will be noted that when $\xi = \gamma$, the amplifier will oscillate. The values of γ for a few values of gain are listed below; it is assumed that $G_0 = 8G_L$. In this case, $\xi = 1$.

A_0 db	γ
5	0.602
10	0.776
15	0.874
20	0.929
30	0.9777

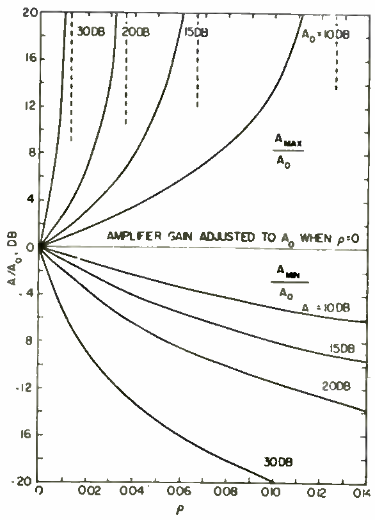

Fig. 2—Maximum and minimum gains as a function of reflection coefficient ρ. (Amplifier gain is adjusted to A_0 when $\rho=0$).

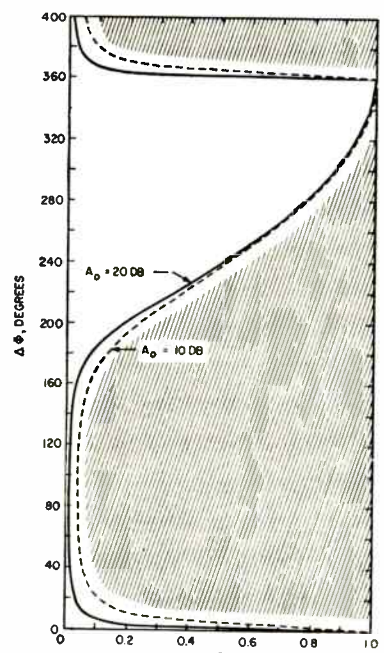

Fig. 3—Phase shift that produces a 3-db increase in gain. Shaded portion indicates region over which oscillation is likely to occur.

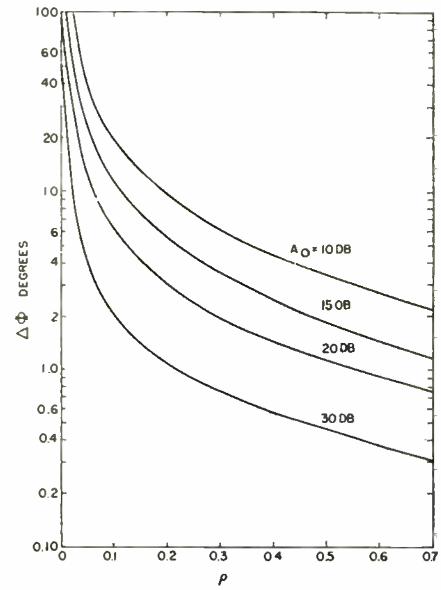

Fig. 4—Phase shift that produces a 3-db increase in gain.

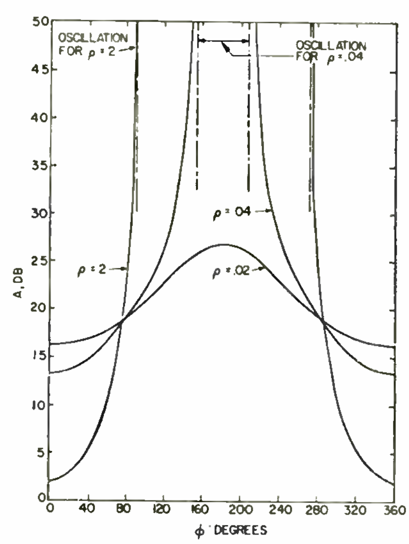

Fig. 5—Gain vs phase for three values of reflection coefficient for an initial gain $A_0=20$ db.

Referring to (11), we see that for $\rho=0$, $G_{g_i}=G_0$; also, if $\cos\phi_0=\rho$, then $G_{g_c}=G_0$. So we see that it is possible to operate with any ρ at the gain we desire as long as $\cos\phi_0=\rho$. However, should the phase ϕ vary slightly from ϕ_0, the gain may rise sharply. This is shown in Figs. 2 through 5. In Fig. 2, we have the maximum and minimum gains attainable for any value of ϕ vs the reflection coefficient ρ. In Figs. 3 and 4 we have the amount of phase shift required to produce a gain increase of 3 db. Fig. 5 shows how the amount of phase over which oscillation can occur increases with increasing ρ. In all the figures, it is assumed that $G_0=8G_L$.

It may be seen that, for high values of ρ, a small phase shift causes the amplifier to oscillate. This effect becomes more pronounced with higher and higher gains.

This analysis applies equally well for either the generator or load conductance, since they enter into the gain expression in the same manner. It should be mentioned again that this analysis assumes that no circulator is used.

The gain expression for a degenerate amplifier considering mismatch effects in the generator conductance cannot be reduced as simply as in the nondegenerate case. Here, the effect of ξ enters into the gain expression more strongly. However, we have essentially the same effect as in the nondegenerate case, but it is more pronounced.

The author is indebted to Rolf D. Weglein and Ronald C. Knechtli, of Hughes Aircraft Company Research Laboratories, for their helpful comments and suggestions.

K. M. Johnson
Research Labs.
Hughes Aircraft Co.
Culver City, Calif.

Parametric Standing Wave Amplifiers*

It has been pointed out by N. M. Kroll[1] and also by G. M. Roe and M. R. Boyd[2] that parametric amplification on nonlinear dispersionless transmission lines does not permit exponential signal growth along the length of the line. The author has come to essentially similar conclusions, based on an analysis which goes beyond those just mentioned, and takes into account the fact that the nonlinearity distorts the propagation of the pump signal. These negative conclusions, however, only characterize the interaction between a pump signal and a small signal which are traveling together along the line. Consider, instead, a line which has a small signal capacitance, $c(t)$, which is varied in time only, but is in phase, all along the length of the line. Let $v(x, t)$, $i(x, t)$, and $q(x, t)$ be the small signal voltage, current, and charge respectively. The relevant transmission line equations are

$$\frac{\partial v}{\partial z} = -l\frac{\partial i}{\partial t}. \qquad (1)$$

$$\frac{\partial i}{\partial z} = -\frac{\partial q}{\partial t} = -\frac{\partial}{\partial t}(c(t)v). \qquad (2)$$

A solution which initially has i, v, and q varying as e^{ikz} will preserve its wavelength as time proceeds. Hence, all solutions can be written as superpositions of such solutions. Letting $q(t)=q_k(t)e^{ikz}$, (1) and (2) lead to

$$\frac{d^2q_k}{dt^2} + \frac{k^2}{lc(t)}q_k = 0. \qquad (3)$$

Let the inductance and capacitance associated with a section of line l/k in length be denoted by

$$L = l/k, \quad C(t) = c(t)/k.$$

Eq. (3) then becomes

$$\frac{d^2q_k}{dt^2} + \frac{q_k}{LC(t)} = 0. \qquad (4)$$

This, however, is just the equation obeyed by the charge on a variable capacitance, $C(t)$, in a simple LC circuit.

Eq. (4) is Hill's equation, if $C(t)$ is periodic, and can have oscillatory solutions with an exponential modulation. This fact has recently been emphasized in connection with parametric amplification and in connection with von Neumann's phase-sensitive computing scheme.[3] Eq. (4) has these exponentially increasing and decreasing solutions if the circuit tuning is in one of a set of frequency ranges, which are located near integral multiples of one half of the frequency with which the capacitance is varied.

The exponentially ascending solutions of (3) and (4) are real functions, approximately of the form $e^{\alpha t}\cos(\omega t+\phi)$, hence after multiplication by the factor e^{ikz}, they represent exponentially growing standing waves.

* Received by the IRE, December 24, 1959.
[1] N. M. Kroll, "Properties of Propagating Structures with Variable Parameter Elements," presented at the ONR Symposium on Microwave Techniques for Computer Systems, Washington, D. C.; March 12, 1959.
[2] G. M. Roe and M. R. Boyd, "Parametric energy conversion in distributed systems," Proc. IRE, vol. 47, p. 1213; July, 1959.
[3] R. L. Wigington, "A new concept in computing," Proc. IRE, vol. 47, pp. 516–523; April, 1959.

Standing waves have a capacitive charge which builds up simultaneously all along the line, and subsequently is discharged simultaneously all along the line. It is therefore possible to have a standing wave synchronize its capacitive charging and discharging action with a pump voltage, just as in a simple lumped circuit. In the particular case where the pump signal has a frequency twice that of the growing signal, the signal must charge the line capacitances when they are large and must discharge the line capacitances when they are small. There will also be a second standing wave solution which has its charging and discharging action phased correctly to cause exponential decay in time.

There are a number of methods[4,5] available for obtaining approximate solutions to (3), all of which give essentially the same answer, if the capacitance variation is taken to be a small fraction of the average capacitance. In a transmission line with a time independent capacitance, the coefficient k^2/lc, which occurs in (3) is exactly ω^2. In our case, where k^2/lc is varying in time, let it be denoted by $\omega^2(t)$. If the capacitance variation is not too large, and is produced by a sinusoidal pumping signal, then we can expect

$$\omega^2(t) = \omega_0^2(1 + 2\epsilon \cos \omega_p t).$$

In this case, exponential gain, to first order in ϵ, turns out to be available only in the one-frequency range in which ω_0 is close to $\omega_p/2$. If we define

$$\delta = \omega_0 - \frac{\omega_p}{2},$$

then the approximate treatments lead to an exponential modulation of the form $e^{\pm\alpha t}$, with $\alpha^2+\delta^2=\epsilon^2\omega_p^2/16$ which gives a maximum value for $\alpha=\epsilon\omega_p/4$ when $\omega_0=\omega_p/2$. The average angular frequency, ω_0, can deviate from $\omega_p/2$ by $\pm\epsilon\omega_p/4$, before the exponential behavior completely disappears.

Additional analysis has shown that if a traveling wave is present on an initially unpumped line, which subsequently has a pumping voltage applied to it, then the initial traveling wave can be resolved into two standing waves, one of which will grow exponentially, while the other will decay. After the pumping voltage has been applied long enough, only the exponentially growing standing wave is left. If the pump voltage is then removed, the standing wave will decompose into traveling waves, each of which is an amplified version of the original signal, except that one will be reversed in its variation with time.

There are a number of conceivable ways of utilizing this standing wave interaction. We will, in this note, confine ourselves to those examples which are most intimately related to the particular way in which we have discussed the standing wave interaction. One practical embodiment would be a ferroelectric crystal, above its Curie point, with transmission line electrodes evaporated on its surface, subject to a dc biasing voltage, and suitably timed pumping voltages. Ferroelectrics, in a narrow temperature range above the Curie point, are strongly nonlinear dielectrics.[6,7] The scheme as described is perhaps of limited practical interest, since it will amplify only in an intermittent fashion. The exponentially growing standing waves can, however, just as well be the resonant modes of a terminated section of line. Thus, one could have a section of line, shorted at both ends, and a half wavelength long at the signal frequency. If excited by a pump signal at twice this frequency, suitably connected so that the capacitance variation is in phase all along the line, this half wave section could serve as one of the bistable "organs" required by von Neumann's phase sensitive computing scheme,[3] in which the lower frequency, building up exponentially, can have one of two phases, 180° apart.

R. Landauer
IBM Research Lab.
Poughkeepsie, N. Y.

[4] M. J. O. Strutt, "Laméche-Mathieusche und Verwandte Funktionen," Julius Springer, Berlin; 1932.

[5] R. Landauer, "Reflections in one-dimensional wave mechanics," *Phys. Rev.*, vol. 82, pp. 80–83; April 1, 1951.

[6] S. Triebwasser, "Study of the second-order ferroelectric transition in tri-glycine sulfate," *IBM J.*, vol. 2, pp. 212–217; July, 1958.

[7] M. E. Drougard, R. Landauer, and D. R. Young, "Dielectric behavior of barium titanate in the paraelectric state," *Phys. Rev.*, vol. 98, pp. 1010–1014; May 15, 1955.

X-Band Super-Regenerative Parametric Amplifier*

Recent experiments at USASRDL have indicated that super-regenerative parametric amplifiers may be capable of operating at K_u or possibly K_a band with the present available varactors.

In order to obtain reasonable gain bandwidth products in parametric amplifiers at X band, a diode Q of 10 ($F_c=100$ kmc) is normally required. The present practical limit to cutoff frequencies in silicon varactor diodes is 100 kmc with an occasional 150-kmc diode. Due to the high-gain bandwidth product available in super-regeneration, a substantial decrease in diode Q can be anticipated for successful operation. The advent of super-regeneration requires only that the diode Q be large enough to produce sufficient negative conductance (via pump voltage) to overcome the positive conductance inherent in the diode and the circuit. To demonstrate this, an X-band super-regenerative parametric amplifier has been constructed using a varactor with a 41-kmc cutoff frequency.

The gain of the amplifier was greater than 50 db at a bandwidth of 2.4 mc. Signal frequency was 8.514 kmc. Pumping was done at 10.15 kmc. A schematic of the circuit used is shown in Fig. 1. The pump was pulsed on for 10 μsec at a PRR of 4.4 kc. Fig. 2 indicates the delay in the start of the free tank oscillations with respect to the pump oscillations. A signal coalescing with the oscillations causes them to build up earlier. The oscillations were quenched after they reached saturation by turning the pump oscillations off. The resultant logarithmic mode of operation was very stable and allowed for a wide range of adjustments. Fig. 3 shows the decrease in oscillation starting time as a logarithmic function of input signal strength. The noise figure of the amplifier was approximately 13 db, as determined by a minimum discernible signal level of -97.5 dbm. No appreciable decrease in noise figure could be accomplished by increasing the diode Q, indicating that

* Received by the IRE, November 27, 1959.

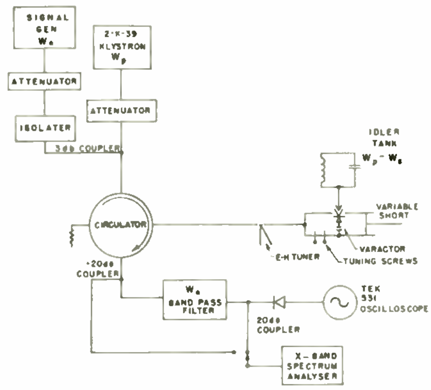

Fig. 1—Diagram of amplifier circuit.

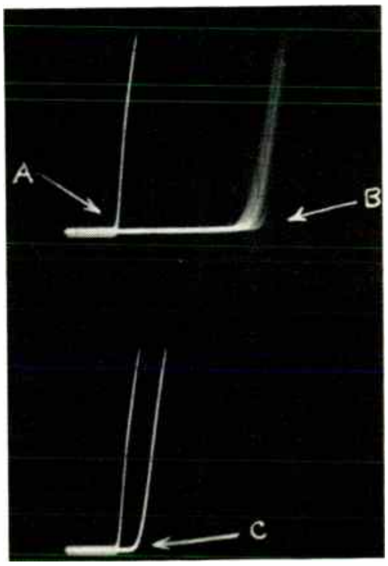

Fig. 2—A=Start of pump oscillation. B=Random start of free tank oscillations under no signal conditions. C=Start of free tank oscillations with signal applied.

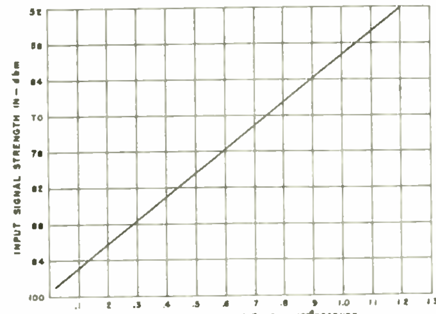

Fig. 3—Advance in oscillation starting time as a function of input signal strength.

the major noise contribution is not the spreading resistance of the diode. Varactor cutoff frequencies of 37, 38, 41, 42, 45, and 57 kmc were utilized in the experiments. No oscillations were observed using varactors with cutoff frequencies below 41 kmc. The high noise figure is apparently due to the high W_s/W_i ratio, the resistive noise in the idler tank which is "up-converted," and to the poor quenching waveform. By simply cooling the idler tank, the noise figure should be considerably lowered. Several techniques are presently being investigated which may lower the noise figure of the receiver.

The results in these experiments are by no means optimum; they merely demonstrate the feasibility of a super-regenerative parametric amplifier at K band utilizing existing varactors. Since pumping was accomplished at a frequency close to the signal, a source of suitable pump power should be available at all system frequencies.

B. B. Bossard
E. Frost
W. Fishbein
U. S. Army Signal Res. and Dev. Lab.
Ft. Monmouth, N. J.

The Effect of Parasitic Diode Elements on Traveling-Wave Parametric Amplification*

In previous analyses,[1-4] the parametric interaction of traveling waves has been formulated by representing the diode elements as ideal nonlinear capacitors which periodically shunt the transmission line structure and couple energy from the pump to the signal and idle waves. The results provide excellent insight into the amplification process but because of the idealized nature of the diode representation are of limited utility for design purposes. In this note a set of design equations are derived based on a circuit representation of the diode which includes the series lead inductance, shunt case capacitance, and dissipative junction losses. Above UHF these diode parameters have an appreciable effect on traveling-wave interaction and must be taken into account in the design of a practical device.

Assume that the voltage across the variable junction capacitance is of the form (Fig. 1)

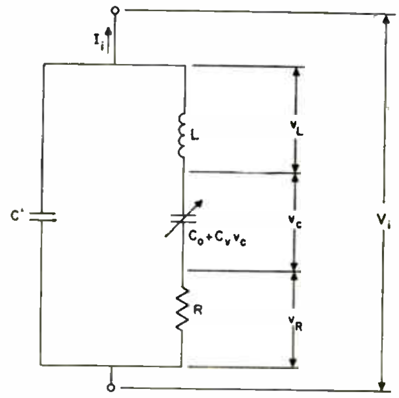

Fig. 1—Equivalent circuit of diode.

$$v_c = v_0 + v_1 e^{j\omega_1 t} + v_{-1}e^{-j\omega_1 t} + v_2 e^{j\omega_2 t} + v_{-2}e^{-j\omega_2 t} + v_3 e^{j\omega_3 t} + v_{-3}e^{-j\omega_3 t} \quad (1)$$

where the subscripts 1, 2, and 3 refer to the signal, idle, and pump waves, respectively. Consistent with small signal and small coupling approximations, the total current through the diode is related to the total voltage across the diode as follows:

$$\begin{pmatrix} I_1 \\ I_{-2} \\ I_3 \end{pmatrix} = \begin{pmatrix} y_{1,1} & y_{1,-2} & 0 \\ y_{-2,1} & y_{-2,-2} & 0 \\ 0 & 0 & y_{3,3} \end{pmatrix} \begin{pmatrix} V_1 \\ V_{-2} \\ V_3 \end{pmatrix} \quad (2)$$

where

$$y_{1,1} = Y_{D1} = j\omega_1 C_0 \left[\frac{1}{\bar{\beta}_1} + \frac{C'}{C_0} + \frac{\omega_2^2\gamma^2}{\omega_0^2 \bar{\beta}_1 \bar{\epsilon}} + j\frac{\omega_2 \gamma^2}{\omega_{c0}\bar{\epsilon}} \right],$$

$$y_{-2,-2} = Y_{-D2} = -j\omega_2 C_0 \left[\frac{1}{\bar{\beta}_2{}^*} + \frac{C'}{C_0} + \frac{\omega_1^2\gamma^2}{\omega_0^2 \bar{\beta}_2{}^* \bar{\epsilon}} - j\frac{\omega_1 \gamma^2}{\omega_{c0}\bar{\epsilon}} \right],$$

$$y_{3,3} = Y_{D3} = j\omega_3 C_0 \left[\frac{1}{\bar{\beta}_3} + \frac{C'}{C_0} \right],$$

$$y_{1,-2} = j\frac{\omega_1 C_V V_3}{\bar{\epsilon}\bar{\beta}_3},$$

$$y_{-2,1} = -j\frac{\omega_2 C_V V_{-3}}{\bar{\epsilon}\bar{\beta}_3{}^*},$$

$$\bar{\epsilon} = \bar{\beta}_1\bar{\beta}_2{}^* - \gamma^2\left(\frac{\omega_1^2}{\omega_0^2} - j\frac{\omega_1}{\omega_{c0}}\right)\left(\frac{\omega_2^2}{\omega_0^2} + j\frac{\omega_2}{\omega_{c0}}\right),$$

$$\gamma^2 = \frac{C_V^2 |V_3|^2}{C_0^2 |\bar{\beta}_3|^2},$$

$$\bar{\beta}_i = 1 - \frac{\omega_i^2}{\omega_0^2} + j\frac{\omega_i}{\omega_{c0}},$$

$\omega_0 = (LC_0)^{-1/2}$ = series resonant angular frequency of diode,

$\omega_{c0} = (RC_0)^{-1}$ = cutoff angular frequency of diode,

and the bar ("-") indicates a quantity is complex.

The quantities $y_{1,1}$, $y_{-2,-2}$, and $y_{3,3}$ relate to the *linear* or *noncoupling* portion of the diode admittance and $y_{1,-2}$, $y_{-2,1}$ relate to the *nonlinear* or *coupling* portion.

The diode loaded traveling-wave structure is represented as shown in Fig. 2(a). Since the loading is periodic, the linear (noncoupling) transmission characteristics may be determined by analysis of a single section [Fig. 2(b)]. The transmission matrix T for this section at ω_i is simply

$$T = \begin{pmatrix} 1 & 0 \\ \frac{Y_{Di}}{2} & 1 \end{pmatrix} \begin{pmatrix} \cos\theta_i & jZ_0 \sin\theta_i \\ jY_0 \sin\theta_i & \cos\theta_i \end{pmatrix} \begin{pmatrix} 1 & 0 \\ \frac{Y_{Di}}{2} & 1 \end{pmatrix}. \quad (3)$$

The diode-loaded π section may be considered equivalent to a new uniform section of transmission line characterized by $\bar{Z}_i$, $\bar{\phi}_i$ [Fig. 2(c)]. Expansion of (3) shows that

$$\bar{Z}_i = Z_0 \frac{\sin\theta_i}{\sin\bar{\phi}_i} \qquad (i = 1, -2, 3) \quad (4)$$

$$\cos\bar{\phi}_i = \cos\theta_i + jZ_0\frac{Y_{Di}}{2}\sin\theta_i \qquad (i = 1, -2, 3) \quad (5)$$

where

$\bar{\phi}_i = \phi_{i\beta} - j\phi_{i\alpha}$ = propagation wave number of traveling wave structure in absence of coupling;

$\bar{\phi}_i = -\bar{\phi}_{-i}{}^*$

$\theta_i = -\theta_{-i}$.

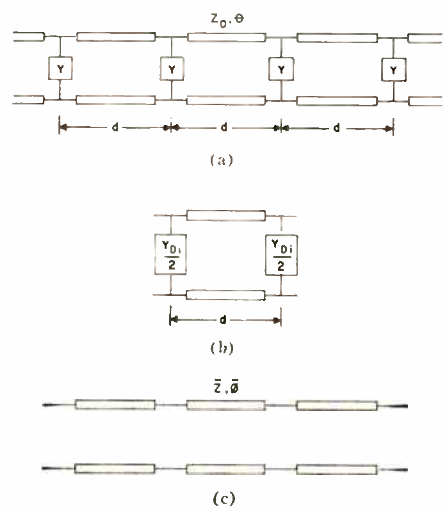

Fig. 2—(a) Periodically-loaded traveling-wave transmission-line structure. (b) π-section formed by linear (noncoupling) portion of diode admittance. (c) Equivalent uniform transmission line.

This uniform line is now considered to be periodically loaded with the nonlinear portion of the diode admittance. The nonlinear admittance may be represented by the four terminal controlled source network[5] of Fig. 3. This network serves to provide coupling between the signal and idle waves. Hence, the equivalent circuit representation of the traveling-wave structure may be depicted as in Fig. 4. Application of Floquet's Theorem relates the voltages across any two successive sections at the signal and idle frequencies. Under the assumption that the pump wave experiences negligible attenuation, it follows that the signal and idle

* Received by the IRE, February 29, 1960; revised manuscript received, March 30, 1960. This work was partially supported by Contract DA-36-039-SC-78114.

[1] K. Kurokawa and J. Hamasaki, "Mode theory of lossless periodically distributed parametric amplifier," IRE Trans. on Microwave Theory and Techniques, vol. MTT-3, pp. 360–365; July, 1959.

[2] G. Heilmeier, "An analysis of parametric amplification in periodic loaded transmission lines," *RCA Rev.*, vol. 20, pp. 442–454; September, 1959.

[3] P. Parzen, "Theory of Filter-Type Parametric Amplifier," presented at the 1959 Natl. Symp. on Microwave Theory and Techniques, Harvard Univ., Cambridge, Mass.; June 1–3.

[4] C. V. Bell and G. Wade, "Circuit considerations in traveling-wave parametric amplifier," 1959 IRE Wescon Convention Record, pt. 2, pp. 75–82.

[5] J. Sie, "Controlled Source Circuit Representation of Parametric Amplifier," RCA, New York, N. Y., Internal Rept.; December, 1959.

Fig. 3—Controlled source circuit representation of nonlinear (coupling) portion of diode admittance.

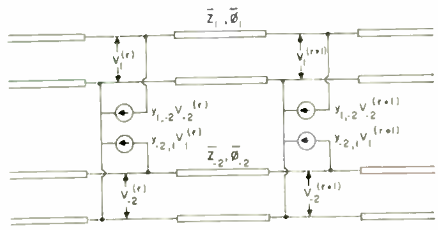

Fig. 4—Equivalent circuit representation of traveling-wave structure.

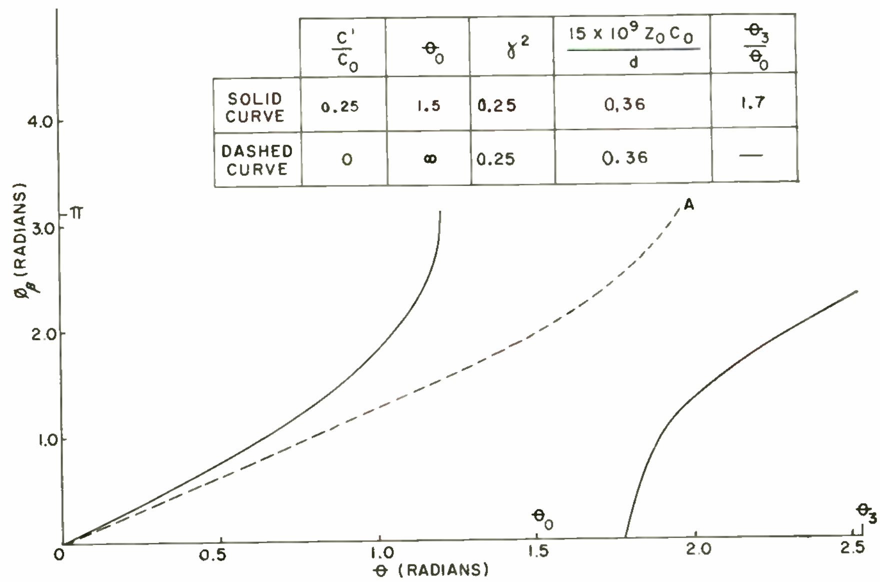

	$\frac{C'}{C_0}$	θ_0	γ^2	$\frac{15 \times 10^9 Z_0 C_0}{d}$	$\frac{\theta_3}{\theta_0}$
SOLID CURVE	0.25	1.5	0.25	0.36	1.7
DASHED CURVE	0	∞	0.25	0.36	—

Fig. 5—Typical phase diagram for traveling-wave structure.

propagate as exponential waves of the form

$$e^{-j\bar{x}} = e^{-j(\bar{\phi}_1-\bar{\Delta}/2)}\left[\cos\frac{\bar{\Delta}}{2} \pm \frac{1}{2}\left(2[\cos\bar{\Delta} - 1] - y_{1,-2}y_{-2,1}\bar{Z}_1\bar{Z}_{-2}\right)^{1/2}\right] \quad (6)$$

where,

$\bar{x} = \beta + j\alpha =$ propagation wave number of traveling-wave structure including coupling;

$\bar{\Delta} = \bar{\phi}_1 + \bar{\phi}_2^* - \phi_3$.

It is seen from (6) that the traveling-wave gain factor per section is

$$\alpha = -\frac{1}{2}(\phi_{1\alpha} + \phi_{2\alpha}) + \ln\left|\cos\frac{\bar{\Delta}}{2} + \frac{1}{2}(2[\cos\bar{\Delta} - 1] - y_{1,-2}y_{-2,1}Z_1Z_{-2})^{1/2}\right|. \quad (7)$$

Eqs. (4), (5), and (7) constitute the general design equations for the traveling-wave parametric amplifier.

Inspection of (7) shows that maximum gain per section obtains when

$$\phi_{1\beta} + \phi_{2\beta} - \phi_{3\beta} = 0,$$

and

$$\phi_{1\alpha} = \phi_{2\alpha} = 0,$$

i.e., when the signal, idle, and pump waves are in perfect synchronism and the diode exhibits no loss. The development of high cutoff frequency parametric diodes has enabled this latter condition to be closely approximated in the microwave range. The synchronism condition can not always be approximated, however, especially if one or more of the operating frequencies are close to the series resonant frequency of the diode. The dashed curve of Fig. 5 illustrates a typical phase characteristic for the traveling-wave structure when periodically loaded with an ideal varactor. The solid curve shows the phase characteristic when the series lead inductance and shunt case capacitance are included in the equivalent diode representation. The diode resonance severely disturbs the linearity of the phase characteristic and introduces a stop band in the region of resonance. At present the resonance of commercially-available diodes ranges from S band to low X band and therefore the idealized analysis is inadequate for design purposes in the microwave region. The stop band exhibited by the dashed characteristic (starting at A) stems from the periodic nature of the traveling-wave structure.

Design of an experimental traveling-wave parametric amplifier has been initiated in our laboratory based on the analysis outlined above. We hope to report our results in a future note.

D. Fleri
J. Sie
Surface Communications Systems Lab.
RCA, Defense Electronic Products
75 Varick St.
New York 13, N. Y.

A Method for Broad-Banding Synchronism in Traveling-Wave Parametric Devices*

In this note, a theoretical method for achieving very broad-band synchronism among signal, idle, and pump waves in a parametric diode traveling-wave amplifier or upconverter is described. The method makes use of the fact that the diode series lead inductance breaks the loaded phase vs frequency curve into two branches, with a stop band, centered at the diode resonant frequency, separating these two branches. Broad-band synchronism can then be attained by choosing the diode parameters in such a way that the two branches referred to above are parallel and more or less linear over the idle and signal frequency ranges. Explicit equations are developed showing how this may be achieved. These equations give the values of diode parameters (case capacitance, series lead inductance, diode capacitance at bias) and idle frequency needed to achieve broad-band synchronism. The efficacy of the method is then demonstrated by calculating synchronism and traveling wave gain vs frequency over the 400–1600-mc band using an 8-kmc pump, with 3630-mc resonant frequency diodes spaced 1.5 cm apart in a 150 Ω coax line. The advantages of the method in achieving very broad-band synchronism are then demonstrated by comparing the results of the above example with the numerical results evaluated for the following two cases: 1) the parameters of the diode (in particular, the diode series lead inductance) are chosen more or less at random; 2) the diode is assumed to have negligible series inductance (previously thought to be the best condition for traveling wave paramp operation). In each of these two cases the synchronism, gain, and bandwidth are considerably poorer than the results achieved by the method we propose.

The basis of the method lies in the work of Fleri and Sie,[1] in which they extend the traveling-wave diode investigations previously reported[2] by including the diode series lead inductance and by giving the diode a more accurate circuit representation. They find that the phase equation for the loaded periodic structure is

$$\cos\phi = \cos\theta - xf(\theta)\theta\sin\theta \quad (1a)$$

$$x = \frac{Z_0 C C'}{2d};$$

* Received by the IRE April 12, 1960. This work is being performed for the Rome Air Dev. Center under Contract No. AF 30(602)2184.

[1] D. Fleri and J. Sie, "The effect of parasitic diode elements on traveling-wave parametric amplification," this issue, pp. 1330–1331.

[2] K. Kurokawa and J. Hamasaki, "Mode theory of lossless periodically distributed parametric amplifiers," IRE Trans. on Microwave Theory and Techniques, vol. MTT-7, pp. 360–365; July, 1959.

G. Heilmeier, "An analysis of parametric amplification in periodically loaded transmission lines," *RCA Rev.*, vol. 20, pp. 442–454; September, 1959.

P. Parzen, "Theory of Filter-Type Parametric Amplifier," presented at the 1959 Natl. Symp. on Microwave Theory and Techniques, Harvard Univ., Cambridge, Mass.; June 1–3.

C. Bell and G. Wade, "Circuit considerations in traveling-wave parametric amplifiers," 1959 IRE WESCON Convention Record, pt. 2, pp. 75–82.

R. S. Engelbrecht, "Nonlinear-reactance (parametric) traveling-wave amplifiers for UHF," presented at the 1959 Solid-State Circuits Conference, University of Pennsylvania, Philadelphia, February 12–13; *Digest of Technical Papers*, pp. 8–9.

$$\theta = \omega \frac{d}{c} \text{ (unloaded line phase constant)} \quad (1b)$$

$$f(\theta) = 1 + \frac{r}{1 - \dfrac{\theta^2}{\theta_0^2}} + \frac{ar\left(\dfrac{\theta_3 - \theta}{\theta_0}\right)^2}{(1 - k_2^2)\left(1 - \dfrac{\theta^2}{\theta_0^2}\right)(1 - k_1^2)};$$

$$a = \left(\frac{\Delta C}{C_0}\right)^2 \quad (1c)$$

$$r = \frac{C_0}{C'}; \quad k_1 = \frac{\omega_1}{\omega_0} = \frac{\theta_1}{\theta_0};$$

$$k_2 = \frac{\omega_2}{\omega_0} = \frac{\theta_2}{\theta_0}; \quad \omega_0 = \frac{1}{\sqrt{L_0 C_0}},$$

where subscripts 1, 2, and 3 refer to signal, idle, and pump frequencies. ΔC is the nonlinear part of the diode capacitance; L_0 is the diode series inductance; ω_0 the diode resonant angular frequency; C_0 the diode capacitance at bias; C' the case capacitance; Z_0 the unloaded line impedance; d the diode spacing; c the speed of light, and ϕ is the loaded line phase constant. Deviation from synchronism is defined as

$$\Delta = \phi_3 - (\phi_1 + \phi_2).$$

The circuit representation of the diode, which leads to the $f(\theta)$ of (1c), and the qualitative nature of the ϕ vs θ curves defined by (1a) are shown in Fig. 1 below, together with the ϕ, θ curve when L_0 is assumed to be negligible.[2] The latter curve is shown dashed; the $f(\theta)$ corresponding to this curve is $f(\theta) = 1 + (C_0/C')$.

The discontinuous ϕ, θ curve in Fig. 1 can be used to advantage to achieve broadband synchronism, as follows: we attempt to make the curves at signal band A–A' and idle band B–B' parallel and as linear as possible. If this can be done, we can then write

$$\phi_1 = A\omega_1, \quad \phi_2 = A(\omega_2 - \omega'), \quad (2)$$
$$\phi_3 = A(\omega_3 - \omega'),$$

where we are assuming the pump is not too far from the idle frequency. Then from (2), $\Delta = \phi_3 - (\phi_1 + \phi_2) \equiv 0$ over the whole band, inasmuch as $\omega_3 = \omega_1 + \omega_2$.

To make the curves linear, we require that $\theta_1 \ll 1$ over the signal range; the linearity over the signal range can then be verified by expanding (1a), using (1b) and (1c), to θ^2 and ϕ^2 terms. Linearity at the idle can be realized by making $f(\theta) = 0$ at one idle frequency, for instance, θ_2^*. Then (1a) and (1c) show that linearity will be achieved over much of the idle range because a four- or five-fold change in signal frequency corresponds to a small percentage change in idle frequency, so that $f(\theta_2) \sim 0$ over the whole idle range. We note that, if these conditions are met, we can afford to use larger line impedance Z_0 (*i.e.*, larger x) and this will not disturb linearity at the signal region where θ_1 is small, nor will it disturb linearity over much of the idle region where $f(\theta_2) \sim 0$. This has the advantage of increasing α and the over-all traveling-wave gain, where

$$\alpha = \left[\frac{\omega_1\omega_2 Z_{01} Z_{02} \sin\theta_1 \sin\theta_2}{(1 - k_1^2)^2(1 - k_2^2)^2 \sin\phi_1 \sin\phi_2} (\Delta C)^2\right]^{1/2} \quad (3)$$

$$\text{traveling-wave gain} = 10 \log_{10} \left[e^{N/2\sqrt{\alpha^2 - \Delta^2}} \mp e^{-N/2\sqrt{\alpha^2 - \Delta^2}}\right]^2 \quad (3a)$$

where N is the total number of sections and the minus sign applies for the upconverter and the plus sign for the straight-through amplifier. To obtain the total gain, we must add $10 \log_{10} \omega_2/4\omega_1$ db for an upconverter, and subtract 6 db for a straight-through amplifier.

The condition that $f(\theta_2^*) = 0$ at one idle frequency $\omega_2^*/2\pi$ gives

$$r = \frac{C_0}{C'} = k_2^* - 1, \quad k_2^* = \frac{\omega_2^*}{\omega_0} = \frac{\theta_2^*}{\theta_0} \quad (4)$$

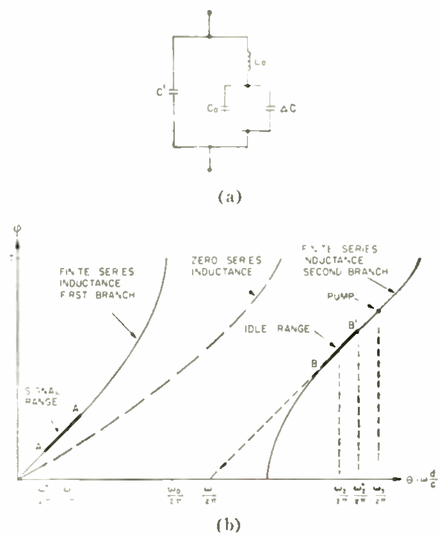

Fig. 1—(a) Circuit representation of diode with its case capacitance C' and series lead inductance L_0. (b), ϕ, θ curves for case of finite series inductance (1a)–(1c) and for case of negligible series inductance. Perfect synchronism is attained when AA' and BB' are linear and parallel, and the pump is close to BB'.

where we have neglected the third term in (1c), as it is generally small when compared to the other terms at the idle frequency in a practical case.

The slopes of the two branches at idle frequency $\omega_2^*/2\pi$ and at signal frequency $\omega_1^*/2\pi$ are readily calculated from (1a)–(1c). This is done at $\omega_1^*/2\pi$ by expanding (1) to θ^2 and ϕ^2 terms with $\theta \ll 1$ and using the value of r in (4). It is accomplished at $\omega_2^*/2\pi$ by differentiating (1a) with respect to θ and then putting $f(\theta) = 0$ at θ_2^* with $\phi = \theta_2^*$ there, and then using the value of r in (4). Setting the two slopes equal and solving for k_2^*, there results

$$k_2^{*2} = 1 + A(1 + x) + \sqrt{[1 + A(1 + x)]^2 - (1 + 2A)} \quad (5)$$

$$A = \frac{1}{1 - a}; \quad x = \frac{Z_0 c C'}{2d}.$$

Thus a given value of $x(Z_0, C', d)$ and $a = (\Delta C/C_0)_2$ determines k_2^*. This in turn determines what the resonant frequency $\omega_0/2\pi$ of the diode must be:

$$\omega_0 = \omega_2^*/k_2^*, \quad (6)$$

where $\omega_2^*/2\pi$ is the idle frequency that the designer proposes to use. The value of C_0 required is determined from (4):

$$C_0 = C'(k_2^{*2} - 1) \quad (7)$$

and this can be achieved by biasing the diode to the correct voltage.

L_0 can then be tailored to achieve the required diode resonant frequency [given in (6)]:

$$L_0 = \frac{1}{\omega_0^2 C_0}. \quad (8)$$

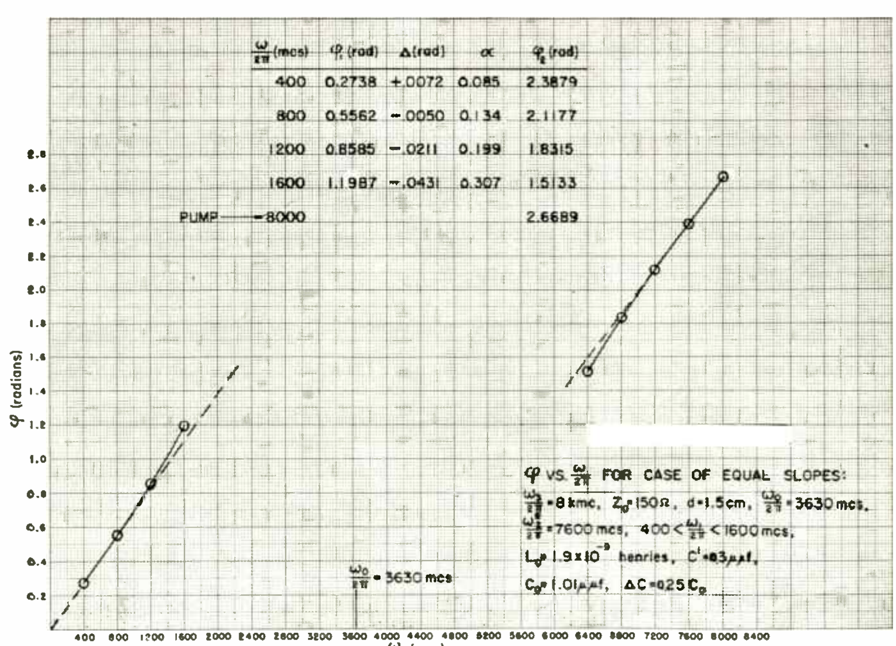

Fig. 2.

Eqs. (5)–(8) determine the choice of the diode and frequency parameters which will guarantee broad-band synchronism, $\Delta \approx 0$.

We illustrate the method by the following example.

Choose

$$400 \text{ mc} \le \frac{\omega_1}{2\pi} \le 1600 \text{ mc}, \quad \frac{\omega_3}{2\pi} = 8000 \text{ mc};$$

$$6400 \text{ mc} \le \frac{\omega_2}{2\pi} \le 7600 \text{ mc}, \tag{9}$$

$Z_{01} = Z_{02} \equiv Z_0 = 150\Omega$ (TEM Mode Line).

$$d = 1.5\text{cm}, \quad C' = 0.3\ \mu\mu f,$$

$$x = \frac{Z_0 c C'}{2d} = 0.45, \quad \frac{\Delta C}{C_0} = 0.25,$$

$$A = \frac{1}{1-a} = 1.067.$$

Taking $\omega_2^*/2\pi = 7600$ mc, (5)–(8) give

$$k_2^* = 2.094, \quad r = 3.378, \quad C_0 = 1.013\ \mu\mu f,$$

$$\frac{\omega_0}{2\pi} = 3630 \text{ mc}, \quad L_0 = 1.9 \times 10^{-9} \text{ henries}. \tag{10}$$

We now use the parameters of (10) to calculate ϕ vs ω from the exact equations (1a)–(1c). Fig. 2 shows the resulting ϕ, ω curve, from which $\Delta = \phi_3 - (\phi_1 + \phi_2)$ can be calculated. A table is presented in Fig. 2 giving Δ and α [see (3)] vs signal frequency over the 400–1600-mc band. We note several things from Fig. 2. 1) The two branches are quite linear and parallel at signal and idle frequencies. 2) The value of Δ is very small—much less than α over the whole band. 3) The nonlinearity in the signal and idle curves are in opposite directions, thus compensating each other so that $\phi_1 + \phi_2$ can be maintained constant over a bandwidth larger than the regions over which the curves are strictly linear. This could not be achieved by working both the signal and idle on the same ϕ, ω branch below the diode resonant frequency. This is an added feature of the method which helps to produce larger bandwidths over which synchronism can be achieved. 4) From (3) and (3a), the remarks below (3a), and the results of Fig. 2 we find, using 20 diodes, that an upconverter would have 12.4 db gain at 400 mc, increasing to 26.4 db gain at 1600 mc. For the straight-through amplifier we would find 5.8 db gain at 400 mc and 33 db gain at 1600 mc using 30 diodes.

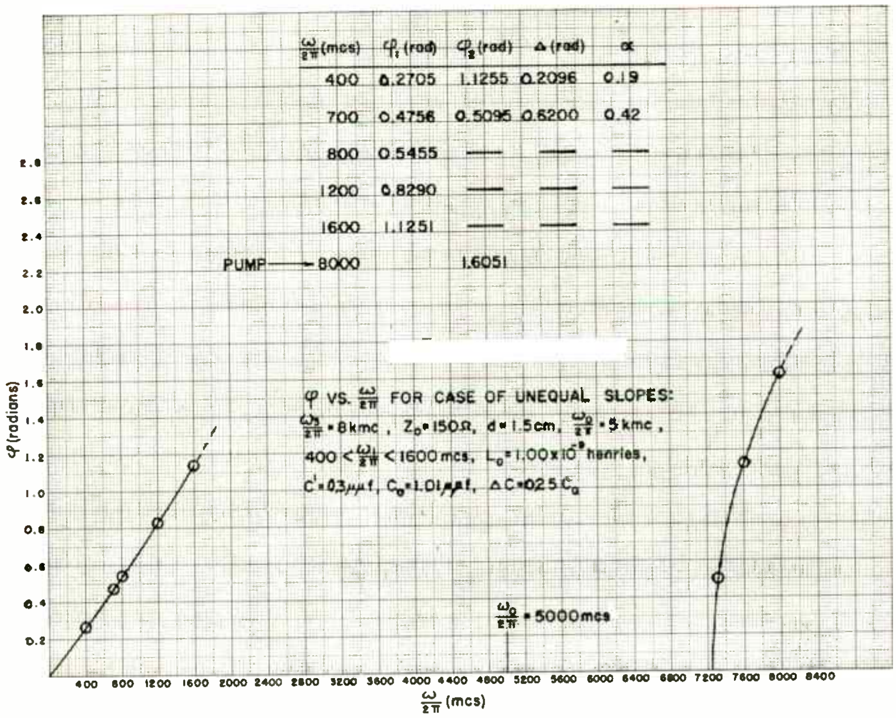

Fig. 3.

Fig. 3 shows the results when the diode is chosen incorrectly. In this case we kept all the parameters the same except the diode series inductance. L_0 was chosen to be 1.00×10^{-9} henries ($\omega_0/2\pi = 5000$ mc) instead of the correct value 1.9×10^{-9} henries.

We note that the two branches are not parallel and are highly nonlinear. In this case we can not find gain for any frequency in the 400–1600-mc range because $\Delta > \alpha$. In fact ϕ_2 does not exist (stop band) for

$$\frac{\omega_2}{2\pi} < 7300 \text{ mc} \left(\frac{\omega_1}{2\pi} > 700 \text{ mc}\right).$$

Finally, Fig. 4 shows the results when the diode series inductance is made negligible, so that there is only one branch of the ϕ, ω curve ($\omega_0 = \infty$: see dashed curve of Fig. 1). All the other parameters were kept the same as in Figs. 2 and 3, except that the pump frequency, of necessity, could be no larger than ~3 kmc. We chose two cases: a 3-kmc pump and a 2-kmc pump. The tables in Fig. 4 show that no gain could be achieved for a 3-kmc pump because $\Delta > \alpha$ for all signal frequencies. For a 2-kmc pump we would get gain at all signal frequencies in the band because Δ is quite small and less than α. However, the gain is poorer than that of Fig. 2 ($\omega_1\omega_2$ product is smaller) and the noise figure above 1000 mc is worse than 3 db (reaching 7 db at 1600 mc), unlike the case of Fig. 2 where the noise figure is less than 1 db over the whole 400–1600-mc band. This latter case is quasi-degenerate operation.

Thus, these examples serve to show the advantages which the method provides compared with the techniques used previously in designing parametric diode traveling-wave structures.

The above examples assumed infinite cutoff frequencies ($R_s = 0$) for the diodes. In the case of a finite diode cutoff frequency (for instance, 100 kmc), the losses have been taken into account. They reduce the gain, of course, but do not affect to any significant degree the broad-band synchronism obtained in Fig. 2.

Other cases have been worked out in which Δ is ~0 and much less than α over as much as 10–1 bandwidths.

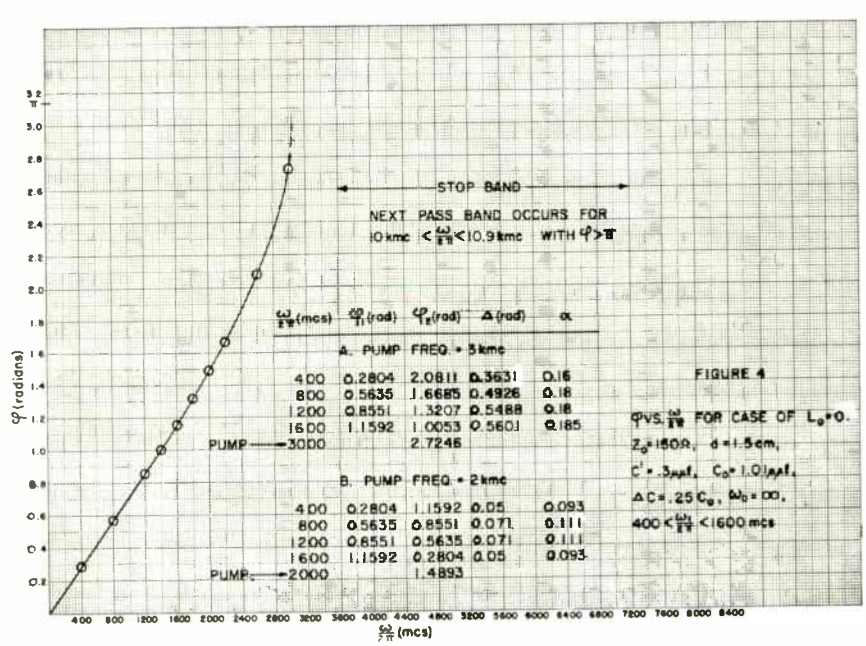

Fig. 4.

H. Boyet
D. Fleri
RCA, Defense Electronic Products
New York, N. Y.

Solid-State Microwave Power Sources Using Harmonic Generation*

The recent development of high-Q variable-reactance diodes has stimulated considerable interest in the efficient, all-solid-state, harmonic generation of microwave power. This letter describes a specific configuration which, for a dc input power of 4 watts, achieves an output power of either 2 mw at 8720 mc or ¼ watt at 1090 mc. The circuit (Fig. 1) can conveniently be divided into the following three parts: 1) a single transistor oscillator operating at 218 mc, 2) a varactor diode fifth-harmonic generator that converts the 218 mc to 1090 mc, and 3) a varactor diode eighth-harmonic generator that converts the 1090 mc to 8720 mc.

The oscillator employs a developmental Bell Telephone Laboratories silicon NPIN transistor[1] in a common-base circuit with pi-network load coupling. For heat dissipation purposes, the header, upon which the collector is mounted, is directly connected to the chassis. The transistor has a room temperature collector-dissipation rating of 6 watts, and, when operated at 2.75 watts input, has a 200-mc collector efficiency of 35 per cent. Thus, an output of 1.5 to 2.0 watts is obtainable at 200 mc.

The two harmonic generation circuits employ two different types of Bell Telephone Laboratories silicon-diffused varactor diodes: a high-breakdown, moderate-Q diode[2] ($C_0 = 5.3\ \mu\mu f$, $R_s = 1.2$ ohms, $V_b = -39$ v) in the fifth-harmonic circuit, and a high-Q, low-breakdown diode ($C_0 = 1.2\ \mu\mu f$, $R_s = 1.8$ ohms, $V_b = -6$ v) in the eighth-harmonic circuit. This combination of diode types comprises an efficient, two-step means of converting VHF to X band at the power levels involved. The first diode, because of its high breakdown voltage and high C_0, is capable of handling a large amount of VHF power (1 to 2 watts) and efficiently converting it to L band. The high-Q diode is capable of efficiently converting the resulting L-band power to X band.

The fifth-harmonic circuit was designed primarily for the measurement of diode input impedance in series-diode harmonic-generation circuits. For this reason, it was constructed as a separate package with the major undesired harmonics short-circuited locally at the pins of the diode, using series resonant traps. To measure input impedance, a 50-ohm load is connected at Y in place of the X-band circuit, the oscillator is disconnected at A–A', and VHF energy is applied at X through a coaxial matching network (triple-stub tuner) and a Byrne bridge or slotted line. The series resonant traps and the RF choke at the input of the diode insure that negligible harmonic energy up to at least the fifth harmonic is reflected toward the source, so that the input matching network functions only as a matching system and not as a harmonic filter.

* Received by the IRE, April 1, 1960.

[1] "Engineering Services on Transistors (1958–1959)," Bell Telephone Labs., Whippany, N. J., Interim Repts. Nos. 11–19, Signal Corps Contract No. DA 36-039-sc-64618; 1958–1959.

[2] D. Leenov and J. Root, "High Power Harmonic Generation with a Silicon Varactor Diode," 1959 IRE Electron Devices Meeting, Washington, D. C.; October 29–30.

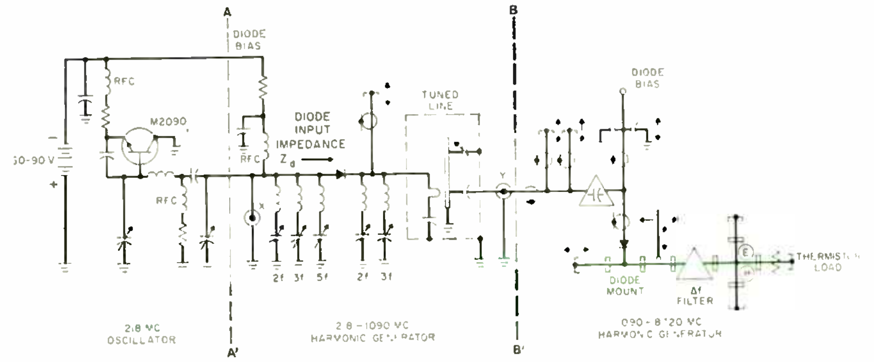

Fig. 1—Solid-state X-band source.

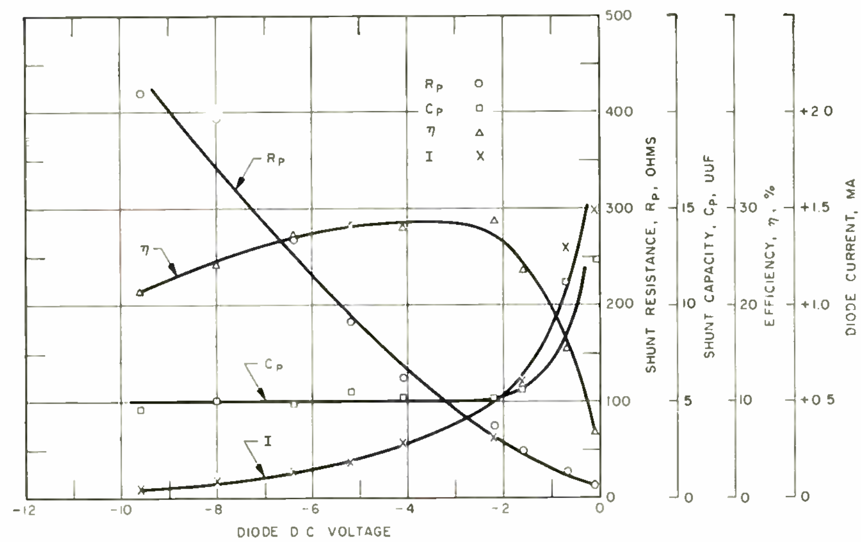

Fig. 2—218-mc–1090-mc harmonic generator, measured values of efficiency, input impedance and diode current (170-mw input power).

The variation in diode input impedance and in conversion efficiency η with bias for fixed input power is shown in Fig. 2. Here input impedance is defined as the impedance "seen" from the left of the diode (Z_d in Fig. 1) and is displayed as a shunt resistance R_p and a shunt capacitance C_p. Note that R_p is a strong function of bias, but that C_p and η are fairly constant over a wide bias range. Other measurements of R_p, C_p, and η with changing input power level, but with bias held fixed, show that R_p is a strong function of power, that η drops slowly with increasing power, and that C_p is almost constant over a wide range. Clearly then, a major problem in the design of a harmonic generator is that of matching into a rapidly varying input impedance. A combination of self and applied bias is helpful in stabilizing input impedance against input level.

Efficiencies as high as 30 per cent at 200-mw input and 22 per cent at 1-watt input have been obtained in the 218- to 1090-mc fifth-harmonic generator. Typical results for a range of input power levels are shown graphically in Fig. 3. In obtaining these data, circuit parameters, bias, and matching elements were adjusted for maximum output at each power level. A further improvement in performance might be realized by operating into an optimum load impedance, but no provisions for adjusting load impedance were incorporated into this design.

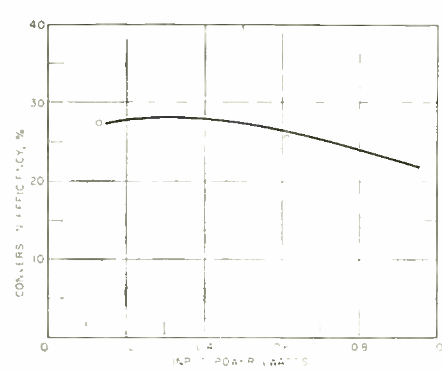

Fig. 3—218-mc–1090-mc harmonic generator, measured values of conversion efficiency.

The eighth-harmonic generator consists of a waveguide-mounted diode with associated matching and filtering components (Fig. 1). No attempt was made to individually terminate each undesired harmonic. The input and output matching elements therefore play dual roles as both matching networks and harmonic filters. With the entire circuit of Fig. 1 functioning as an X-band source, 2 mw at 8720 mc was obtained for a dc power of approximately 4 watts, neglecting bias resistor losses. Approximately 160 mw of 1090-mc power was generated in the process.

In the course of the above measurements, it has been noted that best conversion efficiencies are often obtained with appreciable forward or reverse diode current flowing. The presence of forward current means that the nonlinear depletion-layer capacity is not the only contributor to the efficient generation of harmonics, but that stored charge carriers are also playing a part.[3,4] Reverse current indicates that the diode is undergoing reverse breakdown because of the high level of applied power. However, in this case as well, forward conduction occurs and stored charge effects are probably present.

R. Lowell
M. J. Kiss
Bell Telephone Laboratories
Whippany, N. J.

[3] A. Uhlir, "The potential of semiconductor diodes in high-frequency communications," Proc. IRE, vol. 46, pp. 1099–1115; June, 1958.
[4] A. F. Dietrich and W. M. Goodall, "Solid state generator for 2×10⁻¹⁰ second pulses," Proc. IRE, vol. 48, pp. 791–792; April, 1960.

UHF Harmonic Generation with Silicon Diodes*

P-N junction diodes operated as nonlinear capacitors have proved to be very effective harmonic generators. A number of investigators have obtained efficiencies of 50 per cent or more with junction diodes in the UHF region, though the outputs have only been of the order of milliwatts or tens of milliwatts. These high efficiencies are consistent with the Manley-Rowe theory of lossless nonlinear reactances,[1] which predicts harmonic generation efficiencies of up to 100 per cent for such devices.

A large increase in harmonic power output, along with high efficiency, has been obtained by using a diffused junction silicon diode with a high breakdown voltage. One harmonic generator has delivered 1.1 watts of second harmonic power at 800 mc with an efficiency of 48 per cent. Another gave 166 mw of fourth harmonic at 1600 mc with 17 per cent efficiency. Finally, 2 mw of *X*-band power has been obtained with 0.6 per cent efficiency by multiplying an 1800-mc input.

To investigate the relation between breakdown voltage and power handling ability, a diode with a 7-volt breakdown and one with a 41-volt breakdown were compared. (These were diffused mesa diodes which have been described elsewhere.[2] The different values of breakdown voltage were obtained by choice of impurity gradient—10^{23} cm^{-4} for the former diode, 10^{21} cm^{-4} for the latter.) For some input power levels, the seven volt diode gave efficiencies of over 50 per cent for doubling 400 mc, in the circuit of Fig. 1. The output began to saturate at about 10 mw. The high breakdown diode also gave efficiencies of over 50 per cent for this conversion (but for a wider range of input power levels), and the output began to saturate at about 1.1 watts. These effects can be seen in the plots of maximum output vs input power (Figs. 2 and 3).

* Received by the IRE, December 4, 1959. This work was supported in part by the U. S. Army Signal Corps.
[1] J. M. Manley and H. E. Rowe, "Some general properties of nonlinear elements," Proc. IRE, vol. 44, pp. 904–913; July, 1956.
[2] A. Uhlir, Jr., "The potential of semiconductors in high-frequency communications," Proc. IRE, vol. 46, pp. 1099–1115; June, 1958.

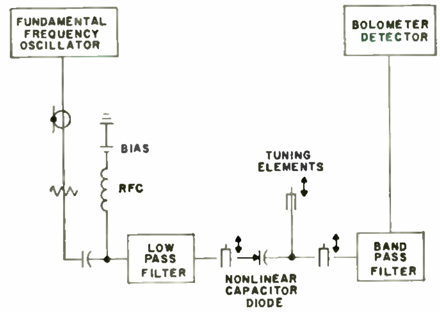

Fig. 1—Tuned harmonic generator.

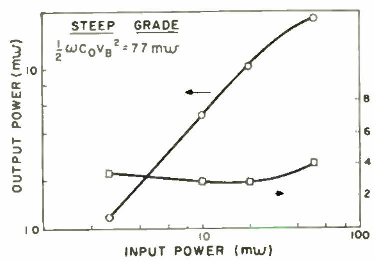

Fig. 2—Second harmonic output power vs input power for the steep grade (low breakdown) diode.

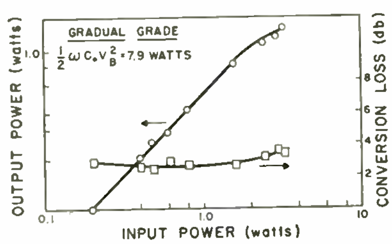

Fig. 3—Second harmonic output power vs input power for the gradual grade (high breakdown) diode.

These high efficiencies, considered in the light of existing theories of nonlinear elements,[1,3] indicate that the diodes acted chiefly as nonlinear capacitors rather than as nonlinear resistors. This conclusion is also consistent with the bias conditions used. To get maximum output power at significant input power levels, it was necessary to back-bias the diodes. At maximum efficiency, the diode current was usually very small, again implying nonlinear capacitor action.

A simple calculation suggests that the observed saturation of output power at high input power sets in when the fundamental voltage amplitude becomes large enough to drive the diode into forward conduction and beyond reverse breakdown, resulting in greater losses. The applied reactive power at this point is given by $P_{max} \approx \frac{1}{2}\omega_1 C_0 V_B^2$, where C_0, the capacitance at zero bias, represents an average capacitance, ω_1 is the fundamental angular frequency, and V_B is the breakdown voltage. P_{max} can be considered an upper limit on the amount of input power that the diode can efficiently convert to harmonics. And in fact, the values of input power at which saturation begins to set in (Figs. 2 and 3) are seen to scale reasonably well with the corresponding values of P_{max} (Table I).

As a preliminary investigation of feasibility of *X*-band harmonic generation, efficiencies have been measured for the following conversions: 400 mc–1600 mc, 800 mc–1600 mc, 1800 mc into *X*-band waveguide. The data are given in Table II. In the last case, no particular harmonics were selected by filtering. The guide cutoff frequency was about 6.5 kmc; hence, the output must have consisted mainly of fourth harmonic.

[3] C. H. Page, "Harmonic generation with ideal rectifiers," Proc. IRE, vol. 46, pp. 1738–1740; October 1958.

TABLE I

	$C_0(\mu\mu f)$	V_B(volts)	P_{max} (Maximum reactive power) $\frac{1}{2}\omega_1 C_0 V_B^2$
Diode 1	1.25	7.0	77 mw
Diode 2	3.76	41.0	7.9 watts

TABLE II

Input frequency (mc)	P_{in} (mw)	Output frequency (mc)	P_{out} (mw)	Conversion loss (db)
400	1000	1600	166	7.8*
400	960	1600	140	8.5†
800	700	1600	245	4.6
1800	340	*X*-band	2	22

* One diode used.
† Two diodes used in two stages of doubling.

The results given here indicate that diode harmonic generators can deliver well over a watt of power at about 1 kmc as well as significant amounts of power at *X*-band. The power-handling ability of nonlinear capacitor diodes has been shown to depend strongly on breakdown voltage.

We are pleased to thank A. E. Bakanowski and R. L. Rulison for the design and fabrication of the gradual grade diode used in these experiments. We also wish to thank Mr. Bakanowski for his helpful advice.

D. Leenov
J. W. Rood
Bell Telephone Labs., Inc.
Murray Hill, N. J.

Boolean Functions Realizable With Single Threshold Devices*

Despite the increasing use of threshold devices such as magnetic cores and parametrons, for digital circuitry, several of the most basic properties of these devices are not fully understood. This paper discusses the properties of the Boolean functions which can be realized with a single threshold de-

* Received by the IRE, February 17, 1960.

vice. Although this discussion is carried out with particular reference to magnetic cores, the conclusions are equally valid for other threshold devices.

Review[1]

The magnetic cores used in pulse-switching circuits possess "rectangular" hysteresis loops such as that shown in Fig. 1. When there is no current in the core windings, the core flux corresponds to either point s or point r of the hysteresis loop. Usually all cores in a group are switched to point r (reset) and then input pulses are allowed to switch certain of the cores to point s (set).

The input leads to the circuit are labeled $x_1, x_1', x_2, x_2', \cdots, x_n, x_n'$ and R. The number of turns on the x_1-winding is N_1, the number of turns on the x_1'-winding is N_1', etc. The current in the x_1-winding is I_1, the current in the x_1'-winding is I_1', etc. (N_i and I_i are not Boolean variables.) If a pulse is present on lead x_1 (and therefore not on lead x_1') we say that $x_1=1(x_1'=0)$ and if a pulse occurs on the x_1'-lead (and not on the x_1-lead) x_1 is equal to 0 and x_1' to 1. A core will be set only if the pulses through the windings of the core produce a magnetomotive force greater than the threshold of the core. The threshold is defined as the smallest magnetomotive force which will cause the core to be set. The setting of the threshold is at the discretion of the designer using the R winding which is either excited with a dc or pulsed every time any of the windings are pulsed. If a core has two windings (x_1 and x_2) and a pulse on either lead will set the core, the setting function of the core is x_1+x_2; if both windings must be pulsed to set the core, the setting function is x_1x_2. The core will be set when the input variables ($x_1, x_2, \cdots$) have values which cause the setting function to equal one. Not all Boolean functions can be the setting function of a single core. For example, $T=x_1x_2+x_1'x_2'$ cannot be a setting function (of a single core). Through this paper, the term setting function will mean setting function for a single core. The purpose of this paper is to discuss the properties of setting functions. A list of symbols which will be used is given in Table I.

Necessary Conditions

In this section, we develop some of the properties of setting functions. These properties are given in three theorems. The first of these, Theorem 1, gives one of the most easily recognized properties of a setting function, unateness. This property will be discussed in detail later. Theorem 2 gives another special property of setting functions, which in Corollary 1 leads to certain constraints on the core windings. Finally, the results of the first two theorems are generalized in Theorem 3 and its corollary.

Theorem 1: A setting function must be unate.

A unate function is defined as one from which one of each pair of complementary literals (x_i, x_i') can be eliminated. By a theorem of Boolean algebra, any switching function can be written in the form $T=x_1t_1+x_1't_0$ where $t_1=T(x_1=1)$ and $t_0=T(x_1=0)$. The function t_1 represents the setting function of the core with a current flowing in the x_1 winding ($x_1=1$). The current in the x_1 winding has the effect of changing the threshold which the core presents to the other windings. If the original threshold of the core was v and the x_1 current produces a magnetomotive force equal to N_1I_1, then the apparent threshold, v_1, with $x_1=1$ will be $v-N_1I_1$ since an additional magnetomotive force of only $v-N_1I_1$ is now necessary to set the core. Similarly, if current in the x_1' winding produces a magnetomotive force of $N_1'I_1'$, the apparent threshold, v_0, with $x_1'=1$, will be $v-N_1'I_1'$.

Either $v_1<v_0$, $v_0<v_1$ or $v_0=v_1$. Let us first assume that $v_1<v_0$. Then t_1 must equal or include t_0 ($t_1 \supseteq t_0$) since any combination of pulses on the input leads (or equivalently any condition of the x_i variables) which provides enough magnetomotive force to overcome the v_0 threshold must surely overcome the smaller v_1 threshold. Similarly, if $v_0<v_1$, t_0 must equal or include t_1, and if $v_1=v_0$, then t_1 must equal t_0. We have thus shown that for all possible relations of v_1 to v_0 t_1 must either equal t_0 ($t_1=t_0$), include t_0 ($t_1 \supset t_0$), or be included in t_0 ($t_1 \subset t_0$).

If t_1 equals t_0, we can let t without a subscript stand for either t_1 or t_0 ($t=t_1=t_0$). The original function can then be written as $T=x_1t_1+x_1't_0=x_1t+x_1't=(x_1+x_1')t=t$. This shows that both x_1 and x_1' can be eliminated from T. If t_1 includes t_0 we can write t_1 as $t_1=t_0+t_d$. Then T can be written as $T=x_1t_1+x_1't_0=x_1(t_0+t_d)+x_1't_0=(x_1+x_1')t_0+x_1t_d=t_0+x_1t_d$. Thus x_1 can be eliminated from T. If t_0 includes t_1, x_1 can be eliminated from T by a similar process. We have thus shown that if T is a setting function, one or both of each pair of complementary literals can be eliminated from T and therefore T must be unate.

A function, T, will be called unate in the literals $x_1^*, x_2^*, \cdots, x_n^*$ (written $T[x_1^*, x_2^*, \cdots, x_n^*]$), if $x_1^*, x_2^*, \cdots, x_n^*$ are the literals which cannot be eliminated from the function. Each symbol x_i^* represents either x_i or x_i'. Thus the function $x_1x_2'+x_2'x_3$ is unate in the literals x_1, x_2', x_3.

Theorem 2: If T is a setting function, unate in the literals $x_1^*, x_2^*, \cdots, x_n^*$, then $T_{10}=T_{01}$, or $T_{01} \supset T_{10}$, or $T_{01} \subset T_{10}$ where $T_{01}=T(x_1^*=0,\ x_2^*=1)$ and $T_{10}=T(x_1^*=1,\ x_2^*=0)$.

T_{10} is the setting function of the core with current in the x_1^*-winding and no current in the x_2^*-winding. The x_1^*-current causes the core to appear to the $x_3^*, x_4^*, \cdots, x_n^*$ windings as if the core had a threshold $v_1=v-N_1I_1$. Thus, T_{10} is the setting function of a core having a threshold v_1. Similarly, T_{01} is the setting function of a core having the same $x_3^*, x_4^*, \cdots, x_n^*$ windings as the original core, but having a threshold $v_2=v-N_2I_2$. As in Theorem 1, $v_1=v_2$, $v_1>v_2$, or $v_2>v_1$, and therefore $T_{01}=T_{10}$, $T_{01} \supset T_{10}$, or $T_{10} \supset T_{01}$.

Corollary 1: If $T_{10} \supset T_{01}$, then $N_1^*I_1^* > N_2^*I_2^*$, and if $T_{10} \subset T_{01}$, then $N_1^*I_1^* < N_2^*I_2^*$.

TABLE I
Definitions of Symbols

Logical	
1)	$\cdot$ and
2)	$+$ or
3)	$\supset$ inclusion
The letters T, t, and x are used for logical variables.	
Arithmetic	
1)	$-$ difference
2)	$+$ sum
3)	$\cdot$ multiplication
4)	$>$ nequality
The letters N, I, R, and v are used for arithmetic variables.	

Note: Although the same symbol is used in some cases for arithmetic and logical operations there is no ambiguity since d fferent symbols are used for arithmetic and logical variables.

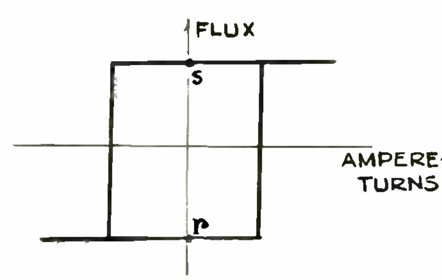

Fig. 1.

TABLE II
Four Variable Setting Functions

	Function	Realization				
		N_1I_1	N_2I_2	N_3I_3	N_4I_4	RI_R
1	X_1	1	—	—	—	0
2	X_1+X_2	1	1	—	—	0
3	$X_1+X_2+X_3$	1	1	1	—	0
4	$X_1+X_2+X_3+X_4$	1	1	1	1	0
5	$X_1+X_2X_3$	2	1	1	—	1.5
6	$X_1+X_2(X_3+X_4)$	3	2	1	1	2.5
7	$X_1+X_2X_3+X_2X_4+X_3X_4$	2	1	1	1	1.5
8	$X_1+X_2+X_3X_4$	2	2	1	1	1.5
9	$X_1(X_2+X_3+X_4)$	3	1	1	1	3.5
10	$X_1(X_2+X_3)+X_2X_3$	2	2	1	—	2.5
11	$X_1(X_2+X_3+X_4)+X_2X_3$	3	2	2	1	3.5
12	$X_1X_2+X_1X_3+X_1X_4+X_2X_3+X_2X_4$	2	2	1	1	2.5
13	$X_1X_2+X_1X_3+X_1X_4+X_2X_3+X_2X_4+X_3X_4$	1	1	1	1	1.5
14	$X_1X_2+X_1X_3+X_1X_4+X_2X_3X_4$	2	1	1	1	2.5
15	$X_1X_2X_3+X_1X_3X_4+X_2X_3X_4+X_1X_2X_4$	1	1	1	1	3.5
16	$X_1X_2+X_1X_3X_4+X_2X_3X_4$	2	2	1	1	3.5
17	$X_1(X_2+X_3)+X_2X_3X_4$	3	2	2	1	4.5
18	$X_1X_2(X_3+X_4)$	2	2	1	1	4.5
19	$X_1(X_2+X_3)(X_2+X_4)(X_3+X_4)$	3	1	1	1	4.5
20	$X_1(X_2+X_3X_4)$	3	2	1	1	4.5
21	$X_1+X_2X_3X_4$	3	1	1	1	2.5
22	$X_1(X_2+X_3)$	2	1	1	—	2.5
23	$X_1X_2X_3X_4$	1	1	1	1	3.5
24	$X_1X_2X_3$	1	1	1	—	2.5
25	X_1X_2	1	1	—	—	1.5

[1] See M. Karnaugh, "Pulse-switching circuits using magnetic cores," Proc. IRE, vol. 43, pp. 570–584; May, 1955.

If $T_{10} \supset T_{01}$, then there is at least one combination of pulses on the input leads which is sufficient to overcome the apparent threshold $v_1 = v - N_1^*I_1^*$, and which is not sufficient to overcome the apparent threshold $v_2 = v - N_2^*I_2^*$. Therefore $v_1 < v_2$ and $N_1^*I_1^* > N_2^*I_2^*$. Similarly if $T_{10} \subset T_{01}$, $v_1 > v_2$ and $N_1^*I_1^* < N_2^*I_2^*$. If $T_{10} = T_{01}$, it might seem that $N_1^*I_1^*$ must equal $N_2^*I_2^*$, but this is not necessarily true. For consider the function $x_1x_3 + x_2x_3$, in which $T_{10} = T_{01}$. This function can be realized by $N_1^*I_1^* = 1$, $N_2I_2 = 2$, $N_3^*I_3^* = 3$, and $v = 3.5$, or by $N_1^*I_1^* = 2$, $N_2^*I_2^* = 1$, $N_3^*I_3^* = 3$, and $v = 3.5$ or by $N_1^*I_1^* = 1$, $N_2^*I_2^* = 1$, $N_3^*I_3^* = 2$ and $v = 2.5$. So that although $T_{10} = T_{01}$, no constraint is implied between $N_1^*I_1^*$, $N_2^*N_2^*$.

This result is important in the design of a core which is to have a specified setting function since it provides a method of determining the restriction on the number of turns for each winding on the core.

The functions T_{00}, T_{01}, T_{10}, T_{11}, which will be called residues, appear in the canonical expansion of the function about the variables x_1^*, x_2^*:

$$T = x_1^*x_2^*T_{11} + x_1(x_2^*)'T_{10} + (x_1^*)'x_2^*T_{01} + (x_1^*)'(x_2^*)'T_{00}.$$

A function can, of course, be expanded about more than two variables. The following theorem, which includes Theorems 1 and 2 as special cases, can be proved by the same proof given for Theorem 2.

Theorem 3: If T is a setting function, then the residues which occur in a canonical expansion of T about any number of variables must be such that for each pair of residues, either one includes the other or both residues are equal.[2]

Corollary 2: If, in a canonical expansion of a setting function, residue T_a includes residue T_b, then the sum of the number of ampere-turns corresponding to literals set equal to 1 in T_a must be greater than the sum of the number of ampere-turns corresponding to literals set equal to 1 in T_b.

The proof of this corollary is analogous to that given for Corollary 1.

Examples

For functions of three or less variables it has been found that Theorem 1 provides both necessary and sufficient conditions for a setting function. For four or more variables, however, the additional conditions of Theorem 3 become necessary. For example, the function $T = x_1x_2 + x_3x_4$ is unate, satisfying Theorem 1, but it is not a setting function since the conditions of Theorem 3 are not satisfied. For example, $T(x_1 = 1, x_3 = 0) = x_2$ and $T(x_1 = 0, x_3 = 1) = x_4$, so for this pair of residues one *does not* include the other nor are they equal.

As an example of the use of Corollary 2 consider the function

$$T = x_1x_2 + x_1x_3 + x_1x_4 + x_1x_5 + x_2x_3x_4x_5.$$

Then

$$T(x_1 = 1, x_2 = 0, x_3 = 0) = x_4 + x_5$$
$$T(x_1 = 0, x_2 = 1, x_3 = 1,) = x_4x_5.$$

Therefore

$$T(x_1 = 1, x_2 = 0, x_3 = 0) \supset T(x_1 = 0, x_2 = 1, x_3 = 1),$$

and by Corollary 2,

$$N_1I_1 > N_2I_2 + N_3I_3.$$

M. C. Paull
Bell Telephone Labs.
Whippany, N. J.
E. J. McCluskey, Jr.
Princeton University
Princeton, N. J.

[2] The converse of this theorem is also true for most of the functions which have been studied, and it was originally conjectured that the conditions of the theorem might be sufficient as well as necessary. That this is not true was demonstrated by E. F. Moore of Bell Telephone Laboratories. Dr. Moore has constructed a function which satisfies the conditions of the theorem but which is not realizable as a setting function.

An equivalent theorem was independently formulated by E. P. Stabler in terms of the set of inequalities which correspond to the magnetomotive forces necessary to realize a given function.

Strip-Line *Y* Circulator*

Waveguide *Y*-junction circulators have been investigated by many authors.[1-4] In this letter the author proposes a new *Y* circulator which consists of the *strip-line Y* junction containing the nonreciprocal element (two pieces of properly magnetized garnet or ferrite) shown in Fig. 1. This is useful especially in the UHF region because it is simple in structure, small in volume, light in weight, and has good characteristics. Experimental results with the proposed circulator in *L* band are discussed.

Garnet (or ferrite) elements of the proper material, shape, and size for the characteristics of a circulator are inserted with correct impedance elements at the right place in the *H*-plane *Y* junction of a balanced strip-line, and a dc external magnetic field is applied to these garnet elements, transverse to the plane of the strip-line junction by an external electromagnet.

When a wave of frequency 1350 mc enters, for example, through arm 3 from a matched generator, it comes out from arms 1 and 2 terminated by matched detectors. Transmission losses are shown against the applied dc magnetic field in Fig. 2. When the external dc magnetic field *Ho* corresponding to point *A* or *B* in this figure is applied, the clockwise or counter-clockwise circulator is completed. In practice, Alnico magnets having the magnetic field *Ho* corresponding to the point *A* are set to this strip-line junction; the frequency characteristics of the circulator are shown in Fig. 3. These data are obtained for the strip-line *Y* circulator

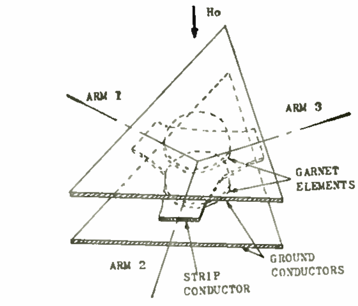

Fig. 1.

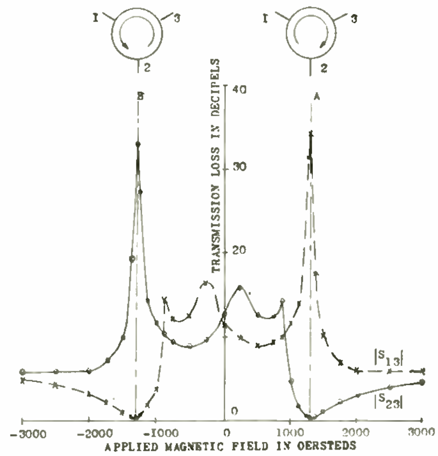

Fig. 2.

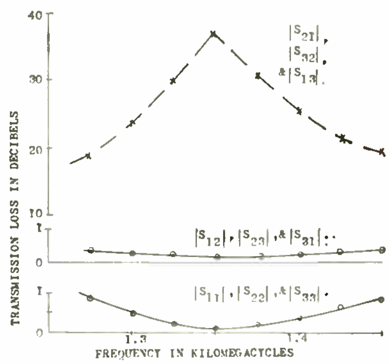

Fig. 3.

with type *N* coaxial connectors. This circulator is designed for use with masers and parametric amplifiers at *L* band with special attention given to minimizing the insertion losses. Typical performance is 0.3 db insertion loss, over 23 db isolation with VSWR less than 0.5 db over 100-mc bandwidth in *L* band, and is 0.2_2 to 37 db with VSWR 0.1_5 db at the center of the band. We can expect to get better characteristics when the strip-line circulator is used without the coaxial connectors and the coaxial-strip-line junctions.

In the above example, disks of yttrium iron garnet made by another group in this laboratory are placed on the inside walls of ground plates at the center of the junction as the nonreciprocal phase shift element; the impedance element (disks of low-loss dielectrics) is useful for improving the characteristics of the circulator.

* Received by the IRE, November 30, 1959.

[1] W. E. Swanson and G. J. Wheeler, "Tee circulator," 1958 WESCON Convention Record, pt. 1, pp. 151–160.

[2] H. N. Chait and T. R. Curry, "Y circulator," *J. Appl. Phys.*, vol. 30, pp. 152s–153s; April, 1959.

[3] B. A. Auld, "The synthesis of symmetrical waveguide circulators," IRE Trans. on Microwave Theory and Techniques, vol. MTT-7, pp. 238–246; April, 1959.

[4] L. Davis, Jr., U. Milano, and J. Saunders, "An *L*-band *Y*-junction circulator," presented at 1959 PGMTT Natl. Symp., Harvard University, Cambridge, Mass.; June 1–3.

The strip-line T circulator, which consists of the strip-line T junction containing the nonreciprocal element, can be made successfully by using almost the same technique, but at present its characteristics are slightly inferior to the strip-line Y circulator, especially in the balance of the characteristics and in the insertion loss.

The other types of circulator can be made by using almost the same technique as in the case of the other types of strip-lines, for example, the unbalanced strip-line, and so on.

A microwave switch can be made by applying the magnetic field corresponding to the points A and B in Fig. 2 alternately to the garnet elements.

The strip-line circulator with the permanent magnet and the coaxial connectors can be made up in small size, for example, less than 4.5 inches in diameter and 2 inches in height.

SHINICHIRO YOSHIDA
Matsuda Research Lab.
Tokyo Shibaura Electric Co.
Kawasaki, Kanagawa, Japan

Influence of Source Distance on the Impedance Characteristics of ELF Radio Waves*

Some interesting features in the propagation of radio waves emerge when the wavelength becomes very great. In the frequency range below 3 kc, which may be described as extremely low frequencies (ELF), the distance from the source to the observer is usually comparable with the wavelength. Under such a condition, it is not permissible to assume that the wavefronts are plane; consequently the ratio of the electric and magnetic field components orthogonal to the direction of propagation are no longer equal to 377 ohms. While this fact has been implicitly recognized by some workers[1-3] in field studies of lightning discharges, little attempt has been previously made to estimate the actual behavior of the fields taking into account both source distance and the influence of the ionosphere.

In this note, quantitative results for the wave impedance at ELF are presented for a typical case. The model chosen consists of a flat perfectly conducting earth and a plane ionospheric reflecting layer at height h. The source is assumed to be equivalent to a vertical electric dipole located on the ground plane. Choosing a conventional cylindrical coordinate system (ρ, ϕ, z), the ground plane is $z=0$, the lower edge of the ionosphere is $z=h$, and the source is at the origin. The ionosphere itself is taken to be a homogeneous ionized medium for $z>h$. Under these assumptions, the expressions for the (nonzero) field components at distance ρ on the surface of the ground may be written[4]

$$E_z = WE_0 \tag{1}$$

and

$$H_\phi = -TE_0/377, \tag{2}$$

where E_0 is numerically equal to the radiation field of the source dipole at a distance ρ on a perfectly flat conducting plane in the absence of a reflecting ionospheric layer. By definition, $E_0 = \text{const.} \times \exp(-i2\pi\rho/\lambda)/\rho$. The dimensionless quantities W and T are given to a high order of approximation[4] by the following series expansions, involving Hankel functions of order zero and one:

$$W = i\pi(\rho/h)\exp(ik\rho)\sum_{n=0}^{\infty}\delta_n S_n{}^2 H_0{}^{(2)}(kS_n\rho), \tag{3}$$

and

$$T = -\pi(\rho/h) \cdot \exp(ik\rho)\sum_{n=0}^{\infty}\delta_n S_n H_1{}^{(2)}(kS_n\rho), \tag{4}$$

where

$$\delta_0 = 1/2, \quad \delta_n = 1 \quad \text{for } n = 1, 2, 3 \cdots,$$
$$S_0 = (1 - i\Delta/kh)^{1/2},$$
$$S_n = [1 - (\pi n/kh)^2 - i2\Delta/kh]^{1/2} \quad n = 1, 2, 3 \cdots,$$
$$k = 2\pi/\lambda,$$
$$\Delta = (i\omega/\omega_r)^{1/2}.$$

In the above, ω_r is an ionospheric conductivity parameter which involves the electron density, collision frequency and earth's magnetic field. On the basis of previous work,[4] its effective value can be expected to range from 10^5 to 10^6. The forms of (3) and (4) are actually modified by earth curvature and finite ground conductivity,[4] but for ELF applications their influence is usually negligible.

The above series formulas for W and T may be regarded as a sum of waveguide modes. In the classical sense, the modes above zero are cut off at ELF since $(\pi n/kh) > 1$, and thus S_n is almost purely imaginary. However, at short distances $(k\rho \ll 1)$, these terms do contribute appreciably to the mode sum. In fact, at very short distances $(\rho \ll h)$, the mode sum becomes very poorly convergent. In this case, however, W and T may be simply computed from the elementary formulas[2]

$$W = 1 - i/(k\rho) - 1/(k\rho)^2, \tag{5}$$

and

$$T = 1 - i/(k\rho), \tag{6}$$

which physically mean that the ionosphere is not a factor.

The wave impedance is, of course, the ratio of E_z to $-H_\phi$. In dimensionless form, this becomes the complex ratio W/T. Using (3) and (4), the magnitude of W/T and the phase lag of W/T are plotted in Figs. 1 and 2 as a function of distance ρ, in km for frequencies of 50 cps to 1600 cps. For these curves, $\omega_r = 5 \times 10^5$ and $h = 90$ km which are typical values for night. (Actually, the phase as plotted is a lag in the sense that the ordinate of Fig. 2 is the $-\arg(W/T)$ and, to avoid negative quantities, 2π radians are added.)

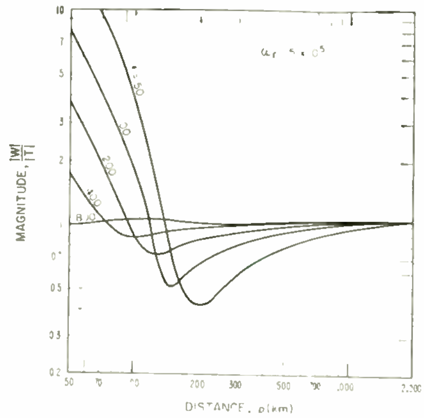

Fig. 1—The magnitude of the normalized impedance ratio W/T as a function of distance ρ, $h = 90$ km.

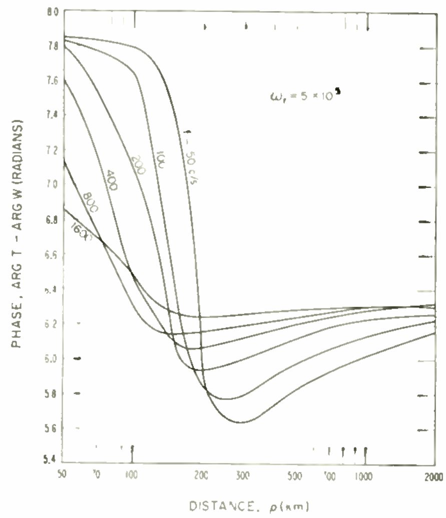

Fig. 2—The phase (lag) of the impedance ratio W/T as a function of distance ρ, $h = 90$ km.

At large distances, the magnitude W/T is approaching unity and the phase is 2π radians. This limiting case corresponds to a plane wavefront and thus W/T may be replaced by unity or E_z/H_ϕ may be replaced by -377 ohms. At the moderately short distances the magnitude of W/T is actually less than unity, and at the very short distances it rises considerably above unity. The curves in Figs. 1 and 2 are actually only appropriate for $\omega_r = 5 \times 10^5$ and $h = 90$ km. Their shape, however, is not appreciably modified if other values of these parameters are chosen.

It has been suggested[5] that the behavior of these curves could be the basis of a range finding device at ELF. For example, if the distance to a lightning stroke is to be estimated from a single station, the following procedure might be used. The waveform of the electric field $e_z(t)$ and the magnetic field

* Received by the IRE, March 11, 1960.

[1] E. T. Pierce, "Electrostatic field-changes due to lightning discharges," *Quart. J. Roy. Met. Soc.*, vol. 81, pp. 211–228; April, 1955, and "Some ELF phenomena," *J. Research NBS*, vol. 64D; July/August, 1960. (In press.)

[2] J. R. Wait, "On the waveform of a radio atmospheric at short ranges," PROC. IRE, vol. 44, p. 1052; August, 1956.

[3] A. D. Watt and E. L. Maxwell, "Characteristics of atmospheric noise from 1 to 100 kc," PROC. IRE, vol. 45, pp. 787–794; June, 1957.

[4] J. R. Wait, "Terrestrial propagation of VLF radio waves—a theoretical investigation," *J. Research NBS*, vol. 64D, pp. 153–204; March/April, 1960. (Gives many references.)

[5] J. R. Wait, "On VLF and ELF mode propagation," paper presented at Commission IV session of Fall URSI meeting, San Diego, Calif.; October 20, 1959.

$h_\phi(t)$ of the event are recorded on an oscilloscope.[6] The frequency spectra of these waveforms are obtained from

$$E_z(f) = \int_0^\infty e_z(t) \exp(-i2\pi ft)dt, \qquad (7)$$

and

$$H_\phi(f) = \int_0^\infty h_\phi(t) \exp(-i2\pi ft)dt, \qquad (8)$$

for $f=50$, 100, 200, 400, 800 and 1600 cps. The amplitude and phase of the ratio of these quantities, which are proportional to W/T, are then plotted in Figs. 1 and 2 and shifted laterally until they give the nearest coincidence with the curves.

The preceding operation might also be performed using tuned receivers with multiple channels.[7] This has the disadvantage, however, that signals radiated from individual strokes could not be easily distinguished.

I would like to thank A. G. Jean for his helpful comments concerning this problem.

J. R. Wait
Nat. Bur. Standards
Boulder, Colo.

[6] W. L. Taylor and A. G. Jean, "Very low-frequency spectra of lightning discharges," *J. Research NBS*, vol. 63D, pp. 199–204; September/October, 1959.

[7] P. W. A. Bowe, "The wave forms of atmospherics and the propagation of VLF radio waves," *Phil. Mag.*, vol. 42, pp. 121–133; February, 1951.

The Minimum-Range Equation and the Maximum Doppler-Frequency Shift for Satellites*

In a previous paper[1] the minimum-range equation for satellites using the Doppler effect was derived from a spherical geometry. The resulting equation was obtained for the case of a satellite orbiting along a circle whose origin lies at the center of the earth. Since this is a special case, a more general treatment is in order. This will be shown for a simple two-dimensional orbiting problem in which the minimum-range equation

$$R_m = -\frac{v^2}{\lambda(\dot{f})_{\max}} \qquad (1)$$

obtained for a linear orbit is modified by a curved orbit. Fig. 1 illustrates the geometry in which R_0 = radius of the earth, ρ = radius of curvature of the circular orbit of the satellite, α = angular distance between satellite and receiving point, v = speed of satellite, λ = wavelength of emitted signal, $(\dot{f})_{\max}$ = maximum rate of change of frequency at $\alpha=0$, R = range between satellite and receiving point ($R=R_m$ for $\alpha=0$), θ = elevation angle to the satellite, and ψ = angle between v and R.

From Fig. 1, it follows

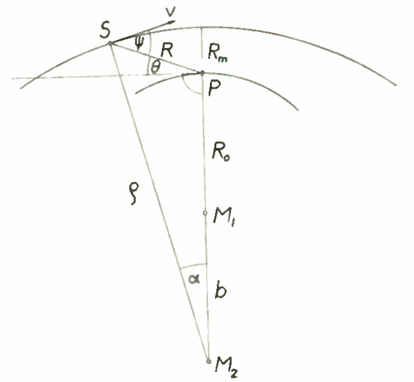

Fig. 1.

$$R = \left[(R_0+b)^2 + \rho^2 - 2(R_0+b)\rho\cos\alpha\right]^{1/2} \qquad (2)$$

and

$$\dot{R} = \frac{dR}{d\alpha}\dot{\alpha} = v\frac{(R_0+b)}{R}\sin\alpha. \qquad (3)$$

Since the observed frequency is

$$f_{\text{observed}} = \frac{\dfrac{c}{\lambda}}{1-\dfrac{v}{c}\cos\psi} \quad \text{for } \frac{v^2}{c^2} \ll 1, \qquad (4)$$

one obtains

$$\Delta f = -\frac{\dfrac{v}{\lambda}\cos\psi}{1-\dfrac{v}{c}\cos\psi} = -\frac{v}{\lambda}\cos\psi \quad \text{for } \frac{v}{c} \ll 1; \qquad (5)$$

and because

$$tg\psi = \frac{1-\dfrac{(R_0+b)}{\rho}\cos\alpha}{\dfrac{(R_0+b)}{\rho}\sin\alpha}, \qquad (6)$$

it follows from (3), (5), and (6)

$$\Delta f = -\frac{\dot{R}}{\lambda} \quad \text{for } \frac{v}{c} \ll 1. \qquad (7)$$

Combining (3) and (7),

$$R = -\frac{(R_0+b)v\sin\alpha}{\lambda(\Delta f)} \qquad (8)$$

and

$$R_m = -\frac{(R_0+b)v}{\lambda}\lim_{\alpha\to 0}\left[\frac{\sin\alpha}{\Delta f}\right]. \qquad (9)$$

Applying the rule of de l'Hospital, using time as the independent variable, one obtains

$$\lim_{\alpha\to 0}\left[\frac{\sin\alpha}{\Delta f}\right] = \frac{\cos\alpha\,\dot{\alpha}}{\dot{\Delta f}} = \frac{\dot{\alpha}}{(\dot{f})_{\alpha=0}}, \qquad (10)$$

and since $\dot{\alpha}=v/\rho$, it follows from (9) and (10)

$$R_m = -\frac{(R_0+b)}{\rho}\,\frac{v^2 f}{\lambda(\dot{f})_{\alpha=0}}. \qquad (11)$$

For the simple case of a circular orbit, it can be seen that the error of determining R_m by neglecting the curvature of the orbit (1) is determined by the ratio $(R_0+b)/\rho$, which approaches unity the further M_2 is removed from M_1 (Fig. 1) while R_m is kept the same.

If v, λ, and $(\dot{f})_{\alpha=0}$ are the measured quantities, (11) can be written in a more general form which includes also the angle ξ between the plane containing the circular orbit and $\dot{R}_m$. Hitherto, ξ was assumed to be 0.

$$\frac{\lambda(\dot{f})_{\alpha=0}}{v^2} = -\frac{1}{R_m} + \frac{\cos\xi}{\rho}. \qquad (12)$$

For $\rho\to\infty$ or $\xi=90°$, (12) and (1) are identical. For smaller values of ρ, the experimental data are influenced by R_m as well as ρ and ξ.

It is of mathematical interest to rewrite (12) for $\rho<R_m$ when $\xi=0$:

$$\frac{\lambda(\dot{f})_{\alpha=0}}{v^2} = \frac{1}{\rho} \quad \text{for } \frac{\rho}{R_m} \ll 1. \qquad (13)$$

For small values of ρ at great distances from P, the knowledge of v, λ, and $(\dot{f})_{\alpha=0}$ enables one to determine the radius of curvature of a moving emitter.

The minimum of the Doppler frequency difference occurs for $R=R_m$; *i.e.*, $\alpha=0$. It is now of interest to determine the value of θ (Fig. 1) for which the Doppler frequency shift is a maximum. For $v/c \ll 1$, and since

$$\cos\psi = \frac{(R_0+b)}{\rho}\cos\theta, \text{ for } \xi=0, \qquad (14)$$

it follows from (5) and (14) that

$$\Delta f = -\frac{v}{\lambda}\,\frac{(R_0+b)}{\rho}\cos\theta = \Delta f_{\max}\cos\theta. \qquad (15)$$

The maximum of $\Delta f(\theta)$ is obtained for $\theta=0$. The $\Delta f(\theta)$-distribution is symmetrical relative to $\theta=0$. Because $R\dot{\alpha}$ is asymmetrical with respect to $\theta=0$, there exists no symmetry in time with respect to $\theta=0$, although

$$\left.\frac{d\Delta f}{dt}\right|_{\theta=0} = \left.f_{\min}\right|_{\theta=0} = 0. \qquad (16)$$

In practice, satellites are more likely to move in elliptic rather than circular orbits. With this in mind, one arrives at the following conclusion:

If a satellite moves with constant speed v over a sufficient length of its orbit along a circle of radius ρ which is centered on M_2 (Fig. 2), and its radio emission is monitored from P in the plane of the orbit, the Doppler-frequency difference is a maximum where the satellite orbit is intersected by a normal to $\overline{M_2P}$ through P. Moreover, if a satellite moves in an elliptic orbit, its speed varies in accordance with Kepler's second law. If P lies in the focal point of the ellipse, the minimum range R_m lies in the direction of the major axis. In this case, the normal ($\theta=0$) to R_m ($\theta=90°$) remains the direction of maximum Doppler-frequency shift and the $\Delta f(\theta)$-distribution also obeys the cosine law.

* Received by the IRE, January 4, 1960.

[1] J. M. Brito, Infante, "A correction necessary for the applications of the Doppler effect to the measurement of distances to satellites," Proc. IRE, vol. 47, p. 2023; November, 1959.

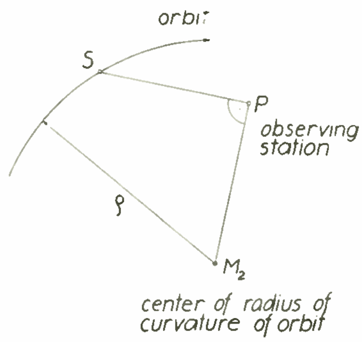

Fig. 2.

In (15), relativistic effects were neglected. It is conceptually of interest to consider relativistic speeds assuming that an emitter can move in a prescribed circle with $v \doteq c$. The observed frequency[2] at P is

$$f_{\text{observed}} = \frac{f\left(1 - \dfrac{v^2}{c^2}\right)^{1/2}}{1 - \dfrac{v}{c}\cos\psi}. \qquad (17)$$

It follows from (14) and (17)

$$\Delta f = f\left[1 - \frac{\left(1 - \dfrac{v^2}{c^2}\right)^{1/2}}{1 - \dfrac{v}{c}\left(1 - \dfrac{R_m}{\rho}\right)\cos\theta} =\right] \qquad (18)$$

For $R_0 = 6378$ km, $\rho = 6878$ km and $b = 0$, curve II of Fig. 3 displays the normalized

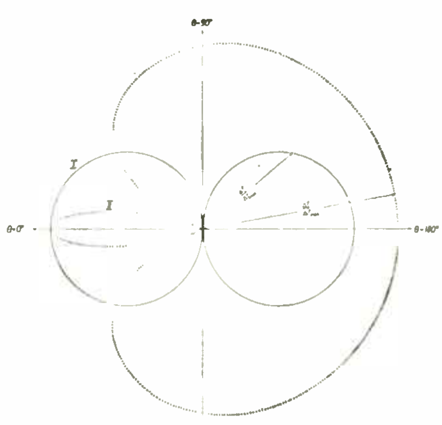

Fig. 3—Normalized Doppler-frequency difference as a function of elevation angle θ for a nonrelativistic (I) and a relativistic (II) case. $R_0 = 6378$ km, $\rho = 6878$ km.

form of (18) for $v = 0.99c$. The radius vector represents $\Delta f/(\Delta f_{\max})_{\theta=0}$. The cosine distribution of (15) for $v \ll c$ is shown for comparison (curve I). For both cases a maximum of the Doppler-frequency difference occurs at $\theta = 0$ and both distributions are symmetrical relative to $\theta = 0$. As v increases from nonrelativistic to relativistic speeds, the maximum of the $\Delta f(\theta)$-distribution for the approaching emitter sharpens while it flattens for the receding portion of the emitter's path. One can conclude that the maximum of $\Delta f(\theta)$ can become a useful supplement to the minimum of $\Delta f(\theta)$ if it were possible to have an emitting body orbit with a relativistic speed. For low speeds the sharpness of the maximum was given by the cosine law of (15).

KURT TOMAN
AF Cambridge Res. Ctr.
Bedford, Mass.

[2] F. A. Jenkins and H. E. White, "Fundamentals of Optics," McGraw-Hill Book Co., Inc., New York, N. Y., p. 402; 1950.

Radiation Effects on Quartz Oscillators*

The effects of X radiation on the oscillatory frequency of quartz crystal plates have been reported by many investigators in recent publications.[1] The purpose of this note is to discuss the frequency shift of quartz oscillators with respect to total dose received, dose rate, and the level of X- and gamma-ray incident energy.

The specimens selected for investigation were BT cut crystals, wire mounted in HC-6/U holders, all having a fundamental frequency of 10 mc. Since the primary objective was to measure the change in frequency due to radiation, reference or "standard" crystals were used, eliminating the need for measurement of exact specimen frequency. The specimen and reference crystals were oscillated in identical circuits. The RF outputs of these circuits were then combined, and the resulting signal was demodulated. This demodulated signal was amplified and fed to an electronic counter whose readout represented the beat frequency between specimen and reference crystals. The difference frequency was measured before irradiation, and at specific dose levels during the irradiation of the specimens. The high degree of temperature sensitivity of BT crystals made it necessary to use temperature controlled ovens during frequency measurements. The specimens were removed from the ovens, irradiated, and returned to the ovens for measurement of frequency shift.

Specimen irradiation was accomplished by the use of 28 kvp, 100 kvp, and 300 kvp X-ray sources and multi-curie gamma emitting isotope sources of 0.66 mev and 1.25 mev. Dose rates varied from 9×10^3 R per hour to 147.6×10^3 R per hour, with total doses up to 1×10^6 R accumulated by the crystals.

BT cut quartz crystal oscillators, which are subjected to X or gamma radiation, shift frequency in proportion to the dose received as illustrated in Fig. 1.

The curve is representative of the change in frequency which occurred when a 300 kvp X-ray source was used to irradiate the crystals. As shown by the graph, the initial rate of frequency shift was greater than the shift

* Received by the IRE, January 27, 1960.
[1] R. Beckmann, "Radiation effects in quartz—a bibliography," *Nucleonics*, vol. 16, pp. 122; March, 1958.

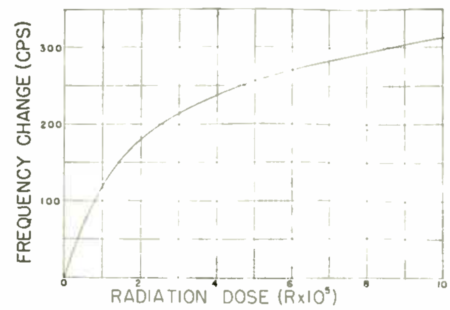

Fig. 1—Change in frequency vs accumulated dose for 300 kvp X radiation.

after a dose had been accumulated, indicating an asymptotic approach to radiation saturation.

The energy level of incident ionizing radiation was also a parameter in determining the radiation-frequency effects as shown in Fig. 2.

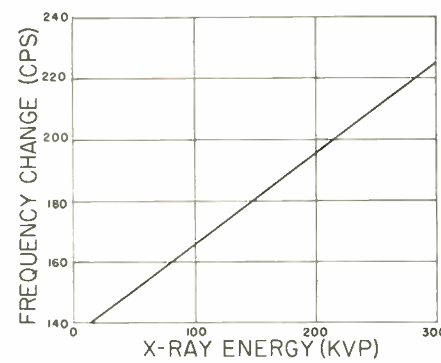

Fig. 2—Change in frequency vs X-ray energy at 300,000 R total dose.

At a dose level of 300,000 R, the frequency shift increased directly with the increase in the peak energy of the incident X radiation. Since X-ray generators produce a continuous spectrum of "white" radiation in addition to a characteristic spectrum, no correlation other than that of peak energy was made. The use of 0.66 mev Cesium 137 and 1.25 (average) mev Cobalt 60 gamma emitting isotopes however, substantiated this effect of radiation energy level upon the frequency shift.

Although dose rate dependence is still being investigated, no frequency changes which can be totally attributed to a change in dose rate have been noted to the present time. Several specimen crystals were irradiated with Cobalt 60 gamma radiation (1.25 mev average), at 9000 R/hour and 19,900 R/hour and measurements at 300,000 R and 600,000 R failed to show any difference in frequency shift. It is anticipated that work now in process will substantiate this.

The authors wish to express their appreciation to D. S. Sarna for his valuable assistance in the measurements performed during the course of this investigation.

O. RENIUS
D. REES
Physical Sciences Lab.
Ordnance Tank-Automotive Command
Detroit, Mich.

The Calculation of Transit Times in Junction Transistors When the Mobilities Are Not Constant*

Varnerin[1] has pointed out that the charge stored in the base for a given emitter current is a convenient way of defining the effective carrier transit time across the base of a junction transistor. Working from various assumptions which can be found from his paper, he showed that for a given base resistance a retarding drift field gives a substantially shorter transit time than an aiding field.

One of the assumptions was that the mobility and diffusion constants were independent of impurity concentration. Since it is necessary to use a very high doping level to obtain a low base resistance in VHF transistors, it is of considerable interest to examine the case of nonconstant mobilities. At high doping levels the diffusion constants and the mobilities vary approximately as $N^{-1/3}$ where N is the impurity concentration. Varnerin mentions this, but, as he points out, he makes a rather crude approximation to the varying mobility, and only attempts to indicate the transit time for a given donor charge. This corresponds to a constant punch-through voltage, but not, of course, to a constant base resistance.

However, it is possible to repeat the analysis on Varnerin's original assumptions except for that of constant mobilities, and to obtain an accurate comparison of the transit time for a given base resistance for different impurity distributions. Using Varnerin's notation

$$J = q\mu_p(x)pE - qD_p(x)\frac{dp}{dx} \tag{1}$$

if

$$n = N \text{ and } \mu_p(x) = \frac{q}{kT}D_p(x)$$

$$J = -qD_p(x)\left(\frac{p}{n}\frac{dn}{dx} + \frac{dp}{dx}\right).$$

Integrating between x and w and writing $p=0$ at $x=w$,

$$p(x) = \frac{J}{qn(x)}\int_x^w \frac{n}{D_p(x)}dx. \tag{2}$$

It is this equation rather than Varnerin's (4) which must be used if D_p is a function of x.

It is instructive to repeat Varnerin's analysis of exponential impurity distributions in the base.

$$\therefore N = n = N_0e^{\alpha x} \tag{3}$$

$$\therefore D_p = D_0e^{-\alpha x/3} \text{ and } \mu_n = \mu_0e^{-\alpha x/3}. \tag{4}$$

It is first necessary to establish the condition of constant base resistance. The sheet conductance of the base (σ) is given by

$$\sigma = q\int_0^w \mu_n n dx$$

$$\therefore \sigma = \frac{3q}{2\alpha}\mu_0N_0[e^{2\alpha w/3} - 1]. \tag{5}$$

It is now necessary to find the total hole charge in the base. From (2), (3) and (4),

$$p_x = \frac{3J}{4qD_0\alpha}\left[e^{4\alpha w/3}e^{-\alpha x} - e^{\alpha x/3}\right]. \tag{6}$$

The total hole charge in the base (Q) is

$$q\int p_x dx;$$

therefore transit time $(t)=Q/J$ is given by

$$t = \frac{3}{4D_0}\left[\frac{3 - 4e^{\alpha w/3} + e^{4\alpha w/3}}{\alpha^2}\right]. \tag{7}$$

From (5)

$$e^{2\alpha w/3} = \left[\frac{2\sigma}{3q\mu_0N_0}\right]\alpha + 1.$$

Let

$$\frac{2\sigma}{3q\mu_0N_0} = Z \quad \therefore e^{2\alpha w/3} = \alpha Z + 1. \tag{8}$$

From (7) and (8)

$$t = \frac{\sigma^2}{3q^2\mu_0^2N_0^2D_0} \cdot\left(\frac{3 - 4\sqrt{\alpha Z + 1} + (\alpha Z + 1)^2}{(\alpha Z)^2}\right). \tag{9}$$

The ratio of doping on the collector side to the emitter side of the base is $e^{\alpha w}$. Therefore, the transit time can be found as a function of this doping ratio and it is plotted in Fig. 1. A large aiding field will in fact be worse than is indicated by the figure because the doping level near the collector will be too low for the assumption of increasing mobility with decreasing impurity concentration to be valid.

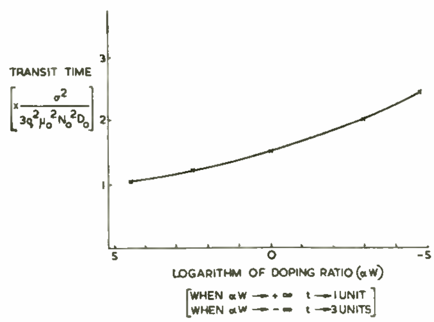

Fig. 1.

It is interesting that an impurity distribution that gives a large reverse drift field gives an advantage over a homogeneous base of only a factor of 1.5. This is much less than the advantage in transit time for a given punch-through voltage indicated by Varnerin's approximation. It would, of course, be possible to use (2), in conjunction with the obvious condition for constant donor charge, to obtain an accurate expression for the transit time for a given punch-through voltage. However, the punch-through voltage can be altered independently of the transit time by changing the doping in the collector depletion layer and is not a fundamental property of the base layer. The base resistance and the transit time are controlled by the doping in the base only.

It should be emphasized that the result of the above analysis in no way contradicts the main conclusions of Varnerin's excellent paper.

J. R. A. Beale
Mullard Research Labs.
Salfords, Redhill
Surrey, Eng.

Author's Comment[2]

In the preceding letter, Beale has presented an interesting extension of my stored charge base transit analysis.[1] He treats rigorously the case for nonconstant mobilities which I had dealt with in an approximate fashion. I am in complete agreement with his analytical contribution. However, it seems worth emphasizing that Beale has made his calculations subject to a boundary condition (constant base resistance, r_b') which is different from mine (constant donor charge per cm², N_T). It is shown below that it is this fact which primarily accounts for the qualitatively different conclusions. In addition, a more detailed design analysis based upon the transistor application provides a basis for further interpretation of these conclusions.

As in Varnerin,[1] the base transit time τ can be expressed as

$$\tau = \frac{w_0^2}{2D_p}f, \tag{10}$$

where w_0 is the base width for uniform doping and D_p is diffusion coefficient for holes (for the case of a p-n-p transistor); $(w_0^2/2D_p)$ is the transit time for uniform doping, while f is a base transit time factor which depends upon the doping profile and actual base width w. For analytical simplicity an exponential base doping was chosen given by $N = N_0 \exp(-\beta x)$ (as does Beale with $\beta = -\alpha$) subject to constant emitter doping N_0 and a constant base donor charge N_T per cm². For the case of constant diffusion coefficient, I showed that by varying β the base transit time factor is given by

$$f \cong \left(\frac{w}{w_0}\right)^{1/3}$$

When $w < w_0$, reverse grading and retarding fields result, but transit time is reduced. In an approximate fashion it was shown in Varnerin[1] that for a nonuniform diffusion coefficient, represented by a $N^{-1/3}$ dependence, f is given approximately by

$$f \cong \frac{w}{w_0}.$$

shown as curve A in Fig. 2.

Also shown as curve B in Fig. 2 are Beale's results for constant base resistance r_b'. As noted by Beale, f is always larger than $\frac{2}{3}$. While these two cases represent different boundary conditions, they would nevertheless appear to present a dilemma in interpretation.

* Received by the IRE, September 8, 1959; revised manuscript received, October 16, 1959.

[1] L. J. Varnerin, "Stored charge method of transistor base transit time analysis," Proc. IRE, vol. 42, pp. 523–527; April, 1959.

[2] Received by the IRE, November 18, 1959.

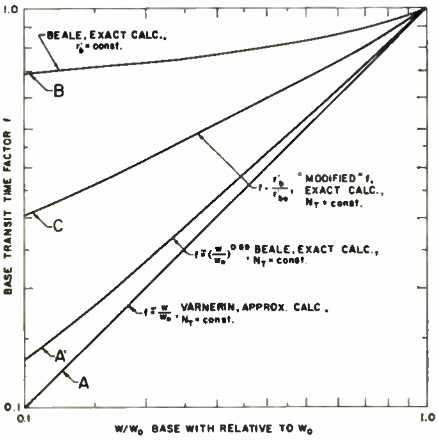

Fig. 2—Base transit time factor as a function of base thickness. Curve A, Varnerin approximate calculation for constant number of donors per cm², N_T; Curve A', same case but using Beale exact calculation; curve B, Beale exact calculation for constant base resistance, r_b'; curve C, "modified" or "figure of merit" base transit factor, $f\cdot(r_b'/r_{b0}')$, based on Beale exact calculation.

As a first step in resolving this dilemma, the degree of approximation in curve A can be checked rather simply. As noted by Beale, his expressions can be used for my constant N_T case. This is presented as curve A'. It is interesting to note that over the range of interest the accurate calculation of f can be represented by

$$f \cong \left(\frac{w}{w_0}\right)^{0.89}$$

which agrees remarkably well with the unity power dependence resulting from my approximation.

Why curves A' and B behave so differently is easy to understand physically. Beale's constant base resistance condition requires that donors be added to compensate for mobility loss as base width is reduced, while I do not require such an addition. An increase in base resistance occurs in the constant donor case; for $w/w_0=0.1$, it amounts to a factor of 2.3. On the other hand, for $w/w_0=0.1$, 4.2 times as many donors must be introduced into the base to maintain constant base resistance. The increased base doping results in a further decrease in diffusion coefficient over the constant donor case. In addition, the larger grading parameter β required by the higher doping results in a larger retarding field than for the constant donor case.

There are some guides to the use of these results. In the case of power amplifier and oscillator applications, the gain-band figure of merit[3,4]

$$\Gamma_0 \cdot B^2 = \frac{f_\alpha}{25 r_b' C_c}$$

can be used to advantage.[5] Γ_0 is the low-frequency common emitter power gain, B the frequency at which the gain is down 3 db, f_α the α cutoff frequency, and C_c the collector capacity. In a transistor in which base transit time exceeds all other time constants, f_α is approximately $(2\pi\tau)^{-1}$. Thus the base transit time factor f, for the purposes of figure of merit comparisons, should be multiplied by the relative increase in base resistance. This is given in Fig. 2 as curve C and represents a "modified" base transit time factor $f(r_b/r_{b0})$ where r_{b0} is the base resistance corresponding to uniform base doping. This curve was calculated using Beale's accurate expressions. The "modified" or "figure of merit" base transit time factor in the range of interest can be represented by

$$f\frac{r_b}{r_{b0}} \cong \left(\frac{w}{w_0}\right)^{1/2}.$$

Here it is seen that the modified base transit time factor does not fall off as rapidly as does curve A' with a decreasing w/w_0, yet it represents a more favorable case than does curve B which approaches asymptotically a minimum value of $\frac{2}{3}$. The modified base transit time factor decreases monotonically with w/w_0 without approaching an asymptotic limit.

The application of these results to iterative amplifiers is somewhat less clear since the case of a maximum gain-band product is quite complicated and has not yet been solved exactly. For the case of germanium *p-n-p* transistors, common emitter output impedance is often larger than base resistance so that mismatch occurs in iterative amplifiers. Increased base resistance in such cases is probably of less importance than decreasing base transit time in a transistor for which, as above, the base transit time exceeds all other time constants. A suitable modified base transit time factor might possibly lie between curves A' and C.

In summary, Beale's contribution of a more rigorous analysis for the case of variable diffusion coefficient is interesting and illuminating. His requirement of constant base resistance seems to me, however, unnecessarily restrictive in many practical cases. It precludes a substantial enhancement in figure of merit available in the case of constant donor charge per cm².

I wish again to thank J. M. Early for helpful discussions.

L. J. VARNERIN
Bell Telephone Labs., Inc.
Murray Hill, N. J.

[3] First presented by R. L. Pritchard at the AIEE Winter Meeting in New York, N. Y., January 20, 1954; also, R. L. Pritchard, "Frequency response of theoretical models of junction transistors," IRE TRANS. ON CIRCUIT THEORY, vol. CT-2, pp. 183–191; June, 1955.

[4] J. M. Early, "PNIP and NPIN junction transistor triodes," *Bell Sys. Tech. J.*, vol. 33, pp. 517–533; May, 1954.

[5] Actually f_T (the frequency for which common emitter current gain is unity) has subsequently been found more useful. f_α is used here, however, since it is generally more familiar.

Direct Reading Noise Figure Measuring Device*

The basic principles used at present in direct reading noise figure meters can be modified to improve the performance.

The principle of gating an auxiliary noise source into the input is maintained in the proposed scheme, but instead of measuring voltages, the modified version measures power.

* Received by the IRE, February 8, 1960.

Fig. 1 shows the block diagram. The input of the system under test is connected to the antenna through a shutter which can be either open or closed, according to whether antenna noise should be included or excluded from the measurement. The noise source is added to the input.

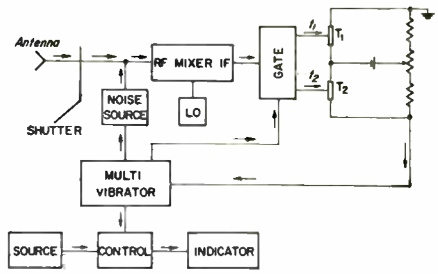

Fig. 1—Block diagram—direct reading noise figure measuring device.

A multivibrator gates the noise source on during a period t_1 and off during a period t_2. Simultaneously, this multivibrator gates the output of the instrument under test during the period t_1 into thermistor T_1, and during the period t_2 into thermistor T_2. An auxiliary amplifier may be needed.

The thermistor bridge is prebalanced. Under balanced conditions, the product of t_1 and the power into T_1 will be equal to the product of t_2 and the power into T_2. The unbalance of the bridge is used to control the ratio of t_1 to t_2 of the multivibrator. Under these conditions, and with sufficient gain in the feedback circuit, the ratio of t_1 to t_2 and knowledge of the power of the noise source are sufficient to compute the noise figure of the instrument under test.

The multivibrator controls the time during which the output of a known source (such as a voltage reference) is applied through a filtering network to an indicator. This indicator reads

$$E = \frac{t_1 E_0}{t_2 + t_1}.$$

E_0 is the reference voltage.

From $R=E/E_0$, the noise figure of the equipment can be computed as

$$F = \frac{RF_0}{1-2R}.$$

where F_0 is the ratio of the power of the noise source to thermal power. This latter value F_0 is fixed for a specific test equipment and, therefore, the output indicator can be calibrated directly for the noise figure.

The system lends itself to a simple performance check by reversing the two thermistors. This can be done by reversing the gate functions and the polarity of the bridge. If the indicator reads the same in both positions, the thermistors are performing properly.

GEORGE BRUCK
Crosley Division
AVCO Corporation
Cincinnati, Ohio

Adoption of the Metric System in the United States*

With very much interest I read the questionnaire about the introduction of the metric system in the United States on page 584 of the April, 1959 issue of PROCEEDINGS OF THE IRE.

I know very well how difficult the whole problem will be for Americans, and that you have to decide yourselves about this question.

However I feel that it might be interesting for you to hear a voice from abroad, and I further would like to draw your attention to the fact that this question concerns not only you, but the whole world and especially us here in Switzerland.

I would like to mention a few facts which will perhaps be of some interest for you. As you perhaps know, our country has a big volume of industry (compared with our population of only about 5,000,000) and we are exporting a very big percentage of our industrial products. In so doing we have to fulfill the standards and rules of our customer countries. For example, we are forced to use the Whitworth screw threads as well as the Unified threads and, of course, as a metric country we must also use the metric thread. So our Swiss standards contain not only metric screws but also screws with inch threads, and all our manufacturers are forced to use and to have in stock many more different parts than are technically necessary. This applies not only to screws but also to other parts, and it is true not only for our own country but for many others, including those "young" countries in Asia and Africa which will buy products from metric and from inch countries.

I am a delegate of my country for different technical committees of ISO, the international body for standardization. Here again I see the disadvantages of having two different measuring systems in our world. Without any exaggeration I can say that this diversity is the most difficult problem we of ISO have to deal with. We spent a great deal of time trying to find ingenious solutions, but most of the time everything failed and finally we had to establish two different ISO Recommendations for metric and inch units, which is, of course, not the aim of international standardization.

I could tell you much more which would confirm the fact that the whole world will be affected by your final decision, and that this world would be very much delighted if you could change over to the metric system.

Of course, the question arises whether it would not be possible to adopt the inch system over the whole world instead of the metric. I think it is unnecessary to point out that this is not only impossible, but would also be a step backwards, as the English system as a whole is a very complicated and inefficient system, especially if we consider not only length but also volume, weight, and so on. I think even English and American people would dislike to speak of a radio wavelength of two inches and similar things.

Now let us talk about a quite different question. Fig. 1 shows the layout of a big

* Received by the IRE, October 30, 1959.

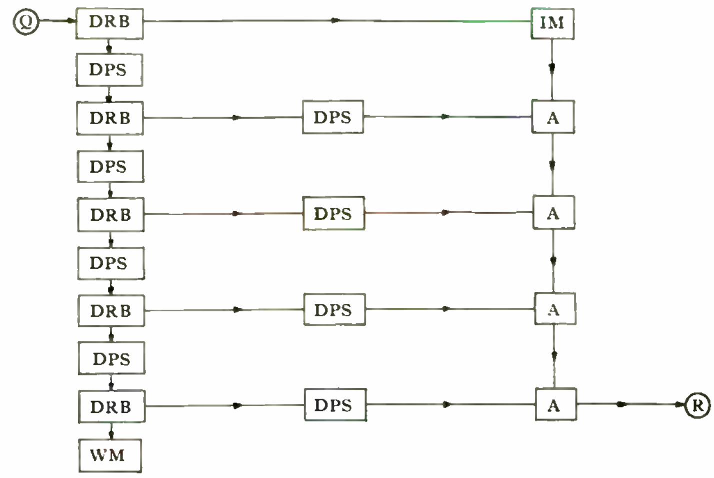

Fig. 1.

Fig. 2.

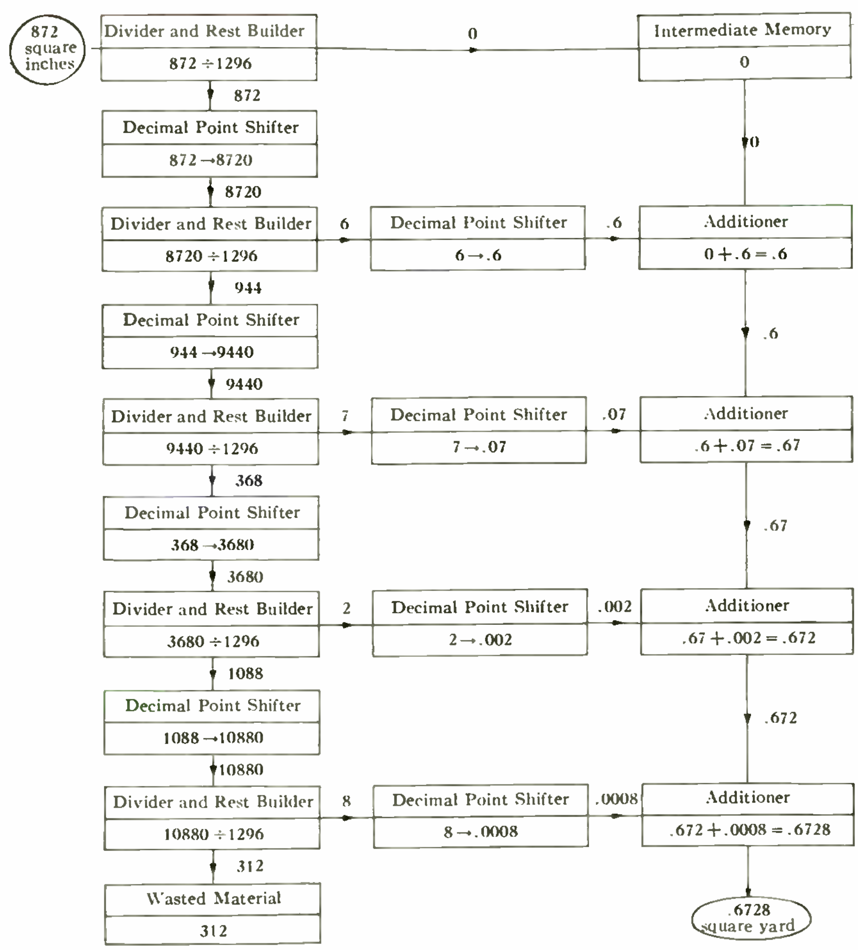

Fig. 3—How many square yards are equal to 872 square inches? (Four significant figures).

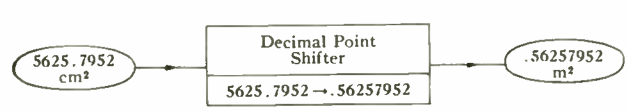

Fig. 4.

workshop where some raw material comes in at point Ⓠ and some finished end product leaves at Ⓡ. Every square represents a machine of a specific design which is indicated by letters. The DPS machines are much simpler and cheaper than DRP, IM and A, but for simplicity let us assume that all blocks are of similar value.

One day a new engineer was engaged. He had very new ideas and after some study he went to the boss and gave him a diagram (see Fig. 2) and stated that this very simple and inexpensive machinery could do a better job than the old crowded workshop, and he was able to prove it. Of course the boss was anxious about the price of the Mysterious Magic Box (MMB) and assumed that it would perhaps cost more than all the previous machines together. But the engineer convinced him that the MMB was not more expensive than the cheapest of all the former machines. In fact, the MMB turned out to be identical with the former DPS machine, there would be no more wasted material (WM), and the operating speed would be much faster than with the old machinery.

Can you imagine a modern boss who would refuse this kind of modernization? I can't.

Now what kind of workshop was it? A quite common institution with the name B.R.A.I.N., sometimes simply called "human brain" and the work it does in this case is the conversion of one square measure into another.

In the first case it has to convert, for example, 872 square inches into square yards, and it does it in the way indicated in Fig. 3. The modernization of the new engineer is nothing but the application of metric units: conversion of 5625.7952 square centimeters (which is the exact equivalent of 872 square inches) into square meters (Fig. 4). Please not that an unlimited number of significant figures can be handled at once, in contrast to the old layout.

Now I hope that you will forgive me this little joke with a very serious matter. I wonder very much what the results of your enquiry will be. The most important point is perhaps the transition time, and I think your proposed 33 years is a period which will be a real possibility, even if we Europeans would be much happier with a much shorter delay.

Ernst Bänninger
Standard Engineer
Landis and Gyr S.A.
Zug, Switzerland

Aperture Antenna Synthesis and Integral Equations*

Recent investigation on the aperture antenna synthesis problem has clarified some aspects of the solution of an integral equation, which may be useful in the other branches of electrical engineering. Some generalizations resulting from the studies on the antenna problem will be presented below.

* Received by the IRE, October 8, 1959; revised manuscript received, November 12, 1959.

The problem of determining the source field over an aperture in order to produce a prescribed radiation pattern leads to the problem of Fredholm equation of the first kind with a finite range of integration. Thus, for a line source, we have

$$g(u) = \int_{-1}^{1} f(x)e^{iux}dx \tag{1}$$

and for a circular aperture we have

$$g(u) = \int_{0}^{1} f(r)J_0(ur)rdr \tag{2}$$

where $g(u)$ is the given radiation pattern, $f(r)$ is the source field function to be determined, x and r are the normalized distance on the aperture surface, and u is proportional to $\sin\theta$, $\pi/2-\theta$ being an angle of elevation.

The exact solution of the integral equation of this type is extremely difficult. Because of the finiteness of the range, the ordinary transform techniques such as Laplace, Fourier, Hankel, and Mellin transforms cannot be used and the available techniques such as Schmidt orthogonalization process are quite involved.[1] In recent years, the art of antenna synthesis has made considerable progress,[2-4] which sheds a new light on the solution of the problem of this type.

Let us consider an integral equation,

$$g(u) = \int_{a}^{b} f(x)\phi(x, u)r(x)dx, \tag{3}$$

where $\phi(x, u)$ satisfies a Sturm-Liouville equation.

$$\frac{d}{dx}\left[p(x)\frac{d\phi}{dx}\right] + [q(x) - u^2r(x)]\phi = 0. \tag{4}$$

Let us assume that $g(u)$ is given in a range $c \leq u \leq d$ and we wish to find $f(x)$ which yields $g(u)$ in this particular range. Now, if we expand $f(x)$ in a series of eigenfunctions $\phi(x, u_m)$,

$$f(x) = \sum_m A_m\phi(x, u_m), \tag{5}$$

we have

$$g(u) = \sum_m A_mG_T(u, u_m) \tag{6}$$

$$G(u, u_m) = \int_{a}^{b} \phi(x, u_m)\phi(x, u)r(x)dx. \tag{7}$$

It can be seen that the orthogonality property of $\phi(x, u_m)$ requires

$$\lim_{u\to u_n} G_T(u, u_m) = \delta_{nm}N_n \tag{8}$$

where

$$N_n = \int_{a}^{b} \{\phi(x, u_n\}^2r(x)dx. \tag{8a}$$

Thus

$$g(u_n) = A_nN_n. \tag{9}$$

Therefore if we can expand the given function $g(u)$ in a form of (6), the solution to (3) will be given by (5) and (9). Now, (7) can be written as

$$G(u, u_m) = \frac{p\left[\phi(x, u_m)\dfrac{\partial}{\partial x}\phi(x, u) - \phi(x, u)\dfrac{\partial}{\partial x}\phi(x, u_m)\right]_a^b}{u_m^2 - u^2}. \tag{10}$$

Often, (10) can be expressed in the following form:

$$G(u, u_m) = \frac{G_1(u)G_2(u_m)}{u_m^2 - u^2}. \tag{11}$$

For example, when

$$\phi(x, u) = J_n(ux),\ 0 \leq x \leq 1, \tag{12}$$

with the homogeneous boundary condition for $\phi(x, u_m)$

$$u_mJ_n'(u_m) + hJ_n(u_m) = 0, \quad h = \text{const},$$

we have

$$G_1(u) = uJ_n'(u) + hJ_n(u),$$
$$G_2(u_m) = J_n(u_m). \tag{13}$$

For

$$\phi(x, u) = \sin ux, \quad 0 \leq x \leq 1$$
$$u_m = m\pi \tag{14}$$
$$G_1(u) = \sin u,$$
$$G_2(u_m) = (-1)^{m+1}u_m \tag{15}$$

For

$$\phi(x, u) = \cos ux,\ 0 \leq x \leq 1$$
$$u_m = (2m + 1)\frac{\pi}{2} \tag{16}$$
$$G_1(u) = \cos u,\ G_2(u_m) = (-1)^m u_m. \tag{17}$$

For $\phi(x, u) = e^{ixu}$, $-1 \leq x \leq 1$, replacing $\phi(x, u_m)$ by its complex conjugate in (10), we have a similar form for $G(u, u_m)$:

$$G(u, u_m) = 2\frac{\sin u(-1)^m}{u - u_m}, \quad u_m = m\pi. \tag{18}$$

Now, if G is given by (11), we can approximate the given function $g(u)$ to any desired degree in the following manner.

[1] P. Morse and H. Feshbach, "Method of Theoretical Physics," McGraw-Hill Book Co., Inc. New York, N. Y., p. 925; 1953.
[2] T. T. Taylor, "Design of line source antennas for narrow beamwidth and low side-lobes," IRE Trans. on Antennas and Propagation, vol. AP-3, p. 16; January, 1955.
[3] A. Ishimaru and G. Held, "Optimum Radiation Pattern Synthesis for Circular Aperture," Dept. of Elec. Engrg., Univ. of Washington, Seattle, Tech. Rept. No. 29; 1958.
[4] A. Ishimaru and G. Held, "Analysis and synthesis of radiation patterns from circular apertures," *Can. J. Phys.* vol. 38; January, 1960.

Let us take a finite number of terms in (6). Using (11), we get

$$g(u) = G_1(u) \sum_{m=0}^{M} A_m \frac{G_2(u_m)}{u_m^2 - u^2} \qquad (19)$$

$$= Q_M(u) P_M(u^2) \qquad (20)$$

$$Q_M = \frac{G_1(u)}{\prod_{m=0}^{M} \left[1 - \left(\frac{u}{u_m}\right)^2\right]} \qquad (21)$$

where P_M is a polynomial in u^2 of order M. $Q_M(u)$ is usually a slowly varying function of u as seen from the above examples. In case of a finite range of u for $g(u)$, Q_M becomes more flat in this range as M increases. We can approximate $g(u)/Q_M$ by P_M in the following manner, thus obtaining the solution to the original integral equation.

Let us divide the range (c, d) of u into M equal sections and call each point

$$c + m \frac{(d - c)}{M} = V_m,$$

$$m = 0, 1, \cdots, M. \qquad (22)$$

Using Lagrange's formula, P_M, to give a correct value of $g(u)$ at V_m, is given by

$$P_M(u^2) = \sum_{i=0}^{M} \frac{g(V_i)}{Q_M(V_i)} \frac{\prod_{m=0, m\neq i}^{M} \left[1 - \left(\frac{u}{V_m}\right)^2\right]}{\prod_{m=0, m\neq i}^{M} \left[1 - \left(\frac{V_i}{V_m}\right)^2\right]}. \qquad (23)$$

Therefore, a solution to (3) is given by

$$f(x) = \sum_{n=0}^{M} Q_M(u_n) P_M(u_n^2) \frac{1}{N_n} \phi(x, u_n). \qquad (24)$$

It may be seen that this solution (24) gives the correct value of $g(u)$ at the discrete points $u = V_m$, $m = 0, 1, \cdots, M$. As we increase M, a number of division, we can approximate $g(u)$ to an arbitrary degree of accuracy.

It must be remembered, however, that the above statement concerning the accuracy is valid only when the finite range of $g(u)$ is considered. We can approximate $g(u)$ in a range (c, d) to any degree of accuracy at the expense of the large unknown values of $g(u)$ outside of this range, which corresponds to the supergaining effect of an antenna. Thus in (1), considering u as a time and x as frequency, we have a problem of determining the frequency spectrum in a finite frequency range in order to produce a given transient function of time. We can produce a pulse of any shape in a range $t_1 < t < t_2$ by using the frequency range $0 \leq \omega \leq \omega_0$, if we can allow the large unspecified function of time outside the range (t_1, t_2). This aspect of synthesis has been discussed and proved by Bouwkamp and De Bruijn.[5]

A. Ishimaru
Dept Elec. Engrg.
Univ. of Washington
Seattle 5, Wash.

[5] C. J. Bouwkamp and N. G. De Bruijn, "The Problem of Optimum Antenna Current Distribution," *Philips Res. Repts.*, vol. 1, p. 135; January, 1946.

Contributors

R. Bechmann

Rudolf Bechmann (SM'54–F'60) was born in Nuremberg, Germany, on July 22, 1902. He received the Ph.D. degree in theoretical physics in 1927 from the University of Munich, Germany.

From 1927 to 1945, he was employed by Telefunken Company for Wireless Telegraphy, Ltd. Berlin, Ger. He was at first particularly concerned with antenna problems, especially with questions of radiation resistance and radiation characteristics of composite antennas. In 1931 he developed the so-called EMF method. Later, he turned his full attention to piezoelectric quartz crystals and developed this field in all directions during the following decade. In 1933 he discovered, independently, several quartz cuts having zero-frequency temperature coefficients—that AT-, BT-, CT- and DT-type resonators. He made many contributions, practical and theoretical, to the field of elasticity and piezoelectricity and its application to quartz. By joining the production of oscillators and resonators to his scientific laboratory activities, Dr. Bechmann became involved in all questions related to quartz crystals. During World War II he directed, in addition to his specified activities with Telefunken, several agencies covering the quartz industry as a whole.

After the war he joined the Oberspree Company in Berlin and directed that company from 1946 to 1948.

Moving to England in 1948, he was Principal Scientific Officer at the British Post Office Research Station, Dollis Hill, London. Here he studied the properties of several water-soluble piezoelectric materials, and developed methods for determining the elastic and piezoelectric constants, using the resonant method applied to various modes of plates. The results of this research are compiled in "Piezoelectricity," General Post Office, Selected Engineering Reports, H. M. Stationery Office, London, 1957.

In 1953, he became associated with the Brush Laboratories Company, now the Clevite Research Center, Cleveland, Ohio, as head of the Dielectric Phenomena Section of the Electrophysical Research Department. He extended his studies on methods of determining the elastic and piezoelectric constants into the field of ferroelectric ceramics. His chief activity, however, was the investigation of properties of synthetic quartz resonators.

In 1956 he joined the Signal Corps Engineering Laboratories, Fort Monmouth, N. J., as a Consultant.

Dr. Bechmann is a Fellow of the American Physical Society, and a Corresponding Member of the German Committee for Standards on Piezoelectric Crystals.

J. N. Cooper

John N. Cooper was born in Kalamazoo, Mich., on February 4, 1914. He received the B.A. degree in physics from Kalamazoo College, Kalamazoo, Mich., in 1935 and the Ph.D. degree in the same field from Cornell University, Ithaca, N. Y., in 1940.

From 1940 to 1943 he was an instructor in physics at the University of Southern California, Los Angeles, and from 1943 to 1946 he was assistant professor of physics at the University of Oklahoma, Norman. He was on leave for eighteen months in 1944 and 1945 as a research physicist, Radiation Laboratory, University of California, Berkeley. From 1946 to 1956 he was successively assistant professor, associate professor, and professor of physics at The Ohio State University, Columbus, where he worked in the Van de Graaff generator program on proton-induced reactions in light elements and on the energy loss of protons in thin films. In 1956 he became professor of physics at the U. S. Naval Postgraduate School, Monterey, Calif., where he has been working on superconductivity in thin films and related topics. For the past three summers he has worked as consultant in the Physical Research Laboratory of Space Technology Labs., Inc., Los Angeles, Calif. on problems related to the Persistor memory element.

Dr. Cooper is a Fellow of the American Physical Society, and a member of the American Association of Physics Teachers and Sigma Xi.

❖

John R. Copeland (S'56–M'59) was born on December 4, 1933, in Findlay, Ohio. He received the B.E.E. and M.S.E.E. degrees in 1956 and 1958, respectively from The Ohio State University, Columbus.

J. R. COPELAND

He has been employed at The Ohio State University Antenna Laboratory since 1955, working in the fields of echo area measurement and analysis, and traveling-wave antenna theory.

Mr. Copeland is a member of Sigma Xi.

❖

Eugene C. Crittenden, Jr., was born in Washington, D. C., on December 25, 1914. He received the B.A. degree in physics in 1934, and the Ph.D. degree in physics in 1938, both from Cornell University, Ithaca, N. Y.

E. C. CRITTENDEN

From 1938 to 1944 he was instructor in physics and later assistant professor of physics at Case Institute of Technology, Cleveland, Ohio. From 1944 to 1946 he was on leave from Case, serving as research physicist at the Radiation Laboratory, University of California, Berkeley. In 1946 he returned to Case Institute of Technology as associate professor of physics and in 1948 became professor of physics. His research at Case dealt with the ferromagnetic properties of thin films. From 1952 to 1953 he was in charge of solid state physics research at the Atomic Energy Research Division of North American Aviation, Downey, Calif. In 1953 he became professor of physics at the U. S. Naval Postgraduate School, Monterey, Calif., where his research has dealt with low temperature solid state physics, crystal imperfections, and superconductivity. Since 1956 he has served as a consultant for the Ramo-Wooldridge Corp. and its subsidiary, Space Technology Labs., Los Angeles, Calif., on problems related to the use of superconductivity in electronic circuits.

Dr. Crittenden is a Fellow of the American Physical Society and a member of Sigma Xi.

❖

Sydney T. Fisher (M'60) was born in Philadelphia, Pennsylvania on July 11, 1931. He received the B.S.E.E. degree from the University of Pennsylvania, Philadelphia, in 1954, and the M.S. and Ph.D. degrees from Cornell University, Ithaca, N. Y. in 1957 and 1959, respectively.

S. T. FISHER

He spent two summers at Philco Research Division, Philadelphia, where he worked on a frequency analysis of radar data, and then on a study of jam-proof communications systems. He also spent a summer at the Moore School of the University of Pennsylvania on a square-law detector project.

As a full-time employee at Philco, he has been conducting a study of parametric amplifiers, including many different types of tuned amplifiers and converters. He has also performed an intensive analysis of semidistributed, traveling-wave parametric amplifiers, and has made analytical studies of pulse code modulation systems.

Dr. Fisher is a member of Sigma Xi.

❖

Armin H. Frei, for a photograph and biography, please see page 1277 of the July, 1959 issue of PROCEEDINGS.

❖

Ferdinand Hamburger, Jr. (A'32–M'39–SM'43–F'53), for a photograph and biography, please see page 846 of the May, 1960 issue of PROCEEDINGS.

❖

Irving Itzkan (M'57) was born in Brooklyn, N. Y. on December 4, 1929. He received the Bachelor of Engineering Physics degree from Cornell University, Ithaca, N. Y. in 1952, where he also did graduate work in electron microscopy during 1955–1956. From 1952 to 1955, he was an engineering and repair officer in the United States Navy.

I. ITZKAN

Since 1956, he has been associated with the Electronic Tube Division of Sperry Gyroscope Company, a Division of Sperry-Rand Corporation, Great Neck, N. Y., working principally on electron beam focusing and interaction problems.

Mr. Itzkan is a member of Tau Beta Pi.

❖

Ronald C. Knechtli (M'54) was born in Geneva, Switzerland, on August 14, 1927. He received the Diploma in electrical engineering in 1950 and the Ph.D. degree in 1955 from the Swiss Federal Institute of Technology, Zurich. He was a research assistant at Massachusetts Institute of Technology, Cambridge from 1951–1952, and a research engineer at Brown Boveri, Switzerland, from 1952 to 1953.

From 1953 to 1958, he worked on low-noise microwave tubes at RCA Laboratories, Princeton, N. J. In 1958, he joined the Hughes Research Laboratories, Culver City, Calif., where he heads the Plasma and Solid-State Research Section.

R. C. KNECHTLI

Dr. Knechtli is a member of the American Physical Society, Sigma Xi, and RESA.

❖

Paul R. McIsaac (A'59), for a photograph and biography, please see page 959 of the May, 1960 issue of PROCEEDINGS.

❖

Jack Munushian (S'52–A'54) was born in Rochester, N. Y. on September 6, 1924. He received the B.S. degree in physics from the University of Rochester, Rochester, N. Y., in 1947 and the Ph.D. degree in electrical engineering from the University of California, Berkeley, in 1954.

J. MUNUSHIAN

In 1946, he worked with the Eastman Kodak Company. He was later associated with the Electronics Research Laboratory at the University of California. In 1954, he joined the Hughes Aircraft Company. Since that time, he has been involved in a wide variety of problems in microwave circuits, systems, instrumentation, traveling-wave tubes and superconductivity. He is head of the Microwave Devices Section of the Microwave Laboratory, and is a part-time lecturer in electrical engineering at the University of Southern California, Los Angeles.

Dr. Munushian is a member of Sigma Xi.

❖

Charles Polk (A'52–SM'56) was born on January 15, 1920, in Vienna, Austria. He came to this country in 1940. From 1943 to 1946 he served in the U. S. Army. He received the B.S.E.E. degree from Washington University in 1948, and the M.S. degree in physics in 1953 and the Ph.D. degree in electrical engineering in 1956, both from the University of Pennsylvania, Philadelphia.

CHARLES POLK

From 1948 until September, 1952, he was employed by RCA, working mostly on problems related to UHF television transmitting antennas. From 1952 to 1956 he was a teaching and research associate at the Moore School of Electrical Engineering of the University of Pennsylvania and from 1957 to 1959, a member of the Technical Staff of RCA Laboratories in Princeton, N. J. He became chairman of the Department of Electrical Engineering at the University of Rhode Island, Kingston, R. I., in September, 1959.

Dr. Polk is a member of Sigma Xi, Tau Beta Pi, AIEE, and ASEE.

❖

Fred W. Schmidlin was born in Maumee, Ohio, on August 28, 1925. He received the B.S. degree in engineering physics from the University of Toledo, Toledo, Ohio, in 1950, and the Ph.D. degree in physics from Cornell University, Ithaca, N. Y., in 1956.

F. W. Schmidlin

Since October, 1956, he has been employed in the Physical Research Laboratory of the Space Technology Labs., Inc. (formerly a division of The Ramo-Wooldridge Corp.), Los Angeles, Calif.

Dr. Schmidlin is a member of Sigma Xi and the American Physical Society.

❖

Walter R. Sooy was born in Boston, Mass. on December 28, 1932. He received the B.S. degree in physics from the Massachusetts Institute of Technology, Cambridge, in 1956 and the M.A. degree in physics from the University of Southern California, Los Angeles, in 1958.

W. R. Sooy

He joined the Hughes Aircraft Company, Culver City, Calif., in 1956 under Hughes Master's Fellowship Program. Since that time, he has been a member of the Microwave Laboratory where he has been working on microwave circuits, stable microwave oscillators and more recently on the high frequency properties of superconductors. He is presently studying for the Ph.D. degree in physics at the University of California at Los Angeles.

Mr. Sooy is a member of the American Physical Society.

❖

Malcom W. P. Strandberg was born in Box Elder, Mont., on March 9, 1919. He received the B.S. degree from Harvard College, Cambridge, Mass. in 1941, and the Ph.D. degree from the Massachusetts Institute of Technology, Cambridge, in 1948.

M. Strandberg

From 1941 to 1945, he was a staff member of the M.I.T. Radiation Laboratory, engaged in advanced development work on microwave radar. The year 1942–1943, he spent in Malvern, England, as a visiting scientist working on radar countermeasures for the Royal Air Force. At M.I.T., he was appointed a research assistant in 1945, and an assistant professor of physics in 1948. Having become an associate professor in 1953, he is also head of a research group in microwave spectroscopy in the Research Laboratory of Electronics at M.I.T.

Dr. Strandberg is a fellow of the American Physical Society, the American Academy of Arts and Sciences, the New York Academy of Arts and Sciences, the AAAS, and has been a Visiting Scientist for the American Institute of Physics in 1957–1958 and 1958–1959. He is also a member of Phi Beta Kappa.

❖

M. J. O. Strutt (SM'46–F'56), for a photograph and biography, please see page 1278 of the July, 1959 issue of Proceedings.

❖

Frank L. Vernon (S'50–A'51–M'57) was born in Dallas, Texas on September 16, 1927. He received the B.S.E.E. degree from Southern Methodist University, Dallas, Tex., in 1949. After working for one and one-half years with the Geophysical Division of the Texas Company, he entered the University of California at Berkeley where he received the M.S.E.E. degree in June, 1952.

F. L. Vernon

In 1951, he joined Hughes Aircraft Company. Since then, he has been associated with the Electronics Research Department of the Microwave Laboratory and has worked on a wide variety of problems in microwave circuits. Most recently he has been investigating the high-frequency properties of superconducting materials. In September, 1953, he entered the California Institute of Technology, Pasadena where he received the Ph.D. degree in electrical engineering and physics in June, 1959.

Dr. Vernon is a member of Sigma Xi and the American Physical Society.

Rolf D. Weglein (S'52–A'55–SM'58) was born in Ichenhausen, Germany, on August 13, 1920. He received the B.S.E.E. and M.S.E.E. degrees in 1953 and 1954, respectively, from the California Institute of Technology, Pasadena. Prior to his formal education, he was actively engaged in AM and TV broadcasting. At the Electron Tube Laboratory at Cal Tech, he performed early experiments in microwave beam tube focusing and power generation.

R. D. Weglein

Since 1954, he has been a member of the technical staff of Hughes Research Laboratories, Culver City, Calif., where his fields of endeavor have been backward-wave oscillator development and, more recently, solid-state circuit research.

Mr. Weglein is a member of Tau Beta Pi, the American Physical Society, Sigma Xi, and RESA.

❖

Martin Wolf (A'52–M'54–SM'56) was born in Wuppertal, West Germany, on August 2, 1922. He received the Vordiplom-Physiker degree in May, 1948, and the Diplom Physiker degree in February, 1952, both from the Georg August University in Goettingen, West Germany.

M. Wolf

From 1943 to 1945, he designed power distribution systems for the Allgemeine Elektrizitaets Gesellschaft, Duesseldorf, Germany. From 1950 to 1952 he developed microwave measuring equipment at the Georg August University and carried out research concerning the input impedances of different antenna configurations in the microwave region. From 1952 to 1955, he was project engineer at the Admiral Corporation, Chicago, Ill., where he developed UHF television tuners and transmitters. Since 1955, he has been with the Semiconductor Division of Hoffman Electronics Corporation, Evanston, Ill., where he has carried out research and development work on general semiconductor problems and on various silicon diffused junction devices. He is presently manager of the Solar Section, which is responsible for all research and development activities of this company in the field of photovoltaic devices.

Mr. Wolf is a member of the American Physical Society. He is co-recipient of the Marconi Award of the British IRE for 1958.

Books

Waves and the Ear, by Willem A. Van Bergeijk, John R. Pierce and Edward E. David, Jr.

Published (1960) by Doubleday and Company, Inc., 575 Madison Ave., N. Y. 22, N. Y. 221 pages+9 index pages+4 suggested reading pages. Illus. 4¼×7⅛. $0.95 (paperback).

This book is a paper-bound pocket book prepared under the Science Study Series of books "designed to provide a survey of physics within the grasp of the young student or the layman." However, the book is really more about physiology and psychology than about physical acoustics. It is an excellent book, being technically competent and accurate, and written in a style that makes for easy reading. The authors are to be congratulated for bringing together in such a succinct and readable manner such a great amount of knowledge; the breadth of the book can be best illustrated by listing the headings of the major chapters: I, To Hear the World (Codes and Communication); II, The Power of Sound; III, Waves, Frequencies and Resonators; IV, What Do We Hear (The Psychology of Perception); V, Ears to Hear With (Physiology of Perception); VI, Nerves and The Brain; VII, Voices (Acoustics and Physiology of Speech); VIII, Quality and Fidelity. A selected list of references is provided.

The book is suitable, it seems to this reviewer, for the high school and college science major and the engineer interested in auditory communications, particularly speech communications. The attempts of the authors to lead the reader "painlessly" through some of the more detailed acoustical and physiological facts will probably not be successful with the average layman. Nevertheless, as an introduction to the science of psychoacoustics, the book is outstanding.

It should be noted that the "Waves and the Ear" is by and large the same (word for word) as "Man's World of Sound," by J. R. Pierce and E. E. David, Jr., Doubleday and Company, Garden City, N. Y. Two or three chapters found in "Man's World of Sound" have been dropped to advantage, and some few pages on the phylogeny of the ear and vocal mechanism have been added to the new book, again to advantage.

KARL D. KRYTER
Bolt Beranek & Newman, Inc.
Cambridge, Mass.

F-M Simplified, Third Edition, by Milton S. Kiver

Published (1960) by D. Van Nostrand Co., Inc., 120 Alexander St., Princeton, N. J. 366 pages+4 index pages+3 bibliography pages+4 appendix pages+vi pages. Illus. 6¼×9¼. $7.50.

In this, his third edition of similar title, the author has vastly expanded and updated his material on frequency-modulation broadcasting and reception. Tracing the concept of F-M, as a mode of transmission, the author then devotes the major portion of his book to a detailed, nonmathematical analysis of all of the circuitry associated with the reception and detection of the frequency-modulated signal.

The chapters dealing with the alignment and the servicing of F-M receivers are thorough and should prove beneficial to technicians and service personnel who are involved in this work. Many modern receivers and tuners of commercial hi-fi manufacturers are treated in detail, and full schematic diagrams are included. It is this portion of the book that is most adequately illustrated.

A brief chapter on audio amplifiers and "high fidelity" is included, more as fill-in material than as a comprehensive treatment of a subject which might of itself warrant several volumes the size of this present edition. On the other hand, no mention whatever is made of F-M multiplex transmission, a subject which is currently much under discussion within the industry, because of the recent popularity of stereophonic music sources.

The author concludes with a brief discussion of F-M transmitters and their circuitry. Here, too, the material is less detailed than the sections dealing with the reception of F-M.

All chapters are followed by a thoughtful list of questions, to aid the beginning student. An excellent bibliography and a rather cursory "list of common troubles and their cures" complete the book.

Mr. Kiver, as always, has managed to present a highly readable treatment of a subject which is normally associated with complex mathematical interjections. Divested of virtually all mathematics, the author skillfully verbalizes on the intricacies of frequency-modulation and gets all the major concepts across by the sheer use of properly chosen prose.

Service technicians will value this book even above their specific servicing diagrams. Engineers not normally exposed to the 88–108 megacycle region may well gain rapid familiarity with the subject through Mr. Kiver's book.

LEONARD L. FELDMAN
Crosby Electronics, Inc.
Syosset, L. I., N. Y.

Value Engineering 1959, EIA Conference on Value Engineering

Published (1959) by Engineering Publishers, Elizabeth, N. J. 165 pages. Illus. 6¼×9¼. $6.00.

This is the official report of this conference sponsored by the Electronic Industries Association. The book is a notable presentation in style and format compared with the reports on some other conferences, but it cannot be reviewed except by reporting on the objectives and program of the conference. Value Engineering—what is it? Value is the lowest total cost to achieve reliably the essential functions. Although defined in several other ways by the various speakers during this camp revival type of meeting, there is no doubt about their conclusions: everybody is in favor of getting and giving VALUE. The word is mentioned at least half a dozen (and up to twenty) times on every page. This reviewer, who was not at the conference, was surprised to note that Value Engineering originated just a couple of years ago, possibly in a committee, and that the idea applies mainly to military equipment. It had seemed that every small company and many of the larger ones, competing in commercial markets, had long applied plain common sense and Yankee ingenuity to their designs, using experienced designers to maintain their positions. Such designers will probably find little help, but considerable amusement, from these pages.

Perusal of the many "before and after" pictures now having "value," indicates that this concept will be hailed by all taxpayers. It is supposed that future designs will be handled in the approved manner by having designated "value engineers," the suggested four such to each hundred designers, advise on new designs, unless by some chance responsible designers with a little common sense gained from wide experience in fabrication methods can be corralled to inject value into their projects, all on their own. The papers seem to be slanted toward management level to show that reliability and economy are not incompatible. One hopes that the concept will back up one or two steps and include circuits and systems, where unneeded parts can often be eliminated completely with no loss in the functioning.

RALPH R. BATCHER
Douglaston, N. Y.

Preservation and Storage of Sound Recordings, by A. G. Pickett and M. M. Lemcoe

Published (1959) by the U. S. Government Printing Office, Washington 25, D. C. 64 pages+4 bibliography pages+6 appendix pages+vii pages. 30 figures. 10¼×8. $0.45.

This publication is a research report in which long term aging and degradation effects in disk and tape recording media are studied and proper storage conditions recommended. As such, it should be of principal interest to librarians and archivists, although recording engineers and private record collectors may also find it worthwhile reading.

The first three sections of the report deal with recording disks. Following some general comments on the manufacture, storage, and shipping of disks is a discussion of the long term chemical changes which can be expected to ensue in plastic disk materials such as cellulose nitrate, shellac, and vinyl polymers. Detailed analytical tests are described in which the degradation effects causing embrittlement and cracking in aged disk materials are assessed by infrared spectroscopy. The samples studied included both naturally aged disks extracted from libraries and disks artificially aged in the laboratory. These disks are also subjected to attack by fungi.

The effects of plastic deformation and internal stresses in vinyl plastic disks are treated next in some detail. From laboratory measurements of stress-strain and plastic creep properties against time and temperature, the warping and embossing tendencies of the various disk materials are inferred.

The results of these studies are neatly summarized in a comparative evaluation of disk materials as to life expectancy which, incidently, was found to range from about fifteen years for cellulose nitrate disks to more than a century for vinyl disks under favorable storage conditions. In addition to the study of aging effects, recommendations are given for the storage of disks with preferred environmental conditions being specified and the requirements for packaging materials and storage compartments treated in detail.

The final section deals with aging effects in magnetic tape, but regrettably, this subject is not treated with the same thoroughness as the previous sections on disks. Following a brief description of the testing conditions is a general discussion of the possible mechanisms of failure in magnetic tape. Winding conditions and the stresses in wound rolls are treated in a general way. The chemical stability of the plastic materials used in tape is also discussed, but no conclusions are made as to life expectancy.

Possible magnetic changes in tape including print through effects are briefly treated in their relationship to signal level, wavelength, time and temperature of storage. The section concludes with a number of recommendations for the proper storage and handling of magnetic tape.

The authors recognize that many of the problems in long term storage of disk and tape materials are not yet fully known, and stress that this current paper is intended as a progress report on their work. In the last section they suggest the formation of a special committee with scientific and industry representation to guide continued research in this area.

R. A. von Behren
Minnesota Mining & Mfg. Co.
St. Paul, Minn.

Physics for Students of Science and Engineering, Part I, by Robert Resnick and David Halliday

Published (1960) by John Wiley and Sons, Inc., 440 Fourth Ave., N. Y. 16, N. Y. 554 pages+8 index pages+4 answer pages+27 appendix pages+xiv pages. Illus. 6¼×9¼. $6.00.

This volume and its companion (Part II) are intended as textbooks for a general physics course for engineers and scientists. The material contained in these books has formed the basis of such a course at Rensselaer Polytechnic Institute, where Robert Resnick is Professor of Physics, and at the University of Pittsburgh, where David Halliday is Head of the Physics Department. The authors bring to their subject not only a wealth of teaching experience, but also the vantage point of creative scientists who have been active in the fields of aerodynamics, nuclear, solid state, and upper atmosphere physics. Parts I and II are available in separate editions, and in a combined edition as well.

The mathematical level of these books assumes a concurrent course in calculus. The fundamental ideas of calculus and vector analysis are introduced gradually, after which they are freely used.

According to the preface, the authors have attempted to improve upon other books of a similar nature in four major respects. In the first place, they have deliberately avoided writing an encyclopedic work which covers too many topics, which treats many topics with insufficient depth, and which contains too many discussions which are largely descriptive rather than explanatory and analytical.

In this book there is a considerable departure from the standard coverage. Many topics such as gravitation and kinetic theory are treated in greater depth than is customary, while much traditional material such as simple machines, surface tension, viscosity, and calorimetry is omitted entirely or treated only indirectly. In addition, the subject matter is consistently enlivened by the inclusion of contemporary material such as basic data on earth satellites.

Second, the authors have drawn their applications and illustrative examples from contemporary physics rather than from past engineering practice. The result is a pleasing reflection of present culture. The student is likely to find many of the problems less burdensome by virtue of their timeliness and current appeal.

Third, the authors have attempted to reveal the essential unity of physics by stressing the similarity of method in different disciplines, and by making frequent appeal to physical and mathematical analogies. Strong emphasis on the various conservation laws also serves this purpose.

Finally, the authors have stressed the connection between theory and experiment wherever possible. In order to accomplish this end, they have deliberately avoided a highly deductive approach which, after all, is perhaps more suitable for an advanced than for an elementary course.

This reviewer applauds the approach taken by the authors: their treatment is solid, lively, well-balanced, and intellectually stimulating. While this reviewer is not sufficient conversant with other textbooks of a similar nature to hazard a detailed comparison, he finds the present volume considerably more interesting and instructive than the one on which he was nurtured some twenty years ago (Hausmann and Slack). He was particularly pleased with the frequent references to related material in such journals as *Scientific American*, *Scientific Monthly*, and the *American Journal of Physics*. The student is given ample opportunity to broaden his perspective by reading introductory accounts written by leading authorities in such journals.

This reviewer was also impressed by the large number of fully worked out problems, as well as by the excellent choice of problem sets which appear at the end of each chapter. Part I contains some extremely useful appendixes on physical constants, dimensions and units, and conversion factors, to mention but a few items.

In summary, this book is warmly recommended to its intended audience.

Frank Herman
RCA Laboratories
Princeton, N. J.

Encyclopedia on Cathode-Ray Oscilloscopes and Their Uses, 2nd Ed., by John F. Rider and Seymour D. Uslan

Published (1959) by John F. Rider, Publisher, Inc. 116 W. 14 St., N. Y. 11, N. Y. 1052 pages+11 index pages+11 bibliography pages+30 appendix pages+xix pages. Illus. 8½×11¼. $21.95.

As the title says, this book is an encyclopedia. It really is. You name it, they have it. To quote from the blurb, "The newly revised second edition of this best selling classic begins with cathode-ray tube construction and theory, then carries you through an analysis of modern oscilloscope circuitry, commercial scope types and maintenance, to a detailed treatment of how the scope is operated for all applications."

Just a list of chapter titles is almost overwhelming. "Basic Characteristics of Cathode-Ray Tubes—Principles of Focusing and Deflection—Deflection Systems and Shot Displacement—Screens of Cathode-Ray Tubes—The Basic Oscilloscope—Vertical and Horizontal Amplifiers—Time Bases—Synchronization—Power Supply Circuits—Auxiliary Equipment—Oscilloscope Circuit Analysis and Maintenance—Special Purpose Cathode-Ray Tubes—Basic Pulse Measurement and Observation—Phase and Frequency Measurements—Audio-Frequency Circuit Testing—Transmitter Testing—Visual Alignment of A-M, F-M, and Television Receivers—Observation of Voltage Waveforms in Television Receivers—Engineering, Medical, and Scientific Applications—Oscilloscope Photography—Complex Waveforms—Square Wave Testing of R-C Coupled Amplifiers and Networks—Specifications and Schematics of Commercial Oscilloscopes."

The book is well written, profusely illustrated, and has an attractive format. The level is that of the technician or serviceman. It would seem to be a must for any group doing electronic testing.

Knox McIlwain
Great Valley Lab.
Burroughs Corp.
Paoli, Pa.

Beam and Wave Electronics in Microwave Tubes, by Rudolf G. E. Hutter

Published (1960) by D. Van Nostrand Co., Inc., Princeton, N. J. 367 pages+10 index pages+xii pages. Illus. 6¼×9¼. $9.75.

This book is devoted to the small signal analysis of beam type microwave tubes. The book begins with a discussion of the frequency limitations of conventional tubes and a brief description of klystrons, magnetrons, and traveling-wave tubes. Simple cavities and waveguides are then analyzed and relations between the fields in waveguides and cavities and the voltages and currents in conventional circuits are presented.

The next section contains approximate field analyses of a wide variety of slow wave structures which are useful in traveling-wave tubes and a review of conventional filter circuits and possible equivalent circuits for periodically loaded waveguides. Electron beams in short gaps are treated and the equations are applied to obtain the velocity modulation produced by the input cavity of a klystron and the power delivered to the output gap. The analysis of space-charge waves on electron beams and the transmission line analog for space-charge waves are covered before the beam analysis is combined with the circuit analysis to describe the interaction between the beam and the circuit in the traveling-wave amplifier and the backward-wave oscillator. Several small signal analyses of beam-type crossed-field amplifiers are presented in the next section and then energy conversion in the various tube types is discussed. Coupled-mode theory is used to point out the basic similarities between different devices and the book concludes with a chapter on noise in beam-type tubes.

The book is intended as a college textbook and as a theoretical book for workers new to the microwave tube field. It does not purport to be useful in the design of microwave tubes other than to provide fundamental understanding of the devices. As a textbook, it gathers most of the important small signal analyses into one place and presents them in a unified fashion. The transmission line analog for space-charge waves, coupled-mode theory, crossed-field analyses including space-charge, and energy conversion are fully treated. The chapter on noise assumes considerable background knowledge and could possibly have been made more understandable by using the transmission line analog for space-charge waves developed earlier in the book.

This book differs from the book "Space-Charge Waves," by Beck, in that it gives only the basic small signal analyses but in sufficient detail to be easily followed by the student. The two books would be good complements for a course on microwave tubes.

J. W. Sedin
Watkins-Johnson Co.
Palo Alto, Calif.

Space Flight, Volume I, by Krafft A. Ehricke

Published (1960) by D. Van Nostrand Co., Inc., 120 Alexander St., Princeton, N. J. 485 pages+7 index pages+20 appendix pages+xiii pages. Illus. 6¼×9¼. $14.50.

Volume I of Krafft Ehricke's 3 volume series "Space Flight" is subtitled "Environment and Celestial Mechanics." By "environment" is meant the general description of the solar system, its gravitational, radiative and particle climate at various points, and the types of mission which may be carried out therein. This first part contains 260 pages and is unusually full of quantitative data concerning the planets, the asteroids, and other features of the solar system. Preceding these data is a 100-page discussion of the applications or missions (called by the author the "utility") of space flight. This latter discussion is sufficiently full to enable a careful reader to feel at home in the solar system, as indeed the author obviously does.

The second half of the book, entitled "celestial mechanics," covers central force fields, orbits, and perturbations of orbits. The material is largely that of classical descriptive astonomy, but written from the point of view of an engineer interested in describing the behavior of a maneuverable space vehicle as well as an inert planet. It is quite quantitative in nature, including the details of transformation of coordinates between geocentric and heliocentric systems, and including also an interesting tabulation of the many algebraic relationships of the central force field, such as those for mean and true anomaly, eccentricity, peri-apsis, etc. The final chapter describes the complex and cumbersome machinery of perturbation analysis.

The entire book is written with the fullness and conscientious attention to detail characteristic of Krafft Ehricke. It is a book for the serious student, and endeavors to give him practical help by the inclusion of many tables and even some formal problems. Good problems in this field are of course scarce, and some of those included here are rather awe-inspiring in the amount of labor involved. (For example, on p. 499 the student is requested to "compute the perturbations of the planetoid *Asia* of Jupiter on Jan. 22, 1868 . . . etc. . . . ").

Vols. II and III of this set are to cover dynamics and operations of space vehicles. The whole will form a monumental encyclopedia of the subject. Ehricke is to be commended for his patience, thoroughness, and organizational skill. His readers will be called upon to display some of these same qualities to reap the maximum benefit from this volume.

Howard S. Seifert
Stanford University
Stanford, Calif.

Laplace Transforms for Electronic Engineers, by James G. Holbrook

Published (1959) by Pergamon Press, 122 E. 55 St., N. Y. 22, N. Y. 208 pages+3 index pages+48 appendix pages+xiii pages. Illus. 5½×8¾. $8.50.

In the preface the author makes an open statement that "this book is written primarily for the practicing electronic engineer." It assumes a background of calculus and elementary circuit analysis. The material is easy to read and suitable for those who want to do some self-study on Laplace transforms.

Chapters 1 and 2 give the necessary mathematical framework on elementary complex variable and Fourier analysis. In the chapter on complex variable, only material essential for the discussion of Laplace transforms is considered. Chapter 2 starts with real and exponential Fourier series and follows with the Fourier integral. The convergence factors are then introduced. Chapter 3 deals with the direct Laplace transforms of simple functions with the inclusion of a simple table. Chapter 4 proceeds with the inverse transforms of rational functions. Chapter 5 contains some important and useful theorems. Chapter 6 gives many circuit applications. In Chapter 7, the transforms of some familiar waveforms and pulses are derived. In Chapter 8, some elementary notions of network synthesis are discussed. An illustrative design of a maximally flat magnitude filter is given based on the method of equating coefficients.

On the whole the presentation is clear and straightforward. The practicing engineers and technicians undoubtedly could learn a great deal about the use of Laplace transforms without getting involved in details.

E. S. Kuh
University of California
Berkeley 4, Calif.

Applications of Thermoelectricity, by H. J. Goldsmid

Published (1960) by John Wiley and Sons, Inc., 440 Fourth Ave., N. Y. 16, N. Y. 115 pages+2 index pages+1 appendix page+xv pages. 32 figures. 4¼×6¾. $2.25.

This is the first short, introductory book on this subject; it also is one more member of the Methuen Monograph series which admirably fulfills its stated aims. In the preface, Dr. Goldsmid states, "One of the aims of this book is the introduction of the subject to those who are entering the field for the first time. It is also hoped that it will prove useful in providing an elementary account of the applications of thermoelectricity for students and those working in other fields." For the reader desiring a treatment described by either of these aims, this book can be highly recommended.

Dr. Goldsmid opens with a brief introductory chapter describing thermoelectric effects and the relations among them. This is followed by an elementary treatment of the theory of thermoelectric devices and the thermoelectric properties of semiconductors. The figure of merit for a thermoelectric material is first discussed in Chapter II, and is covered in detail in Chapter IV. Chapters V and VI cover the selection and properties of semiconductor alloys suitable for thermoelectric applications. The final three chapters describe the preparation and evaluation of materials, various applications of the Peltier effect and thermoelectric generation.

The book is beautifully written. In fact, its near glibness is apt to give the reader the impression that he has heard the last (and only) word on the subject. This brings up another minor objection: one could wish that Dr. Goldsmid had more access to more of the American work which is largely unpublished, or published only in government reports. Figures of merit higher than those stated as maxima for certain systems have been achieved in this country and some of the applications given as "suggested" have been proved.

Finally, the experienced worker will find little new in this book. Even for the beginner, extensions to the treatment given will be difficult to find in the references listed at the end of the chapters; only a very few references are given to the later work on transport phenomena.

However, these objections are minor and do not detract from the achievement of the aims stated in the preface. For an introduction to the field, or for a working knowledge of thermoelectricity, this book is highly recommended.

F. E. Jaumot, Jr.
Delco Radio Div.
General Motors Corp.
Kokomo, Indiana

Physique et Technique des Tubes Electroniques, Tome II, by R. Champeix

Published (1960) by Dunod Editeur, 92 Rue Bonaparte, Paris (6e), France. 394 pages+3 index pages+24 appendix pages+5 problem pages+xvi pages. Illus. 6¼×9¾. $11.84.

Dr. Champeix' book attempts to cover a broad field. In its first part, it deals with the theory of electron tubes. Tube technology is the subject of the second part.

Starting with an elementary introduction into modern physics, Dr. Champeix explains the principles of thermionic emission on a level accessible even to the least specialized reader. The theory and design principles of thermionic cathodes and heaters are presented on the same rather elementary level. A brief chapter (about 25 pages) on electron dynamics and electron optics completes the background upon which the theory and design principles of the vacuum diode, triode, and multigrid tubes are treated. High frequency and microwave tubes are compressed into 16 pages, hardly enough for even the most superficial discussion. Cathode ray tubes, phototubes, and gas tubes are considered at some more length, although not much more.

The second part of this book, devoted to tube technology, consists of a compilation of the properties of the more common vacuum tube materials, and of the more standard techniques and tube assembly procedures.

This book will probably provide excellent reading to an intelligent technician who does not have the benefit of a full undergraduate college curriculum in engineering or science. For any college graduate, the introductory chapters are superfluous, and most of the book too elementary. Because of the quantity of material treated in these 394 pages, this book could hardly be more than an introduction to the subject.

R. C. Knechtli
Hughes Research Labs.
Malibu, Calif.

Electronic Computers, Principles and Applications, 2nd edition, by T. E. Ivall

Published (1960) by Philosophical Library Inc., 15 E. 40 St., N. Y. 16, N. Y. 259 pages+3 index pages+viii pages. Illus. 5¾×8¾. $15.00.

As an introduction to analog computation, the book provides a brief history and develops circuit diagrams used for summing, integrating, multiplying, limiting and function-generating. Requirements for the operational amplifier are given in some detail, and patching and indication are touched upon. Examples of British applications are described, ranging from the RAE's missile-and-target simulator to such statistical uses as auto-correlation and product inspection.

The advantages of readily changed parameters, immediate read-out, and incorporation of nonlinear or physical hardware are all pointed out. An excellent discussion of recent developments includes automatic correlation, fast repetitive solution, punched tape read-in and digital printout, and the digital differential analyzer.

About three-quarters of the book is devoted to digital computers. Descriptions of logic circuits, core stores, ferroelectric stores, magnetic tape or drum recorders, and cathode-ray tube stores begin with basic circuit diagrams and waveforms and progress through logic diagrams and system block diagrams. Various commercially available computers and auxiliary equipments are described and illustrated in photographs.

A short chapter on programming introduces the basic ideas including English language input to automatic programs. Applications to business data processing, industrial control, optimizing operations, research, and simulation are described. Two final chapters on recent developments and computers of the future are remarkably up to date.

Though a specialist may be startled by some glosses used to cover so much material in so little space, the explanations are usually clear, as far as they go, relative emphasis appropriate, and reasoning in comparative evaluations valid.

The book is excellent as a broad, first introduction to electronic computers for a reader grounded in electronics or radio techniques. He should, of course, read much further to acquire depth.

R. D. Elbourn
H. L. Mason
National Bureau of Standards
Washington 25, D. C.

Scanning the Transactions

One man show. The Medical Electronics Group has come forth with an issue which is unique in the publication annals of the IRE. All eleven articles in the issue were written by the same man. What is more surprising, the papers cover a wide range of subjects of interest to many groups. Not only is this a compliment to the versatility of the author, it is a most convincing demonstration that in the bio-medical electronics field the individual investigator has an unusual opportunity to contribute to a large variety of problems. Consider for a moment the wide assortment of topics treated in this issue. A general summary on negative resistance is given in one paper on nerve impulses; the same paper includes a discussion of switching in bistable circuits that resembles an Electronic Computers Transactions paper. A discussion of motion transducers makes up part of a paper on detecting oncoming blindness. Miniaturization and antenna design are included in a paper on small FM transmitters that are swallowed to telemeter internal information. (The omnidirectional antenna system using nonlinear circuits could have general application.) The making of X-ray movies and the use of spectral information involve two papers in which some effects of linear and nonlinear circuits on the flow of information is considered. The use of sound waves in finding kidney stones and other hard objects in the body occupies one paper and the electron optics of focussing electron microscopes another. A summary of hazards found in a laboratory is given as is a discussion of certain aspects of electric shock. (Papers by R. S. Mackay, IRE Trans. on Medical Electronics, April, 1960.)

What was the world's first technical report? The answer is revealed on the cover of the last issue of the IRE Transactions on Engineering Writing and Speech. Shown thereon is a photograph of a clay tablet which was excavated in Iraq in 1950. We are told that the tablet contains instructions from a father to his son concerning the technical details for growing a successful crop. The tablet was inscribed about 1700 B.C. This evidence of the dawn of technical writing was obtained by PGEWS Editor, H. J. Michaelson, who must have done considerable excavating himself to find it. He finally tracked it down among a collection of ancient tablets at the University of Pennsylvania Museum. Editor's Michaelson's search also uncovered an ancient document that shows how little times have changed. Written about 97 A.D., and entitled "The Aqueducts of Rome," it describes the great water system which yielded taxes for Augustus Caesar's Roman Empire. The report reveals that 40 per cent of the water supply was stolen by citizens who tapped the conduits illegally—clearly an age-old case of tax money going down the drain. (IRE Trans. on Engineering Writing and Speech, April, 1960.)

Nuclear rocket propulsion has been under study in the U. S. for five years. Although the first experimental reactor was successfully tested last summer, the era of the nuclear rocket must still be considered to be in an early stage, with many practical problems yet to be solved. Nevertheless, it is now possible to predict with some confidence the most likely ways that nuclear rockets will first be used. An interesting study has been made of the performance advantages and the practical problems involved in substituting nuclear-powered stages for various chemical stages of two rockets, the Saturn and the Nova. The Saturn, now under development, is to be a four-stage $1\frac{1}{2}$-million-pound-thrust vehicle, with a 4630-pound payload, intended for planet probes. The Nova has been suggested for landing a two-man crew on the moon and returning them to earth. It would have five stages, 9-million pounds of thrust, and a carry payload of 8000 pounds. The study suggests that the development of these two vehicles would proceed using conventional chemical rockets, but that a single nuclear stage might later be used in place of the top two chemical stages to provide added simplicity and a payload increase of 150 to 170 per cent. This strongly suggests that the early application of nuclear rockets will be for the propulsion of the upper stages of space vehicles. (H. R. Schmidt and R. S. Decker, "Factors which will influence early application of nuclear rockets," IRE TRANS. ON NUCLEAR SCIENCE, March, 1960.)

What will engineering college enrollment be in the future? One recent study took a fresh approach to this question by proposing as an index the growth of engineering societies (chemical, electrical, civil, mechanical, automotive, and IRE). It was found that the over-all society growth rate is exponential and is $7\frac{1}{2}$ per cent per year. A similar growth rate in engineering college enrollment would mean that most previous forecasts should be revised upward by a substantial amount. The study also showed that IRE growth was the fastest, about 14 per cent per year, with the American Institute of Chemical Engineers the next fastest. (W. B. Swift, "An alarmist view of engineering college enrollment," IRE TRANS. ON EDUCATION, June, 1960.)

The corner-reflector antenna is being discussed with increasing regularity in the technical literature. This interest stems from the fact that this antenna has been found to be particularly well suited for ionospheric scatter communication systems. It is simple in form, consisting of two plane reflecting surfaces joined at one edge to form a corner, with the driving element placed in the aperture between the two planes. An important advantage of the corner reflector over other types of antennas is that it can be designed to have extremely low back radiation, an important requirement for ionospheric scatter work. It also offers high gain, broad frequency response, narrow beam width, low cost, and ease of construction. One of the drawbacks of the corner-reflector antenna has been a scarcity of quantitative experimental data on the effects of the various parameters, such as lengths and widths of the reflecting surfaces and the magnitude of the corner angle, on the performance of the antenna. This deficiency has now been amply corrected by publication of the results of a comprehensive program of radiation pattern measurements of a variety of corner-reflector antennas. The report features no less than 56 graphs, from which beam widths and back radiation levels for any combination of surface lengths and widths can easily be determined. (A. C. Wilson and H. V. Cottony, "Radiation patterns of finite-size corner-reflector antennas," IRE TRANS ON ANTENNAS AND PROPAGATION, March, 1960.)

Fusion research efforts, as everyone knows, are now being directed on a large scale toward the tremendously challenging problem of achieving a controlled thermonuclear reaction in order to provide mankind with an unlimited and inexpensive source of energy. These efforts have brought with them some rather challenging design problems that involve the electronics engineer. All of the fusion methods currently being pursued require enormous energy storage and switching systems. If design engineers think they have problems, perhaps they would like the job of designing an energy storage system with peak power requirements exceeding 1000 megawatts and switches capable of passing several hundred thousand amperes for intervals ranging from a microsecond to as long as one second. At present, the development of suitable energy storage systems seems to be leading the means of switching. Capacitors have been used almost exclusively for energy storage, although for extremely large energy storage, inductive means are beginning to look more attractive. As for switching, the ignitron tube has proved the most satisfactory to date. (V. L. Smith, "Electronic engineering design problems in fusion research," IRE TRANS. ON NUCLEAR SCIENCE, March, 1960.)

Abstracts of IRE Transactions

The following issues of TRANSACTIONS have recently been published, and are now available from the Institute of Radio Engineers, Inc., 1 East 79th Street, New York 21, N. Y. at the following prices. The contents of each issue and, where available, abstracts of technical papers are given below.

Sponsoring Group	Publication	Group Members	IRE Members	Non Members*
Aeronautical and Navigational Electronics	ANE-7, No. 1	$0.55	$0.85	$1.65
Antennas and Propagation	AP-8, No. 2	2.00	3.00	6.00
Audio	AU-8, No. 2	0.70	1.25	2.10
Broadcast and Television Receivers	BTR-6, No. 1	1.30	1.95	3.90
Education	E-3, No. 2	1.50	2.25	4.50
Engineering Writing and Speech	EWS-3, No. 1	1.15	1.70	3.45
Medical Electronics	ME-7, No. 2	1.50	2.25	4.50
Nuclear Science	NS-7, No. 1	1.80	2.70	5.40

*** Libraries and colleges may purchase copies at IRE Member rates.**

Aeronautical and Navigational Electronics

VOL. ANE-7, NO. 1, MARCH, 1960

The Editor Reports (p. 2)

Automatic Radio Flight Control (Reproduction of Historic Paper)—F. L. Mosley and C. B. Watts, Jr. (p. 3)

This reproduction of an historic 1946 paper discusses the general problem of automatic control of aircraft flight on radio-defined tracks as an aid to point-to-point navigation, traffic control, and final approach and landing. Practical systems which have been extensively tested are described, and their operation is explained on both operational and theoretical grounds. A brief outline is given of the various radio navigational facilities which are available to define suitable tracks for automatic aircraft guidance. Effects of cross winds are analyzed, and a complete discussion of damping problems is given.

The improvements in accuracy, reliability, and safety in flight which accrue through the use of automatic instead of manual control are described, and supported by results of operational tests. The paper recommends widespread adoption of automatic radio flight control systems as an indispensable aid to all-weather operation of aircraft.

Basic Air Traffic Control System Concepts—Howard K. Morgan (p. 12)

The basic need for air traffic control for aircraft and missiles results from the inability of any pilot or missile control agency to digest and handle information concerning many aircraft, even if presented perfectly, since judgment must be centrally controlled. Only in wholly controlled space is separation safely handled, a system necessity. Positive Occupancy systems define occupied space most safely and economically. Area control has uniform application for universal use. The interlocking function to maintain separation can be handled most efficiently and safely by a computer, while trained controllers can expedite most economically with such automatic protection. The flight plan used for control can consist of much more limited data than those for an entire trip, a saving over methods of transmitting full plans with updating. The fundamental basis of presentation of ATC information to the pilot can be simplified by either automatic flag presentations or, for voice, equivalent short phrases. Clear distinction is necessary between the control data and monitoring data, and the two methods should be used as a cross check.

Uncontrolled space, with speed restriction, is required for certain users and restricted space is required for others in certain areas. Methods of handling space on an area basis utilize all space with maximum freedom.

A universal coordinate system for control has many advantages and can be easily introduced. Aircraft and missile identity numbers can contain useful additional information. Frequency, time, and space assignments are necessary considerations for control communications.

An example of the Bendix Positive Area Occupancy procedure shows its relative simplicity. Methods of expediting in a Positive Area Occupancy system are explained.

A Statistical Analysis of Cross-Track Errors in a Navigation System Utilizing Intermittent Fixes—H. Staras and R. W. Klopfenstein (p. 15)

A model is developed relating navigational instrument errors to the actual cross-track error of an aircraft. At a set of equispaced points, fixes on precisely known landmarks are obtained whose accuracy is assumed independent of the length of the flight. An optimum procedure is developed for utilizing these fixes to calibrate the compass on board the aircraft. Finally, the accuracy of arriving at a predetermined destination after the last checkpoint is evaluated.

Because of the complexity of the problem, numerical calculations using the IBM 650 were used. Two interesting conclusions were reached: 1) for a fixed spacing between fixes the accuracy of arriving at the destination is improved as the length of the flight (and therefore the number of fixes taken) is increased, and 2) for a fixed length of flight, the accuracy of arriving at the destination is almost independent of the number of fixes.

Abstracts (p. 20)
PGANE News (p. 22)
Contributors (p. 23)

Antennas and Propagation

Vol. AP-8, No. 2, March, 1960

Frontispiece (p. 128)
John B. Smyth, Retiring Editor (p. 129)
Editorial Comment (p. 130)
Theory of Coupled Folded Antennas—C. W. Harrison, Jr. and Ronold King (p. 131)

Formulas for the mutual and self-impedance of two identical nonstaggered parallel-folded dipoles are developed. A generalization of the theory permits determination of these impedances for any identical dual configuration of wires, no matter how complicated, provided the structures are symmetrical with respect to the driving points. If the impedance of any single-conductor solid-wire element in a symmetrical circular array of linear radiators is known, the impedance of each element in a similar array consisting of folded-wire structures is readily obtained. Two obvious practical uses of the theory are: 1) the determination of the performance of a two-element folded antenna array, when one antenna is a tuned parasite, functioning as a director or reflector; and 2) determination of the driving-point impedance of a folded antenna parallel to a highly-conducting plane.

The Slot Antenna with Coupled Dipoles—R. W. P. King and G. H. Owyang (p. 136)

The problem of an array consisting of a slot antenna and two symmetrically-located cylindrical dipoles is formulated. The approximate distribution of the current along each antenna is obtained by a method of iteration. The radiation function, the coupling coefficients between the slot and the dipole, the relation between the magnetic current in the slot and the electric current in the dipole, and the input impedance of the slot in the presence of the dipoles have been obtained. An experimental setup for measuring the radiation patterns is described and measured and theoretical patterns are displayed.

Radiation Patterns of Finite-Size Corner-Reflector Antennas—A. C. Wilson and H. V. Cottony (p. 144)

Radiation patterns were measured for corner-reflector antennas having various combinations of widths and lengths of the reflecting surfaces. The widths of these ranged from 1 to 10 wavelengths, the lengths from 0.5 to 5 wavelengths. The aperture angle was, in general, set at a value required to maximize the gain. Radiation patterns are arranged according to the size of the reflecting surfaces. The effect of the widths and lengths of the surfaces on the widths of the main lobe and on the level of the radiation to the rear is summarized in a series of curves. A corner-reflector antenna with a collinear array of dipoles was designed, constructed, and tested to have sidelobe radiation below −40-db level.

The Flight Evaluation of Aircraft Antennas—George W. Leopard (p. 158)

Flight evaluation of communication-navigation-identification antennas installed on new types of aircraft is required to confirm model measurements. The paper reviews the parameters involved in such an evaluation under both standard and nonstandard propagation conditions. The predicted signal level across the receiver terminals connected to an isotropic antenna is employed as the standard of comparison with the scale-model antenna patterns. The procedures employed and the results obtained are briefly discussed.

Reciprocity and Scattering by Certain Rough Surfaces—W. S. Ament (p. 167)

Reciprocity theorems are developed for the average field specularly reflected, and the average power randomly scattered, to a point by a statistically described array of objects. A reciprocal quasivariational expression for the average power is developed for use when the self-consistent method applies to calculating currents in the individual objects. This formula is applied to calculate differential scattering cross sections for two idealized arrays bounded by plane "rough surfaces." General conclusions, relating to reciprocity, power conservation, grazing behavior, etc., for rough surface scattering, are made and applied heuristically to show that grazing reflection and backscatter from the rough ocean should be independent of polarization.

Backscattering from a Finite Cone—Joseph B. Keller (p. 175)

Backscattering is calculated for an acoustic wave incident on a hard or soft finite cone, and for an electromagnetic wave incident on a perfectly-conducting finite cone. Two shapes of cone are treated, one with a flat base and the other with a rounded base. The calculation is based on the geometrical theory of diffraction. It is probably valid for wavelengths as large as the cone dimensions or smaller. Graphs of the backscattering cross section vs cone angle and vs wavelength are given for axial incidence on the flat-based cone. Suggestions for shaping an object to minimize its backscattering are also included.

Optimim Radar Integration Time—J. M. Flaherty and E. Kadak (p. 183)

The practice of integrating periodic low-level signals with time in order to improve the SNR of a coherent signal in an ambient of incoherent noise is extremely useful and generally understood. In cases where the signal continues as long as the observer desires to integrate, the SNR can of course be improved by lengthening the integration period without limit. However, in the case of a radar system trying to detect a very rapidly-approaching target, it is obvious that one does not have an unlimited length of time to perform the signal integration and arrive at a decision. The authors have derived an expression which reveals what the optimum integration period is when the radius of the region to be protected, and the velocity of the approaching target are known.

Power Spectra of Temperature, Humidity and Refractive Index from Aircraft and Tethered Balloon Measurements—Earl E. Gossard (p. 186)

Fifty-seven spectra of temperature, vapor pressure and refractive index were computed from captive balloon data taken at elevations up to 3000 feet MSL. Eight spectra of refractive index were obtained using an aircraft equipped with a microwave refractometer. It was found that atmospheric stability apparently has a pronounced effect on the variation of turbulent intensity with height. Although the spectra of all three parameters generally approach a $-5/3$ power law at high wave numbers, stability seems to have a controlling influence on spectral form at the low-frequency end of the wave number range studied. It is therefore concluded that methods of computing microwave scattered fields from the mean square dielectric perturbations and scale size obtained from the auto covariance are unreliable. The forms of the experimental auto covariances appear to be best represented by an exponential function or perhaps by a Modified Bessel Function of the second kind and 1/3 order. The temperature-humidity cospectrum may influence the shape of the refractive index spectrum, especially under unstable conditions. The equivalence of Eulerian space and time spectra is verified for refractive index by a series of aircraft-balloon fly-bys.

Aircraft Scintillation Spectra—Robert B. Muchmore (p. 201)

Using the model of aircraft reflection developed by DeLano, the spectra of the reflection signals are found. Spectra for the amplitude of the rectified return, for the angular fluctuation signal associated with a fixed radar line-of-sight (effective radar center fluctuation), and for the angular fluctuation signal associated with a zero time constant servo (apparent radar center fluctuation) are derived. Several types of target motion are considered: uniform rotation, random rotation, and rectilinear velocity toward the radar itself. Each of these motions produces a characteristic spectrum and the properties of these spectra are pointed out and their significance in radar system design emphasized. In particular, the importance of the spectral density at zero frequency of the apparent radar center is shown in relation to systems using very rapid automatic gain control (AGC). It is shown that such use of very fast AGC may increase this noise density by a factor of approximately three, and thus increase the system noise.

Apparent Thermal Noise Temperatures in the Microwave Region—Eric Wegner (p. 213)

The necessary equations are presented for obtaining the noise temperature due to thermal radiation which would be sensed by a receiver with an antenna located at some altitude above the earth. Emission and absorption of radiation by the atmosphere is considered. Calculated over-all absorptivities and apparent atmospheric temperatures are given as a function of antenna observation angle for beam paths through the atmosphere. Six wavelengths in the microwave band and three types of weather conditions were chosen for the calculations. Some typical antenna temperatures are presented as examples of the magnitudes of the effects to be expected as a function of the type of surface being viewed, the weather, and polarization.

Patterns of a Radical Dipole on an Infinite Circular Cylinder: Numerical Values—Curt A. Levis (p. 218)

Linear Arrays with Arbitrarily Distributed Elements—H. Unz (p. 222)

A linear array with general *arbitrarily* distributed elements is discussed. A matrix relationship is found between the elements of the array and its far-zone pattern. The lower bound of the stored energy and the Q factor of the array are found. A figure of merit for the array is defined.

Synthesis of Nonseparable Two-Dimensional Patterns by Means of Planar Arrays—A. Ksienski (p. 224)

A Method to Reduce Antenna Ground Reflections—David Sabih (p. 225)

Impulse Excitation of a Conducting Medium—J. Galejs (p. 227)

The depth of penetration into a conducting medium, where sinusoidal surface excitations generate peak magnetic fields or derivatives equal to those of an impulse-type surface excitation, are calculated. Finite pulses generate fields similar to those of a surface impulse provided they are sufficiently short. The maximum permissible pulse duration is proportional to the square of the specified penetration depth. In order to exhibit minimum attenuation, the excitation fields must be unipolar over a time period comparable with the transient duration. Such fields may be generated within the induction field of the source.

Electromagnetic Transients in Conducting Media—S. H. Zisk (p. 229)

In a recent paper, Richards derives expressions for the electric and magnetic fields of a short pulse of electric or magnetic dipole moment in a conducting medium. An alternative analysis is given which explains certain unusual results of the original work as arising from dispersion in the conducting medium and from the frequency dependence of the attenuation factor of the fields. The conclusion drawn is that communication by pulses is expected to be inferior to that by low-frequency continuous waves.

Audio

Vol. AU-8, No. 2, March–April, 1960

The Editor's Corner—Marvin Camras (p. 37)

PGA News—J. Ross Macdonald (p. 38)

A Comparison of Several Methods of Measuring Noise in Magnetic Recorders for Audio Applications—John G. McKnight (p. 39)

The various methods of measuring noise in audio magnetic recorders are discussed, and data are shown comparing the numbers observed for the different methods (IRE Standard Methods, and others) when applied to the same recorder. This data will enable one to compare other data taken by one method with data taken by another method.

The present audio specifications based only on broad-band noise are shown to be inadequate, as the equipment noise in the range of low hearing sensitivity masks any improvements which may be made in tape noise, or with the Ampex Master Equalization. A measure of relative audible noise level should be added to the present broad-band measurement.

Magnetic Recording and Reproduction of Pulses—Donald F. Eldridge (p. 42)

The most widely used techniques for recording digital information on a moving magnetic medium are return-to-zero (RZ) and non-return-to-zero (NRZ). Both techniques have some peculiar advantages and disadvantages. Although sophisticated coding methods may be utilized to increase information density, the density achievable by any method is determined by the basic resolution of the record and reproduce processes.

An expression is derived for the output of a reproduce head when an ideally recorded pulse is passed over it. The output is a function of the head fringing field in the region occupied by the recorded medium, and is the sum of the outputs produced by the longitudinal and perpendicular components of magnetization. A novel technique is used to measure the relative magnitudes of the components in a typical saturated recording tape. The perpendicular component is 11 per cent of the longitudinal component and may be neglected for the practical case.

From a combination of experimental and theoretical data the width and height of the reproduced pulse are computed for variable gap width, medium thickness, and head-to-medium spacing. The effect of a nonideal pulse with a finite recorded width is considered. The total output pulse width is shown to the be sum of the computed ideal reproduce pulse width and the width of the actual recorded pulse. From the curves presented, one may observe that only a slight increase in resolution can be achieved by utilizing very small reproduce head gaps.

Data are presented on the measured initial magnetization characteristics of a typical oxide. The characteristic may be approximated by either an offset linear curve up to about 60 per cent of saturation or a fourth power curve up to about 30 per cent of saturation. Data are also presented to show the effect of previous magnetization upon the transfer characteristic.

The record process is analyzed with a step-by-step technique utilizing measured data on the head field and oxide magnetization characteristics. It is shown that both the shape and location of the recorded pulse are functions of the medium magnetization characteristic, the record head gap width, the record current, the medium thickness, and the head-to-medium spacing. The effect of each of these variables is computed. The computed results are verified experimentally. It is shown that under a wide range of conditions the reproduce pulse width obtained from a given head is approximately five times the width of a pulse ideally recorded by the same head. It is further shown that when the spacing between head and medium is larger than the gap width, the resulting over-all reproduced pulse width is approximaetly seven times the head-to-medium spacing.

Previous recording history of the medium has a significant effect upon the pulse location. Data presented indicate that the record current must be approximately twice the current required for medium saturation to make the pulse location error unmeasurable.

High-Density Magnetic Recording—James J. Brophy (p. 58)

By improving the mechanical properties of magnetic recording heads and recording media, it has been possible to demonstrate consistent recordings at information densities up to 40,000 cycles per inch. No fundamental magnetic limit to the maximum recording density has been detected. The major mechanical limitation appears to be the effective head-tape separation due to mechanical surface roughness of the medium. Tape noise arises from both body and surface effects, but their relative importance is not clear. High-frequency recording in the region of several megacycles introduces no special problems with heads of suitable design, such as the outside coil head. Based on present experimental results, a maximum recording density of the order of 100,000 cycles per inch is predicted.

A Compatible Tape Cartridge—Marvin Camras (p. 62)

Magnetic recording is recognized as a superior medium for stereophonic entertainment, but its popularity has been handicapped by inconvenience of threading and high cost. A new approach is a tape cartridge of very low cost, which is compact, and fully protects the record. The cartridge is completely automatic on a machine designed for its use, and yet will operate manually on present tape recorders.

Correspondence (p. 67)

Contributors (p. 68)

Broadcast and Television Receivers

Vol. BTR-6, No. 1, May, 1960

Meet Our New Chairman (p. 1)

Professional Group on Broadcast and Television Receivers, Administrative Committee (p. 2)

Minutes of PGBTR Administrative Committee Meeting, March 22, 1960 (p. 3)

Excerpts from Minutes of PGBTR Administrative Committee Meeting, November 10, 1959 (p. 5)

Chicago Spring Conference (p. 6)

A Transistorized Portable Television Receiver—A. R. Curll, Philco, (p. 9)

A Transistor TV I-F Amplifier—John G. Humphrey, General Electric (p. 17)

Designing Solar Power Supplies for Transistorized Radio Receivers—Jerome Kalman, Solar Products (p. 21)

The Video Processing Circuits of an All Transistor Television Receiver—C. D. Simmons and C. R. Gray, Lansdale Tube (p. 25)

Transistorized Vertical Scan System for Magnetic Deflection—Fuad L. Abboud, Sylvania (p. 33)

Linearization of a Transistorized Vertical Deflection System—R. B. Ashley, General Electric (p. 39)

Improvement of Picture Quality by Means of Beam Spot Stretch—H. Kogo, H. Nakatsukasa and T. Kawase, Chiba University (p. 48)

Mixer-Oscillator Considerations for Nuvistors in the VHF Band—C. Gonzalez, RCA (p. 49)

Performance of Nuvistor Small-Signal Tetrodes in Television Video I-F Amplifiers—W. H. Mead, RCA (p. 50)

Calendar of Coming Events (p. 51)

Education

Vol. E-3, No. 2, June, 1960

Evaluation Report on the New York City Academic High School Program in Physics—Engineering Advisory Committee (p. 31)

The physics syllabus being offered in the academic high schools of New York City has aroused considerable interest as to its value as prerequisite to baccalaureate programs in science and engineering.

To gather certain facts, the Engineering Advisory Committee was organized, comprised of members selected from the New York Metropolitan sections of the professional engineering societies. The members visited numerous schools to arrive at a broad appraisal of high-school physics as a pre-engineering preparation. They inspected class schedules, laboratory facilities and libraries. They examined laboratory schedules, textbooks in use, teaching load assignments, and procedures for ordering laboratory equipment. They evaluated the qualifications of teachers and methods for motivating gifted students. Their findings are described in this report which includes a listing of recommendations.

A Look at the New Electrical Engineering Laboratory Program at the Hopkins—Theodore A. Bickart (p. 36)

The undergraduate electrical engineering program at The Johns Hopkins University has undergone extensive revision. The most striking revision has been in the laboratory program. Laboratory courses which are distinct from the lecture courses have been developed. These laboratory courses embrace the fields of basic and advanced electrical measurements, transducers, passive circuits, active networks, communications, microwaves, materials, computers, servomechanisms, and energy conversion. The experiments in each one of these fields are designed to give the student insight into both the basic and advanced concepts involved. The sequence of presentation of the experiments is chosen to allow the most complete coverage of a subject as possible, based on the order in which the electrical engineering lecture courses are taken. The use of laboratory manuals, notebooks, reports, and examinations has been given careful thought and some significant ideas have been evolved with regard to their use in establishing a successful laboratory course.

Linear Graph Theory—A Fundamental Engineering Discipline—H. E. Koenig and W. A. Blackwell (p. 42)

Current techniques for formulating the mathematical characteristics of physical systems vary greatly from one type to another (mechanical, electrical, thermal, etc.). Of these techniques, those used in electrical network analysis have proven to be the more orderly and generally applicable as evidenced by repeated efforts on the part of the system analyst to first establish an electrical analog of the system in question.

This paper presents the basis of an operational concept of system analysis embracing all types of systems and presents an orderly, sure, and relatively simple basis for extending the discipline of linear graph theory (abstracted form of network theory) to the analysis and synthesis of all types of lumped-parameter systems without the artifice of analogies. It is indicated that these procedures and concepts also provide a means for extending electrical network theory beyond current applications to include systems of multiterminal components.

Part-Time Graduate Electrical Engineering Programs in the San Francisco Bay Area—Joseph M. Petit (p. 49)

The San Francisco Bay area has been rapidly growing in size and stature as one of the national centers of the electronics industry. In particular, the growth has been in companies and laboratories with a strong emphasis on research and development, in contrast to volume production. Such industry needs and seeks opportunities for graduate education for its engineers. The manner in which such opportunities have developed in the San Francisco area, especially at Stanford where the great majority of the part-time students are enrolled, provides an interesting example of how the needs of industry can be served within the academic objectives of an educational institution which serves primarily the full-time day student.

The Functional Context Method of Instruction—Harry A. Shoemaker (p. 52)

This is a discussion of a method of instruction designed to replace conventional methods for training radio repairmen. In traditional radio repair instruction, basic electronics has been taught as a block of instruction preceding instruction on intact equipment and maintenance operations. This approach is criticized for its failure to provide the student with meaningful and relevant contexts for the learning of basic electronics and for the obstacles it presents to the assimilation of basic electronics knowledge into maintenance skills. A new approach, entitled the functional context method, is offered as a means for avoiding these shortcomings. This is accomplished through a topic sequence wherein basic electronics is taught in the broader contexts of over-all equipment functions and maintenance operations.

An Alarmist View of Engineering College Enrollment—W. B. Swift (p. 58)

Engineering college enrollment is in some measure a response to the demand for trained people. The forecasting of enrollment may thus be improved if it is based upon trends in the demand for trained people. One way to measure these trends, which does not seem to have been explored, comes from consideration of the membership in technical societies. The trends found in this way are very marked. The over-all rate of growth so indicated is exponential and is about $7\frac{1}{2}$ per cent per year. The indicated growth rate in electrical engineering is much greater than in any of the other major subdivisions of engineering except chemical engineering.

Contributors (p. 63)

Announcement of the 1960 Special Summer Session (p. 64)

Engineering Writing and Speech

Vol. EWS-3, No. 1, April, 1960

The Cover (p. 2)

Background to Scientific Communication—M. M. Kessler (p. 3)

The need for more efficient communication of engineering and scientific information is traced to the increase in the number and variety of people who have the need to know. The change in the position of science from a significant source of power to a major instrument of power makes the distribution of scientific information a matter of competitive necessity and logistics. It is stressed that we need a communications systems that will satisfy the needs of the scientific community at large rather than isolated and specialized pockets of retrieval. An experimental system is suggested that will provide a realistic test facility for the evaluation of ideas and components. Some problem areas in need of research and invention are discussed.

Space-Technology: Reporting the New Dimension—R. E. Hohmann (p. 7)

How the Graphic Arts Can Help Engineering Communication—A. N. Spence (p. 16)

Technical Journalism and the Business Press—James Girdwood (p. 20)

This paper discusses the aims of business publications in the electronics engineering field, and their obligations to readers and to the electronics industry. It also discusses the obligations of engineers to disseminate information quickly and accurately. Engineers who wish to write for the business press should consider the nature of the "publication image" of the magazine, the best approach to set forth the findings, and the appropriate style of writing for a given readership.

Language as an Engineering Tool—J. R. Gould (p. 24)

In an analysis of the use of language as an engineering tool, the writing problem is divided into three phases: the preparation, the act of writing, and the results achieved. Questions of empathy for the reader, writing style for effective expression, and organization for clarity are discussed. Some criteria are given for mature, professional prose and for measuring the effectiveness of engineering literature.

Organizing and Complex Technical Proposal Effort—E. M. Smith (p. 28)

A complex proposal is a document which offers to a potential customer an approach to a problem involving the activities of more than one department, division or company working toward that goal. This paper discusses the organization of a hypothetical complex proposal and shows the nature of management responsibilities, the use of a "systems approach" to subdivide the workload, and the role of the Publications Project Leader.

The Authors (p. 31)

Information for Authors (Inside Back Cover)

Medical Electronics

Vol. ME-7, No. 2, April, 1960

Editorial—L. B. L. (p. 60)

Fast, Automatic Ocular Pressure Measurement Based on an Exact Theory—R. Stuart Mackay and Elwin Marg (p. 61)

Several tonometers are described which are simultaneously faster, more accurate and more gentle than previous forms. They are easier to use and more convenient to read, and do not generally require anesthesia since their indication is recorded a fraction of a second after they contact the eye. Their principle is such that they can be used while covered with a sterilizable rubber film, thus minimizing risk of infection and clogging of the instrument. New systems of tonography are also described. The factors which allow readings by a component insensitive to variations in corneal curvature, bending forces, tissue tension and surface tension of tears suggest other biological applications such as blood pressure monitoring through intact vessels. A discussion of a number of electronic motion and pressure transducers is included.

Endoradiosondes: Further Notes—R. Stuart Mackay (p. 67)

This paper is to supplement last year's summary on swallowable radio transmitters. Included are general comments on procedure as well as specific items such as temperature sensitivity, the use of tunnel diodes in pH measurement, the use of multiple transmitters, and the design of a nondirectional receiving antenna system. The latter not only simplifies unattended recording in some cases but also helps in relaying the signal from a small booster transmitter carried by the subject. The frequency shift needed in relaying action is here a frequency doubling provided by suitable nonlinear receiver circuits.

Foreign Body and Kidney Stone Localizer—R. Stuart Mackay (p. 74)

Various probes are described that will amplify the sound of contact with any hard object in the body and thus signify its presence. One of the most useful forms consists of a sound transducer that clamps to the handle of any pair of forceps so that the surgeon knows when he is grasping a kidney stone or gall stone or other hard body. Almost mentioned are active probes in which loading of a bilateral sound transducer, which is being driven by an external electrical circuit, causes an indication of contact as an apparent change in impedance. These forms seem especially sensitive when fitted into the end of a catheter.

X-Ray Visualization and Analysis Using Spectral Information—R. Stuart Mackay (p. 77)

An electronic X-ray system is described which allows more information to be obtained than do the usual radiographic methods which lump together the effects of different wavelengths. It gives high contrast images and allows otherwise unnoticeable detail to be detected with a quantitative evaluation of composition. The system has been used to visualize a normal thyroid and analyze it for normal iodine distribution, though a thyroid gland cannot usually be seen at all in a radiograph. An analogy with a new electrocardiographic method is noted.

Television X-Ray Movies: Dose and Contrast Factors—R. Stuart Mackay (p. 80)

A television link with nonlinear circuits aids X-ray movie production by allowing concentration on a small brightness range, and dose can be determined by the detail to be observed rather than by film properties. A continuously-moving-film camera viewing a single line on the kinescope, or a video tape recorder, need lose the effect of no interacting quantum. The frame rate aspect is considered and a systematic exposure procedure is given. An X-ray beam monitor is also described.

The probable course of certain future developments is given as well as suggestions for the best use of existing detectors.

Deflection Focusing of Electron Microscopes—R. Stuart Mackay (p. 87)

An image is an electron microscope is made to move in response to manipulation of a switch if the image is slightly out of focus. Because of the sensitivity of the eye to motion, even low contrast or dim images can thus be focused very accurately by noting lack of motion. This method is helpful in all cases, but with certain specimen types or with a biased electron gun it is essential. Construction information is given for a magnetic beam deflection unit that has performed well in regular use for over ten years. The electron optics of certain corrections are discussed briefly.

What is a Nerve?—R. Stuart Mackay (p.94)

Many of the observed properties of a nerve are summed up by noting that it appears to be a cascaded series of bistable elements. This implies an electrical negative resistance property which is observed to be tetrode-like, as opposed to arc-like. A time dependent element in the regenerative feedback loop is involved in such things as anode-break stimulation. New nerve analogs are suggested by this view, and the common factor in previous ones is seen. Many excitable plant and animal cells show these properties. A brief general discussion of negative resistance is given. No new biological data is presented.

Switching in Bistable Circuits—R. Stuart Mackay (p. 98)

Switching or triggering in certain nonlinear circuits having two stable states is studied in graphic detail. The minimum and maximum pulse requirements are discussed and some of the general ideas of bistability considered. A convenient technique for studying the response of circuits, apparently in slow motion, is described. A classroom demonstration relating to nerve impulse generation is given.

Physiological Effects of Condenser Discharges With Application to Tissue Stimulation and Ventricular Difibrillation—R. Stuart Mackay and Sanford E. Leeds (p. 104)

The experiments reported in this paper served three major purposes: 1) They defined that property of an electrical discharge upon which the ability to stimulate living tissue depends, in particular the ability to produce a saturation stimulation of the heart. 2) They demonstrated that intense condenser discharges through the chest need not produce any deleterious effects. 3) They showed that one can produce defibrillation of the ventricles of a canine heart, through the closed chest, by such a discharge.

Some Electrical and Radiation Hazards in the Laboratory—R. Stuart Mackay (p. 111)

Some electrical and radiation hazards which are present in the laboratory are discussed. A constant reminder concerning some of the common dangers is worthwhile since even experienced workers may forget about them and injury or death can result.

Letter to the Editor—R. Stuart Mackay

Correction—L. B. L.

Nuclear Science

Vol. NS-7, No. 1
March, 1960

Signal-Flow Graphs and Stability Analysis of Nuclear Reactors—A. B. VanRennes (p. 1)

Signal-flow graphs have long been exploited in feedback-control analysis, and can greatly aid in kinetic studies of nuclear reactors and nuclear reactor systems. The signal-flow graph is a means for conveniently and compactly displaying a set of linear differential equations. Such a flow graph can be easily and quickly formulated from a set of equations, or, with experience, directly by inspection from the physical system. A powerful method developed by S. J. Mason permits rapid determination of the transfer function between any two points in the system.

The above techniques are illustrated for an elementary nuclear reactor. The usual transfer function is quickly obtained, as is also the transfer function for a reactor operating in a sub- or supercritical condition. Other methods of reactor control suggested by the analysis are discussed.

Factors Which Will Influence Early Application of Nuclear Rockets—Lt. Col. H. R. Schmidt and Major R. S. Decker (p. 6)

An approach to the application of nuclear rocket systems is to consider the integration of such systems into the national space vehicle program. Within the framework of the general configuration and the various missions for which these space vehicles are planned, the potential performance which nuclear rockets may provide is illustrated. Although a wide range of potential applications is apparent within the limits of consideration, certain practical and technical matters tend to reduce the scope of logical and reasonable choice for initial use. Many of the practical problems involved in nuclear rocket development are reviewed to provide an appreciation for the effort required.

Electronic Engineering Design Problems in Fusion Research—Vernon L. Smith (p. 13)

Design problems peculiar to fusion research are discussed. Particular emphasis is placed on the development of large energy storage systems, and transfer and utilization of this energy. In addition, design criteria for data reduction systems, and other problems related to our fusion research program are discussed.

Nonsaturating Transistor Circuitry for Nanosecond Pulses—Robert M. Sugarman (p. 23)

A system is described for pulse testing of transistors in the 10^{-10} to 10^{-9} sec range. Based on these measurements, a nanosecond, current switching, multiple coincidence system has been constructed. It is dc coupled and has input pulse limiters and clipping stubs. A ten-nanosecond scaler-discriminator stage is discussed which also employs current switching techniques. One output is scaled for pulse counting; another unscaled output is used to drive coincidence circuitry.

Nuclear Rocket Engine Controls in an Orbital Transfer Role—B. P. Hegelson (p. 29)

It is assumed that the mission for a nuclear rocket upper-stage vehicle is the transfer from a 300-mile earth orbit to a corotational earth orbit.

An engine of the solid fuel, heat exchanger type is assumed and briefly described.

The engine duty cycle requirements are deduced from the incremental velocity requirements of the mission. Controls attention is fixed on the thrust programmer without discussion of the equally important sequence control aspects. A constant specific impulse, variable thrust controls approach is taken. Basic principles underlying this approach are discussed. Fineness of control and restart capability are pointed out as inherent features of the engine. These augment the well-known performance advantages due to the high specific impulse of nuclear rocket engines.

Background Pulse Pile-Up in Neutron Counting Channels—J. L. Burkhardt and R. C. Wilson (p. 36)

An experimental study of background pulse pile-up in neutron counting channels has been performed. Neutron- and gamma-produced pulses from two BF_3-filled counters and one boron-lined counter were photographed for several input circuit time constants. Several measurements were made for each of ten counting channels: five commercially available circuits, three Bettis reactor source range channels, and two experimental systems. Integral bias curves taken with simulated neutron and gamma pulses were the major comparison criterion. Wide differences in performance were found, even among very similar circuits. The results indicate that small pulse pile-up in the test circuitry may greatly influence data taken with counters operating in high-background gamma fluxes. Recommendations are made for the design of circuitry with reduced pile-up.

Digital Storage of Statistical Data—Fred H. Irons (p. 43)

In the field of nuclear instrumentation, there is need for an economical instrument capable of storing data compactly in digital form. This paper describes a magnetic tape recorder which can store binary numbers from one to a maximum of eleven digits in parallel on a continuously rotating loop of tape. The tape is operated at a constant speed of 30 inches per second and a packing density of 667 bits/inch/track and can be used in loops of two to 1000 feet. For these operating conditions, the average storage access time for random inputs is 25 μsec. Stored data are read back from the tape into a core-memory matrix at a 20-kc rate. The operational reliability for the recording and reading processes has been found to vary between 4 and 14 parts/million. Higher reliability may be obtained by using the tape at lower packing densities.

Contributors(p. 49)

Annual PGNS Meeting (p. 50)

Abstracts and References

Compiled by the Radio Research Organization of the Department of Scientific and Industrial Research, London, England, and Published by Arrangement with that Department and the *Electronic Technology* (incorporating *Wireless Engineer* and *Electronic and Radio Engineer*) London, England

NOTE: The Institute of Radio Engineers does not have available copies of the publications mentioned in these pages, nor does it have reprints of the articles abstracted. Correspondence regarding these articles and requests for their procurement should be addressed to the individual publications, not to the IRE.

The number in heavy type at the upper left of each Abstract is its Universal Decimal Classification number. The number in heavy type at the top right is the serial number of the Abstract. DC numbers marked with a dagger (†) must be regarded as provisional.

UDC NUMBERS

Certain changes and extensions in UDC numbers, as published in PE Notes up to and including PE 666, will be introduced in this and subsequent issues. The main changes are:

Artificial satellites:	551.507.362.2	(PE 657)
Semiconductor devices:	621.382	(PE 657)
Velocity-control tubes, klystrons, etc.:	621.385.6	(PE 634)
Quality of received signal, propagation conditions, etc.:	621.391.8	(PE 651)
Color television:	621.397.132	(PE 650)

The "Extensions and Corrections to the UDC," Ser. 3, No. 6, August, 1959, contains details of PE Notes 598–658. This and other UDC publications, including individual PE Notes, are obtainable from The International Federation for Documentation, Willem Witsenplein 6, The Hague, Netherlands, or from The British Standards Institution, 2 Park Street, London, W.1, England.

The Index to the Abstracts and References published in the PROC. IRE from February, 1959 through January, 1960 is published by the PROC. IRE, June, 1960, Part II. It is also published by *Electronic Technology* (incorporating *Wireless Engineer* and *Electronic and Radio Engineer*) and included in the April, 1960 issue of that Journal. Included with the Index is a selected list of journals scanned for abstracting with publishers' addresses.

ACOUSTICS AND AUDIO FREQUENCIES

534.2 1840

Propagation of Band-Limited Noise in a Layered Waveguide—C. S. Clay. (*J. Acoust. Soc. Am.*, vol. 31, pp. 1473–1479; November, 1959.) The normal mode solution of the problem of the radiation field of a simple harmonic point source in a layered waveguide is extended to the case of a band-limited noise source. This theory is used to calculate the radiation field of a simple harmonic point source and a point noise source in shallow water over a thick layer of unconsolidated sediments; calculations are compared with experimental data.

A list of organizations which have available English translations of Russian journals in the electronics and allied fields appears at the end of the Abstracts and References section.

534.232 1841

Measurements of the Total Acoustic Radiation Impedance of Rigid Pistons in an Array—J. S. M. Rusby. (*Nature*, vol. 186, pp. 144–145; April 9, 1960.) The admittance diagram for a single sound projector in a square 36-element array has been measured. Near resonance the admittance increases suddenly and the conductance may become negative. This phenomenon is thought to be due to large changes in the relative phase of the diaphragm velocities of neighboring projectors nears resonance.

534.232-8:546.431'824-31 1842

Performance of High-Frequency Barium Titanate Transducers for Generating Ultrasonic Waves in Liquids—H. J. McSkimin. (*J. Acoust. Soc. Am.*, vol. 31, pp. 1519–1522; November, 1959.) The effect of electrical damping on the performance of transducers operating at 10 mc is discussed. A composite layer of thickness $\lambda/4$ introduced between transducer and liquid improves the performance.

534.283-8:538.6 1843

Ultrasonic Absorption in Metals in a Magnetic Field: Part 1—V. L. Gurevich. (*Zh. Eksp. Teor. Fiz.*, vol. 37, pp. 71–82; July, 1959.) The absorption coefficient can show periodic variations of two types: oscillations and periodic increments. The determination of the Fermi surface from an investigation of these variations is discussed.

534.322.3 1844

Curves of Equal Loudness for Octave-Band Noise—G. Jahn. (*Hochfrequenz. und Elektroak.*, vol. 67, pp. 187–189; March, 1959.) The results of subjective tests are given and discussed with reference to the work of other authors, in particular Stevens (1302 of 1957). The adoption of a standard reference level of loudness for such measurements is advocated to facilitate comparisons.

534.613 1845

Measurements of Acoustic Radiation Force—K. Budal, E. Höy and H. Olsen. (*J. Acoust. Soc. Am.*, vol. 31, pp. 1536–1538; November, 1959.) "The acoustic radiation force of a plane wave impinging on a rigid sphere of diameter 10 cm and on a circular disk of diameter 7.4 cm has been measured in the wavelength interval 4 to 40 cm. The agreement with theory is satisfactory."

534.75 1846

Detection of a Pulsed Sinusoid in Noise as a Function of Frequency—D. M. Green, M. J. McKey and J. C. R. Licklider. (*J. Acoust. Soc. Am.*, vol. 31, pp. 1446–1452; November, 1959.) Detectability measurements have been made using 1) 0.1-second pulses at 16 frequencies in the range 250–4000 cps, and 2) compound pulses. Results are discussed in relation to the mechanism of the auditory system in integrating signal energy over a frequency band.

534.76 1847

Stereophonic Sound Systems—D. M. Leakey. (*Wireless World*, vol. 66, pp. 154–160, 238–240; April/May, 1960.) Extension of work described earlier [1946 and 2607 of 1956 (Brittain and Leakey)] and a brief analysis of practical two-channel systems. (See also 1472 of 1960.)

534.78 1848

Minimal Rules for Synthesizing Speech—A. M. Liberman, F. Ingemann, L. Lisker, P. Delattre and F. S. Cooper. (*J. Acoust. Soc. Am.*, vol. 31, pp. 1490–1499; November, 1959.)

534.78:681.142 1849

Results Obtained from a Vowel Recognition Computer Program—J. W. Forgie and C. D. Forgie. (*J. Acoust. Soc. Am.*, vol. 31, pp. 1480–1489; November, 1959.)

534.844.1 1850

Measurement of Sound Diffusion in Reverberation Chambers—M. R. Schroeder. (*J. Acoust. Soc. Am.*, vol. 31, pp. 1407–1414; November, 1959.) A variety of methods for the measurement of the diffusion of sound fields using simple sound-pressure or pressure-gradient microphones are described.

534.845 1851

The Sound Transmissivity of Fabric Screens, Wood Strip Mesh and Cinema Screens—J. Steinert. (*Hochfrequnz. und Elektroak.*, vol. 67, pp. 169–174; March, 1959.) A formula for the sound transmission coefficient is derived which allows for properties of the screen such as hole size, perforation, strength and mass of material. Test results are given for a number of screen materials, which show that only tests in an anechoic chamber produce reliable results in agreement with calculated values.

534.845 1852

The Absorption of Single Resonators for Different Arrangements in a Closed Room (Centre of Wall, Edge, Corner)—W. Wöhle. (*Hochfrequenz. und Elektroak.*, vol. 67, pp. 180–

187; March, 1959.) Calculations of sound absorption for resonators on an infinitely large wall (*ibid.*, vol. 67, pp. 140–146; January, 1959) are modified to apply to a closed room. Measurements in a model chamber with Helmholtz resonators distributed over the walls are discussed.

621.395.61 1853
Fluctuation Threshold of Microphone Sensitivity—A. O. Sall'. (*Akust. Z.*, vol. 5, no. 3, pp. 351–354; 1959.) An expression is derived for the sensitivity threshold due to thermodynamic fluctuations. At sufficiently low frequencies the noise level due to thermodynamic and temperature fluctuations of the gas behind the membrane of the microphone can be larger than the noise due to molecule collisions on this membrane.

621.395.616:534.26 1854
Method for Measuring and Calculating the Diffraction Coefficient of Microphones—A. N. Rivin and V. A. Cherpak. (*Akust. Z.*, vol. 5, no. 3, pp. 345–350; 1959.) A direct method is described based on the use of two similar capacitor microphones, one radiating and the other receiving. The diffraction coefficient is derived from the ratio of the potentials generated at the output of the receiving microphone in a free field and in a closed chamber of small dimensions.

621.395.623.7 1855
A Corner Loudspeaker with Coaxial Acoustical Line—T. S. Korn. (*J. Audio Eng. Soc.*, vol. 5, pp. 138–141; July, 1957.) A corner-cabinet loudspeaker system is described in which the loudspeaker is coupled to a quarter-wave coaxial re-entrant acoustic line. Full acoustic loading is obtained at 38 cps in an enclosure with a volume of 2.2 ft^3.

621.395.623.7:534.76 1856
Psychoacoustics Applied to Stereophonic Reproduction Systems—P. C. Goldmark and J. M. Hollywood. (*J. Audio Eng. Soc.*, vol. 7, pp. 72–74; April, 1959.) Results of subjective listening tests show that the stereophonic component may be eliminated below 250 cps. Experimental systems are described using two HF loudspeakers for the stereophonic component and a single LF loudspeaker. A resistive bridge circuit suitable for providing "sum" and "difference" signals is briefly described.

621.395.625.3 1857
The Method of Differential Measurement in Magnetic Sound Recording—K. Schönbrunn. (*Elektron. Rundschau*, vol. 13, pp. 80–84; March, 1959.) Methods of simplifying the alignment procedure of recording and reproducing heads and sound track are considered. These are based on the use of test tapes; design features are discussed.

621.395.625.3 1858
Time Errors in Magnetic Tape Recording—R. H. Prager. (*J. Audio Eng. Soc.*, vol. 7, pp. 81–88; April, 1959.) Autocorrelation techniques have been used to predict and measure time errors due to random noise and flutter.

681.84.087.7 1859
A Single-Element Stereophonic Cartridge—J. N. Wood. (*J. Audio Eng. Soc.*, vol. 7, pp. 92–96; April, 1959.) The principle of operation and characteristics of a ceramic element sensitive to displacement along two coordinates is described.

681.85:621.391.822 1860
Surface and Groove Noise in Disk Recording Media: Parts 1 and 2—D. H. Howling. (*J. Acoust. Soc. Am.*, vol. 31, pp. 1463–1472, 1626–1637; November/December, 1959.) A generalized noise equation involving the physical parameters of the recording medium and the playback stylus is derived. This shows reasonable agreement with measured playback noise spectra for different plastic surfaces. The theory of surface noise is extended to include modulation noise, and the evaluation of a theoretically realizable SNR. At 1000 lines per inch information density a SNR of 50 db at a linear velocity of 15 cm should be realized.

ANTENNAS AND TRANSMISSION LINES

621.372.2:621.372.54 1861
Ring-Type Transmission-Line Networks—G. J. Phillips. (*Electronic Technologist*, vol. 37, pp. 150–155; April, 1960.) Theory is developed for relating filter networks comprising closed rings of transmission line or waveguide to lumped-impedance networks.

621.372.22:621.372.51 1862
Contribution on Transformation with Inhomogeneous Transmission Lines—E. Baur. (*Arch. elekt. Übertragung*, vol. 13, pp. 114–120; March, 1959.) An approximation method of impedance transformation is considered based on that given by Willis and Sinha (1614 of 1956). Other methods are briefly reviewed.

621.372.8:621.372.413 1863
Some Properties of Travelling-Wave Resonance—J. R. G. Twisleton. (*Proc. IEE*, pt. B, vol. 107, pp. 108–118; March, 1960.) Resonance conditions in a waveguide ring circuit excited through a directional coupler are studied. The theory is confirmed by experiments with moving probes.

621.372.81.09 1864
Some Comments on the Classification of Waveguide Modes—A. E. Karbowiak. (*Proc. IEE*, pt. B, vol. 107, pp. 85–90, discussion pp. 91–93; March, 1960.) A distinction is drawn between the modes which apply to an idealized loss-free waveguide, and those which exist in physical systems. The expression of the physical properties of a real system in mathematical terms is discussed. Particular attention is given to the radiation field.

621.372.832.4 1865
Elliptic Waveguide Window—R. V. Harrowell. (*Electronic Technologist*, vol. 37, pp. 163–166; April, 1960.) An empirical approach to the problem of designing elliptic resonant windows for rectangular waveguide is described. Resonance frequencies are predicted with a maximum error of about 4 per cent.

621.372.832.43 1866
Long-Slot Directional Coupler for *H*-Mode Waves—H. Pascher. (*Arch. elekt. Übertragung*, vol. 13, pp. 76–82; February, 1959.) Theoretical consideration of long-slot directional couplers of any cross-sectional shape. Results of measurements on an experimental rectangular-circular coupler are in good agreement with theoretical values.

621.396.67:537.226 1867
Some Investigations on Dielectric Aerials: Part 4—B. R. Rao. (*J. Indian Inst. Sci.*, sec. B, vol. 41, pp. 23–29; October, 1959.) Variations of the propagation constant and radiation characteristic for the HE_{11} mode as a unction of the dielectric constant and diameter of a dielectric rod antenna are shown graphically. There is good agreement between theoretical and experimental values for the beamwidth of the major lobe and the positions of the maxima and minima of sidelobes. [Pt. 3, 2118 of 1959 (Rao *et al.*).]

621.396.67.095 1868
Analysis and Synthesis of Radiation Patterns from Circular Apertures—A. Ishimaru and G. Held. (*Canad. J. Phys.*, vol. 38, pp. 78–99; January, 1960.) The source distribution over a circular aperture is determined for a required radiation pattern. From this an improved design of narrow broadside beam is obtained. Expressions are also derived for the analysis and synthesis of radiation patterns from an annular aperture having a traveling-wave type source distribution. Narrow- and shaped-beam designs are discussed.

621.396.674–428 1869
The Unidirectional Equiangular Spiral Antenna—J. D. Dyson. (IRE TRANS. ON ANTENNAS AND PROPAGATION, vol. AP-7, pp. 329–334; October, 1959. Abstract, PROC. IRE, vol. 48, p. 269; February, 1960.)

621.396.674.3 1870
The Conductance of Dipoles of Arbitrary Size and Shape—K. Fränz and P. A. Mann. (IRE TRANS. ON ANTENNAS AND PROPAGATION, vol. AP-7, pp. 353–358; October, 1959. Abstract, PROC. IRE, vol. 48, p. 270; February, 1960.)

621.396.674.3:621.372.21 1871
A Dipole Antenna Coupled Electromagnetically to a Two-Wire Transmission Line—S. R. Seshadri and K. Iizuka. (IRE TRANS. ON ANTENNAS AND PROPAGATION, vol. AP-7, pp. 386–392; October, 1959. Abstract, PROC. IRE, vol. 48, p. 270; February, 1960.)

621.396.677.1:523.164 1872
Development of Highly Directive Aerials in Radio Astronomy—W. N. Christiansen. (*Proc. IRE* (*Australia*), vol. 20, pp. 519–528; September, 1959.) A number of fixed and steerable antennas and interferometer systems are briefly described.

621.396.677.3 1873
Successive Variational Approximations of Impedance Parameters in a Coupled Antenna System—M. K. Hu and Y. Y. Hu. (IRE TRANS. ON ANTENNAS AND PROPAGATION, vol. AP-7, pp. 373–379; October, 1959. Abstract, PROC. IRE, vol. 48, p. 270; February, 1960.)

621.396.677.3 1874
On the Use of Uniform Circular Arrays to Obtain Omnidirectional Patterns—Ta-Shing Chu. (IRE TRANS. ON ANTENNAS AND PROPAGATION, vol. AP-7, pp. 436–438; October, 1959.) A theoretical investigation of the relation between the number of radiating elements and the fluctuations in azimuthal pattern as the radius of curvature of the array varies.

621.396.677.3:621.396.965 1875
Scanning Antenna Arrays of Discrete Elements—E. A. Blasi and R. S. Elliott. (IRE TRANS. ON ANTENNAS AND PROPAGATION, vol. AP-7, pp. 435–436; October, 1959.) The advantage of increased aperture control obtained by using discrete elements may be entirely offset by the effect of variations in driving-point impedance.

621.396.677.32 1876
The Radiation Characteristics of a Sinuate Antenna—S. C. Loh. (*Canad. J. Phys.*, vol. 38, pp. 119–127; January, 1960.) Rigorous expressions for the radiation field of an antenna of sinusoidal shape are derived assuming a traveling-wave-type current distribution. The design of a practical end-fire antenna is described and test results are given.

621.396.677.5:621.318.134 1877
Radiation Properties of a Thin-Wire Loop Antenna Embedded in a Spherical Medium—O. R. Cruzan. (IRE TRANS. ON ANTENNAS AND PROPAGATION, vol. AP-7, pp. 345–352; October, 1959. Abstract, PROC. IRE, vol. 48, p. 270; February, 1960.)

621.396.677.71 1878
Closely-Spaced Transverse Slots in Rectangular Waveguide—R. F. Hyneman. (IRE Trans. on Antennas and Propagation, vol. AP-7, pp. 335–342; October, 1959. Abstract, Proc. IRE, vol. 48, p. 269; February, 1960.)

621.396.677.71:621.372.826 1879
The Launching of Surface Waves by a Parallel-Plate Waveguide—C. M. Angulo and W. S. C. Chang. (IRE Trans. on Antennas and Propagation, vol. AP-7, pp. 359–368; October, 1959. Abstract, Proc. IRE, vol. 48, p. 270; February, 1960.)

621.396.677.75 1880
Leaky-Wave Antennas: Part 1—Rectangular Waveguides—L. O. Goldstone and A. A. Oliner. (IRE Trans. on Antennas and Propagation, vol. AP-7, pp. 307–319; October, 1959. Abstract, Proc. IRE, vol. 48, p. 269; February, 1960.)

621.396.677.75 1881
A Flush-Mounted Leaky-Wave Antenna with Predictable Patterns—R. C. Honey. (IRE Trans. on Antennas and Propagation, vol. AP-7, pp. 320–329; October, 1959. Abstract, Proc. IRE, vol. 48, p. 269; February, 1960.)

621.396.677.75 1882
High-Dielectric Rod Antenna Arrays for U.H.F.—C. W. Morrow and J. L. Moore. (*Electronics*, vol. 33, pp. 60–62; February 5, 1960.) The performance of various ceramic rods as UHF antennas and array elements is discussed.

621.396.677.8:551.521.2 1883
The Thermal Radio Emission of the Ground and the Atmosphere at 1420 Mc/s and its Influence on Aerial Noise—Mezger. (See 2013 of 1960.)

621.396.677.81 1884
A New Method for Obtaining Maximum Gain from Yagi Antennas—H. W. Ehrenspeck and H. Poehler. (IRE Trans. on Antennas and Propagation, vol. AP-7, pp. 379–386; October, 1959. Abstract, Proc. IRE, vol. 48, p. 270; February, 1960.)

AUTOMATIC COMPUTERS

681.142 1885
Generators and Storage Devices for Functions of the Form $y=f(x)$ and $z=f(x, y)$—A. Haug. (*Nachrichtentech. Z.*, vol. 12, pp. 147–152, 192–200; March/April, 1959.) Comprehensive review, up to the end of 1957, of function devices for use in analog computers. Over 90 references.

681.142:537.312.62 1886
Relaxation Times in Lead-Film, Superconductive, Storage Elements—R. F. Broom and O. Simpson. (*Brit. J. Appl. Phys.*, vol. 11, pp. 78–80; February, 1960.) An experiment is described to measure the critical current of a Pb-film Crowe cell during the first microsecond after switching; different substrates are used.

681.142:621.318.424 1887
Ferroresonant Systems of Circuit Logic—J. G. Santesmases, M. Alique and J. L. Lloret. (*Proc. IEE*, pt. B, vol. 107, pp. 190–198; March, 1960.) *I/V* characteristics for coupled inductors are presented, and computer circuits based on these elements are described, with oscillograms illustrating practical operation.

681.142:621.372.44:537.227 1888
Ferroelectric Memory in the Parametron Circuits—K. Husimi and K. Kataoka. (*Rep. elect. Commun. Lab., Japan*, vol. 7, pp. 213–217; July, 1959.) Difficulties experienced in the use of ferroelectric materials in pulse-type storage systems are shown to be partly overcome in parametron circuits. The present limitation is due to unsuitable ferroelectric materials: $BaTiO_3$ shows a high fatigue phenomenon and triglycine sulphate a low switching velocity.

681.142:621.374.3 1889
Direct Digital Conversion of Pulse-Width Multiplexed Data—Chambers. (See 1912 of 1960.)

681.142:621.382.3 1890
An Analogue Electronic Multiplier using Transistors as Square-Wave Modulators—P. Gleghorn. (*Proc. IEE*, pt. B, vol. 107, pp. 94–99; March, 1960. Discussion, p. 100.) The multiplier is designed for high-speed operation at reasonable cost, and has an accuracy within ±2 per cent. Protection circuits for the transistors are provided.

681.142:621.385.3:621.317.3 1891
Indicator Triode for Direct Data Read-Out—H. Rodriques de Miranda and I. Rudich. (*Electronics*, vol. 33, pp. 52–54; February 5, 1960.) The triode (Amperex 6977) combines amplifier and indicator in one envelope. A triode-and-transistor bistable circuit is described with a required input trigger level of 30 μw, and also a shift register in which these circuits are cascaded.

681.142:621.385.832 1892
Character Generator for Digital Computers—E. D. Jones. (*Electronics*, vol. 33, pp. 117–118, 120; February 12, 1960.) A monoscope-tube apparatus is described which operates in the speed range of computers and storage devices, and provides read-out directly on a CRO or on paper.

CIRCUITS AND CIRCUIT ELEMENTS

621.3.011.3:621.375.13 1893
Simulation of Inductance by an Integrating Circuit—D. Midgley and J. M. Stewart. (*Elec. Rev. (London)*, vol. 166, pp. 281–285; February 12, 1960.) An operational amplifier used as integrator has an inductive input impedance when a resistive feedback loop is added between input and output. Theoretical and measured values of inductance, *Q*-factor and self-capacitance are given, and the possibility of raising *Q* by positive feedback is examined.

621.3.049.7 1894
Design Consideration for Integrated Electronic Devices—J. T. Wallmark. (Proc. IRE, vol. 48, pp. 293–300; March, 1960.) Discussion of fundamental factors affecting the design of integrated electronic devices [see e.g. 3213 of 1959 (Wallmark and Marcus)] with consideration of the effect of shrinkage and methods of overcoming it.

621.3.049.75:[621.396.62+621.397.62 1895
Printed Circuits in Radio and Television Receivers—W. Taeger. (*Frequenz*, vol. 13, pp. 57–59; February, 1959.) Review of printed-circuit design features in German receivers.

621.316.86:551.58 1896
The Climatic Fitness of Carbon-Film Resistors for Use in Electrical Communications and Measurements—H. J. Goldschmidt. (*Nachrichtentech. Z.*, vol. 9, pp. 125–128; March, 1959.) Equipment for climatic tests is described; effects observed in resistors subjected to such tests are discussed.

621.318.4:551.58 1897
Coils and Transformers Under Normal Room Climatic Conditions—H. Kreuzberger. (*Nachrichtentech. Z.*, vol. 9, pp. 111–116; March, 1959.) The influence of environmental conditions on the operating characteristics of wire-wound components with magnetic cores is investigated. Methods of reducing inductance and *Q*-factor changes caused by climatic effects are considered.

621.372:621.391.822:530.162 1898
On the Problem of Brownian Motion of Nonlinear Systems—C. T. J. Alkemade. (*Physica*, vol. 24, pp. 1029–1034; December, 1958.) A kinetic derivation is given of the spectral noise intensity in first-order approximation and for relatively high frequencies, for a nonlinear RC circuit consisting of an idealized diode tube in thermal equilibrium and a capacitor. The discrepancy with the results obtained by MacDonald (*Phys. Rev.*, vol. 108, pp. 541–545; November 1, 1957) and van Kampen (2651 of 1958) is discussed.

621.372.412:621.372.54 1899
Filter Crystals for the Frequency Range 7–30 Mc/s—R. Bechmann. (*Arch. elekt. Übertragung*, vol. 13, pp. 90–93; February, 1959.) The requirements for crystals used in filter networks are considered. For AT-cut crystals operating in the range 7–30 mc a triangular shape gives a satisfactory reduction of unwanted modes.

621.372.44 1900
The Stability of Negative-Resistance Two-Poles—L. Piglione. (*Alta Frequenza*, vol. 28, pp. 25–36; February, 1959.) Stability conditions are considered on the basis of the static characteristics of the two-pole.

621.372.5:621.376.3:621.3.018.78 1901
Fundamental and Harmonic Distortion of Waves Frequency-Modulated with a Single Tone—Medhurst. (See 2159 of 1960.)

621.372.54 1902
"Echostant" Matching, a New Method of Matching Image-Parameter Filters—T. Laurent. (*Arch. elekt. Übertragung*, vol. 13, pp. 132–140; March, 1959.) With the type of impedance matching described, better matching conditions are obtained and fewer reactance elements are required than with the use of double *m*-derived image impedances. The simulation of Tchebycheff-type insertion loss, and the compensation of losses by this method are also considered.

621.372.54 1903
Unified Formulae for Filters with Tchebycheff-Type Insertion Loss—G. Bosse and W. Nonnenmacher. (*Frequenz*, vol. 13, pp. 33–44; February, 1959.) Formulas are derived for the determination of zeros and poles of the transfer function based on the Tchebycheff polynomial or on Cauer parameters. The characteristics and treatment of elliptic functions are discussed, and curves are given for relating the insertion-loss requirements to the parameters of the transfer function.

621.372.543.2:621.372.412 1904
The Image-Parameter Theory as a Simple Aid to the Realization of Crystal Band-Pass Filters of Branch-Network Type—W. Poschenrieder. (*Nachrichtentech. Z.*, vol. 12, pp. 132–138; March, 1959.) Design formulas and curves are given for ladder-type networks with the crystal in the shunt arms. (See also 2365 of 1957.)

621.372.543.2:621.372.414 1905
A New Coaxial Resonator Filter—K. G. Dean and A. G. Hancock. (*Proc. IRE (Australia)*, vol. 20, pp. 622–631; October, 1959.) A band-pass filter with an *m*-derived type of characteristic is described, consisting of loop-coupled coaxial resonators in a re-entrant ar-

rangement. Performance may be described in terms of an equivalent lattice network. Good agreement is shown between the experimental and theoretical insertion-loss characteristics at 200 mc.

621.372.63:512.831 1906
Analysis of Active Networks by Admittance Matrices—M. N. Srikantaswamy and K. K. Nair. (*J. Inst. Telecommun. Engrs., India*, vol. 5, pp. 186–193; September, 1959.) Admittance matrices of valves and transistors are derived directly and from their indefinite admittance matrices. [See 642 of 1953 (Shekel).]

621.373.4.029.62:621.397.62 1907
Considerations on Oscillator Stability—G. Förster and W. Spyra. (*Elektron. Rundschau*, vol. 13, pp. 46–50; February, 1959.) Methods of reducing microphony effects and temperature dependence of oscillators in television tuners working at about 200 mc are considered.

621.373.421.13 1908
A Procedure for Tuning a Bridge-Stabilized Crystal Oscillator—M. Boella. (*Alta Frequenza*, vol. 28, pp. 3–9; February, 1959.) A Meacham bridge circuit is used in which the lamp is replaced by a thermistor, and a second thermistor is added to compensate for ambient temperature fluctuations. A sensitive method of tuning input and output transformers in this circuit is described.

621.373.421.13 1909
Theoretical Investigation of a Tuning Procedure for Bridge-Stabilized Crystal Oscillators—G. Gennaro and G. C. Patrucco. (*Alta Frequenza*, vol. 28, pp. 10–24; February, 1959.) The tuning method described in 1908 of 1960 is analyzed.

621.373.43 1910
Pulse Generator for the Production of a Spectrum with Constant Amplitude in the Frequency Range 0.1–30 Mc/s—G. Bittner. (*Elektrotech. Z.*, vol. 80, pp. 762–764; November 1, 1959.) The equipment described conforms to the German specifications for radio-interference measuring sets. Five different pulse repetition frequencies can be selected in the range 1–100 cps.

621.373.43:621.375.23 1911
On the Regenerative Pulse Generator—V. Met. (PROC. IRE, vol. 48, pp. 363–364; March, 1960.) An analysis of the mμsec pulse generator of Cutler (1293 of 1955) as a multimode oscillator.

621.374.3:681.142 1912
Direct Digital Conversion of Pulse-Width Multiplexed Data—F. T. Chambers. (*Electronic Equip. Engrg.*, vol. 7, pp. 55–58; November, 1959.) Pulse-width data are converted to a binary form by relating the incidence of leading and trailing pulse edges to the state of a counter driven by an asynchronous oscillator.

621.375.227.029.3:621.395.623.7 1913
A Further Method of Coupling Loudspeakers to a So-Called Transformerless Push-Pull Output Stage—W. Auer. (*Elektron. Rundschau*, vol. 13, p. 93; March, 1959.) In the single-ended push-pull circuit described, two pairs of series-connected 800-Ω loudspeakers or loudspeaker groups are connected across screen grid and anode of the output pentodes.

621.375.3 1914
Parallel-Connected Magnetic Amplifier—K. J. Srivastava. (*J. Inst. Telecommun. Engrs, India*, vol. 5, pp. 200–206; September, 1959.) "A mathematical analysis of parallel-connected magnetic amplifiers with an inductive and capacitive load is presented. The analysis is based on the representation of the normal magnetization curve of the core material by polynomials of third and fifth degree respectively."

621.375.3 1915
The Dynamic Hysteresis Loop as a Cause of the Free Demagnetization in Magnetic Amplifiers—R. Weppler. (*Elektrotech. Z.*, vol. 80, pp. 850–854; December 11, 1959.) Self-demagnetization effects are considered with reference to a hysteresis loop modified as a result of eddy-current losses.

621.375.4+621.376.23 1916
Design of Transistor I.F. Amplifier Detector Stages with Stabilized Band-Pass Characteristics—M. V. Joshi. (*J. Inst. Telecommun. Engrs, India*, vol. 5, pp. 223–229; September, 1959.) An extension of work described earlier. (See 2517 of 1959.)

621.375.422 1917
Junction-Transistor Circuits—J. J. Ward. (*Electronic Technologists*, vol. 37, pp. 109–115, 143–145; March/April, 1960.) A method is described for calculating current drift due to changes of junction temperature in a direct-coupled transistor circuit with series negative feedback. The design of drift-compensating circuits is considered and a brief comparison is made with parallel-feedback circuits.

621.375.9:[538.569.4+621.372.44 1918
The Noise and Gain Properties of Molecular and Parametric Amplifiers—E. D. Farmer. (*J. Electronics Control*, vol. 7, pp. 214–232; September, 1959.) Analysis is sufficiently general to include both types of amplifier as special cases. The concepts of negative noise temperature and negative quality factor are introduced by analyzing the energy exchange between a general sample of matter and a quantized cavity field. The three-level maser of Bloembergen and the ferrimagnetic amplifier of Suhl are discussed in some detail.

621.375.9:538.569.4 1919
The Present State of Solid-State Molecular Amplifiers—K. G. McKay. (*Nachrichtentech. Z.*, vol. 12, pp. 61–67; February, 1959.) The principles and properties of solid-state masers with two and three energy levels are discussed. Recent developments and future applications are considered.

621.375.9:538.569.4 1920
Operating Characteristics of a Molecular-Beam Maser—H. G. Venkates and M. W. P. Strandberg. (*J. Appl. Phys.*, vol. 31, pp. 396–399; February, 1960.) "General expressions for the emitted power and the frequency pulling in an ammonia maser have been deduced. The operating characteristics of the maser have been deduced by introducing a mean-square time of flight of molecules in the cavity."

621.375.9:538.569.4 1921
Ammonia Maser Oscillator—A. M. J. Mitchell, K. G. Roots and G. Phillips. (*Electronic Technologists*, vol. 37, pp. 136–143; April, 1960.) The principle of operation and constructional details of an ammonia maser are described. Four parameters affecting the frequency of operation have been investigated: ammonia flow, separator voltage, magnetic fields and cavity tuning. The difference frequency between two masers operating at 23,870 mc was found to be stable to within 12 cps over 4 hours with higher stability over shorter periods.

621.375.9:538.569.4:621.391.822 1922
Noise Temperature Measurement on a Travelling-Wave Maser Preamplifier—R. W. DeGrasse and H. E. D. Scovil. (*J. Appl. Phys.*, vol. 31, pp. 443–444; February, 1960.) The measured noise temperature was 10.7 ± 2.3°K, but it is estimated that a noise temperature of 9 ± 1°K is produced by the input cable losses.

621.375.9:538.569.4.029.65 1923
Pulsed-Field Millimetre-Wave Maser—L. R. Momo, R. A. Myers and S. Foner. (*J. Appl. Phys.*, vol. 31, p. 443; February, 1960.) The frequency range of the pulsed-field ruby maser [3623 of 1959 (Foner *et al.*)] has been extended to 70 kmc, and the peak output power has been increased to several milliwatts.

621.375.9:538.569.4.029.66 1924
Submillimetre-Wave Maser—S. M. Bergmann. (*J. Appl. Phys.*, vol. 31, pp. 275–276; February, 1960.) A proposal is made for operation of a maser at a frequency of 5.18×10^{11} cps, corresponding to the $3^2P_{3/2}$–$3^2P_{1/2}$ transition in Na, using a dielectric tube resonator as a cavity. Coupling schemes are discussed.

621.375.9:621.372.44 1925
Some Possible Arrangements of Parametric Amplifiers Employing Lower-Frequency Pumping—N. B. Chakrabarti and K. D. Dikshit. (*Indian J. Phys.*, vol. 33, pp. 431–451; October, 1959.) Two arrangements are analyzed in detail: 1) combination of a mixer and an amplifier using one pump and two idlers; 2) combination of a mixer and an amplifier using two pumps and two idlers.

621.375.9:621.372.44:621.372.2 1926
Theory of the Travelling-Wave Parametric Amplifier—A. L. Cullen. (*Proc. IEE*, pt. B, vol. 107, pp. 101–107; March, 1960. Discussion, pp. 123–126.) The theory is based on a nonlinear distributed capacitance excited by a traveling wave. Losses in the capacitance and the effects of saturation on large signals are considered. (See 2353 of 1958.)

621.375.9:621.372.44:621.372.2 1927
Saturation Effects in a Travelling-Wave Parametric Amplifier—A. Jurkus and P. N. Robson. (*Proc. IEE*, pt. B, vol. 107, pp. 119–122; March, 1960. Discussion, pp. 123–126.) Equations of voltage distribution are solved in terms of elliptic functions, and an expression for the maximum power gain is derived. The positions of gain maxima are calculated.

621.375.9:621.372.44:621.385.6 1928
Theory of Fast-Wave Parametric Amplification—Johnson. (See 2203 of 1960.)

621.375.9:621.372.44:621.385.6 1929
A Microwave Adler Tube—Bridges and Ashkin. (See 2204 of 1960.)

621.376.2:621.397.132 1930
Double Push-Pull Modulator with Valves—Beckmann. (See 2170 of 1960.)

621.376.223 1931
Rectifier Modulators—D. P. Howson. (*Electronic Technologist*, vol. 37, pp. 158–162; April, 1960.) A method for reducing the complexity of equations for the series rectifier modulator without undue loss of accuracy is postulated. The simplified equations are shown to be soluble by successive approximations. The process is applied to a modulator with 1) constant-resistance termination, 2) purely capacitive termination.

621.376.32:621.373 1932
The Frequency Modulation of Tuned-Circuit and Relaxation Oscillators—E. Kettel. (*Arch. elekt. Übertragung*, vol. 13, pp. 95–100; March, 1959.) The problem of distortionless frequency modulation of oscillators for any modulating frequency is considered. The conditions for an ideal nonlinear frequency modulator are formulated and applied to the con-

stant-amplitude and relaxation oscillator. (See also 784 of 1960.)

GENERAL PHYSICS

530.14:538.3 1933
Classical Electrodynamic Equations of Motion with Radiation Reaction—G. N. Plass. (*Phys. Rev. Lett.*, vol. 4, pp. 248–249; March 1, 1960.) A physically reasonable solution for the equations exists for any force field that satisfies certain conditions.

535.215:537.531 1934
Sauter Theory of the Photoelectric Effect—U. Fano, K. W. McVoy and J. R. Albers. (*Phys. Rev.*, vol. 116, pp. 1147–1156; December 1, 1959.) The photoelectric-effect cross section for arbitrary X-ray polarization and arbitrary initial and final orientations of electron spin is expressed in the form of a transition matrix. Approximation shows its relation to bremsstrahlung theory.

535.215:537.531 1935
High-Frequency Limit of Bremsstrahlung in the Sauter Approximation—U. Fano. (*Phys. Rev.*, vol. 116, pp. 1156–1158; December 1, 1959.) The photoelectric process is shown, to a first order in $Z/137$, to be inverse to the process of X-ray emission at the high-frequency limit of the spectrum.

535.215:537.531 1936
Interference of Orbital and Spin Currents in Bremsstrahlung and Photoelectric Effect—U. Fano, K. W. McVoy and J. R. Albers. (*Phys. Rev.*, vol. 116, pp. 1159–1167; December 1, 1959.) Interpretation of angular distribution, X-ray polarization, and spin orientation in terms of interference between orbital and spin currents.

535.215:537.531 1937
Bremsstrahlung and the Photoelectric Effect as Inverse Processes—K. W. McVoy and U. Fano. (*Phys. Rev.*, vol. 116, pp. 1168–1184; December 1, 1959.) A detailed theoretical examination of the inverse processes of the photoelectric effect and of bremsstrahlung at the high-frequency limit of the spectrum.

537.228:538.63 1938
The Motion of an Electron in a Crystal Located in an External Field—G. E. Zil'berman. (*Zh. Eksp. Teor. Fiz.*, vol. 36, pp. 1465–1471; May, 1959.) Extension of an earlier analysis (3444 of 1957) to the case of uniform magnetic and arbitrary electric fields.

537.311.1 1939
Exclusion Factors in Transport Theory—E. I. Blount. (*Phys. Rev.*, vol. 116, pp. 1365–1368; December 15, 1959.)

537.311.31:535.39 1940
The Problem of the Optical Constants of Conductors—V. P. Silin. (*Zh. Eksp. Teor. Fiz.*, vol. 36, pp. 1443–1450; May, 1959.) A mathematical analysis showing that the optical constants of an isotropic conductor comprise, in addition to the index of refraction and of the absorption coefficient, two real quantities corresponding to a complex boundary impedance. The real part of this boundary impedance represents the surface losses in the conductor, and the imaginary part of the dielectric constant, the volume losses.

537.312.62 1941
High-Current Superconductivity—R. H. Parmenter. (*Phys. Rev.*, vol. 116, pp. 1390–1399; December 15, 1959.) "The Bardeen, Cooper and Schrieffer theory of superconductivity (1386 of 1958) is extended to the case of high current densities by explicitly including in the phonon-induced electron-electron attraction the modification of the phonon spectrum in a moving coordinate system. This modification results from the Doppler effect."

537.523.3 1942
Investigation of the High-Frequency Spectrum of Periodic Discharges—W. Heintz. (*Z. angew. Phys.*, vol. 11, pp. 51–57; February, 1959.) The frequency spectrum of HV corona pulse discharges is investigated.

537.525 1943
Electric Field in a Microwave Plasma as a Function of Time—V. E. Mitsuk and M. D. Koz'minykh. (*Zh. Eksp. Teor. Fiz.*, vol. 36, pp. 1603–1604; May, 1959.) Investigation of the transient state in a pulsed discharge at 9400 mc in deuterium at pressures of 4 and 23 mm Hg. Field strength was determined by an optical method by noting the Stark effect on the Balmer lines in the external oscillating field.

537.525:538.56 1944
The Plasma Capacitor—W. C. Schumann. (*Z. Naturforsch.*, vol. 13a, pp. 888–895; October, 1958.) The measurements of Dattner on a plasma resonator (418 of 1958) are discussed.

537.525:538.69 1945
Electron Temperature in Electrodeless Discharge Subjected to a Transverse Magnetic Field—S. N. Goswami. (*Indian J. Phys.*, vol. 33, pp. 452–455; October, 1959.)

537.525:538.69 1946
Ion Energies in a Cold-Cathode Discharge in a Magnetic Field—J. Backus and N. E. Huston. (*J. Appl. Phys.*, vol. 31, pp. 400–403; February, 1960.) The current flow after a discharge revealed an approximately Maxwellian distribution of velocities at the cathodes with a temperature of about 0.5 ev. This gives an ion density in the discharge of about 20 per cent.

537.525:546.212–13 1947
Microwave Study of Afterglow Discharge in Water Vapour—S. Takeda and A. A. Dougal. (*J. Appl. Phys.*, vol. 31, pp. 412–416; February, 1960.) Electron loss processes prevailing in decaying water-vapour plasmas are interpreted.

537.525:621.391.822.08 1948
Possibility of Determining the Potential Distribution of a Plasma from the Characteristics of the Noise Generated in a Gaseous Discharge—A. A. Zaĭtsev, M. Ya. Vasil'eva and V. N. Mnev. (*Zh. Eksp. Teor. Fiz.*, vol. 36, pp. 1589–1591; May, 1959.) A note of noise measurements made on oxide-cathode discharges in krypton at pressures between 0.01 and 1 mm Hg and at discharge currents 6–140 ma. The variation of potential along the axis of the discharge is in close agreement with results obtained by conventional probe methods.

537.56 1949
Scattering Potential in Fully Ionized Gases—O. Theimer and R. Gentry. (*Phys. Rev.*, vol. 116, pp. 787–792; November 15, 1959.) A discussion of recent methods for calculating 1) the scattering potential, and 2) the probability, $W(E)dE$, that a test particle experiences an electrical field of magnitude $E \pm \frac{1}{2}dE$.

537.56 1950
The Stability of Plasma Configurations of Cylindrical Symmetry with Volume Currents—K. Hain and R. Lüst. (*Z. Naturforsch.*, vol. 13a, pp. 936–940; November, 1958.) The stability is investigated by the method of small perturbations.

537.56:537.533 1951
Energy Losses of Charged Particles due to Excitation of Plasma Oscillations—Yu. L. Klimontovich. (*Zh. Eksp. Teor. Fiz.*, vol. 36, pp. 1405–1418; May, 1959.) A kinetic equation is derived describing the interaction between beam elements and plasma under equilibrium conditions. For nonequilibrium conditions a nonlinear theory of plasma oscillations excited by an electron beam is developed and results are applied to account for the rapid energy transfer from the beam.

537.56:537.533:621.385.6 1952
Collision Damping of Space-Charge Waves in a Plasma—S. V. Yadavalli. (*J. Electronics Control*, vol. 7, pp. 261–267; September, 1959.) The general determinantal equation applicable to the propagation of space-charge waves including the effect of collisions (in the absence of a velocity distribution) in a plasma is derived. Suggestions arising from the solutions are discussed.

537.56:538.56 1953
Absorption and Reflect on Spectrum of a Plasma—W. D. Hershberger. (*J. Appl. Phys.*, vol. 31, pp. 417–422; February, 1960.) A re-evaluation of the experimental results of Rommel (1618 of 1951) and Dattner (418 of 1958) and a development of theory to account for additional resonance peaks.

537.56:538.56 1954
Penetration of an Electromagnetic Field into a Plasma—K. N. Stepanov. (*Zh. Eksp. Teor. Fiz.*, vol. 36, pp. 1457–1460; May, 1959.) Calculation of the penetration depth for a semi-infinite plasma located in a magnetic field perpendicular to the plasma boundary.

537.56:538.561 1955
Incoherent Microwave Radiation from Plasmas—G. Bekefi, J. L. Hirshfield and S. C. Brown. (*Phys. Rev.*, vol. 116, pp. 1051–1056; December 1, 1959.) A study of incoherent radiation from an isotropic quiescent plasma of a low degree of ionization. The three cases of transparent, semi-opaque, and opaque plasmas are considered theoretically. Good experimental agreement is obtained at 3 kmc using dc glow discharges in helium and hydrogen.

537.56:538.566 1956
Microwave Determination of Plasma Density Profiles—C. B. Wharton and D. M. Slager. (*J. Appl. Phys.*, vol. 31, pp. 428–430; February, 1960.) "A method for the rapid determination of the average electron density and of the spatial electron density distribution in plasmas is presented. The technique employed permits time-resolved measurements over a wide range of electron densities, introducing little or no perturbation into the gaseous discharge."

537.56:538.6 1957
Structure of a Magnetohydrodynamic Shock Wave in a Partially Ionized Gas—S. B. Pikel'ner. (*Zh. Eksp. Teor. Fiz.*, vol. 36, pp. 1536–1541; May, 1959.) An approximate solution of the equation for the transition zone is given for some special cases.

537.56:538.6 1958
The Structure of Hydromagnetic Shock Waves: Part 1—Nonlinear Hydromagnetic Waves in a Cold Plasma—L. Davis, R. Lüst and A. Schlüter. (*Z. Naturforsch.*, vol. 13a, pp. 916–936; November, 1958. In English.) Waves in a quasi-neutral gas consisting of ions and electrons are investigated neglecting collisions but not the inertial effects of the electric current. The relation of these waves to hydromagnetic shock waves in low-density plasmas is considered.

537.56:551.510.536:538.566 1959
Electromagnetic Properties of High-Temperature Air—M. P. Bachynski, T. W. John-

ston and I. P. Shkarofsky. (Proc. IRE, vol. 48, pp. 347–356; March, 1960.) If the parameters are normalized, the em characteristics of plasmas can be represented in a universal form in the complex dielectric-coefficient plane or the complex propagation-constant plane.

538.221:538.569.4 **1960**
Fine Structure in the Decline of the Ferromagnetic Resonance Absorption with Increasing Power Level—E. Schlömann. (*Phys. Rev.*, vol. 116, pp. 828–837; November 15, 1959.) A theory of ferromagnetic resonance at high signal powers is developed which accounts quantitatively for observed effects. [See 4139 of 1959 (Schlömann and Green).]

538.222:538.566.029.64:538.612 **1961**
On the Phenomenological Theory of the Voigt Effect in Paramagnetics—L. M. Tsirul'nikova. (*Zh. Eksp. Teor. Fiz.*, vol. 36, pp. 1428–1434; May, 1959.) A macroscopic calculation of the Voigt effect in paramagnetic media at centimeter wavelengths.

538.222:538.569.4 **1962**
Influence of Exchange Interaction on Paramagnetic Relaxation Times—J. P. Goldsborough, M. Mandel and G. E. Pake. (*Phys. Rev. Lett.*, vol. 4, pp. 13–15; January 1, 1960.)

538.222:538.569.4:621.375.9 **1963**
Relaxation Effects in a Maser Material, $K_3(CoCr)(CN)_6$—S. Shapiro and N. Bloembergen. (*Phys. Rev.*, vol. 116, pp. 1453–1458; December 15, 1959.) The rate equations for the occupation of spin levels are augmented to include cross-relaxation processes, which can impair maser action.

538.561:537.533 **1964**
Radiation Produced by an Electron Beam Passing Through a Dielectric Medium—J. Neufeld. (*Phys. Rev.*, vol. 116, pp. 785–787; November 15, 1959.) An electron beam passing through a dielectric medium may produce an instability that is associated with the growth of longitudinal waves having a velocity close to the velocity of the beam. If homogeneities are present these longitudinal waves may be converted into transverse waves and radiated into space. Thus there is a possibility of a luminous effect at "Bohr frequencies" that differ from the Vavilov-Cherenkov frequencies.

538.566 **1965**
On the Doppler Effect in an Anisotropic and Gyrotropic Medium—K. A. Barsukov. (*Zh. Eksp. Teor. Fiz.*, vol. 36, pp. 1485–1491; May, 1959.) Investigation of the Doppler effect during the motion of an oscillator along the axis of a gyrotropic anisotropic crystal. Expressions are derived for the radiation energy applicable to the Cherenkov radiation field of an electron and of a dipole.

538.566 **1966**
The Increase in Frequency Bandwidth of Thin "λ/4-Layer" Absorbers for Centimetre Electromagnetic Waves—R. Pottel. (*Z. angew. Phys.*, vol. 11, pp. 46–51; February, 1959.) A type of absorber is investigated which can be made thinner than 1/30 of the wavelength in free-space. If the dielectric constant, or permeability, of the lossy material is independent of frequency the effective bandwidth of the absorber decreases with absorber thickness. To obtain a thin absorber covering a frequency range of ratio $\geq 1:2$, dielectric constant or permeability would have to follow a frequency law of the type given, but no practical material is known which meets these requirements.

538.566:535.42 **1967**
A Note on Diffraction by an Infinite Slit—R. F. Millar. (*Canad. J. Phys.*, vol. 38, pp. 38–47; January, 1960.) Previous results for plane waves at longer wavelengths are extended to obtain transmission coefficients at oblique angles of incidence. Cylindrical waves are considered briefly.

538.566:535.42 **1968**
Diffraction by a Spheroid—B. R. Levy and J. B. Keller. (*Canad. J. Phys.*, vol. 38, pp. 128–144; January, 1960.) The diffracted field is determined by two methods for wavelengths small compared to the spheroid. Results are applied to evaluate the back-scattered fields.

538.566.2.029.6:537.226 **1969**
Investigations on Artificial Dielectrics at Microwave Frequencies: Part 2—B. V. Rao. (*J. Indian Inst. Sci.*, sec. B, vol. 41, pp. 36–45; October, 1959.) The expression for the phase change in transmission of an em wave incident on a parallel-plate-type artificial dielectric, as a function of the plate spacing, has been verified experimentally. [See pt. 1, 1385 of 1956 (Chatterjee and Rao).]

538.567.4:534.13–14 **1970**
On the Reflection of Electromagnetic Waves from a Medium Excited by Acoustic Waves—H. J. Schmitt and D. L. Sengupta. (*J. Appl. Phys.*, vol. 31, pp. 439–440; February, 1960.) Theory is developed for the variation of density and temperature (in a liquid) caused by an acoustic wave generating regions of maximum and minimum dielectric constant. Modulation of a 3.2-cm wave reflected from an acoustically disturbed water surface is observed.

538.569:539.12 **1971**
Confinement of Charged Particles by Plane Electromagnetic Waves in Free Space—C. M. Haaland. (*Phys. Rev. Lett.*, vol. 4, pp. 111–112; February 1, 1960.) Confining forces associated with nonuniform fields are shown to occur when two plane waves intersect in free space.

538.569.4:621.373.421.1 **1972**
Nuclear-Resonance-Absorption Circuit—F. N. H. Robinson. (*J. Sci. Instr.*, vol. 36, pp. 481–487; December, 1959.) The principles of detecting nuclear resonance absorption in a specimen surrounded by a coil forming part of a tuned circuit are discussed in detail, and various methods are compared. A new circuit is described and two practical designs are given for operation 1) between 20 and 60 mc, and 2) between 200 kc and 20 mc.

539.2 **1973**
Correlation Effects in Impurity Diffusion—J. R. Manning. (*Phys. Rev.*, vol. 116, pp. 819–827; November 15, 1959.)

539.2 **1974**
The Shielding of a Fixed Charge in a High-Density Electron Gas—J. S. Langer and S. H. Vosko. (*J. Phys. Chem. Solids*, vol. 12, pp. 196–205; January, 1960.) A closed expression for the density of displaced electrons is derived by a systematic application of the many-body perturbation theory.

539.2:538.566:538.6 **1975**
Magnetoplasma Reflection in Solids—B. Lax and G. B. Wright. (*Phys. Rev. Lett.*, vol. 4, pp. 16–18; January 1, 1960.) The splitting of the reflection edge at the plasma frequency, in the presence of a magnetic field, has been used to measure the effective mass of the electrons.

GEOPHYSICAL AND EXTRATERRESTRIAL PHENOMENA

523.164:621.396.677.1 **1976**
Development of Highly Directive Aerials in Radio Astronomy—Christiansen. (See 1872 of 1960.)

523.165 **1977**
On the Long-Term Variation in the Cosmic Radiation—J. A. Lockwood. (*J. Geophys. Res.*, vol. 65, pp. 19–25; January, 1960.) The variation seems to occur in a series of sudden decreases rather than gradually. A possible solar modulating mechanism is discussed.

523.165 **1978**
Decrease of Cosmic-Ray Intensity on February 11, 1958—J. A. Lockwood. (*J. Geophys. Res.*, vol. 65, pp. 27–37; January, 1960.) The sudden decrease followed by a temporary recovery is attributed to disordering of the outer geomagnetic field by the increase of the solar wind.

523.165:550.38 **1979**
Geomagnetic Effects on Cosmic Radiation for Observation Points Above the Earth—J. E. Kasper. (*J. Geophys. Res.*, vol. 65, pp. 39–53; January, 1960.) Störmer and Lemaitre-Vallarta theories of the principal shadow cone have been adapted for observational points above the earth's surface.

523.3 **1980**
Question of the Existence of a Lunar Magnetic Field—M. Neugebauer. (*Phys. Rev. Lett.*, vol. 4, pp. 6–8; January 1, 1960.) A lunar magnetic field would be distorted by solar corpuscular radiation. On the sunlit side it would not extend to high altitudes, and would be difficult to detect.

523.72:523.165 **1981**
Observations on the General Solar Plasma Instability—L. Reiffel. (*Phys. Rev. Lett.*, vol. 4, pp. 136–138; February 1, 1960.) Suggestions are made for satellite experiments during occasional very intense solar streams to determine the nature and geometry of the plasma barrier.

523.745:550.385.4 **1982**
A Relationship Between the Life of *M*-Regions and the Rate of Change of Solar Activity—D. W. G. Chappell. (*J. Atmos. Terr. Phys.*, vol. 17, pp. 315–319; February, 1960.) An inverse relation is established between the rate of decay of the cycle of solar activity and the lifetime of *M*-regions as manifested by the persistence of the recurrence of magnetic storms.

523.75:523.165 **1983**
Small Effects of Solar Flares and the Energy Spectrum of the Primary Variation of Cosmic Rays—E. V. Kolomeets. (*Zh. Eksp. Teor. Fiz.*, vol. 36, pp. 1351–1353; May, 1959.) Investigation of the relation between small solar flares and the intensity of cosmic-ray neutrons during 1957 at four stations at different latitudes.

523.75:550.389.2 **1984**
Survey of Number of Solar Flares Observed During the International Geophysical Year—H. W. Dodson and E. R. Hedeman. (*J. Geophys. Res.*, vol. 65, pp. 123–131; January, 1960.) The IGY flare data show a very high rate of occurrence between 0500 and 1600 U.T. Many of these flares would probably have been classified as subflares by photographic observers.

550.38:523.165 **1985**
Motion of Geomagnetic Field Lines—C. J. Loughnan. (*Nature*, vol. 186, pp. 33–34; April 2, 1960.) Motion of the impact regions of the upper atmosphere can only be very slow since the high conductivity of the earth's interior limits the field distortion: this is at variance with the hypothesis of Rees and Reid (4063 of 1959).

550.38:551.507.362.2 1986

Current Systems in the Vestigial Geomagnetic Field: Explorer VI—C. P. Sonett, E. J. Smith, D. L. Judge, and P. J. Coleman, Jr. (*Phys. Rev. Lett.*, vol. 4, pp. 161–163; February 15, 1960.) The results indicate the existence of a temporally and spatially variable current system at 5–7 earth radii.

550.38:551.510.535 1987

Some Characteristics of the Upper-Air Magnetic Field and Ionospheric Currents—A. J. Smuda. (*J. Geophys. Res.*, vol. 65, pp. 69–84; January, 1960.) Magnetic scalar intensity from rocket data is compared with that derived by extrapolation from the surface vector field. The agreement is good for equatorial regions but is only fair for White Sands, New Mexico. The data also show that the equatorial current density has a maximum of about 21 A/km² while that of the electrojet is about 130 A/km².

550.38:551.510.536 1988

A Radial Rocket Survey of the Distant Geomagnetic Field—C. P. Sonett, D. L. Judge, A. R. Sims and J. M. Kelso. (*J. Geophys. Res.*, vol. 65, pp. 55–68; January, 1960.) Analysis of the earth's field to 14.8 earth radii shows that an inverse cube field exists to 13.6 radii, beyond which the field rapidly decreases. Analysis of the field fluctuations in this latter region indicate a particle density of 100 cm⁻³.

550.385.3 1989

Fluctuations in the Geomagnetic Horizontal Field Near the Magnetic Equator—A. Onwumechilli. (*J. Atmos. Terr. Phys.*, vol. 17, pp. 286–294; February, 1960.) Earlier work (861 of 1960) is continued to cover the diurnal characteristics of fluctuations and to examine how they compare with fluctuations due to solar flare effects.

550.385.37 1990

Occurrence Frequency of Geomagnetic Micropulsations, *Pc*—J. A. Jacobs and K. Sinno. (*J. Geophys. Res.*, vol. 65, pp. 107–113; January, 1960.) Analysis of the diurnal occurrence frequency shows that 1) the frequency increases and time of maximum occurrence gets earlier as the auroral zones are approached; 2) the diurnal distribution of frequency depends on universal time as well as local time.

550.385.37 1991

A Giant Geomagnetic Pulsation—J. Veldkamp. (*J. Atmos. Terr. Phys.*, vol. 17, pp. 320–324; February, 1960.) The characteristics of the event of July 17, 1958 are studied from magnetograms recorded at a large number of European observatories. Observed effects are compared with existing theories of the cause of giant pulsations.

550.385.37 1992

On the Theory of Giant Pulsations—J. G. J. Scholte. (*J. Atmos. Terr. Phys.*, vol. 17, pp. 325–336; February, 1960.) A mathematical analysis of the propagation of a magneto-ionic disturbance originating in the exosphere shows that only the rotational movement, perpendicular to the geomagnetic field, is propagated without great loss of energy. The observed characteristics of giant pulsations suggest that they are mainly caused by this rotational component of the primary disturbance.

550.385.4 1993

Geomagnetic Storm Theory—J. H. Piddington. (*J. Geophys. Res.*, vol. 65, pp. 93–106; January, 1960.) The penetration of solar ions into the geomagnetic field during the main phase of storms is discussed. A model is suggested, the principal feature of which is a "magnetic tail" extending from the earth on the dark side. This model would help to explain the gegenschein electrons with auroral energies, the position of the Van Allen zones and diurnal cosmic-ray variations.

550.385.4 1994

The Simultaneity of Sudden Commencements of Magnetic Storms—V. L. Williams. (*J. Geophys. Res.*, vol. 65, pp. 85–92; January, 1960.) Geographic analysis of magnetograms shows that 1) sudden commencements always occur first in high or middle latitudes, 2) the average values of their apparent propagation velocity around the magnetic equator lie between 1145 and 2835 km.

551.507.362.2 1995

Charge and Magnetic-Field Interaction with Satellites—D. B. Beard and F. S. Johnson. (*J. Geophys. Res.*, vol. 65, pp. 1–7; January, 1960.) When satellite motion is parallel to a magnetic field the satellite will become negatively charged to a potential of about 0.25 v. For motion perpendicular to the field this will be modified by an induced emf which may be as large as 0.2 v per meter with satellite length. The drag caused by induced currents is found to be negligible except for very large satellites.

551.507.362.2 1996

Satellite Orbits in an Oblate Atmosphere—D. G. Parkyn. (*J. Geophys. Res.*, vol. 65, pp. 9–17; January, 1960.)

551.507.362.2 1997

Variation of Upper-Atmosphere Density with Latitude and Season: Further Evidence from Satellite Orbits—D. G. King-Hele and D. M. C. Walker. (*Nature*, vol. 185, pp. 727–729; March 12, 1960.) [See also 485 of 1960 (King-Hele)].

551.510.535 1998

Atmospheric Tides and Ionospheric Electrodynamics—M. L. White. (*J. Geophys. Res.*, vol. 65, pp. 153–171; January, 1960.) A semi-empiricial treatment of winds in the height range 0–105 km showing their dependence on latitude and height. The extension of modern tidal theory into the dynamo region is discussed.

551.510.535 1999

Electron Density of the Ionosphere Utilizing High-Altitude Rockets—O. C. Haycock, J. I. Swigart and D. J. Baker. (IRE TRANS. ON ANTENNAS AND PROPAGATION, vol. AP-7, pp. 414–418; October, 1959. Abstract, PROC. IRE, vol. 48, pp. 270–271; February, 1960.)

551.510.535 2000

The Comparison Method of the Station Lindau/Harz for the Determination of the True Distribution of Electron Density in the Ionosphere—W. Becker. (*Arch. elekt. Übertragung*, vol. 13, pp. 49–57; February, 1959.) An extension of the method described earlier (115 of 1957) is discussed. The advantages of using the extraordinary-ray traces for comparisons are shown. Details are given of the method of calculation and the equipment used for analysis; the tables included are calculated for a geomagnetic inclination of 67°6′.

551.510.535 2001

Group Refractive Index of the Ionosphere at Low Frequency—Y. S. N. Murty and S. R. Khastgir. (*J. Atmos. Terr. Phys.*, vol. 17, pp. 309–314; February, 1960.) A general expression for the group refractive index at LF is obtained which, for the limiting case when electron collisional frequency is small, is identical with an approximate expression due to Gibbons and Rao (1415 of 1958).

551.510.535 2002

A Theoretical Current-Density Ansatz for the Quiet-Day Solar Semidiurnal Tidal Mode of Oscillation of the Ionosphere—S. Shanack. (*J. Atmos. Terr. Phys.*, vol. 17, pp. 337–344; February, 1960.) Theoretical expressions, which embody the generalized atmospheric dynamo mechanism of the origin of upper atmospheric current systems, are derived for the current density vector. By numerical integration methods, approximate expressions may be obtained for the current density over an ionized shell concentric with the earth.

551.510.535 2003

Use of Green's Function in the Solution of Ionospheric Diffusion Problems—J. E. C. Gliddon. (*Quart. J. Mech. Appl. Math.*, vol. 12, pp. 347–353; August, 1959.) The mathematical analogy between diffusion of ions in the ionosphere and heat conduction in a rod (see 2004 of 1960) is used to solve the problem of diffusion with an attachment-type law of electron loss.

551.510.535 2004

Diffusion of Ions in a Static F_2 Region—J. E. C. Gliddon. (*Quart. J. Mech. Appl. Math.*, vol. 12, pp. 340–346; August, 1959.) "The vertical diffusion of ions under the action of gravity and a rate of electron loss which decreases exponentially with height is shown to correspond to heat conduction in a rod with a heat-source distribution and radiation from the lateral surface. Electron density is determined as a time-periodic function of the height and is expressed in the form of an infinite series."

551.510.535 2005

A Model of the F Region Above $h_{max}F_2$—J. W. Wright. (*J Geophys. Res.*, vol. 65, pp. 185–191; January, 1960.) The electron density distribution above the F_2-layer maximum is approximated using a Chapman distribution. The scale height has been chosen to agree with the sparse data available for this region. This approximation has been used to extrapolate vertical-incidence ionospheric data for a chain of observatories along the 75°W meridian.

551.510.535 2006

Correlation of Spread-F Activity with F-Region Height Changes—M. S. V. G. Rao, B. R. Rao and P. R. R. Pant. (*J. Atmos. Terr. Phys.*, vol. 17, pp. 345–347; February, 1960.) The analysis employs a new index of spread-F activity suited to equatorial phenomena.

551.510.535:523.75 2007

Ionospheric Effects Associated with the Solar Flare of July 10, 1959—V. A. W. Harrison. (*Nature*, vol. 186, pp. 228–229; April 16, 1960.) Report of observations made in Singapore of ionospheric effects associated with the flare which commenced at 0210 U.T. A positive pulse in the measured values of f_0F_2 similar to that studied by Minnis and Bazzard (2733 of 1958) was observed immediately after the period of high absorption.

551.510.535:550.383 2008

Variation of Electron Density in the Ionosphere with Magnetic Dip—S. Croom, A. Robbins and J. O. Thomas. (*Nature*, vol. 185, pp. 902–903; March 26, 1960.) Extension of work described earlier (882 of 1960) to include the northern winter solstice. Results show a sharp maximum in the average electron density N_h and peak electron density N_mF_2 centered on a dip angle of 70°N.

551.510.535:551.507.362.2 2009

The Electron Content and Distribution in the Ionosphere—T. G. Hame and W. D. Stuart. (PROC. IRE, vol. 48, pp. 364–365; March, 1960.) Electron content and distribution are determined from an analysis of measurements of the Faraday rotation rate on transmissions received near Columbus, Ohio, November, 1958 to May, 1959, from satellite 1958 δ2.

551.510.535:621.391.812.63 2010
Some Observations of Ionospheric Faraday Rotation on 106.1 Mc/s—R. A. Hill and R. B. Dyce. (*J. Geophys. Res.*, vol. 65, pp. 173–176; January, 1960.) A comparison with vertical-incidence ionosonde data suggests that the ratio of the electron contents above and below the level of maximum ionization of the *F* region does not remain constant between sunrise and noon.

551.510.535:621.391.812.63 2011
Measurement of the Ionospheric Absorption on 2.5 Mc/s at Ahmedabad—J. S. Shirke. (*J. Inst. Telecommun. Engrs, India*, vol. 5, pp. 115–120; June, 1959.) The mean monthly values of the absorption plotted against cos χ for each month from August, 1957 to July, 1958 obeyed a relation of the type log $\rho \alpha \cos^n \chi$, where the mean value for n is 0.73. The results are in agreement with those obtained by Appleton and Piggott (3220 of 1954).

551.510.535(98/99) 2012
On the Rotation of the Polar Ionospheric Regions—C. O. Hines. (*J. Geophys. Res.*, vol. 65, pp. 141–143; January, 1960.) The depth to which the drag of the interplanetary gas (1556 of 1959) might be expected to penetrate is examined. Levels as low as the E region may be involved.

551.521.2:621.396.677.8 2013
The Thermal Radio Emission of the Ground and the Atmosphere at 1420 Mc/s and its Influence on Aerial Noise—P. G. Mezger. (*Z. angew. Phys.*, vol. 11, pp. 41–46; February, 1959.) The measurements of radio noise discussed were made with the 25-m radio telescope on the Stockert (see 835 of 1960). A "radio image" of the horizon is obtained from the thermal emission and compared with the optical image.

551.594.21 2014
The Electrical Sandstorm and Related Phenomena—D. Müller-Hillebrand. (*Elektrotech. Z.*, vol. 80, pp. 837–844; December 11, 1959.) The mechanism of electrical charge generation in sandstorms and volcanic eruptions is discussed with reference to thunderstorm phenomena. The world-wide distribution of thunderstorms is examined and related to the distribution of land masses over the globe and to the daily fluctuations of atmospheric electricity.

551.594.5 2015
Polar Auroral, Geomagnetic, and Ionospheric Disturbances—E. H. Vestine. (*J. Geophys. Res.*, vol. 65, pp. 360–362; January, 1960.) An integral invariant of auroral particle motion which appeared to predict successfully features associated with auroral isochasms [*ibid.*, vol. 64, pp. 1338–1339; September, 1959 (Vestine and Sibley)] is used to explain other other polar effects.

551.594.5 2016
The Nightly Variation of Auroras at a Subauroral Station—J. W. Chamberlain and H. M. Thorson. (*J. Geophys. Res.*, vol. 65, pp. 133–136; January, 1960.) The maximum frequency of auroras occurs near local magnetic midnight. The problem of particle bombardment on the dark hemisphere is considered.

551.594.6 2017
Doppler-Shifted Cyclotron-Frequency Radiation from Protons in the Exosphere—W. B. Murcray and J. H. Pope. (*Phys. Rev. Lett.*, vol. 4, pp. 5–6; January 1, 1960.) These protons are a possible source of VLF "dawn chorus" and hiss. Making reasonable assumptions regarding the physical processes in the outer ionosphere theoretical dispersion curves are obtained which are similar to those observed. [See 3311 of 1959 (MacArthur).]

551.594.6 2018
Observations on Atmospheric Radio Noise—G. R. A. Ellis. (*Nature*, vol. 186, p. 229; April 16, 1960.) Observations made at Camden, N.S.W., in the range 4–6 kc show that the start of noise bursts usually coincides with bay-like variations in the magnetic-field. [See also 1227 of 1960 (Aarons, *et al.*).]

551.594.6:550.386 2019
Correlation of Occurrence of Whistlers with Geomagnetic Activities—A. Kimpara. (*Nature*, vol. 186, p. 230; April 16, 1960.) The frequency of occurrence of whistlers has a seasonal variation upon which are superposed daily variations which reach a maximum on the second day after a geomagnetic disturbance.

LOCATION AND AIDS TO NAVIGATION

621.396.946 2020
Location and Guidance in Space—E. Rehbock. (*Nachrichtentech. Z.*, vol. 12, pp. 85–92; February, 1959.) Passive and active DF methods, radar, and inertial navigation systems are considered and the limits set to remote- and self-guidance systems are discussed.

621.396.96 2021
The Radar Cross-Section of a Semi-Infinite Body—H. Brysk. (*Canad. J, Phys.*, vol. 38, pp. 48–56; January, 1960.) The problem is formulated from the basic definition of cross section and applied to bodies of revolution nose-on and circular cylinders broadside-on. Values for cones and paraboloids are obtained.

621.396.96 2022
Geometrical-Optics Approximation of Near-Field Back-Scattering—F. S. Holt. (IRE TRANS. ON ANTENNAS AND PROPAGATION, vol. AP-7, pp. 434–435; October, 1959.) A target in the far field of a radar will have a back-scattering cross section which is a function of range if the radar is in its near field.

621.396.962.3 2023
Pulse Compression—Key to More Efficient Radar Transmission—C. E. Cook. (PROC. IRE, vol. 48, pp. 310–316; March, 1960.) A technique is suggested for increasing the average power capability of a pulse radar without increasing the peak power or degrading the pulse resolution. It consists in transmitting a wide pulse with a linearly swept carrier frequency and using a time-delay filter which delays one end of the pulse relative to the other; this gives a much narrower pulse of greater peak amplitude. Spectra and time functions of the signals are analyzed and filter design is discussed.

621.396.963:621.395.625.3 2024
Storage of Compressed Radar Images on Magnetic Tape—H. Groll and E. Vollrath. (*Nachrichtentech. Z.*, vol. 12, pp. 113–120; March, 1959.) The development of tape recorders for recording bandwidth-compressed radar images with a bandwidth of up to 100 kc at a tape speed of 30 inches per second is described. [See also 3874 of 1957 (Groll, *et al.*).] Test results using a method of signal-controlled carrier modulation (1630 of 1960) are given.

621.396.969.3 2025
Radar "Ring Angels" and the Roosting Movements of Starlings—E. Eastwood, G. A. Isted and G. C. Rider. (*Nature*, vol. 186, pp. 112–114; April 9, 1960.) Simultaneous visual and radar observations show that "ring-angel" echoes at sunrise are caused by the departure of starlings in successive groups from their roosts. Analysis of the time variation of echoes observed during 1959 shows a maximum during July and August. The manner of assembly of the birds into a roost is also discussed.

621.396.969.35 2026
Over-Horizon Radar's Role in Defence—(*Electronics*, vol. 33, pp. 28–29; February 5, 1960.) Describes the U. S. Naval Research Laboratory's early-warning radar, "Madre."

MATERIALS AND SUBSIDIARY TECHNIQUES

535.215 2027
Physics and Applications of Photoconduction—F. Stöckmann. (*Z. angew. Phys.*, vol. 11, pp. 68–80; February, 1959.) Fundamental theory and principal applications are reviewed. 45 references.

535.215:538.63 2028
Photoconductive and Photoelectromagnetic Lifetime Determination in Presence of Trapping: Part 1—Small Signals—A. Amith. (*Phys. Rev.*, vol. 116, pp. 793–802; November 15, 1959.) The effects of traps, located in the forbidden energy gap, upon the steady-state photoconductance and photoelectromagnetic effect are discussed.

535.215:546.47'221 2029
Effects of Polarized Light on Photocurrents and Photovoltages in ZnS—G. Cheroff, R. C. Enck and S. P. Keller. (*Phys. Rev.*, vol. 116, pp. 1091–1093; December 1, 1959.) Measurements are described of the anomalous short-circuit photo-currents in ZnS, for light polarized perpendicular and parallel to the *c* axis. An explanation in terms of a double valence-band model is suggested.

535.215:546.48'221 2030
Hole Conduction and Photovoltaic Effects in CdS—J. Woods and J. A. Champion. (*J. Electronics Control*, vol. 7, pp. 243–253; September, 1959.) The preparation and properties of crystals in which the conduction current is carried predominantly by positive holes are described. Conduction appears to take place in impurity levels.

535.37:546.47.48'221 2031
Dependence of the Forbidden Gap and Luminescence Ground-State Energies of (ZnCd)S:Ag on the Concentration of CdS—G. E. Gross. (*Phys. Rev.*, vol. 116, pp. 1478–1480; December 15, 1959.)

535.376:546.47'221 2032
Efficiency of Electroluminescence in ZnS—G. Neumark. (*Phys. Rev.*, vol. 116, pp. 1425–1432; December 15, 1959.) Theoretical calculation of efficiency, based on a model of impact ionization in a barrier. Reasonable agreement with experiment is obtained.

535.376:546.47'221:539.23 2033
Electroluminescence at Low Voltages—W. A. Thornton. (*Phys. Rev.*, vol. 116, pp. 893–894; November 15, 1959.) The effect is observed in ZnS films at a peak voltage of 2.2 v.

537.226:621.319.2 2034
Resin Electrets—J. Euler. (*Elektrotech. Z.*, vol. 11, pp. 359–364; September 21, 1959.) The formation process and characteristics of electrets are described. The properties of various dielectric materials are compared with regard to their suitability as electrets, and some suggested applications of this device are reviewed. 32 references.

537.226:621.319.2 2035
Decay of Wax Electrets—M. M. Perlman. (*J. Appl. Phys.*, vol. 31, pp. 356–357; Febru-

ary, 1960.) Experiments with resin-wax electrets show that the charge decay observed upon unshielding electrets is caused primarily by volume polarization due to internal field rather than by external ion collection.

537.227:546.431'824-31 2036

Polarized Light Transmission of $BaTiO_3$ Single Crystals—R. C. Casella and S. P. Keller. (*Phys. Rev.*, vol. 116, pp. 1469–1473; December 15, 1959.)

537.227:546.431'824-31 2037

Detailed Study of Switching Current in Barium Titanate—M. E. Drougard. (*J. Appl. Phys.*, vol. 31, pp. 352–355; February, 1960.) It is shown that the switching current depends on the applied field and the state of the net polarization. The form of the law suggests that sideways motion of domain walls plays a predominant part in the switching process, the wall velocity increasing exponentially in the early stages. This is shown to agree with a theory of domain-wall motion governed by nucleation.

537.311.31 2038

Electrical Resistivity of Yttrium Single Crystals—P. M. Hall, S. Legvold and F. H. Spedding. (*Phys. Rev.*, vol. 116, pp. 1446–1447; December 15, 1959.) Measurements over the temperature range 1.3°–300°K, in directions parallel and perpendicular to the c-axis, show a large anisotropy.

537.311.33 2039

Correlation Energy in a Model Semiconductor—J. Callaway. (*Phys. Rev.*, vol. 116, pp. 1368–1371; December 15, 1959.) Calculation of the reduction in the correlation energy of electrons, in a simple model of a semiconductor, compared with a metal of the same electron density.

537.311.33 2040

Phenomena of Injection and Extraction of Minority Carriers in a Nearly Intrinsic Semiconductor—M. R. Boite. (*Rev. HF, Brussels*, vol. 4, no. 7, pp. 151–156; 1959.) The phenomena are studied in the case of a nearly intrinsic semiconductor subjected to pulses of such amplitude that the thermal diffusion of the carriers is negligible compared to the electric-field conduction. Applications of minority-carrier extraction for the calculation of lifetime and for the determination of the type of conduction are outlined.

537.311.33 2041

Ion Drift in an *n-p* Junction—E. M. Pell. (*J. Appl. Phys.*, vol. 31, pp. 291–302; February, 1960.) Reverse bias is applied to an *n-p* junction at an elevated temperature: ions drift in the electric field of the junction to produce an intrinsic semiconductor region between the *n* and *p* regions. This offers a means for studying diffusion constants and may also be useful in device technology.

537.311.33 2042

Zener Tunnelling in Semiconductors—E. O. Kane. (*J. Phys. Chem. Solids*, vol. 12, pp. 181–188; January, 1960.) The Zener current in a constant field is calculated both with and without the Wannier-Adams reduction of the interband-coupling terms. The Zener current is only slightly different in the two cases. The apparent reduction of interband coupling is interpreted as a polarization correction. A detailed calculation of the Zener current is made for a simple two-band model which is applicable to InSb

537.311.33 2043

The Isoelectronic Series of Semiconducting Compounds with the Zinc Blende Structure—A. Raychaudhuri. (*Proc. Natl. Inst. Sci. India*, pt. A, vol. 25, pp. 201–205; July 26, 1959.) The increase of energy gap and the monotonic decrease of hole mobility with increasing charge difference between constituent nuclei are explained on the basis of a three-dimensional model. (See *Z. Phys.*, vol. 148, pp. 435–442; June 22, 1957.)

537.311.33 2044

The Influence of Polarization on the Semiconductor Properties of $A^{III}B^{V}$ Compounds—O. G. Folberth. (*Z. Naturforsch.*, vol. 13a, pp. 856–865; October, 1958.) The valence electrons in $A^{III}B^{V}$ compounds are polarized in the direction of the B^{V} atom. This explains some peculiarities of the properties of these compounds with regard to forbidden band, electron mobility, and mobility ratio.

537.311.33 2045

Effect of the Polarity of the III–V Intermetallic Compounds on Etching—J. W. Faust, Jr., and A. Sagar. (*J. Appl. Phys.*, vol. 31, pp. 331–333; February, 1960.)

537.311.33 2046

Three-Element Semiconductor Materials—J. H. Wernick and R. Wolfe. (*Electronics*, vol. 33, pp. 103–108; February 12, 1960.) Methods of assessing new semiconductor materials are described and basic properties of various ternary compounds are listed. Particular properties of $AgSbTe_2$ are discussed.

537.311.33 2047

Improvement of Semiconductor Surfaces by Low-Melting Glasses, Possibly Functioning as Ion Getters—S. S. Flaschen, A. D. Pearson and I. L. Kalnins. (*J. Appl. Phys.*, vol. 31, pp. 431–432; February, 1960.) Experiments designed to reduce the activity and concentration of surface contaminants by coating with low-melting-point sulphide and iodide inorganic glasses are described.

537.311.33:534.2-8 2048

Resonance of Charge Carriers under the Action of an Ultrasonic Wave—E. P. Pokatilov. (*Zh. Eksp. Teor. Fiz.*, vol. 36, pp. 1461–1464; May, 1959.) Theoretical treatment of the effect of ultrasonic waves on the electron gas of a semiconductor in a magnetic field. The power absorbed in unit volume is calculated for charges with scalar and tensor effective masses.

537.311.33:535.215 2049

The Surface Photovoltage of Semiconductors—A. Surduts. (*J. Phys. Radium*, vol. 20, pp. 980–981; December, 1959.) Mathematical treatment of surface potential as a function of the number of photons actually absorbed. Two cases are considered: 1) when the densities of donor and acceptor fast traps can be neglected; and 2) when their density ratio remains finite. Experimental results for *n*-type Ge tend to conform to the first case.

537.311.33:535.215 2050

Photoelectron Emission from the Surface of Semiconductor Catalysts—F. Wilessow and A. Terenin. (*Naturwiss.*, vol. 46, pp. 167–168; March, 1959.) The displacement of the photoeffect frequency limits due to adsorption was measured on ZnO, NiO and Cr_2O_3 in vacuum and in the presence of gases or vapors.

537.311.33:546.23 2051

Structure of Solid Amorphous and Molten Selenium in the Temperature Range — 180° to 430°C—H. Richter and F. Herre. (*Z. Naturforsch.*, vol. 13a, pp. 874–885; October, 1958.)

537.311.33:546.26-1 2052

Crystal Potential and Energy Bands of Semiconductors: Part 1—Self-Consistent Calculations for Diamond—L. Kleinman and J. C. Phillips. (*Phys. Rev.*, vol. 116, pp. 880–884; November 15, 1959.) Crystal potentials are constructed, first with exchange ignored, and then with exchange included on the basis of previous theoretical work.

537.311.33:[546.28+546.289 2053

The Field-Dependence of Carrier Mobility in Silicon and Germanium—A. C. Prior. (*J. Phys. Chem. Solids*, vol. 12, pp. 175–180; January, 1960.) "The variation of mobility with electric field has been measured for *n*- and *p*-type silicon and germanium with fields up to 10^6 volts/cm. For *p*-type silicon the variation is found to depend on hole concentration. For the other materials any variation with concentration must be smaller, and these experiments are inconclusive as to its existence."

537.311.33:[546.28+546.289 2054

Structure of Amorphous Germanium and Silicon—H. Richter and G. Breitling. (*Z. Naturforsch.*, vol. 13a, pp. 988–996; November, 1958.) Investigations of atomic structure were made on vapour-deposited Ge and Si films using different types of radiation.

537.311.33:546.28 2055

Diffusion of Boron into Silicon—A. D. Kurtz and R. Yee. (*J. Appl. Phys.*, vol. 31, pp. 303–305; February, 1960.) Investigation over a temperature range 1050°–1350°C using an open-tube technique gave lower diffusivities than those previously reported. The difference is attributed to variation of diffusivity with surface concentration.

537.311.33:546.28 2056

Effect of Oxide Layers on the Diffusion of Phosphorus into Silicon—R. B. Allen, H. Bernstein and A. D. Kurtz. (*J. Appl. Phys.*, vol. 31, pp. 334–337; February, 1960.) Analysis of experimental data in terms of a simple model shows that the diffusion constant of P in the oxide layer is three orders of magnitude smaller than for P in bulk Si.

537.311.33:546.28 2057

Recombination Radiation from Hot Electrons in Silicon—L. W. Davies. (*Phys. Rev. Lett.*, vol. 4, pp. 11–12; January 1, 1960.) Observed spectral distributions of radiation are considered to indicate that recombination of electrons and holes does not take place directly but through the intermediate formation of an exciton.

537.311.33:546.28 2058

Electron Pair Production at High Energy in a Silicon Single Crystal—G. Bologna, G. Diambrini and G. P. Murtas. (*Phys. Rev. Lett.*, vol. 4, pp. 134–135; February 1, 1960.) Preliminary results of an experiment to measure the number of symmetrical pairs as a function of angle between crystal axis and photon direction are given.

537.311.33:546.28 2059

Internal Impurity Levels on Semiconductors: Experiments on *p*-Type Silicon—S. Zwerdling, K. J. Button, B. Lax and L. M. Roth. (*Phys. Rev. Lett.*, vol. 4, pp. 173–176; February 15, 1960.) A discussion of localized impurity levels and of the nature of higher bands in Si.

537.311.33:546.28:537.533 2060

Electron Emission from Silicon *p-n* Junctions—B. Senitzky. (*Phys. Rev.*, vol. 116, pp. 874–879; November 15, 1959.) Experiments on uncoated, reverse-biased, Si *p-n* junctions are described. A simple mechanism is proposed to explain the effect of the electric field, lattice temperature and total current on electron emission.

537.311.33:546.289 2061

The Electrical Conductivity of Germanium in High Electric Fields at Low Temperatures—É. I. Abaulina-Zavaritskaya. (*Zh. Eksp. Teor. Fiz.*, vol. 36, pp. 1342–1350; May, 1959.) Investigation of the electrical properties of Ge single crystals doped with Sb, Bi and Zn in the temperature range 2°–10°K. Three conductivity regions are distinguished. The sharp increase in conductivity in the third of these, the breakdown region, is attributed to the development of an avalanche in the conduction band.

537.311.33:546.289 2062

Influence of Degeneracy on Recombination Radiation in Germanium—J. I. Pankove. (*Phys. Rev. Lett.*, vol. 4, pp. 20–21; January 1, 1960.) Changes of radiation spectrum with current in a tunnel diode are explained.

537.311.33:546.289 2063

Far-Infrared Electron-Ionized Donor Recombination Radiation in Germanium—S. H. Koenig and R. D. Brown, III. (*Phys. Rev. Lett.*, vol. 4, pp. 170–173; February 15, 1960.) A discussion of measurements of 100-μ radiation at a temperature of 4.2°K using a sample biased at various points in the breakdown region.

537.311.33:546.289 2064

Optical Absorption in Germanium—J. C. Phillips. (*J. Phys. Chem. Solids*, vol. 12, pp. 208–209; January, 1960.) Optical constants of Ge obtained by Philipp and Taft (2659 of 1959) are related to energy-band models.

537.311.33:546.289 2065

Origin of the Photomagnetism Anomaly in Germanium—A. R. Moore and J. O. Kessler. (*Phys. Rev. Lett.*, vol. 4, pp. 121–123; February 1, 1960.) Experiments are described which suggest that the transport of energy over relatively long distances via an excitonic mechanism is responsible for the anomaly. [See also 2300 of 1959 (Kessler and Moore).]

537.311.33:546.289:539.12.04 2066

Monoenergetic Neutron Irradiation of Germanium—O. L. Curtis, Jr., and J. W. Cleland. (*J. Appl. Phys.*, vol. 31, pp. 423–427; February, 1960.) Describes a study made on Ge irradiated with 14-mev neutrons, using lifetime, Hall effect and resistivity measurements to determine the nature of the radiation-induced defects, and to compare the damage with that produced by neutrons from a fission specimen.

537.311.33:546.289:539.12.04 2067

Recombination Centres Formed in Ge by Fast Neutrons—Nguyen van Dong and A. Barraud. (*J. Electronics Control*, vol. 7, pp. 275–288; September, 1959.)

537.311.33:546.289:539.12.04 2068

Radiation Recombination in Germanium Crystals Subjected to Fast Electron Bombardment—V. S. Vavilov, A. A. Gunnius, M. M. Gorshkov and B. D. Kopylovskii. (*Zh. Eksp. Teor. Fiz.*, vol. 37, pp. 23–26; July, 1959.) The relative intensity of the emission band with a peak at 2.35 μ increases with increasing concentration of Frenkel defects caused by fast electron bombardment.

537.311.33:[546.681'19+546.863'221 2069

Photoelectronic Analysis of High-Resistivity Crystals: (a) GaAs, (b) Sb_2S_3—R. H. Bube. (*J. Appl. Phys.*, vol. 31, pp. 315–322; February, 1960.) The results provide data on the band gap, the majority-carrier lifetime, the activation energy for dark conductivity, and the density and depth of trapping centers. Both crystals show trapping of photoexcited carriers by compensated donor centers.

537.311.33:546.681'19 2070

The Reverse Characteristics of Gallium Arsenide *p-n* Junctions—J. W. Allen. (*J. Electronics Control*, vol. 7, pp. 254–260; September, 1959.) "A method of making *p-n* junctions in GaAs by diffusion of zinc is described. On the basis of their reverse characteristics the junctions can be divided into two groups. 'Hard' junctions have a sharp breakdown, their breakdown voltage increases with increasing temperature and their capacity varies as the inverse cube root of the bias voltage. 'Soft' junctions do not show a rapid change of slope in their current-voltage curve, their voltage at a given current decreases with increasing temperature and their capacity-voltage characteristic is anomalous."

537.311.33:546.681'86 2071

Optical Properties of Gallium Antimonide—D. F. Edwards and G. S. Hayne. (*J. Opt. Soc. Amer.*, vol. 49, pp. 414–415; April, 1959.) A note of measurements made on a single-crystal sample grown by the modified Czochralski method, for which the Hall mobility was 50 per cent greater than has been previously reported for relatively pure material.

537.312.62:537.311.62 2072

Analysis of Experimental Data relating to the Surface Impedance of Superconductors—A. A. Abrikosov, L. P. Gor'kov and I. M. Khalatnikov. (*Zh. Eksp. Teor. Fiz.*, vol. 37, pp. 187–191; July, 1959.) Experimental results are in agreement w th theory [see 3758 of 1958 (Mattis and Bardeen)] except at VLF where the real part of the impedance near the critical temperature is several times larger than the theoretical value.

537.312.62:538.569.4 2073

Millimetre-Wave Absorption in Superconducting Aluminium—M. A. Biondi and M. P. Garfunkel. (*Phys. Rev.*, vol. 116, November 15, 1959.)

Part 1: Temperature Dependence of the Energy Gap (pp 853–861).

Part 2: Calculation of the Skin Depth (pp. 862–867).

537.583 2074

Anomalous Thermionic Emission of Some Borides and Carbides of Rare Earth and Transition Elements—E. A. Kmetko. (*Phys. Rev.*, vol. 116, pp. 895–896; November 15, 1959.)

538.22 2075

Magnetization Reversal and Asymmetry in Cobalt Vanadate (IV)—N. Menyuk, K. Dwight and D. G. Wickham. (*Phys. Rev. Lett.*, vol. 4, pp. 119–120; February 1, 1960.)

538.22:538.569 2076

Microwave Faraday Rotation in Antiferromagnetic MnF_2—A. M. Portis and D. Teaney. (*Phys. Rev.*, vo . 116, pp. 838–845; November 15, 1959.)

538.221 2077

Pseudodipo ar Anisotropy in Cubic Ferromagnets at Low Temperatures—S. H. Charap and P. R. Weiss. (*Phys. Rev.*, vol. 116, pp. 1372–1380; December 15, 1959.)

538.221 2078

High-Resistivity Nickel-Iron Alloys with Rectangular Hysteresis Loops—A. Hart. (*Brit. J. Appl. Phys.*, vol. 11, pp. 58–60; February, 1960.) A method of magnetic annealing is described for an alloy containing up to 3 per cent Mo with Ni and Fe in the ratio 65:35. This has similar magnetic properties to a 65/35 per cent Ni-Fe alloy but higher resistivity.

538.221 2079

Magnetic Measurements on Ferromagnetic Nickel Amalgams—W. Henning. (*Z. Naturforsch.*, vol. 13a, pp. 897–898; October, 1958.) Measurements of magnetization and of the temperature dependence of coercive force made on three different specimens are discussed. For earlier work on Fe and Co amalgams see *ibid.*, vol. 12a, p. 754; September, 1957. (Henning and Vogt.)

538.221:539.12.04 2080

Polarization of Cobalt and Iron Nuclei in Ferromagnetics—B. N. Samoĭlov, V. V. Sklyarevskiĭ, and E. P. Stepanov. (*Zh. Eskp. Teor. Fiz.*, vol. 36, pp. 1366–1367; May, 1959.) The anisotropy of gamma rays from ^{60}Co in a magnetized permendur alloy was measured in the temperature range 0.03°–0.1°K. No anisotropy was detected in similar experiments on ^{59}Fe nuclei in Armco iron.

538.221:539.23 2081

"Spontaneous Magnetic Anisotropy" in Polycrystalline Thin Films—W. Andrä, Z. Málek, W. Schüppel and O. Stemme. (*J. Appl. Phys.*, vol. 31, pp. 442–443; February, 1960.) Thin ferromagnetic films produced in a magnetic field parallel to their surface show a uniaxial magnetic anisotropy.

538.221:539.23 2082

Observation of Néel Walls in Thin Films—H. Rubinstein, H. W. Fuller and M. E. Hale. (*J. Appl. Phys.*, vol. 31, pp. 437–438; February, 1960.) Néel walls were observed in a 450-Å film from a 4–79 permalloy melt deposited on glass substrate heated to a temperature of 150°C.

538.221:539.23 2083

Saturation Magnetization of Nickel Films of Thickness Less than 100 Å—C. A. Neugebauer. (*Phys. Rev.*, vol. 116, pp. 1441–1446; December 15, 1959.) No decrease in saturation magnetization from that of bulk Ni was observed for films down to 20 Å thick, at room temperature. Behavior of thinner films suggests super-paramagnetism rather than a decrease in the saturation magnetization.

538.221:539.23 2084

Observations on MnBi Films during Heat Treatment—L. Mayer. (*J. Appl. Phys.*, vol. 31, pp. 346–351; February, 1960.) These observations give a visual demonstration of the nascent state of ferromagnetism.

538.221:539.23:621.385.833 2085

Determination of Magnetization Distribution in Thin Films Using Electron Microscopy—H. W. Fuller and M. E. Hale. (*J. Appl. Phys.*, vol. 31, pp. 238–248; February, 1960.) Developments in technique and some results for a Ni-Fe film are described.

538.221:621.318.12/.13 2086

The Role of Magnetic After-Effects in Engineering Materials—K. Sixtus. (*Elektrotech. Z.*, vol. 80, pp. 565–570; September 1, 1959.) Various types and causes of magnetic after-effects are reviewed and some applications of these phenomena in high-frequency techniques are discussed.

538.221:[621.318.124+621.318.134 2087

The Behaviour of Scattered Stabilized Bloch Walls in Magnetization Cycles—A. v. Kienlin. (*Z. angew. Phys.*, vol. 11, pp. 118–120; March, 1959.) Irregular magnetization changes observed in Ni-Cu ferrites are discussed and considered as a "freezing" of a diffusion after-effect. Measurements on Co ferrites with stabilized Bloch walls indicate strongly pronounced irreversible Bloch-wall jumps which occur independently of each other.

538.221:621.318.124 2088

Applications of Barium Ferrite Magnets—

W. Hotop and K. Brinkmann. (*Elektrotech. Z.*, vol. 80, pp. 609–615; September 1, 1959.) 30 references, mainly to German applications.

538.221:621.318.13 **2089**
Two Examples of Further Development of Magnetically Soft Materials—G. Hellbardt and H. Stäblein. (*Elektrotech. Z.*, vol. 80, pp. 570–576; September 1, 1959.) Si-Fe cube-textured sheet material, and 50 per cent Co-Fe alloy with rectangular hysteresis loop are discussed.

538.221:621.318.134 **2090**
Recent Development of Ferrites—F. Berlinghoff. (*Elektrotech. Z.*, vol. 80, pp. 600–605; September 1, 1959.) Improvements in electrical and magnetic properties and new methods of core construction are described.

538.221:621.318.134 **2091**
Perminvar Ferrites—M. Kornetzki. (*Elektrotech. Z.*, vol. 80, pp. 605–609; September 1, 1959.) The characteristics of constricted-loop ferrites and their advantages are described.

538.221:621.318.134 **2092**
A Resonance Phenomenon in Perminvar Ferrites Annealed in a Magnetic Field—H. Rabl. (*Z. angew. Phys.*, vol. 11, pp. 57–63; February, 1959.) Numerous sharp resonances in the frequency range 1–14 mc have been observed in perminvar ferrites annealed in a transverse magnetic field. These may be due to small magnetostrictive resonator elements distributed in the material.

538.221:621.318.134 **2093**
Contribution to the Classification of the Diffusion After-Effect in Ferrites with Divalent and Trivalent Manganese—W. Gieseke. (*Z. angew. Phys.*, vol. 11, pp. 91–95; March, 1959.) Results of measurements of activation energy as a function of ferrite composition are discussed with reference to ordering conditions and diffusion processes in the crystal lattice according to the theory of Goodenough and Loeb (3016 of 1955).

538.221:621.318.134 **2094**
A Relation between Magnetic After-Effect and Hysteresis Losses in Ferrites—W. Metzdorf. (*Z. angew. Phys.*, vol. 11, pp. 95–102; March, 1959.) The Jordan after-effect is considered and a quantitative relation between after-effect loss-factor and relative hysteresis coefficient is found. This relation is discussed with reference to results of measurements on various ferrites and the findings of other authors.

538.221:621.318.134 **2095**
The Electron-Diffusion After-Effect in Oversintered High-Permeability Ferrites—D. Köhler. (*Z. angew. Phys.*, vol. 11, pp. 103–111; March, 1959.) The complex permeability at temperatures in the range $-183°$ to $+60°C$ was measured on Ni-Zn ferrites of equal composition but sintered at normal and higher-than-normal temperatures. The additional losses observed at low temperatures are due to diffusion after-effects which are more pronounced the higher the sintering temperature. The variation with temperature of activation and after-effect energies is discussed with reference to existing theory.

538.221:621.318.134 **2096**
Crystal Chemical and Magnetic Studies of Garnet Systems $M_3^{2+}Fe_2Sn_3O_{12}$–$Y_3Fe_2Fe_3O_{12}$—S. Geller, R. M. Bozorth, M. A. Gilleo and C. E. Miller. (*J. Phys. Chem. Solids*, vol. 12, pp. 111–118; January, 1960.)

538.221:621.318.134 **2097**
Method for the Detection of Flaws in Yttrium Iron Garnet Crystals—E. Buehler and M. Tanenbaum. (*J. Appl. Phys.*, vol. 31, pp. 388–390; February, 1960.)

538.221:621.318.134 **2098**
Optical Observation of Exchange Splitting in Ytterbium Iron Garnet—K. A. Wickersheim and R. L. White. (*Phys. Rev. Lett.*, vol. 4, pp. 123–125; February 1, 1960.) Splitting of the Yb^{3+} transition is shown in high-resolution spectra to be of large size and large anisotropy.

538.221:621.318.134:538.569.4 **2099**
What is Ferromagnetic Resonance?—R. A. Waldron. (*Brit. J. Appl. Phys.*, vol. 11, pp. 69–73; February, 1960.) Two distinct resonance effects may take place in ferrites, ferromagnetic resonance and Kittel resonance. These two effects are analyzed in terms of the permeability tensor, and show different energy losses.

538.221:621.318.134:538.569.4 **2100**
High-Power Effects in Ferrimagnetic Resonance—P. E. Seiden and H. J. Shaw. (*J. Appl. Phys.*, vol. 31, pp. 432–433; February, 1960.) Experiments with Y-Fe garnet have shown discontinuous decreases in susceptibility superposed on the continuous decline as the power increases. (See also 1320 of 1960.)

538.221:621.318.134:538.569.4 **2101**
Ferromagnetic Relaxation Mechanism for M_z in Yttrium Iron Garnet—M. Sparks and C. Kittel. (*Phys. Rev. Lett.*, vol. 4, pp. 232–234; March 1, 1960.)

538.221:621.318.134:538.569.4 **2102**
Spin-Lattice Relaxation in Yttrium Iron Garnet—E. G. Spencer and R. C. LeCraw. (*Phys. Rev. Lett.*, vol. 4, pp. 130–131; February 1, 1960.) Low-temperature measurements show the existence of a process not included in present theories.

538.221:621.318.134:538.569.4 **2103**
Temperature Dependence of Ferromagnetic Resonance in Yttrium Ferrite-Garnets—L. A. Malevskaya and G. M. Nurmukhamedov. (*Zh. Eksp. Teor. Fiz.*, vol. 36, pp. 1600–1601; May, 1959.) Experimental investigation of the temperature dependence of the width of ferromagnetic resonance absorption lines in "substituted" ferrites. (See 2104 of 1960.)

538.221:621.318.134:538.569.4 **2104**
Magnetic and Resonance Properties of Yttrium Ferrite-Garnets with Replacement of Fe^{3+} Ions by Cr^{3+} and Al^{3+} Ions—K. P. Belov, M. A. Zaĭtseva and L. A. Malevskaya. (*Zh. Eksp. Teor. Fiz.*, vol. 36, pp. 1602–1603; May, 1959.) The dependence of absorption line width on Cr and Al content is shown graphically.

538.221:621.318.4.042 **2105**
Metallic Magnetic Materials and Core Shapes in Telecommunications—R. Boll. (*Elektrotech. Z.*, vol. 80, pp. 582–588; September 1, 1959.) Materials and core shapes for relays, transformers, switching, counting and storage devices are reviewed.

538.222:538.56 **2106**
Paramagnetic Absorption and Rotation of the Plane of Polarization for Certain Salts in the Microwave Band—A. I. Kurushin. (*Zh. Eksp. Teor. Fiz.*, vol. 37, pp. 297–298; July, 1959.) A report of experiments carried out at 9150 mc on powdered paramagnetic salts at room temperature. Absorption is plotted as a function of the magnitude of a constant field 1) perpendicular, and 2) parallel to the high-frequency field. In fields up to 6000 oersteds the curves for case 1) lie above those for case 2). Polarization-rotation curves do not show the reversal of sign reported by Imamutdinov *et al.* (776 of 1959).

538.222:538.569.4 **2107**
Spin-Lattice Relaxation Times in Ruby at 34.6 kMc/s—J. H. Pace, D. F. Sampson and J. S. Thorp. (*Phys. Rev. Lett.*, vol. 4, pp. 18–19; January 1, 1960.)

538.222:538.569.4 **2108**
Paramagnetic Resonance of Exchange-Coupled Cr^{3+} Pairs in Ruby—L. Rimai, H. Statz, M. J. Weber, G. A. deMars and G. F. Koster. (*Phys. Rev. Lett.*, vol. 4, pp. 125–128; February 1, 1960.) Measurements at 10 and 16 kmc are reported.

538.222:538.569.4 **2109**
Electron Nuclear Double-Resonance Experiments with Ruby—R. W. Terhune, J. Lambe, G. Makhov and L. G. Cross. (*Phys. Rev. Lett.*, vol. 4, pp. 234–236; March 1, 1960.) Describes polarization effects observed by scanning the frequency of an RF generator connected to a coil around the crystal.

538.222:538.569.4 **2110**
Single-Crystal Tungstates for Resonance and Emission Studies—L. G. Van Uitert and R. R. Soden. (*J. Appl. Phys.*, vol. 31, pp. 328–330; February, 1960.)

538.222:538.569.4 **2111**
Paramagnetic Resonance and Crystal Field in Two Nickel Chelate Crystals—M. Peter. (*Phys. Rev.*, vol. 116, pp. 1432–1435; December 15, 1959.)

538.633:537.311.31 **2112**
Experimental Investigation of the Magnetoresistance Effect in Corbino Disks of Copper and Gold at Low Temperatures—G. Lautz and E. Tittes. (*Z. Naturforsch.*, vol. 13a, pp. 866–874; October, 1958.) Results obtained on disk- and strip-shaped specimens are compared with those of other authors. The relation between magnetoresistance effect and Hall effect is discussed. 47 references.

MATHEMATICS

512.3 **2113**
A Method for the Hurwitz Factorization of a Polynomial—R. Unbehauen. (*Arch. elekt. Übertragung*, vol. 13, pp. 58–62; February, 1959.) The method gives the factorization without an explicit determination of the zeros of the Hurwitz factor.

517.512 **2114**
Dual Fourier-Bessel Series—J. C. Cooke and C. J. Tranter. (*Quart. J. Mech. Appl. Math.*, vol. 12, pp. 379–386; August, 1959.) A method is given for determining the coefficients in a dual Fourier-Bessel series arising in the solution of potential problems in which the application of a finite Hankel transform is appropriate and in which one of the boundary conditions is a "mixed" one. The method is applied to find the potential due to an electrified circular disk situated inside an earthed coaxial infinite hollow cylinder.

517.512.2 **2115**
Fourier Series associated with Duty Cycles—C. G. Mayo and J. W. Head. (*Brit. J. Appl. Phys.*, vol. 11, pp. 103–106; March, 1960.) A mathematical investigation of the Fourier series of an arbitrary periodic function and the way in which the behavior of the function in various parts of the period affects the series.

517.63 **2116**
The Evaluation of Integrals of Products of Linear System Responses: Part 1—A. Talbot. (*Quart. J. Mech. Appl. Math.*, vol. 12, pp. 488–503; November, 1959.) For cases when the functions $x(t)$ and $y(t)$ have rational Laplace transforms, simple methods are presented for the evaluation of the integrals $\int_0^\infty xydt$ and

$\int_0^\infty x^2 dt$ in terms of the transform coefficients. The results are extended to the moment integrals $\int_0^\infty t^r xy dt$ and $\int_0^\infty t^r x^2 dt$.

517.63 2117
The Evaluation of Integrals of Products of Linear System Responses: Part 2—Continued-Fraction Methods—A. Talbot. (*Quart. J. Mech. Appl. Math.*, vol. 12, pp. 504–520; November, 1959.) The method described in pt. 1 (2116 of 1960) depends on the determination of polynomials u, v such that $fv+gu=N$, where f, g and N are prescribed polynomials. A method of solution of this equation by means of continued fractions is described.

MEASUREMENTS AND TEST GEAR

621.3.018.41(083.74) 2118
Measurements of the Frequency of an Ammonia Maser in England and Australia—A. M. J. Mitchell and E. Sandbach. (*Nature*, vol. 185, pp. 833–834; March 19, 1960.) Measurements made in Australia by comparison with transmissions from Rugby show the maser frequency to be 2.2 parts in 10^9 higher than it was in England. This frequency difference is comparable to the error due to propagation variations over the path Rugby–Melbourne.

621.317.2:389.2:621.373.44 2119
A Timing-Pulse Generator—C. S. Fowler. (*J. Brit. IRE*, vol. 20, pp. 125–126; February, 1960.) "The equipment described generates timing pulses for general laboratory use. By reference to the MSF standard-frequency transmissions, the pulses serve as time signals which do not differ from Universal Time (UT 2) by more than ±0.05 ms."

621.317.3:621.385.001.4 2120
Simplified Electrical Measurement and Test Methods in the Mass Production of Receiver Valves—Kirachke. (See 2190 of 1960.)

621.317.328.029.6 2121
Field-Strength Measurements in High-Frequency Fields—H. Fricke. (*Arch. tech. Messen*, pp. 15–16, 89–92, 133–136; January/May/July, 1959.) Pt. 1 comprises definitions of standard terminology and 42 references. In pts. 2 and 3 methods in which the aerial or the generator is used as reference standard, and specialized equipment are described.

621.317.33 2122
A Novel, High-Accuracy Circuit for the Measurement of Impedance in the A. F., R.F., and V.H.F. Ranges—W. H. P. Leslie and D. Karo. (*Proc. IEE*, vol. 107, pp. 225–226; March, 1960.) Comment on 554 of 1959 and author's reply.

621.317.335 2123
Improvements in the Precision Measurement of Capacitance—G. H. Rayner and L. H. Ford. (*Proc. IEE*, pt. B, vol. 107, pp. 185–189; March, 1960.) A Wien bridge operating at 1 kc gives a repeating accuracy of about 2 parts in 10^6, which is much better than the stability of available standard capacitors. A second, more versatile type of bridge has rather lower accuracy.

621.317.34.029.6 2124
A Method of Amplitude and Phase Measurement in the V.H.F.-U.H.F. Band—G. D. Monteath, D. J. Whythe and K. W. T. Hughes. (*Proc. IEE*, pt. B, vol. 107, pp. 150–154; March, 1960.) The measurements relate to changes in the transmission characteristics of a network in the frequency range 41–1000 mc, and are made with a modified commercial instrument. Phase errors are mainly within ±3°, and the maximum error vector is 6 per cent of the full-scale reading.

621.317.361.029.6:621.396.1 2125
Definition and Measurement of Bandwidth in Radio Engineering—Schröck. (See 2162 of 1960.)

621.317.4 2126
Coaxial Measurement-Line Inserts of High Precision for the Frequency Range 1–13 Gc/s—M. Ebisch. (*Frequenz*, vol. 13, pp. 52–56; February, 1959.) Two interchangeable inserts of 50- and 60-Ω impedance for swr measuring equipment are described. Particular attention is given to the design of insulating supports and connectors.

621.317.411.088 2127
A Technique for Reducing Errors in Permeability Measurements with Coils—B. L. Danielson and R. D. Harrington. (PROC. IRE, vol. 48, pp. 365–366; March, 1960.) The errors, which are independent of the permeability value, may be eliminated through measurements of the inductance of the magnetic-core coil and of a similar polystyrene-core coil.

621.317.43 2128
Calorimetric Measurement of Magnetic-Reversal Losses in Ring Cores—F. Koppelmann and G. Unger. (*Elektrotech. Z.*, vol. 80, pp. 773–777; November 11, 1959.) A toroidal calorimeter is described and details of the test procedure are given. A comparison with electrical measurements of losses shows that a high accuracy can be achieved with the calorimetric method.

621.317.442 2129
Noise-Voltage Measurements on Transformer Laminations—G. Strasser. (*Nachrichtentech. Z.*, vol. 9, pp. 134–137; March, 1959.) A noise-meter circuit for the frequency range 900–2100 cps is described. Curves of noise voltage as a function of field strength, and signal/noise ratio as a function of excitation are given for different lamination materials.

621.317.79:681.142:621.385.833 2130
An Improvement to the Electron-Trajectory Tracer—J. Vine and R. T. Taylor. (*Proc. IEE*, pt. B, vol. 107, pp. 181–184; March, 1960.) An interpolation method for electric-field determination with a resistance network is described. [See 614 of 1960 (Haine and Vine).]

OTHER APPLICATIONS OF RADIO AND ELECTRONICS

621.365.5.029.6 2131
The Application of Microwave Energy in Industry—W. Schmidt. (*Nachrichtentech. Z.*, vol. 12, pp. 79–84; February, 1959.) Magnetron circuits for dielectric-heating applications are considered.

621.373:531.787:616–07 2132
Electronic Tonometer for Glaucoma Diagnosis—R. S. Mackay and E. Marg. (*Electronics*, vol. 33, pp. 115–116; February 12, 1960.) A servo-controlled plunger and associated circuitry for rapid pressure measurement are described.

621.383.5:531.715 2133
Method of Measuring Displacement Using Optical Gratings—D. L. A. Barber and M. P. Atkinson. (*J. Sci. Instr.*, vol. 36, pp. 501–504; December, 1959.) Two diffraction or shadow gratings are used with a third "comparison" grating mounted on a drum rotating at constant speed. Fringe patterns are detected by two photocells. The change in the phase difference between the alternating signals from the photocells is a measure of the displacement.

621.385.833 2134
Use of an Image Converter in Negative-Ion Emission Microscopy—R. Bernard, R. Goutte and C. Guillaud. (*J. phys. radium*, vol. 20, pp. 981–982; December, 1959.) A negative-ion image obtained by positive-ion bombardment of a metal surface is formed on a polished brass or Be cathode. The secondary electrons emitted from this cathode are focused on a screen between the objective and converter giving an enlarged electronic image of the original one.

621.385.833 2135
A 70-KV Electron Microscope with Cold Cathode and Electrostatic Lens—M. Gribi, M. Thürkauf, W. Villiger and L. Wegmann. (*Optik*, vol. 16, pp. 65–86; February, 1959.)

621.385.833 2136
Calculation of the Aberration Coefficients of Magnetic Electron Lenses as a Function of Pole-Piece Geometry and Operational Data—O. Jandeleit and F. Lenz. (*Optik*, vol. 16, pp. 87–107; February, 1959.)

621.385.833 2137
Existence Ranges of Rotationally Symmetric Electron Lenses—W. Tretner. (*Optik*, vol. 6, pp. 155–184; March, 1959.) The effects of field parameters and optical characteristics on the limits of chromatic aberration and aperture error in an electron-optical system are determined.

621.385.833.032.362 2138
The Problem of Interpretation of Field-Emission Patterns of Metal-Film Cathodes—V. N. Shrednik. (*Fiz. Tverdogo Tela*, vol. 1, pp. 1134–1139; July, 1959.) Investigation shows that the distribution of intensities on the field emission patterns in an electron projector depends on the distribution of the work function and on the distribution of local changes in the electric field on the surface of the sample. The emission patterns of the systems Zr-W and Ba-W are examined.

PROPAGATION OF WAVES

621.391.812.3 2139
Statistical Analysis of Fading on Short-Wave Transmissions—K. K. Aggarwal. (*J. Inst. Telecommun. Engrs, India*, vol. 5, pp. 230–237; September, 1959.) Analyses of fading records taken on oblique-incidence broadcast transmissions and on pulsed transmissions at vertical incidence show the amplitude distributions to be of the Rayleigh, Gaussian and log-normal type.

621.391.812.6 2140
Fading and Attenuation of High-Frequency Radio Waves Propageted over Long Paths Crossing the Auroral, Temperate and Equatorial Zones—K. C. Yeh and O. G. Villard, Jr. (*J. Atmos. Terr. Phys.*, vol. 17, pp. 255–270; February, 1960.) Propagation modes made possible by ionospheric layer tilts are suggested as the reason for a minimum in fading speed which is observed on auroral paths during 2130–0300 U.T. The same reason can explain the fact that during this period the attenuation of the waves cannot be attributed to the absorption which causes "blackouts." Some explanations are also offered for the marked diurnal variation in fading speed observed on temperate latitude and transequatorial paths.

621.391.812.6.029.62 2141
Transequatorial Propagation of V.H.F. Signals—R. G. Cracknell. (*QST*, vol. 43, pp. 11–17; December, 1959.) Details are given of the results of observations in Europe and Africa of long-distance transmission across the geomagnetic equator in the range 30–75 mc during the period 1957–1958.

621.391.812.61.029.64 2142
Analysis of 3-cm Radio Height-Gain Curves

Taken Over Rough Terrain—H. T. Tomlinson and A. W. Straiton. (IRE Trans. on Antennas and Propagation, vol. AP-7, pp. 405–413; October, 1959. Abstract, Proc. IRE, vol. 48, p. 270.)

621.391.812.62 2143

Sweep-Frequency Studies in Beyond-the-Horizon Propagation—W. H. Kummer. (IRE Trans. on Antennas and Propagation—vol. AP-7, pp. 428–433; October, 1959. Abstract, Proc. IRE, vol. 48, p. 271; February, 1960.)

621.391.812.62:621.397 2144

V.H.F. Field-Strength Measurements Over Paths in the Irish Sea Involving Mountain Obstacles—J. K. S. Jowett. (*Proc. IEE*, pt. B, vol. 107, pp. 141–149; March, 1960.) Statistical properties of the fading signals were studied in relation to a channel-sharing problem in television. Signals over an obstructed path had a higher median field strength and showed less fading than those over a similar path with no obstruction.

621.391.812.621 2145

An Analysis of Time Variations in Tropospheric Refractive Index and Apparent Radio Path Length—M. C. Thompson, Jr., H. B. Janes and A. W. Kirkpatrick. (*J. Geophys. Res.*, vol. 65, pp. 193–201; January, 1960.) The experimental results are presented for two paths which show differences in length, climate and angle of elevation.

621.391.812.624 2146

A Scatter Propagation Experiment Using an Array of Six Paraboloids—L. H. Doherty. (IRE Trans. on Antennas and Propagation, vol. AP-7, pp. 419–428; October, 1959. Abstract, Proc. IRE, vol. 48, p. 271; February, 1960.)

621.391.812.63 2147

A Note on Fourth Reflection Condition in the Ionosphere—B. Chatterjee. (*J. Atmos. Terr. Phys.*, vol. 17, pp. 271–275; February, 1960.) A "ray treatment" method is used to show that no reflection of the wave takes place under the condition $\mu=\infty$.

621.391.812.63 2148

Ionospheric Models as an Aid for the Calculation of Ionospheric Propagation Quantities—A. H. de Voogt. (Proc. IRE, vol. 48, pp. 341–346; March, 1960.) Continuation of earlier work (3691 of 1953). The models are derived assuming various critical frequencies of the E and F_2 layers; calculated and experimental ionograms are compared and the model giving the best fit is used to calculate the propagation conditions.

621.391.812.63 2149

An Ionospheric Ray-Tracing Technique and its Application to a Problem in Long-Distance Radio Propagation—D. B. Muldrew. (IRE Trans. on Antennas and Propagation, vol. AP-7, pp. 393–396; October, 1959. Abstract, Proc. IRE, vol. 48, p. 270; February, 1960.)

621.391.812.63 2150

The Propagation of High-Frequency Radio Waves to Long Distances—F. Kift. (*Proc. IEE*, pt. B, vol. 107, pp. 127–140; March, 1960.) The parabolic-layer transmission equation of Appleton and Beynon has been solved for a wide range of its main parameters. A method of applying this equation to any long-distance circuit, in which the successive hop lengths of each transmitted ray are adjusted to accord with ionospheric variations along the path, is described. Results are displayed on mode plots showing the vertical angles of arrival and the time delays of the predominant modes. Experimental results for the paths Ascension Island–Slough and Colombo–Slough agree well with data obtained from the mode plots, provided that the effect of the tropical E_s layer is included. The technique is useful for aerial design and in choosing an optimum frequency for reduction of delay distortion.

621.391.812.63 2151

The Lower Frequency Limits for F-Layer Radio Propagation—B. Fulton, O. Sandoz and E. Warren. (*J. Geophys. Res.*, vol. 65, pp. 177–183; January, 1960.) Methods are discussed for calculating the lowest frequencies propagated by high-angle and low-angle rays.

621.391.812.63 2152

Ionospheric Irregularities and Propagation at Frequencies Above the "Classical" M.U.F.—A. K. Saha. (*J. Inst. Telecommun. Engrs, India*, vol. 5, pp. 136–139; June, 1959.) A review with 17 references.

621.391.812.63:551.510.535 2153

Some Observations of Ionospheric Faraday Rotation on 106.1 Mc/s—Hill and Dyce. (See 2010 of 1960.)

621.391.812.63.029.45 2154

The Propagation of Radio Waves of Frequency Less Than 1 KC—E. T. Pierce. (Proc. IRE, vol. 48, pp. 329–331; March, 1960.) Agreement between mode theory and experimental results at night is improved by assuming that the effective height of ionospheric reflection increases as the frequency is reduced.

621.391.812.63.029.51:523.75 2155

Some Investigations on Long-Wave Propagation—S. N. Mitra. (*J. Inst. Telecommun. Engrs, India*, vol. 5, pp. 121–135; June,1959.) An analysis of observations made on a frequency of 164 kc over a propagation path of 1650 km during the period August 9th to December 16th, 1958 shows that solar flares of all classes of importance give rise to sudden increases in amplitude of the received signal.

RECEPTION

621.391.821 2156

On the Need for Revision of Noise Grades for India—B. B. Ghosh and S. N. Mitra. (*J. Inst. Telecommun. Engrs, India*, vol. 5, pp. 194–199; September, 1959.) Noise grades predicted in C.C.I.R. Rept. No. 65 are low by comparison with measured values (2743 of 1959): the difference has at times exceeded 40 db.

STATIONS AND COMMUNICATION SYSTEMS

621.376:621.396:681.84.087.7 2157

Interrelation and Combination of Various Types of Modulation—W. D. Meewezen. (*Proc. IRE (Australia)*, vol. 20, pp. 582–590; October, 1959.) An examination of the frequency distribution of the power in typical broadcast signals shows that low-deviation PM should have advantages over AM and FM. A stereophonic broadcasting system is proposed in which the sum of the two channels is transmitted as AM and the difference as PM.

621.376.22 2158

New Suppressed-Carrier Modulation Technique—J. Dysinger, W. Whyland and R. Wood. (*Electronics*, vol. 33, pp. 47–49; February 5, 1960.) Balanced modulation by the clipped AF signal gives phase reversal at a low level, and can be followed by frequency changing or Class-C ampl fication. The envelope is modulated in the final amplifier.

621.376.3:621.3.018.78:621.372.5 2159

Fundamental and Harmonic Distortion of Waves Frequency-Modulated with a Single Tone—R. G. Medhurst. (*Proc. IEE*, pt. B. vol. 107, pp. 155–164; March, 1960.) An approximate formula is developed for distortion in passive networks whose amplitude and phase characteristics vary nonlinearly with frequency. [See also 1581 of 1957(Brown).]

621.391 2160

Information Processing by Man—K. Küpfmüller. (*Nachrichtentech. Z.*, vol 12, pp. 68–74; February, 1959.) From observations of human behavior the speed and limitations of human information processing as controlled by the nervous system are assessed.

621.391 2161

The Fundamental Theorems of Information Theory Arising From the Error Propagation Laws in the Solution of Convolution Integral Equations—H. Wolter. (*Arch. elekt. Übertragung*, vol. 13, pp. 101–113; March, 1959.) A study of formulations of more general validity than those given by the basic theorems of information theory. Evaluation of the time function observed at the distant end of a communication channel taking account of error propagation laws may give better information on the message present at the input than the conventional use of the information theorems. (See also 3852 of 1959.)

621.396.1:621.317.361.029.6 2162

Definition and Measurement of Bandwidth in Radio Engineering—U. Schröck. (*Nachrichtentech. Z.*, vol. 12, pp. 139–146; March, 1959.) A comparison of bandwidth definitions for telegraphy and telephony transmission shows that the time-frequency spectrum is a better basis of reference than the line spectrum function. C.C.I.R. recommendations for various types of transmission and appropriate methods of bandwidth measurement are discussed.

621.396.1:621.391.826.2 2163

The Effect of Multipath Distortion on the Choice of Operating Frequencies for High-Frequency Communication Circuits—D. K. Bailey. (IRE Trans. on Antennas and Propagation, vol. AP-7, pp. 397–404; October, 1959. Abstract, Proc. IRE, vol. 48, p. 270; February, 1960.)

621.396.43:551.507.362.2 2164

Long-Distance Communication—R. J. Hitchcock. (*Wireless World*, vol. 66, pp. 161–163; April, 1960.) A general discussion of problems of long-distance communications using earth satellites.

621.396.65 2165

French Transhorizon Radio-Link Systems—(*Onde élect.*, vol. 40; January, 1960.)

1) **Transhorizon Radio Links, Present and Future Position**—F. du Castel (pp. 9–18).

2) **Program for the Installation of Transhorizon Radio Links in Algeria and the Sahara**—A. G. Pluchard (pp. 19–23).

3) **Transhorizon Links: Operating Conditions and Performance**—R. Cabessa (pp. 24–31).

4) **The Media-Laghouat-Ouargla Radio Link**—M. Olivier and J. Pellerin (pp. 32–38).

5) **Discussion of a West African Transhorizon Radio Link**—L. Boithias and F. du Castel (pp. 39–45.)

6) **The THC 953 Transhorizon Radio Link**—B. Fostoff and J. Iltis (pp. 46–57).

7) **900-Mc/s Transhorizon Radio-Link Equipment of the Compagnie Générale d'Électricité**—P. Mandel (pp. 58–64).

8) **Equipment for a Transhorizon Radio Link in the 170-Mc/s Band**—R. Bayot and A. Forest (pp. 65–73).

9) **Radiotelephony Equipment for Propagation by Tropospheric Scatter**—G. Andrieux, J. Cayzac and C. Ducot (pp. 74–81).

10) **A Prototype Transhorizon Radio-Link Equipment in the 2000-Mc/s Band**—F. du Castel, G. Broussaud, L. Malnar and R. Baud (pp. 82–99).

11) **Transhorizon Radio Links in the 4 400–5000-Mc/s Band**—J. Dockes and W. Koreicho (pp. 100–105).

12) **Transhorizon Television Transmission Tests at 4000-Mc/s**—A. Laurens, J. D. Koenig and C. Carzan (pp. 106–111).

13) **A Diversity Combiner for Transhorizon Links**—P. Lemoine (pp. 112–115).

14) **Radio-Climatic Influences on Transhorizon Links**—P. Misme (pp. 116–123).

621.396.65:6211.376.55 2166

Modulation Equipment Type PPM 24 with Pilot-Tone Synchronization—H. M. Christiansen and R. Senft. (*Frequenz*, vol. 13, pp. 44–52; February, 1959.) A radio-telephony pulse phase modulation system for 24 channels usable for the transmission of broadcast programs over radio links is described.

621.396.934:629.19 2167

Radio Communication with a Space Probe—W. T. Blackband. (*J. Brit. Interplanetary Soc.*, vol. 17, pp. 159–161; November/December, 1959.) "The various sources of noise with which a radio signal from a space probe must compete are discussed and evaluated. The power requirements for transmitting television pictures from the Moon or Mars are calculated for several possible systems."

SUBSIDIARY APPARATUS

621.3–71:537.322.1 2168

Thermoelectric Temperature Stabilization of Electrical Circuit Elements—G. Lautz. (*Elektrotech. Z.*, vol. 80, pp. 741–745; November 1, 1959.) The application of the Peltier effect to the cooling of semiconductor rectifiers and transistors is discussed.

621.316.722 2169

Low-Noise Electronic Voltage Stabilizers with Low Internal Resistance—G. Giachino. (*Alta Frequenza*, vol. 28, pp. 37–56; February, 1959.) The design of low-output-impedance stabilizers for voltages between 150 and 600 v is discussed.

TELEVISION AND PHOTOTELEGRAPHY

621.397.132:621.376.2 2170

Double Push-Pull Modulator with Valves—W. Beckmann. (*Z. angew. Phys.*, vol. 11, pp. 89–91; March, 1959.) A circuit is described for suppressing the carrier and the modulating signal while providing an adequate level of modulated output for use in the NTSC system of color television. This forms part of the experimental equipment described earlier [1372 of 1959 (Mayer)].

621.397.132.001.4 2171

A Precision Colour-Television Signal Source for Research Purposes—J. E. Benson. (*Proc. IRE* (*Australia*), vol. 20, pp. 472–486; August, 1959.) Equipment is described for producing color video signals with sufficient precision and stability to serve as a reference standard.

621.397.331.21 2172

Signal Distortion in the Supericonoscope—W. Dillenburger. (*Arch. elekt. Übertragung*, vol. 13, pp. 63–75; February, 1959.) The faults are considered which arise in image iconoscopes with potential equalization by the method of "electron irrigation." [See 2632 of 1952 (Cope, *et al.*).] A quantitative investigation of distortion effects is made and conclusions regarding optimum operating conditions are drawn.

621.397.331.21 2173

The Image Shape resulting from a Reduction of Electron-Optical Scale of Reproduction in Image Iconoscopes—U. Schmidt. (*Nachrichtentech. Z.*, vol. 9, pp. 64–67; February, 1959.) The reduction of image distortion by modifications of the magnetic and electrostatic field distributions is discussed.

621.397.61:621.372.542 2174

A New Vestigial-Sideband Filter for Television Transmitters in Band I—H. Menzel. (*Nachrichtentech. Z.*, vol. 9, pp. 90–94; February, 1959.) The design calculations for such a filter are given, and means of achieving conformity to CCIR and OIR specifications are described.

621.397.62 2175

The Determination of Power Losses in Valves for the Vertical and Horizontal Deflection Circuits in Television Receivers—E. Hartmann. (*Nachrichtentech. Z.*, vol. 9, pp. 61–63; February, 1959.) A method of determining the losses from an analysis of oscillograms is described.

621.397.62:621.382.2 2176

New Applications of Germanium Diodes in Television Receivers as Switches, Limiters, and Interference Inverters—W. Bruch. (*Elektron. Rundschau*, vol. 13, pp. 39–45; February, 1959.) Applications described include methods for interference suppression by signal limiting or inversion, and for remote control of oscillator frequency.

621.397.62:621.396.662 2177

The Design of Experimental Tuners for Bands IV and V—K. H. Smith. (*J. Telev. Soc.*, vol. 9, pp. 103–114; July-September, 1959. Discussion, p. 123.) The general principles, construction and performance of experimental UHF tuners are described and compared with models developed in the U.S.A. and Germany.

TRANSMISSION

621.396.61:621.375.2 2178

An Accurate Calculation of Current Amplitudes in Transmitter Amplifiers—D. Thielicke. (*Nachrichtentech. Z.*, vol. 9, pp. 50–55; February, 1959.) A general solution of the current-flow angular function is derived.

621.396.712.029.62:621–523.8 2179

Automatic Control of U.S.W. Transmitter Operation—J. Brose. (*Elektrotech. Z.*, vol. 11, pp. 342–345; August 21, 1959.) Automatic equipment for switching on stand-by transmitters in unmanned stations is described. [See also 1576 of 1958 (Zehnel and Brose).]

TUBES AND THERMIONICS

621.382 2180

The Tunnel-Emission Amplifier—C. A. Mead. (Proc. IRE, vol. 48, pp. 359–361; March, 1960.) Theoretical considerations supported by experimental results for metal-insulator junctions, indicate that tunnel diodes and triodes may be operated at extremely high frequencies; but more development work is required to realize their theoretical capabilities.

621.382.2:621.318.57 2181

A Gallium Arsenide Switching Diode—R. I. Walker, F. A. Cunnell, C. H. Gooch and J. J. Low. (*J. Electronics Control*, vol. 7, pp. 268–269; September, 1959.) The method of making the diode and some electrical properties are given. Switching time from a low- to a high-impedance state is less than 2 mμsec.

621.382.2:621.375.9:621.372.44 2182

Frequency Dependence of the Equivalent Series Resistance for a Germanium Parametric-Amplifier Diode—S. T. Eng and R. Solomon. (Proc. IRE, vol. 48, pp. 358–359; March, 1960.) Measurements on diodes in ozone, and wet and dry oxygen over the frequency range 0.2–2.0 kmc show the resistance to be proportional to $1/f^2$. The results can be explained by assuming a constant surface resistance shunting the transition capacitance.

621.382.23:621.375.9 2183

Tunnel (Esaki) Diode Amplifiers with Unusually Large Bandwidths—E. W. Sard. (Proc. IRE, vol. 48, pp. 357–358; March, 1960.) An analysis, supported by measurements, is given for three connections of negative-conductance amplifier operated with lumped-constant filters that give an over-all maximally flat response.

621.382.33 2184

Field Effect on Silicon Transistors—B. Schwartz and M. Levy. (Proc. IRE, vol. 48, pp. 317–320; March, 1960.) A direct method of calculating the surface recombination velocity of an operating device is developed.

621.382.33 2185

Maximum Stable Collector Voltage for Junction Transistors—R. A. Schmeltzer. (Proc. IRE, vol. 48, pp. 332–340; March, 1960.) The voltage is calculated for a given circuit configuration, mode of emitter bias, rate of heat generation and ambient temperature. Measurements confirm the validity of the theory.

621.382.33 2186

Transistor Equivalent-Circuit Modification due to Non-equipotential Base—L. J. Giacoletto. (*J. Electronics Control*, vol. 7, pp. 233–242; September, 1959.) The assumption of an equipotential base region is generally not valid even at small currents. The effects of the voltage gradient can be accommodated by introducing a resistance into the equivalent circuit. A formula for this resistance is derived and the consequences of its presence are studied in relation to measurements.

621.382.333 2187

Semiconductors—(*Electronic Technologist*, vol. 37, pp. 148–149; April, 1960.) The form of construction of two types of Si transistor is described pictorially:

1) a mesa-type transistor suitable for HF operation;

2) a four-layer *p-n-p-n* switching device.

621.382.333.33 2188

The Characteristic Frequencies of a Drift Transistor—J. M. Rollett. (*J. Electronics Control*, vol. 7, pp. 193–213; September, 1959.) Specific characteristic frequencies are related to each other, to basic transistor parameters and to minority carrier time constants using theory of the simple one-dimensional model. Approximations are given for the frequency variations of current gain, and effects of junction capacitances and base resistance are considered. The maximum frequency of oscillation is discussed.

621.383.4:621.391.822 2189

Current Fluctuations in PbS Cells—F. M. Klaassen and J. Blok. (*Physica*, vol. 24, pp. 975–984; December, 1958.) Results are given of measurements of the noise spectrum and response of PbS photoconductive cells in the range 1 cps–20 kc.

621.385.001.4:621.317.3 2190

Simplified Electrical Measurement and Test Methods in the Mass Production of Re-

ceiver Valves—W. Kirschke. (*Nachrichtentech. Z.*, vol. 9, pp. 71–76; February, 1959.) Test methods and equipment suitable for use with automatic production techniques are described which have been developed on the basis of statistical analyses of tube faults.

621.385.004.6 2191
Problems relating to the Life of Receiver Valves with Oxide Cathode—S. Dietel. (*Nachrichtentech. Z.*, vol. 9, pp. 76–80; February, 1959.) The changes occurring in the structure and composition of oxide cathodes during the operation of the tube, and their effect on the life of the tube are reviewed.

621.385.032.213.13 2192
Evaporation and Diffusion Rate Measurements on Cathodes of Sintered Nickel Containing Alkaline-Earth Oxides—J. F. Richardson and F. A. Vick. (*Brit. J. Appl. Phys.*, vol. 11, pp. 73–77; February, 1960.) Measurements have been made using ^{140}Ba and tracer techniques. Activation energy of evaporation is 2.2–2.5 ev. Two diffusion processes operate, one predominant in the range 875°–1020°C and one below 875°C.

621.385.032.213.13 2193
Anode Surface Effects in Diodes Containing Oxide-Coated Cathodes—B. J. Hopkins. (*Brit. J. Appl. Phys.*, vol. 11, pp. 124–128; March, 1960.) A contact-potential-difference method was used to follow the changes in anode work function during activation of the cathode at different anode potentials. Emission poisoning effects are attributed to two separate contaminating films on the anode surface.

621.385.3:534.29 2194
Microphony Effects in some Amplifier Valves—H. Köhler and G. Uhlenbrok. (*Nachrichtentech. Z.*, vol. 9, pp. 80–83; February, 1959.) Methods of investigating microphony are discussed including the white-noise method described by Valkó, *et al.* (1981 and 3356 of 1957), which gives the most complete picture of the effects.

621.385.3:621.317.3:681.142 2195
Indicator Triode for Direct Data Read-Out.—Rodriques de Miranda and Rudich. (See 1891 of 1960.)

621.385.3:621.396.61 2196
The Triode in Class-C Transmitter Amplifiers—W. Junge. (*Nachrichtentech. Z.*, vol. 9, pp. 56–61; February, 1959.) A method is given of determining the operational power conditions from the characteristic curves of the triode.

621.385.3:621.396.61 2197
High-Power Transmitting Valves with Thoriated Filaments for Use in Broadcasting—H. S. Walker, W. H. Aldous, R. G. Roach, J. B. Webb and F. D. Goodchild. (*Proc. IEE*, pt. B, vol. 107, pp. 172–180; March, 1960.) Comparison with tubes having pure tungsten cathodes shows improved economy in operation and often longer life.

621.385.5 2198
Modern Double Triodes and their Application in Electronic Equipment—L. Starke. (*Elektronik*, vol. 8, pp. 45–48; February, 1959.) The principal data on some 30 different types of double triode are tabulated, and their properties and suitability for specific applications are summarized.

621.385.5:621.395.64 2199
Post Office Valves for Deep-Water Submarine Telephone Repeaters—M. F. Holmes and F. H. Reynolds. (*Proc. IEE*, pt. B, vol. 107, pp. 165–171; March, 1960.) The construction details and performance specification are given for two pentode tubes, types 10P1 and 10P2, for input and output use respectively. Particular attention is paid to long-term stability, avoidance of internal breakdown and efficient operation at low anode voltage.

621.385.6:537.533 2200
Knowledge in Physics as a Basis for the Technique of Modern Thermionic Valves—K. Pöschl. (*Nachrichtentech. Z.*, vol. 12, pp. 93–97; February, 1959.) The laws of physics underlying the development of drift tubes and traveling-wave tubes are considered. In particular, problems of statistics, nonlinear processes and electron-beam guidance are discussed.

621.385.6:537.533 2201
Single-Velocity Equivalents for Multivelocity Electron Streams—G. A. Gray. (*J. Appl. Phys.*, vol. 31, pp. 370–380; February, 1960.) Several problems are treated; in each case the actual multivelocity stream is replaced by an equivalent single-velocity stream. For a traveling-wave tube, it is found that a distribution of dc electron velocities has the same effect as an increase in the space-charge parameter QC. A class of re-entrant beam devices is examined and experimental results are cited which support the theory.

621.385.6:537.533 2202
On the Concept of Fictitious Surface Charges of an Electron Beam—E. L. Chu. (*J. Appl. Phys.*, pp. 381–388; February, 1960.) The electrodynamic phenomena in the boundary strip of a sharply focused electron beam are simplified for analysis by postulating a layer of surface current on the boundary of the imperturbed beam and eliminating the boundary strip; a layer of electric dipoles should also be postulated. Second-order quantities are included in all equations, so that the small-signal beam kinetic quantities can be calculated reliably.

621.385.6:621.375.9:621.372.44 2203
Theory of Fast-Wave Parametric Amplification—C. C. Johnson. (*J. Appl. Phys.*, vol. 31, pp. 338–345; February, 1960.) The fast-cyclotron wave in a beam-type parametric amplifier can be made relatively noiseless. An analytical description of the device is presented which includes a discussion of parametric amplification of the fast-cyclotron wave. A method of coupling to cyclotron waves is investigated, and design procedures for establishing optimum low-noise characteristics are outlined.

621.385.6:621.375.9:621.372.44 2204
A Microwave Adler Tube—T. J. Bridges and A. Ashkin. (Proc. IRE, vol. 48, pp. 361–363; March, 1960.) A description is given of the construction of an amplifier operating at 4140 mc with a noise figure of 2.3 db for double-channel operation and gains up to 24 db with a bandwidth of 67 mc.

621.385.62 2205
Drift Tube and Mutual Conductance of Klystron Amplifiers—R. Krönert. (*Nachrichtentech. Z.*, vol. 9, pp. 84–90; February, 1959.) The relation between drift-tube parameters and slope is determined theoretically treating the velocity-modulated electron beam as plasma and assuming Brillouin conditions for the focusing field. The application of the equations and curves derived is discussed, and consideration is given to large-signal conditions.

621.385.632.029.65 2206
A Half-Watt C.W. Travelling-Wave Amplifier for the 5–6 Millimetre Band—H. L. McDowell, W. E. Danielson and E. D. Reed. (Proc. IRE, vol. 48, pp. 321–328; March, 1960.) Description of the mechanical and electrical techniques used in the design of a practical CW power amplifier with a bandwidth of 10 kmc centred at 55 kmc.

Translations of Russian Technical Literature

Listed below is information on Russian technical literature in electronics and allied fields which is available in the U. S. in the English language. Further inquiries should be directed to the sources listed. In addition, general information on translation programs in the U. S. may be obtained from the Office of Science Information Service, National Science Foundation, Washington 25, D. C., and from the Office of Technical Services, U. S. Department of Commerce, Washington 25, D. C.

PUBLICATION	FREQUENCY	DESCRIPTION	SPONSOR	ORDER FROM:
Acoustics Journal (Akusticheskii Zhurnal)	Quarterly	Complete journal	National Science Foundation—AIP	American Institute of Physics 335 E. 45 St., New York 17, N. Y.
Automation and Remote Control (Avtomatika i Telemekhanika)	Monthly	Complete journal	National Science Foundation—MIT	Instrument Society of America 313 Sixth Ave., Pittsburgh 22, Pa.
	Monthly	Abstracts only		Office of Technical Services U. S. Dept. of Commerce Washington 25, D. C.
Journal of Abstracts, Electrical Engineering (Reseratívnyy Zhurnal: Electronika)	Monthly	Abstracts of Russian and non-Russian literature		Office of Technical Services U. S. Dept. of Commerce Washington 25, D. C.
Journal of Experimental and Theoretical Physics (Zhurnal Eksperimentalnoi i Teoreticheskoi Fiziki)	Monthly	Complete journal	National Science Foundation—AIP	American Institute of Physics 335 E. 45 St., New York 17, N. Y.
Journal of Technical Physics (Zhurnal Tekhnicheskoi Fiziki)	Monthly	Complete journal	National Science Foundation—AIP	American Institute of Physics 335 E. 45 St., New York 17, N. Y.
Proceedings of the USSR Academy of Sciences: Applied Physics Section (Doklady Akademii Nauk SSSR: Otdel Prikladnoi Fiziki)	Bimonthly	Complete journal		Consultants Bureau, Inc. 227 W. 17 St., New York 22, N. Y.
Radio Engineering (Radiotekhnika)	Monthly	Complete journal	National Science Foundation—MIT	Pergamon Institute 122 E. 55 St., New York 22, N. Y.
	Monthly	Abstracts only		Office of Technical Services U. S. Dept. of Commerce Washington 25, D. C.
Radio Engineering and Electronics (Radiotekhnika i Elektronika)	Monthly	Complete journal	National Science Foundation—MIT	Pergamon Institute 122 E. 55 St., New York 22, N. Y.
	Monthly	Abstracts only		Office of Technical Services U. S. Dept. of Commerce Washington 25, D. C.
Solid State Physics (Fizika Tverdogo Tela)	Monthly	Complete journal	National Science Foundation—AIP	American Institute of Physics 335 E. 45 St., New York 17, N. Y.
Telecommunications (Elekprosviaz')	Monthly	Complete journal	National Science Foundation—MIT	Pergamon Institute 122 E. 55 St., New York 22, N. Y.
	Monthly	Abstracts only		Office of Technical Services U. S. Dept. of Commerce Washington 25, D. C.
Automation Express	10/year	A digest: abstracts, summaries, annotations of various journals		International Physical Index, Inc. 1909 Park Ave., New York 35, N. Y.
Electronics Express	10/year	A digest: abstracts, summaries, annotations of various journals		International Physical Index, Inc. 1909 Park Ave., New York 35, N. Y.
Physics Express	10/year	A digest: abstracts, summaries, annotations of various journals		International Physical Index, Inc. 1909 Park Ave., New York 35, N. Y.
Express Contents of Soviet Journals Currently being Translated into English	Monthly	Advance tables of contents of translated journals		Consultants Bureau, Inc. 227 W. 17 St., New York 22, N. Y.
Technical Translations	Twice a month	Central directory in the U. S. of translations available from all major sources in the U. S.	OTS and Special Libraries Assoc.	Superintendent of Documents U. S. Gov't Printing Office Washington 25, D. C.

Section Meetings

(Continued from page 98A)

Lubbock

"Angular Modulation," Mr. Green, Panhandle Elec. 4/26/60.

Miami

Tour of WTHS-TV facilities emphasizing video tape equipment, Herb Evans, Dade County Board of Education. 4/19/60.

Montreal

"Ultra-Directional Microphones," Robert Ramsay, Electro-Voice, Inc. 4/27/60.

New York

"The Fledgling Engineer—Physicist or Technician," Dr. R. L. McFarlan, President of the IRE; Fellow Award Presentation. 1/17/60.

"Computer Applications in Space Vehicles," G. C. Randa, IBM. 2/3/60.

"Microwave Research & Development in Japan," A. A. Oliner, Microwave Inst. 3/2/60.

"A Probabilistic Network Approach to Reliability," Fred Moscowitz, Lab. for Electronics. 4/6/60.

"Esaki Diodes," G. C. Dacey, Bell Telephone Labs.; Election of Officers. 5/4/60.

Northern Alberta

"Handling High Speed Data on Microwave Systems," F. B. Bramhall, Lenkurt Elec. 4/26/60.

"Recent Research & Development in Geophysical Instrumentation," John Zowtiak, Accurate Exploration Ltd. 5/17/60.

Northern New Jersey

"Solid State Tunnel Diode," D. J. Donahue. RCA. 1/13/60.

"Present Status of Mechanized Information Retrieval Systems," H. P. Luhn, IBM; Tour of NCE facilities; Election of officers. 4/13/60.

"Satellite Systems for Commercial Communications," J. R. Pierce, Bell Telephone Labs. 5/11/60.

Northwest Florida

"Theory & Application of Digital Encoders," Daniel Griffin, United Aircraft Corp.; Joint Meeting with IRE-PGMIL and ARS. 3/29/60.

"Computation of Coasting Time From Measured Velocity of Missile During Powered Flight," Donald Colbert, Electronic Communications, Inc. 4/26/60.

Orlando

"Man in Space," G. M. Knauf, USAF, MC, Patrick Air Force Base. 4/20/60.

Ottawa

"How Much Space," J. E. Keister, GE Co. 4/8/60.

Philadelphia

"Satellite Technology," Sidney Sternberg, RCA, 4/6/60.

Phoenix

"Wireless Transmission of Microwave Power to Maintain a High Platform," Dr. R. L. McFarlan, President of IRE. 4/19/60.

Pittsburgh

"The Engineer's Place in Management," P. R. Sprowl, Westinghouse Elec. Corp.; Joint meeting with AIEE Pittsburgh Section. 4/18/60.

"The WBTR," M. A. Schultz, Westinghouse Elec. Corp.; Joint meeting with ANS. 4/19/60.

"An Introduction to the Analogue Computer," A. I. Katz, Electronic Associates, Inc. Joint meeting with IRE PGEC. 5/11/60.

(Continued on page 106A)

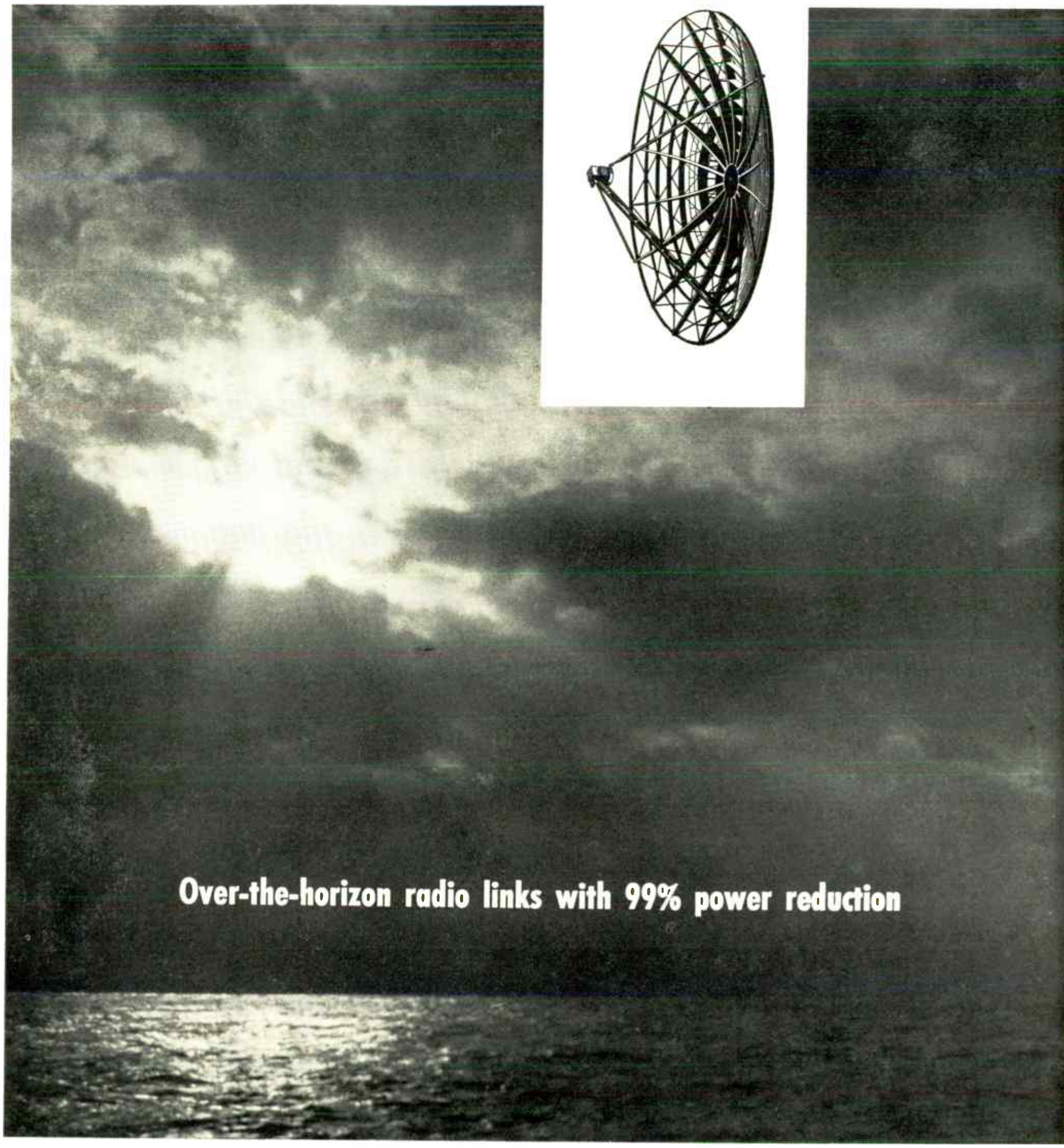

Here is an important new advance in microwave communications —NEC's High Sensitivity Reception system. By combining high sensitivity reception, parametric amplifier, low feeder loss design, and the high antenna gain possible at 2000 mc, this system improves S/N ratio by more than 20 db.

This permits hops at 1/1000 of the power required for conventional links. For example, a 400 W OH-2000 using a 33-ft dish and quadruple diversity is capable of a 300-mile hop at 99.0% reliability, or 99.9% reliability at 260 miles.

The OH-2000 is drastically reducing installation and maintenance costs of over-the-horizon links in capacities up to 60 voice channels. A descriptive brochure is available on request.

OH-2000 in military communications

First major OH-2000 installation will be a 17-station system for the United states Air Force linking radar sites on the three main islands of Japan. The system contains no active repeaters. Longest hop is 145 miles at 100 W output. Guaranteed reliability is a character error of no more than 1:10,000 for 99.9% of a year's hours.

OH-2000

The compact 100W transmitter uses economical planar tubes in the final stage. A quadruple diversity station requires a radio room of only 100 Sq. ft. NEC can also supply completely transistorized carrier equipment.

NEC *Nippon Electric Company Ltd.* Tokyo, Japan

Components / Systems

DONALD G. MACKEY, ROBERT J. BOWES, JR., Sylvania Picture Tube Operations, in the library at Seneca Falls, N.Y.

PROCEEDINGS *really takes a beating . . . FROM ITS READERS!*

If you've been in many company libraries, we're sure you've seen "dog-eared" copies of *Proceedings*. It's not a case of poor paper and printing—we use the best quality—it's just an example of pass-along readership taken to extremes!

Of course, 57,334 (ABC) professionally qualified men receive individual copies of *Proceedings* at home each month, as well as 13,976 students in engineering colleges. What's the reason for this important following?

Proceedings of the IRE enlisted the aid of the John Fosdick Organization to take a survey of its many readers to find out what they thought. Here are some of their reactions. "We use *Proceedings* as a reference. It's really a text. Has the largest amount in proportion of text, the highest quality text, and the largest amount of informational advertising of any book in the industry." And, of special interest to advertisers, one chief engineer said, "I've saved half-a-million dollars by buying from ads in *Proceedings,* and I've bought a quarter of a million dollars worth of equipment from the ads."

Fact is, 100% of those interviewed said they have some purchasing responsibility! And, as a further indication of the effectiveness of using *Proceedings* to reach buying factors of electronic equipment, components and supplies, these readers expressed a 2 to 1 preference for *Proceedings* when compared with mentions of all the electronic books. (Survey available upon request—ask for it!)

Are *you* now reaching this important, select audience for your product? You can, you know, reach them 12 times a year in *Proceedings* for just $8,640. (1960 rates). A similar schedule in a semi-monthly would cost $29,087.50 . . . and in a weekly, $46,280! Call or write today for all the facts. Find out what selling power *Proceedings* really has! Reach 61,957 (net paid circulation) top-level radio-electronics men each and every month throughout the year!

For a share in the present, and a stake in the future, make your product NEWS in

Proceedings of the IRE

The Institute of Radio Engineers

Adv. Dept. 72 West 45th St., New York 36, N. Y. • MUrray Hill 2-6606

BOSTON • CHICAGO • MINNEAPOLIS • SAN FRANCISCO • LOS ANGELES

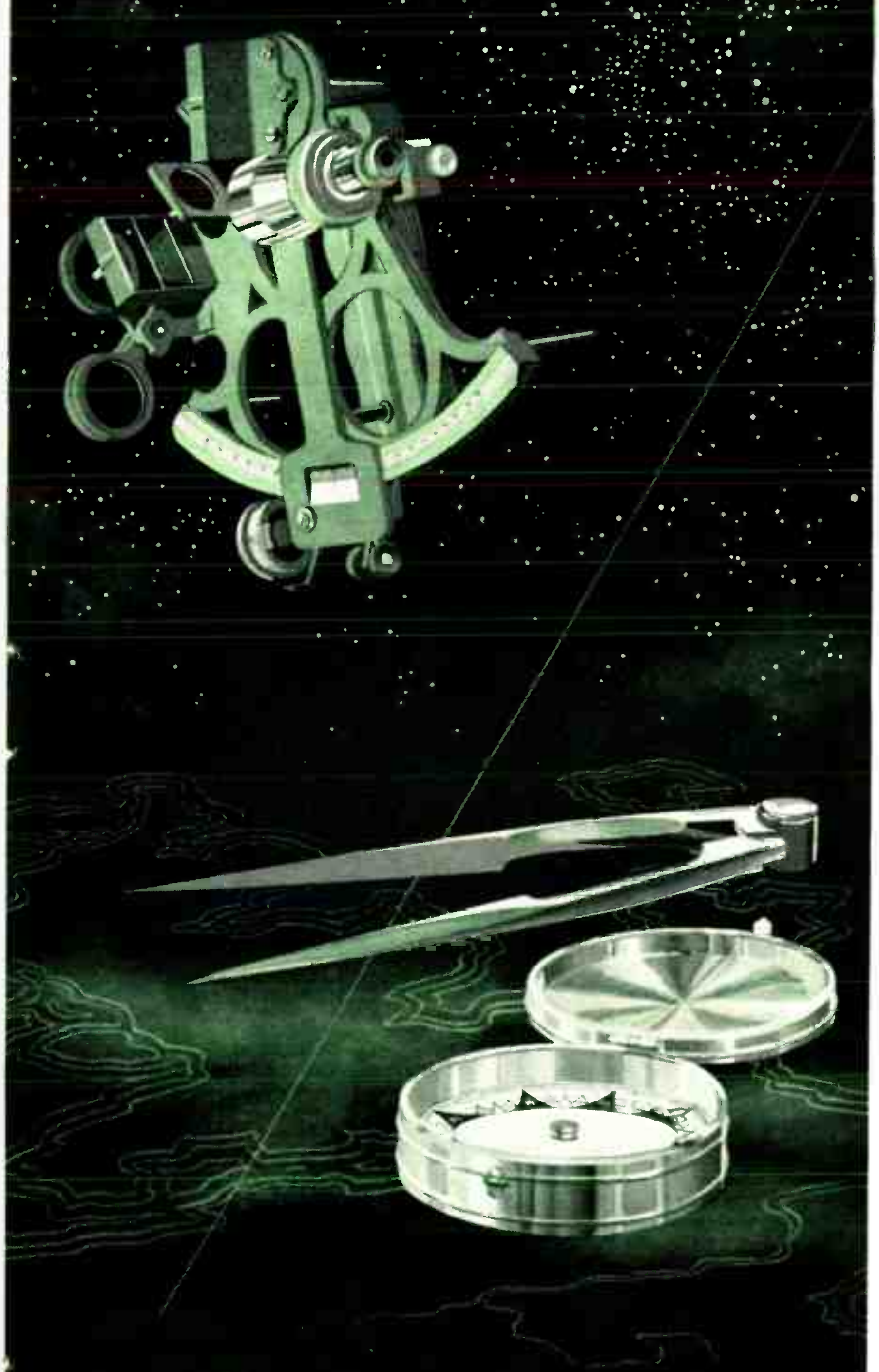

LFE

is experienced . . . in Advanced Systems

In times past, the leader in man's challenge of the unknown was the mariner with compass and sextant, and the vision to follow the stars.

Today, this challenge is being met by scientists with advanced training working in well-equipped laboratories.

At LFE, where one man in five is a physicist, mathematician or engineer, 2,700 years of advanced technical training are combined with 8,000 years of systems experience. This know-how has been a major factor in the frequent choice of LFE as prime contractor on Advanced Systems projects.

LFE has recently prepared a new series of Technical Data Digests covering each area of Company activity. Write the Vice-President of Marketing for series No. 6065.

LABORATORY FOR ELECTRONICS, INC., Boston 15, Massachusetts

SYSTEMS, EQUIPMENT & COMPONENTS FOR

AIRBORNE NAVIGATION • RADAR and SURVEILLANCE • ELECTRONIC DATA PROCESSING • AUTOMATIC CONTROLS • GROUND SUPPORT

Section Meetings

(Continued from page 102A)

PORTLAND

"Esaki Diode Principles and Application," C. N. Winningstad, Tektronix, Inc. 4/21/60.

PRINCETON

"Experiments Exploring the Mechanisms of Color Vision," E. H. Land, Polaroid Corp. 4/21/60.

QUEBEC

"Manufacture of Electric Meters & Permanent Magnets," I. Inculet and J. Morrison, Canadian GE Co. 4/9/60.

RIO DE JANEIRO

"1959 U.I.T. Conference in Genebra," J. Guriao Neto, Brazilian Navy. 4/13/60.

"Public Services," Gustavo Corcao, Escola Nacional de Engenharia: Election of Officers. 5/11/60.

ROCHESTER

"The Hall Effect and Its Applications," T. R. Lawson, Jr., Westinghouse Elec. Corp. 1/7/60.

"Synchronous Communication Systems," G. A. Franco, General Dynamics. 1/21/60.

"Human Factors Engineering in Electronic Systems," Jesse Orlansky, Dunlap Associates, Inc. 2/18/60.

"Numerical Machine Tool Control," F. A. Mitchell, and J. S. Fondrk, General Dynamics Corp. 3/17/60.

"The Eastman Kodak Minicard System," J. E. Morse, Eastman Kodak Co. 4/21/60.

ROME-UTICA

"The RCA Microminiaturization Program," Donald Mackey. 4/13/60.

SCHENECTADY

"Testing the SAGE System," S. J. Hauser, Jr.; Mitre Corp. 4/26/60.

SHREVEPORT

"Modern Stereo," P. W. Klipsch, Klipsch Associates, Demonstration of the "Brussels System." 4/5/60.

"Hycalog Products and Services," J. H. Hartwell and H. R. Chism, Hycalog Inc., Plant Tour. 5/3/60.

SOUTH BEND-MISHAWAKA

"Human Attitudes & Reliability," Dave Christian, Bendix Products Div. 1/28/60.

"Parametric Amplifiers," R. S. Englebrecht, Bell Telephone Labs. 2/25/60.

"Electronic Applications in Heavy Industry," Jerry Roedel, The Hallicrafters Co. 3/31/60.

SOUTH CAROLINA

Résumé of IRE International Convention by W. R. Boehm, U. S. Navy; Tour of WUSN-TV. 3/31/60.

"Manufacture of Carbon Deposited Resistors," J. Appleby, Western Elec. Co. 4/25/60.

SYRACUSE

"The Fledgling Engineer—Physicist or Technician?" Dr. R. L. McFarlan, President IRE; "Thermoplastic Recording," I. C. Abrahams, GE Co.; Student Awards Presentation; Election of Officers. 5/10/60.

TOLEDO

Plant Tour—Sylvania Electric. 4/21/60.

(Continued on page 110A)

ALITE®

CERAMIC-TO-METAL SEALS

Standard Bushings or Special Designs

FROM ONE COMPLETELY INTEGRATED SOURCE

ALITE — with its completely equipped facilities for producing high quality, vacuum-tight, ceramic-to-metal seals — is geared to meet all your requirements for high alumina ceramic-metal components. From design to finished assembly, every manufacturing step — including formulating, firing, metalizing and testing—is carefully supervised in our own plant. Result: effective quality control and utmost reliability.

Hermetic seals and bushings made of high alumina Alite are recommended for electromechanical applications where service conditions are extremely severe or critical. Alite has high mechanical strength and thermal shock resistance. It maintains low-loss characteristics through a wide frequency and temperature range. It resists corrosion, abrasion and nuclear radiation. Its extra-smooth, hard, high-fired glaze assures high surface resistivity.

To simplify design problems and speed delivery, Alite high voltage terminals, feed-throughs and cable end seals are available in over 100 standard sizes. However, when specifications call for special units for unusual applications, you can rely on expert assistance from Alite engineers to help you take full advantage of Alite's superior properties.

Write us about your specific requirements today.

WRITE FOR HELPFUL FREE BULLETINS

Bulletin A-7R gives useful comparative data. Bulletin A-40 describes Alite facilities and complete line of Alite Standard Bushings.

ALITE DIVISION

U. S. STONEWARE

BOX 119 ORRVILLE, OHIO

New York Office — 60 East 42nd St.

102-G

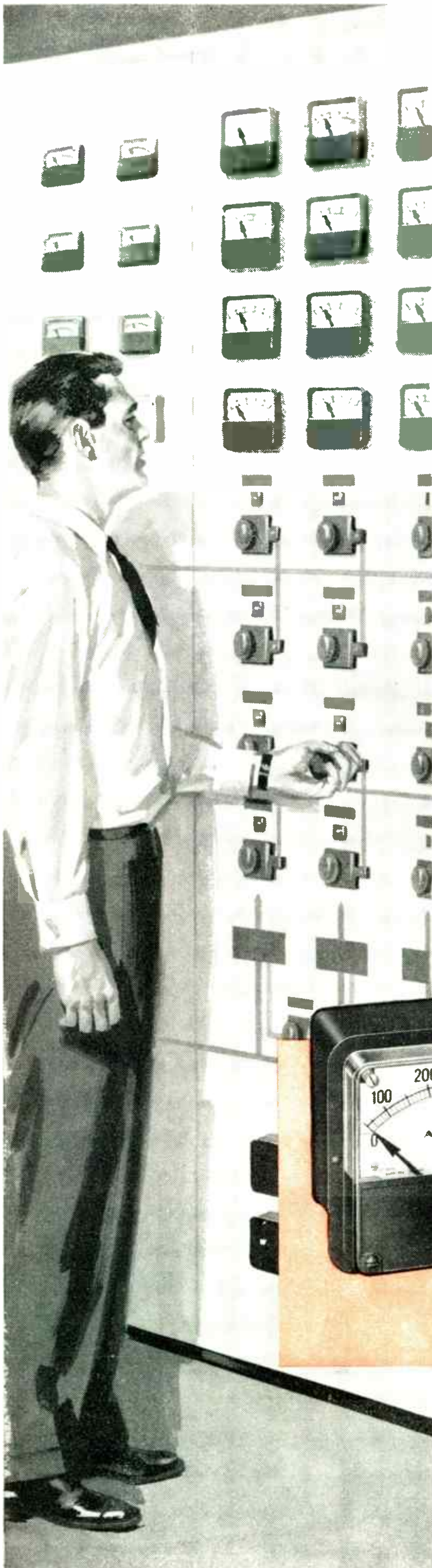

WESTON SWITCHBOARD INSTRUMENTS SOLVE PROBLEMS OF RANGE, ACCURACY, SPACE

Models and types available for every application

Weston Switchboard Instruments provide basic accuracies of ±1% full scale, and can be made to meet more exacting requirements. They are supplied in groups of matching units in a wide variety of models and ranges.

All models are available with internal illumination, or with clear plastic fronts for exceptional visibility. "In-line" pointers and scales eliminate reading errors caused by parallax. For even more precise measurement, they can be supplied with knife-edge pointers and mirror scales.

Model 610 Group is supplied with 4 x 4.5″ Bakelite cases. Scales are 3.5″ long. CORMAG® mechanisms permit mounting on magnetic or non-magnetic panels without special adjustment. These instruments are ideal for compact installations where one operator controls a large number of circuits.

Model 921 Group consists of 5.75 x 6″ instruments with 5.21 scales. Rugged steel cases provide shielding against external magnetic fields. This group is particularly suitable where good readability under adverse conditions is required.

Call your Weston representative for details on how these instruments can be adapted to your most critical specifications, or write for Catalog 01-200. Daystrom, Incorporated, Weston Instruments Division, Newark 12, New Jersey.
International Sales Division, 100 Empire St., Newark 12, N. J.
In Canada: Daystrom Ltd., 840 Caledonia Rd., Toronto 19, Ontario.

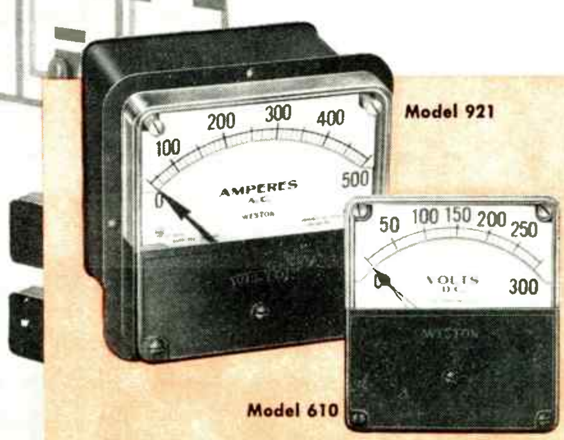

Model 921

Model 610

Model 610 and 921 Groups have 90° arc movements, high torque to weight ratios, can withstand heavy overloads. Available as: AC and DC voltmeters and ammeters, rectifier-type instruments, single element and polyphase wattmeters and varmeters, power factor and frequency meters, and thermocouple instruments.

DAYSTROM, INCORPORATED
WESTON INSTRUMENTS DIVISION
Reliability by Design

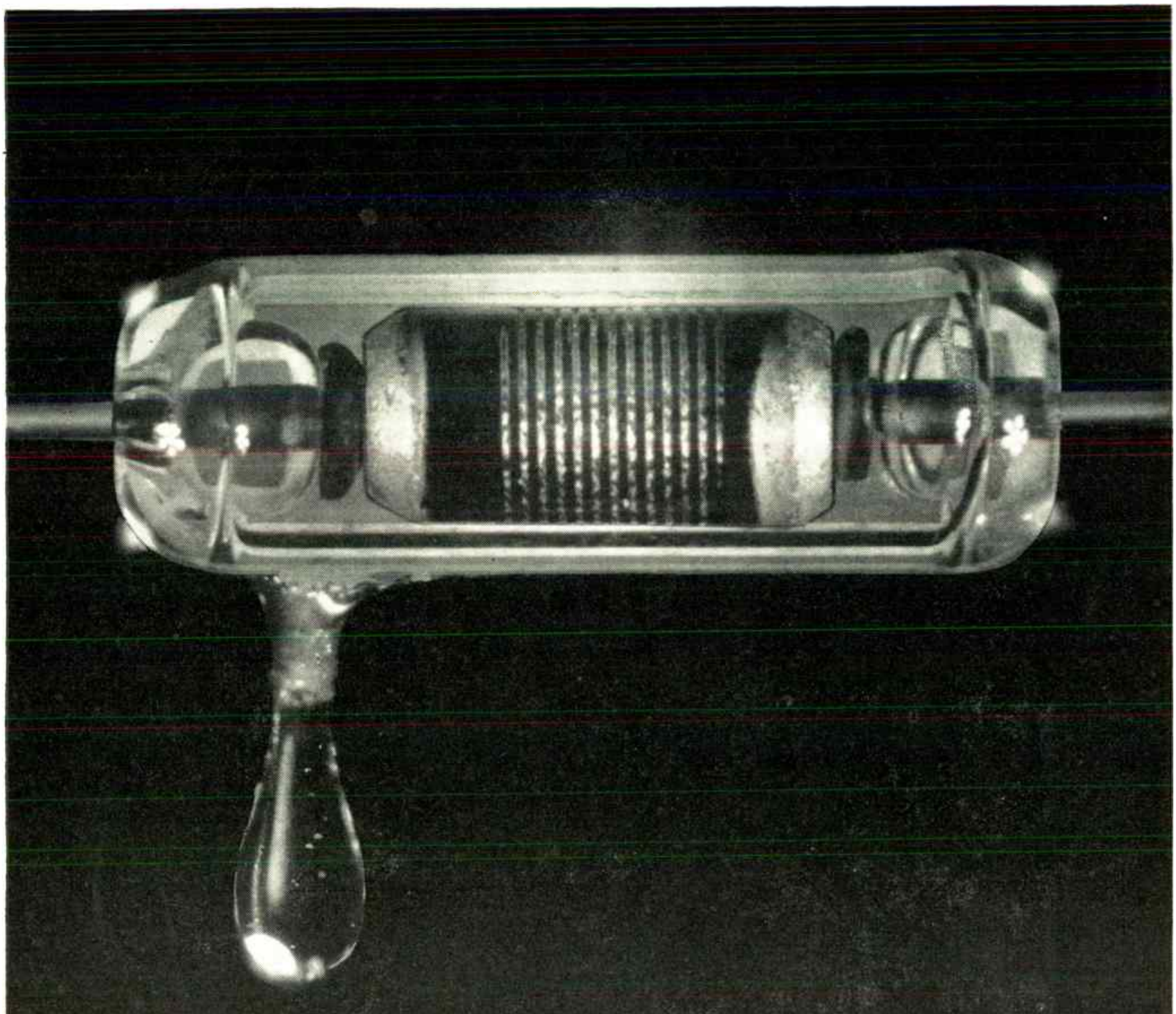

MOISTURE ABSORPTION
IS NAUGHT, NIL, ZERO
IN CORNING NF RESISTORS

Glass-enclosed, fusion-sealed Corning NF resistors have boiled merrily in salt water for days without showing a jot of change in their electrical characteristics.

These are resistors that are rugged, completely moisture resistant, highly vibration resistant . . . in short, resistors that exceed the requirements of MIL-R-10509C, Char. B, better than any we've seen or heard of.

The key to such fortitude is our NF structure. We start with glass rods with metal oxide applied under heat. This in itself makes a moisture-resistant, almost abnormally stable resistor, as you well know if you have ever used our regular N-style resistors.

We encapsulate this basic unit in a glass envelope and apply glass-to-metal seals at the leads . . . comparable to those in a vacuum tube.

IMMEDIATE DELIVERY • There are two models of this gem in production, ready for *quick shipment:* the ⅛-watt NF-60 and the ¼-watt NF-65. Resistance ranges from 100 ohms to 360K ohms. Voltage ratings are 250v and 300v. Full rating at 70°C. with derating to 150°C. More data:

Load life 0.3%
Voltage coefficient 0.001%/v
Temp. coefficient . . . . . . 0.03%/°C.
Insulation resist. . 100,000 megohms

To get this and other data for your file, just write and ask for Data Sheet CE-2.02. Address: Corning Glass Works, 542 High Street, Bradford, Pennsylvania.

CORNING ELECTRONIC COMPONENTS

CORNING GLASS WORKS, BRADFORD, PA.

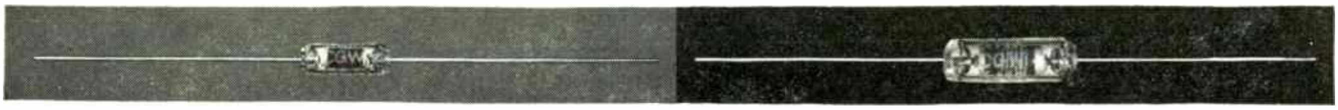

⅛-WATT NF-60 ACTUAL SIZE ¼-WATT NF-65

Section Meetings

(Continued from page 106A)

TUCSON

"The Orbiting Astronomical Observatory Program of AURA, Inc.," Russell Niday, AURA, Inc. 4/12/60.

"Guided Missile Systems," D. T. Wangsgard, Hughes Aircraft Co. 5/10/60.

VANCOUVER

"Communications for a Gas Pipeline," T. G. Lynch, Westcoast Transmission Co., Ltd. 3/21/60.

"Power Line Carrier Systems," Roland Reader, B. C. Elec. Co., Joint meeting with AIEE Vancouver Section. 4/11/60.

Field Trip—Dominion Radio Astrophysical Observatory. 4/30/60.

WESTERN MASSACHUSETTS

"Extra High Voltage Instrumentation," A. H. Foley, GE. 3/13/60.

"New Telephone Equipment for the Home," E. S. Moss, New England Telephone Co. 5/11/60.

WILLIAMSPORT

Election of Officers. 4/20/60.

"The IRE Today and Tomorrow," J. N. Dyer, Airborne Instrument Lab.; "Satellite Studies of the Ionosphere," W. J. Ross, Pa. State Univ.; Joint meeting with Central Pa. and Emporium Sections. 5/17/60.

SUBSECTIONS

EASTERN NORTH CAROLINA

"Cold Logic: The Story of the Persistatron," C. R. Vail, Duke University. 3/13/60.

KITCHENER-WATERLOO

"R-C Synthesis of Transistor Networks," B. R. Myers, Univ. of Waterloo; Election of Officers. 4/4/60.

General Tour of Nuclear Reactor, W. H. Fleming, McMaster Univ. 4/14/60.

LANCASTER

"The Tunnel Diode," Jack Hillebrand, RCA. 3/17/60.

MEMPHIS

Plant Tour, Fryling Electric Co. 4/28/60.

"A Single Side-Band Exciter Employing a New Beam Tube," Mr. Vance, RCA. 5/2/60.

MERRIMACK VALLEY

"Standards & Specifications? Yes!," R. L. Keller, GE Co., L. V. Porter, GE, A. Rosenwald, Raytheon. 3/21/60.

MID-HUDSON

"Instrumentation for Space Vehicles," John O'Hara, GE Co.; Joint meeting with AIEE. Mid-Hudson Section. 1/18/60.

"Glass in Electronics," G. W. McLellan, Corning Glass Works. 2/17/60.

"FM Reception in Fringe Areas," L. F. B. Carini, Apparatus Development Co.; Election of Officers. 3/9/60.

"The International Electro-Technical Commission," H. J. Geisler, IBM. 3/15/60.

MONMOUTH

"The Evolution of High Fidelity Sound Reproduction," H. F. Olson, RCA Labs.; Presentation of Fellow Awards. 2/17/60.

Field Trip.—I.T.&T. Labs. 3/16/60.

"Signal Detection with Matched Filters," G. S. Sebestyen, Melpar Communications Research Lab. 4/20/60.

(Continued on page 112A)

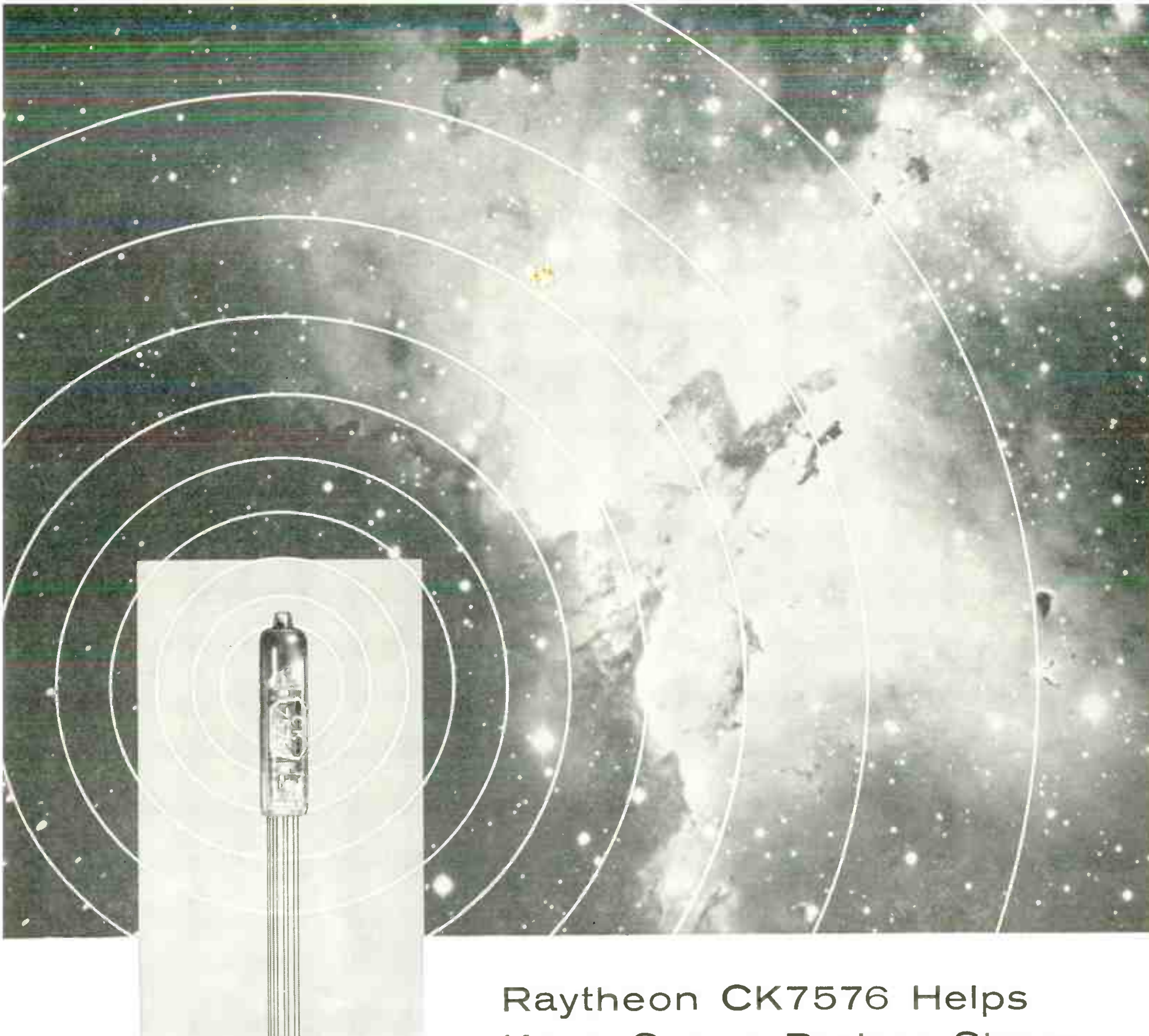

CK7576 CHARACTERISTICS AND TYPICAL OPERATION: 235Mc GROUNDED GRID RF AMPLIFIER

Filament Voltage	6.3 ± 5% volts
Plate Voltage	200 volts
Cathode Resistance	150 ohms
Peak RF Grid to Cathode Voltage	14 volts
Grid Current	10 mAdc
Plate Current	37 mAdc
RF Driving Power (Approx.)	0.5 watts
Useful Power Output	3.25 watts

RAYTHEON

Raytheon CK7576 Helps Keep Space Probes Sharp

Effective missile operation depends on compact, reliable telemetering made possible by components such as the CK7576.

The Raytheon CK7576 is a subminiature triode providing over 3 watts output at 235Mc in grounded grid RF power amplifier service. It offers designers of spaceborne telemetering equipment the advantages of excellent isolation between input and output circuits, high transconductance, high amplification factor, and impressive power-handling capabilities.

If your area of design interests includes airborne communication and navigation applications make it a point to investigate the CK7576 as well as the other versatile types in Raytheon's full line of subminiature tubes. For technical information, please write to: Raytheon, Industrial Components Division, 55 Chapel St., Newton 58, Massachusetts.

For Small Order or Prototype Requirements See Your Local Franchised Raytheon Distributor.

RAYTHEON COMPANY

INDUSTRIAL COMPONENTS DIVISION

Section Meetings

(Continued from page 110A)

NEW HAMPSHIRE

"Micro Wave Cooking," Mr. & Mrs. Roger French, Servodyne Corp.; Election of Officers. 4/27/60.

NORTHERN VERMONT

"High Fidelity—Acoustic Suspension Speaker," Maurice Rotstein and Chuck Israels, Acoustic Research Lab. 4/25/60.

PANAMA CITY

"Percos—Performance Coding System," E. A. Keller, Motorola, Inc. 5/18/60.

SANTA BARBARA

"Report from Geneva," James Hacke, GE (TEMPO). 4/19/60.

WESTCHESTER

"Medical Electronics," Carl Berkely, Rockefeller Inst. 4/20/60.

WESTERN NORTH CAROLINA

"The Three-Two Plan for Engineering Training," C. J. Pietenpal, Davidson College; Tour of Dana Science Lab. & Language Lab. 4/22/60.

NEWS New Products

(Continued from page 28A)

Ferrite Components

A new line of millimeter-wave ferrite components is now available from **T.R.G., Inc., Microwave Component and Antenna Dept.,** 9 Union Square, Somerville 43, Mass., to the microwave engineer working in the V-Band, covering 60–75 kmc. The new components include a compact ferrite isolator, a fast-operating ferrite on-off-switch or variable attenuator, a ferrite circulator, and a ferrite high-power reciprocal switch.

These are believed to be the first V-Band components of this type to be available commercially.

Lightweight and miniaturized, each component will withstand pressurization to 30 psi.

Ferrite Isolator, Model V-FL 1, is used to isolate generator from load. It operates as a non-reciprocal 45° rotator with a permanent magnet supplying the bias field. Isolation is larger than 17 db over at least a 3% band with insertion loss less than .6 db.

Ferrite On-Off Switch or Variable Attenuator, Model V-FSW 1, is a low-power lightweight fast-operating switch with high isolation when off, low loss when turned on. Switching is accomplished by a coil in 1 to 2 microseconds.

Ferrite Circulator, Model V-FC 1, is a lightweight four-port device using polarization rotation as the basic non-reciprocal element. A non-reciprocal 45° rotator combined with dual-mode transducers plus input and output taper sections make up the complete circulator. Peak power unpressurized is 10 kw, average power 2 watts.

The Ferrite High-Power Reciprocal Switch, Model V-FSW 2, is a reciprocal lightweight ferrite rotator switch. By means of a ferrite rotator and dual-mode transducer an input signal may be switched to either of two arms. Switching time is 1 to 2 microseconds. Peak power is at least 10 kw, unpressurized.

All components are available from stock and are designed to meet military standards. A catalogue complete with detailed specifications is available by writing to the firm.

(Continued on page 130A)

The new model RD-190 16-32 Mc Continuous Coverage Synthesizer incorporates 8 million discrete crystal frequencies to choose from.

Highly stable, continuous coverage of the 16-32 Mc spectrum is accomplished by the Manson RD-190 Crystal Synthesizer, with a single one-megacycle crystal as the internal reference. Double superheterodyne circuitry is employed in the indirect method of synthesis to discipline freerunning oscillators, the RD-190 is of unique character in that the fundamental crystal frequency is linearly tuned over a range of 62.5 parts per million — without degradation of stability — in order to offset the internal harmonic reference spectrum precisely as needed for "Cycles" accuracy.

Three variable frequency oscillators, providing tuning increments of 100 kc, 10 kc, and 1 kc, are phase-locked to the reference in an all-electronic system in which no mechanical servos are used. Pull-in and hold-in characteristics are equal and instantaneous over the entire band. The setting of frequency to cycles is accomplished by direct control of the crystal, which is capacitively trimmed to an accuracy of better than 1 part in 10^7.

Frequency readout is displayed by means of counter-type dials across the front panel, assuring zero error readability and resettability. Fast drive lever knobs permit the setting of any frequency in a matter of seconds, and since tuning condensers are linear, the unit is adaptable to remote operation.

MANSON PROVIDES EIGHT MILLION DISCRETE CRYSTAL FREQUENCIES IN ONE SPACE-SAVING UNIT!

FREQUENCY STABILITY: Better than 1 part in 10^8 per day
OUTPUT FREQUENCY RANGE: 16 to 32 Mc, continuously tunable (non-incremental).
TUNABILITY ACCURACY: Better than 1 part in 10^7.
RESETTABILITY ACCURACY: Zero error
READABILITY ACCURACY: Zero error
SPURIOUS SIGNALS: Down a minimum of 80 db, except for harmonics of the output
OPERATING AMBIENT TEMPERATURE RANGE: 0 to +50°C
OUTPUT POWER: 100 milliwatts minimum
OUTPUT IMPEDANCE: 50 ohms nominal
NUMBER OF QUARTZ CRYSTALS: One
INPUT POWER REQUIRED: 105/125 volts, 60 or 400 cps, 1 phase
DIMENSIONS: 18" W x 12" H; depth, 16"
MOUNTING: For rack or bench use

manson

MANSON LABORATORIES, INC.

375 FAIRFIELD AVENUE / STAMFORD, CONNECTICUT / DAvis 5-1391

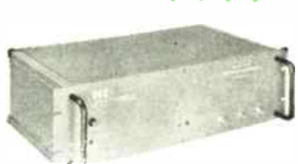

Model RD-170
1000 Mc reference generator

Model RD-141
1 Mc transistorized oscillator in mercury switch oven

Model N-317
2 Mc to 34 Mc crystal frequency synthesizer

Positions Open

The following positions of interest to IRE members have been reported as open. Apply in writing, addressing reply to company mentioned or to Box No. . . . .

The Institute reserves the right to refuse any announcement without giving a reason for the refusal.

Proceedings of the IRE
1 East 79th St., New York 21, N.Y.

TEACHING POSITIONS

The E.E. Dept. of The City College of New York has several positions available on the teaching staff beginning September 1960. Rank and salary commensurate with qualifications and experience. Opportunity for graduate study. Applicants must be present resident of the U.S. Address inquiry to Prof. H. Taub, Dept. of E.E., The City College, Convent Ave., & 139th St., New York 31, N.Y.

ENGINEERS

The University of Denver's Research Institute is seeking graduate electronic engineers in the areas of circuit design and development, system design, and field engineering. Openings exist at all levels from engineers with advanced degrees and several years experience to recent graduates. Opportunities are available for advanced study or part-time teaching in the College of Engineering. Address inquiries to C. A. Hedberg, Head, Electronics Div., Denver Research Institute, University of Denver, Denver 10, Colo.

ELECTRONICS PATENT ATTORNEY OR AGENT

Eastern U.S. company engaged in a broad line of developments in the electronics field has an opening for a patent attorney or agent. Applicant should have excellent comprehension of electronics, together with some experience in patent prosecution. Salary and position will be dependent on background and indicated ability. In reply please supply information as to education, experience and salary expected. Box 2017.

ANALOG COMPUTER ENGINEER

The Standard Oil Co. (Ohio) has an immediate opening for an Analog Computer Engineer. A minimum of a B.S. in E.E. or Physics and 2-5 years analog experience is required. Applications are in the field of simulation and study of chemical and refining processes and process control systems. Salary commensurate with experience. Apply Mr. C. A. Bruggers, The Standard Oil Co. (Ohio), 1737 Midland Bldg., Cleveland, Ohio.

MEDICAL ENGINEERING

Electronics Engineer or Physicist. Permanent position in Dept. of Surgical Research of a large eastern university, involves design of new instruments, supervision of maintenance of equipment, and consulting with physicians. Salary range open. Send complete resume to Box 2019.

ENGINEER

Engineer to conduct a research and development program on instrumentation for data accumulation, reduction, and processing in geology, water resources investigations, photogrammetry, and allied fields including the development of new equipment and techniques for sensing, digitizing, logging, transmitting, storing, and processing of mass data. Contact Personnel Officer, U.S. Geological Survey, Washington 25, D.C.

(Continued on page 118A)

SURFACE STUDIES:

qualified research men wanted at T/I...

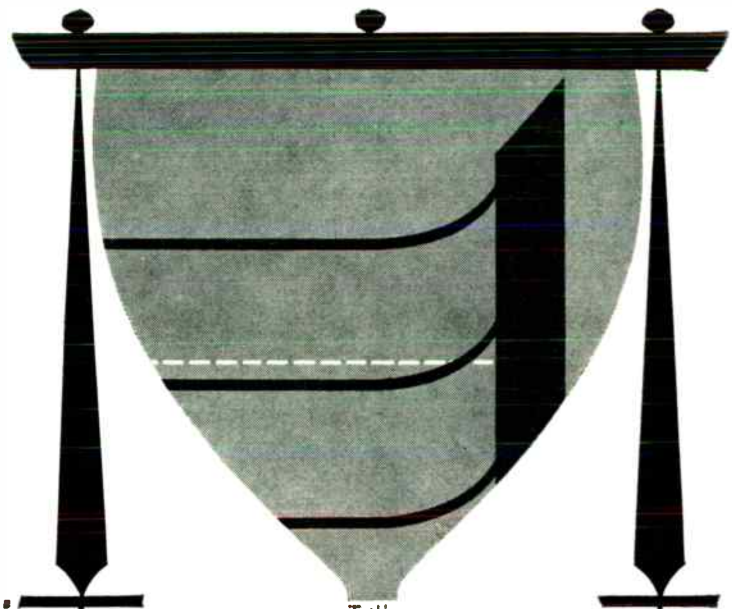

T/I's expanding Semiconductor-Components division is looking for experienced scientists whose background qualifies* them for advanced research in the fields of silicon, germanium and intermetallic semiconductor surfaces. At Texas Instruments the scientist will find a creative environment ready to make immediate use of his present capabilities. It offers him the challenge of making significant contributions to an expanding field. These characteristics of the T/I climate constantly demand and renew the scientist's own highest level of achievement. If a responsible post in this sort of environment intrigues you, send in the coupon below with a statement of your particular interests and background.

*******You qualify for one of these key posts in semiconductor surface research if you have an advanced degree with related experience.* We have openings for Chemists, Physicists, Electrical Engineers, Metallurgists. Background in one or more of the following fields is desirable: surface physics, surface chemistry, electrochemistry, corrosion, etching, ohmic contacts, noise. Actual semiconductor experience, while valuable, is not essential. Surface studies research at T/I offers the opportunity to work on a wide range of theoretical and applied problems.

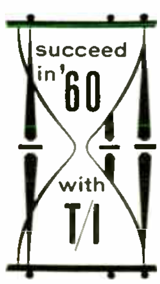

INTERVIEWS in your area will be held in the near future. If you qualify for positions described, please send resume immediately to C. A. BESIO, Dept. 120.

TEXAS INSTRUMENTS INCORPORATED

SEMICONDUCTOR - COMPONENTS DIVISION
POST OFFICE BOX 312 • DALLAS, TEXAS

For complete information about T/I's Semiconductor-Components division, send coupon for "TIPS" today.

TEXAS INSTRUMENTS INCORPORATED
Semiconductor-Components division
P. O. Box 312, Dept. 120, Dallas, Texas

Please send me "TIPS" containing complete information about currently available T/I S-C professional careers in my field, and related information.

NAME ______________________

ADDRESS ______________________

CITY ______________ STATE ______

My professional field is ______________________

My specialty is ______________________

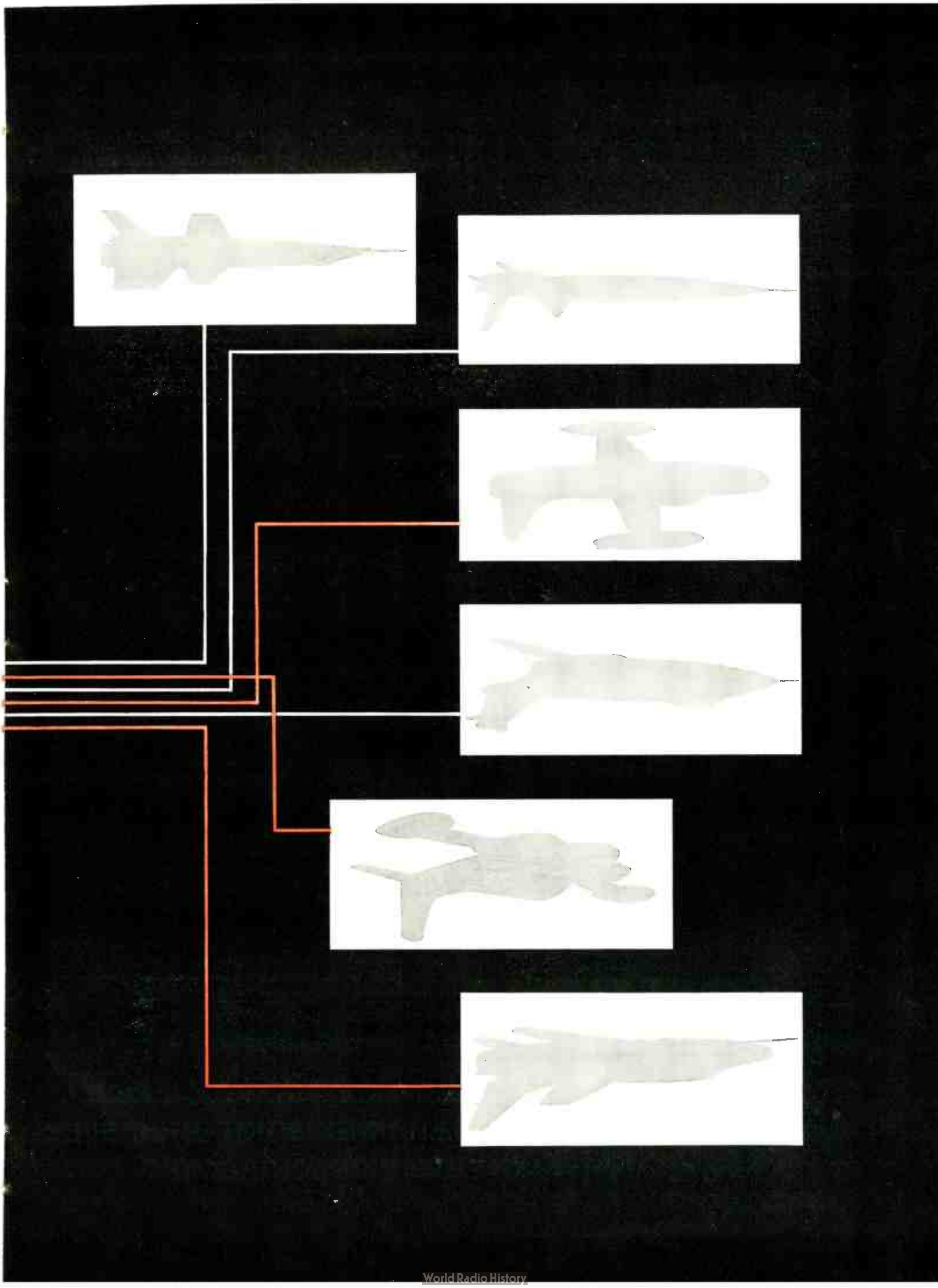

working . . .
with systems that know how to adapt

Like man—Honeywell's Adaptive Autopilot can accommodate, in fact, can adapt. Anthropomorphic? Perhaps—nonetheless, this system has the capacity to change its own parameters through an internal process of measurement, evaluation, and adjustment. It operates independently of air data information and complex gain scheduling—and is unaffected by changes in aerodynamic characteristics. Simply, it adjusts itself in response to its own performance.

Without major modifications, the Adaptive Autopilot can be adapted to air vehicles of all types—from business aircraft, helicopters, drones, supersonic fighters and bombers, and missiles—to the latest hypersonic research vehicles.

Adaptive flight control systems are another example of Honeywell Aeronautical's accomplishments in advanced control. Other developments include electrically suspended gyros, guidance control and environmental control systems, and "decision-making" pre-launch checkers. The division's competence has been demonstrated by contributions to Sergeant, Thor, Atlas, Titan, Polaris, Centaur, Wagtail, F-104, B-58, WS 117L, X-15, F-101, B-66 and WF2. Current expansion has created openings for engineers and scientists in these and similar programs throughout the country and abroad.

Examples of the variety of aircraft and missiles that can be flown with Honeywell Adaptive Autopilots

living . . .
with people that know how to live

Honeywell engineers and their families find facilities are readily accessible for the things they enjoy.

For the sports minded, the Twin Cities offer Big Ten Football, professional hockey, and in 1961, National League Football. And with its Metropolitan Stadium, one of the country's finest baseball parks, major league baseball seems inevitably near.

Outdoor enthusiasts enjoy this area for its easy access to hunting, fishing, golfing, tennis, swimming, boating—or in winter, skating, skiing, sledding, ice fishing, and ice boating. And the popularity of sailing and yachting is evidenced by the existence of many fine clubs of this type.

Those who appreciate the arts enjoy the Twin Cities as a cultural center . . . listening to the Minneapolis Symphony Orchestra—browsing through the Minneapolis Institute of Art or Walker Art Center—enjoying opera and ballet at Northrup Memorial Auditorium, or legitimate theatre at one of the area's fine playhouses.

These are some of the activities that make this an area for "living." And they're an important part of the life enjoyed by Honeywell engineers and their families.

Inquiries on opportunities with Honeywell Aeronautical will get prompt and confidential attention. Write Mr. James A. Burg, Technical Director, Dept. 729A, Aeronautical Division, 1433 Stinson Blvd. N.E., Minneapolis 13, Minnesota.

Honeywell

H HONEYWELL *Military Products Group*

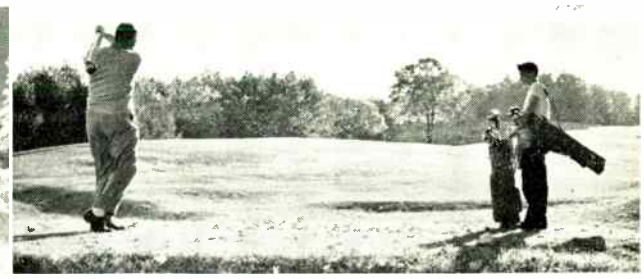

To explore professional opportunities in other Honeywell operations coast to coast, send your application in confidence to H. K. Ekstrom, Honeywell, Minneapolis 8, Minn.

Positions Open

(Continued from page 114A)

ELECTRONIC ENGINEER

Electronic Engineer to teach lecture and laboratory courses. Up-to-date knowledge of the field required. Working and living conditions excellent; salary and opportunity very attractive. Write to Dean of Engineering, California State Polytechnic College, San Luis Obispo, Calif.

ELECTRICAL ENGINEERING

Excellent opportunities for qualified Ph.D.'s in logical design, network synthesis and other areas. Rank and salary commensurate with research and teaching qualifications. Teaching loads at all ranks are low. They are reduced further for those handling sponsored research projects. Each faculty member is expected to develop and maintain a strong research program. Send complete resume including research publications to Chairman, Dept. of E.E., Northwestern University, Evanston, Ill.

ELECTRICAL ENGINEERS

Electrical Engineering staff openings. Both graduate and undergraduate courses. M.S. required, Ph.D. desirable. Modern facilities. Active research program. Write: Joseph C. Michalowicz, Head, E.E. Dept., Catholic University, Washington 17, D.C.

ELECTRONIC ENGINEERS—TECHNICIANS

The Federal Aviation Agency needs qualified Electronic Engineers and Technicians in Alaska for installation and maintenance of electronic equipment and systems for air navigation, air traffic control, telecommunications, etc. Career Federal Civil Service qualification requirements and benefits. Moving costs paid. Annual compensation $6700 and up depending upon qualifications. Contact F.A.A., P.O. Box 440, Anchorage, Alaska.

ENGINEERS—PHYSICISTS

Company engaged in research, production and development of camera tubes, infrared devices and image amplifiers seeks graduate engineers and physicists to work in new laboratories at beautiful Fort Washington, Pa. Reply to Box 2020.

PROFESSOR

Rapidly expanding engineering school located in snow-free, smog-free area with ideal climate needs electronic engineer to teach undergraduate courses and to help develop graduate program. MS. minimum requirement. Salary dependent upon industrial experience and graduate degree. Modern facilities and equipment with new building under construction. Apply to Prof. M. P. Capp. Engineering Div., San Diego State College, San Diego 15, Calif.

TEACHING—RESEARCH

Positions at all ranks for well qualified persons with MS. or Ph.D. in developing department in an engineering school with a new program which emphasizes engineering sciences and interdepartmental teaching. Research presently in areas of signal detection and propagation with others being developed. 9 month or full year appointments available. Salary to $13,500 on full year basis. Write to A. T. Murphy, School of Engineering, University of Wichita, Wichita, Kansas.

(Continued on page 120A)

Engineers
Physicists
Mathematicians

submarines to satellites

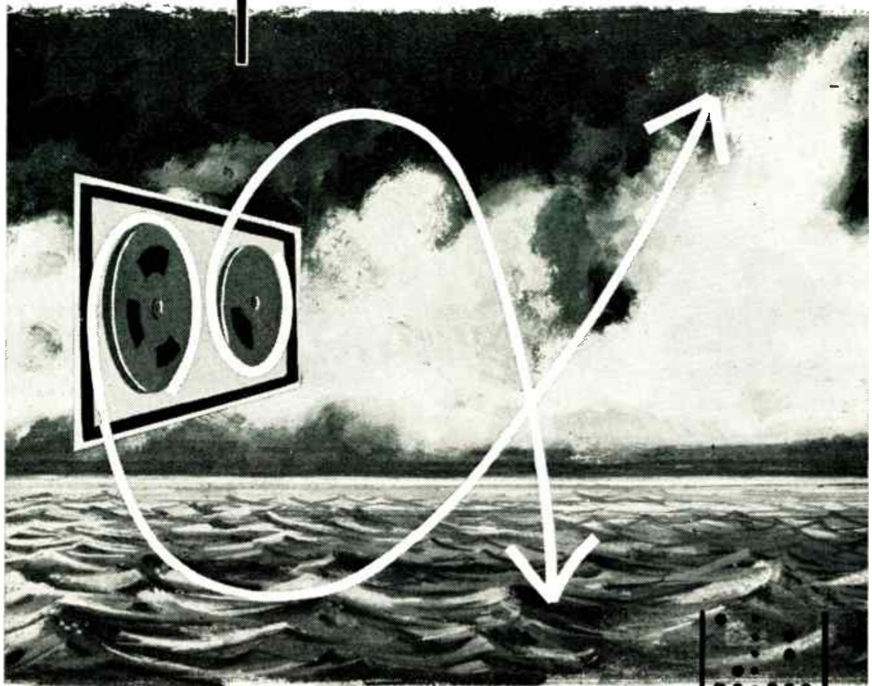

computer applications

To fully exploit the problem-solving potential of modern high speed. high capacity computers requires men with vision, high analytical abilities and a strong background in electronics. physics or mathematics. Engineers and scientists with these capacities will find an opportunity in the Research & Development Department at Electric Boat to explore and develop improved methods of computer applications to problems of data reduction and control systems for a wide range of programs from satellite communications to submarine weapons systems.

Training or experience is essential in the analytical aspects of at least one of the following:

1. Theory of electroacoustic transducers
2. Theory of non-linear control systems
3. Theory of inertial sensors
4. Propagation of sound through water
5. Mathematical computations based on statistical data
6. Conceptual design of digital processing and control systems

Positions are immediately available, providing opportunity to grow in professional knowledge and status ... and to live and work on the beautiful Connecticut Shore near New London. To arrange a convenient interview. send a resume. including salary requirements, to Peter Carpenter

ELECTRIC BOAT
A DIVISION OF **GENERAL DYNAMICS**
Groton, Connecticut

Positions Open

(Continued from page 118A)

TECHNICAL MANAGER

Advanced Data Processing Systems. Direct planning requirements for organization of comprehensive business information processing systems. Requires a Ph.D. in E. E., physics or math., plus several years experience in digital data processing systems. Managerial experience desirable. Attractive salary. Forward resume to Box 2021.

ASSISTANT PROFESSOR

Assistant Professor of Electrical Engineering. Ph.D. required with interest in circuit theory, physical electronics or solid state. Active research and graduate program. Contact W. P. Smith, Chairman, E. E. Dept., University of Kansas, Lawrence, Kansas.

ELECTRICAL OR ELECTRONICS ENGINEER

Large medical institution is interested in employing an engineer to direct the maintenance and trouble-shooting of a large variety of complex electrical instrumentation, and to make modifications in existing equipment. Position requires a person with a degree in E.E. and a minimum of 4 years experience in one or more of the following fields: electrical instrumentation; field engineering or electrical instruments; computers, f.m. tape equipment; telemetering equipment; radiation equipment and counters. Write Personnel Section, Mayo Clinic, Rochester, Minnesota.

(Continued on page 122A)

Engineers

SUPERVISOR SPACE SYSTEMS ANALYSIS

A long established California research organization has an immediate opening for a supervisor of a staff of analysts skilled in engineering, physics and mathematics and conducting mission-oriented lunar and interplanetary system and studies involving trajectories, error sensitivities, maneuvering requirements and guidance equations. The position also affords opportunity for individual research.

Advanced degree and related experience required.

Send resume today to Box 2023
Institute of Radio Engineers
1 East 79th St.
New York 21, N.Y.

Positions Open

(Continued from page 120A)

PHYSICIST

M.S. or Ph.D. Solid background in both optics and electronics. Research on techniques and phenomena for application to space navigation. Send resume to Personnel Director, The Franklin Institute, Phila. 3, Pa.

RADIO ENGINEERS

Design and development positions for Circuit Designers, Development Engineers, Antenna Engineers in connection with direction finding equipment, ECM devices, advanced communication systems, air traffic control, multi-channel receiver development, advanced filter design, R.F. systems analysis and simulation. Apply Servo Corporation of America, 111 New South Road, Hicksville, L.I., New York.

ENGINEERS

Electrical engineering staff openings in an expanding undergraduate program. (1) Instructor: to teach undergraduate courses to sophomore and junior engineering students. Candidate must have B.S. degree and be willing to take graduate work at nearby university. (2) Assistant, associate or full professor: to teach electronics and senior E.E. electives. Candidate should possess a graduate degree (M.S. or Ph.D.) specializing in electronics and/or communications. Encouragement given to private research and consultation. Rank and salary commensurate with academic attainment and experience. Apply: L. M. Gonsalves, chairman, Dept. of E.E., New Bedford Institute of Technology, New Bedford, Mass.

ASSISTANT OR ASSOCIATE PROFESSOR

Assistant or Associate Professor for E. E. Dept. M.S. or Ph.D. degree required. Opening in electronics. Salary commensurate with qualifications. Position available Sept. 1960. Write, Head, E.E. Dept., South Dakota School of Mines and Technology, Rapid City, South Dakota.

SENIOR ANALOG COMPUTER ENGINEER

Milgo Electronic Corporation of Miami, Florida has an opening for a senior level engineer, with a minimum of 5 years experience in the field of analog circuitry design. This individual would become the nucleus of a new products design group, with unlimited opportunity for advancement. Interested candidates forward resumes to Mr. R. H. Mattox, Milgo Electronic Corp., 7620 N.W. 36th Ave., Miami 47, Florida.

ELECTRONICS ENGINEERS—PHYSICISTS

The Cambridge Electron Accelerator, a joint undertaking of Massachusetts Institute of Technology and Harvard University, has openings for electronic engineers for research and development in instrumentation and circuitry from d.c. to millimicrosecond; physicists interested in instrumentation and nucleonics. 2 years minimum experience. Citizenship not required. Applications from abroad also invited. Write to Director, Cambridge Electron Accelerator, Harvard University, 42 Oxford St., Cambridge 38, Mass.

Use your IRE DIRECTORY! It's valuable!

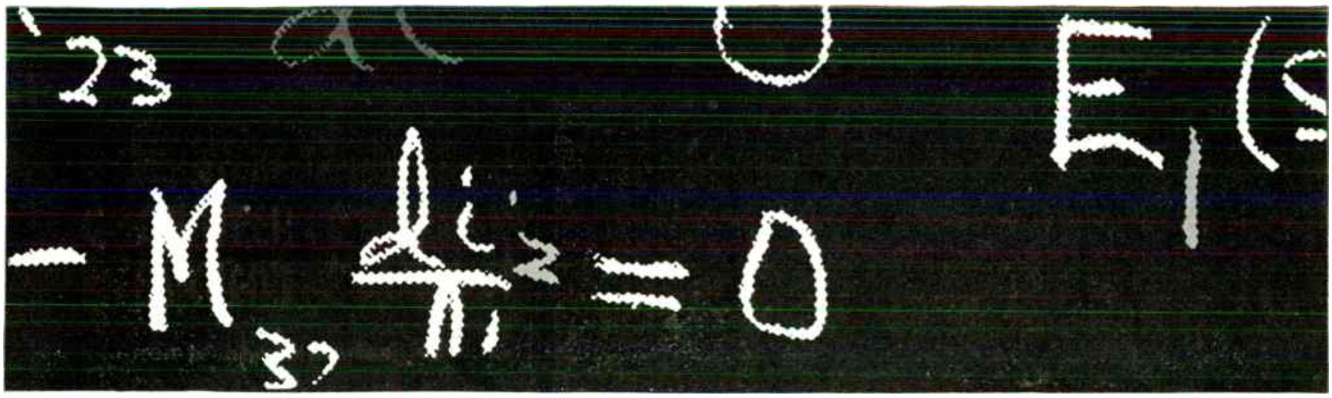

General Motors pledges

AC QUESTMANSHIP

AC Seeks and Solves the Significant—AC Design and Development is moving far ahead in new technology—the result of GM's commitment to make ever larger contributions to the defense establishment. AC plans to resolve problems even more advanced than AChiever inertial guidance for Titan / This is AC QUESTMANSHIP. It's a scientific quest for the development of significant new components and systems . . . to advance AC's many projects in guidance, navigation, control and detection / Dr. James H. Bell, AC's Director of Navigation and Guidance, sees this as a "creative challenge". His group takes new concepts and designs them into producible hardware having performance, reliability and long life. He strongly supports the fact that an AC future offers scientists and engineers "a great opportunity to progress with a successful and aggressive organization" / If you have a B.S., M.S., or Ph.D. in the electronics, scientific, electrical or mechanical fields, plus related experience, you may qualify for our specially selected staff. If you are a "Seeker and Solver", write the Director of Scientific and Professional Employment, Mr. Robert Allen, Oak Creek Plant, 7929 So. Howell Ave., Milwaukee, Wisconsin.

GUIDANCE / NAVIGATION / CONTROL / DETECTION / AC SPARK PLUG *The Electronics Division of General Motors*

Positions Wanted

By Armed Forces Veterans

In order to give a reasonably equal opportunity to all applicants and to avoid overcrowding of the corresponding column, the following rules have been adopted:

The IRE publishes free of charge notices of positions wanted by IRE members who are now in the Service or have received an honorable discharge. Such notices should not have more than five lines. They may be inserted only after a lapse of one month or more following a previous insertion and the maximum number of insertions is three per year. The IRE necessarily reserves the right to decline any announcement without assignment of reason.

Address replies to box number indicated, c/o IRE, 1 East 79th St., New York 21, N.Y.

ELECTRONIC ENGINEER

BSEE, 1948. Heavy experience in industry controls and allied fields. Desires managerial position with strong and growing company in the field of industrial electronics. Location anywhere. Box 2067 W.

(Continued on page 128A)

How to take a satellite

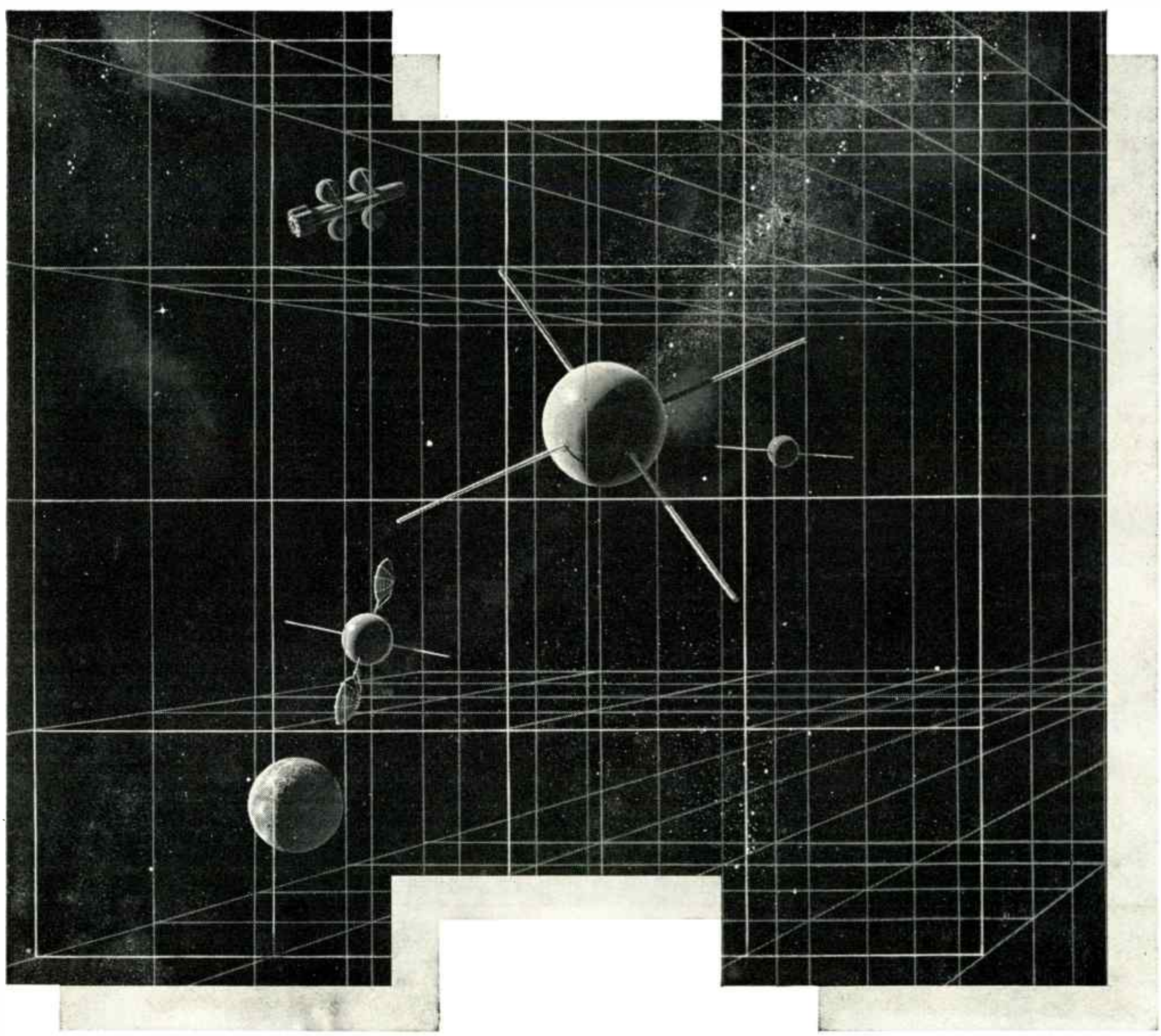

census

At present rates, man will soon have space cluttered with all sorts of orbiting objects. Keeping track of these thousands of new satellites will be a major factor in the success of future space explorations.

This extra-atmospheric clutter can be resolved, sorted, and classified at great range by a new systems concept of satellite intelligence developed by Hughes-Fullerton engineers. The prime sensor is a flexible, computer-programmed radar which can chop space into billions of small information cells on thousands of simultaneous beams.

This enormous multiple-beam capacity permits search, track, and examination of huge numbers of targets—in addition to providing the capability for transmitting control information to defense systems or satellite platforms.

This capability requires a new beam scanning technique, a major step beyond frequency or phase control of arrays. Such advances are typical of the Hughes engineers who pioneered electronic scanning. Here, thinking is not limited to today's problems, or even next year's but toward the next generation of information gathering systems—systems which will not be obsolete by the time they are operational.

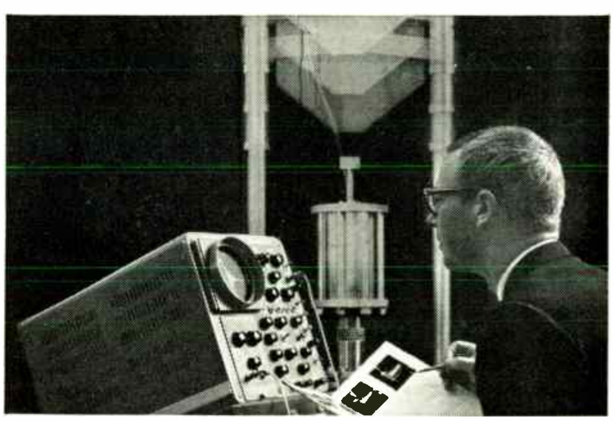

Shown recording shock test data, the MEMO-SCOPE® Oscilloscope is one of the many commercial products developed by Hughes. Precise trace measurement is made possible by the Hughes-built MEMOTRON® Storage Tube.

As a means for studying r-f containment concepts for use in thermonuclear machines, dense cesium plasmas are generated in this tube at the Hughes Research Laboratories in Malibu, California.

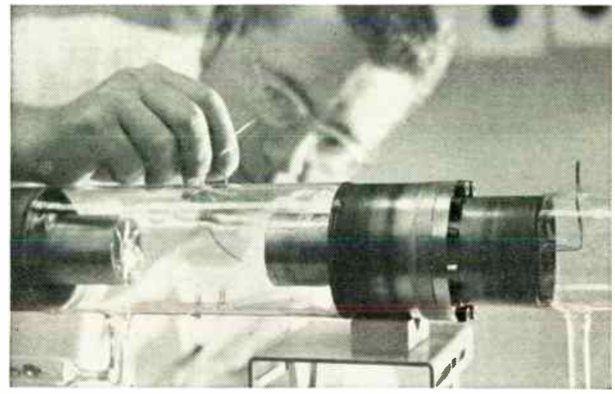

Numerous other Hughes projects, in virtually every area of advanced electronics, provide similarly stimulating outlets for your abilities. Current areas of activity include: advanced electronic display systems, microminiaturized semiconductors, nuclear electronics, space vehicles, ASW systems, hydrofoil system, infrared devices, advanced control systems—and many others.

This variety of advanced projects makes Hughes the ideal environment for the engineer or scientist who wishes to increase his professional stature and personal growth.

Newly instituted programs at Hughes have created immediate openings for engineers experienced in the following areas:

Electroluminescence	RF Network Engineering
Infrared	Microwave & Storage Tubes
Solid State Physics	Communications Systems
Digital Computers	Inertial Guidance
Reliability & Quality Assurance	Field Engineering
Systems Design & Analysis	Circuit Design & Evaluation

Write in confidence to Mr. M. W. Welds
Hughes General Offices, Bldg. 6-E7, Culver City, Calif.

Creating a new world with ELECTRONICS

HUGHES

HUGHES AIRCRAFT COMPANY
Culver City, El Segundo, Fullerton, Newport Beach, Malibu, Oceanside, Santa Barbara and Los Angeles, California; Tucson, Arizona.

3-Question Quiz for Senior Level Electronic Engineers and Physicists

(1) Do you enjoy the full measure of creative freedom to which experienced men are entitled?

(2) Do you have a high degree of respect for your top management's technical competence?

(3) What about the projects you're working on—are they stimulating enough to fully challenge your talents?

At General Mills R and D Laboratories in Minneapolis, engineers and physicists answer an enthusiastic "yes" to all these questions.

For nearly two decades we have been developing and manufacturing weapons, sub-systems, and electro-mechanical and electronic instrumentation systems for both military and commercial use. Our growth has been impressive, and it promises to be even more impressive. Right now we have several technical supervisory and purely technical opportunities open to senior level engineers and physicists in the fields of:

- Digital System Configuration
- Electronic Circuit Design
- Micro-wave Development
- Digital Computer Logic
- Electronic Packaging
- Advanced Pulse and Video Circuit Development
- Advanced Inertial Navigational System Development
- Optical and Infra-Red Equipment Engineering

Perhaps you are one of the men we seek. Ideally, you have a graduate degree and 5 to 8 years experience in electronic instrumentation systems development. In any event, if you now hold a technical supervisory position or are capable of doing so, if you have initiative and drive, if you enjoy exploring the unknown in order to find better ways of doing things—we are genuinely interested in you. And you should be interested in us, because we promise you a creative environment in which you can quickly achieve the full measure of professional and personal recognition that your finest talents demand.

You'd like living in Minneapolis—some of the nation's most beautiful fishing, hunting and camping sites are just an hour's drive away. We enjoy a friendly, neighborly way of life and, at the same time, have all the advantages a major cosmopolitan center can offer. Our people spend long evenings with their families because travel to and from work is easy, uncongested. Children grow strong and healthy in this wholesome vacationland. And they're educated in fine, trouble-free schools.

Send today for more information.

Mr. G. P. Lambert
Manager Professional Personnel
MECHANICAL DIVISION
2003 East Hennepin Avenue,
Dept. PI-7
Minneapolis 13, Minnesota

General Mills

LINCOLN LABORATORY

invites inquiries from persons with superior qualifications.

SOLID STATE Physics, Chemistry, and Metallurgy

RADIO PHYSICS and ASTRONOMY

NEW RADAR TECHNIQUES

COMMUNICATIONS:

Techniques
Psychology
Theory

INFORMATION PROCESSING

SYSTEMS:

Space Surveillance
ICBM Detection and Tracking
Strategic Communications
Integrated Data Networks

SYSTEM ANALYSIS

Research and Development
LINCOLN LABORATORY
Massachusetts Institute of Technology
BOX 16 · LEXINGTON 73, MASSACHUSETTS

Positions Wanted

(Continued from page 124A)

ELECTRONIC ENGINEER

BSEE, 1957, 1/Lt. USAF. Electronic instructor while on active duty. Some graduate work completed. Desires an R & D position in the mid Atlantic area. Age 24, married, 1 child. Box 2068 W.

SALES ELECTRONICS

Experienced sales and engineering background in electronics to distributors. OEM and direct customers. Age 38 with excellent sales record in product and components. Experienced in sales promotion. Desires position with responsibility and future. Box 2069 W.

ELECTRICAL ENGINEER

BSEE. 1958. Lt. (JG) USNR. Completing 2 years as Electrical & Engineer officer afloat and ashore. Experience in repair and maintenance of various types of equipment and in personnel management. Married. Desires position in south west. Available August 1960. Box 2070 W.

ENGINEERING EXECUTIVE

At 35, holding SBEE and MSEE electronics, and wonderfully settled with family in Honolulu, desires a position in this area. Unusually familiar with resources, limitations and energetic future of Hawaii. 15 years experience with shipboard, missile and management of Naval Electronics. Box 2086 W.

SENIOR ENGINEER

MS., solid supervisory experience in transistor applications and technology, desires technical or administrative position in Europe with U.S. or European semiconductor manufacturer. Fluent French, some Italian; married with family. Box 2087 W.

SENIOR PROJECT ENGINEER—CHIEF

BSEE, all requirements MS but thesis. Age 36, married, 2 children. 10 years design and project supervision experience in air navigation systems, HF and VHF communications and industrial TV systems. Also teaching experience in transistors. Member IRE and Tau Beta Pi. Prefer location south or southwest. Box 2088 W.

ENGINEERING TECHNICIAN

Graduate of DeVry Technical Institute in Electronic Technology and Design; married; age 26. 5 years experience in radar and TV repair; 17 months experience as Service Manager for large

(Continued on page 130A)

1961
International Radio and Electronics Show
and
IRE International Convention
March 20-23, 1961
New York Coliseum and Waldorf-Astoria Hotel
New York City

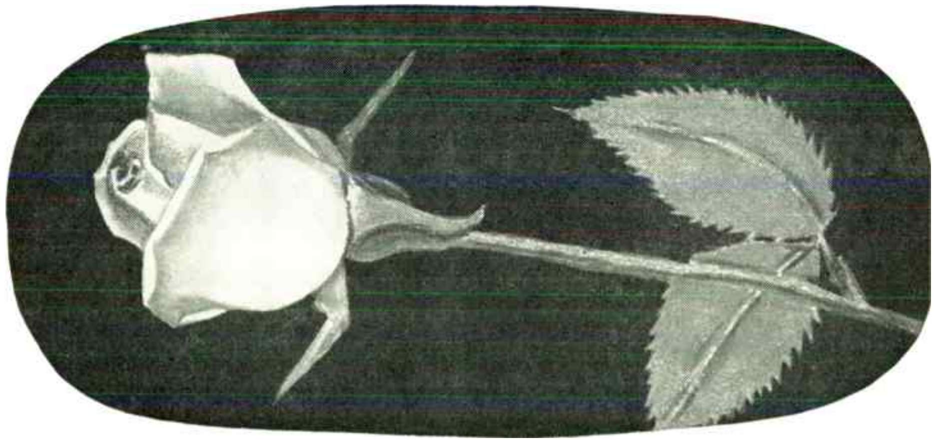

At Bendix York, we have a number of immediate openings for Electronic Engineers and Physicists.

There are many worthwhile advantages awaiting the Professional Engineer who chooses to advance his career with us at Bendix York.

A white rose . . .

The white rose is a symbol at Bendix York . . . a symbol with two meanings. Both of vital importance to *your* future.

First, the white rose is the official flower of York, Pennsylvania. It is a symbol of the good life in our dynamic community, located in the heart of the scenic Pennsylvania Dutch region. It is a wholesome, happy area with excellent schools, delightful recreational opportunities and many cultural advantages. Here—away from high-pressure, high-cost, big-city living—you will enjoy the fuller, more rewarding life that you want for yourself and for your family.

Second, the white rose is a symbol of perfection . . . the perfection for which we strive at Bendix York—perfection in the engineering and scientific pioneering and development in missile electronics that is our principal objective.

We offer a small Division's assurance of individual recognition and advancement, and yet you have the security and employee benefits of a large corporation.

We would like to have the opportunity to tell you more about Bendix® York. We invite you to contact us—by dropping us a post card, by giving us a call or, if you will, by sending us a brief resume. Address Professional Employment: Dept. P

THE Bendix CORPORATION

YORK DIVISION

York, Pennsylvania
Phone: York 47-1951

Positions Wanted

(Continued from page 128A)

Detroit electronic distributor; wants position with up-and-coming firm that is going places. Opportunity for further study and advancement desirable. Available July 1960. Box 2089 W.

JUNIOR ELECTRONIC ENGINEER

No degree but 8 years of test and design experience aircraft navigational, communications, and radar equipment. 1st class radiotelephone and advanced class radio amateur licenses. CREI graduate. Member IRE. Age 27. Married. Desires challenging position. Box 2094 W.

PATENTS OR CONTRACT ADMINISTRATION

Desire to enter field combining the legal and technical. 7 years technical experience (4 years technical writing). Liberal arts degree including 59 credits physical sciences and electronics. Law degree. East coast preference. Resume upon request. Box 2095 W.

ELECTRONICS PATENT LAWYER

Electronics patent lawyer, engineer, etc., 15 years patent experience, desires position handling patent work, and also other responsibilities as time permits, in small dynamic east coast company. Box 2096 W.

SEMICONDUCTORS

Age 34. 7 years background engineering supervisor and factory superintendent, transistor diode and rectifier production. B.S. in chemistry, graduate work and management training. Earlier experience quartz oscillators. Desires more responsibility. Box 2097 W.

BASIC RESEARCH

BSEE. (electronics option). University of Michigan 1948. Age 36. Member IRE. Wide industrial and some college teaching experience in electronics. Have a great desire to do basic research in such fields as atom structure and atom particles, propagation of light energy, magnetism, and gravitation. Seek college research assistantship or fellowship for the 1960-1961 academic year. Box 2098 W.

NEWS New Products

These manufacturers have invited PROCEEDINGS readers to write for literature and further technical information. Please mention your IRE affiliation.

(Continued from page 112A)

Near-Perfect Light Amplifier

A small electronic tube, developed by scientists at the Westinghouse research laboratories, reaches the near ultimate in the ability to amplify ordinary light. The tube, known as the Astracon, is so sensitive that it makes visible a single electron, released at the tube's input by an individual photon—the smallest unit quantity of light that exists.

The electronic development was described by Dr. J. W. Coltman, manager of

(Continued on page 132A)

fmc offers

COMPUTER ENGINEERS

immediate opportunities on the San Francisco Peninsula

FMC Central Engineering Laboratories' commercial product development program has started a major digital activity using the latest techniques in the design of special purpose computers and memory devices.

Project Manager, Group Leader, and Engineer openings require top creative professionals with BS or advanced degrees in EE or Physics with experience in:

Systems Design
Logical Design
Transistor Circuitry
Memory Systems
Input/Output Equipment

Central Engineering's expanding program in non-military products requires engineers and specialists to staff our new million-dollar R & D laboratories now under construction in the Santa Clara Valley in the FMC complex. Forward-looking management provides environment for and encourages individual contributions, personal recognition, and professional advancement.

Interested? Send a resume of your educational and professional background to E. M. Card, Jr., FMC Central Engineering, 1105 Coleman Ave., San Jose, Calif. Phone: CYpress 4-8124.

Putting Ideas to Work

Central Engineering Laboratories

FOOD MACHINERY AND CHEMICAL CORPORATION

alpha is an experienced systems organization

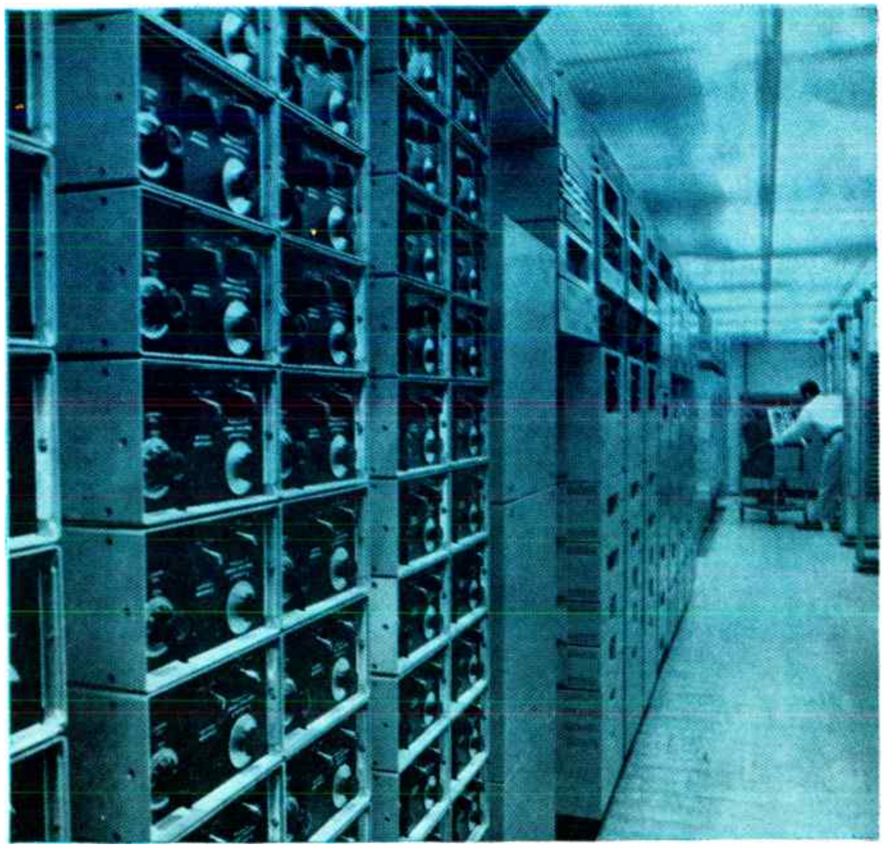

How Much Systems Experience Do You Have?

Alpha's facilities consist of its collection of top system management and technical talents together with the physical facilities necessary to most effectively design, engineer and implement systems of high reliability.

Alpha technical experience, know-how and creative talent is exemplified by the fact that more than eighty percent of Alpha project employees hold degrees in science or engineering. Alpha systems management talent is exemplified by the Alpha Project Directors whose average age is 40 and average years of systems experience is more than 10.

Would your capabilities be more significant in a completely systems-oriented organization where facilities must be measured in terms of talent? Do you have technical talent with the specialized capabilities needed to select system parameters; integrate a complex of equipments; direct a team of subsystem suppliers?

Write:

C. P. Nelson
Employment Manager

Alpha CORPORATION
A SUBSIDIARY OF COLLINS RADIO COMPANY

SYSTEMS DESIGNERS, ENGINEERS, CONSTRUCTORS, WORLD-WIDE • RICHARDSON, TEXAS • TELEPHONE DALLAS ADams 5-2331

NEWS New Products

These manufacturers have invited PROCEEDINGS readers to write for literature and further technical information. Please mention your IRE affiliation.

(Continued from page 130A)

the electronics and nuclear physics department of the **Westinghouse Electric Corp.**, research laboratories in Pittsburgh, Pa.

The Astracon tube operates upon an amplifying principle discovered at the research laboratories five years ago. The image of an object, so dim that it is invisible to the naked eye, is focused by lenses onto a light-sensitive screen, called a photosurface, at the input end of the tube. The individual particles of light, or photons, arriving from the scene strike the surface and eject electrons from it.

Each ejected electron is then accelerated forward by 2000 volts and strikes head-on into a thin two-layer film, only a few millionths of an inch thick. The front surface of the film is aluminum; on its back surface is deposited a slightly thicker layer of an insulating material. When a high-speed electron crashes into the film it penetrates into the insulator and releases four or five additional electrons. These are accelerated into a second film, or dynode, where the electron multiplication is repeated.

By using five such steps, a single electron is multiplied into about 3000. These are given a final 20,000-volt boost and are aimed into a thin layer of fluorescent material at the output end of the tube. Here they release 20,000 or more photons of visible light.

"This ability to record photons makes the Astracon useful in many fields of research. In astronomy it will increase the effective size, or light gathering ability, of the largest telescopes. In nuclear physics it will permit the viewing of the tracks of high-energy cosmic rays and other particles. Until now there has been no practical method for observing these particles as they flash through solid crystals with a feeble glow."

Integrated Equalizer-Analyser System

The first independent laboratory random vibration facility utilizing the latest Ling analyser-equalizer system has been installed by **Rototest Laboratories, Inc.**, 2803 Los Flores, Lynwood, Calif.

(Continued on page 134A)

NEWS New Products

These manufacturers have invited PROCEEDINGS readers to write for literature and further technical information. Please mention your IRE affiliation.

(Continued from page 132A)

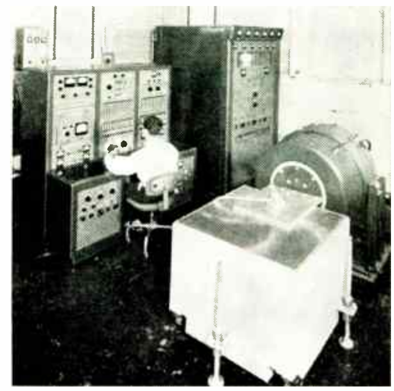

This new facility enables random vibration tests to be run so that unknown variations can be analyzed at a glance and spectrum shifts equalized while test is still in progress.

The facility consists of an elaborate system integrating four major units—control console with equalizer-analyzer, shaker, amplifier, and oil table, plus supporting equipment.

The entire facility enables the following to be accomplished: (1) equalization time is greatly reduced; (2) equalization may be done on the actual test specimen; (3) many different power spectral density curves may be readily shaped; (4) constant narrow band monitoring is carried out to detect changes in test specimen behavior; (5) equalization read-out is directly in G^2/cps. No mathematical conversions are required; (6) random and sine wave excitations may be readily superimposed.

Exciter capabilities are as follows: RMS force pound output, 5000 pounds (sine wave); 3500 pounds (random), and peak force pound output 10,500 pounds (random).

The equipment features 29 filters covering the range from 10 to 2000 cps and one for 2000–5000 cps with individual controls for each. Sine wave cycling is completely automatic with adjustable sweep rate and servo control of acceleration level.

Small-Area Infrared Detector

A new infrared detector of extremely small area (0.1×0.1 mm^2) is now being produced by **Radiation Electronics Co.,** 5600 Jarvis Ave., Chicago 48, Ill., a division of Comptometer Corp. Utilizing the photovoltaic effect in indium antimonide at liquid nitrogen, the Model J-02 detector exhibits typical NEP values of 2×10^{-12} watt at 5 microns and 7×10^{12} watt for 500° K Blackbody. The J-02 responds from the visible region to 5.7 microns with a time constant of less than one microsecond.

(Continued on page 136A)

FROM AN ENGINEER'S NOTE PAD

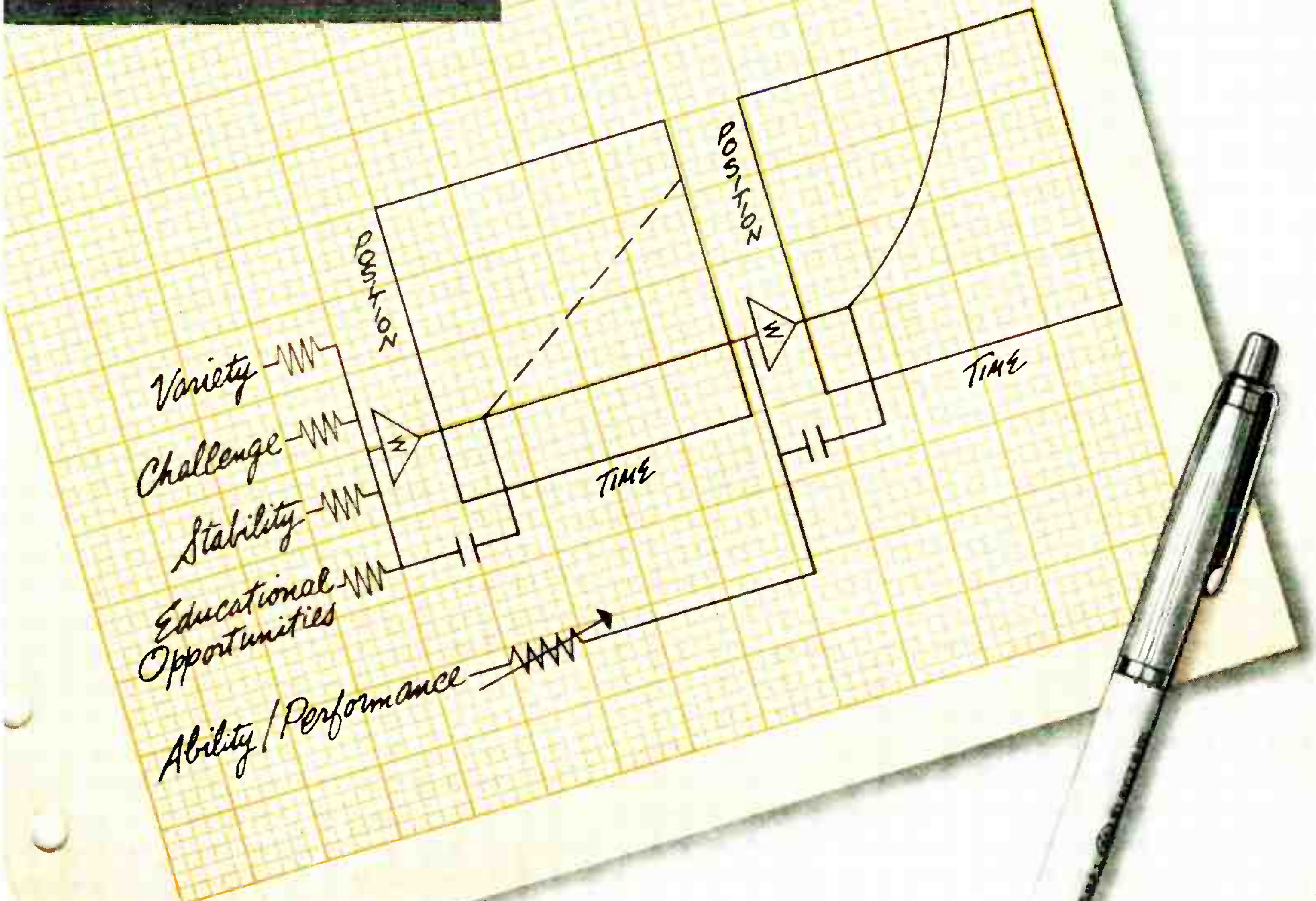

"You plot your own curve at HMED"

ENGINEERS ARE a curious lot: a breed apart. Their natural preferences for facts, their talents for logic have been trained and disciplined.

The result many times…an uncommon, refreshing way of expressing the well known…a direct, succinct method of stating the complex.

Here is an actual example. It is a composite of sketches made by one of our Engineering Supervisors during a discussion of General Electric's unique Salary Administration Program.

Circuit engineers will have little trouble in reading it. Others may have more difficulty. All may wish additional detail. For this, as well as other information regarding the unusual professional and outstanding personal opportunities awaiting you at General Electric's Heavy Military Electronics Department, write in confidence to George B. Callender.

HEAVY MILITARY ELECTRONICS DEPARTMENT

GENERAL ELECTRIC

Div. 53-MG, Syracuse, New York

There are openings for graduate engineers at intermediate (3 or more years) and high levels of experience in the following areas: **Weapons Systems Analysis; Mathematical Analysis of Engineering Problems; Military Communications Systems; Radar Systems; Weapons Control Systems; Electronic Circuitry; Experimental Psychology — Human Factors; Instrumentation.**

NEWS New Products

These manufacturers have invited PROCEEDINGS readers to write for literature and further technical information. Please mention your IRE affiliation.

(Continued from page 134A)

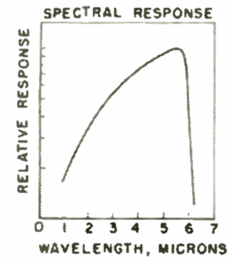

Because of its small area, fast response, and sensitivity, the J-02 detector permits the design of infrared systems with high optical gain, high resolution, and very rapid scanning rates. Having an impedance between 1,000 and 40,000 ohms, the J-02 is efficiently coupled to both transistor and vacuum tube pre-amplifiers. Linear arrays of detection elements can be fabricated for special applications.

For more information, write for bulletin J-02.

Tuller Memorial Award to O'Meara

Dr. Thomas R. O'Meara, **Hughes Aircraft Company** electrical engineer, has been informed by the IRE that he will receive the first Dr. William G. Tuller Memorial award May 10, the company announced here today. The award is "in recognition of the most outstanding technical paper dealing with electrical component parts published in professional journals in 1959."

IRE's professional group on component parts will present Dr. O'Meara with a scroll and $250 at the organization's annual electric component conference in Washington, D. C., May 10. Dr. Tuller was one of the founders of the presenting group.

Dr. O'Meara's paper was described as "one of the first general studies of the common methods of extending low frequency transformation to high frequency, wide band operation using a lumped parameter, wide band, high frequency transformer."

He developed the paper from a thesis written for the University of Illinois, where he received the doctorate in philosophy in 1957. It appeared in the June, 1959, issue of the IRE professional group's publica-

(Continued on page 138A)

Use Your IRE DIRECTORY! It's Valuable!

NEWS New Products

These manufacturers have invited PROCEEDINGS readers to write for literature and further technical information. Please mention your IRE affiliation.

(Continued from page 136A)

tion, TRANSACTIONS ON COMPONENT PARTS.

Any technical paper dealing specifically with an electronic component part presented either at the IRE symposium or in an IRE publication is eligible for the annual Tuller award.

Hull Honored by General Electric

Dr. Albert W. Hull, formerly assistant director of the **General Electric Research Laboratory,** was honored on his eightieth birthday April 19 at the Laboratory. Dr. Hull has been credited with the invention of more types of electron tubes than any other man.

At a luncheon in his honor, Dr. Hull was presented with a memorial album commemorating some of the high points of his career. Dr. Guy Suits, vice president and director of research, made the presentation.

Dr. Hull has been with the Research Laboratory since 1914, first as a physicist, then from 1928 until his retirement in 1949 as assistant director, and, since retirement, as a consultant. His work with electron tubes forms the basis for much of modern electronics.

One of Dr. Hull's inventions is the magnetron tube, originally developed in 1921, which was the forerunner of power tubes used in radar systems during World War II. He also is the inventor of the screen-grid tube, which made possible modern radio and television receivers. Perhaps the most important of his tubes is the thyratron, used for automatic control of many industrial processes.

In addition to his work with electron tubes, Dr. Hull has made many contributions to the fundamentals of physical science. He was a pioneer in crystal studies using x-rays, and developed a new method of x-ray crystal analysis in 1916. The technique, which was independently discovered in Europe, is still one of the principal tools used in crystal studies.

During World War I he originated the use of Rochelle salt crystals in devices for underwater detection of submarines. Similar methods were used in World War II.

Many honors have come to Dr. Hull during his long scientific career. He received IRE's highest technical award, the Medal of Honor, in 1958, and in 1930 was awarded the Morris Liebmann Memorial Prize for his work on vacuum tubes. He is a past president of the American Physical

(Continued on page 140A)

NEWS New Products

These manufacturers have invited PROCEEDINGS readers to write for literature and further technical information. Please mention your IRE affiliation.

(Continued from page 138A)

Society and a member of the National Academy of Sciences. He has received several honorary degrees, including a D. Sc. from his alma mater, Yale University. Other awards include the Potts Medal from the Franklin Institute for his work on crystal analysis. His scores of scientific papers and more than 90 patents form one of the most important bodies of work contributed by any individual to the development of the electronics industry.

Power Supply

Power Instruments Corp., 235 Oregon St., El Segundo, Calif., announces a new completely transistorized laboratory power supply which features an automatic current limiting circuit as well as precision voltage regulation. Short circuit current can be selected (40, 100, 200, and 350 ma) on front panel. Voltage regulation is better than 0.1%. Voltage range 0–32 vdc. Ripple is less than 1 mv. Output impedance is less than 0.2 ohms. Input 105–125 volts, 50–400 cps.

Vibration Pickup

Southwestern Industrial Electronics Co., a division of **Dresser Industries, Inc.,** 10201 Westheimer Rd., P.O. Box 22187, Houston 27, Texas, announces the introduction of its new Model TD-6 Vibration Pickup.

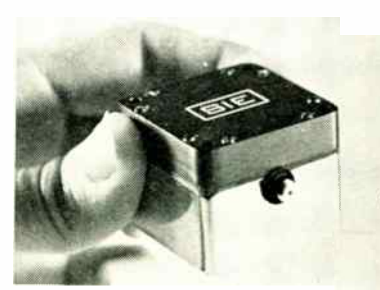

The TD-6 is said to be different from any vibration pickup previously manufactured by SIE or any other manufacturer. It incorporates a newly developed magnetic circuit which combines the temperature stability of magnetic damping

(Continued on page 142A)

Take...

- forefront work essential to National defense
- varied "doing" as well as "thinking" projects
- the academic atmosphere of a great University
- big Company orderliness plus small-group freedom
- inspirational elbow-rubbing with outstanding men
- stability, permanence, most fortunate living conditions
- California, Stanford nearby for advanced work

blend—and know why so many leading engineers and scientists come to, and remain at

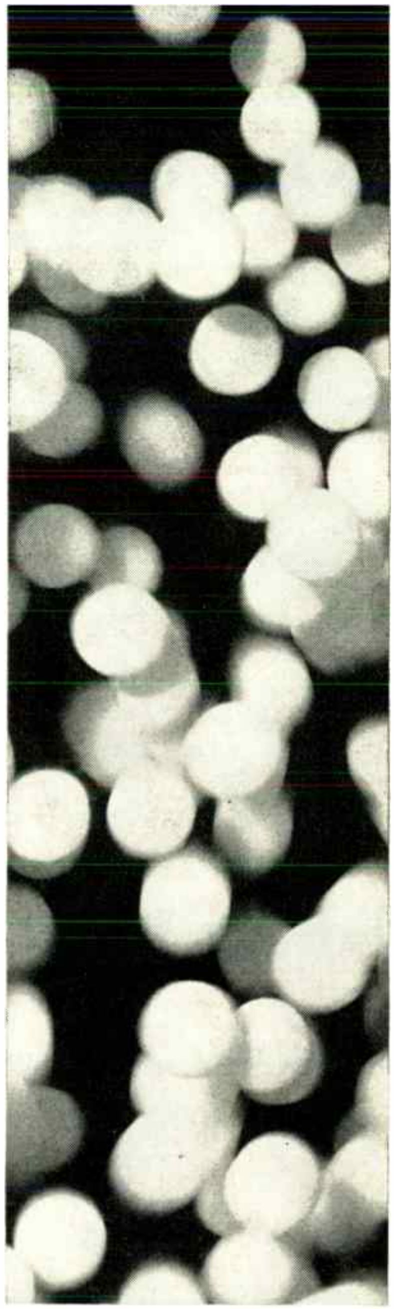

Large-scale dynamical model of gas in operation

SYLVANIA MOUNTAIN VIEW OPERATIONS

on the San Francisco Peninsula

Rewarding assignments at B. S., M. S., Ph. D levels in the following: Evaluation, Concept, Design of Systems, Circuits, Receivers, Transmitters. Receiver Design, Antenna Systems Design. Theoretical, Experimental and Solid State Physics. Microwave Tube R & D. Sales Engineering. Engineering Writing. Interested? Mr. Wayne Pearson will welcome your letter and/or resume, and answer quickly in confidence.

Electronic Systems Division

SYLVANIA

Subsidiary of GENERAL TELEPHONE & ELECTRONICS

Dept. B-7, Box 188, Mountain View, California

6203

(Continued from page 140A)

with the sensitivity previously available only in fluid damped units.

Some of the features of this pickup are its size ($1\frac{1}{2}'' \times 1\frac{1}{2}'' \times 1\frac{5}{32}''$), weight (6.5 ozs), frequency range (20–2000 cps) and low price. It has a threshold velocity of essential y zero.

The TD-6 will be available from stock in June 1960. Its list price is $175.00 and quantity discounts are available.

G. Barron Mallory President of P. R. Mallory

The Board of Directors of **P. R. Mallory & Co., Inc.**, Indianapolis, Ind., announces the election of G. Barron Mallory to the office of president, succeeding Joseph E. Cain, who has been president since 1946 and prior to that was executive vice president from 1935 to 1946.

Philip R. Mallory was re-elected chairman of the board of directors with Mr. Cain elec-

(Continued on page 144A)

NEWS New Products

These manufacturers have invited PROCEEDINGS readers to write for literature and further technical information. Please mention your IRE affiliation.

(Continued from page 142A)

ted co-chairman. Cain was also elected chairman of the executive committee, succeeding J. F. Riley who remains a member of the executive committee together with C. Harvey Bradley and G. B. Mallory.

G. Barron Mallory, son of company founder and board chairman, P. R. Mallory, has been administrative vice president since October 1958. Active in Mallory Company affairs for many years, Mallory was a director of the company before his election as administrative vice president.

Mallory was formerly a partner in the law firm of Brown, Wood, Fuller, Caldwell & Ivey, New York City general counsel for P. R. Mallory & Co., Inc. He is a graduate of Yale College and Yale Law School. He served in the Naval Reserve during World War II and was retired as Lt. Commander.

Precision Potentiometric Microvoltmeter

Smith-Florence, Inc., 4228—23rd Ave. Seattle 99, Wash., introduces the transistorized Model 951 Microvoltmeter. This instrument is a differential voltmeter which compares a precise internal voltage with the unknown voltage to be measured. Since the two voltages are adjusted to be equal, no current will flow from the unknown into the instrument, thus the input impedance is determined by the leakage resistance of the internal insulation.

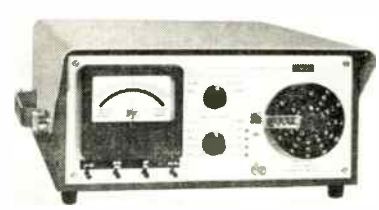

The instrument is capable of measuring voltages between 10 volts and one microvolt. The reference voltage to the precision voltage divider covers four ranges: 10 volts, 1 volt, 100 millivolts and 10 millivolts. The divider is a four-dial device reading from 0 to 9 on the three outer dials, and 0 to 10 on the inner dial. Thus to set the reference voltage to 10 volts, the Reference Voltage Switch is operated to this position and the dials set to 9.9910. Indicator lamps controlled by the Reference Voltage Switch indicate volts (V) or millivolts (MV) about the dials, and provide a properly positioned decimal point on the readout graticule.

The null indicating meter operates over seven ranges, from 10 volts full scale to 10 microvolts full scale. Size is approximiately 5¼" H × 17" W × 11" D. Price is $1,350 f.o.b. factory.

(Continued on page 146A)

active programs in 19 critical electronic areas

Offer You Opportunities To Participate In Significant Advances at STROMBERG-CARLSON Division of General Dynamics

Top-calibre research and development teams at Stromberg-Carlson are tackling the prime problem areas in electronics affecting commercial communities and national defense. Programs and R & D staffs are expanding, backed by the vast resources of General Dynamics and the Stromberg-Carlson engineer-oriented management.

Every senior engineer and scientist who feels he can contribute to the expansion of man's capabilities in any of the following areas is invited to contact us.

We are particularly interested in people with advanced degrees in Physics, Electrical Engineering or Mathematics and experience in one or more of the areas listed. Please send resume in confidence to Technical Personnel Department.

ENGINEERING AND ADVANCED DEVELOPMENT

Advanced ICBM Communications
Electronic Switching
Nuclear Instrumentation
High-Speed Digital Data Communications
Electronic Reconnaissance Systems
Single Sideband Communications
Synchronous Data Transmission
Advanced ASW Techniques
Machine Tool Automation
Radio Data Links • Tacan Equipment
High Intensity Sound Generators
Advanced Air Acoustics
Shaped Beam Display Systems
High-Speed Automatic Missile Check-Out Equipment
Super-Speed Read-Out and Printing Equipment

RESEARCH

Paramagnetic Resonance • Ferroelectricity
Thin Photoconductor Films
Propagation and Coding • Speech Analysis
Bandwidth Compression • Hydro-Acoustic Transducers
Defect Solid State Physics
Parametric Devices • Molecular Electronics
Tunnel Diode Logic • Scatter Propagation Analysis

STROMBERG-CARLSON
A DIVISION OF **GENERAL DYNAMICS**
1476 N. Goodman St., Rochester 3, New York

These manufacturers have invited PROCEEDINGS readers to write for literature and further technical information. Please mention your IRE affiliation.

(Continued from page 144A)

Transistorized Oscillator-Amplifier

The development of a transistorized plug-in bias oscillator-direct record amplifier has been announced by the **Applied Magnetics Corp.**, P.O. Box 368, Goleta, Calif. The unit, Model DO-70, is designed for use in the direct record mode in instrument-type tape recorders. Power consumption is 100 ma at 24 vdc.

The bias oscillator section operates at a nominal frequency of 70 kc and provides an output of 10 ma. The output ratings of both the oscillator and amplifier are based on working into an impedance consisting of a five to ten mh recording head and a 1000 ohm resistor.

Amplifier input impedance is 100,000 ohms, unbalanced to ground, and frequency response is 50 to 8000 cps, within 2 db. The amplifier, which requires a minimum input voltage of 0.7 volts RMS, will provide an output of 1 ma.

The packaged unit measures $1\frac{7}{8}$ square by $3\frac{3}{4}$ inches long, including the plug. Although normally provided with an Amphenol Blue Ribbon 26-182, other plugs are available on special request.

Further information and specifications are available from the firm.

Nylon Parts Catalog

A new six-page catalog, illustrating molded Nyon parts available from stock molds, is now offered by **Nylomatic Corp.**,

(Continued on page 148A)

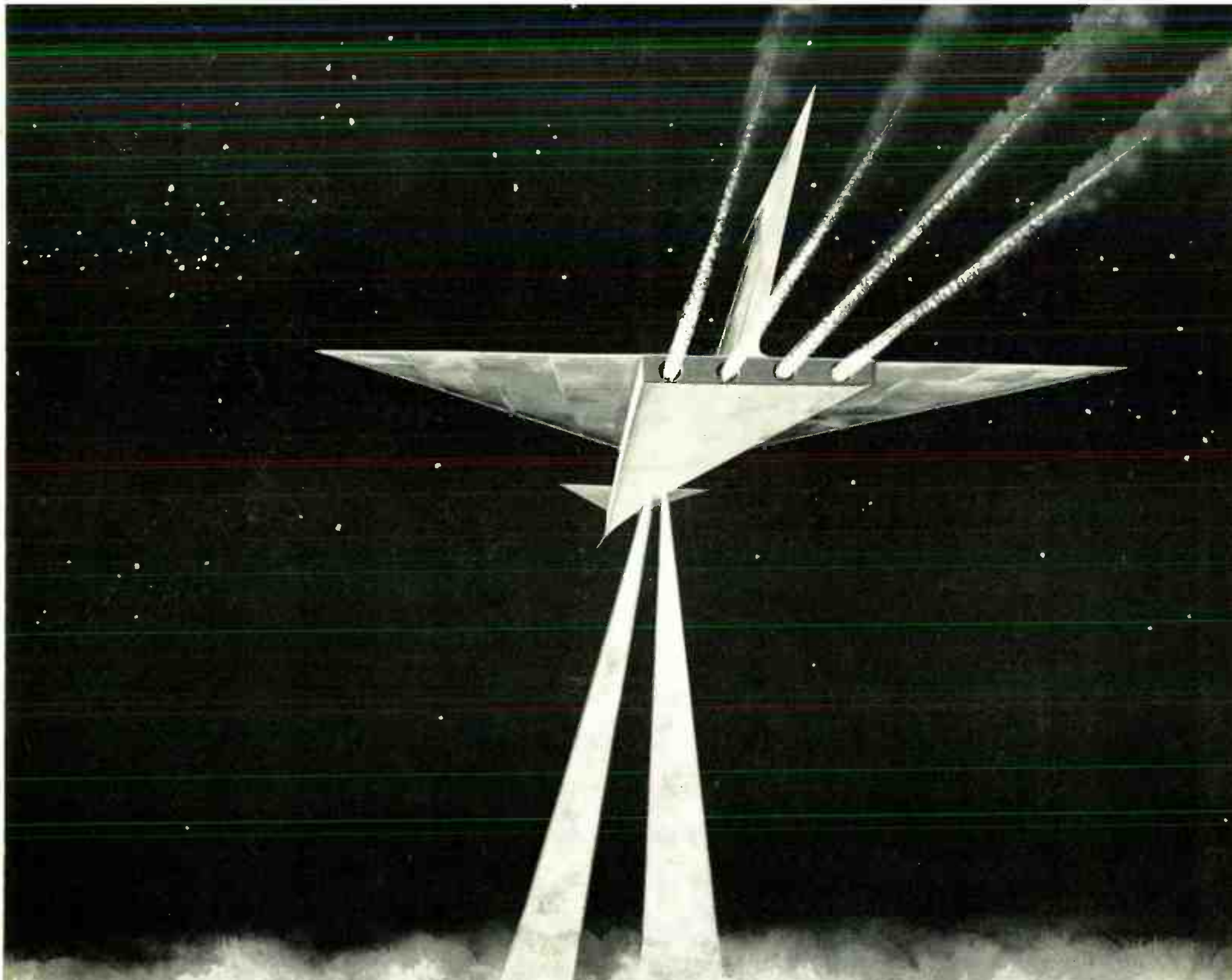

How to keep Mach 3 airliners on course...

A CHALLENGE TO EXCITE ANY ELECTRONICS ENGINEER WORTH HIS SALT... THE KIND RYAN NEEDS RIGHT NOW

Present navigational techniques are not fast enough nor accurate enough to navigate jet transports hurtling passengers across the world at three times the speed of sound.

Yet Ryan Electronics, geared to the future, has already conceived such flight instrumentation control, combining Ryan-pioneered C-W doppler techniques with advanced inertial methods. This is another reason Ryan is the largest electronics firm in San Diego — *and the fastest growing!* If you are an electronics engineer ambitious to help advance the art, as well as your own career, we want you *right now* at Ryan Electronics.

Ryan Electronics employs over 2000 people and has over one-third of the company's $149-million backlog of business. Under the leadership of some of America's most prominent scientists and engineers, Ryan is probing beyond the known . . . seeking solutions to vital problems of space navigation.

Expanding facilities of Ryan Electronics at San Diego and Torrance in Southern California are among the most modern in the West. You enjoy living that's envied everywhere, plus facilities for advanced study. Send your resume or write for brochure today: Ryan Electronics, Dept. 2, 5650 Kearny Mesa Road, San Diego 11, Calif.

DIVISION OF RYAN AERONAUTICAL COMPANY
SAN DIEGO & TORRANCE • CALIFORNIA

RYAN ELECTRONICS

NEWS New Products

(Continued from page 146A)

189 W. Trenton Ave., Morrisville, Pa. Among the assortment are numerous bushings, washers, rollers, gears, bearings, glides, etc. Also, several parts designed for specific applications. Many of the parts can be supplied in Delrin as well as Nylon and the number of parts offered is constantly increasing with additional catalog sheets being sent out periodically. Write to the firm for details.

Strain Gage Input Conditioning Unit

A new Input Conditioning (Bridge Balance and Calibrating) module for feeding oscillographs directly or front ends of data acquisition systems has recently been announced by **B & F Instruments, Inc.**, 3644 N. Lawrence St., Philadelphia 40, Pa.

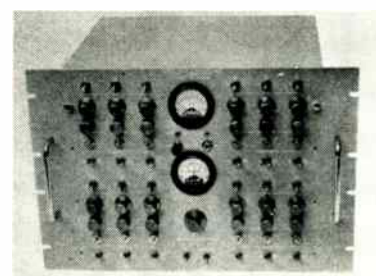

(Continued on page 150A)

wanted:

engineers

FOR CAREERS WITH

PAN AM

in **florida**

Since 1953 Pan Am's Guided Missiles Range Division has had prime responsibility to the Air Force Missile Test Center for operation and maintenance of the 5000-mile Atlantic Missile Range extending from Cape Canaveral through the Bahamas to Ascension Island and beyond.

The electronics, electrical, mechanical, civil or industrial engineer, the physicist, or the mathematician will discover here a unique opportunity to play an intimate, vital role in the nation's major missile test and astronautical exploration activities.

He will discover that the Florida way of life offers him and his family modern recreations and conveniences in the unparalleled vacation setting of our sunshine and seashores.

He will discover that beyond normal employee benefits—paid vacation, sick leave, retirement plan, group life insurance, etc., Pan Am's Guided Missiles Range Division offers a unique travel advantage.

If you seek a meaningful career in missiles and astronautics, investigate these opportunities in Florida, with Pan Am.

Please address your resume in confidence to Director of Technical Employment, Pan American World Airways, Inc., Dept. C-30, Patrick Air Force Base, Florida.

PAN AM

GUIDED MISSILES RANGE DIVISION

PATRICK AIR FORCE BASE, FLORIDA

NEWS New Products

(Continued from page 148A)

Known as Model 12-200BX, the unit will accommodate twelve (12) resistance type transducers, 1, 2, or 4 active arms, employing 3, 5, 4, or 6 wire input techniques thus providing for the cancellation of cable temperature effect. Sensitivity losses due to cable length are calibrated out.

The 12-200BX will feed sensitive oscillograph galvanometers directly, or high frequency oscillograph galvanometers and voltage controlled oscillators via single ended or differential amplifiers.

For further information write to the firm.

Membership

The following transfers and admissions have been approved and are now effective:

Transfer to Senior Member

Arndt, R. B., Saint Paul, Minn.
Bashara, N. M., Lincoln, Neb.
Bawer, R., Alexandria, Va.
Berger, D. C., Philadelphia, Pa.
Boecker, A., East Norwich, L. I., N. Y.
Boyd, J. A., Ann Arbor, Mich.
Caldwell, E. E., Baltimore, Md.
Campbell, A. T., Downey, Calif.
Campbell, W. O., Towson, Md.
Carroll, J. M., Huntington, L. I., N. Y
Carroll, T. J., Baltimore, Md.
Chapman, C. W., Houston, Tex.
Chen, K., Pittsburgh, Pa.
Damon, E. K., Columbus, Ohio
Damonte, J. B., Belmont, Calif.
Dossey, J. L., Albuquerque, N. M.
Dunklee, L. H., Garden Grove, Calif.
Dunn, E. B., Philadelphia, Pa.
Fluhr, F. R., Washington, D. C.
Fowler, C. A., East Norwich, L. I., N. Y.
Gardner, L. B., North Hollywood, Calif.
Gartner, W. W., Fort Monmouth, N. J.
Gray, J. O., Patrick Air Force Base, Fla.
Greenbaum, J. R., Syracuse, N. Y.
Greene, W. E., Point Mugu, Calif.
Gruen, H. E., Geneva, Ill.
Hayter, W. R., Jr., Elmira, N. Y.
Heenan, N. I., Ottawa, Ont., Canada
Horsch, J. R., North Syracuse, N. Y.
Houghton, H. V., Jr., Los Angeles, Calif.
Huebler, M. A., Belmont, Calif.
Jackson, R. W., Montreal, Que., Canada
James, D. B., Far Hills, N. J.
Ko, H. C., Columbus, Ohio
Ludwig, J. T., St. Petersburg, Fla.
Rector, J. D., Denver, Colo.
Saslow, S., Saratoga Springs, N. Y.
Sheppard, G. E., Wichita, Kan.
Weiss, M. M., Whippany, N. J.
Zappacosta, A. D., Havertown, Pa.

Admission to Senior Member

Adey, W. R., Los Angeles, Calif.
Barnett, W. P., North Syracuse, N. Y.
Bossers, C., Emporium, Pa.
Boucheron, P. H., Jr., Syracuse, N. Y.
Brower, G. H., Lutherville, Md.

(Continued on page 152A)

RESEARCH AT COLLINS

$$p(\lambda)d\lambda = \frac{C_1}{\lambda^5} \frac{d\lambda}{\exp(C_2/\lambda T)-1}$$

$$C_1 = 8\pi hc$$

$$C_2 = \frac{hc}{k}$$

THE UNUSUAL SHAPE OF PROGRESS

The principles of spectral energy distribution of the radiation from a black body, announced by Max Planck in 1900, were of intense interest to the theoretical physicists of the day. Since then, these principles have paved the way for major advances in marine navigation and radio astronomy. For example, Collins new Radio Sextant pictured here is capable of continuously tracking the sun or the moon under any weather conditions, furnishing both the ship's location and heading with high precision.

Max Planck's work was done in an atmosphere of unrestricted scientific freedom. Such an atmosphere is provided in Collins Radio Company Research laboratories for physicists, mathematicians and engineers engaged in basic research. These are men capable of looking beyond man's present limitations, with the ability and ambition to analyze man's progress and envision his future environment. To further implement the advancement of scientific knowledge at Collins, with the resultant development of new technologies, unique professional opportunities are now being offered in the fields of radio astronomy, circuits, advanced systems, antennas and propagation, mechanical sciences and mathematics. Your inquiry is invited.

COLLINS

COLLINS RADIO COMPANY • CEDAR RAPIDS, IOWA • DALLAS, TEXAS • BURBANK, CALIFORNIA

Membership

(Continued from page 150A)

Button, K. J., Lexington, Mass.
Caldecott, R., Columbus, Ohio
Cauvin, G. A., New York, N. Y.
Crook, G. M., Canoga Park, Calif.
Edelman, F. H., Philadelphia, Pa.
Faralla, R. A., Long Branch, N. J.
Feldman, N. W., Fort Monmouth, N. J.
Hiebert, A. L., Santa Monica, Calif.
Hugle, W. B., Youngwood, Pa.
Johnson, E. H., Chicago, Ill.
Kaiser, J., Jr., Bethesda, Md.
Kanbergs, J. V., East Palo Alto, Calif.
Kincaid, M. M., Newton, Mass.
Kline, F. W., Jr., Minneapolis, Minn.
Kravetz, J., Pasadena, Calif.
Kumpfer, B. D., Salt Lake City, Utah
Leake, C. E., Los Altos, Calif.
Lemmerman, E. R., Schenectady, N. Y.
Li, Y. T., Cambridge, Mass.
Lyon, R. P., Auburn, N. Y.
McMath, J. P. C., Winnipeg, Manitoba, Canada
McMullin, E. K., Inglewood, Calif.
Miera, S. M., Los Angeles, Calif.
Moncrief, L. E., North Syracuse, N. Y.
Munson, J. C., Silver Spring, Md.
Parker, D. J., Mershantville, N. J.
Redmond, W. G., Jr., Dallas, Tex.
Rove, G., Sherman Oaks, Calif.
Sann, K. H., Washington, D. C.
Schurr, P. M. E., Den Haag, Nederland
Seybold, A. M., West Caldwell, N. J.
Shima, S., Tokyo, Japan
Sobey, A. E., Jr., Dallas, Tex.
Stokes, R. G., Derwood, Md.
Stralser, B. J., Las Vegas, Nev.
Strelow, R. E., Los Alamitos, Calif.
Sundaram, P. S. M., Geneva, Switzerland

Transfer to Member

Abeson, I. S., Los Angeles, Calif.
Adey, A. W., Ottawa, Ont., Canada
Ahman, A. J., Huntington Station, L. I., N. Y.
Ahmann, R. M., Marshall, Minn.
Alderete, C. T., Anaheim, Calif.
Alton, J. M., Saint Paul, Minn.
Anderson, M. A., Tucson, Ariz.
Andrews, B. L., Haddonfield, N. J.
Andrews, R. C., Anaheim, Calif.
Apelbaum, J. H., Waban, Mass.
Asch, B., White Plains, N. Y.
Avrin, J. S., Ontario, Calif.
Baker, L. C., Brooklyn, N. Y.
Baker, P. A., Summit, N. J.
Ball, R. H., Washington, D. C.
Banhagel, E. W., Santa Monica, Calif.
Banta, F. D., Kettering, Ohio
Barrios, A. A., Red Bank, N. J.
Batterman, S., Delaware Township, N. J.
Beisel, F. A., Upper Montclair, N. J.
Bello, P. A., Needham, Mass.
Belluck, R. E., Brooklyn, N. Y.
Bengston, P. S., Silver Spring, Md.
Bentley, A. W., LaJolla, Calif.
Bessen, A. S., Brooklyn, N. Y.
Blum, C. M., Wynnewood, Pa.
Bowles, C. H., Jr., Cedar Rapids, Iowa
Bramble, C. A., Jr., Cincinnati, Ohio
Brooks, M. S., Hicksville, N. Y.
Brule, R. J., London, Ont., Canada
Bryan, G. E., Murray Hill, N. J.
Bublitz, A. T., Ann Arbor, Mich.
Buckler, P. F., Baltimore, Md.
Buley, T. L., Poughkeepsie, N. Y.
Bullock, A. J., Jr., Ithaca, N. Y.
Bush, B. A., Jr., Upper Darby, Pa.
Cabot, J. H., Woodside, L. I., N. Y.
Carros, J. R., Johnson City, N. Y.
Casey, S. D., Riverside, Calif.
Castellucci, A. H. E., George Air Force Base, Calif.

(Continued on page 154A)

Membership

(Continued from page 152A)

Castro, S. J., Flushing, L. I., N. Y.
Caswell, J. R., Lincoln, Mass.
Cederberg, R. D., Evanston, Ill.
Chait, H. N., Los Angeles, Calif.
Chang, C. M., Dallas, Tex.
Cheek, W. A., Hamilton, Ont., Canada
Chisholm, D. A., Murray Hill, N. J.
Chmiel, B. A., Pompton Lakes, N. J.
Chong, C. F., Philadelphia, Pa.
Churchill, O. R., Los Angeles, Calif.
Cimerman, L., Haddonfield, N. J.
Clark, N. F., Wakefield, Mass.
Clark, P. S., Newport Beach, Calif.
Clemence, C. R., Ottawa, Ont., Canada
Colburn, D. S., Palo Alto, Calif.
Collins, M., Woodstock, N. Y.
Connelly, E. McD., Springfield, Va.
Craig, J. P., Lubbock, Tex.
Cummins, E. L., San Jose, Calif.
Curtiss, R. H., Norwalk, Conn.
Daly, W. P., Glen Cove, L. I., N. Y.
D'Angelo, F., South Ozone Park, L. I., N. Y.
Davis, J. M., Sr., Bel Air, Md.
Davis, R. S., Levittown, N. J.
De Paola, G. E., New Shrewsbury, N. J.
Dillon, M. M., Gardena, Calif.
Di Nardo, A., Jr., Commack, L. I., N. Y.
Doerner, R. C., Wheaton, Ill.
Dorsay, T. A., Levittown, N. J.
Dougherty, R. L., Kingston, N. Y.
Douglas, J. W., Collingswood, N. J.
Drexel, A., Miami, Fla.
Due, R. C., Racine, Wis.
Duval, A. N., Orlando, Fla.
Edwards, D. J., Lubbock, Tex.
Ellinthorpe, A. W., Sudbury, Mass.
Erickson, T., Little Neck, L. I., N. Y.
Falknor, F. B., Jr., New York, N. Y.
Ferris, W. C., Jr., Belmont, Calif.
Finken, K. R., Jr., Massapequa Park, L. I., N. Y.
Finlay, R. S., Kansas City, Mo.
Fischer, D. H., Phoenix, Ariz.
Fitzgerald, J. F., Palo Alto, Calif.
Fountain, J. G., Manhattan Beach, Calif.
Frank, F. P. E., Amityville, L. I., N. Y.
Gallo, E. F., Santa Maria, Calif.
Garcia, G., West Covina, Calif.
Garson, E. L., New York, N. Y.
Gerardi, F. R., Los Angeles, Calif.
Ginsling, A. A., Palo Alto, Calif.
Goldsberry, P. E., Lexington, Ky.
Goldstein, A., Livingston, N. J.
Greco, N. A., Menlo Park, Calif.
Greene, A. A., Santa Maria, Calif.
Greig, W. J., Jr., Somerville, N. J.
Griffiths, J. D., Rome, N. Y.
Guilford, R. P., Albuquerque, N. M.
Gullatt, S. P., Jr., Santa Barbara, Calif.
Guthrie, E. E., Santa Clara, Calif.
Hacker, P. S., Silver Spring, Md.
Hahn, J., Dumont, N. J.
Hann, J. D., Silver Spring, Md.
Harcar, A. R., Rome, N. Y.
Harjes, F. W., Westbury, L. I., N. Y.
Harris, E. L., Westerville, Ohio
Haselton, E. F., Waltham, Mass.
Hastings, D. F., Smithtown, N. Y.
Hata, J. H., New York, N. Y.
Hays, F. R., Whippany, N. J.
Hayward, W. S., Jr., Westfield, N. J.
Heinzinger, J. P., Mountain View, Calif.
Heislein, J. T., Andover, Mass.
Hertz, K. L., New Brunswick, N. J.
Hill, M. E., Alexandria, Va.
Ho, E-C., Pacific Palisades, Calif.
Hofler, J. J., Hurley, N. Y.
Holm, W. E., Inglewood, Calif.
Hook, G. E., Speedway, Ind.
Horn, R. E., Severna Park, Md.

(Continued on page 158A)

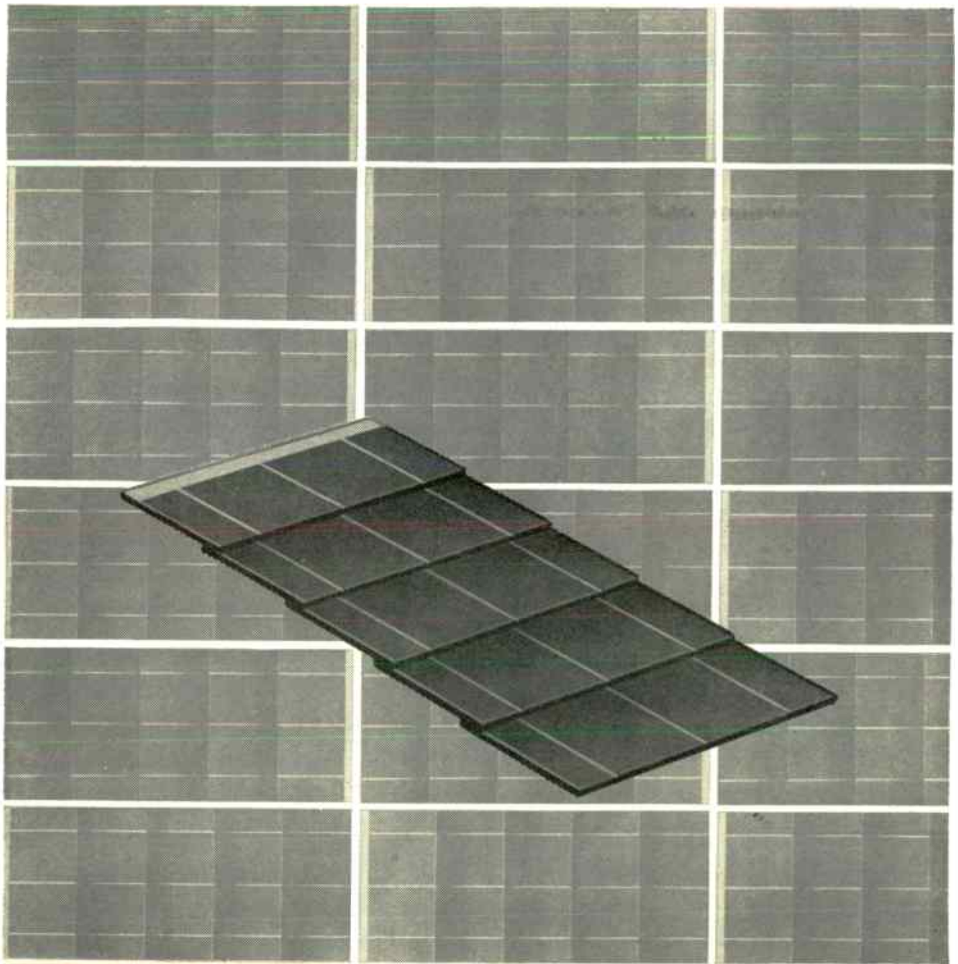

Hoffman solar-power series.

SOLAR-SHINGLE®† ASSEMBLY/POWER CURVES IN SPACE

90% area utilization, spatial solar input in vicinity of earth's orbit (140 mW/cm²)

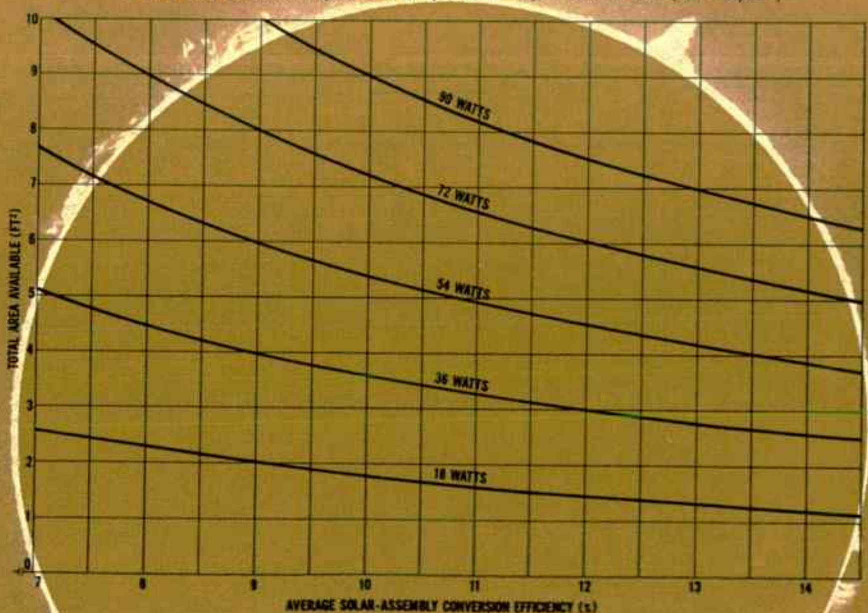

ELECTRICAL CHARACTERISTICS

Test Conditions: 100 mW/cm² solar input (at earth's surface)

SILICON SOLAR CELLS (TYPE 120C)				SILICON SOLAGRID* CELLS (TYPE 120CG)			
Type No.	Load Voltage mV	Minimum Output mA	Conversion Efficiency %	Type No.	Load Voltage mV	Minimum Output mA	Conversion Efficiency %
120C-7	400	31.5	7.0	120CG-11	485	40.8	11.0
120C-8	400	36.0	8.0	120CG-12	485	44.5	12.0
120C-9	400	40.5	9.0	120CG-13	485	48.2	13.0
120C-10	400	45.0	10.0	120CG-14	485	51.9	14.0

†A Patented Device (U.S. Patent No. 2,938,938)

*Trade Mark Hoffman Electronics Corporation

ONLY HOFFMAN GIVES YOU THIS MUCH DESIGN RANGE IN SILICON SOLAR-POWER ASSEMBLIES

No longer need unconventional solar-power requirements cause procurement problems. Hoffman's broad range of conversion efficiencies — widest in the industry — helps you achieve the optimum solution. Now you can specify size, shape, power output and conversion efficiency in an unprecedented number of combinations. ■ The curves at the left show you how much design flexibility is possible. To determine the minimum assembly efficiency necessary, relate the area available to the desired power output. For details, consult your Hoffman sales engineer or request Data Sheet 126-660S.

Hoffman

ELECTRONICS CORPORATION

Semiconductor Division

1001 Arden Drive, El Monte, California

TWX: El Monte 9735

Plants: El Monte, California and Evanston, Illinois

28 Fields of Special Interest-

The 28 Professional Groups are listed below, together with a brief definition of each, the name of

Aeronautical and Navigational Electronics

Annual fee: $2.

The application of electronics to operation and traffic control of aircraft and to navigation of all craft.

Mr. W. P. McNally, Chairman, Servo Corp., Hicksville, L.I., N.Y.

35 Transactions, *5, *6, & *9, and *Vol. ANE-1, No. 3; Vol. 2, No. 1-3; Vol. 3, No. 2; Vol. 4, No. 1, 2, 3,; Vol. 5, No. 2, 3, 4; Vol. 6, No. 1, 3, 4; Vol. 7, No. 1.

Antennas and Propagation

Annual fee: $4.

Technical advances in antennas and wave propagation theory and the utilization of techniques or products of this field.

Prof. Edward C. Jordan, Chairman, Electrical Engineering Dept., University of Illinois, Urbana, Ill.

29 Transactions, *Vol. AP-2, No. 2; AP-4, No. 4; AP-5, No. 1-4; AP-6, No. 1, 2, 3, 4; AP-7, No. 1, 2, 3, 4; AP-8, No. 1, 2.

Audio

Annual fee: $2.

Technology of communication at audio frequencies and of the audio portion of radio frequency systems, including acoustic terminations, recording and reproduction.

Mr. H-S. Knowles, Chairman, Knowles Electronics, 9400 Belmont Ave., Franklin Park, Ill.

52 Transactions, *Vol. AU-1, No. 6; *Vol. AU-2, No. 4; Vol. AU-3, No. 1, 3, 5; Vol. AU-4, No. 1, 5-6; Vol. AU-5, No. 1, 2, 3, 4, 5, 6; AU-6, No. 1, 2, 3, 4, 5, 6; AU-7, No. 1, 2, 3, 4, 5, 6; AU-8, No. 1, 2.

Automatic Control

Annual fee: $3.

The theory and application of automatic control techniques including feedback control systems.

Mr. John M. Salzer, Chairman, 909 Berkeley St., Santa Monica, Calif.

8 Transactions, PGAC-3-4-5-6, AC-4, No. 1, 2, 3; AC-5, No. 1.

Bio-Medical Electronics

Annual fee: $3.

The use of electronic theory and techniques in problems of medicine and biology.

Dr. Herman P. Schwan, Chairman, University of Pennsylvania, School of Elec. Engrg., Philadelphia 4, Pa.

16 Transactions, 8, 9, 11, 12; ME-6, No. 1, 2, 3, 4; ME-7, No. 1.

Broadcast & Television Receivers

Annual fee: $4.

The design and manufacture of broadcast and television receivers and components and activities related thereto.

Mr. Robert R. Thalner, Chairman, Sylvania Home Electronics, Batavia, N.Y.

25 Transactions, *7, 8; BTR-1, No. 1-4; BTR-2, No. 1-2-3; BTR-3, No 1-2; BTR-4, No. 2, 3-4; BTR-5, No. 1, 2, 3; BTR-6, No. 1.

Broadcasting

Annual fee: $2.

Broadcast transmission systems engineering, including the design and utilization of broadcast equipment.

Mr. George E. Hagerty, chairman, Westinghouse, 122 E. 42nd St., New York 17, N.Y.

15 Transactions, No. 2, 6, 7, 8, 10, 11, 12, 13, 14; BC-6, No. 1.

Circuit Theory

Annual fee: $3.

Design and theory of operation of circuits for use in radio and electronic equipment.

Mr. Sidney Darlington, Chairman, Bell Tel. Labs., Murray Hill, N.J.

26 Transactions, CT-3, No. 2; CT-4, No. 3-4; CT-5, No. 1, 2, 3, 4, CT-6, No. 1, 2, 3, 4; CT-7, No. 1.

Communications Systems

Annual fee: $2.

Radio and wire telephone, telegraph and facsimile in marine, aeronautical, radio-relay, coaxial cable and fixed station services.

Capt. C. L. Engleman, Chairman, Engleman & Co., Inc., 2480 16th St., N.W., Washington 9, D.C.

17 Transactions, CS-5, No. 2, 3; CS-6, No. 1, 2; CS-7, No. 1, 3, 4; CS-8, No. 1.

Component Parts

Annual fee: $3.

The characteristics, limitation, applications, development, performance and reliability of component parts.

Mr. Floyd E. Wenger, Chairman, Headquarters ARDC, Andrews AFB, Washington 25, D.C.

19 Transactions, CP-4, No. 1, 2, 3-4; CP-5, No. 1, 2, 3, 4; CP-6, No. 1, 2, 3, 4; CP-7, No. 1.

Education

Annual fee: $3.

To foster improved relations between the electronic and affiliated industries and schools, colleges, and universities.

Dr. John G. Truxal, Chairman, Dept. of EE, PIB, Brooklyn, N.Y.

10 Transactions, Vol. E-1, No. 3, 4; E-2, No. 1, 2, 3, 4; E-3, No. 1, 2.

Electron Devices

Annual fee: $3.

Electron devices, including particularly electron tubes and solid state devices.

Mr. A. K. Wing Jr., Chairman IT&T Labs, Nutley, N.J.

28 Transactions, *Vol. ED-1, No. 3-4; ED-3, No. 2-4; ED-4, No 2-3, 4; ED-5, No. 2, 3, 4; ED-6, No. 1, 3; ED-7, No. 1, 2.

Electronic Computers

Annual fee: $4.

Design and operation of electronic computers.

Dr. A. A. Cohen, Chairman, Remington-Rand Univac, St. Paul 16, Minn.

33 Transactions, EC-6, No. 2, 3; EC-7, No. 1, 2, 3, 4; EC-8, No. 1, 2, 3, 4; EC-9, No. 1.

Engineering Management

Annual fee: $3.

Engineering management and administration as applied to technical, industrial and educational activities in the field of electronics.

Dr. Henry M. O'Bryan, Sylvania Elec. Products, 730 3rd Ave., New York 17, N.Y.

17 Transactions, EM-3, No. 2, 3; EM-4, No. 1, 3, 4; EM-5, No. 1-4; EM-6, No. 1, 2, 3; EM-7, No. 1.

Engineering Writing and Speech

Annual fee: $2.

The promotion, study, development, and improvement of the techniques of preparation, organization, processing, editing, and delivery of any form of information in the electronic-engineering and related fields by and to individuals and groups by means of direct or derived methods of communication.

Mr. T. T. Patterson, Jr., Chairman, RCA Bldg. 13-2, Camden, N.J.

6 Transactions, Vol. EWS-1, No. 2; EWS-2, No. 1, 2, 3; EWS-3, No. 1.

THE INSTITUTE OF RADIO

-IRE's 28 Professional Groups

the group chairman, and publications to date.

* Indicates publications still available

Human Factors in Electronics
Annual fee: $2.

Development and application of human factors and knowledge germane to the design of electronic equipment.

Mr. Robert R. Riesz, Chairman, Bell Tel. Labs, Murray Hill, N.J.

1 Transaction, HFE-1, No. 1.

Industrial Electronics
Annual fee: $3.

Electronics pertaining to control, treatment and measurement, specifically, in industrial processes.

Mr. J. E. Eiselein, Chairman, RCA Victor Dev., Camden, N.J.

11 Transactions, *PGIE 1, 3, 5, 6, 7, 8, 9, 10, 11.

Information Theory
Annual fee: $3.

The theoretical and experimental aspects of information transmission, processing and utilization.

Dr. Paul E. Green, Jr., Chairman, Lincoln Lab., MIT, Lexington, Mass.

21 Transactions, PGIT-4, IT-1, No. 2-3; IT-2, No. 3; IT-3, No. 1, 2, 3, 4; IT-4, No. 1, 2, 3, 4; IT-5, No. 1, 2, 3, 4; IT-6, No. 1, 2.

Instrumentation
Annual fee: $2.

Measurements and instrumentation utilizing electronic techniques.

Mr. C. W. Little, Jr., Chairman, C-Stellerator Assoc., Princeton, N.J.

16 Transactions, 4; Vol. 1-6, No. 2, 3, 4; Vol. 1-7, No. 1, 2; Vol. 1-8, No. 1, 2.

Microwave Theory and Techniques
Annual fee: $3.

Microwave theory, microwave circuitry and techniques, microwave measurements and the generation and amplification of microwaves.

Dr. Kiyo Tomiyasu, Chairman, General Electric Microwave Lab., Palo Alto, Calif.

30 Transactions, MTT-4, No. 3; MTT-5, No. 3, 4; MTT-6, No. 1, 2, 3, 4; MTT-7, No. 2, 3, 4; MTT-8, No. 1, 2, 3.

Military Electronics
Annual fee: $2.

The electronics sciences, systems, activities and services germane to the requirements of the military. Aids other Professional Groups in liaison with the military.

Mr. Edward G. Witting, Chairman, R&D Dept. U.S. Army, Pentagon, Wash. 25, D.C.

8 Transactions, MIL-1, No. 1; MIL-2, No. 1; MIL-3, No. 2, 3, 4.

Nuclear Science
Annual fee: $3.

Application of electronic techniques and devices to the nuclear field.

Dr. A. B. Van Rennes, Chairman, United Research, Inc., Cambridge, Mass.

16 Transactions, NS-1, No. 1; NS-3, No. 2; NS-4, No. 2; NS-5, No. 1, 2, 3, NS-6, No. 1, 2, 3, 4; NS-7, No. 1.

Production Techniques
Annual fee: $2.

New advances and materials applications for the improvement of production techniques, including automation techniques.

Mr. Warren D. Novak, Chairman, General Precision Labs, Pleasantville, N.Y.

6 Transactions, No. 2-3, 4, 5, 6.

Radio Frequency Techniques
Annual fee: $2.

Origin, effect, control and measurement of radio frequency interference.

Professor Ralph M. Showers, Chairman, Moore School of Elec. Eng., 200 S. 33rd St., Philadelphia 4, Pa.

1 Transaction, RF-1, No. 1.

Reliability and Quality Control
Annual fee: $3.

Techniques of determining and controlling the quality of electronic parts and equipment during their manufacture.

Mr. P. K. McElroy, Chairman General Radio Co., West Concord, Mass.

17 Transactions, *3, 5-6, 10, 11, 12, 13, 14, 15, 16; RQC-9, No. 1.

Space Electronics and Telemetry
Annual fee: $2.

The control of devices and the measurement and recording of data from a remote point by radio.

Mr. Robert V. Werner, Cubic Corp. Chairman, San Diego, Calif.

14 Transactions, TRC-1, No. 2-3; TRC-2, No. 1; TRC-3, No. 2, 3; TRC-4, No. 1; SET-5, No. 1, 2, 3, 4; SET-6, No. 1.

Ultrasonics Engineering
Annual fee: $2.

Ultrasonic measurements and communications, including underwater sound, ultrasonic delay lines, and various chemical and industrial ultrasonic devices.

Mr. David L. Arenberg, Chairman, Arenberg Ultrasonic Lab. Inc., Jamica Plains, Mass.

8 Transactions, PGUE, 5, 6, 7; UE-7, No. 1.

Vehicular Communications
Annual fee: $2.

Communications problems in the field of land and mobile radio services, such as public safety, public utilities, railroads, commercial and transportation, etc.

Mr. A. A. MacDonald, Chairman, Motorola, Inc., 4545 W. Augusta Blvd., Chicago 51, Ill.

13 Transactions, 5, 6, 8, 9, 10, 11, 12, 13.

USE THIS COUPON

PG-7-60

Miss Emily Sirjane
IRE—1 East 79th St., New York 21, N.Y.

Please enroll me for these IRE Professional Groups

.... $ ....
.... $ ....

Name ....
Address ....
Place ....

Please enclose remittance with this order.

ENGINEERS **1 East 79th Street, New York 21, N.Y.**

Membership

(Continued from page 154A)

Houldin, R. J., Poughkeepsie, N. Y.
Hoyt, E. P., Arlington, Calif.
Hricko, R. M., Nicholson, Pa.
Hunt, M. J., Salt Lake City, Utah
Hunter, H. H., Columbus, Ohio
Ittenbach, L. J., Jr., Phoenix, Ariz.
Ives, W. J., Belleville, Ont. Canada
Jackson, A. S., Hinsdale, Ill.
Jayson, E. L., Falmouth, Mass.
Johannesen, W., Richmond Hill, L. I., N. Y.
Johnson, F. L., Glens Falls, N. Y.
Johnson, S. L., Cochituate, Mass.
Jones, B. J., Sherman Oaks, Calif.
Kalin, F., North Bergen, N. J.
Kalisky, A., Sudbury, Mass.
Kellar, J. B., Seattle, Wash.
Kerns, G. P., Ithaca, N. Y.
King, P. F., Webster, N. Y.
Knocklein, H. P., Mineola, L. I., N. Y.
Koenig, M., Camden, N. J.
Kuskowski, L. J., East Northport, L. I., N. Y.
Lamb, J. M., Newton, N. J.
Lamere, B. E., Manchester, N. H.
Landman, R. M., Sherman Oaks, Calif.
Landry, A. P., New Orleans, La.
Lanford, L. D., Kansas City, Kan.
Larney, J. L., Chicago, Ill.
Layden, O. P., Shrewsbury, N. J.
Leahy, G. F., Dumont, N. J.
Lehman, G. C., Wayne, N. J.
Leibholz, S. W., Huntington, L. I., N. Y.
Lewicki, W. M., Cheektowaga, N. Y.
Liebermann, J., Haddonfield, N. J.
Liebold, F. A., Glendora, N. J.
Lind, M. S., Houghton, Mich.
Lockyer, J. E., Thistletown, Ont., Canada
Lohkemper, O. A., New Hyde Park, L. I., N. Y.
Low, R. C., Nashua, New Hampshire
Luehring, E. L., Cleveland, Ohio
Lyuta, G. R., Georgetown, Conn.
Mack, C. L., Jr., Lexington, Mass.
MacLeod, D. S., Vestal, N. Y.
Macomber, G. R., Largo, Fla.
Malitz, E., Collingswood, N. J.
Maloy, M., Fair Lawn, N. J.
Malvin, M. A., Medford, N. J.
Mandell, M., New York, N. Y.
Margulies, H. H., Hazelwood, Mo.
Marshall, J. A., Sunnyvale, Calif.
Marshall, J., Warren, Mich.
Martin, A. L., II, Woodside, L. I., N. Y.
Mattes, A. J., Eatontown, N. J.
Maxwell, J. W., Dallas, Tex.
Mayhew, J. A., Randallstown, Md.
Mays, C. H., Pomona, Calif.
McBride, N. G., Hamburg, N. Y.
McClure, R. W., Newark, Del.
McDonald, M., Houston, Tex.
McDuff, B. G., Ft. Worth, Tex.
McPhail, J. H., Santa Clara, Calif.
McPherson, R. T., Sault Ste. Marie, Mich.
Mealey, G. J., San Diego, Calif.
Mesecher, M. G., Huntington Sta., L. I., N. Y.
Metzelaar, P. N., Pacific Palisades, Calif.
Metzler, D. H., Syracuse, N. Y.
Metzner, J. J., Rego Park, L. I., N. Y.
Michon, G. J., Waterford, N. Y.
Miles, H. L., Houston, Tex.
Miller, R. L., Whitesboro, N. Y.
Millunzi, P. T., Minneapolis, Minn.
Miner, J. H., Munster, Ind.
Mirick, H. L., Jr., West Hurley, N. Y.
Mitchell, C. A., II, Los Angeles, Calif.
Mitchell, J. M., Los Angeles, Calif.
Mitchell, W. F., Fairfield, Conn.
Monshaw, J. H., New York, N. Y.
Moore, P. G., Los Angeles, Calif.
Morey, G. A., Poughkeepsie, N. Y.
Morrow, A. J., Huntington Station, L. I., N. Y.
Munt, I., New Brunswick, N. J.
Murray, P. C., Franklin Park, N. J.

(Continued on page 160A)

IT TALKS BACK THROUGH A RYPINSKI DUPLEXER

The highly-instrumented Pioneer V would lose most of its effectiveness if we could not communicate with it at will from Earth. Fortunately, the spaceborne hardware works; it talks back from megamiles when Earthbound technicians trigger it. The C. A. Rypinski Co. is proud to have supplied the UHF Duplexer that makes it possible to share a single efficient antenna in the STL-designed Pioneer V for transmitting and receiving. Rypinski specializes in the design and manufacture of filters that work. Write for our descriptive brochure and product bulletins.

C. A. RYPINSKI CO.
2005 No. Fair Oaks Ave.
Pasadena, California
MU 1-4423

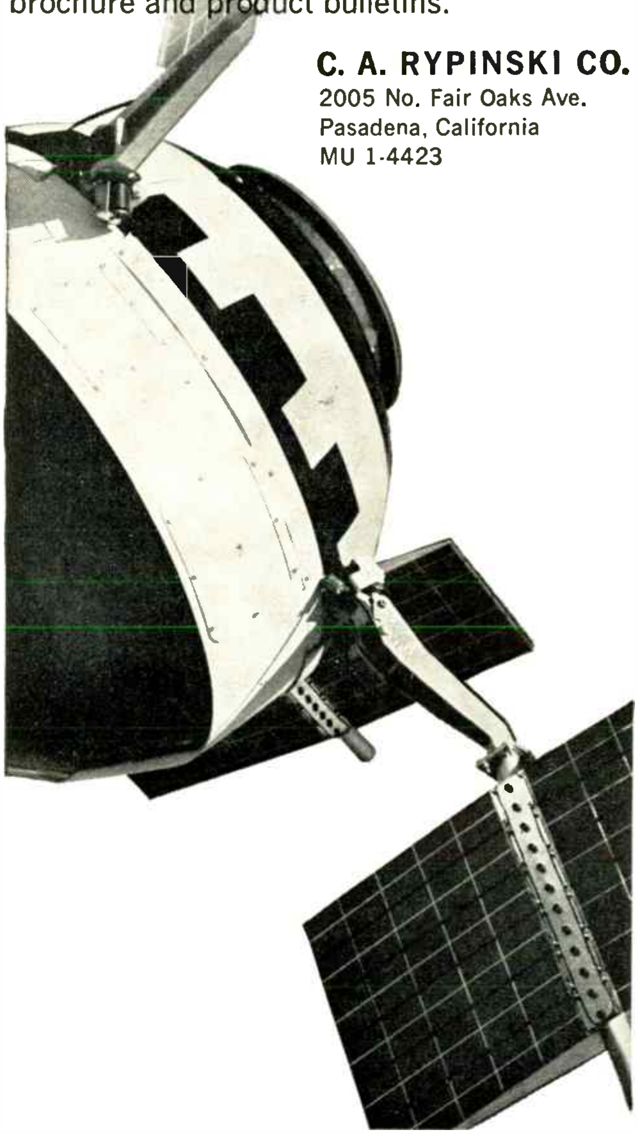

Applied Research inc.

LOW NOISE RF AMPLIFIERS

NOISE FIGURES

LESS THAN 1 DB at 30 MC
3 DB at 300 MC

No Blowers

No Critical Alignment

Amplifier Model UH-2(A)SP is available at any preset frequency between 30 and 300 MC. This amplifier is a two tube unit with broadband response, high gain, and low noise figure. The unit requires no additional air cooling supply, as natural ventilation is used. The amplifier and its power supply are assembled on a 19" L x 3½" H panel suitable for rack mounting. Small size and low weight are featured in the rugged amplifier chassis.

Specifications of the amplifier are given below.

SPECIFICATIONS—MODEL UH-2(A)SP AMPLIFIERS

Frequency range:	Center frequency between 30 MC and 300 MC
Bandwidth:	Up to 10% of center frequency
Gain:	Greater than 20 DB (function of freq. and BW)
Noise figure:	<1 DB at 30 MC to <3 DB at 300 MC (function of freq. and BW)
Source impedance:	50 ohms
Output impedance:	50 ohms
Connectors: input	Type BNC, or N
output	Type BNC, or N
power	2 prong motor base receptacle
Power requirements:	115 VAC, 60 cps, 25 W
Dimensions:	19" L x 3½" H x 6½" D
Weight:	12¾ lbs.
Finish:	Gray enamel panel

For additional information write

Applied Research inc.

76 South Bayles Avenue, Port Washington, N. Y.

Membership

(Continued from page 158A)

Murray, W. A., Seattle, Wash.
Neumann, L. R., Philadelphia, Pa.
Nidus, L. S., Fort Lee, N. J.
Ohlmann, G. A., Palos Verdes Estates, Calif.
Okwit, S., Melville, L. I., N. Y.
Oldfield, R. L., Chicago, Ill.
Oliver, E. F., El Cajon, Calif.
Oman, R. M., Saint Paul, Minn.
Ostrowski, R. E., North Syracuse, N. Y.
Otis, G. E., Ocean Springs, Miss.
Pace, R. A., Jericho, L. I., N. Y.
Pantazelos, P. G., Somerville, Mass.
Pape, A. E., Melrose Park, Ill.
Paquette, G. A., Wetherfield, Conn.
Park, J. H., Jr., Minneapolis, Minn.
Parkinson, R. W., Newport Beach, Calif.
Pate, G. W., Jr., Clearwater, Fla.
Perry, W. C., Los Angeles, Calif.
Peterson, J. A., Reseda, Calif.
Pfeiffer, J. H., Jr., Cincinnati, Ohio
Pinkstaff, J. R., Peabody, Mass.
Plumridge, R. F., Lexington, Mass.
Podell, R. L., Oradell, N. J.
Polgar, E. A., Sacramento, Calif.
Polkosnik, C. F., Jr., Union, N. J.
Porter, H., Jr., Denver, Colo.
Potter, F. J., Penfield, N. Y.
Power, H. J., Whitesboro, N. Y.
Presutti, B., Erie, Pa.
Ralidis, G. W., Bayside, L. I., N. Y.
Raman, S., Poona, India
Ramsey, J. T., Dayton, Ohio
Ratner, A., Philadelphia, Pa.
Rawdin, E., Morrestown, N. J.
Redfield, D. D., Charlottesville, Va.
Regniere, J-P., Ste. Foy, Que., Canada
Reilly, M., Glendora, Calif.
Rhamy, J. D., San Diego, Calif.
Richard, C. A., Jr., Pequannock, N. J.
Ritchie, R. W., Ontario, Calif.
Roder, A., Mountain View, Calif.
Rosenberg, H. S., San Pedro, Calif.
Rosenthal, M. L., Natick, Mass.
Rothenstein, E. M., New York, N. Y.
Rothwell, T. L., Jr., Gardena, Calif.
Sackett, R. W., Milwaukee, Wis.
Sackson, M. M., New York, N. Y.
Sanders, J. J., Rochester, Minn.
Saunders, W. K., Bethesda, Md.
Savoie, L. P., Burlington, N. C.
Saxe, H. A., Whippany, N. J.
Schlechter, L., Forest Hills, L. I., N. Y.
Schneider, R. W., Rockville, Conn.
Schodowski, S. S., Asbury Park, N. J.
Searcy, J. H., Melbourne, Fla.
Shear, H., Palo Alto, Calif.
Shelton, P. W., Baldwin, L. I., N. Y.
Siddall, W. D., Havana, Cuba
Sigelmann, R. A., Seattle, Wash.
Simon, H., Brooklyn, N. Y.
Simons, S. C., West Peabody, Mass.
Sirkis, M. D., New Brunswick, N. J.
Skerritt, J. W., Kingston, N. J.
Skinner, D. D., Turtle Creek, Pa.
Smith, W. F., Jr., Syracuse, N. Y.
Smith, W. L., Palmyra, N. J.
Sorkin, C. S., Bala Cynwid, Pa.
Spector, G., New York, N. Y.
Spector, N., Little Neck, L. I., N. Y.
Sperling, L., Panorama City, Calif.
Spieler, A., Huntington Valley, Pa.
Spink, P. G., Arnold, Md.
Sprouse, P. J., Mishawaka, Ind.
Stankovich, D., San Fernando, Calif.
Steed, W. P., Lafayette, Calif.
Steele, K. P., Eden, N. Y.
Stelene, L. H., Jr., Orlando, Fla.
Stengel, C. J., Jr., Buffalo, N. Y.
Stern-Montagny, F. H., Hurley, N. Y.
Stevenson, D. D., China Lake, Calif.
Street, E. L., Hamilton, Mass.
Strinkowski, N. W., Riverton, N. J.
Strumer, J. N., Briarcliff Manor, N. Y.
Stuart, H. D., Utica, N. Y.
Swain, W. H., Sarasota, Fla.
Swisher, B. F., Seattle, Wash.
Szirmay, S. Z., Altadena, Calif.
Szupillo, R. E., Corning, N. Y.
Tatsuguchi, I., Whippany, N. J.
Taylor, E. H., North Hollywood, Calif.
Temple, K. H., Freeville, N. Y.
Templeton, H. S., Hopewell Junction, N. Y.
Terashi, T., Aberdeen, Md.
Thomas, D. C., Northridge, Calif.
Thomas, E. K., Sudbury, Mass.
Thurston, R. N., Murray Hill, N. J.
Tockey, R. J., Livermore, Calif.
Troiano, A., Raritan, N. J.
Turchiano, M. W., New York, N. Y.
Van Den Berg, W. J., Jr., Las Vegas, Nev.
Vlasak, W. R., Ft. Lauderdale, Fla.
Vodopia, S. N., Los Angeles, Calif.
Voelcker, H. B., Jr., London, England
Wall, R. D., Madison, N. J.
Ward, V. E., Jr., Buffalo, N. Y.
Warren, W. L., Haddonfield, N. J.
Watson, J. T., Dallas, Tex.
Webb, W. J., Ossining, N. Y.
Weber, V. F., Elmhurst, Ill.
Weems, S., Chatsworth, Calif.
Weinstein, D. A., El Sobrante, Calif.
Wentz, J. L., Albuquerque, N. M.
Werner, W., Minneapolis, Minn.
Westman, W. W., Jr., Albuquerque, N. M.
Wexler, P. S., New York, N. Y.
Wible, P. E., Jr., Fort Wayne, Ind.
Williamson, R. T., Belle Harbor, L. I., N. Y.
Williamson, W., Youngstown, Ohio
Wilson, H. S., Haddonfield, N. J.
Wolber, W. G., Detroit, Mich.
Woods, E. L., Tustin, Calif.
Worth, F. L., Van Nuys, Calif.
Worthington, R. L., East Orange, N. J.
Wright, W. L., Monroeville, Pa.
Wynne, J. J., Washington, D. C.
Yaeger, W. O., Orange, N. J.
Young, E. A., Rochester, N. Y.
Zadoff, S. A., Jericho, L. I., N. Y.
Zemenick, C. J., Whittier, Calif.
Zirkle, R. E., Jr., Minneapolis, Minn.
Zola, M. J., Pleasantville, N. Y.
Zuck, R. A., Lafayette Hill, Pa.

Admission to Member

Aitken, T. B., Wynnewood, Pa.
Argondelis, E., Chicago, Ill.
Ascione, A., Rome, Italy
Baker, J. R., Jr., Ipswich, Mass.
Barron, C. L., Minneapolis, Minn.
Bates, R. H. T., Arlington, Mass.
Beagle, C. K., Torrance, Calif.
Beetem, J. M., Portland, Ore.
Blomeyer, L. S., Reseda, Calif.
Blount, G. H., Oak View, Calif.
Bonasera, J. T., Commack, L. I., N. Y.
Bonin, D., Seattle, Wash.
Booker, S. R., Albuquerque, N. M.
Bossard, C. L., Perkasie, Pa.
Brass, R. L., Morristown, N. J.
Broniwitz, L. E., Syracuse, N. Y.
Brooks, R. R., Denver, Colo.
Brown, R. J., Jr., Tempe, Ariz.
Brummer, E. A., Warwick, Va.
Bryan, R. K., Oklahoma City, Okla.
Bumstorf, T. A., Bradford, Pa.
Carlson, J. W., Baltimore, Md.
Casazza, C. A., Brooklyn, N. Y.
Castle, B. B., West Keansburg, N. J.
Chaffee, B. A., Wethersfield, Conn.
Chandler, J. A., Little Ferry, N. J.
Chang, Y. G., Long Branch, N. J.
Cleary, F. W., Pacific Palisades, Calif.
Cluggish, W. H., Indianapolis, Ind.
Coccoli, J. C., Upper Providence, Media, Pa.
Cook, A. W., East Brunswick, N. J.
Cook, P. G., Bradford, Pa.

(Continued on page 162A)

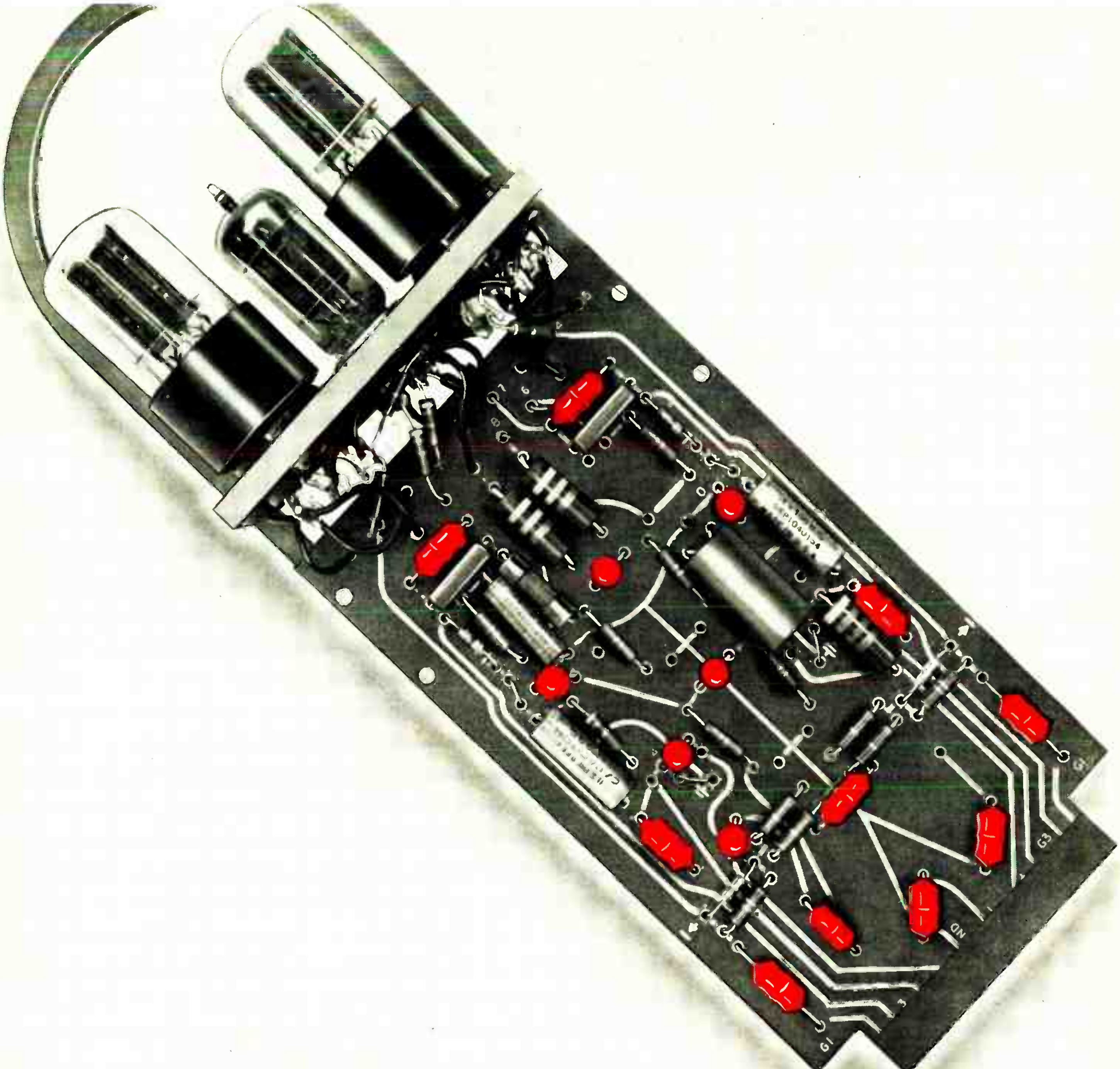

Top reliability in miniature size...

Daven wire wound resistors

For printed circuit boards, miniature plug-in packages . . . any tight place in which you must have a really small wire wound resistor, check Daven for the Super Davohm Miniatures that can solve your problem. For example . . .

1273
"Lollypop"
Up to 400 K

1274
Up to 100 K

1250
Up to 900 K

SHOWN ACTUAL SIZE

These resistors meet and exceed all requirements, except physical size, of MIL-R-93-B, and MIL-R-9444.

The overall stability of Daven Miniature Resistors is possible because of an entirely new approach to subminiature production techniques. A unique spool design permits low-stress winding of fine resistance wire . . . obtaining 2 to 3 times the resistance value previously supplied on a miniature bobbin. This is done under the most stringent quality control and inspection.

The industry's widest range of sizes, temperature coefficients, and tolerances is available for your requirements. Write today for further information and a complete resistor catalog.

THE DAVEN CO. **LIVINGSTON, NEW JERSEY**

TODAY, MORE THAN EVER, THE DAVEN Ⓓ STANDS FOR DEPENDABILITY

Membership

(Continued from page 160A)

Cooper, D. J., Hicksville, N. Y.
Cortez De Lobao, F. J., Den Haag, Netherlands
Cory, I. W., Charleston, S. C.
Craig, J. C., Waco, Tex.
Craig, P. H., Jr., Gainesville, Fla.
Davies, M. C., North Harrow, Middx., England
Delzer, C. L., Las Vegas, Nev.
Dempsey, R. J., Manhattan Beach, Calif.
Domchick, R. J., Huntington Station, L. I., N. Y.
Donaldson, R. W., Jr., Glen Burnie, Md.
Draper, I. K., San Jose, Calif.
Druschel, W. H., Pittsfield, Mass.
Duncan, R. D. P., Bedford, Mass.
Dupen, D. W., Menlo Park, Calif.
Durham, A. F., Levittown, Pa.
Durnovo, C. P., Flushing, L. I., N. Y.
Earleywine, E., Midland, Mich.
Edson, A. P., Chatham, N. J.
Ellett, J. D., Ft. Worth, Tex.
Elliott, Brother J., New York, N. Y.
Eng, D. Y., Farmingdale, L. I., N. Y.
Engert, M., Baltimore, Md.
Erb, G. H. C., Somerville, N. J.
Erdag, J. M., Los Angeles, Calif.
Erickson, W. L., San Diego, Calif.
Fahey, W. P., Commack, L. I., N. Y.
Farey, L., Richmond, B. C., Canada
Farkas, B., McKeesport, Pa.
Feavearyear, J. E., Huntington Sta., L. I., N. Y.
Feidelman, L. A., Willow Grove, Pa.
Fejer, J. A., Ottawa, Ont., Canada
Fennel, C. K., Dallas, Tex.
Fiecki, R. F., Audubon, N. J.
Fields, H. R., Inglewood, Calif.
Filley, W. H., Jr., Newmarket, Ont., Canada
Fischer, R. E., West Webster, N. Y.
Fischler, H., Rehovoth, Israel
Foldis, G., Napoli, Italy
Forbes, R. F., Jr., Fullerton, Calif.
Forry, S. H., East Syracuse, N. Y.
Foster, L. E., Springfield, Va.
Freilich, A., Brooklyn, N. Y.
Friedman, J. W., Merrick, L. I., N. Y.
Fuschetto, A. N., Collingswood, N. J.
Gallagher, B. D., Syracuse, N. Y.
Galler, H., Buffalo, N. Y.
Geissler, F. X., Bayside, L. I., N. Y.
Gershon, G. S., Ridgefield, N. J.
Gibilisco, P. J., Reading, Pa.
Gilbeau, L. E., Sherbrooke, Que., Canada
Glassberg, R., Los Angeles, Calif.
Gliessman, J. R., Corona Del Mar, Calif.
Goj, W. W., Goodyear, Ariz.
Gonzalez, C. P., Ivyland, Pa.
Graybill, H. R., Arlington, Va.
Greenberg, S. N., Philadelphia, Pa.
Grubbs, C. L., Fort Worth, Tex.
Guscott, J. K., Great Neck, L. I., N. Y.
Hackbarth, E., Houston, Tex.
Halverson, H. L., Palo Alto, Calif.
Hansen, E. N., Nutley, N. J.
Hart, G. H., Jr., Wayland, Mass.
Hart, J. C., Watertown, Mass.
Hart, R. R., Los Angeles, Calif.
Hayashi, I., Kitatama-gun, Tokyo, Japan
Hechler, V., IV, Northfield, Ill.
Helliwell, J., Berlin, N. J.
Henson, M. J., Covina, Calif.
Hermann, G. L., Ste. Genevieve, Mo.
Herrington, L. H., Winnipeg, Man., Canada
Heyser, L. S., Linthicum Heights, Md.
Hoffman, S. P., Graham, N. C.
Holmes, J. C., Scotch Plains, N. J.
Holzman, J., Los Angeles, Calif.
Hoppel, T. O., Nicktown, Pa.
Howard, J. A., Los Angeles, Calif.
Howard, M. G., Macon, Ga.
Hoyt, R. S., South Plainfield, N. J.
Hughes, D. W., La Crescenta, Calif.
Hull, C. E., Kansas City, Mo.

(Continued on page 164A)

Lab setup shows SB-15a versatility. (1) FM display measures dynamic deviation. (2) & (3) are AM and SSB signals, respectively, with sine wave modulation.

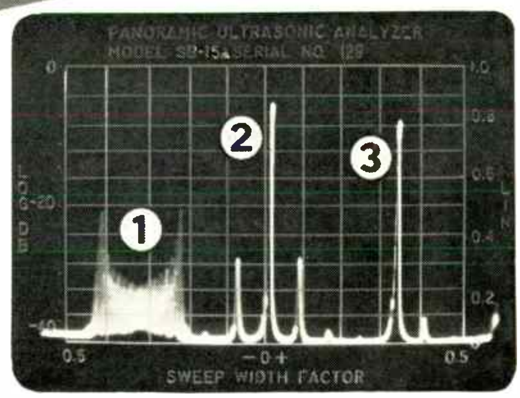

NOT JUST ULTRASONIC . . .

ULTRA-Compact (only 8¾" high)
ULTRA-Versatile (so many applications)
ULTRA-Fast • Easy-to-read • Economical

Panoramic's advanced Model SB-15a automatically and repetitively scans spectrum segments from 1 kc to 200 kc wide through the entire range (0.1 kc to 600 kc) . . . plots frequency and amplitude along the calibrated X and Y axes of a long persistence CRT, or on a 12 x 4½" chart (optional RC-3a/15). Sweep rates are adjustable from 1 to 60 cps.

Adjustable resolution enables selection and detailed examination of signals as close as 100 cps. Self-checking internal frequency markers every 10 kc. Also internal amplitude reference • Only 8¾" high, the SB-15a is completely self-contained, needs no external power supply or regulator.

PANORAMIC PRESENTATION MEANS
- quick signal location, minimum chance of missing weak signals or holes in spectrum
- faster measurements—no tedious point-by-point plots
- reliable spotting of low level discrete signals in noise
- positive identification and dynamic analysis of all types of modulation

ALL THESE APPLICATIONS . . .
- Noise, vibration, harmonic analysis
- Filter & transmission line checks
- Telemetry analysis
- Communication System Monitoring . . . and more
- Power Spectral Density Analysis (with Model PDA-1 Analyzer)
- Frequency Response Plotting (with Model G-15 Sweep Generator)

SUMMARY OF SPECIFICATIONS

Frequency Range: 0.1 kc to 600 kc.
Sweepwidth: Variable, calibrated from 1 kc to 200 kc.
Center Frequency: Variable, calibrated from 0 to 500 kc.
Markers: crystal controlled, 10 kc and 100 kc plus harmonics.
IF Bandwidth: Variable, 100 cps to 5 kc.
Sweep Rate: Variable, 1 cps to 60 cps.
Amplitude Scales: Linear, 40 db log (extendable to 60 db) and 2.5 db expanded.
Sensitivity: 200 μv to 200 v full scale deflection.
Accuracy: $\pm$ 0.5 db.
Input Impedance: 50,000 ohms

Write now for specifications, other applications of PANORAMIC's Model SB-15a. Get on our regular mailing list for THE PANORAMIC ANALYZER, featuring application data.

PANORAMIC's
SB-15a
SPECTRUM ANALYZER
0.1 KC TO 600 KC

THE MARK OF THE ORIGINAL PANORAMIC

Panoramic
RADIO PRODUCTS, INC.

PANORAMIC RADIO PRODUCTS, INC.
522 So. Fulton Avenue, Mount Vernon, N.Y.
Phone: OWens 9-4600 TWX: MT-V-NY-5229
Cables: Panoramic, Mt. Vernon, N.Y. State

the pioneer is the leader

WE CATALOG IN eem electronic engineers master
Sec. 2900

dependable CERTIFIED SPECIFICATIONS for accurate data

Membership

(*Continued from page 162A*)

Hull, D. H., Trenton, N. J.
Ireland, G. C., Ottawa, Ont., Canada
Jacobowitz, H., New York, N. Y.
Jambor, L. D., Cincinnati, Ohio
Jennings, E. R., Medford, N. J.
Juodikis, P., Chicago, Ill.
Kaufman, F. M., Richmond Hill, N. Y.
Kauppi, D. K., Midland, Mich.
Kelly, J. A., Arlington, Mass.
Kidman, R. D., Cedar Rapids, Iowa
Kilimnik, B., Brooklyn, N. Y.
Kirkpatrick, E. E., Brooklyn, N. Y.
Klahr, S., Baldwin, L. I., N. Y.
Knudsen, A. R., Valparaiso, Ind.
Koehler, K. G., East Northport, L. I., N. Y.
Kozma, J. A., Edison, N. J.
Kuchela, K. S., Bombay, India
LaBahn, R. W., Corona, Calif.
Landis, R. B., Allentown, Pa.
Lange, T. J., Bellevue, Wash.
Lassetter, W. L., Charlottesville, Va.
Lathbury, C. W., Encino, Calif.
Lieber, R., Moorestown, N. J.
Mackway, H. J., Haddon Heights, N. J.
MacLean, W. F., Jr., Marion, Mass.
Marmar, G., Cedar Grove, N. J.
Marshall, J. P., Rome, N. Y.
Matty, H. B., Ashland, N. J.
Maxham, K. E., San Antonio, Tex.
McCarthy, G. F., Teaneck, N. J.
McCormick, T. C., Falls Church, Va.
McGarry, J. J., Jr., Albuquerque, N. M.
Meeker, T. R., Dayton, Ohio
Melhado, W. K., Great Neck, L. I., N. Y.
Meredith, C. M., Canoga Park, Calif.
Meyers, S. D., Fresh Meadows, L. I., N. Y.
Michener, R. E., Warrington, Pa.
Mickey, L. W., Richardson, Tex.
Miksit, G. L., Paoli, Pa.
Miles, P. A., Cambridge, Mass.
Moe, J. L., St. Paul, Minn.
Montresor, R. L., Hyde, Pa.
Moorhouse, D. M., Hawthorne, Calif.
Morden, R. E., New York, N. Y.
Morris, A. A., Arlington, Va.
Morrison, C. O., Pittsburgh, Pa.
Mower, L., Baltimore, Md.
Moyer, E. P., Bath, Pa.
Myers, W. D., Chelmsford, Mass.
Nace, P. L., Berkeley Heights, N. J.
Nalbandian, A., Hawthorne, Calif.
Nathanson, H. C., Pittsburgh, Pa.
Niquette, R. P., Somers Point, N. J.
Nurnberger, W. H., Glendale, Calif.
Oliver, W., New Milford, N. J.
Ornstein, S., New Milford, N. J.
Orr, W. C., Winston-Salem, N. C.
Osterhues, G. D., Maywood, Calif.
Pacl, R. A., Willow Grove, Pa.
Pagni, G., Rome, Italy
Parks, D. G., Palo Alto, Calif.
Parrish, L. J., Triangle, Va.
Parsegyan, B. L., St. Paul, Minn.
Paufve, E. H., Binghamton, N. Y.
Pfizenmayer, H. L., Jr., Cincinnati, Ohio
Phillips, P. C., Medford Lakes, N. J.
Poldoian, J. C., Waltham, Mass
Poulin, D. J., Andover, Mass.
Powell, J. F., Murray Hill, N. J.
Prant, A., Moorestown, N. J.
Pulford, S. R., Owego, N. Y.
Raynor, J. E., Islip, L. I., N. Y.
Reich, A., Haddonfield, N. J.
Robey, M. J., New York, N. Y.
Robinson, R. F., Alexandria, Va.
Roche, G. B., Philadelphia, Pa.
Rodieck, R. H., San Diego, Calif.
Rodriquez, R. A., Jr., Winston-Salem, N. C.
Ruffing, N. E., Shaw Air Force Base, S. C.
Rybicki, R. J., Sr., Baltimore, Md.

(*Continued on page 166A*)

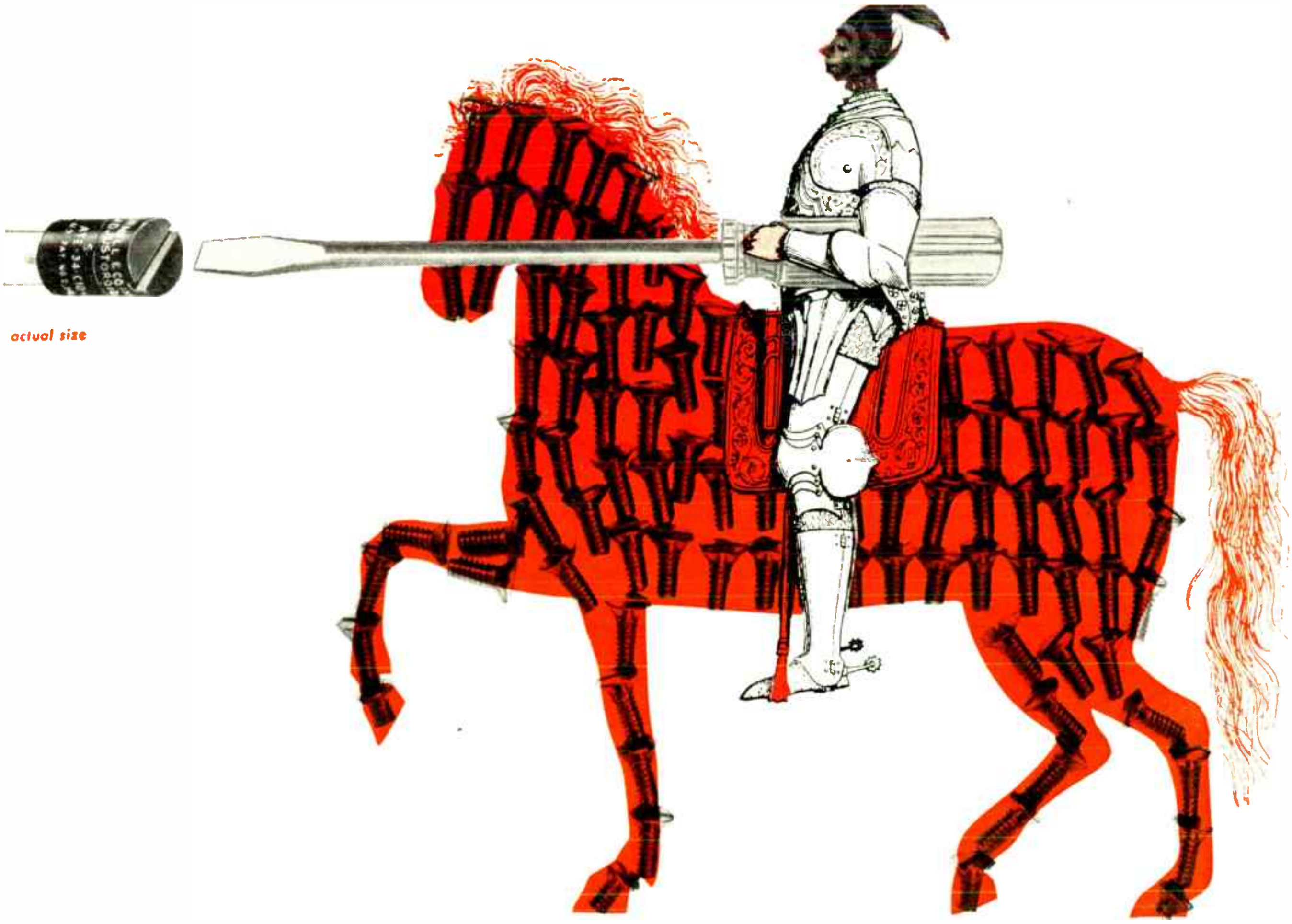

actual size

TAMING OF THE SCREW

Newest additions to the Burnell Adjustoroid® line, the microminiaturized Kernel ATE 34 and the miniatures ATE 11, ATE 0, ATE 4, represent an important contribution to printed circuit design.

These new Adjustoroids possess the exclusive advantage of flush-slotted heads which serve to eliminate adjusting screws — provide maximum economy of height — insure ease of adjustment. Besides high Q, they also offer high stability of inductance versus dc.

The new microminiature Kernel ATE 34 and the miniature ATE 11, ATE 0 and ATE 4 Adjustoroids are variable over a 10% range of their inductance. Fully encapsulated, they will withstand high acceleration and vibration environments. These Adjustoroids meet specifications MIL-T 27 Grade 4, Class R and MIL-E 15305 A as well as MIL-E 5272 for humidity and thermal shock. Write for Adjustoroid Bulletin ATE-7.

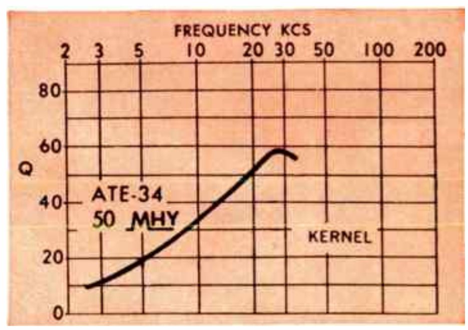

SEND NOW FOR HANDY 24" x 36" TOROIDAL INDUCTOR WALL REFERENCE CHART

Lists more than 100 types of toroidal inductors and adjustoroids. Gives performance characteristics, mechanical specifications, including case sizes, types of sealing, etc. Attach coupon to company letterhead. And if you haven't already done so — send for your free membership in the Space Shrinkers Club.

Burnell & Co., Inc. Dept. P17
10 Pelham Parkway, Pelham, New York

Gentlemen:

☐ I am interested in your new universal toroidal reference chart.

☐ I am interested in a Space Shrinkers Club membership.

name..

title..

company..

address..

PAT. 2,762,020

Burnell & Co., Inc.

PIONEERS IN microminiaturization OF TOROIDS, FILTERS AND RELATED NETWORKS

Eastern Division
Dept. P17
10 Pelham Parkway
Pelham, N. Y.
PElham 8-5000
Teletype Pelham 3633

Pacific Division
Dept. P17
720 Mission St.
South Pasadena, Cal.
MUrray 2-2841
Teletype Pasacal 7578

Membership

(*Continued from page 164A*)

Salenius, A. G., Port Washington, N. Y.
Sapp. R. S., Cincinnati, Ohio
Sasaki, T., New York, N. Y.
Scheelar, J. M., Patrick Air Force Base, Fla.
Schiring, E. E., Pittsburgh, Pa.
Schmall, D., Nutley, N. J.
Schmidt, C. H., Albuquerque, N. M.
Schmidt, J. D., Jr., Baldwinsville, N. Y.
Scholz, M. P. E., Den Haag, Nederland
Schwier, J. P., Torrance, Calif.
Seaford, R. P., Sr., Hampton, Va.
Shahan, V. T., Wappingers Falls, N. Y.
Shattuck, D. L., Wichita, Kan.
Sheridan, T. B., Cambridge, Mass.
Shoop, G. N., Marlton, N. J.
Sims, J. V., Winston-Salem, N. C.
Slattery, M. C., Bellflower, Calif.
Smith, F. P., Belmont, Mass.
Solomon, H. W., Nashua, N. H.
Somers, O. H., Wayland, Mass.
Soriano, S. M. B., Verona, Italy
Sparks, R. A., Silver Spring, Md.
Stauber, M. C., Garden City, L. I., N. Y.
Stewart, Brother B. J., New York, N. Y.
Strom, J. A., Chelmsford, Mass.
Stumpf, F. J., Jr., Fair Lawn, N. J.
Sudduth, J. F., Woodbridge, Va.
Sumida, W. S., Gardena, Calif.
Sundry, J. L., Glenburnie, Md.
Swan, W. O., Jr., Pleasant Ridge, Mich.
Tarr, R., Reseda, Calif.
Tenenberg, S. E., Sepulveda, Calif.
Testerman, W., Oklahoma City, Okla.
Thomas, S. F., Palo Alto, Calif.
Tozier, R. E., Cleveland, Ohio
Treat, C. J., Las Cruces, N. M.
Tulloh, C. F., Denver, Colo.
Tvrdy, J. J., Anchorage, Alaska
Unwin, A. M., Bellevue, Wash.
Vammen, C. M., Riverside, N. J.
van Leeuwen, C. J. T., St. Lambert, P. Q., Canada
Vannucchi, G., Bologna, Italy
Veerkamp, L. J., Grosse Pointe, Mich.
Vickers, W. H., San Jose, Calif.
Vogel, M. D., Montgomery, Ala.
Walsh, B. D., Albany, N. Y.
Watson, D. C., Fort Worth, Tex.
Weaver, R. C., Jr., Towson, Md.
Weiss, R., Long Beach, L. I., N. Y.
Westerman, R. L., Walnut Creek, Calif.
Westmark, C. I., Albuquerque, N. M.
Whicker, L. R., Clearwater, Fla.
Williams, R. P., Andover, Mass.
Williamson, V. R., Dallas, Tex.
Wippermann, D. R., San Antonio, Tex.
Wise, C. M., Rochester, N. Y.
Wishengrad, H. S., King of Prussia, Pa.
Worth, J. H., Rochester, N. Y.
Yandell, D., Fort Worth, Tex.
Young, D. T., Holmdel, N. J.
Zanella, F. H., Hollywood, Calif.
Zartman, N. B., Westmont, N. J.
Zinn, S. V., Jr., Medford Lakes, N. J.
Zushin, A. R., Annandale, Va.

Admission to Associate

Abney, L. J., Portland, Ore.
Adducci, A. J., Chicago, Ill.
Anderson, J. E., Billerica, Mass.
Ando, A., San Jose, Calif.
Aniskovicz, S., Milltown, N. J.
Antonoplos, P. A., Pittsburgh, Pa.
Avery, E. R., Stronghurst, Ill.
Bennett, N. A., Goldsboro, N. C.
Betson, C., Auckland, New Zealand
Blanchard, E. P., Jr., New York, N. Y.
Boonin, L. I., Philadelphia, Pa.
Boutin, J. J., Quebec, P. Q., Canada
Bowen, A. L., Beaumont, Tex.
Bowen, J. S., New York, N. Y.
Brashear, J. E., Pittsburgh, Pa.
Brown, W. T., Reading, Mass.
Bruster, H. E., 11, Horseheads, N. Y.
Brzezinski, W. H., West Acton, Mass.
Burk, A. J., Bethpage, L. I., N. Y.
Canavan, J. F., Ozone Park, L. I., N. Y.
Cantor, H. J., Baltimore, Md.
Carriger, J. R., Topeka, Kan.
Cassar, C. J., London, Ont., Canada
Castelli, E., Roma, Italy
Cawley, A., Philadelphia, Pa.
Church, A., Paramus, N. J.
Crutchfield, A. E., Fort Myer, Arlington, Va.
Davis, J. R., Shreveport, La.
DeSciscio, J. W., Roselle, N. J.
Dickinson, A. F., Fort Huachuca, Ariz.
Draudin, R. R., Scotland, Conn.
Duncan, A. J. H., Port of Spain, Trinidad, West Indies
Ericsson, O. E., Garfield Heights, Ohio
Filion, L. J., Montreal, P. Q., Canada
Fleckles, D. E., Northridge, Calif.
Foster, J. R., Granada Hills, Calif.
Fraher, R. J., Vandenberg Air Force Base, Calif.
Frank, W. F., Bethesda, Md.
Gaffney, D. T., New Rochelle, N. Y.
Ganger, G. M., Dayton, Ohio
Garton, A. V., Sunnyvale, Calif.
Gayhart, M. F., Springdale, Pa.
Geartner, J., Miami Beach, Fla.
Grisoff, S. F., Poughkeepsie, N. Y.
Guntsch, F. R., Konstanz, Germany
Harris, G. E., Wichita, Kan.
Harvey, R. R., Utica, N. Y.
Hayes, G. V., Rochester, N. Y.
Henderson, W. C., 111, Greensburg, Pa.
Holm, C., Skedsmokorset, Norway
Honess, C. B., Charlotte, N. C.
Horowitz, P., Los Angeles, Calif.
Houck, J. W., Jr., Towson, Md.
Howell, W. W., Lake Charles, La.

(*Continued on page 168A*)

Two completely new, transistorized, differential Data Amplifiers, Types 491 and 492, by Offner Electronics Inc. Their high precision makes possible an accuracy and simplification of data reduction previously impossible. Sixteen channels of data reduction (Type 492) requires only 8¾″ of rack space. Power supply occupies only 5¼″. The combination of accuracy, stability, fast response, and size is unmatched.

1/100% accuracy

1/100% gain stability

1/100% linearity

OFFNER

Type 491 and 492 *Differential* Data Amplifiers

Type 492 Amplifier (left) provides 2 channels of precision amplification per unit. The Type 491 (right) is a single channel unit, with input coupler for added versatility.

featuring

1/100% accuracy

1/100% gain stability—for 1,000 hours at normal ambients
1/100% linearity—for full output
All-transistor construction
1/400th second response—to step input
Very low output impedance—less than 0.1 ohm
Infinite rejection—of common d-c signals
120db rejection—at 60 cps
16 channels in 8¾ inches of rack space (Type 492)
Versatile input couplers (Type 491)

OFFNER ELECTRONICS INC.
3912 River Road, Schiller Park, Ill. (Suburb of Chicago)

PROFESSIONAL CONSULTING SERVICES

Membership

(*Continued from page 166A*)

Iida, M., Nakamura-ku, Nagoya, Japan
Jeanes, P. M., Houston, Tex.
Johnson, R. D., Sierra Vista, Ariz.
Jones, R. E., Jr., Irwin, Pa.
Kaltman, A. H., New York, N. Y.
Kessler, K. L., Seattle, Wash.
Klein, G. P., Forest Hills, N.Y.
Kojak, C. S., Beaumont, Tex.
Kopteros, G. B., Cambridge, Mass.
Kramer, C., Cincinnati, Ohio
Kruger, B., Galion, Ohio
Lapp, M. C., Corning, N. Y.
Lawrence, O., San Francisco, Calif.
L'Ecuyer, J. J., Dover, N. H.
Londis, J. J., Arlington, Va.
Margerum, R. A., Winston-Salem, N. C.
Marron, D. B., New York, N. Y.
Michels, H. P., Livingston, N. J.
Miles, A. G., Clarkson, Ont., Canada
Monteith, W. W., Horsham, Pa.
Morrow, R. L., Lubbock, Tex.
Ohlrich, J. H., Dallas, Tex.
Oliver, R. A., Montreal, Que., Canada
Pearson, W. H., III, Devon, Pa.
Perkins, D. L., Fort Walton Beach, Fla.
Radhakrishnan, T., Mysore State, India
Read, M. E., Philadelphia, Pa.
Ribeiro, G. D., Rio de Janeiro, Brazil
Riedel, J., Princeton Junction, N. J.
Riley, F. J., Palo Alto, Calif.
Rodgers, T. S., Alexandria, Va.
Rohde, F. S., Johnstown, Pa.
Salik, C. E., San Diego, Calif.
Smith, E. O., Eau Gallie, Fla.
Smith, J. Skokie, Ill.
Sneider, R. R., Edgewater, Md.
Spackman, I. H., Auckland, New Zealand
Stevens, P. L., River Vale, N. J.
Stickan, F., Waterloo, Ont., Canada
Sweeney, J. A., Philadelphia, Pa.
Takeo, O., Amagasaki, Hyogo Pref., Japan
Taylor, L. L., South Windham, Conn.
Trone, G. R., Rome, N. Y.
Tucker, T. L., Eau Gallie, Fla.
Umstead, D. L., Jr., Westminster, Calif.
Van Cleef, H. H., Jr., Cambridge, Mass.
Vega, J. C., Woodland Hills, Calif.
Vlaeminck, N. J. C., Antwerpen, Deurne-Z, Belgium
Vogelzang, J. J., Manhattan Beach, Calif.
Wakeford, F. B., St. Petersburg, Fla.
Weinberg, H. J., Chicago, Ill.
Wilson, J. F., Glen Cove, N. Y.
Winning, R. M., Van Nuys, Calif.
Wisniewski, L. R., Springfield, Va.
Woerz, M. W., Honolulu, Hawaii
Wolfe, E. M., Reading, Pa.
Wong, E. S., Los Angeles, Calif.
Wood, M. A., Beaumont, Tex.
Woods, D. L., Livermore, Calif.
Yamada, T., New York, N. Y.

Advertising Index

DISPLAY ADVERTISERS

Advertising Index

Advertising Index

STANDARD SIGNAL GENERATOR

MODEL 65-B

RANGE 75 KC to 30 MC

Individually Calibrated Scale

OUTPUT: Continuously variable, .1 microvolt to 2.2 volts.
OUTPUT IMPEDANCE: 5 ohms to .2 volt, rising to 15 ohms at 2.2 volts.

MODULATION: From zero to 100%. 400 cycles, 1000 cycles and provision for external modulation. Built-in, low distortion modulating amplifier.

POWER SUPPLY: 117 volts, 50-60 cycles, AC.

DIMENSIONS: 11" high, 20" long, 10¼" deep, overall.

WEIGHT: Approximately 50 lbs.

PRICE OF THE MODEL 65B IS $875.00; MODEL 58AS, $925.00. PRICES F.O.B. BOONTON, NEW JERSEY.

MANUFACTURERS OF
Standard Signal Generators
Pulse Generators
FM Signal Generators
Square Wave Generators
Vacuum Tube Voltmeters
UHF Radio Noise & Field Strength Meters
Capacity Bridges
Megohm Meters
Phase Sequence Indicators
Television and FM Test Equipment

MEASUREMENTS' *improved*

VHF Radio Noise and Field Strength Meter

FREQUENCY RANGE 15 MC TO 150 MC

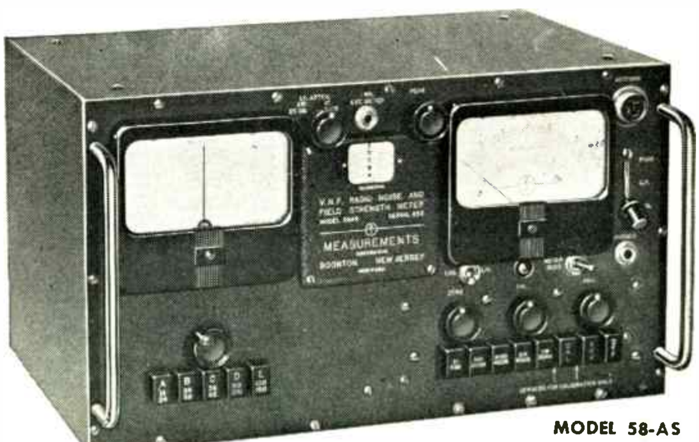

MODEL 58-AS

USES

- For measuring electrical noise
- As a tuned r-f voltmeter
- As a null indicator for r-f bridges and slotted lines
- For directional-antenna pattern measurements
- For signal-to-noise ratio measurements
- For measurement of harmonics
- As a carrier-voltage meter
- As a field-strength meter

Laboratory Standards

Write for Bulletin

MEASUREMENTS
A McGraw-Edison Division
BOONTON, NEW JERSEY

Advertising Index

CDE *Consistently Dependable Capacitors*

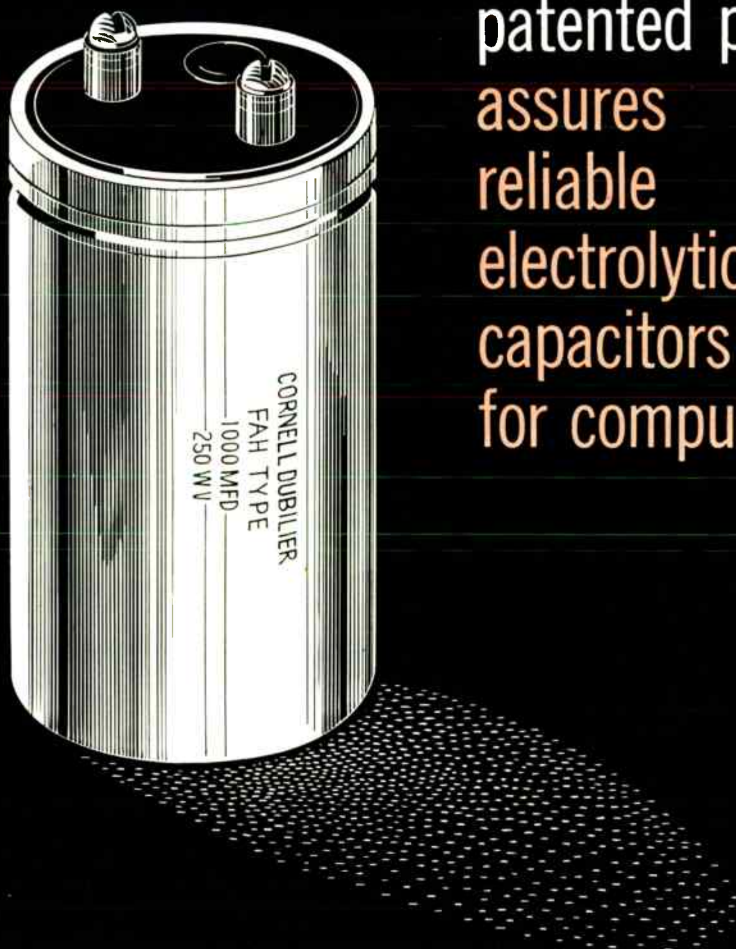

Cornell-Dubilier's patented process assures reliable electrolytic capacitors for computers

Cornell-Dubilier now combines highest purity aluminum foil with a *patented cleaning process* to eliminate all impurities in making electrolytic capacitors for power supplies and control circuits in military and industrial computers, electronic controls and other high-reliability electronic equipment. The process, specially developed for Type FAH high-reliability capacitors, achieves a freedom from corrosion that heretofore was considered impossible in foil-type electrolytics. This combination of highest-purity foil with complete freedom from contaminants also assures you that C-D electrolytic capacitors will have low leakage current and long shelf life. For complete engineering data, write for Bulletin 538 to Cornell-Dubilier Electric Corporation, South Plainfield, New Jersey. *Manufacturers of consistently dependable capacitors, filters and networks for electronics, thermonucleonics, broadcasting and utility use for 50 years.*

SPECIFICATIONS AND FEATURES

• Heavier tabs and longer staking lengths for excellent current-carrying characteristics. • Hermetically sealed, aluminum cans with molded cover. • Also available with outer insulating tube of wax-impregnated Kraft board or plastic. • Hermetically sealed with Hycar rubber gaskets. • Tapped terminal inserts or solder lug terminals. • Standard diameters: 1⅜", 2", 2½" and 3". • Can height: 4⅛". • Voltages: 3 to 450 VDC. • Capacitances: to 65,000 mfd. depending on voltage. • Temperature range: —20°C to +85°C.

CDE CORNELL-DUBILIER ELECTRIC CORPORATION

AFFILIATED WITH FEDERAL PACIFIC ELECTRIC COMPANY

How to Control
TIME, FREQUENCY and SPACE

A radio-guidance system, built by Space Technology Laboratories, Inc., played an important role in the successful launching of Pioneer V. This new ground-controlled guidance system, based on doppler-shift techniques, obtains and uses velocity and position data to control the missile.

The system relies on an accurately-controlled, stable, primary frequency — instability, f-m noise, or harmonic interference in the primary frequency could impair system performance. The G-R 1112-A Standard-Frequency Multiplier was picked by STL to help generate this frequency. It serves in an important in-line role as an element of the frequency synthesizer for this radio-guidance system. STL also uses the Frequency Multiplier in its world-wide network of tracking stations.

Telemetering, missile tracking, spectroscopy and atomic-resonance investigations, radar, and navigation-systems applications are but a few of the other areas where the 1112-A and its companion frequency multiplier, the 1112-B, find use.

U.S. Sun Orbiter Right on Beam

WASHINGTON, March 12 (AP) — Pioneer V hurtled through space today toward its destined place as a tiny new sister planet between earth and Venus in a giant orbit about the sun.

Good Operation

Pioneer V was speeding away at 6,487 m.p.h. This carried it to an estimated 213,140 miles out from earth at noon.

All equipment was reported operating perfectly. Giant radios, triggered from earth approximately once an hour, sent back loud and clear signals from which scientists computed speeds and distances.

Later today the instru-packed space vehicle ...nge into its giant five- ... orbit around the sun. ...t orbit will be a 514,- ...0-mile circle through ... between the orbits of ...arth and the planet ...

... the orbit Pioneer V will ...ach to about 74,967,000 ... the sun, compared ... the ...

Type 1112-A Standard-Frequency Multiplier . . . $1450

1-Mc, 10-Mc, and 100-Mc output frequencies are generated by separate crystal oscillators that are phase locked to the input frequency to insure extremely low f-m noise levels.

INPUT: 1-volt, 100-kc sine wave from G-R 1100-A Frequency Standard or equivalent. Can be driven by 1-Mc, 2.5-Mc, or 5-Mc standard frequency as well.

OUTPUT: 1-Mc, 10-Mc, and 100-Mc sine-wave signals; output level of each independently adjustable with maximum of 20 mw into 50 ohms.

STABILITY: Long-term stability dependent only upon driving source.

F-M NOISE: Less than 1 part in 10^9.

Type 1112-B Standard-Frequency Multiplier . . . $1360

1000-Mc output is generated directly by a klystron oscillator that is phase-locked to the 100-Mc input. Phase stability of the output is comparable to that of the input signal.

INPUT: 20-mw, 100-Mc sine wave from 1112-A or equivalent.

OUTPUT: 1000-Mc sine wave; at least 50 mw into a 50-ohm load.

STABILITY and F-M NOISE: Same as 1112-A.

Write For Complete Information

GENERAL RADIO COMPANY
WEST CONCORD, MASSACHUSETTS

our 45th year in Electronics

NEW YORK, WOrth 4-2722 District Office in Ridgefield, N. J. WHitney 3-3140	CHICAGO Oak Park Village 8-9400	PHILADELPHIA Abington HAncock 4-7419	WASHINGTON, D.C. Silver Spring JUniper 5-1088	SAN FRANCISCO Los Altos WHitecliff 8-8233	LOS ANGELES Los Angeles HOllywood 9-6201	IN CANADA Toronto CHerry 6-2171